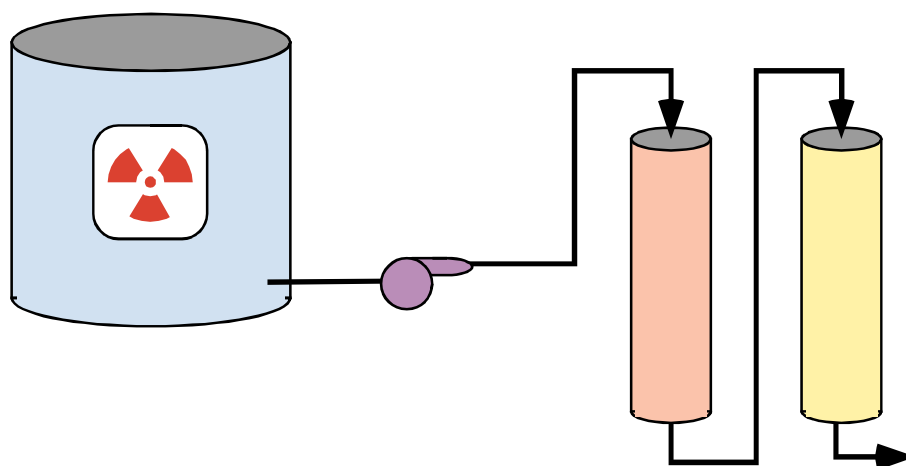


## Preliminary Ion Exchange Modeling for Removal of Cesium from Hanford Waste Using Hydrrous Crystalline Silicotitanate Material



Westinghouse Savannah River Company  
Savannah River Site  
Aiken, SC 29808



**This document was prepared in conjunction with work accomplished under Contract No. DE-AC09-96SR18500 with the U. S. Department of Energy.**

#### **DISCLAIMER**

**This report was prepared as an account of work sponsored by an agency of the United States Government. Neither the United States Government nor any agency thereof, nor any of their employees, makes any warranty, express or implied, or assumes any legal liability or responsibility for the accuracy, completeness, or usefulness of any information, apparatus, product or process disclosed, or represents that its use would not infringe privately owned rights. Reference herein to any specific commercial product, process or service by trade name, trademark, manufacturer, or otherwise does not necessarily constitute or imply its endorsement, recommendation, or favoring by the United States Government or any agency thereof. The views and opinions of authors expressed herein do not necessarily state or reflect those of the United States Government or any agency thereof.**

**This report has been reproduced directly from the best available copy.**

**Available for sale to the public, in paper, from: U.S. Department of Commerce, National Technical Information Service, 5285 Port Royal Road, Springfield, VA 22161,  
phone: (800) 553-6847,  
fax: (703) 605-6900  
email: [orders@ntis.fedworld.gov](mailto:orders@ntis.fedworld.gov)  
online ordering: <http://www.ntis.gov/help/index.asp>**

**Available electronically at <http://www.osti.gov/bridge>  
Available for a processing fee to U.S. Department of Energy and its contractors, in paper, from: U.S. Department of Energy, Office of Scientific and Technical Information, P.O. Box 62, Oak Ridge, TN 37831-0062,  
phone: (865)576-8401,  
fax: (865)576-5728  
email: [reports@adonis.osti.gov](mailto:reports@adonis.osti.gov)**

**WSRC-TR-2001-00400**  
**SRT-RPP-2001-00134**

**KEYWORDS:**

*Hanford River Protection Project*  
*Ion Exchange Technology*  
*Crystalline Silicotanate Resins*  
*Technetium*  
*Cesium*  
*VERSE Code*  
*Column Modeling*

**RETENTION - Permanent**

# **Preliminary Ion Exchange Modeling for Removal of Cesium from Hanford Waste Using Hydrous Crystalline Silicotitanate Material**

*SAVANNAH RIVER TECHNOLOGY CENTER*

L. Larry Hamm  
Thong Hang  
Daniel J. McCabe  
William D. King

Publication Date: July 2002

Westinghouse Savannah River Company  
Savannah River Site  
Aiken, SC 29808



---

**SAVANNAH RIVER SITE**

**This page was intentionally left blank**

## TABLE OF CONTENTS

<b>1.0 Executive Summary .....</b>	<b>1</b>
<b>2.0 Introduction and Background.....</b>	<b>11</b>
2.1 Test Specification Objectives .....	13
2.2 IONSIV® IE-910/IE-911 CST Versus SuperLig® 644.....	13
2.3 Ion Exchange Modeling.....	14
2.4 Report Overview .....	15
<b>3.0 Column Model Formulations .....</b>	<b>19</b>
3.1 The Multi-Component Model .....	20
3.2 The Single-Component Model .....	22
3.3 The Cesium-IONSIV® IE-911 CST System .....	22
<b>4.0 Equilibrium Cesium Isotherms .....</b>	<b>27</b>
4.1 The Isotherm Model .....	28
4.2 Batch Feed Compositions .....	29
4.3 The Beta Parameter Values .....	30
4.4 Isotherm Model for VERSE-LC Application .....	31
<b>5.0 Column Properties .....</b>	<b>39</b>
5.1 Basic Constraint Functions .....	39
5.2 Densities .....	40
5.3 Porosities.....	41
<b>6.0 Particle Size Distributions .....</b>	<b>47</b>
6.1 MicroTrac® Laser Technology Data.....	47
6.2 Lasentec® Laser Technology Data .....	48
<b>7.0 Pore Diffusion.....</b>	<b>53</b>
7.1 Waste Solution Density and Viscosity .....	53
7.2 Molecular Diffusion Coefficients .....	54
7.3 Pore Diffusion Coefficients.....	55
7.3.1 CST Conceptual Model .....	55
7.3.2 The Tortuosity Factor .....	56
7.3.3 Comparison to Previous Studies .....	57
7.4 VERSE-LC Simulations for Batch Kinetics Tests .....	58
7.4.1 PNNL Kinetics Studies.....	59
7.4.2 SRS Kinetics Studies .....	59
7.4.3 Particle Size Impact on Kinetics.....	60
7.4.4 ORNL Kinetics Studies .....	61
<b>8.0 Axial Dispersion and Film Diffusion.....</b>	<b>75</b>

<b>8.1</b>	<b>Film Diffusion.....</b>	<b>75</b>
<b>8.2</b>	<b>Axial Dispersion .....</b>	<b>75</b>
8.2.1	Radial Flow Maldistribution.....	76
8.2.2	Headspace and Short Column Impacts .....	76
<b>9.0</b>	<b>Laboratory-Scale Column Assessments.....</b>	<b>77</b>
<b>9.1</b>	<b>CST Pore Diffusion Coefficient .....</b>	<b>78</b>
9.1.1	Tortuosity Factor Optimization Strategy .....	78
9.1.2	Tortuosity Factor Optimization Results.....	79
9.1.3	Tortuosity Factor Coefficient Recommendation.....	80
<b>9.2</b>	<b>Column Assessment Studies.....</b>	<b>80</b>
9.2.1	SRS Tank 44 Tests .....	80
9.2.2	SRS Average Simulant Tests.....	81
9.2.3	SRS High OH Simulant Tests.....	83
9.2.4	PNNL Hanford Sample Tests .....	83
9.2.5	ORNL MVST Sample Tests .....	83
<b>10.0</b>	<b>Full-Scale Column Predictions and Design .....</b>	<b>101</b>
<b>10.1</b>	<b>IONSIV® IE-911 CST versus SuperLig® 644 Ion-Exchanger Performance .....</b>	<b>101</b>
<b>10.2</b>	<b>Basic Flowsheet.....</b>	<b>103</b>
<b>10.3</b>	<b>VERSE-LC Modeling of the Full-Scale Facility .....</b>	<b>104</b>
10.3.1	Volumetric Flowrate on an Envelope Basis.....	104
10.3.2	Cesium-137 Exit Concentration Criterion on an Envelope Basis.....	105
10.3.3	Input Concentration and Flowrate Boundary Conditions .....	106
<b>10.4</b>	<b>Mass Transfer Zone Concept for Column Design .....</b>	<b>106</b>
<b>10.5</b>	<b>The Global Optimization Strategy .....</b>	<b>107</b>
<b>10.6</b>	<b>Theoretical Minimum Spent CST Material .....</b>	<b>108</b>
<b>10.7</b>	<b>Spent CST Material Dependency on Geometry.....</b>	<b>109</b>
<b>10.8</b>	<b>CST Column Design and Performance.....</b>	<b>111</b>
10.8.1	Nominal Case Results for 2-Column Carousels .....	111
10.8.2	Nominal Case Results for 3-Column Carousels .....	113
10.8.3	Impact of Slow Kinetics on Design .....	113
<b>10.9</b>	<b>Cesium Column Inventory.....</b>	<b>114</b>
A.....		117
B.....		117
<b>11.0</b>	<b>References .....</b>	<b>139</b>
<b>Appendix A</b>	<b>(BBI Phase 1 LAW Feed Solution Definitions).....</b>	<b>145</b>
<b>A.1</b>	<b>Altered Tank Solutions.....</b>	<b>145</b>
<b>A.2</b>	<b>Isotopic Dilution Process for Strontium-90 .....</b>	<b>147</b>
<b>A.3</b>	<b>Adjusted Tank Solutions for K<sub>d</sub> Modeling.....</b>	<b>148</b>
<b>A.4</b>	<b>Feed Solution Densities.....</b>	<b>149</b>
<b>Appendix B</b>	<b>(Cesium Isotherms for LAW Phase 1 Batch Feeds) .....</b>	<b>167</b>
<b>B.1</b>	<b>Molar Ratios of Na/Cs, K/Cs, and SrOH/Cs .....</b>	<b>168</b>

<b>B.2 Isotherm Predictions using the ZAM Model .....</b>	<b>168</b>
<b>B.3 Isotherm Model for VERSE-LC Application .....</b>	<b>169</b>
<b>B.4 Isotherm Parameter Estimation Technique .....</b>	<b>171</b>
<b>B.5 The Least Favorable Isotherm.....</b>	<b>172</b>
<b>B.6 “Effective” Single-Component Isotherm Models.....</b>	<b>173</b>
B.6.1 PHASE 1 Envelope A LAW Isotherms .....	174
B.6.2 PHASE 1 Envelope B LAW Isotherms .....	174
B.6.3 PHASE 1 Envelope C LAW Isotherms .....	174
B.6.4 Comparison of Least Favorable Isotherms .....	174
B.6.5 LAW-1 Feed (KNO <sub>3</sub> precipitation Issue) .....	175
B.6.6 Impact of Strontium on Envelope C Isotherms.....	176
<b>B.7 Cesium Isotherm Sensitivity Study and Error Analysis.....</b>	<b>177</b>
B.7.1 The Uncertainty Approach Taken .....	177
B.7.2 Feed Composition Uncertainties.....	178
B.7.3 Feed Density and Process Temperature Uncertainties.....	179
B.7.4 Dilution Factor Uncertainty .....	179
B.7.5 Sensitivity Results and Error Estimates .....	180
<b><i>Appendix C (Dilution Factor for IONSIV<sup>®</sup> IE-911) .....</i></b>	<b><i>217</i></b>
<b>C.1 Cesium loading on IONSIV<sup>®</sup> IE-911 versus IONSIV<sup>®</sup> IE-910.....</b>	<b>218</b>
<b>C.2 Averaged Dilution Factor for Baseline IE-911 CST Material .....</b>	<b>219</b>
<b>C.3 Dilution Factor Variability.....</b>	<b>221</b>
C.3.1 Impact of Cesium Concentration .....	221
C.3.2 Impact of Temperature.....	222
<b>C.4 Cesium Loading Curve Comparisons .....</b>	<b>223</b>
<b>C.5 Strontium Loading Curve Comparisons.....</b>	<b>224</b>
<b><i>Appendix D (VERSE-LC Input Files for Phase 1 Batch Feeds) .....</i></b>	<b><i>239</i></b>
Makefile for NMAKE Utility (2 nominal case runs of VERSE-LC).....	243
VERSE-LC Input for Phase 1 LAW-1 Batch Feed (nominal case; 2000 L).....	249
VERSE-LC Input for Phase 1 LAW-2a Batch Feed (nominal case; 2000 L).....	249
VERSE-LC Input for Phase 1 LAW-2b Batch Feed (nominal case; 2000 L).....	250
VERSE-LC Input for Phase 1 LAW-3 Batch Feed (nominal case; 2000 L).....	250
VERSE-LC Input for Phase 1 LAW-4 Batch Feed (nominal case; 2000 L).....	251
VERSE-LC Input for Phase 1 LAW-5 Batch Feed (nominal case; 2000 L).....	251
VERSE-LC Input for Phase 1 LAW-6 Batch Feed (nominal case; 2000 L).....	252
VERSE-LC Input for Phase 1 LAW-7 Batch Feed (nominal case; 2000 L).....	252
VERSE-LC Input for Phase 1 LAW-8 Batch Feed (nominal case; 2000 L).....	253
VERSE-LC Input for Phase 1 LAW-9 Batch Feed (nominal case; 2000 L).....	253
VERSE-LC Input for Phase 1 LAW-10 Batch Feed (nominal case; 2000 L).....	254
VERSE-LC Input for Phase 1 LAW-11 Batch Feed (nominal case; 2000 L).....	254
VERSE-LC Input for Phase 1 LAW-12 Batch Feed (nominal case; 2000 L).....	255
VERSE-LC Input for Phase 1 LAW-13 Batch Feed (nominal case; 2000 L).....	255
VERSE-LC Input for Phase 1 LAW-14 Batch Feed (nominal case; 2000 L).....	256
VERSE-LC Input for Phase 1 LAW-15 Batch Feed (nominal case; 2000 L).....	256
VERSE-LC Output for Phase 1 LAW-1 Batch Feed (nominal case; 2000 L).....	257
VERSE-LC Output for Phase 1 LAW-2b Batch Feed (nominal case; 2000 L).....	258
VERSE-LC Output for Phase 1 LAW-3 Batch Feed (nominal case; 2000 L).....	259

<b>Appendix E (Batch Kinetics Test Input and Output Files)</b>	<b>261</b>
<b>E.1 PNNL Kinetics Studies</b>	<b>261</b>
<b>E.2 SRS Kinetics Studies</b>	<b>261</b>
<b>E.3 Particle Size Impact on Kinetics</b>	<b>261</b>
<b>E.4 ORNL Kinetics Studies</b>	<b>261</b>
VERSE Input for Powder Test (Brown et al., 1996)	269
VERSE Output for Powder Test (Brown et al., 1996)	270
VERSE Input for Engineered -08 Test (Brown et al., 1996)	271
VERSE Input for Engineered -38b Test (Brown et al., 1996)	272
VERSE Input for Batch Kinetic Test (Fondeur et al., 2000)	273
VERSE Output for Batch Kinetic Test (Fondeur et al., 2000)	274
VERSE Input for Cs Uptake Test (Anthony et al., 1996; 112 $\mu\text{m}$ )	276
VERSE Input for Cs Uptake Test (Anthony et al., 1996; 334 $\mu\text{m}$ )	277
<b>Appendix F (ZAM Code Description)</b>	<b>279</b>
<b>F.1 About the Model</b>	<b>279</b>
<b>F.2 I/O Files and Running the ZAM Code</b>	<b>282</b>
<b>F.3 Input File Structure</b>	<b>283</b>
<b>F.4 Installation, Verification &amp; Validation</b>	<b>285</b>
F.4.1 ZAM Verification of Total Ionic Capacities	286
F.4.2 ZAM Validation to Hanford LAW Solutions	287
F.4.3 Version-4 Versus Version-5 Comparison	288
<b>F.5 ZAM Version-4 or Version-5 Input for 5 M Na AW-101 Feed)</b>	<b>302</b>
<b>F.6 ZAM Version-4 Output for 5 M Na AW-101 Feed)</b>	<b>302</b>
<b>F.7 ZAM Version-4 or Version-5 Input for Phase 1 LAW-1 Batch Feed)</b>	<b>302</b>
<b>F.8 ZAM Version-4 Output for Phase 1 LAW-1 Batch Feed)</b>	<b>303</b>
<b>F.9 ZAM Version-5 Output for Phase 1 LAW-1 Batch Feed)</b>	<b>303</b>
<b>Appendix G (ZAM Input Files for Phase 1 Batch Feeds)</b>	<b>305</b>
ZAM Input for Phase 1 LAW-1 Batch Feed (Envelope A; nominal case)	306
ZAM Input for Phase 1 LAW-5 Batch Feed (Envelope A; nominal case)	306
ZAM Input for Phase 1 LAW-6 Batch Feed (Envelope A; nominal case)	306
ZAM Input for Phase 1 LAW-8 Batch Feed (Envelope A; nominal case)	306
ZAM Input for Phase 1 LAW-9 Batch Feed (Envelope A; nominal case)	307
ZAM Input for Phase 1 LAW-10 Batch Feed (Envelope A; nominal case)	307
ZAM Input for Phase 1 LAW-11 Batch Feed (Envelope A; nominal case)	307
ZAM Input for Phase 1 LAW-12 Batch Feed (Envelope A; nominal case)	307
ZAM Input for Phase 1 LAW-13 Batch Feed (Envelope A; nominal case)	308
ZAM Input for Phase 1 LAW-14 Batch Feed (Envelope A; nominal case)	308
ZAM Input for Phase 1 LAW-15 Batch Feed (Envelope A; nominal case)	308
ZAM Input for Phase 1 LAW-2a Batch Feed (Envelope B; nominal case)	308
ZAM Input for Phase 1 LAW-2b Batch Feed (Envelope B; nominal case)	309
ZAM Input for Phase 1 LAW-3 Batch Feed (Envelope C; nominal case)	309
ZAM Input for Phase 1 LAW-4 Batch Feed (Envelope C; nominal case)	309
ZAM Input for Phase 1 LAW-7 Batch Feed (Envelope C; nominal case)	309
ZAM Input for Phase 1 LAW-1 Batch Feed (Envelope A; with 4 M $\text{Na}^+$ )	310
ZAM Input for Phase 1 LAW-1 Batch Feed (Envelope A; with 6 M $\text{Na}^+$ )	310



ZAM Input for Phase 1 LAW-3 Batch Feed (Envelope C; with $\text{Sr}^{+2}$ ) .....	310
<b>Appendix H (Column Test Input Files) .....</b>	<b>311</b>
<b>H.1 SRS Tank 44 Studies.....</b>	<b>311</b>
<b>H.2 SRS Average Simulant Studies .....</b>	<b>311</b>
<b>H.3 SRS High OH Simulant Studies.....</b>	<b>312</b>
<b>H.4 PNNL AW-101 Sample Studies .....</b>	<b>312</b>
<b>H.5 ORNL MVST Sample Tests.....</b>	<b>312</b>
VERSE Input for SRS-Tank44-Test1a .....	327
VERSE Input for SRS-Tank44-Test1b .....	327
VERSE Input for SRS-Avg-Test1 .....	328
VERSE Input for SRS-Avg-Test2 (single-component approach) .....	328
VERSE Input for SRS-Avg-Test2 (ternary-component approach).....	329
VERSE Input for SRS-Avg-Test3 .....	329
VERSE Input for SRS-Avg-Test4 .....	330
VERSE Input for SRS-Avg-Test5 .....	330
VERSE Input for SRS-Avg-Test6 .....	331
VERSE Input for SRS-Avg-Test7 .....	332
VERSE Input for SRS-High-OH-Test1a .....	332
VERSE Input for SRS-High-OH-Test1b .....	333
VERSE Input for PNNL-AW101-Test1 .....	333
VERSE Input for ORNL-W27-Test1.....	334
VERSE Input for ORNL-W27-Test2.....	334
VERSE Input for ORNL-CsRD-Run2.....	335
VERSE Input for ORNL-CsRD-Run3.....	335
VERSE Input for ORNL-CsRD-Run4a.....	336
VERSE Input for ORNL-CsRD-Run4b.....	337

(This Page Intentionally Left Blank)

## LIST OF TABLES

Table 2-1. Key batch processing information on the Phase 1 Low activity waste (LAW) feeds listed in their scheduled order to be processed. ....	17
Table 4-1. Summary of the Phase 1 batch feed compositions in molarity units (on a 5M sodium basis) highlighting those ionic species who are dominant contributors to the effectiveness of CST material for cesium loading. <sup>a</sup> .....	33
Table 4-2. Estimated beta parameter values and error estimate for a one-component (total cesium) homovalent algebraic isotherm model based on CST in its powder-form (IE-910) where the data sets used were created using the ZAM code. ....	34
Table 4-3. Parameter settings for an “effective” single component Freundlich/Langmuir Hybrid equilibrium isotherm model for total cesium on CST based on the 1-component homovalent model. ....	35
Table 5-1. Key CST exchange properties taken from literature for various ion exchangers. ....	42
Table 5-2. Estimated particle density based on measured densities taken from slurry mixtures of CST and water by Qureshi (1999). ....	43
Table 5-3. “Best estimate” and upper/lower bounds of total porosity or particle density based on available measured densities or bed/particle porosities for IE-911 CST material. ....	43
Table 5-4. Particle porosity as a function of bed porosity at three different total porosity values for the IONSIV <sup>®</sup> IE-911 CST material. ....	44
Table 6-1. Particle size distributions <sup>a</sup> of CST material in its engineered-form (batch number not recorded) based on MicroTrac <sup>®</sup> Laser Technology. ....	49
Table 6-2. Chord size distributions <sup>a</sup> of CST material in its engineered-form (Baseline Lot #9090-76) based on Lasentec <sup>®</sup> Laser Technology. ....	49
Table 6-3. Estimated average particle radius of CST material in its engineered-form (Baseline Lot #9090-76) based on Lasentec <sup>®</sup> Laser Technology. ....	51
Table 7-1. Fluid density and dynamic viscosity for water and simulated Envelope A 5 M sodium waste solution. ..	61
Table 7-2. Measured fluid density and dynamic viscosity for various SRS waste solutions. ....	62
Table 7-3. Limiting ionic conductances in water at 25 °C (Reid et al., 1977; Perry, 1973, Glasstone and Lewis, 1960). ....	62
Table 7-4. Best estimate binary molecular <sup>a</sup> diffusion coefficients at 25 °C for a solution containing essentially only cesium cations and anion of one particular species. ....	63
Table 7-5. Phase 1 LAW feed anion concentrations and relative mole fractions <sup>a</sup> for Envelope A used in determining “effective” binary molecular diffusion coefficients with cesium. ....	64
Table 7-6. Phase 1 LAW feed anion concentrations and relative mole fractions <sup>a</sup> for Envelopes B and C used in determining “effective” binary molecular diffusion coefficients with cesium. ....	65
Table 7-7. Simulant or sample anion concentrations and relative mole fractions <sup>a</sup> for various solutions <sup>b</sup> used in determining “effective” binary molecular diffusion coefficients with cesium. ....	66
Table 7-8. Best estimate cesium effective molecular and pore diffusion coefficients at 25 °C for each Phase 1 LAW batch feed. ....	67
Table 7-9. Best Estimate cesium effective molecular and pore diffusion coefficients at 25 °C for various solutions used in column transport assessments. ....	68
Table 9-1. Key features of Cesium-CST IE-911 fixed bed small-scale columns considered. ....	85
Table 9-2. Summary of recommended nominal parameter settings for Cesium-IONSIV <sup>®</sup> IE-911 CST system column modeling. ....	87
Table 9-2. Summary of recommended nominal parameter settings for Cesium-IONSIV <sup>®</sup> IE-911 CST system column modeling (continued). ....	88
Table 9-3. Root-mean-square residuals for each column study as a function of the ratio of pore to free diffusion coefficients ( $\eta$ ). ....	89
Table 10-1. Comparison of key parameters <sup>a</sup> between IONSIV <sup>®</sup> IE-911 CST material and SuperLig <sup>®</sup> 644 resin for removal of cesium from LAW by ion exchange. ....	117
Table 10-2. Ion-exchange facility cesium exit concentration criterion on an envelope basis. ....	117
Table 10-3. Processing information on the Phase 1 Low activity waste (LAW) feeds listed in their scheduled order to be processed. ....	118
Table 10-4. Ion-exchange facility total cesium exit concentration criterion on a batch feed basis. ....	119

Table 10-5. Estimate of the theoretical minimum amount of spent CST material required to process each Phase 1 LAW batch feed. ....	120
Table 10-6. Impact of L/D geometry on estimated amount of total spent CST material generated to process the Phase 1 LAW inventory and the number of cycles required per batch of feed (i.e., based on a 2000 L 2-column carousel facility operating at 25 C under nominal parameter settings <sup>a</sup> , except for those parameters explicitly listed in this table). ....	121
Table 10-7. Geometric L/D ratios and resulting geometries considered in CST column design simulations using VERSE-LC based on a 2-column carousel configuration. ....	122
Table 10-8. Geometric L/D ratios and resulting geometries considered in CST column design simulations using VERSE-LC based on a 3-column carousel configuration. <sup>a</sup> ....	122
Table 10-9. Estimated amount of total spent CST material generated to process the Phase 1 LAW inventory and the number of cycles required per batch of feed (i.e., based on a 2-column carousel facility operating at 25 C under nominal parameter settings <sup>a</sup> ). ....	123
Table 10-10. Estimated amount of total spent CST material generated to process the Phase 1 LAW inventory and the number of cycles required per batch of feed (i.e., based on a 3-column carousel facility operating at 25 C under nominal parameter settings <sup>a</sup> ). ....	124
Table 10-11. Impact of mass transfer limitations on estimated amount of total spent CST material generated to process the Phase 1 LAW inventory and the number of cycles required per batch of feed (i.e., based on a 2-column carousel facility operating at 25 C under nominal parameter settings <sup>a</sup> , except for those parameters explicitly listed in this table). ....	125
Table 10-12. Estimated amount of total spent CST material generated to process the Phase 1 LAW inventory and the number of cycles required per batch of feed (i.e., based on a 2-column carousel facility operating at 25 C under nominal parameter settings <sup>a</sup> , except for the cesium pore diffusivity coefficient). ....	126
Table 10-13. Estimated amount of total spent CST material generated to process the Phase 1 LAW inventory and the number of cycles required per batch of feed (i.e., based on a 2-column carousel facility operating at 25 C under nominal parameter settings <sup>a</sup> , except for the cesium pore diffusivity coefficient). ....	127
Table A-1. Best Basis Inventory (BBI) Phase 1 LAW feed solution data for Envelope A where stated alterations were made to minimize inventory inconsistencies and to establish an ionic charge balance (a value of zero implies that no information was provided on species). ....	152
Table A-2. Best Basis Inventory (BBI) Phase 1 LAW feed solution data for Envelopes B and C where stated alterations were made to minimize inventory inconsistencies and to establish an ionic charge balance (a value of zero implies that no information was provided on species). ....	154
Table A-3. Best Basis Inventory (BBI) Phase 1 LAW feed solution data for Envelope C where the impact from the isotopic dilution pretreatment process for Strontium-90 and permanganate addition for TRUs separation have been taken into account. ....	156
Table A-4. Ionic species available within the ZAM CST ion-exchange equilibrium model. ....	159
Table A-5. Best estimate Phase 1 LAW feed solution data for Envelope A adjusted to 5 M Na <sup>a</sup> and used as input to the CST equilibrium model. ....	160
Table A-6. Best estimate Phase 1 LAW feed solution data for Envelopes B and C adjusted to 5 M Na <sup>a</sup> and used as input to the CST equilibrium model. ....	162
Table A-7. Hanford and SRS measured liquid-phase densities for several LAW liquid samples and simulants considered. ....	164
Table A-8. Comparison of measured to predicted liquid-phase densities for several Hanford LAW liquid samples and simulants based on available correlations. ....	165
Table B-1. Key CST exchange properties taken from literature. ....	181
Table B-2. Key molar ratios for the various LAW batch feed solutions. ....	181
Table B-3. “Extrapolated” ZAM equilibrium isotherm model predictions for CST material in the powder form (IE-910) in contact with Envelope A’s LAW-1 feed solution at 5 M [Na <sup>+</sup> ]. <sup>a</sup> ....	182
Table B-4. ZAM equilibrium isotherm model predictions for CST material in the powder form (IE-910) in contact with Envelope A’s LAW-5 feed solution at 5 M [Na <sup>+</sup> ]. <sup>a</sup> ....	182
Table B-5. ZAM equilibrium isotherm model predictions for CST material in the powder form (IE-910) in contact with Envelope A’s LAW-6 feed solution at 5 M [Na <sup>+</sup> ]. <sup>a</sup> ....	183

Table B-6. ZAM equilibrium isotherm model predictions for CST material in the powder form (IE-910) in contact with Envelope A's LAW-8 feed solution at 5 M [Na <sup>+</sup> ]. <sup>a</sup>	183
Table B-7. ZAM equilibrium isotherm model predictions for CST material in the powder form (IE-910) in contact with Envelope A's LAW-9 feed solution at 5 M [Na <sup>+</sup> ]. <sup>a</sup>	184
Table B-8. ZAM equilibrium isotherm model predictions for CST material in the powder form (IE-910) in contact with Envelope A's LAW-10 feed solution at 5 M [Na <sup>+</sup> ]. <sup>a</sup>	184
Table B-9. ZAM equilibrium isotherm model predictions for CST material in the powder form (IE-910) in contact with Envelope A's LAW-11 feed solution at 5 M [Na <sup>+</sup> ]. <sup>a</sup>	185
Table B-10. ZAM equilibrium isotherm model predictions for CST material in the powder form (IE-910) in contact with Envelope A's LAW-12 feed solution at 5 M [Na <sup>+</sup> ]. <sup>a</sup>	185
Table B-11. ZAM equilibrium isotherm model predictions for CST material in the powder form (IE-910) in contact with Envelope A's LAW-13 feed solution at 5 M [Na <sup>+</sup> ]. <sup>a</sup>	186
Table B-12. ZAM equilibrium isotherm model predictions for CST material in the powder form (IE-910) in contact with Envelope A's LAW-14 feed solution at 5 M [Na <sup>+</sup> ]. <sup>a</sup>	186
Table B-13. ZAM equilibrium isotherm model predictions for CST material in the powder form (IE-910) in contact with Envelope A's LAW-15 feed solution at 5 M [Na <sup>+</sup> ]. <sup>a</sup>	187
Table B-14. ZAM equilibrium isotherm model predictions for CST material in the powder form (IE-910) in contact with Envelope B's LAW-2a feed solution at 5 M [Na <sup>+</sup> ]. <sup>a</sup>	187
Table B-15. ZAM equilibrium isotherm model predictions for CST material in the powder form (IE-910) in contact with Envelope B's LAW-2b feed solution at 5 M [Na <sup>+</sup> ]. <sup>a</sup>	188
Table B-16. ZAM equilibrium isotherm model predictions for CST material in the powder form (IE-910) in contact with Envelope C's LAW-3 feed solution at 5 M [Na <sup>+</sup> ]. <sup>a</sup>	188
Table B-17. ZAM equilibrium isotherm model predictions for CST material in the powder form (IE-910) in contact with Envelope C's LAW-4 feed solution at 5 M [Na <sup>+</sup> ]. <sup>a</sup>	189
Table B-18. ZAM equilibrium isotherm model predictions for CST material in the powder form (IE-910) in contact with Envelope C's LAW-7 feed solution at 5 M [Na <sup>+</sup> ]. <sup>a</sup>	189
Table B-19. Parameter identities between a 4-component VERSE-LC Freundlich/Langmuir Hybrid equilibrium isotherm model and the "effective" single-component homovalent isotherm model.	190
Table B-20. Estimated selectivity coefficients for the Cesium-CST system based on ZAM predictions and the 4-component homovalent isotherm model for the Envelope A feed solutions.	191
Table B-21. The resulting correlation coefficient matrix for the fit of the selectivity coefficients for the Cesium-CST system, ZAM produced data, and the 4-component homovalent isotherm model for the Envelope A feed solutions.	192
Table B-22. Estimated beta parameter values and error estimate for a one-component (total cesium) homovalent algebraic isotherm model based on CST in its powder-form (IE-910) where the data sets used were created using the ZAM code.	192
Table B-23. Parameter settings for an "effective" single component Freundlich/Langmuir Hybrid equilibrium isotherm model for total cesium on CST based on the 1-component homovalent model.	193
Table B-24. "Extrapolated" ZAM equilibrium model versus algebraic model cesium loading predictions for CST material in contact with Envelope A's LAW-1 feed solution at 5 M [Na <sup>+</sup> ]. <sup>a</sup>	193
Table B-25. ZAM equilibrium model versus algebraic model cesium loading predictions for CST material in contact with Envelope A's LAW-5 feed solution at 5 M [Na <sup>+</sup> ]. <sup>a</sup>	194
Table B-26. ZAM equilibrium model versus algebraic model cesium loading predictions for CST material in contact with Envelope A's LAW-6 feed solution at 5 M [Na <sup>+</sup> ]. <sup>a</sup>	194
Table B-27. ZAM equilibrium model versus algebraic model cesium loading predictions for CST material in contact with Envelope A's LAW-8 feed solution at 5 M [Na <sup>+</sup> ]. <sup>a</sup>	195
Table B-28. ZAM equilibrium model versus algebraic model cesium loading predictions for CST material in contact with Envelope A's LAW-9 feed solution at 5 M [Na <sup>+</sup> ]. <sup>a</sup>	196
Table B-29. ZAM equilibrium model versus algebraic model cesium loading predictions for CST material in contact with Envelope A's LAW-10 feed solution at 5 M [Na <sup>+</sup> ]. <sup>a</sup>	196
Table B-30. ZAM equilibrium model versus algebraic model cesium loading predictions for CST material in contact with Envelope A's LAW-11 feed solution at 5 M [Na <sup>+</sup> ]. <sup>a</sup>	197
Table B-31. ZAM equilibrium model versus algebraic model cesium loading predictions for CST material in contact with Envelope A's LAW-12 feed solution at 5 M [Na <sup>+</sup> ]. <sup>a</sup>	197

Table B-32. ZAM equilibrium model versus algebraic model cesium loading predictions for CST material in contact with Envelope A's LAW-13 feed solution at 5 M [Na <sup>+</sup> ]. <sup>a</sup>	198
Table B-33. ZAM equilibrium model versus algebraic model cesium loading predictions for CST material in contact with Envelope A's LAW-14 feed solution at 5 M [Na <sup>+</sup> ]. <sup>a</sup>	198
Table B-34. ZAM equilibrium model versus algebraic model cesium loading predictions for CST material in contact with Envelope A's LAW-15 feed solution at 5 M [Na <sup>+</sup> ]. <sup>a</sup>	199
Table B-35. ZAM equilibrium model versus algebraic model cesium loading predictions for CST material in contact with Envelope B's LAW-2a feed solution at 5 M [Na <sup>+</sup> ]. <sup>a</sup>	200
Table B-36. ZAM equilibrium model versus algebraic model cesium loading predictions for CST material in contact with Envelope B's LAW-2b feed solution at 5 M [Na <sup>+</sup> ]. <sup>a</sup>	200
Table B-37. ZAM equilibrium model versus algebraic model cesium loading predictions for CST material in contact with Envelope C's LAW-3 feed solution at 5 M [Na <sup>+</sup> ]. <sup>a</sup>	201
Table B-38. ZAM equilibrium model versus algebraic model cesium loading predictions for CST material in contact with Envelope C's LAW-4 feed solution at 5 M [Na <sup>+</sup> ]. <sup>a</sup>	201
Table B-39. ZAM equilibrium model versus algebraic model cesium loading predictions for CST material in contact with Envelope C's LAW-7 feed solution at 5 M [Na <sup>+</sup> ]. <sup>a</sup>	202
Table B-40. Cesium isotherm (engineered-form) sensitivity results based on the ZAM model for deviations about the nominal settings for the Phase 1 LAW-15 feed solution at 5.0 M Na <sup>+</sup> , 25 C, and 4.552x10 <sup>-5</sup> M Cs <sup>+</sup> (100% of feed value).	203
Table B-41. Cesium isotherm (engineered-form) sensitivity results based on the ZAM model for deviations about the nominal settings for the Phase 1 LAW-15 feed solution at 5.0 M Na <sup>+</sup> , 25 C, and 2.276x10 <sup>-5</sup> M Cs <sup>+</sup> (50% of feed value).	204
Table B-42. Error estimates associated with feed compositions for the key species of interest.	205
Table B-43. Phase 1 LAW-15 feed solution data used as input to the CST equilibrium model sensitivity study.	205
Table C-1. Ionic species molar concentrations for simulated waste solutions used in ZAM batch contact simulations for estimating the dilution factor.	225
Table C-2. Cesium batch contact test data taken by Walker et al. (2001) for various batches of CST material in contact with SRS-average simulated waste samples at 36.2 C.	226
Table C-3. Cesium batch contact test data taken by Walker et al. (2001) for various batches of CST material in contact with SRS-average simulated waste samples at different temperatures.	227
Table C-4. Cesium batch contact test data taken by Fondeur et al. (2000) for two batches of CST material in contact with SRS-average simulated waste samples at 25 C.	227
Table C-5. Power-law coefficients based on cesium loading data taken by Walker et al. (2001) for various batches of CST material in contact with SRS-average simulated waste samples at 36.2 C.	228
Table C-6. Estimated dilution factors based on an "effective" single component homovalent isotherm model of the cesium loading curve computed for selected SRS batch contact data <sup>a</sup> .	228
Table C-7. Cesium batch contact test data taken by Walker et al. (1997) for the Baseline CST material in contact with SRS Tank 44 actual waste samples at 31 C. <sup>a</sup>	229
Table C-8. Cesium batch contact test data taken by McCabe (1995 & 1997) for two CST materials in contact with a SRS simulant at 25 C. <sup>a</sup>	230
Table C-9. Key CST exchange properties taken from literature.	230
Table C-10. Strontium batch contact test data taken by Walker et al. (2001) for various batches of CST material in contact with SRS-average simulated waste samples at 36.2 C.	231
Table D-1. Listing of batch feed sequence and VERSE-LC I/O transferring.	240
Table D-2. VERSE-LC nominal input parameters settings used in the Envelope A batch feed simulations at 25 C.	241
Table D-3. VERSE-LC nominal input parameters settings used in the Envelopes B and C batch feed simulations at 25 C.	242
Table E-1. Cesium uptake measurements made at 25 C during the batch kinetics tests of Brown et al., 1996 (initial cesium concentration of 1.0x10 <sup>-4</sup> M).	262
Table E-2. Key parameters measured or specified during the batch kinetics tests of Brown et al. (1996) and used to establish the cesium isotherms used in VERSE-LC kinetic modeling.	263
Table E-3. Cesium uptake measurements made at 25 C during the batch kinetics tests of Fondeur et al., 2000. Also included are estimated conditions at earlier contact times.	263

Table E-4. Key parameters measured or specified during the batch kinetics tests of Fondeur et al. (2000) and used to establish the cesium isotherm used in VERSE-LC kinetic modeling.....	264
Table E-5. Cesium uptake measurements made at 25 C during the transient cesium uptake tests of Miller and Brown (1997) and Anthony et al., 1996. ....	265
Table E-6. Key parameters measured or specified during the transient cesium uptake tests of Miller and Brown (1997) and Anthony et al. (1996) and used to establish the cesium isotherm used in VERSE-LC kinetic modeling. ....	266
Table E-7. Cesium uptake measurements made at 25 C during the batch kinetics tests of Davidson et al., 1998...	267
Table E-8. Key parameters measured or specified during the batch kinetics tests of Davidson et al. (1998) and used to establish the cesium isotherm used in VERSE-LC kinetic modeling.....	268
Table F-1. Ionic species available within the ZAM CST ion-exchange equilibrium model. ....	289
Table F-2. ZAM ionic species used in CST modeling of Phase 1 LAW batch feeds.....	290
Table F-3. Equilibrium data for cesium on CST powder (IE-910) based on batch contact tests performed at 25 C in simulated and actual AW-101 solutions (Brown et al. (1996), 0.475 M potassium). <sup>a</sup> .....	290
Table F-4. Equilibrium data for cesium on CST engineered-form (IE-911 –38b) based on batch contact tests performed at 25 C in simulated and actual AW-101 solutions (Brown et al. (1996), 0.475 M potassium). <sup>a</sup> .....	291
Table F-5. Equilibrium data for cesium on CST engineered-form (IE-911 –08) based on batch contact tests performed at 25 C in simulated AW-101 solutions (Brown et al. (1996), 0.475 M potassium). <sup>a</sup> .....	293
Table F-6. ZAM predictions for cesium on CST powder (IE-910) based on simulated batch contact tests performed at 25 C in AW-101 solutions. <sup>a</sup> .....	294
Table F-7. AW-101 simulant and actual solution compositions used to perform ZAM predictions for cesium on CST powder (IE-910) at 25 C. <sup>a</sup> .....	296
Table E-1. Listing of ZAM input files provided in this appendix for reference. ....	305
Table H-1. Ionic species molar concentrations for various simulated and actual waste solutions used in ZAM batch contact simulations to generate a cesium isotherm data used for estimating the beta factor. .	313
Table H-2. Key column parameters for CST IE-911 packed columns using SRS high OH simulant and SRS Tank 44 supernate waste taken by Walker et al. (1999) at 31. <sup>a,b</sup> .....	314
Table H-3. Cesium breakthrough data for CST IE-911 (Lot 98-05) and actual SRS Tank 44 waste taken by Walker et al. (1999) at 31 C. ....	314
Table H-4. Key column parameters for CST IE-911 packed columns using SRS-Avg simulant taken by Wilmarth et al. (1999) at 25 C ( $\pm 5$ C). <sup>a</sup> .....	315
Table H-5. Cesium breakthrough data for CST IE-911 and SRS-Avg waste simulant taken by Wilmarth et al. (1999) at ~25 C. ....	316
Table H-6. Cesium breakthrough data for CST IE-911 (with and without prior exposure to humid air) and SRS-Avg waste simulant taken by Wilmarth et al. (1999) at ~25 C. ....	317
Table H-7. Key column parameters for CST IE-911 packed columns using SRS-Avg simulant taken by Walker et al. (1998) at 22 C. <sup>a,b</sup> .....	318
Table H-8. Cesium breakthrough data for CST IE-911 and SRS-Avg waste simulant taken by Walker et al. (1998) at ~22 C. ....	318
Table H-9. Cesium breakthrough data for CST IE-911 (Lot 98-05) and SRS high OH simulant taken by Walker et al. (1999) at 31 C. ....	320
Table H-10. Key column parameters for CST IE-911 packed columns using PNNL diluted AW-101 sample taken by Hendrickson (1997) at 25 C. <sup>a</sup> .....	321
Table H-11. Cesium breakthrough data for CST IE-911 and PNNL diluted AW-101 sample taken by Hendrickson (1997) at ~25 C. ....	321
Table H-12. Key column parameters for CST IE-911 packed columns using MVST W-27 sample taken by Lee et al. (1997b) at 25 C. <sup>a,b</sup> .....	322
Table H-13. Cesium breakthrough data for CST IE-911 and MVST W-27 waste sample taken by Lee et al. (1997b) at ~25 C. ....	323
Table H-14. Key column parameters for CST IE-911 packed pilot-scale two-column carousel facility using MVST W-29 waste streams taken by Walker, Jr., et al. (1998) at 25 C. <sup>a</sup> .....	323
Table H-15. Cycle 1 ORNL-CsRD-Run2 cesium breakthrough data for CST IE-911 and MVST W-29 waste streams taken by Walker, Jr., et al. (1998) at ~25 C.....	324

<i>Table H-16. Cycle 1 ORNL-CsRD-Run3 cesium breakthrough data for CST IE-911 and MVST W-29 waste streams taken by Walker, Jr., et al. (1998) at ~25 C.....</i>	<i>325</i>
<i>Table H-17. Cycle 1 ORNL-CsRD-Run4 cesium breakthrough data for CST IE-911 and MVST W-29 waste streams taken by Walker, Jr., et al. (1998) at ~25 C.....</i>	<i>326</i>
<i>Table H-18. Cycle 2 ORNL-CsRD-Run4 cesium breakthrough data for CST IE-911 and MVST W-29 waste streams taken by Walker, Jr., et al. (1998) at ~25 C.....</i>	<i>326</i>



## LIST OF FIGURES

Figure 1-1. Computed total spent CST material required to process the entire Phase 1 LAW inventory based on a two-column carousel configuration at 25 C and nominal parameter settings (solid circles are VERSE-LC results while the solid line represents its average behavior). .....	7
Figure 1-2. Computed lead column exit cesium concentration breakthrough curves during the processing of the entire Phase 1 LAW inventory based on a two-column carousel configuration at 25 C and nominal parameter settings (2000 L bed volumes). .....	8
Figure 1-3. Normalized (to feed inlet conditions; $c/c_0$ ) lead column exit cesium concentration breakthrough curves during the processing of the entire Phase 1 LAW inventory based on a two-column carousel configuration at 25 C and nominal parameter settings (2000 L bed volumes). .....	9
Figure 2-1. Simplified material flowsheet overview highlighting the ion-exchange units used for removal of cesium from a candidate LAW stream. ....	18
Figure 2-2. Cesium loading performance comparison between IONSIV® IE-911 CST and SuperLig® 644 exchanger materials at 25 C by Bray et al. (1995). ....	18
Figure 3-1. The basic building blocks of a porous particle ion exchange column model. ....	24
Figure 3-2. Graphical representation of the various mass transport mechanisms considered important for Cesium-IONSIV® IE-911 CST system ion exchange column modeling. ....	25
Figure 3-3. Estimated $\text{Cs}^+$ , $\text{K}^+$ , and $\text{Na}^+$ exit breakthrough curves for the test SRS-Avg-Test2 performed by Wilmarth et al. (1999) based on a porous particle multi-component (i.e., ternary) ion exchange column model for SRS Average simulant using IONSIV® IE-911 CST. ....	26
Figure 3-4. Measured versus predicted $\text{Cs}^+$ column exit breakthrough curves based on the ternary and “effective” single-component ion exchange column models (test SRS-Avg-Test2 performed by Wilmarth et al. (1999) in a SRS Average simulant liquid at $1.24 \times 10^{-4}$ M Cs and at 25 C). ....	26
Figure 4-1. The estimated Phase 1 feed beta values used in the cesium effective single-component isotherm model for CST powder-form and engineered-form materials. The beta values are grouped by envelope and are based on feeds assuming zero $\text{Rb}^+$ and $\text{SrOH}^+$ present. ....	36
Figure 4-2. Comparison of the ZAM generated database for cesium loading onto IE-910 CST (powder) versus the algebraic model fit for the Phase 1 LAW-15 feed. Also shown is the algebraic model when applied to the engineered-form using a dilution factor of 68%. ....	36
Figure 4-3. Comparison of Envelope A isotherms for the CST material in its engineered-form (IE-911). The lines represent predictions based on the single-component Freundlich/ Langmuir Hybrid isotherm model and symbols indicate the feed concentrations of cesium. ....	37
Figure 4-4. Comparison of Envelope B isotherms for the CST material in its engineered-form (IE-911). The lines represent predictions based on the single-component Freundlich/ Langmuir Hybrid isotherm model and symbols indicate the feed concentrations of cesium. ....	37
Figure 4-5. Comparison of Envelope C isotherms for the CST material in its engineered-form (IE-911). The lines represent predictions based on the “effective” single-component Freundlich/ Langmuir Hybrid isotherm model and symbols indicate the feed concentrations of cesium. ....	38
Figure 4-6. Comparison of the least favorable isotherms for Envelope A, B, and C feeds for the CST material in its engineered-form (IE-911). The lines represent predictions based on the “effective” single-component Freundlich/ Langmuir Hybrid isotherm model. ....	38
Figure 5-1. Functional behavior between bed porosity and particle porosity for the IONSIV® IE-911 CST material for various assumed total porosity values. The nominal settings used for the majority of column studies performed are shown by the solid circle. ....	45
Figure 6-1. Volume percent of particles as a function of particle size for one sample of the CST material in its IE-911 engineered-form (batch # not recorded) based on MicroTrac® laser technology (data from Qureshi, 1999). ....	52
Figure 6-2. Chord length percent of particles as a function of chord size for one sample of the CST material in its IE-911 engineered-form (Baseline Lot # 9090-76) based on Lasentec® laser technology. ....	52
Figure 7-1. Cesium $K_d$ measurements obtained from batch kinetics tests performed by Brown et al. (1996) at 25 C and in a 70% AW-101 DSSF simulant liquid at $1 \times 10^{-4}$ M Cs and 5 M Na. ....	69
Figure 7-2. Estimation of the cesium pore diffusion coefficient based on batch kinetics tests performed by Brown et al. (1996) at 25 C for cesium uptake on IONSIV® IE-910 CST (powder-form). ....	69

Figure 7-3. Estimation of the cesium pore diffusion coefficient based on batch kinetics tests performed by Brown et al. (1996) at 25 C for cesium uptake on IONSIV® IE-911 CST (engineered-form 08).....	70
Figure 7-4. Estimation of the cesium pore diffusion coefficient based on batch kinetics tests performed by Brown et al. (1996) at 25 C for cesium uptake on IONSIV® IE-911 CST (engineered-form 38b).....	70
Figure 7-5. Cesium $K_d$ measurements obtained from batch kinetics tests performed by Fondeur et al. (2000) at 25 C and in a SRS average simulant liquid at $1.4 \times 10^{-4}$ M Cs and 5.6 M Na. Also shown is an estimated behavior at early times for the Fondeur et al. (2000) data.....	71
Figure 7-6. A comparison of the cesium $K_d$ measurements obtained from batch kinetics tests performed by Brown et al. (1996) and Fondeur et al. (2000) on various CST materials at 25 C.....	71
Figure 7-7. Estimation of the cesium pore diffusion coefficient based on batch kinetics tests performed by Fondeur et al. (2000) at 25 C for cesium uptake on IONSIV® IE-911 CST (engineered-form Baseline).....	72
Figure 7-8. Comparison of VERSE-LC predictions to measured cesium concentrations during approach to equilibrium based on batch kinetics tests performed by Fondeur et al. (2000) at 25 C for the Baseline form of CST material (IONSIV® IE-911).....	72
Figure 7-9. The effect particle size has on rates of cesium uptake by IONSIV® IE-910 (Miller and Brown, 1997) and by IONSIV® IE-911 (Anthony et al., 1996) CST materials based on transient cesium uptake testing.....	73
Figure 7-10. The effect phase ratio has on rates of cesium uptake by IONSIV® IE-910 CST material (Davidson et al., 1998) based on batch kinetics testing.....	73
Figure 9-1. Measure of error for individual tests in predicting column exit cesium breakthrough as a function of the ratio of pore to free stream diffusion coefficients. Average behavior of the top eight tests is also plotted. ....	89
Figure 9-2. Overall measure of error in predicting column exit cesium breakthrough as a function of the pore to free stream diffusion coefficient ratio (8 column tests considered in summation). ....	90
Figure 9-3. Measured versus predicted cesium column exit breakthrough for three assumed pore diffusion coefficient values (test SRS-Avg-Test2 performed by Wilmarth et al. (1999) in a SRS Average simulant liquid at $1.24 \times 10^{-4}$ M Cs and at 25 C). ....	90
Figure 9-4. Measured versus predicted cesium column exit breakthrough for two assumed pore diffusion coefficient values (test SRS-Avg-Test2 performed by Wilmarth et al. (1999) in a SRS Average simulant liquid at $1.24 \times 10^{-4}$ M Cs and at 25 C). ....	91
Figure 9-5. A direct comparison of predicted versus measured cesium loadings on IONSIV® IE-911 CST material for diluted SRS Tank 44 waste (Walker et al., 1999). The algebraic model is plotted for both the powder (solid-curve) and engineered (dashed-curve) forms. ....	91
Figure 9-6. VERSE-LC cesium exit breakthrough curves compared to data from Walker et al. (1999) for SRS Tank 44 waste: $D = 1.59$ cm, $L = 10$ cm and 85 cm, $U = 5.319$ cm/min, $T = 31$ °C.....	92
Figure 9-7. VERSE-LC cesium exit breakthrough curve compared to data from SRS-Avg-Test1 (Wilmarth et al., 1999): $D = 1.5$ cm, $L = 10$ cm, $U = 5.5$ cm/min, $T = \sim 25$ °C.....	92
Figure 9-8. VERSE-LC cesium exit breakthrough curve compared to data from SRS-Avg-Test2 (Wilmarth et al., 1999): $D = 1.5$ cm, $L = 10$ cm, $U = 7.0$ cm/min, $T = \sim 25$ °C.....	93
Figure 9-9. VERSE-LC cesium exit breakthrough curve compared to data from SRS-Avg-Test3a and Test3b (Wilmarth et al., 1999): $D = 1.5$ cm, $L = 10$ cm, $U = 4.1$ cm/min, $T = \sim 25$ °C. ....	93
Figure 9-10. VERSE-LC cesium exit breakthrough curve compared to data from Wilmarth et al. (1999) for 98-05 CST material and Walker et al. (1998) for 96-04 CST material: $D = 1.5$ cm, $L = 10$ cm, $U = \sim 4.1$ cm/min, $T = \sim 25$ °C.....	94
Figure 9-11. VERSE-LC cesium exit breakthrough curve compared to data from SRS-Avg-Test4 (Wilmarth et al., 1999): $D = 2.5$ cm, $L = 10$ cm, $U = 4.1$ cm/min, $T = \sim 25$ °C.....	94
Figure 9-12. VERSE-LC cesium exit breakthrough curve compared to data from SRS-Avg-Test5 (Walker et al., 1998): $D = 1.5$ cm, $L = 10$ cm, $U = 0.47$ cm/min, $T = \sim 22$ °C.....	95
Figure 9-13. VERSE-LC cesium exit breakthrough curve compared to data from SRS-Avg-Test6 (Walker et al., 1998): $D = 1.5$ cm, $L = 10$ cm, $U = 0.98$ cm/min, $T = \sim 22$ °C.....	95
Figure 9-14. VERSE-LC cesium exit breakthrough curve compared to data from SRS-Avg-Test7 (Walker et al., 1998): $D = 1.43$ cm, $L = 11$ cm, $U = 4.1$ cm/min, $T = \sim 22$ °C.....	96

Figure 9-15. VERSE-LC cesium exit breakthrough curve compared to data from SRS-High-OH-Test1 (Walker et al., 1999): $D = 1.5$ cm, $L = 10$ cm and 85 cm, $U = 5.43$ cm/min, $T = \sim 31$ °C. ....	96
Figure 9-16. VERSE-LC cesium exit breakthrough curve compared to data from PNNL-AW101-Test1 (Hendrickson, 1997): $D = 1.5$ cm, $L = 10$ cm and 85 cm, $U = 5.43$ cm/min, $T = \sim 31$ °C. ....	97
Figure 9-17. VERSE-LC cesium exit breakthrough curve compared to data from ORNL-W27-Test1 (Lee et al., 1997b): $D = 1.5$ cm, $L = 5.659$ cm, $U = 0.283$ cm/min, $T = \sim 25$ °C. ....	97
Figure 9-18. VERSE-LC cesium exit breakthrough curve compared to data from ORNL-W27-Test2 (Lee et al., 1997b): $D = 1.5$ cm, $L = 5.659$ cm, $U = 0.566$ cm/min, $T = \sim 25$ °C. ....	98
Figure 9-19. VERSE-LC cesium exit breakthrough curve compared to data from ORNL-CsRD-Run2 (Walker, Jr., et al., 1998): $D = 30.6$ cm, $L = 51.67$ cm per column, $U = 2.584$ cm/min, $T = \sim 25$ °C. ....	98
Figure 9-20. VERSE-LC cesium exit breakthrough curve compared to data from ORNL-CsRD-Run3 (Walker, Jr., et al., 1998): $D = 30.6$ cm, $L = 51.67$ cm per column, $U = 5.167$ cm/min, $T = \sim 25$ °C. ....	99
Figure 9-21. VERSE-LC cesium exit breakthrough curve compared to data from ORNL-CsRD-Run4a (Walker, Jr., et al., 1998): $D = 30.6$ cm, $L = 51.67$ cm per column, $U = 5.167$ cm/min, $T = \sim 25$ °C. ....	99
Figure 9-22. VERSE-LC cesium exit breakthrough curve compared to data from ORNL-CsRD-Run4b (Walker, Jr., et al., 1998): $D = 30.6$ cm, $L = 51.67$ cm per column, $U = 5.167$ cm/min, $T = \sim 25$ °C. ....	100
Figure 10-1. Comparison of cesium loading curves for IONSIV® IE-911 CST material and SuperLig® 644 resin in contact with LAW-12 feed solution (241-AN-103) both on a mass and bed volume basis. ....	128
Figure 10-2. Comparison of normalized cesium breakthrough curves for IONSIV® IE-911 CST packed and SuperLig® 644 packed columns at 25 C using LAW-12 feed solution (i.e., 241-AN-103, identical 2-column carousel configuration, 1000 L columns, $L/D=3$ ). ....	128
Figure 10-3. Basic flowsheet for a full-scale (two-column carousel configuration) ion-exchange facility for removal of cesium using IONSIV® IE-911 CST material. ....	129
Figure 10-4. VERSE-LC model representing a (two-column or three-column carousel configuration) full-scale facility for removal of cesium using IONSIV® IE-911 CST material. The locations where the inlet feed conditions are applied and the exit breakthrough curves are monitored is shown. ....	130
Figure 10-5. Phase 1 LAW batch feed inlet flowrates and cesium concentrations used as input boundary conditions for VERSE-LC CST column design simulations. Constant values are applied over each batch process period. ....	131
Figure 10-6. The conceptual model defining the length of the mass transfer zone based on a 2-column carousel configuration with specified exit criteria for both columns. ....	131
Figure 10-7. Typical impact on mass transfer zone length (i.e., concentration profiles) due to envelope cesium concentration and flowrate differences based on VERSE-LC model predictions when using the IONSIV® IE-911 material. ....	132
Figure 10-8. Sensitivity of spent CST to the bed $L/D$ geometric ratio for the total processing of the Phase 1 LAW inventory (i.e., a 2-column carousel configuration operating at 25 C with 2000 L columns of varying $L/D$ geometries). ....	132
Figure 10-9. VERSE-LC cesium concentration predictions at the exit of the lead column based on CST and the Phase 1 LAW inventory (i.e., a 2-column carousel configuration operating at 25 C with 1000 L columns for a total of 78 carousel cycles performed). ....	133
Figure 10-10. VERSE-LC normalized cesium concentration predictions at the exit of the lead column based on CST and the Phase 1 LAW inventory (i.e., a 2-column carousel configuration operating at 25 C with 1000 L columns for a total of 78 carousel cycles performed). ....	133
Figure 10-11. VERSE-LC cesium concentration predictions at the exit of the lead column based on CST and the Phase 1 LAW inventory (i.e., a 2-column carousel configuration operating at 25 C with 2000 L columns for a total of 31 carousel cycles performed). ....	134
Figure 10-12. VERSE-LC normalized cesium concentration predictions at the exit of the lead column based on CST and the Phase 1 LAW inventory (i.e., a 2-column carousel configuration operating at 25 C with 2000 L columns for a total of 31 carousel cycles performed). ....	134
Figure 10-13. VERSE-LC normalized cesium concentration predictions at the exit of the lead column based on CST and the Phase 1 LAW inventory (i.e., a 2-column carousel configuration operating at 25 C with 3000 L columns for a total of 20 carousel cycles performed). ....	135

Figure 10-14. VERSE-LC cesium concentration predictions at the exit of the lead column based on CST and the Phase 1 LAW inventory (i.e., a 2-column carousel configuration operating at 25 C with 3000 L columns for a total of 20 carousel cycles performed).	135
Figure 10-15. VERSE-LC cesium concentration predictions at the exit of the lead column based on CST and the Phase 1 LAW inventory (i.e., a 2-column carousel configuration operating at 25 C with 4000 L columns for a total of 15 carousel cycles performed).	136
Figure 10-16. VERSE-LC normalized cesium concentration predictions at the exit of the lead column based on CST and the Phase 1 LAW inventory (i.e., a 2-column carousel configuration operating at 25 C with 4000 L columns for a total of 15 carousel cycles performed).	136
Figure 10-17. Computed total spent CST material required to process the entire Phase 1 LAW inventory based on a two-column carousel configuration at 25 C and nominal parameter settings (solid circles are VERSE-LC results while the solid line represents its average behavior).	137
Figure 10-18. Computed total spent CST material required to process the entire Phase 1 LAW inventory at 25 C and nominal parameter settings (VERSE-LC results for 2-column and 3-column carousels and limiting cases).	137
Figure 10-19. Computed total spent CST material required to process the entire Phase 1 LAW inventory based on a two-column carousel configuration at 25 C and nominal parameter settings (VERSE-LC results for various pore diffusivity coefficients and limiting cases).	138
Figure 10-20. Estimated total cesium inventory contained within a lead column during the worst case process cycle for a two-column carousel configuration (results for 3 differing column sizes are shown; worst case cycles occur primarily in the LAW-2a processing period).	138
Figure B-1. Molar ratios of Na/Cs versus K/Cs for the Envelope A candidate feed solutions.	208
Figure B-2. Molar ratios of Na/Cs versus K/Cs for the Envelope B candidate feed solutions.	208
Figure B-3. Molar ratios of Na/Cs versus K/Cs for the Envelope C candidate feed solutions.	209
Figure B-4. Molar ratios of Na/Cs versus K/Cs for all Envelope A, B, and C candidate feed solutions. The least favorable feed solutions for each envelope are highlighted by open symbols.	209
Figure B-5. LAW molar ratios of Na/Cs versus K/Cs for all 177 Hanford waste tanks. The Phase 1 LAW batch feeds are highlighted using larger symbols.	210
Figure B-6. Comparison of ZAM model versus “effective” single-component Freundlich/Langmuir Hybrid isotherm model predictions for cesium loadings on CST material in the powder-form (IE-910) for the eleven Envelope A candidate feed solutions.	210
Figure B-7. Comparison of ZAM model versus “effective” single-component Freundlich/Langmuir Hybrid isotherm model predictions for cesium loadings on CST material in the powder-form (IE-910) for the two Envelope B candidate feed solutions.	211
Figure B-8. Comparison of ZAM model versus “effective” single-component Freundlich /Langmuir Hybrid isotherm model predictions for cesium loadings on CST material in the powder-form (IE-910) for the three Envelope C candidate feed solutions.	211
Figure B-9. The estimated Phase 1 feed beta values used in the cesium effective single-component isotherm model for CST powder-form and engineered-form materials. The beta values are grouped by envelope and are based on feeds assuming zero $Rb^+$ and $SrOH^+$ present.	212
Figure B-10. Comparison of Envelope A isotherms for the CST material in its engineered-form (IE-911). The lines represent predictions based on the “effective” single-component Freundlich/ Langmuir Hybrid isotherm model and symbols indicate the feed concentrations of cesium.	212
Figure B-11. Comparison of Envelope B isotherms for the CST material in its engineered-form (IE-911). The lines represent predictions based on the “effective” single-component Freundlich/ Langmuir Hybrid isotherm model and symbols indicate cesium feed concentrations.	213
Figure B-12. Comparison of Envelope C isotherms for the CST material in its engineered-form (IE-911). The lines represent predictions based on the “effective” single-component Freundlich/ Langmuir Hybrid isotherm model and symbols indicate cesium feed concentrations.	213
Figure B-13. Comparison of the least favorable isotherms for Envelope A, B, and C feeds for the CST material in its engineered-form (IE-911). The lines represent predictions based on the “effective” single-component Freundlich/Langmuir Hybrid isotherm model.	214
Figure B-14. Comparison of ZAM model predicted versus experimental (Washburn et al., 1928) $KNO_3$ solubility limit at 25 C (also shown is OLI version 6.5 prediction). For ZAM predictions NaOH was added to see the ionic strength effect.	214

Figure B-15. Predicted impact for cesium loading on CST engineered-form material upon a swapping of nitrate with nitrite starting with a nominal solution of LAW-1 feed at 5.0 M Na <sup>+</sup> and 25 C (the effect with [solid line] and without [dashed line] KNO <sub>3</sub> precipitation is shown).	215
Figure B-16. Estimated impact of aqueous strontium hydroxide on cesium loadings for CST engineered-form material starting with a nominal solution of LAW-3 feed at 5.0 M Na <sup>+</sup> and 25 C (zero SrOH <sup>+</sup> present [solid line] and upper bound of SrOH <sup>+</sup> present [dashed line]).	215
Figure B-17. Predicted impact of solution density on ZAM prediction of cesium loading on CST material based on LAW-2a and LAW-2b feeds at 5.0 M Na <sup>+</sup> and 25 C (the modified HTWOS density model values represent nominal conditions).	216
Figure B-18. Predicted impact for cesium loading on CST engineered-form material upon an increase in potassium concentration starting with a nominal solution of LAW-15 feed at 5.0 M Na <sup>+</sup> and 25 C (the effect with [solid line] and without [dashed line] KNO <sub>3</sub> precipitation is shown).	216
Figure C-1. Comparison of measured cesium K <sub>d</sub> values for several CST batches taken by Walker et al. (2001) in contact with a SRS-average simulated waste sample at 36.2 C.	232
Figure C-2. Comparison of measured cesium loading values for several CST batches taken by Walker et al. (2001) in contact with a SRS-average simulated waste sample at 36.2 C.	232
Figure C-3. Comparison of SRS-Avg simulant cesium CST loading data recently taken by Walker et al. (2001) to power-law fits through the data sets at 36.2 C.	233
Figure C-4. Comparison of SRS-Avg simulant cesium CST loading data recently taken by Walker et al. (2001) to both best estimate and adjusted ZAM predictions at 36.2 C.	233
Figure C-5. Comparison of dilution factor for several CST batch contact data sets with respect to equilibrium cesium concentration.	234
Figure C-6. Comparison of SRS-Avg simulant cesium CST (new powder-form) loading data taken by Fondeur et al. (2000) and Walker et al. (2001) to best estimate ZAM predictions at 26.7, 30.2, and 36.2 C.	234
Figure C-7. Comparison of dilution factor for several CST batch contact data sets with respect to equilibrium contact temperature.	235
Figure C-8. Comparison of UOP simulant cesium CST loading data recently taken by Walker et al. (2001) to both best estimate and adjusted ZAM predictions at 36.2 C.	235
Figure C-9. A close-up comparison of UOP simulant cesium CST loading data recently taken by Walker et al. (2001) to both best estimate and adjusted ZAM predictions at 36.2 C.	236
Figure C-10. Comparison of SRS-Avg simulant cesium CST loading data taken by Fondeur et al. (2000) to both best estimate and adjusted ZAM predictions at ~25 C.	236
Figure C-11. Comparison of SRS-Tank 44 sample cesium CST loading data taken by Walker et al. (1997) to both best estimate and adjusted ZAM predictions at 31 C.	237
Figure C-12. Comparison of SRS simulant cesium loading data on CST powder and an early on engineered-form material taken by McCabe (1995 [powder data] and 1997 [engineered-form data]) to both best estimate and adjusted ZAM predictions at ~25 C.	237
Figure C-13. Comparison of SRS-Avg simulant strontium CST loading data recently taken by Walker et al. (2001) to both best estimate and adjusted ZAM predictions at 36.2 C.	238
Figure F-1. A comparison of measured versus ZAM predicted cesium K <sub>d</sub> values for simulated AW-101 feed in contact with CST in its power-form (IE-910) over a range of sodium concentration levels [data by Brown et al. (1996)].	297
Figure F-2. A comparison of measured versus ZAM predicted cesium K <sub>d</sub> values for 5 M sodium simulated and actual AW-101 feeds in contact with CST in its power-form (IE-910) [data by Brown et al. (1996)].	297
Figure F-3. A comparison of measured versus ZAM predicted cesium K <sub>d</sub> values for simulated AW-101 feed in contact with CST in one of its engineered-forms referred to as "08" (IE-911) over a range of sodium concentration levels [data by Brown et al. (1996)].	298
Figure F-4. A comparison of measured versus ZAM predicted cesium K <sub>d</sub> values for simulated AW-101 feed in contact with CST in one of its engineered-forms referred to as "38b" (IE-911) over a range of sodium concentration levels [data by Brown et al. (1996)].	298
Figure F-5. A comparison of measured versus ZAM predicted cesium K <sub>d</sub> values for 5 M sodium simulated and actual AW-101 feeds in contact with CST in one of its engineered-forms referred to as "038b" (IE-911) [data by Brown et al. (1996)].	299

Figure F-6. A comparison of measured versus ZAM predicted cesium loadings for simulated AW-101 feed in contact with CST in its power-form (IE-910) over a range of sodium concentration levels [data by Brown et al. (1996)]. .....	299
Figure F-7. A comparison of measured versus ZAM predicted cesium loadings for simulated AW-101 feed in contact with CST in one of its engineered-forms referred to as "08" (IE-911) over a range of sodium concentration levels [data by Brown et al. (1996)]. .....	300
Figure F-8. A comparison of measured versus ZAM predicted cesium loadings for simulated AW-101 feed in contact with CST in one of its engineered-forms referred to as "38b" (IE-911) over a range of sodium concentration levels [data by Brown et al. (1996)]. .....	300
Figure F-9. A comparison of measured versus ZAM predicted cesium loading values for 5 M sodium simulated and actual AW-101 feeds in contact with CST in its power-form (IE-910) [data by Brown et al. (1996)]. .....	301

## TABLE OF NOTATION

$A, B$	Binding constants for Langmuir isotherm, $M^{-1}$ .
$CV, BV$	Active column (bed) volume, ml.
$c_{bi}$	Species $i$ conc. in bed fluid, $M$ .
$c_{pi}$	Species $i$ conc. in pore fluid, $M$ .
$\bar{c}_{pi}$	Species $i$ solid surface conc. (or loadings), $gmole/g_{resin}$ or $mmole/g_{resin}$ .
$\bar{C}_{pi}$	Species $i$ solid surface conc. based on column volume, $gmole/L_{CV}$ or $M$ .
$\bar{C}_T$	Total ion-exchange capacity of resin, $mmole/g_{resin}$ .
$\bar{C}_{Ti}$	Species $i$ ion-exchange capacity of resin, $mmole/g_{resin}$ .
$C_T$	Total cationic strength of solution, $M$ .
$cdf(x)$	Cumulative distribution function for the variable $x$ .
$D$	Column diameter, cm.
$D.F.$	Decontamination factor.
$D_{pi}$	Species $i$ pore diffusion coefficient, $cm^2/min$ .
$\tilde{D}_{pi}$	Species $i$ “overall” pore diffusion coefficient, $cm^2/min$ .
$D_{\pm}^{\infty}$	Binary diffusion coefficient at infinite dilution, $cm^2/s$ .
$D_{AB}$	Binary diffusion coefficient for $A$ diffusing through solvent $B$ , $cm^2/s$ .
$D_{\infty i}$	Species $i$ diffusion coefficient, $cm^2/min$ .
$E_{bi}$	Species $i$ axial dispersivity, $cm^2/min$ .
$F$	Ratio of dry-to-“as received” resin mass
$\mathcal{F}$	Faraday constant, 96,500 C/g-equiv.
$J$	“J factor” analogy dimensionless number.
$k_f$	Liquid film mass transfer coefficient, $cm/min$ .
$K_{di}$	Species $i$ distribution coefficient, $M^{-1}$ or $ml/g$ .
$K_{ji}$	Equilibrium constant between species $j$ and $i$ .
$\tilde{K}_{ji}$	Selectivity coefficient between species $j$ and $i$ .
$L$	Axial length of active bed of column, cm.
$m_i$	Mass of species $i$ , g.
$m_{resin}$	Mass of resin, g.
$M_i$	Species $i$ molecular weight, g/gmole.
$M_{ai}, M_{bi}$	Freundlich/Langmuir Hybrid model exponents for species $i$ .

$N_s$	Total number of cations of interest.
$N_c$	Total number of chemical reactions.
$\text{pdf}(x)$	Probability distribution function for the variable $x$ .
$Q$	Column volumetric flow rate, ml/min.
$q_i$	Species $i$ fractional surface site loading.
$r$	Radial coordinate within avg. size particle, cm.
$R$	Ideal gas constant, 8.314 J/gmole-K.
$R_i$	Isotherm model residual for $i^{\text{th}}$ data point.
$R_A$	Radius of diffusing particle, cm.
$Re$	Reynolds Number.
$< R_p >$	Average particle radius, $\mu\text{m}$ .
$Sc_i$	Species $i$ Schmidt Number.
$t$	Time.
$T$	Absolute temperature, K.
$u$	Linear interstitial velocity, cm/min.
$u'$	Retarded linear interstitial velocity, cm/min.
$u_{\text{peak}}$	Peak radial velocity, cm/min.
$u_{\text{CL}}$	Column centerline velocity, cm/min.
$U$	Superficial (Darcy) velocity, cm/min.
$V_{\text{bed}}$	Total volume of active column, ml.
$V_{\text{void}}$	Total volume of voids within active column, ml.
$V_{\text{pore}}$	Total volume of pores within particles, ml.
$V_{\text{part}}$	Total volume of particles within active column, ml.
$V_{\text{sld}}$	Total volume of solid resin within active column, ml.
$V_{\text{CSTR}}$	Volume of inlet/outlet headspaces, ml.
$z$	Axial coordinate, cm.
$z_+, z_-$	valences of cation and anion, respectively.

## **Greek**

$\beta$	Isotherm parameter constant.
$\hat{\beta}_i$	Langmuir “effective” single isotherm model constant.
$\beta_i, a_i, b_i$	Freundlich/Langmuir Hybrid model coefficients for species $i$ .
$\eta_{\text{df}}$	Dilution factor for converting from IE-910 cesium loading to IE-911 value.



$\kappa$	Boltzmann's constant.
$\tau_p$	Particle tortuosity.
$\lambda$	Lambda value ( $\equiv K_d\rho_b$ ), ml <sub>resin</sub> /ml <sub>BV</sub> .
$\nu_j$	Species j stoichiometric coefficient.
$\varepsilon_b$	Bed porosity.
$\varepsilon_p$	Particle porosity.
$\varepsilon_T$	Total porosity within column bed.
$\sigma_q$	Isotherm model standard deviation.
$\sigma_{K_{ji}}$	Selectivity coefficient standard deviation.
$\mu_B$	Dynamic viscosity of solvent mixture.
$\mu_w$	Dynamic viscosity of feed solution, centi-poise.
$\rho_w$	Density of feed solution, g/ml.
$\rho_b$	Bed density of active column, g/ml.
$\rho_s$	Solid (particle) density of resin, g/ml.
$\lambda_+^0, \lambda_-^0$	Limiting ionic conductance for cation and anion, mhos/equiv.

## Data Set Labeling

SRS-Avg-Test1	Test 1 reported by Wilmarth et al., 1999.
SRS-Avg-Test2	Test 2 reported by Wilmarth et al., 1999.
SRS-Avg-Test3	Test 3 reported by Wilmarth et al., 1999.
SRS-Avg-Test4	Test 4 reported by Wilmarth et al., 1999.
SRS-Avg-Test5	Test 5 reported by Walker et al., 1998.
SRS-Avg-Test6	Test 6 reported by Walker et al., 1998.
SRS-Avg-Test7	Test 7 reported by Walker et al., 1998.
SRS-High-OH-Test1	Test 1 reported by Walker et al., 1999.
PNNL-AW101-Test1	Test 1 reported by Hendrickson, 1997.
ORNL-W27-Test1	Test 1 reported by Lee et al., 1997b.
ORNL-W27-Test2	Test 2 reported by Lee et al., 1997b.
ORNL-CsRD-Test1	Test 1 reported by Walker, Jr., et al., 19978.
ORNL-CsRD-Test2	Test 2 reported by Walker, Jr., et al., 19978.
ORNL-CsRD-Test3	Test 3 reported by Walker, Jr., et al., 19978.

(This Page Intentionally Left Blank)

## 1.0 Executive Summary

For the current pretreatment facility design of the River Protection Project (RPP) Waste Treatment Plant (WTP), the removal of cesium from low activity waste (LAW) is achieved by ion-exchange technology based on SuperLig<sup>®</sup> 644 resin. Due to recent concerns over potential radiological and chemical degradation of SuperLig<sup>®</sup> 644 resin and increased pressure drops observed during pilot-scale column studies, an increased interest in developing a potential backup ion-exchanger material has resulted. Ideally, a backup ion-exchanger material would replace the SuperLig<sup>®</sup> 644 resin and have no other major impacts on the pretreatment facility flowsheet. Such an ideal exchanger has not been identified to date.

However, Crystalline Silicotitanate (CST) ion-exchanger materials have been studied for the removal of cesium from a variety of DOE wastes over the last decade. CST ion-exchanger materials demonstrate a high affinity for cesium under high alkalinity conditions and have been under investigation for cesium removal specifically at Hanford and SRS during the last six years. Since CST is an inorganic based material (with excellent properties in regard to chemical, radiological, and thermal stability) that is considered to be practically non-elutable (while SuperLig<sup>®</sup> 644 is an organic based elutable resin), the overall pretreatment facility flowsheet would be impacted in various ways. However, the CST material is still being considered as a potential backup ion-exchanger material. The performance of a proposed backup ion-exchange column using IONSIV IE-911 (CST in its engineered-form) material for the removal of cesium from Hanford high level radioactive alkaline waste is discussed. This report focuses attention only on the ion-exchange aspects and only addresses the loading phase of the process cycle.

Available bench-scale column tests, batch kinetics tests, and batch equilibrium experiments using CST materials were utilized (wherever possible) in the development and validation of an analysis methodology. The methodology employed and the results of the study are discussed.

The major accomplishments and conclusions are:

- The planned waste treatment processing of the Phase 1 LAW tank inventory consists of processing 16 separate batches of feeds from the ten targeted waste tanks in a sequential fashion. The sequence chosen is reflected in the numbering sequence used to label each batch feed (i.e., LAW-1, LAW-2a, LAW-2b, LAW-3, ..., LAW-15). Each batch represents a fixed amount of liquid waste volume whose volume includes all planned dilution processes. The ionic composition of all 16 candidate feed solutions were determined based on the Tank Farm COUP report, Best Basis Inventory (BBI) Phase 1 database, more recent PNNL and SRTC analytical analysis of available samples. The necessary adjustments to achieve an ionic charge balance (consistent with the demands of the isotherm model used) was performed. The various estimation methods used focused on those waste feed ions that have a direct impact on cesium loading. The batch feed compositions for <sup>137</sup>Cs were decay corrected from ~1999 to the date of scheduled waste processing in the Waste Treatment Plant.

- A sensitivity study and error analysis were performed to estimate an overall uncertainty value of ~30% for predicted cesium loadings based on the engineered-form (IE-911) of CST material. The predicted cesium isotherms are based on the Texas A&M ZAM model coupled with a dilution factor. The ZAM model solves the appropriate liquid-solid equilibrium equations for the Cesium-CST system where its modeling parameters were determined based on batch contact tests using CST powder. The dilution factor is based on the measured deviations of engineered-form contact test data when compared to ZAM predicted powder behavior. To evaluate the impact on the cesium isotherms resulting from uncertainties in the composition of the various Phase 1 LAW feeds, a sensitivity analysis was performed. Using the sensitivity results, a “simplified” error analysis was performed where an estimate of the overall uncertainty in a cesium isotherm was computed. Much of this effort is based on a good engineering judgement approach where errors in various variables are stated based on an assumed/implied confidence level of approximately 2-sigma. Where available, supporting data were used in establishing these error estimates. Verification and validation analyses were performed for the ZAM code based on available Hanford AW-101 simulant and actual waste samples.
- To accommodate batch variability in CST engineered-form material, a dilution factor of 68% was used in the column sizing study. The 68% dilution factor is consistent with the measured impact of the inert binder for baseline IE-911 engineered-form CST material and is statistically conservative (i.e., ~85% confidence) with respect to the majority of batch material data available. The use of 68% for the dilution factor sets a CST material acceptance criterion that should be reasonably achieved by the manufacturer of the CST engineered-forms.
- Originally, batch kinetics test data were going to be used to establish an acceptable value for the cesium pore diffusion coefficient; while, available laboratory-scale column test data were going to be used for assessment purposes only. Unfortunately, significant inconsistencies exist within the available batch kinetics tests such that no conclusive value for the pore diffusion coefficient could be determined. The kinetics data also indicate that simple Fickian diffusion through pores of a homogeneous material is in question. Surface diffusion and heterogeneous pores (between the powder and the binder) may play an important role in establishing the overall mass transfer rate. For this analysis effort it was decided that an “effective” value of the cesium pore diffusion coefficient (based on a purely Fickian formulation) would be determined based on assessment directly to available lab-scale column test data. Based on ten lab-scale column tests a “best estimate” value of ~20% of its free (molecular) stream diffusion coefficient value was computed with a standard deviation of approximately 5%.
- It is assumed that the cesium isotherms for CST material are true solid-liquid equilibrium curves that are unique and are ultimately approached either from above or from below (i.e., no form of hysteresis exists). Limited data exist indicating that this should be a reasonable assumption. Also, it is assumed that the kinetics involved for CST material is directional independent (i.e., diffusion rates are equal for the adsorbing and de-adsorbing processes).

- Early column performance (say the first 5 to 10 column volumes or so) requires the use of multi-component modeling formulations (i.e., ternary component isotherms and transport equations). However, long-term performance should be adequately handled using the simpler single-component formulations. Justification for this simplification is provided. Since significant CPU savings are achieved when the single-component model is used and the differences are well within our current predictive capabilities, the majority of column analyses presented in this report were performed using the single-component approach. This simplification only applies to the loading cycle, while for future elution studies a multi-component version would be required due to the strong concentration gradients that would be present throughout the columns. Elution of CST is not normally possible or conducted.
- Based on the specified Envelope A, B, and C flowrates (i.e., 52.6, 9.4, and 16.2 L/min, respectively) and estimated feed volumes when adjusted to a common 5 M Na<sup>+</sup> basis, an overall processing time of ~4.2 years is required to process the entire Phase 1 LAW inventory. This processing time yields a 42% utilization requirement for the ion-exchange facility over the scheduled 10-year project lifecycle. If the Envelope A feeds are processed at the 30 MT/day production rate, an overall processing time of ~5.8 years is required.
- Surface film diffusion along with pore diffusion place mass transfer limitations on the kinetics of an ion-exchange material. At the flowrates of interest, the CST material is primarily pore diffusion limited. Since the CST columns are not film diffusion limited, the impact on estimated spent CST material is insensitive to geometrical variations (e.g., length to diameter ratio). Therefore, total column “bed” volume is the key parameter for design purposes. For design purposes, the bed L/D ratio can be established based on other operational considerations than column performance in terms of the exit breakthrough curves (e.g., overall column pressure drop or sweeping out of generated gases).
- From the standpoint of minimizing the spent CST material to be sent to the melters versus the physical bed size of an individual column, the column transport results indicate that an ~2 m<sup>3</sup> column is near the optimum value. At this column size an estimated 66,000 kg (66 MT) of spent CST material would be generated corresponding to an ~2.5 wt% of waste sodium oxide in the final glass product (assuming 2651 MT of glass to be produced).
- Also, these results indicate that the current column design based on SuperLig<sup>®</sup> technology (i.e., ~1 m<sup>3</sup> in volume with an ~3 L/D ratio) is adequate, even though not optimal (i.e., ~20% increase in spent CST, ~80 MT), for use if CST material was later chosen as a backup ion-exchanger. Increasing the bed volume up to its current design maximum of ~1.5 m<sup>3</sup> results in only an increase of ~10% in spent CST (~72 MT). In terms of the total number of carousel cycles required the 1 m<sup>3</sup>, 1.5 m<sup>3</sup>, and 2 m<sup>3</sup> column volume designs required 78, 46, and 31 cycles, respectively.
- Historically, it has been stated that CST overall has relatively slow kinetics. However, for the 2 m<sup>3</sup> bed volume design using a two-column carousel, the resistances associated with mass transfer only increases the computed spent CST by ~14%. Impacts of this magnitude would suggest that further reduction in particle size or in bed L/D is not warranted based on improving the “kinetics” alone. Based on the theoretical minimum in spent CST required

(which can not be reached using practical designs, but helps gage how efficient or inefficient the current CST material and carousel designs are), the actual/practical design only increases the computed spent CST by ~19%. These numbers are based on a nominal value for the cesium pore diffusivity coefficient of 20% of its free diffusion value. However, uncertainty in the actual value of the pore diffusivity coefficient can result in larger impacts. For larger coefficient values its impact on spent CST becomes more aggressive. Future efforts should be focused on obtaining better confidence in the magnitude of this diffusivity coefficient.

- The CST column sizing results are based on the sixteen different Phase 1 batch feeds being processed sequentially in the order of their current schedule. However, the actual processing order of the 16 feeds has only a marginal impact on the above results.
- Under the current batch feed process schedule, Envelope B feeds (LAW-2a and LAW-2b, which refer to tank waste from AZ-101 and AZ-102, respectively) are to be processed early on. The inlet feed concentrations for the Envelope B feeds are approximately one order of magnitude greater than values for Envelopes A and C. Under this processing strategy a significant amount of cesium inventory will be held up within the columns throughout much of the total period.
- The majority of analyses performed were based on a two-column carousel configuration. A smaller subset of analyses was performed using a three-column carousel configuration to determine the potential benefit associated with more column stages. Only marginal gains can be achieved when a 3-column versus 2-column carousel facility is considered. Theoretically, increased column stages will reduce the amount of spent CST generated; however, the predicted gains are within the expected accuracy of the methodology and the increased staging is not warranted.
- A homovalent cation exchange process occurs between the batch feeds and the CST material where the cations  $\text{Cs}^+$ ,  $\text{K}^+$ ,  $\text{Na}^+$ ,  $\text{Rb}^+$ , and  $\text{SrOH}^+$  are in direct competition (i.e., the stated total ionic exchange capacities are 0.58, 1.2, 4.6, 1.18, and 1.0 mmole/g<sub>CST</sub>, respectively). Only trace amounts of  $\text{Rb}^+$  are present within the batch feeds and its concentration within these feeds was set to zero. Due to the complex formation of strontium with various complexants (e.g., EDTA), the actual amount of free  $\text{SrOH}^+$  present within a batch feed is currently unknown and was assumed to be zero for the best estimate analyses. To a first approximation  $\text{SrOH}^+$  competes equally for CST sites with  $\text{Cs}^+$  and should be accounted for in any future design efforts. For example, if equal amounts of  $\text{SrOH}^+$  and  $\text{Cs}^+$  are present within the feed, then a column approximately twice the size of one handling  $\text{Cs}^+$  alone would be required. In this work the impact of competition from  $\text{Cs}^+$ ,  $\text{K}^+$ , and  $\text{Na}^+$  was addressed.
- The estimated selectivity coefficients between  $\text{Cs}^+$  and  $\text{K}^+$ , and  $\text{Cs}^+$  and  $\text{Na}^+$ , for CST material are very similar in magnitude to (i.e., only slightly better than) those measured for SuperLig<sup>®</sup> 644. However, on a fixed bed volume basis the CST material contains over twice the number of cesium active exchange sites than SuperLig<sup>®</sup> 644, since its bed density is more than double.

- For each of the 16 batch feeds cesium isotherms were generated using the ZAM model. For each batch feed a simple algebraic model based on the homovalent cation exchange process was found to provide an excellent prediction of the ZAM results. Based on the excellent agreement achieved with the algebraic model, the assumption that the selectivity coefficients are constants over the entire cesium concentration range appears to be reasonable.
- From an equilibrium loading consideration only, batch feeds LAW-1 and LAW-15 (i.e., feeds from tanks AP-101 and AW-101, respectively) exhibit the least favorable isotherms. The primary reason for this is due to their high potassium levels (i.e., 0.71 and 0.41 M, respectively, at 5 M Na<sup>+</sup> conditions).
- Cesium total inventories within the column (i.e., cesium content in the liquid-phase plus adsorbed onto the solid-phase) as a function of time were computed during the loading cycle corresponding to worst case conditions. This inventory estimate can be used in subsequent analyses (beyond the scope of this report) for estimating conservative exposure levels. For design purposes a maximum loading of  $\sim 250 \text{ mmole}_{\text{Cs}}/\text{L}_{\text{bed}}$  over an approximate 150 day exposure time should be considered. At a 30% isotopic fraction of <sup>137</sup>Cs the loading becomes  $\sim 75 \text{ mmole}_{\text{Cs-137}}/\text{L}_{\text{bed}}$  (or  $\sim 889 \text{ Ci}/\text{L}_{\text{bed}}$ ).
- A bed porosity of 0.50 and particle porosity of 0.24 were used for the majority of column simulations performed within this report. These values yield a total column porosity of 62%. Based on recent access to measured particle and bed densities, we estimate that the total porosity is in the range of 29% to 53%. The 62% we assumed earlier is outside this range indicating that the results from our column models are based on total bed voids that are larger than they should have been. This would normally imply that the column models contain less CST material by mass than they should have had. Fortunately, the manner in which VERSE-LC handles the isotherms enforces the bed density to be the value used in creating the isotherms (i.e., typically 1 g<sub>CST</sub>/ml<sub>bed</sub>). The net effect is larger bed and/or pore volumes that can have a secondary effect on the predicted breakthrough curves (e.g., typical impacts are less than  $\pm 10\%$ ). Future design efforts should be based on more up to date porosity values based on measured bed and particle densities consistent with the engineered-form under consideration.

A few of the above listed conclusions deserve some addition clarification. The methodology used in estimating the column performance of CST in removal of cesium is not an overall bounding analysis, but better represents an approximate “best estimate” analysis for columns packed with modest performance CST material. Significant variability among the available batches in engineered-form can be seen. Therefore, the parameter settings were “nominally” established with the intent to represent in a conservative manner the majority of these CST batches.

The major objective of this study was to estimate the quantity of CST material (in its engineered-form) that would be required to process the entire Phase 1 LAW feed solution inventory. It is assumed that these feeds are all adjusted to a 5 M Na<sup>+</sup> basis prior to entering the ion-exchange facility and that the facility will operate at 25 C. In determining the required quantity of CST

material (i.e., spent CST) an exit criterion for  $^{137}\text{Cs}$  was placed on each Envelope along with a design volumetric flowrate as:

- Envelope A  $1.75 \times 10^{-5}$  Ci/gmole of Na (0.088  $\mu\text{Ci/ml}$ ) 52.6 L/min 25%  $^{137}\text{Cs}$
- Envelope B  $5.00 \times 10^{-5}$  Ci/gmole of Na (0.250  $\mu\text{Ci/ml}$ ) 9.4 L/min 30%  $^{137}\text{Cs}$
- Envelope C  $1.75 \times 10^{-5}$  Ci/gmole of Na (0.150  $\mu\text{Ci/ml}$ ) 16.2 L/min 25%  $^{137}\text{Cs}$

Since these CST columns are not film diffusion limited, the bed volume of an individual column is sufficient for defining the performance of a given carousel configuration (i.e., performance is nearly independent of L/D). From a theoretical perspective the amount of spent CST will exhibit a unique minimum with respect to column volume. The minimum point corresponds to the column volume where the cesium exit criterion in the lag column is reached at the same point in time that the last drop of Phase 1 LAW inventory enters the lead column without the need to perform any carousel cycles. Unfortunately, this minimum point represents a significantly large column (i.e., probably greater than 20  $\text{m}^3$ ) and is unpractical from a cost or operational perspective. Fortunately, for smaller column volumes the actual shape of the spent CST versus column volume curve remains relatively flat until a knee in the curve occurs as shown in Figure 1-1.

In Figure 1-1 the solid circles represent VERSE-LC two-column carousel simulation results where the number of carousel cycles performed for each simulation case is provided. The solid line shown represents an average behavior. Carousel cycles are discrete operations that occur each time the exit cesium criterion is reached at the exit of a lag column. During a carousel cycle, the lead column is removed from the column train (i.e., adding to the total spent CST material) and replaced with the current partially loaded lag column, while a fresh column is placed into the lag column position. Therefore, if a sufficient number of simulations at varying column volumes were run the actual shape of this curve would be somewhat saw-toothed. Some of this saw-toothed appearance can be seen at the higher column volumes in Figure 1-1 (note that the magnitude of this saw-toothed behavior diminishes at the smaller column volumes). If the maximum utilization of CST material could be achieved theoretically for each batch feed, an estimated ~56,000 kg of spent CST would be generated (see the dashed line in Figure 1-1).

Based on the location of the “knee”, the optimal column size appears to be approximately 2  $\text{m}^3$ . This corresponds to the smallest column size where only a negligible increase in spent CST results. For column sizes smaller than ~2  $\text{m}^3$  a rapid increase in spent CST is observed. A very similar (i.e., only slightly reduced) curve exists for a three-column carousel configuration.

Based on the order of batch feeds to be processed and a 2  $\text{m}^3$  in size bed volume, the total cesium concentration exiting the lead column (i.e., which provides some measured on its loading level) is shown in Figure 1-2 for the 16 feeds (i.e., each envelope is color-coded). The process time is given in months where the time interval for each batch feed is shown by the various vertical lines provided. Each carousel operation (cycle) resets the exit cesium concentration back to zero (i.e., 31 cycles in total resulting in a total of 33 bed volumes of spent CST). Since Envelope B feeds contain cesium approximately one order larger than in Envelope A and C feeds, cesium loadings within the lead columns are significantly impacted over a sizable range of the entire process



period. As shown in Figure 1-2, for several carousel cycles after the Envelope B feeds have been processed, de-adsorption on the lead columns occur where re-adsorption then takes place on the lag columns (i.e., redistribution of cesium within the carousel). This is a direct result of the significant reduction in inlet cesium concentration after the Envelope B feeds.

By looking at the lead column loadings during each carousel operation, an indication as to the degree of utilization of the CST material can be seen. Under standard operations, a column approaches saturation with respect to its feed when its exit concentration approaches its feed value (i.e., when  $c/c_0$  approaches unity). For a 2 m<sup>3</sup> in size bed volume the results shown in Figure 1-2 are also plotted in Figure 1-3 where the appropriate cesium feed concentrations have been used to normalized the breakthrough curves. Redistribution within the carousel occurs for those cycles whose normalized concentrations ( $c/c_0$ ) exceed unity. The peak values during each cycle indicate the degree of utilization. For example, 100% utilization occurs for the Envelope B feeds, >100% for the Envelope C feeds, and ~45% for the Envelope A feeds.

If a sizing strategy based on worst case feed conditions had been used, the design would have been set based on the Envelope A's AP-101 or AW-101 feeds where a significantly larger column volume would be required to up Envelope A's utilization to the typical 90-95% goal. A mass transfer zone (MTZ) approach to sizing the columns was inappropriate here since the basic assumptions required in determining the MTZ length are invalidated/limited (i.e., inlet conditions are time varying, for many feeds the degree of non-linearity in their isotherms were marginal, and significant variability within feed isotherms).

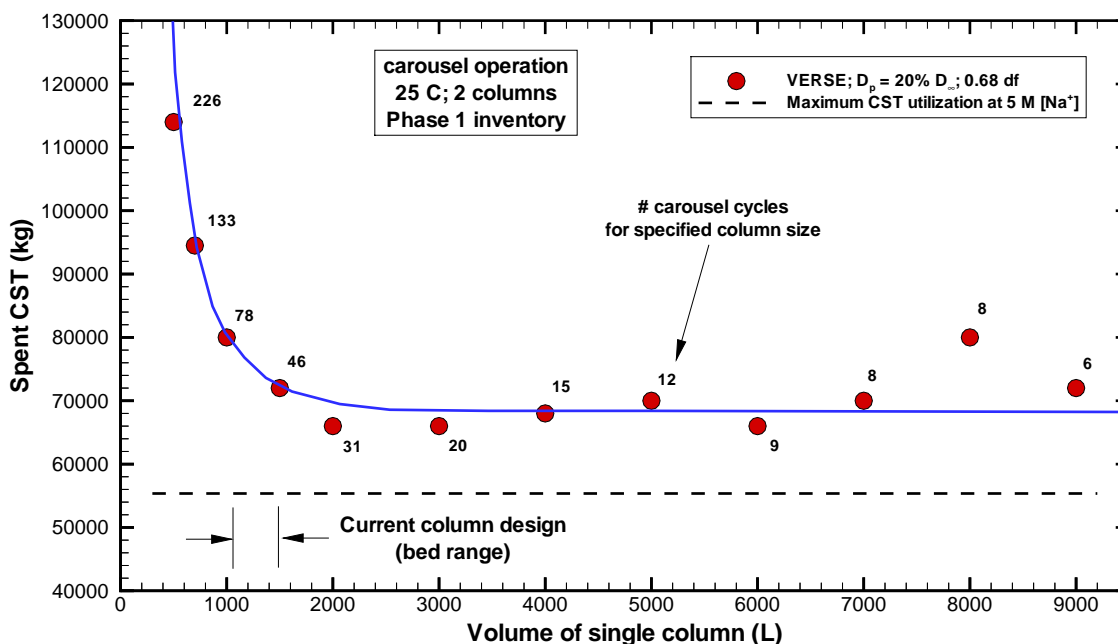


Figure 1-1. Computed total spent CST material required to process the entire Phase 1 LAW inventory based on a two-column carousel configuration at 25 C and nominal parameter settings (solid circles are VERSE-LC results while the solid line represents its average behavior).

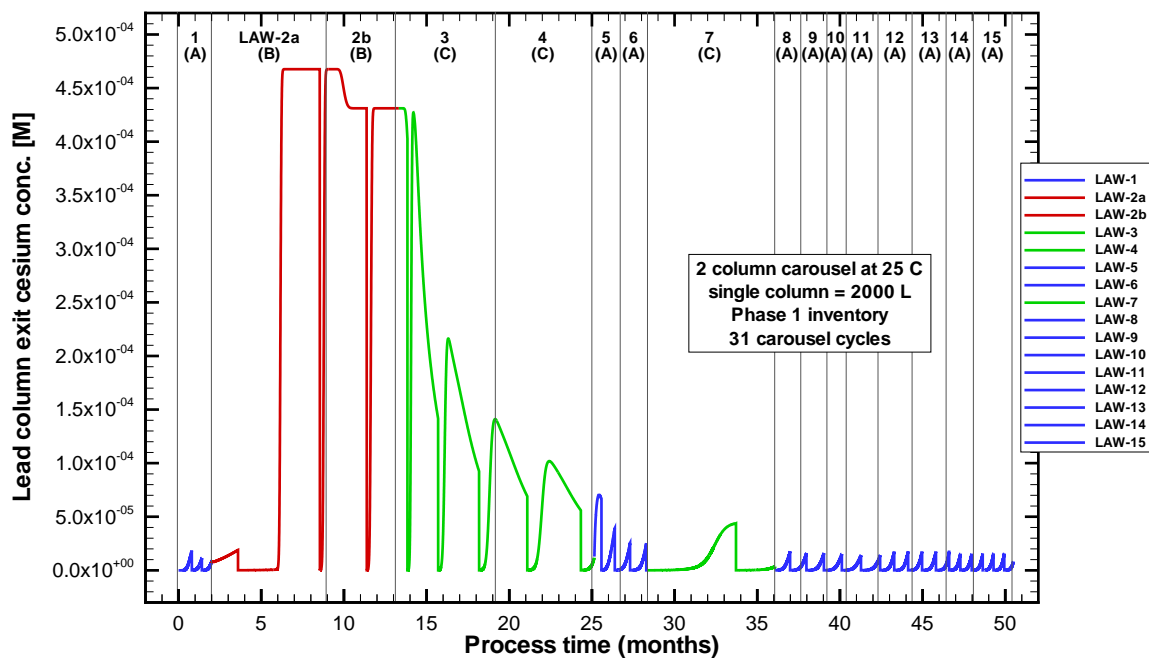


Figure 1-2. Computed lead column exit cesium concentration breakthrough curves during the processing of the entire Phase 1 LAW inventory based on a two-column carousel configuration at 25 C and nominal parameter settings (2000 L bed volumes).

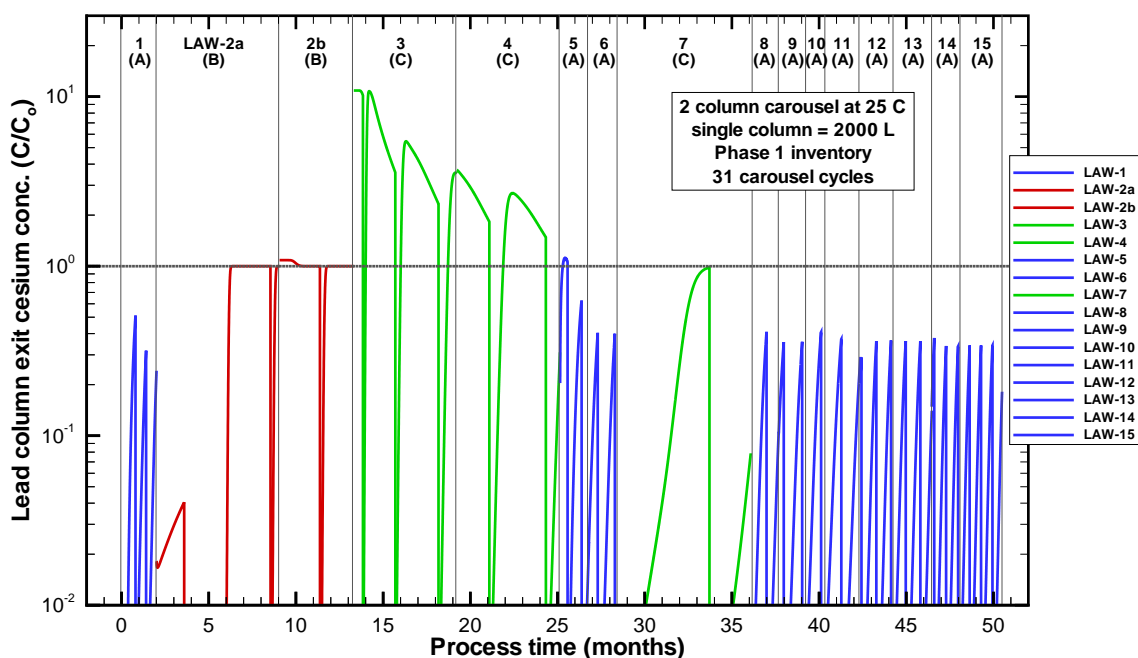


Figure 1-3. Normalized (to feed inlet conditions;  $c/c_0$ ) lead column exit cesium concentration breakthrough curves during the processing of the entire Phase 1 LAW inventory based on a two-column carousel configuration at 25 C and nominal parameter settings (2000 L bed volumes).

(This Page Intentionally Left Blank)

## 2.0 Introduction and Background

A proposed facility is being designed for the immobilization of radioactive waste contained within Hanford underground storage tanks. The waste is pretreated to split it into Low Activity Waste (LAW) and High Level Waste (HLW) streams for separate vitrification. One unit process in the overall pretreatment facility is designed to remove radioactive cesium (therefore total Cs) by ion-exchange from a highly alkaline aqueous phase. A resin specifically designed with moderately high selectivity for cesium under high pH conditions is being investigated. For the current pretreatment facility design of the River Protection Project (RPP) Waste Treatment Plant (WTP), the removal of cesium from low activity waste (LAW) is achieved by ion-exchange technology based on SuperLig<sup>®</sup> 644 resin. This resin is elutable under lower pH conditions (e.g., adequate elution occurs under water or dilute nitric acid conditions). The proposed design of the facility consists of two sets of two packed columns placed in series (i.e., a lead column followed by a lag column configuration). It should be noted that the WTP Contractor has more recently modified the design subsequent to this effort to include a third column within the carousel. During operation, upon reaching a specified cesium concentration criterion at the exit of the lag column, operation is switched to the second set of lead and lag columns. The cesium-loaded lead column is processed (i.e., washed and eluted) and switched to the lag position. The previous lag column is then placed in the lead position (without eluting) and the system is ready for use in the next cycle. For a well designed process, the loading and elution processes result in significant volume reductions in aqueous high level waste. A third column is provided within the facility's footprint for the option to perform three-column carousel operations if needed.

Due to chemical and radiological degradation of the exposed resin, at some point the resin must be replaced. Current design requirements placed on the SuperLig<sup>®</sup> 644 resin assume that adequate removal performance from the resin can be achieved for up to 10 process cycles. Due to recent concerns over potentially high rates of radiological and chemical degradation of SuperLig<sup>®</sup> 644 resin and increased pressure drops observed during pilot-scale column studies, an increased interest in developing a potential backup ion-exchanger material has resulted. Ideally, a backup ion-exchanger material would replace the SuperLig<sup>®</sup> 644 resin and have no other major impacts on the pretreatment facility flowsheet. Such an ideal exchanger would have a high affinity for cesium under high pH conditions and would be elutable. No such exchanger has been identified to date.

However, Crystalline Silicotitanate (CST) ion-exchanger materials have been studied for the removal of cesium from a variety of DOE wastes over the last decade. CST ion-exchanger materials demonstrate a high affinity for cesium under high alkalinity conditions and have been under investigation for cesium removal at specifically Hanford and SRS during the last six years. Since CST is an inorganic based material (with excellent properties in regard to chemical, radiological, and thermal stability and also little swelling/shrinking) that is considered to be practically non-elutable (while SuperLig<sup>®</sup> 644 is an organic based elutable resin), the overall pretreatment facility flowsheet would be impacted in various ways. However, the CST material is still being considered as a potential backup ion-exchanger material. The performance of proposed backup ion-exchange columns using IONSIV IE-911 (CST in its engineered-form)

material for the removal of cesium from Hanford high level radioactive alkaline waste is the main purpose of this analysis report. This report focuses attention only on the ion-exchange aspects and only addresses the loading phase of the process cycle.

From the viewpoint of being an ion-exchange material that is elutable or non-elutable, here we are referring to the level of cesium loading on the exchanger over a wide range of pH. Due to this behavior with respect to pH, the CST material is used only once and then becomes “spent CST” material that must be disposed of by vitrification in the IHLW glass melters. A simplified material flowsheet of the proposed CST based facility is shown in Figure 2-1. As shown in Figure 2-1, a spent CST material stream leaves this facility and ultimately contributes to the composite feed entering the IHLW glass melters.

One of the major questions being answered in this analysis report is the total amount of CST material being consumed (i.e., spent CST) in processing the entire Phase 1 LAW inventory. The current design estimates for the number of glass logs (cans) to be generated based on the use of SuperLig<sup>®</sup> technology is ~866 (see Table 4.1-1 of Kirkbride et al., 2000, the COUP document). This number of glass logs corresponds to 2651 MT (metric tons) of glass product. Due to concerns as to the allowable amount of waste sodium oxides that can be placed into the glass matrix, minimization of the spent CST material is of prime importance in the optimum column design. The feasibility of using CST material rests predominately upon the amount of spent CST generated.

The maximum loadings for waste sodium oxide ( $\text{Na}_2\text{O}$ ) currently planned for ILAW glass forms are envelope dependent. Therefore, the volumetric flowrate of the LAW stream passing through the ion-exchange facility during the loading phase is envelope dependent. The current processing plan for the Phase 1 LAW inventory is to batch process the entire inventory. The Phase 1 campaign constitutes the processing of ten waste tanks that are broken up into 16 batch feeds (i.e., 11 are Envelope A feeds, 2 Envelope B feeds, and 3 Envelope C feeds). The source tank and volume of solution to be processed on a batch feed basis (i.e., shown here on a 5 M sodium basis) are listed in Table 2-1. The envelope dependent flowrates used in the VERSE-LC design calculations are also listed in Table 2-1 for the 16 batch feeds. The basis for the flowrates centers on the production goals of glass and the allowable limits of waste sodium oxide loading within the glass matrix.

Constraints on the allowable levels of  $^{137}\text{Cs}$  contained within the aqueous effluent stream exiting the ion-exchange facility are also envelope dependent. Based on these  $^{137}\text{Cs}$  concentration limits total cesium exit criteria can be computed based on the isotopic content of cesium within each feed (i.e., it is assumed that the isotopic fraction of  $^{137}\text{Cs}$  to  $^{137}\text{Cs}_{\text{total}}$  is 25 mole% for Envelopes A and C and 30% for Envelope B). These total cesium exit criteria are also listed in Table 2-1.

From the viewpoint of determining an optimal ion-exchange facility based on CST packed columns, a minimization of spent CST strategy has been chosen. In this strategy all 16 batch feeds are being addressed individually. Specifically, we are addressing the following key varying attributes: (1) volume of solutions to be processed; (2) feed volumetric flowrates; (3) composition of key constituents; (4) cesium exit criteria; (5) the geometry of the columns; and (6) the number of columns used within a carousel configuration. The methodology used to

perform the design (i.e., minimization) is discussed in detail in Chapter 10 where the supporting bases are provided throughout the remainder of the report.

## 2.1 Test Specification Objectives

The main objectives of this report were defined in the original test specification document by Johnson (2000) and restated in the Task Technical and QA Plan by Hang et al. (2001). In summary, these objectives are:

- To predict the quantity of IONSIV<sup>®</sup> IE-911 CST needed to treat the candidate Phase 1 LAW batch feed solutions (16 feeds in total);
- To predict the number and dimensions of CST ion-exchange columns (i.e., bed geometry) required to reduce the  $^{137}\text{Cs}$  concentrations to  $1.75 \times 10^{-5}$  Ci  $^{137}\text{Cs}$  per gmole of Na after treatment of a selected candidate LAW solution; and
- To compare the dimensions of the CST material bed to the RPP-WTP reference resin bed design based on SuperLig<sup>®</sup> 644 resin.

Based on updated information from Mike Johnson the exit cesium criterion was made envelope dependent:

- $1.75 \times 10^{-5}$  Ci  $^{137}\text{Cs}$  per gmole of Na for Envelope A feeds
- $5.00 \times 10^{-5}$  Ci  $^{137}\text{Cs}$  per gmole of Na for Envelope B feeds
- $2.90 \times 10^{-5}$  Ci  $^{137}\text{Cs}$  per gmole of Na for Envelope C feeds

These criteria are reflected in the exit criteria listed in Table 2-1. Within the Test Specification document no specific criterion as the degree of cesium loading within the lead columns was provided. Based on discussions with Mike Johnson, and after some up front scoping analyses, the traditional +90% loading requirement (established using a mass transfer zone (MTZ) concept) was abandoned in favor of a more robust global optimization strategy alluded to in the previous section and discussed in Chapter 10 where the justification for its use versus the MTZ approach is provided.

## 2.2 IONSIV<sup>®</sup> IE-910/IE-911 CST Versus SuperLig<sup>®</sup> 644

In Chapter 10 a detailed look at the loading performance (both from an equilibrium and a kinetics viewpoint) is provided for IONSIV<sup>®</sup> IE-911 CST material versus SuperLig<sup>®</sup> 644 resin. In brief summary, we see that the IONSIV<sup>®</sup> IE-911 CST material has an increased cesium capacity of ~30% on a per mass basis and ~640% on a per bed volume basis. The significant difference being the higher average bed density of IONSIV<sup>®</sup> IE-911 CST material (i.e., ~1.0 g/ml) when compared to SuperLig<sup>®</sup> 644 resin (i.e., ~0.224 g/ml). The overall kinetics for IONSIV<sup>®</sup> IE-911 CST material appears to be slower than for SuperLig<sup>®</sup> 644 resin, due primarily to a ~3.5 factor smaller cesium pore diffusivity coefficient.

These comparisons were made focusing on the cesium loading phase where the feed solution is near 5 M sodium. The organic based SuperLig<sup>®</sup> 644 resin is considered an elutable resin, while the inorganic based IONSIV<sup>®</sup> IE-911 CST material is considered to be a non-elutable exchanger. The definition of elutable versus non-elutable is based on the exchanger's cesium loading performance under reduced pH conditions. In Figure 2-2 the cesium  $K_d$  values for both exchanger materials are shown as a function of pH for a fixed cesium concentration of  $5 \times 10^{-4}$  M. This data was taken by Bray et al. (1995) at 25 C, where an initial screening comparison was made of the loading performance of five different exchanger materials for Hanford applications.

As shown in Figure 2-2 and stated elsewhere, at high alkalinity conditions the two exchangers have similar loading performances. However, as the pH of the liquid-phase is reduced the two exchangers exhibit opposite behavior. The SuperLig<sup>®</sup> 644 resin shows a systematic drop in cesium loading where it bottoms out for solutions whose pH are at or below pH of  $\sim 7$ . For the IONSIV<sup>®</sup> IE-910 CST material, it rises to an approximate plateau for solutions whose pH are at or below pH of  $\sim 7$ . As such, the pretreatment flowsheet will be impacted due to this unique pH effect between these two exchangers. Other factors are briefly highlighted in Chapter 10.

The ZAM model for describing the loading performance of CST material addresses the pH effect as shown in Figure 2-2. Its Supersite model (i.e., three neighboring surface sites) conceptually handles this effect assuming steric limitations of cations within a supersite. For example, under high pH conditions the supersite is fully occupied by sodium cations. At reduced pH conditions one or more of the sites is occupied by hydrogen cations which have a smaller radius of hydration. At these reduced pH conditions the ability of cesium displacing one of the remaining sodium cations is greater due to the improved steric conditions. Thus, an increased  $K_d$  is observed.

Based on analytical data of the eluate retrieved from elution cycles, the major competitors for exchange sites appear to be  $\text{Cs}^+$ ,  $\text{K}^+$ , and  $\text{Na}^+$  for both exchanger types. For the IONSIV<sup>®</sup> IE-911 CST material  $\text{Rb}^+$  and  $\text{SrOH}^+$  are also potential major competitors however, their impact on performance is assumed to be small due to the low concentrations present within the feeds (i.e., further investigation is required to determine how low the  $\text{SrOH}^+$  really is). The relative affinities of these two exchanger types are quite similar for the three major competitors. Our current estimates for these relative affinities are (1) 1,200 to 1,400 for cesium versus potassium and (2) 24,000 to 26,000 for cesium versus sodium.

## 2.3 Ion Exchange Modeling

This ion-exchange system is one of many unit operations within a larger process flowsheet. Experimental efforts are currently underway to characterize the exchangers and the ion-exchange process in support of the overall design. Modeling the ion-exchange process in detail provides key supporting information needed in establishing the overall flowsheet. For example, cycle (time) average decontamination factors are required at the overall flowsheet level. Separate (off-line) detailed transient column modeling provides these average decontamination factors where the detail of the analysis is not restricted due to constraints imposed by the flowsheet runtime and storage requirements.



In addition, modeling:

- Reduces the overall number of experiments required;
- Provides guidance on experimental efforts and focuses attention on the critical parameters;
- Evaluates the adequacy and consistency of multiple data sets;
- Consolidates available information on a particular ion exchange system; and
- Establishes then confirms full-scale facility design and operational requirements.

## **2.4 Report Overview**

This report focuses on the cesium-loading phase of a complete cycle. An analysis methodology is developed where as much of the available and pertinent data on the Cesium-IONSIV<sup>®</sup> IE-911 CST system is incorporated. Many of the model parameters are currently defined by direct experimentation. However, some of these parameters are based on limited data or significant uncertainties with regard to the data existed. In several cases assumptions had to be made prior to the assessment efforts (e.g., column test exit breakthrough curves). The methodology can easily be updated as new information becomes available (e.g., measured bed and pore porosities or mean particle radius).

This document represents a status report on our current knowledge and capability to model the ion-exchange process for the Cesium-IONSIV<sup>®</sup> IE-911 CST system under various Hanford feed conditions. The methodology, its justification, assessment, and application to the proposed facility is discussed in the following chapters. Supporting information has also been provided in several appendices and wherever possible references to available published data/information pertinent to the discussion has been cited.

Chapter 3 briefly discusses the transport model chosen for modeling column behavior. The governing equations and an appropriate simplification is presented. For the modeling efforts presented in this report the VERSE-LC code was chosen (Berninger et al., 1991) based on its availability and widespread (and accepted) use in this field. Essentially, a very similar methodology was used in earlier analyses for the Cesium-SuperLig<sup>®</sup> 644 system as presented by Hamm et al. (2000a).

Local equilibrium between the pore fluid and its neighboring surface sites is assumed where equilibrium adsorption isotherm(s) must be specified. The algebraic isotherm model(s) used for each of the 16 batch feeds and the database employed in its creation are discussed in Chapter 4. The batch contact test databases in support of isotherm model development are numerically derived based on the ZAM code. The current version of ZAM is based on CST powder and a dilution factor must be applied to address CST in its engineered-forms. Due to batch variability observed in the manufacturing of CST material in its engineered-form(s), a statistically conservative cesium isotherm is used to accommodate the production range of expected CST material. This is accomplished by using a 68% dilution factor. The methods and results for creating charge-balanced compositions of the 16 batch feeds are presented in Appendix A. With these feed compositions cesium isotherm databases were generated and are presented in

Appendix B. The justification for using a dilution factor of 68% is discussed in Appendix C. A description, along with limited verification and validation assessments, for the ZAM code is provided in Appendix F.

Key column properties (i.e., densities and porosities) are addressed in Chapter 5 where the constraint between the porosities is highlighted. Particle size distribution and the average particle radius used for the IONSIV<sup>®</sup> IE-911 CST (i.e., the Baseline CST in its engineered-form) is addressed in Chapter 6.

Pore diffusion and Brownian motion are discussed in Chapter 7 where an assessment to batch kinetics data is provided. The VERSE-LC code input and output files for the batch kinetics simulations are provided in Appendix E. In summary, we see inconsistencies among the available batch contact test data and deficiencies with using the homogeneous particle concept (and perhaps without addressing surface diffusion) currently within VERSE-LC. As such the particle tortuosity factor chosen (i.e., 5.0) for our design efforts is not based on these batch kinetics tests, but rather is based on the assessment of available column tests as discussed in Chapter 9. Future efforts to determine the important diffusional aspects of CST in its most common engineered-forms are recommended.

In Chapter 8 the constitutive models for axial dispersion and film diffusion are presented. Headspace and short column impacts are also briefly discussed. For each column an inlet headspace of 25% based on bed volume is assumed. From the loading perspective the size of this headspace has little impact on the predicted cesium breakthrough curves.

Chapter 9 contains the laboratory-scale (including pilot-scale) column assessments (15 in total). Appendix H contains the VERSE-LC code input files for each of the laboratory-scale and pilot-scale simulations. To perform column transport analyses for sizing the CST columns, a method of estimating an “effective” cesium pore diffusion coefficient value is required (i.e., the tortuosity factor approach is chosen here). We had hoped that available batch kinetics test data would provide us the appropriate values. Unfortunately, the pore diffusion values based on existing kinetics data did not compare favorably when used in laboratory-scale column performance assessments. Given this situation, we are now estimating the pore diffusion coefficient values using a tortuosity factor based on the laboratory-scale column data directly. The tortuosity factor computed and the basis behind its creation are provided in Chapter 9. Also, a brief assessment to pilot-scale experiments is provided.

Based on the test specification objectives for the design of full-scale columns packed with CST material, Chapter 10 presents full-scale column performance predictions where the entire Phase 1 Low inventory is considered. The VERSE-LC code input and output files for the full-scale facility simulations are contained in Appendix D. The basis behind the need to use a global optimization strategy versus the more traditional mass transfer zone concept is provided. A comparison is made of facility performance between columns packed with SuperLig<sup>®</sup> 644 resin versus IONSIV<sup>®</sup> IE-911 CST material. Both 2-column and 3-column carousel configurations are considered. In order to bound the IONSIV<sup>®</sup> IE-911 CST material’s radioactive exposure levels associated with radioactive decay of cesium-137, cesium inventories within the column (i.e., cesium content in the liquid-phase plus adsorbed onto the solid-phase) are estimated during

the loading cycle corresponding to the worst case conditions. This inventory estimate can be used in subsequent analyses (beyond the scope of this report) for estimating conservative exposure levels. The impact of geometry (i.e. L/D, length to diameter ratio) on column performance is also addressed in Chapter 10.

A reasonable complete listing of pertinent literature references is provided in Chapter 11.

Table 2-1. Key batch processing information on the Phase 1 Low activity waste (LAW) feeds listed in their scheduled order to be processed.

Envelope	Source Tank	LAW batch feed (id)	Flowrate <sup>b</sup> (L/min)	Cesium feed conc. [M]	Batch volume to be processed <sup>a,c</sup> (m <sup>3</sup> )	Total Cs exit criterion <sup>b</sup> [M]
A	AP-101	LAW-1	52.62	3.598E-05	4,626	2.953E-08
B	AZ-101	LAW-2a	9.4	4.676E-04	2,906	7.032E-08
B	AZ-102	LAW-2b	9.4	4.311E-04	1,755	7.032E-08
C	AN-102	LAW-3	16.2	3.967E-05	4,200	4.894E-08
C	AN-102	LAW-4	16.2	3.779E-05	4,200	4.894E-08
A	AN-104	LAW-5	52.62	6.283E-05	3,820	2.953E-08
A	AN-104	LAW-6	52.62	6.328E-05	3,540	2.953E-08
C	AN-107	LAW-7	16.2	4.455E-05	5,498	4.894E-08
A	AN-105	LAW-8	52.62	4.324E-05	3,700	2.953E-08
A	AN-105	LAW-9	52.62	4.444E-05	3,600	2.953E-08
A	SY-101	LAW-10	52.62	3.692E-05	2,600	2.953E-08
A	SY-101	LAW-11	52.62	3.739E-05	4,600	2.953E-08
A	AN-103	LAW-12	52.62	4.831E-05	4,720	2.953E-08
A	AN-103	LAW-13	52.62	4.831E-05	4,720	2.953E-08
A	AW-101	LAW-14	52.62	4.569E-05	3,940	2.953E-08
A	AW-101	LAW-15	52.62	4.552E-05	5,360	2.953E-08

<sup>a</sup> The volume of each batch feed represents the volume of solution entering the ion-exchange facility at a 5 M sodium basis and includes the volume changes that occur upstream to this facility (i.e., pretreatment activities).

<sup>b</sup> The volumetric flowrates and batch process times are based on the 30 MT/day operation schedule for Envelopes B and C and on the expanded capability of 60 MT/day operation for Envelope A.

<sup>c</sup> The total amount of processing time is ~4.2 years. If the Envelope A feeds are processed at 30 MT/day, then the total amount of processing time is ~5.8 years.

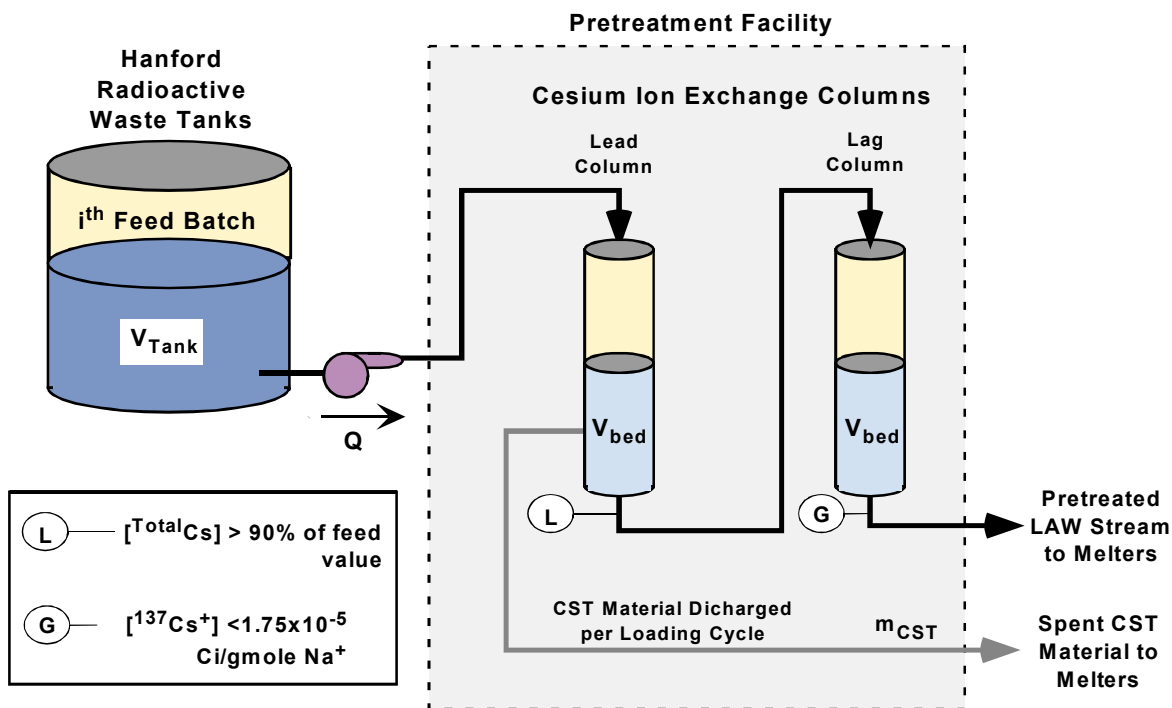


Figure 2-1. Simplified material flowsheet overview highlighting the ion-exchange units used for removal of cesium from a candidate LAW stream.

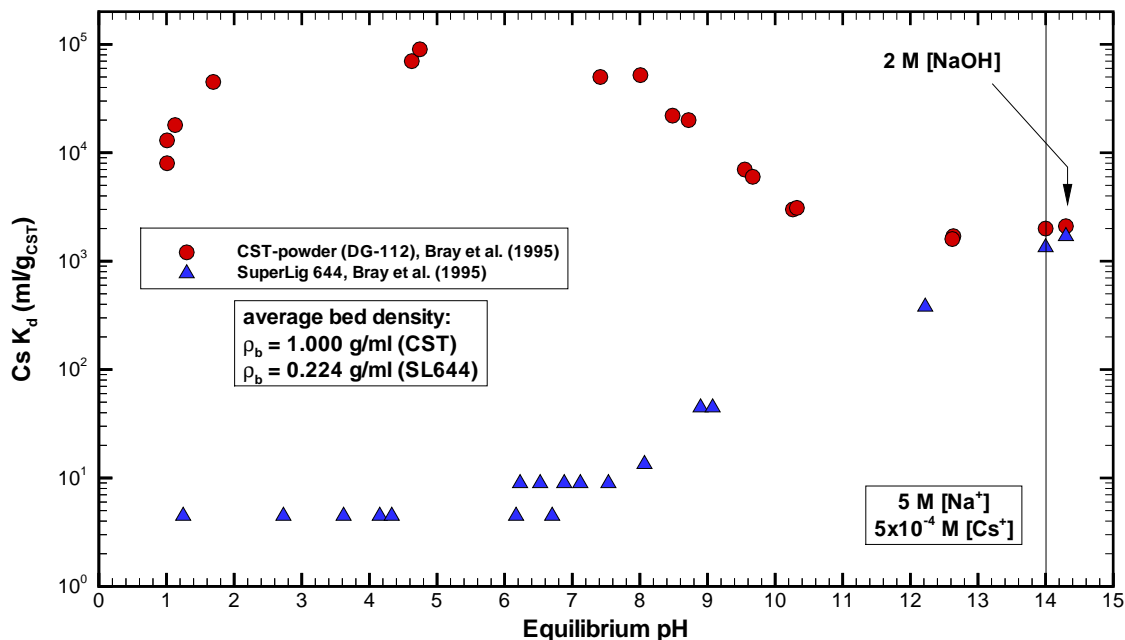


Figure 2-2. Cesium loading performance comparison between IONSIV® IE-911 CST and SuperLig® 644 exchanger materials at 25 C by Bray et al. (1995).

### 3.0 Column Model Formulations

The modeling of ion exchange columns is typically broken up into two basic categories:

- An equilibrium model generally highly empirical in nature, and
- A column model based on one-dimensional solute transport.

In this section the equations for the multi-component and the simpler “effective” single-component ion exchange column models are addressed. Justification for use of the simpler “effective” single-component column model is provided where its use is limited to the loading cycle of the process only. Chapter 4 of this report addresses both equilibrium models considered (i.e., the ternary isotherm model and the “effective” single-component isotherm model).

To take into account the various mechanisms for ion transport and adsorption as it travels down an ion exchange column, a porous particle solute transport formulation has experienced widespread use and acceptability. For this class of column models five basic aspects of the ion exchange column are addressed as highlighted in Figure 3-1. In order of their importance with respect to predicting exit breakthrough curves for the Cesium-IONSIV® IE-911 CST system, they are:

- **Bed Definition** (high impact) – column size, geometry and resin mass have a very direct impact on overall column performance, with particle geometry having a slightly less important impact (Shifts entire breakthrough curve with respect to number of column volumes required to reach a specified concentration level);
- **Adsorption Isotherms** (high impact) – resin affinities for the various competing ions of interest have a very direct impact on overall column performance (Shifts entire breakthrough curve with respect to number of column volumes required to reach a specified concentration level and for non-linear isotherms alters breakthrough curve shape as well as its sensitivity with respect to inlet feed conditions);
- **Pore Diffusion** (high impact) – intra-particle mass transport by pore diffusion to available surface sites has a moderate impact on overall column performance, with particle geometry having a slightly less important impact (under non-limiting mass transfer conditions it alters the shape of exit breakthrough curves typically by a rotation about the ~50% relative concentration level with slight shifting; under limiting mass transfer conditions the rotation is generally at a point higher than 50%);
- **Film Diffusion** (low impact) – liquid mass transport by film diffusion across the particle-to-bed boundary has a low impact on overall column performance (Alters the shape of exit breakthrough curves typically by a rotation about the ~50% relative concentration level with slight shifting);
- **Axial Dispersion** (low impact) – mass transport along the column by axial dispersion has a low impact on overall column performance (Alters the shape of exit breakthrough curves typically by a rotation about the ~50% relative concentration level with slight shifting);

The above stated levels of impact are based on sensitivity studies and are relative values. Mechanisms such as surface migration or adsorption kinetics are not included in our column model since their impacts were considered to be negligible or already indirectly incorporated into the other features during our parameter estimation process. Pore heterogeneity within the CST particles is not explicitly handled as well. A simple graphical representation of the various transport mechanisms listed above and considered important for the Cesium-IONSIV® IE-911 CST system is shown in Figure 3-2.

### 3.1 The Multi-Component Model

For the Cesium-IONSIV® IE-911 CST system a porous particle multi-component ion exchange column model was considered. In this model we assume that the kinetics associated with local ion exchange at an active resin site are very fast (faster than the various liquid mass transfer mechanisms that transport ions to that site). Assuming radial effects to be negligible within the active region of the packed bed (i.e., a large column-to-particle diameter ratio), a one-dimensional species (ion) transport equation for the mobile phase (within the bed) becomes

$$\underbrace{\varepsilon_b \frac{\partial c_{bi}}{\partial t}}_{\text{storage}} + \underbrace{\varepsilon_b u \frac{\partial c_{bi}}{\partial z}}_{\text{advection}} = \underbrace{\varepsilon_b E_{bi} \frac{\partial^2 c_{bi}}{\partial z^2}}_{\text{axial dispersion}} - \underbrace{\left( \frac{3}{\langle R_p \rangle} \right) (1 - \varepsilon_b) k_f \left( c_{bi} - c_{pi} \Big|_{r=R_p} \right)}_{\text{liquid film diffusion (mass transfer)}}, \quad (3-1a)$$

with boundary and initial conditions

$$z = 0, \quad \varepsilon_b E_b \frac{\partial c_{bi}}{\partial z} = uL \left[ c_{bi} - c_{bi}^{\text{feed}}(t) \right], \quad (3-1b)$$

$$z = 1, \quad \varepsilon_b E_b \frac{\partial c_{bi}}{\partial z} = 0, \quad (3-1c)$$

$$t = 0, \quad c_{bi} = c_{bi}(0, z). \quad (3-1d)$$

Assuming uniformly sized spherical particles with a homogeneous distribution of pores, a one-dimensional species transport equation for the pore phase (within an average sized particle of resin) becomes

$$\underbrace{\varepsilon_p \frac{\partial c_{pi}}{\partial t}}_{\text{storage}} + \underbrace{(1 - \varepsilon_p) \overline{C}_T \sum_{j=1}^{N_s} \left[ \left( \frac{\partial q_i}{\partial c_{pj}} \right) \frac{\partial c_{pj}}{\partial t} \right]}_{\text{surface adsorption}} = \underbrace{\varepsilon_p D_{pi} \frac{1}{r^2} \frac{\partial}{\partial r} \left[ r^2 \frac{\partial c_{pi}}{\partial r} \right]}_{\text{Fickian pore diffusion}}, \quad (3-2a)$$

with boundary and initial conditions

$$r = 0, \quad \varepsilon_p D_p \frac{\partial c_{bi}}{\partial r} = 0, \quad (3-2b)$$

$$r = \langle R_p \rangle, \quad \varepsilon_p D_p \frac{\partial c_{bi}}{\partial r} = k_f (c_{bi} - c_{pi}), \quad (3-2c)$$

$$t = 0, \quad c_{pi} = c_{pi}(0, r). \quad (3-2d)$$

In Eq. (3-2) it is assumed that the pore diameters are large relative to the size of migrating ions of interest. Therefore, Fickian diffusion is acceptable and surface migration is considered to be small (or incorporated into the apparent pore diffusivity coefficient) when compared to pore diffusion. Unfortunately, for high affinity exchangers such as CST, which exhibit nonlinear isotherms, an apparent pore diffusivity coefficient is composition dependent as discussed by Ma et al. (1996). As discussed in Chapter 7, in this report we assumed that a cesium composition independent pore diffusivity value can be adequately chosen. Future efforts addressing surface migration and pore heterogeneity should be considered.

Assuming local equilibrium between the pore fluid and its neighboring surface sites, an equilibrium isotherm model for the ion exchange between the pore and solid phases can be generically expressed as:

$$q_i = F_i(\bar{C}_T, \bar{K}_{ij}, c_{p1}, c_{p2}, \dots, c_{pN_s}), \quad i = 1, N_s, \quad (3-3)$$

**multi-component isotherm**

where it has been assumed that surface loadings for the  $i^{\text{th}}$  species can be explicitly related to the liquid concentrations locally. The  $K_{ij}$  values are selectivity coefficients that specify the relative affinity between species  $i$  versus species  $j$ . The number of species required to model the behavior of the  $i^{\text{th}}$  species depends upon its dependence on other species through the functional form (i.e.,  $F_i$ ) of the isotherm model [Eq. (3-3)]. Specific application of Eq. (3-3) to the cesium-IONSIV<sup>®</sup> IE-911 CST system is discussed in Chapter 4 and Appendices B and C. Initial and boundary conditions for Eqs. (3-1) and (3-2) must also be specified. For further details on these equations and their solution in VERSE-LC see Berninger et al. (1991). Helfferich and Carr (1993) provide an excellent review paper describing the behavior of non-linear waves in chromatography and also a brief listing of available algorithms (see their Table I.4). Their paper provides very clear insight into how the above equation set behaves for non-linear isotherms consistent with the system of interest discussed in this report.

For the modeling efforts presented in this report the VERSE-LC code was chosen (Berninger et al., 1991) based on its availability and widespread (and accepted) use in this field. Prior to applying VERSE-LC to the ion exchange modeling presented in this report a verification process was completed and the results of that effort are reported in Hamm et al. (1999). The verification process provided us quality assurance that the installed PC Window95<sup>™</sup> version of VERSE-LC (i.e., version 7.80) was capable of adequately solving the above mentioned equations and also helped us to better understand how to accurately use the VERSE-LC code (e.g., mesh refinement requirements and input/output options). For all column results presented in this report numerical errors associated with the results of VERSE-LC should be very small when compared to the uncertainties associated with various model input parameters (bed density, particle radius, pore diffusion, etc.).

### 3.2 The Single-Component Model

Under certain situations the porous particle multi-component transport equations discussed in Section 3.1 can be adequately decoupled to a series of single-component transport equations. The reduction to single-component equations is:

- valid when the total ionic strength,  $C_T$ , is the same between the column's native and feed solutions; or
- a reasonable approximation when one ion absorbs significantly more onto the resin than others.

Making the same basic assumptions as in Section 3.1 the single-component equations can be derived. For each species a one-dimensional species (ion) transport equation for the mobile phase (within the bed) becomes

$$\underbrace{\varepsilon_b \frac{\partial c_b}{\partial t}}_{\text{storage}} + \underbrace{\varepsilon_b u \frac{\partial c_b}{\partial z}}_{\text{advection}} = \underbrace{\varepsilon_b E_b \frac{\partial^2 c_b}{\partial z^2}}_{\text{axial dispersion}} - \underbrace{\left( \frac{3}{\langle R_p \rangle} \right) (1 - \varepsilon_b) k_f (c_b - c_p)|_{r=R_p}}_{\text{liquid film diffusion (mass transfer)}}, \quad (3-4)$$

where initial and boundary conditions are consistent with Eqs. (3-1b,c,d). A one-dimensional species transport equation for the pore phase (within a particle of resin) becomes

$$\underbrace{\varepsilon_p \frac{\partial c_p}{\partial t}}_{\text{storage}} + \underbrace{(1 - \varepsilon_p) \bar{C}_T \left( \frac{\partial q}{\partial c_p} \right) \frac{\partial c_p}{\partial t}}_{\text{surface adsorption}} = \underbrace{\varepsilon_p D_p \frac{1}{r^2} \frac{\partial}{\partial r} \left[ r^2 \frac{\partial c_p}{\partial r} \right]}_{\text{Fickian pore diffusion}}, \quad (3-5)$$

where initial and boundary conditions are consistent with Eqs. (3-2b,c,d).

The equilibrium isotherm model for species  $i$  for the ion exchange between the pore and solid phases becomes:

$$q = \frac{c_p}{\beta + c_p}, \quad (3-6)$$

**single-component isotherm**

where Eq. (3-6) is of the Langmuir form and  $\beta$  (the beta parameter) is a function of the feed conditions.

### 3.3 The Cesium-IONSIV® IE-911 CST System

Based on our current understanding, for the Cesium-IONSIV® IE-911 CST system the competition for cation exchange loading (under high alkaline conditions) at the CST sites is



primarily between cesium ( $\text{Cs}^+$ ), strontium hydroxide ( $\text{SrOH}^+$ ), rubidium ( $\text{Rb}^+$ ), potassium ( $\text{K}^+$ ), and sodium ( $\text{Na}^+$ ). For the analyses presented in this report it is assumed that rubidium and strontium hydroxide presence within the feeds is negligible for our modeling purposes. For rubidium this is a reasonable assumption due to its trace amounts within the Phase 1 LAW feeds; however, for strontium hydroxide its concentration depends upon the concentrations of  $\text{Sr}^{+2}$  and potential complexants within the feeds. Further studies must be performed to determine actual levels of strontium hydroxide present. Given these assumptions a ternary component feed (i.e., component 1 being  $\text{Cs}^+$ , component 2 being  $\text{K}^+$ , and component 3 being  $\text{Na}^+$ ) must be addressed.

Prior to the loading phase the initial sodium and potassium levels in the pretreatment solution are approximately 0.25 M and 0 M, respectively. During the loading phase these concentration levels increase to approximately ~5.0 M sodium and 0.0-to-1.0 M potassium. Therefore, initially a total ionic concentration wave will pass through the column. Based on available batch equilibrium studies estimates for the relative affinities for ion-exchange with the CST material have been computed as discussed in Chapter 4 and Appendix B (i.e., the CST exchanger affinities are  $\text{Cs}^+ \gg \text{K}^+ > \text{Na}^+$ ). For the Envelope A Phase 1 LAW batch feeds, selectivity coefficients have been estimated to be ~1,400 for cesium versus potassium ( $K_{12}$ ) and ~26,000 for cesium versus sodium ( $K_{13}$ ). Based on this selectivity coefficient values the three ternary isotherms and the one “effective” single-component cesium isotherm at 25 C were generated (see Chapter 4 for more details).

Given the above information, early column performance (say the first 5 to 10 column volumes or so) probably will require the use of the multi-component (i.e., ternary modeling) formulations of Section 3.1. Long-term performance should be adequately handled using the simpler single-component formulations of Section 3.2. To check the validity of these statements, cesium exit breakthrough curves from several column simulations were compared where both the multi-component and single-component formulations were used. Very similar results were obtained. To illustrate the differences in timing for the three ionic species, the exit breakthrough curves for each species is plotted in Figure 3-3 for a multi-component (i.e., ternary model) simulation of one of the experimental column tests (test SRS-Avg-Test2 performed by Wilmarth et al., 1999). The SRS-Avg-Test2 test was performed using a packed column containing an engineered-form of CST operating at 25 C with a feed composition of  $1.24 \times 10^{-4}$  M  $\text{Cs}^+$ , 0.015 M  $\text{K}^+$ , and 5.6 M  $\text{Na}^+$ . Under this feed composition the selectivity coefficients were estimated to be approximately  $K_{12} = 1,400$  and  $K_{13} = 24,270$  and a beta parameter of  $\beta = 2.4145 \times 10^{-4}$  M. Using these isotherms both VERSE-LC ternary and single-component transport simulations were performed. The VERSE-LC input files for both modeling approaches are provided in Appendix H.

As expected sodium breakthrough is the fastest, quickly followed by potassium, and then an order of magnitude later by cesium. Similar behavior is observed for the Cesium-SuperLig<sup>®</sup> 644 resin system (an ion-exchange process, see Hamm et al., 2000a). When the single-component formulations are used, the cesium breakthrough curve is only very slightly altered. Compare the ternary system cesium breakthrough curve prediction in Figure 3-4 (open circles) to the single-component result also provided in Figure 3-4 (solid curve). The VERSE-LC parameter settings chosen are all set to their nominal values (e.g., pore diffusion coefficients are 20% of their free

molecular values and a dilution factor of 68%). The two modeling approaches result in cesium breakthrough curves that are essentially identical.

Since significant CPU savings are achieved when the single-component model is used and the differences are well within our current predictive capabilities, the majority of column analyses presented in this report were performed using the single-component model. This simplification only applies to the loading cycle and for future elution studies a multi-component version will be required due to the short process timing and strong concentration gradients that will be present throughout the columns.

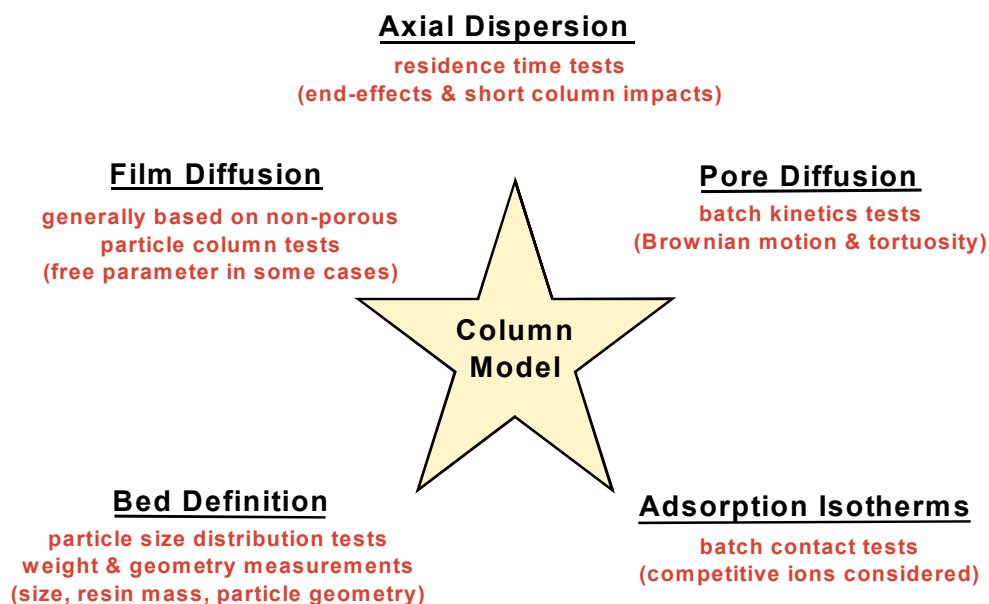


Figure 3-1. The basic building blocks of a porous particle ion exchange column model.

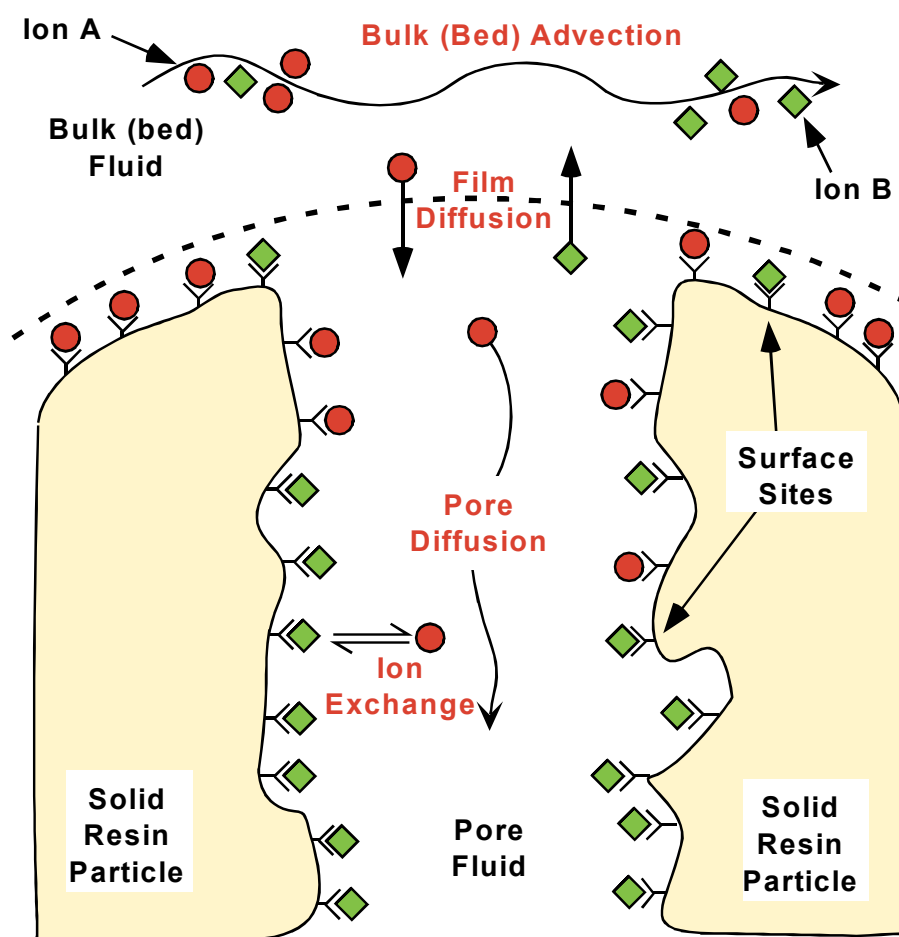


Figure 3-2. Graphical representation of the various mass transport mechanisms considered important for Cesium-IONSIV<sup>®</sup> IE-911 CST system ion exchange column modeling.

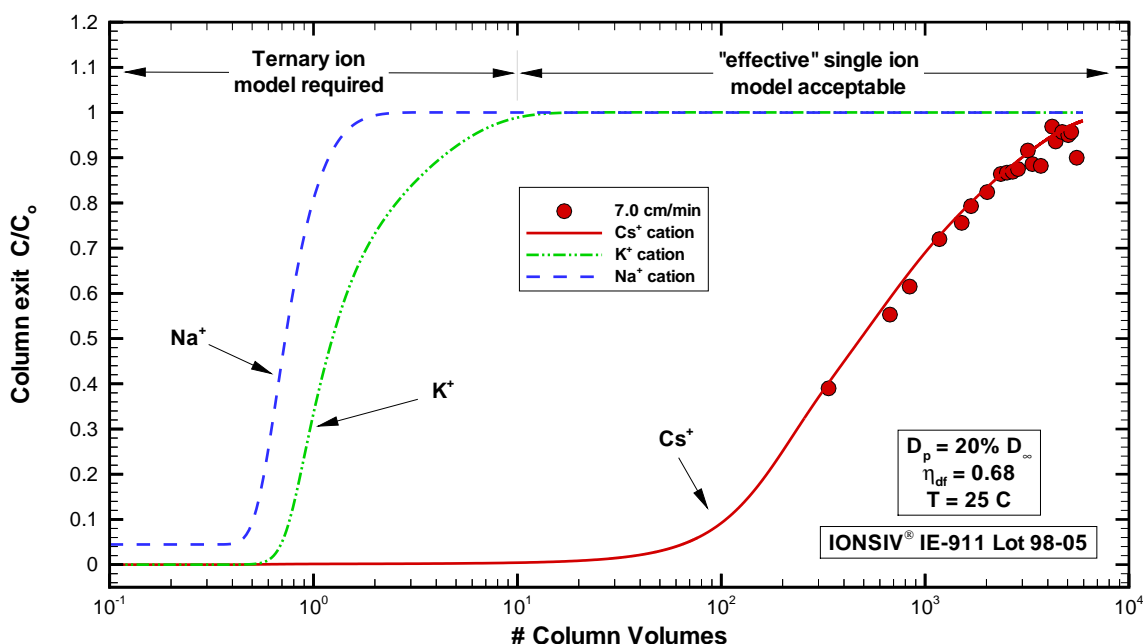


Figure 3-3. Estimated  $\text{Cs}^+$ ,  $\text{K}^+$ , and  $\text{Na}^+$  exit breakthrough curves for the test SRS-Avg-Test2 performed by Wilmarth et al. (1999) based on a porous particle multi-component (i.e., ternary) ion exchange column model for SRS Average simulant using IONSIV® IE-911 CST.

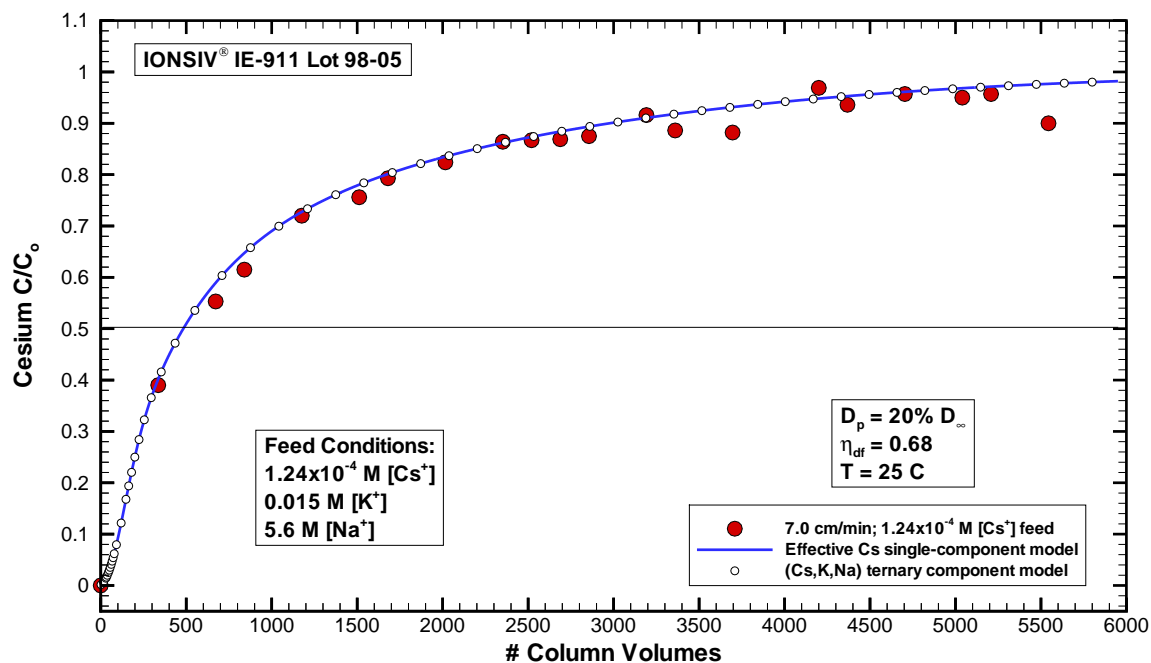


Figure 3-4. Measured versus predicted  $\text{Cs}^+$  column exit breakthrough curves based on the ternary and “effective” single-component ion exchange column models (test SRS-Avg-Test2 performed by Wilmarth et al. (1999) in a SRS Average simulant liquid at  $1.24 \times 10^{-4}$  M Cs and at 25 C).

## 4.0 Equilibrium Cesium Isotherms

In our column modeling efforts we assume that the rate of ion exchange (i.e., exchange of ions at a surface site) is very fast when compared to the rates of diffusion within the pore fluid and mass transfer across the liquid film at the outer boundaries of the particles. In other words, we assume that local equilibrium exists between the pore fluid and its neighboring surface sites. With this assumption an algebraic expression relating ionic (or species) concentrations between the pore fluid and the solid CST material (i.e., surface sites) can be established. No explicit attempt is made in this report to verify this assumption. In an indirect manner this assumption is either verified or incorporated into some of the model parameters. In addition, we assume that the cesium total ionic capacity (i.e., active sites for cesium per gram of CST material) is independent of total ionic strength or solution composition.

The total cation exchange capacity of the CST material in its powder-form (batch IE-910) is species dependent. Two types of exchange sites exist on the CST solid. The total ion exchange capacity is stated to be  $\sim 4.6$  mmole/g<sub>CST</sub>, but the cesium exchange capacity is much less indicating that not all sites are available for cesium exchange (see, Zheng et al., 1996). In the ideal solid region (i.e., prior to the first step of the isotherm), the apparent total capacities are  $\sim 0.58$  mmole/g<sub>CST</sub> for Cs<sup>+</sup>,  $\sim 1.2$  mmole/g<sub>CST</sub> for K<sup>+</sup>,  $\sim 1.18$  mmole/g<sub>CST</sub> for Rb<sup>+</sup>, and  $\sim 1.0$  mmole/g<sub>CST</sub> for SrOH<sup>+</sup>. For the expected feed concentrations it is anticipated that the entire columns will be operating within this ideal solid region. For additional information on this see Appendix C or Zheng et al., (1996).

In column sizing one of two possible design strategies are typically considered: (1) bounding analysis where “worst case” feed compositions are used or (2) global optimization where best estimate feed compositions for each individual batch are used. Each approach has its own advantages and disadvantages. For example, the bounding approach requires less analysis overall but it may be difficult to establish a reasonable bound that is not too excessive. Since the amount of waste to be processed, flowrate, and key feed compositions depend significantly on which envelope is being considered, the global optimization strategy is taken. To use this global optimization strategy “best estimate” cesium isotherms for each of the 16 batch feeds must be determined. In deriving an appropriate generic isotherm model for use with each batch feed the following items were considered:

- To keep reasonable runtimes an algebraic form of an isotherm model was desired that would be compatible/consistent with standard column models;
- The form of the isotherm model is to be thermodynamically consistent with the local mass-action equations where appropriate;
- The effects of competing anions within possible feed solutions needed to be easily addressed (i.e., able to handle the expected range of Hanford waste feeds without major alterations required);
- Batch equilibrium “K<sub>d</sub>” databases needed to be generated for each individual batch feed; and

- Batch variability must be handled by establishing a dilution factor that conservatively incorporates the various potential engineered forms of CST; and

Based on these considerations a binary homovalent isotherm model was developed and is presented in this section. Overall the model meets all of the above items; however, the confidence intervals for the model are higher than hoped. In Appendix C, further discussion of the isotherm model is given, where the effects associated with uncertainties and confidence levels are investigated. These isotherms are for the loading phase applications only.

The isotherm model development discussed below follows very closely to the development efforts presented by Hamm et al. (2000) for the Cesium-SuperLig<sup>®</sup> 644 ion-exchange system. For the Cesium-SuperLig<sup>®</sup> 644 ion-exchange system, batch equilibrium “K<sub>d</sub>” data was used in generating the isotherm models that were then used in VERSE-LC column transport simulations. For the Cesium-IONSIV<sup>®</sup> IIE-911 CST ion-exchange system, batch equilibrium “K<sub>d</sub>” data for each batch feed is not available and the ZAM computer code is used to numerically generate the necessary “K<sub>d</sub>” databases. A description of the ZAM code is given in Appendix F where some limited validation results are shown for use with Hanford LAW solutions. The details of generating these cesium isotherms can be found in Appendix B.

In the next subsection the “effective” cesium isotherm model is discussed based on an ion-exchange process and in the following subsection its specific application to the Cesium-IONSIV<sup>®</sup> IIE-911 CST ion-exchange system is discussed.

#### 4.1 The Isotherm Model

As demonstrated by Hamm et al. (2000a, Figure 3-3), for ion exchange competitors with affinities significantly less than the value for cesium, a single-component transport modeling approach is adequate for the cesium loading phase. To perform single-component transport simulations, an “effective” binary isotherm model in an algebraic form must be available for use in the VERSE-LC code. Based on our previous experience using VERSE-LC for modeling SuperLig<sup>®</sup> 644 and SuperLig<sup>®</sup> 639 resins (Hamm et al., 2000a and 2000b), the VERSE-LC Freundlich/Langmuir Hybrid isotherm model was chosen. As described by Hamm et al. (2000a, see Chapter 4), the cations cesium, potassium, sodium, and strontium hydroxide form a 4-component homovalent system where the surface loading for cesium on the CST material can be expressed as:

$$Q_{Cs} = \frac{\eta_{df} \bar{C}_T c_{Cs}}{c_{Cs} + [\tilde{K}_{21} c_K + \tilde{K}_{31} c_{Na} + \tilde{K}_{41} c_{SrOH} + \dots]} \Rightarrow \frac{\eta_{df} \bar{C}_T c_{Cs}}{c_{Cs} + \beta} \quad , \quad (4-1)$$

where the beta parameter for cesium becomes dependent upon the other ionic competitors for CST adsorption (i.e., K<sup>+</sup>, Na<sup>+</sup>, SrOH<sup>+</sup>, and Rb<sup>+</sup>). The beta parameter contains the selectivity coefficients making it dependent upon temperature and liquid composition of all of the ionic species in solution. The larger the beta parameter the less favorable (and lower loadings) an isotherm will be (have). The dilution factor (η<sub>df</sub>) is unity when considering a specific power-form and is less than one upon addition of an inert binder. Based on analyses discussed in

Appendix C the best estimate dilution factor for the engineered-form is set to 0.68. The total cesium capacity term is only a function of which batch of powder-form material is being considered and is set to 0.58 mmole<sub>Cs</sub>/g<sub>CST</sub>. Based on the work of Zheng et al., (1996). With the dilution factor and the total cesium capacity set, Eq. (4-1) contains only one free parameter (beta) that need to be specified. The beta parameter to determined through nonlinear regression using a ZAM generated database for each batch feed.

## 4.2 Batch Feed Compositions

In order to generate the cesium loading databases (i.e., “K<sub>d</sub>” databases) using the ZAM code, the feed compositions for the 16 candidate batch feeds were determined based on available Best Basis Inventory (BBI) Phase 1 LAW feed solution data. Alterations and adjustments were necessary to the raw BBI data in order for it to conform to current pretreatment plans and for overall charge balancing. Charge balancing is required due to the ZAM code input limitations placed on an ionic solution. The alterations and adjustments made focused on only those ionic species who have a direct impact on cesium loading (i.e., those ionic species considered in the cesium isotherm modeling – ZAM code input options).

A homovalent cation exchange process occurs between the ionic solution and the CST material where the dominant cations competing for exchange sites are Cs<sup>+</sup>, SrOH<sup>+</sup>, Rb<sup>+</sup>, K<sup>+</sup>, H<sup>+</sup>, and Na<sup>+</sup> (where the order presented here is somewhat consistent with the degree of selectivity). For the 16 Phase 1 batch feeds, Table 4-1 lists the key ionic species that play an important role in determining the cesium loading levels on CST material. The following basic assumptions were made in generating the batch feed compositions:

- Rb<sup>+</sup> is only present in trace amounts and was assumed to be zero in the development of cesium isotherms.
- CST has a strong affinity for SrOH<sup>+</sup>; however, the actual amount of total Sr<sup>+2</sup> available in solution to form SrOH<sup>+</sup> is currently believed to be small but is unknown at this time. In this report the Sr<sup>+2</sup> concentration has been set to zero. Future work will need to address this issue. Further discussion on this is given in Appendix B.
- Total Cs<sup>+</sup> concentrations estimated based on the <sup>137</sup>Cs<sup>+</sup> content assuming isotopic fractions of 25% for Envelope A and C feeds and 30% for Envelope B feeds.
- Only those species that are handled within the ZAM code are charge balanced. The concentration of free OH<sup>-</sup> was allowed to vary in order to achieve charge balance.
- The ZAM generated cesium loading databases are based on 25 C column operation. In order to generate one isotherm database, the cesium concentration within a feed solution was varied over a wide range. This was accomplished by adding or removing CsCl from the original LAW feed solution. The choice of CsCl, versus some other salts, was confirmed by the excellent fits achieved using the algebraic model (i.e., selectivity coefficients remained relatively constant over the entire range considered).

The complete list of assumptions made is provided in Appendix A, along with the feed compositions of the original BBI inventories (i.e., obtained from the test specification document)

and the final 5M basis batch feeds. The details and results of the creation of the 16 candidate feed compositions are provided in Appendix A. Tables A-5 and A-6 contain the feed compositions on a 5M sodium basis used as input to the ZAM code.

### 4.3 The Beta Parameter Values

As mentioned above, a nonlinear regression analyses was used to determine the beta value, given in Eq. (4-1), for each of the 16 batch feeds. A non-linear regression analysis based on the maximum likelihood principle (see Anderson et al., 1978) was chosen consistent with earlier work (Hamm et al., 2000a and 2000b). The details and results of the regression analyses are provided in Appendix B.

As shown by Eq. (4-1), it is assumed that the beta parameter is only temperature and composition dependent and does not depend on the CST form under consideration (i.e. powder or engineered material). The dilution factor addresses which particular form is being considered. The ZAM code performs a numerical batch contact simulation for a specific solution composition and temperature (i.e., solves the appropriate liquid-solid equilibrium and mass balance equations for each competitor). The ZAM generated loadings are for the powder-form CST material.

The results of the nonlinear regression analyses are listed in Table 4-2 for the 16 batch feeds. Table 4-2 contains the “best estimate” value of the beta parameter, the standard error in the beta parameter estimate, and the root-mean-square (rms) in cesium loading (i.e., in terms of %). The fitting results are grouped by envelope where overall averages of the three values are also given. Variability within an envelope can be seen, as well as between envelopes. This variability can easily be seen in the barchart of the beta values shown in Figure 4-1. The least favorable isotherm corresponds to batch feed LAW-1 (AP-101 source tank) with the next being LAW-15 (source tank AW-101). As indicated in Table 4-1, these two batch feeds have the highest competitor (specifically potassium) concentrations.

As the standard errors in beta indicate in Table 4-2, the algebraic model fits the ZAM generated database quite accurately. For example, in Figure 4-2 the cesium loading curve (i.e., the 25 C isotherm) for powder-form CST in contact with the LAW-15 batch feed is shown. The solid circles represent the ZAM generated database, while the solid curve is the algebraic model for CST powder. For application to CST column design a cesium loading curve for the engineered-form must be used and also shown in Figure 4-2 by the dashed curve is the isotherm for the LAW-15 batch feed. The location of the cesium feed concentration for LAW-15 is also shown by the gradient symbol on this dashed curve. Here a dilution factor of 68% is employed which shifts the loading curve downward. The basis for this value of the dilution factor is given in Appendix C.

The ZAM generated databases and their corresponding fits to Eq. (4-1) are provided in Appendix B for each of the 16 batch feeds. Also in Appendix B, are graphical comparisons of these isotherms grouped by envelope and by comparing the least favorable between envelopes.



#### 4.4 Isotherm Model for VERSE-LC Application

In order to perform column transport simulations, the algebraic model given by Eq. (4-1) above must be converted into one of the available VERSE-LC isotherm modeling options. Based on our previous experience using VERSE-LC for modeling SuperLig<sup>®</sup> 644 and SuperLig<sup>®</sup> 639 resins (Hamm et al., 2000a and 2000b, respectively), the VERSE-LC Freundlich/Langmuir Hybrid isotherm model was chosen. See Hamm et al. (2000a, see Chapter 4) for further descriptions of the multi-component homovalent isotherm approach.

For a 4-component homovalent isotherm, the VERSE-LC Freundlich/Langmuir Hybrid model is expressed as:

$$\bar{C}_{pi} = \frac{a_i c_{pi}^{M_{ai}}}{\beta_i + b_1 c_{p1}^{M_{b1}} + b_2 c_{p2}^{M_{b2}} + b_3 c_{p3}^{M_{b3}} + b_4 c_{p4}^{M_{b4}}} \quad \text{for } i = 1, 4, \quad (4-2)$$

where the model parameters ( $a_i$ ,  $b_i$ ,  $M_{ai}$ ,  $M_{bi}$ , and  $\beta_i$  for  $i=1,4$ ) can be determined from the parameter values associated with the 4-component homovalent model.

The Freundlich/Langmuir Hybrid model can also be used for an “effective” single-component case as well. Here the potassium, sodium, and strontium hydroxide concentrations throughout the column are assumed to be at their feed concentration levels. For an “effective” single-component total cesium isotherm, Eq. (4-2) under these conditions reduces to:

$$\bar{C}_{p1} = \frac{a_1 c_{p1}^{M_{a1}}}{[\beta_i + b_2 c_{p2}^{M_{b2}} + b_3 c_{p3}^{M_{b3}} + b_4 c_{p4}^{M_{b4}}] + b_1 c_{p1}^{M_{b1}}} \Rightarrow \frac{a_1 c_{p1}^{M_{a1}}}{\hat{\beta}_i + b_1 c_{p1}^{M_{b1}}}, \quad (4-3)$$

where the beta parameter for cesium becomes dependent upon the potassium, sodium, and strontium hydroxide feed concentrations. The relationship between the two models expressed by Eqs. (4-2) and (4-3) (i.e., 4-component homovalent and “effective” single-component isotherm models, respectively) is provided in Appendix B. The dilution factor,  $\eta_{df}$ , is set to unity when CST in its powder-form is being considered.

The modeling parameter values for a cesium single-component isotherm is listed in Table 4-3 for each of the 16 batch feeds. The  $a_1$  parameter of Eq. (4-3) is computed by:

$$a_1 = \rho_b \eta_{df} \bar{C}_T. \quad (4-4)$$

For the CST column design analyses performed in Chapter 10, an average density of 1 g/ml, a total cesium capacity of 0.58 mmole/g<sub>CST</sub> for CST powder, and a dilution factor of 0.68 for CST in its engineered-form are assumed. The  $a_1$  parameter values for both CST powder and its engineered-form are listed in Table 4-3.

Based on CST in its engineered-form the cesium isotherms for the 16 batch feeds, using the parameter settings listed in Table 4-3, are plotted in Figure 4-3 (for Envelope A), Figure 4-4 (for Envelope B), and Figure 4-5 (for Envelope C). In Figure 4-6 the least favorable isotherm taken from each envelope is plotted together for a direct comparison. The feed concentration of cesium is also shown on the figures.

Looking at Figure 4-6 we see that Envelope A's LAW-1 isotherm is the least favorable overall. However, Envelope B's cesium feed concentration is significantly larger than the other two. In addition, in Envelope C we have assumed that the impact of  $\text{SrOH}^+$  is negligible (an assumption that needs to be verified in the future). Therefore, a clear determination as to which feed results in the worst case isotherm for design purposes is difficult to determine based on this information alone.

Table 4-1. Summary of the Phase 1 batch feed compositions in molarity units (on a 5M sodium basis) highlighting those ionic species who are dominant contributors to the effectiveness of CST material for cesium loading. <sup>a</sup>

Env	Batch Name	Staging Tank	Cs <sup>+</sup> <sup>e</sup> (total)	K <sup>+</sup>	Rb <sup>+</sup> <sup>e</sup>	SrOH <sup>+</sup> <sup>b</sup>	pH <sup>d</sup>	OH <sup>-</sup> (free)	NO <sub>3</sub> <sup>-</sup>	NO <sub>2</sub> <sup>-</sup>	Al(OH) <sub>4</sub> <sup>-</sup>	CO <sub>3</sub> <sup>2-</sup>
A	LAW-1	AP-101	3.60E-05	0.71	-	-	14.2	1.55	1.87	0.81	0.23	0.48
A	LAW-5	AN-104	6.28E-05	0.06	-	-	13.9	0.86	1.38	1.19	0.57	0.39
A	LAW-6	AN-104	6.33E-05	0.06	-	-	14.0	0.95	1.36	1.19	0.57	0.36
A	LAW-8	AN-105	4.32E-05	0.07	-	-	14.1	1.34	1.28	1.20	0.64	0.20
A	LAW-9	AN-105	4.44E-05	0.06	-	-	13.8	0.57	1.41	1.21	0.45	0.55
A	LAW-10	SY-101	3.69E-05	0.04	-	-	13.9	0.87	1.43	1.31	0.49	0.28
A	LAW-11	SY-101	3.74E-05	0.04	-	-	14.0	0.93	1.20	1.39	0.47	0.36
A	LAW-12	AN-103	4.83E-05	0.12	-	-	14.2	1.54	1.22	1.13	0.75	0.16
A	LAW-13	AN-103	4.83E-05	0.13	-	-	14.2	1.54	1.22	1.13	0.76	0.16
A	LAW-14	AW-101	4.57E-05	0.32	-	-	14.2	1.75	1.32	1.06	0.49	0.25
A	LAW-15	AW-101	4.55E-05	0.41	-	-	14.3	2.14	1.30	1.01	0.50	0.15
B	LAW-2a	AZ-101	4.68E-04	0.12	-	-	13.2	0.16	1.28	1.48	0.42	0.59
B	LAW-2b	AZ-102	4.31E-04	0.14	-	-	13.4	0.27	0.67	1.18	0.10	1.03
C	LAW-3	AN-102	3.97E-05	0.04	-	-	14.0	1.03	1.74	0.80	0.26	0.51
C	LAW-4	AN-102	3.78E-05	0.04	-	-	14.0	1.03	1.74	0.80	0.26	0.51
C	LAW-7	AN-107	4.45E-05	0.02	-	-	13.9	0.79	1.97	0.70	0.14	0.66

<sup>a</sup> For CST material homovalent cation exchange takes place where the dominant species are Cs<sup>+</sup>, SrOH<sup>+</sup>, Rb<sup>+</sup>, K<sup>+</sup>, H<sup>+</sup>, and Na<sup>+</sup>.

<sup>b</sup> CST has a strong affinity for SrOH<sup>+</sup>; however, the actual amount of total Sr<sup>+2</sup> available in solution to form SrOH<sup>+</sup> is currently believed to be small but is unknown at this time. In this report the Sr<sup>+2</sup> concentration has been set to zero. Future work will need to address this issue.

<sup>c</sup> Rb<sup>+</sup> is only present in trace amounts and was assumed to be zero in the development of cesium isotherms.

<sup>d</sup> pH is only being estimated here without properly accounting for the water activity; however, ZAM correctly computes the H<sup>+</sup> concentration based on the inputted free OH<sup>-</sup>.

<sup>e</sup> Total Cs<sup>+</sup> concentrations estimated based on the <sup>137</sup>Cs<sup>+</sup> content assuming isotopic fractions of 25% for Envelope A and C feeds and 30% for Envelope B feeds.

Table 4-2. Estimated beta parameter values and error estimate for a one-component (total cesium) homovalent algebraic isotherm model based on CST in its powder-form (IE-910) where the data sets used were created using the ZAM code.

Feed Solution	"Best Estimate" $\beta_i$ [M]	Standard Error in $\beta_i$ [M]	Root Mean Square in Cs loading <sup>a</sup> (% difference)
<b>Envelope A</b>			
LAW-1	4.3376E-04	$\pm 8.3713\text{E-}07$	0.3912
LAW-5	2.3431E-04	$\pm 2.0648\text{E-}08$	0.0137
LAW-6	2.3668E-04	$\pm 2.2931\text{E-}08$	0.0202
LAW-8	2.5147E-04	$\pm 3.8060\text{E-}08$	0.0270
LAW-9	2.2453E-04	$\pm 2.8251\text{E-}08$	0.0220
LAW-10	2.2135E-04	$\pm 2.2209\text{E-}08$	0.0161
LAW-11	2.0543E-04	$\pm 2.4697\text{E-}08$	0.0229
LAW-12	2.9196E-04	$\pm 3.2849\text{E-}08$	0.0177
LAW-13	2.9328E-04	$\pm 3.2820\text{E-}08$	0.0184
LAW-14	3.6283E-04	$\pm 4.0017\text{E-}08$	0.0262
LAW-15	3.8513E-04	$\pm 3.7129\text{E-}08$	0.0219
Overall avg.	2.8552E-04	$\pm 1.0334\text{E-}07$	0.0543
<b>Envelope B</b>			
LAW-2a	2.6230E-04	$\pm 2.9902\text{E-}08$	0.0173
LAW-2b	2.1296E-04	$\pm 2.3999\text{E-}08$	0.0138
Overall avg.	2.3763E-04	$\pm 2.6951\text{E-}08$	0.0156
<b>Envelope C</b>			
LAW-3	2.1769E-04	$\pm 2.4699\text{E-}08$	0.0135
LAW-4	2.1769E-04	$\pm 2.4646\text{E-}08$	0.0132
LAW-7	1.9258E-04	$\pm 2.0511\text{E-}08$	0.0166
Overall avg.	2.0932E-04	$\pm 2.3285\text{E-}08$	0.0144

<sup>a</sup> Based on a percent difference in Cs loading [i.e.,  $100(\text{algebraic-ZAM})/\text{ZAM}$ ].

Table 4-3. Parameter settings for an “effective” single component Freundlich/Langmuir Hybrid equilibrium isotherm model for total cesium on CST based on the 1-component homovalent model.

Feed Solution	“Powder-form” (IE-910) $a_i$ (gmoles/L <sub>CV</sub> )	“Engineered-form” (IE-911) <sup>a</sup> $a_i$ (gmoles/L <sub>CV</sub> )	$b_i$ (M <sup>-1</sup> )	$M_{ai}$ (-)	$M_{bi}$ (-)	“Effective” <sup>b</sup> $\beta_i$ (-)
<b>Envelope A</b>						
LAW-1	0.580	0.3944	1.0	1.0	1.0	4.3376E-04
LAW-5	0.580	0.3944	1.0	1.0	1.0	2.3431E-04
LAW-6	0.580	0.3944	1.0	1.0	1.0	2.3668E-04
LAW-8	0.580	0.3944	1.0	1.0	1.0	2.5147E-04
LAW-9	0.580	0.3944	1.0	1.0	1.0	2.2453E-04
LAW-10	0.580	0.3944	1.0	1.0	1.0	2.2135E-04
LAW-11	0.580	0.3944	1.0	1.0	1.0	2.0543E-04
LAW-12	0.580	0.3944	1.0	1.0	1.0	2.9196E-04
LAW-13	0.580	0.3944	1.0	1.0	1.0	2.9328E-04
LAW-14	0.580	0.3944	1.0	1.0	1.0	3.6283E-04
LAW-15	0.580	0.3944	1.0	1.0	1.0	3.8513E-04
<b>Envelope B</b>						
LAW-2a	0.580	0.3944	1.0	1.0	1.0	2.6230E-04
LAW-2b	0.580	0.3944	1.0	1.0	1.0	2.1296E-04
<b>Envelope C</b>						
LAW-3	0.580	0.3944	1.0	1.0	1.0	2.1769E-04
LAW-4	0.580	0.3944	1.0	1.0	1.0	2.1769E-04
LAW-7	0.580	0.3944	1.0	1.0	1.0	1.9258E-04

<sup>a</sup> A dilution factor of 68% is assumed when going from the powder-form to the engineered-form and a bed density of 1.0 g/ml assumed.

<sup>b</sup> These are “best estimate” values based on the maximum likelihood algorithm.

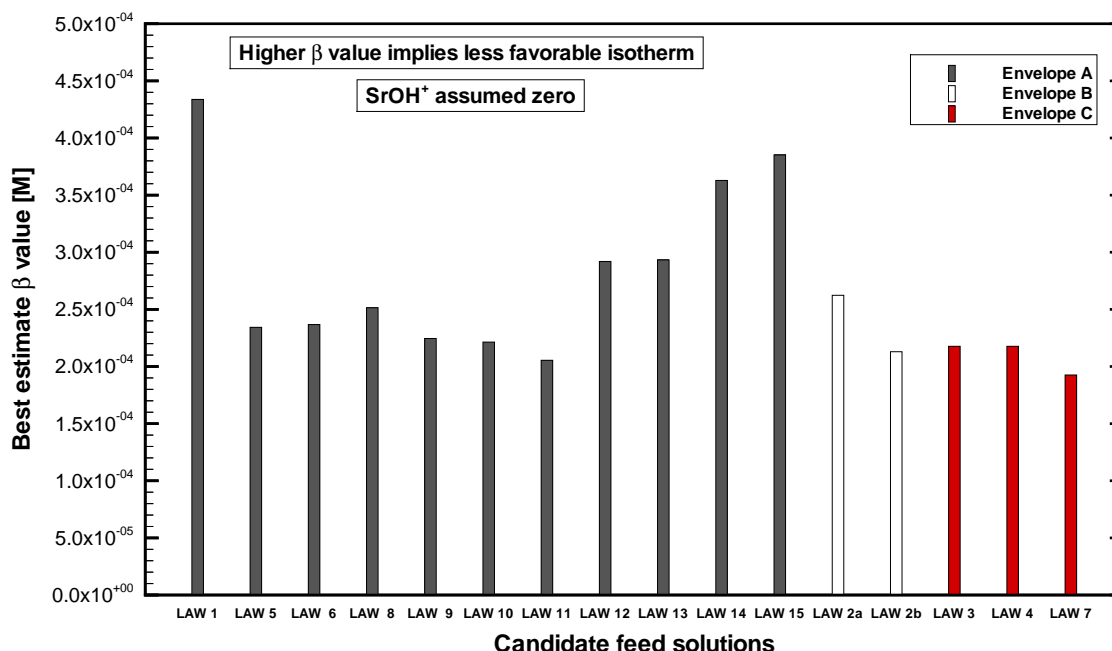


Figure 4-1. The estimated Phase 1 feed beta values used in the cesium effective single-component isotherm model for CST powder-form and engineered-form materials. The beta values are grouped by envelope and are based on feeds assuming zero  $\text{Rb}^+$  and  $\text{SrOH}^+$  present.

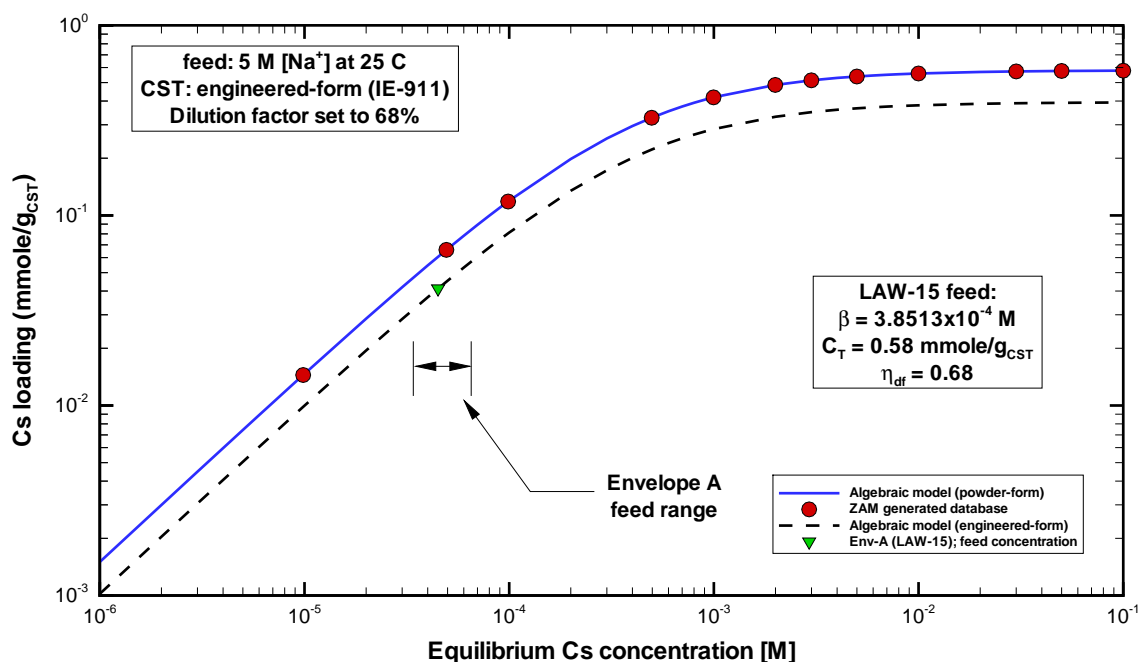


Figure 4-2. Comparison of the ZAM generated database for cesium loading onto IE-910 CST (powder) versus the algebraic model fit for the Phase 1 LAW-15 feed. Also shown is the algebraic model when applied to the engineered-form using a dilution factor of 68%.

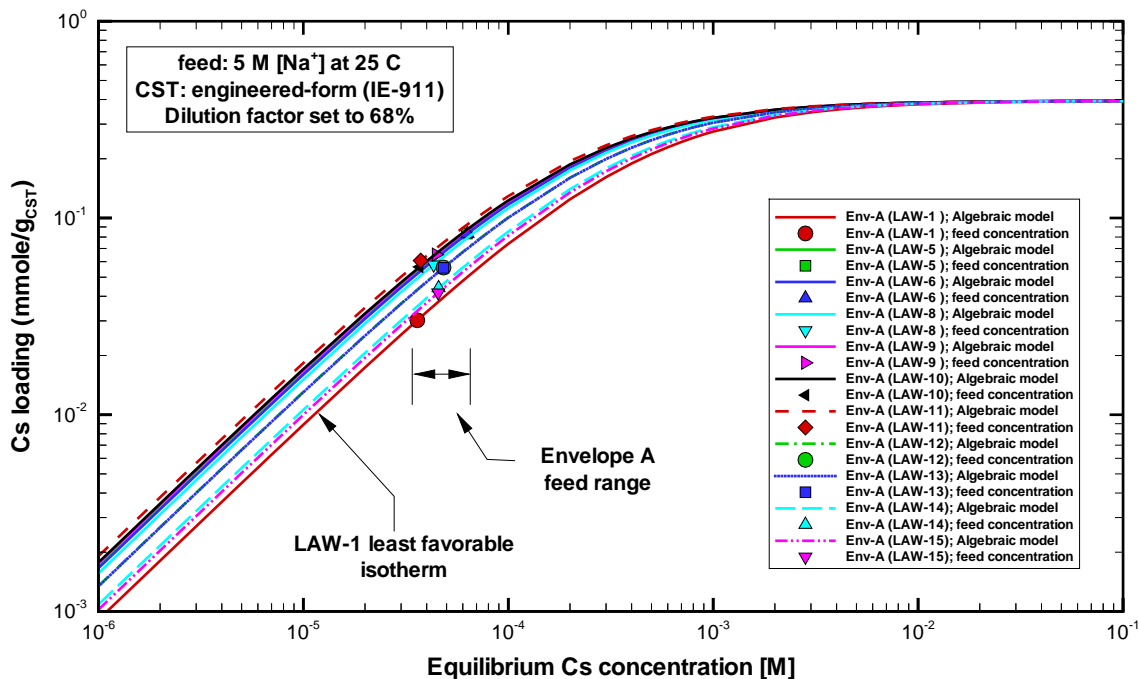


Figure 4-3. Comparison of Envelope A isotherms for the CST material in its engineered-form (IE-911). The lines represent predictions based on the single-component Freundlich/ Langmuir Hybrid isotherm model and symbols indicate the feed concentrations of cesium.

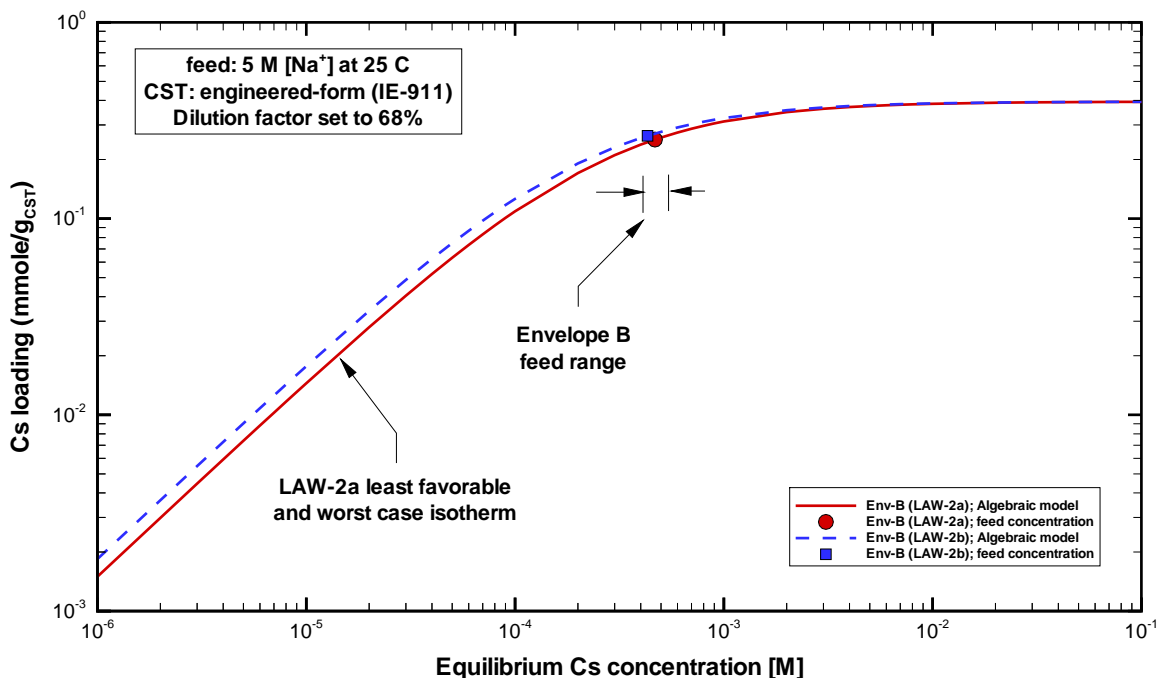


Figure 4-4. Comparison of Envelope B isotherms for the CST material in its engineered-form (IE-911). The lines represent predictions based on the single-component Freundlich/ Langmuir Hybrid isotherm model and symbols indicate the feed concentrations of cesium.

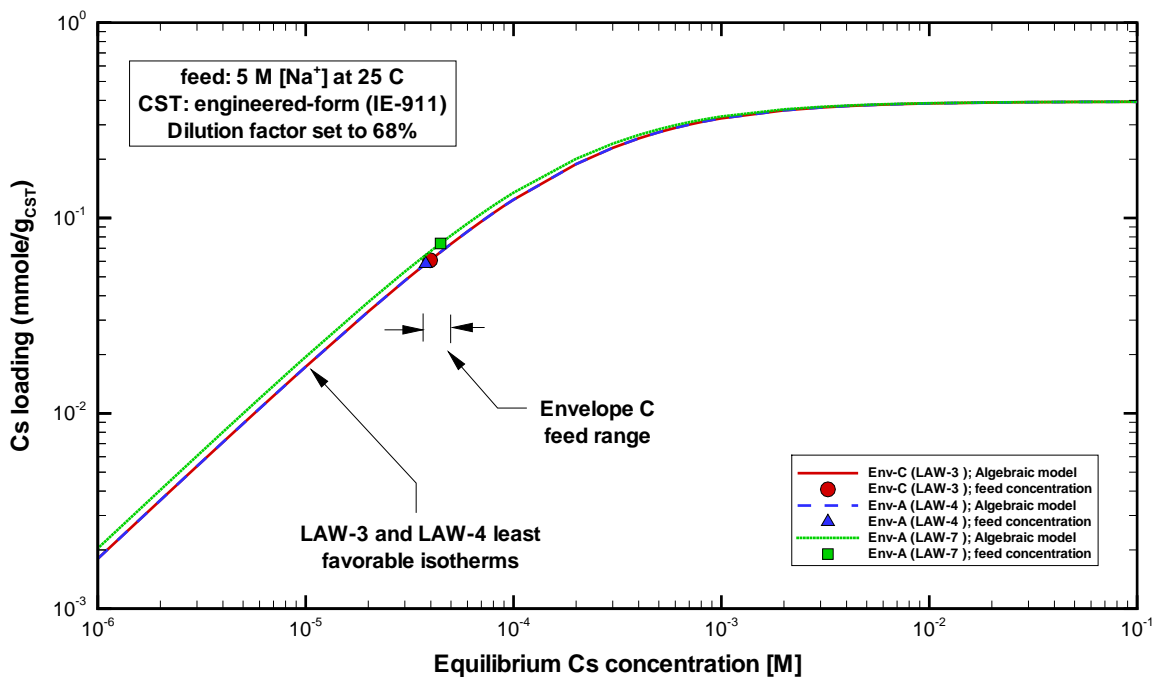


Figure 4-5. Comparison of Envelope C isotherms for the CST material in its engineered-form (IE-911). The lines represent predictions based on the “effective” single-component Freundlich/Langmuir Hybrid isotherm model and symbols indicate the feed concentrations of cesium.

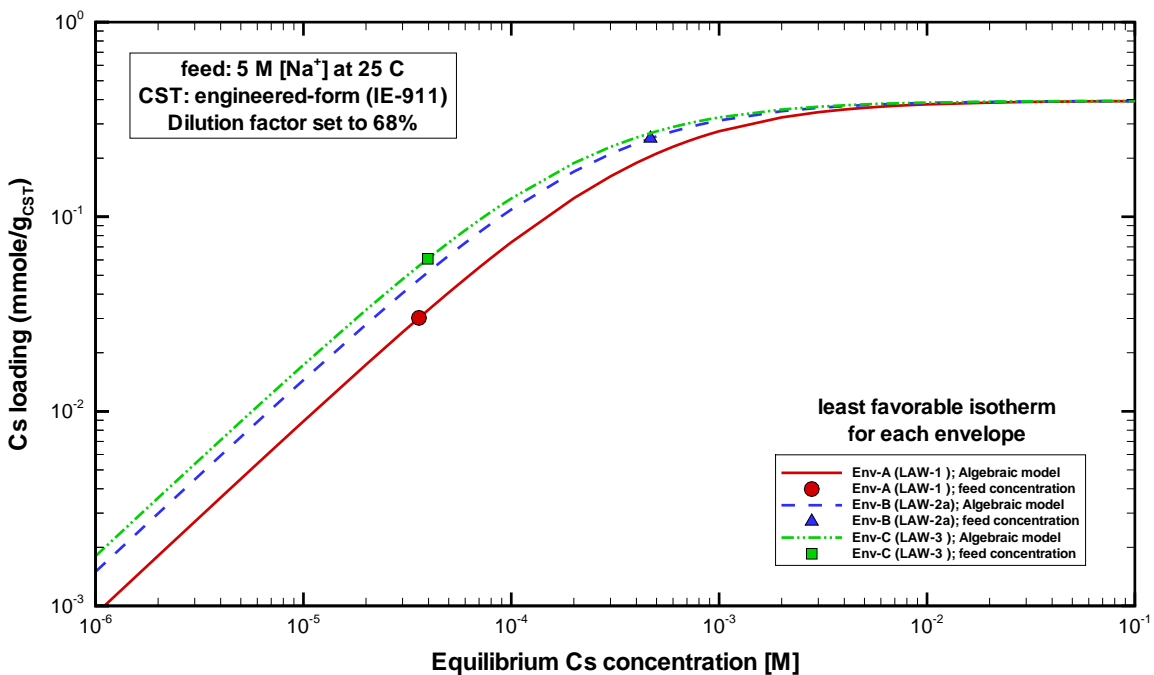


Figure 4-6. Comparison of the least favorable isotherms for Envelope A, B, and C feeds for the CST material in its engineered-form (IE-911). The lines represent predictions based on the “effective” single-component Freundlich/Langmuir Hybrid isotherm model.



## 5.0 Column Properties

Certain material properties (such as, solid particle density and total ionic capacity) are unique to the ion-exchange material and vary only between batches. On the other hand, composite properties associated with an ion-exchange column (such as, bed density or porosities) are inherently column specific resulting from how it was packed for example. Even when different columns are made from the same batch of material, column properties can and will vary. During operation upflow and then downflow can result in changes in particle packing arrangements (see, Steimke, 2000). During operational cycles where a significant variation in total ionic strength of the feed occurs, the active bed size of a column can change. The discussion that follows focuses on the column properties required when performing column transport simulations during the loading phase of a column cycle.

UOP (1996) states that the bulk density of the IE-911 exchanger is approximately 1 g/ml (i.e., a typical range of 0.8 to 1.13 g/ml) and that typically water contents are about 12 wt% for the IE-910 powder and about 20 wt% for the IE-911 engineered-form exchangers. Since the IE-910 and IE-911 materials have rigid inorganic structures, they resist significant swelling or shrinkage due to exposure to changes in temperature, pH, ionic strength, and ion exchange levels. The engineered-forms contain about 20% to 30% inert binder with the rest being CST powder.

The bed porosity of 0.50 and particle porosity of 0.24 were used for the majority of column simulations performed within this report. These porosity values have been used by numerous investigators in earlier analysis efforts (e.g., see Hritzko et al., 1998). These values yield a total bed porosity of 62%. During the writing of this chapter estimates of the particle density for IE-911 material were made available to the authors (i.e., actually slurry densities were provided which were then used to estimate particle density, Qureshi, 1999). Based on the limited measured particle and bed densities available, we estimate that the total porosity is in the range of 29% to 53%. The 62% we assumed earlier is outside this range indicating that the results from our column models are based on total bed voids that are larger than they should have been. This would normally imply that the column models contain less CST material by mass than they should have had. Fortunately, the manner in which VERSE-LC handles the isotherms enforces the bed density to be the value used in creating the isotherms (i.e., as shown in Chapter 4 bed density is part of the isotherm itself). The net effect is larger bed and/or pore volumes that can have a secondary effect on the predicted breakthrough curves (e.g., typical impacts are less than  $\pm 10\%$ ). Future design efforts should be based on more up to date porosity values based on measured bed and particle densities consistent with the engineered-form under consideration.

### 5.1 Basic Constraint Functions

Effective bed and particle porosity values for the powder-form and the engineered-forms will vary. The average particle radius for the powder-form is significantly less than for the engineered-forms (e.g.,  $\sim 0.8 \mu\text{m}$  versus  $\sim 344 \mu\text{m}$ ). Based on geometrical considerations not all densities and porosities are independent. The following two expressions place constraints on the densities and porosities:

$$\varepsilon_T = \varepsilon_b + (1 - \varepsilon_b)\varepsilon_p, \quad (5-1)$$

and

$$\rho_b = \rho_s(1 - \varepsilon_T), \quad (5-2)$$

where

- $\varepsilon_T$  - total porosity of active column, [-]
- $\varepsilon_b$  - bed porosity of active column, [-]
- $\varepsilon_p$  - particle porosity of CST particles, [-]
- $\rho_b$  - bed density of active column, g/ml
- $\rho_s$  - solid (particle) density of CST material, g/ml

and

$$\rho_b \equiv \frac{m_{CST}}{V_{bed}}. \quad (5-3)$$

For the five variables listed above only three are independent. The various porosities used in Eq. (5-1) are defined as:

$$\varepsilon_b = \frac{V_{void} - V_{pore}}{V_{bed}}; \quad \varepsilon_p = \frac{V_{pore}}{V_{part}}; \quad \varepsilon_T = \frac{V_{void}}{V_{bed}} = \frac{V_{bed} - V_{sld}}{V_{bed}}, \quad (5-4)$$

where

- $V_{bed}$  - total volume of active (bed) column, ml
- $V_{void}$  - total volume of voids within active column, ml
- $V_{pore}$  - total volume of pores within particles, ml
- $V_{part}$  - total volume of particles within active column, ml
- $V_{sld}$  - total volume of solid material within active column, ml

The above constraint equations provide a means to internally check for consistency between the various parameters. Below, just such a consistency check is performed where it can be seen that some of the available parameter values fall outside the limited measured data.

## 5.2 Densities

The actual amount of CST material present within a column is a parameter of prime importance with respect to column performance (i.e., exit breakthrough curves). For the column studies assessed within this report no direct measure of the total amount of CST residing within the active beds was available for most columns. For those columns whose original CST mass was not measured, the bed density was assumed to be the nominal value of 1.0 g<sub>CST</sub>/ml<sub>bed</sub>. The specific values for bed density from various data sources are listed in Table 5-1.

The particle (“material”) density of the CST IE-911 material can be estimated based on the measured slurry densities taken by Qureshi (1999) for CST and water mixtures. A summary of the results is given in Table 5-2. From this data an average particle density of ~1.65 g/ml is seen.

As Eq. (5-2) indicates, particle density, along with bed density, can be used to assist in determining the total porosity of a packed bed. Based on the Baseline CST material listed in Table 5-1 (and assumed properties for the majority of column simulations performed within this report), a particle density of ~1.62 g/ml can be back-calculated using Eq. (5-2). Based on these two different methods and data sources, the consistency of the estimates indicates that particle density is in the range of 1.6 to 1.7 g/ml. We assumed an average value of 1.65 g/ml for the Baseline material.

### 5.3 Porosities

No direct measured bed, particle (i.e., sometimes referred to as pore), or total porosities have been consistently reported for the various column studies considered. Table 5-1 contains some of the values found within the literature. Values of 50% bed porosity and 24% particle porosity have been used in many of the existing column analyses to date reported by Hritzko et al. (1998) and many other sets of reported analyses throughout the literature. Within the Hritzko et al. (1998) report they reference their values to personal communications with R. A. Anthony at Texas A&M University. These two porosity values were assumed to be our nominal values used in the majority of VERSE-LC column simulations reported within this report. As stated above, given the recent access to slurry data listed in Table 5-2, a consistency check of the porosity values chosen can be made.

Based on Eq. (5-2) the total porosity of a column is known once the particle and bed densities are specified. Using the values presented in the above subsections and listed in Tables 5-1 and 5-2, the total porosity becomes:

$$\varepsilon_T \equiv 1 - \frac{\rho_b}{\rho_s} , \quad (5-5)$$

where several values are given in Table 5-3. In Table 5-3 four cases are considered. Based on the available data, the first case represents a lower bound, the second case a best estimate, and the third case an upper bound. The fourth case corresponds to the nominal value used in the column simulations reported with Chapters 9 and 10. As Table 5-3 indicates our nominal value for total porosity is greater than the expected range based on available data.

A range of possible void distributions exists between the bed and particle porosities constrained by Eq. (5-1) and any specified total porosity computed by Eq. (5-5). In Table 5-4 Eq. (5-1) is used to compute particle porosity for the four different resulting total porosity values tabulated in Table 5-3. The results provided in Table 5-4 are also plotted in Figure 5-1. In Figure 5-1 the solid curve represent our best estimate, while the solid circle represent our nominal porosity values used in the majority of VERSE-LC simulations.

Also shown in Figure 5-1 is the average measured porosity for dense packing of mono-sized hard spheres (i.e., widely accepted value of 0.363) as reported by German (1989, page 106). Two thirds of the reported values lie between 0.356 and 0.364. Greater packing fractions (or smaller bed porosities) can be achieved when multi-sized spheres are employed. Given the non-uniform sizes of the CST particles, no specific lower limit can be uniquely specified. However, the nominal bed porosity value of 0.50 versus the mono-sized value of 0.363 would appear to be somewhat high.

As stated above, the nominal bed porosity value of 0.50 and the nominal value for particle porosity of 0.24 were taken from the available literature. Based on Eq. (5-1) this corresponds to a nominal value for the total porosity of 62%. However, our best estimate value for total porosity, based on measured densities, is 38%. Notice that the nominal value of 38% and the best estimate value of 62% suggest that an error was made in the earlier literature work where in Eq. (5-2) the one minus total porosity term was assumed to be just total porosity. Assuming this incorrect form for Eq. (5-2) would give the 62% value based on the measured densities.

Table 5-1. Key CST exchange properties taken from literature for various ion exchangers.

Exchanger Form	Batch Name	F Factor <sup>a</sup> (-)	Bulk Dry Density <sup>a</sup> (g <sub>CST</sub> /ml <sub>bed</sub> )	Avg. Particle Diameter (μm)	Bed Porosity (-)	Particle Porosity (-)
SuperLig <sup>®</sup> 644	10-SM-171	0.9751	0.2238	664 <sup>b</sup>	0.450 <sup>b</sup>	0.614 <sup>b</sup>
Powder	IE-910	0.9680	0.7738	0.4 to 0.8 <sup>d</sup>	0.41 <sup>c</sup>	0.1 <sup>c</sup>
Engineered	IE-911 (38b)	0.8870	1.13	-	-	-
Engineered	IE-911 (08)	0.8990	0.8999	-	-	-
Engineered	Nominal <sup>d</sup>	0.80	1.0	200 to 600	0.3 to 0.5 <sup>c</sup>	0.22 <sup>c</sup>
Engineered	Baseline	-	1.0 (avg) <sup>c</sup>	344 (see Chapter 6)	0.50 (assumed) <sup>c</sup>	0.24 (assumed) <sup>c</sup>

<sup>a</sup> Data obtained from Brown et al. (1996, Table 3.1).

<sup>b</sup> Data obtained from Hamm et al. (2000) based on available data and supporting analyses.

<sup>c</sup> These are values used in many of the existing column analyses to date reported by Hritzko et al. (1998) and many other sets of reported analyses throughout the literature. Within the Hritzko et al. (1998) report they reference their values to personal communications with R. A. Anthony at Texas A&M University.

<sup>d</sup> The average properties of IONSIV<sup>®</sup> IE-911 exchanger as stated by UOP (1996).

<sup>e</sup> Other porosity and particle sizes are given by Thibaud-Erkey and Anthony, 1999.

Table 5-2. Estimated particle density based on measured densities taken from slurry mixtures of CST and water by Qureshi (1999).

Test ID	CST wt%	Measured slurry density (g/ml)	Estimated CST particle density (g <sub>CST</sub> /ml <sub>bed</sub> )
1	5	1.030	1.60
2	10	1.067	1.67
3	15	1.105	1.70

Table 5-3. "Best estimate" and upper/lower bounds of total porosity or particle density based on available measured densities or bed/particle porosities for IE-911 CST material.

Parameter being estimated	Bed density (g <sub>CST</sub> /ml <sub>bed</sub> )	Particle density (g <sub>CST</sub> /ml <sub>bed</sub> )	Total porosity (%)	Comments
Lower bound for total porosity	1.13	1.60	29.4	Lower estimated bound for total porosity based on upper measured bed density and lower measured particle density.
Best estimate for total porosity	1.0	1.613	38.0	Best estimate value for total porosity based on average measured bed and particle densities.
Upper bound for total porosity	0.8	1.70	52.9	Upper estimated bound for total porosity based on lower measured bed density and upper measured particle density.
Particle density consistent with current bed and particle porosities	1.0	2.632	62.0	Estimated value for particle density based on average measured bed density and a total porosity computed using a bed porosity of 50% and particle porosity of 24%.

Table 5-4. Particle porosity as a function of bed porosity at three different total porosity values for the IONSIV® IE-911 CST material.

Bed porosity (-)	Particle porosity given $\epsilon_T = 0.294$ (-)	Particle porosity <sup>b</sup> given $\epsilon_T = 0.380$ (-)	Particle porosity given $\epsilon_T = 0.529$ (-)	Particle porosity <sup>a</sup> given $\epsilon_T = 0.620$ (-)
0.00	0.294	0.380	0.529	0.620
0.05	0.257	0.347	0.505	0.600
0.15	0.169	0.271	0.446	0.553
0.20	0.117	0.225	0.412	0.525
0.25	0.058	0.173	0.373	0.493
0.30	na	0.114	0.328	0.457
0.35	na	0.046	0.276	0.415
0.40	na	na	0.216	0.367
0.45	na	na	0.144	0.309
0.50	na	na	0.059	0.240
0.55	na	na	na	0.156
0.60	na	na	na	0.050
0.65	na	na	na	na
Bed density (g/ml) =	1.13	1.0	0.8	1.0
Particle density (g/ml) =	1.6	1.613	1.7	2.632

<sup>a</sup> This total porosity value corresponds to the value used in the majority of column simulations performed.

<sup>b</sup> This total porosity value corresponds to the value most consistent with the available data.

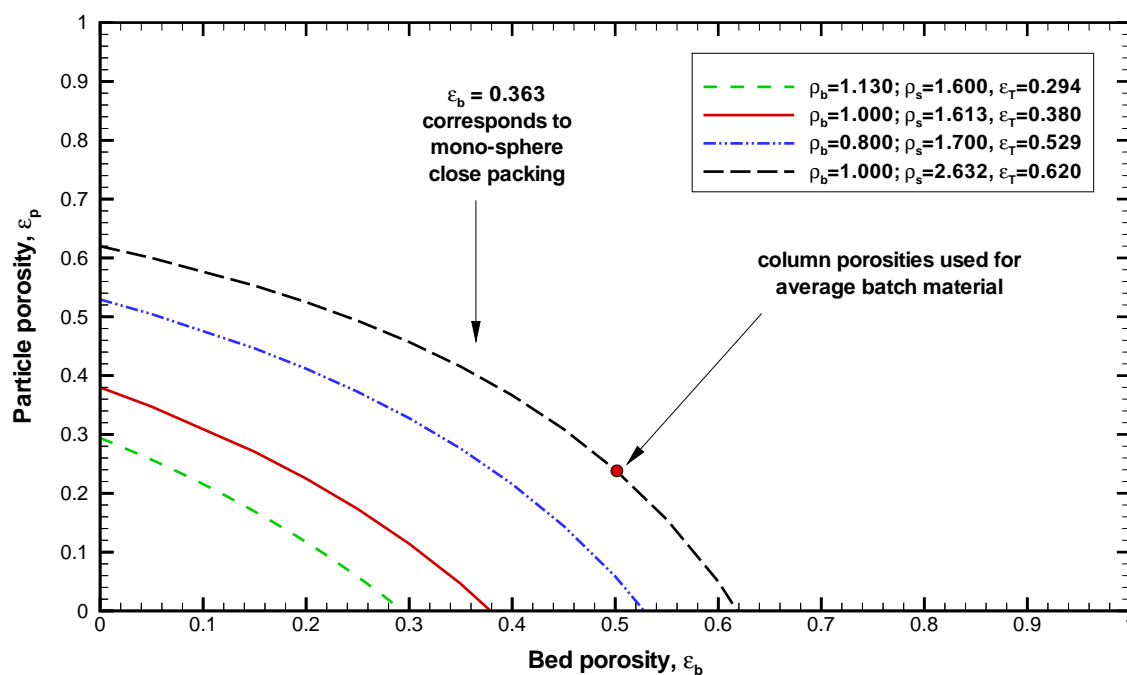


Figure 5-1. Functional behavior between bed porosity and particle porosity for the IONSIV® IE-911 CST material for various assumed total porosity values. The nominal settings used for the majority of column studies performed are shown by the solid circle.

(This Page Intentionally Left Blank)



## 6.0 Particle Size Distributions

Since CST exchanger material has been determined to be mass transfer limited, as a result of pore diffusion, the particle size of its engineered forms is important. The rate of kinetics and particle size are inversely related. The commercial development of IE-911 exchanger has focused on achieving optimum mass transfer efficiency through varying particle size (see UOP, 1996). Based on optimization studies, where a balance between ion exchange kinetics and design engineering requirements (e.g., column pressure drop) was achieved, 30x60 mesh (i.e., 250 to 595  $\mu\text{m}$  diameter) particles produce an engineering optimum (see Miller and Brown, 1997). Unlike organic ion exchange resins, the rigid inorganic structure of IE-910 and IE-911 materials resist significant swelling or shrinkage due to changes in temperature, pH, and ion exchange levels.

The particle size distribution, and therefore its average, vary between batches. For example, for cesium removal assessments the following average particle radiuses have been used in previous column performance analyses :

- 187.5  $\mu\text{m}$  by Hritzko et al. (1998) for the design of a carousel process for handling SRS waste; and
- 123.0  $\mu\text{m}$  by Thibaud-Erkey and Anthony for evaluating laboratory-scale experiments (1999).

Since the particle size distribution varies with batch ID, “as received” Baseline IE-911 material was analyzed using more recent laser technologies. Based on the laser testing a mean particle diameter of 172  $\mu\text{m}$  has been chosen for use in the column transport analysis efforts presented within this report. Uncertainties in this mean diameter exist resulting from potential batch variability and the issue of how representative is a particular tested sample to the entire batch population.

The CST exchanger material is approximately spherical, as assumed in the governing equations used to model the ion-exchange process. The column models also assume that the mass transfer and pore diffusion processes can be modeled using a single average size particle to represent the entire population of CST particles. Given the level of knowledge with regard to particle size and shape distributions, the above assumptions should be acceptable.

### 6.1 MicroTrac<sup>®</sup> Laser Technology Data

Based on MicroTrac<sup>®</sup> technology particle size distributions have been measured by Qureshi (1999) during a mixing and sampling study of sludge-frit-CSR slurries. In particluar, a particle size distribution is provided in Qureshi (1999) for “as received” CST in its engineered-form (batch number not recorded). This sample contained CST only. Percent by volume for a series of particle size ranges are provided by Qureshi (1999, see Figure 9). These volume fractions were first normalized where the average particle radius for each size bracket was set to the

bracket's mid-point value. The resulting normalized volume fractions are then used as weights for estimating the mean particle radius for this sample.

The results of these conversions are tabulated in Table 6-1. The volume fraction measurements for this sample are also plotted in Figure 6-1. An average particle radius of 163  $\mu\text{m}$  was computed for this sample.

## 6.2 Lasentec® Laser Technology Data

Chord length distributions have been measured on a single CST sample with a Lasentec® FBRM at the Savannah River Technology Center. The mean chord length measured for the "as-received", engineered-form of CST (IE-911, Baseline Lot #9090-76) by FBRM was 312  $\mu\text{m}$ . Based on the probabilities of measuring chords that are not representative of the full particle diameter (such as particle edges), a standard correction of +10% is often applied to the mean chord length value obtained for approximately spherical particles. (Note: The true-mean chord length is expected to be in the range 310–390  $\mu\text{m}$ .) After correction, the mean chord length is estimated to be 343  $\mu\text{m}$ , which corresponds to a mean particle radius of 172  $\mu\text{m}$ . Chord length data below 70  $\mu\text{m}$  was not utilized for the calculation of the mean value, since these fine particles are generally readily washed away from the CST bed prior to or during column operation.

For plotting purposes only, the chord length data were normalized where the average particle diameter for each size bracket was set to the bracket's mid-point value. The chord length distribution for this sample is also plotted in Figure 6-2 and tabulated in Table 6-2. The results of the chord length to particle diameter conversions are tabulated in Table 6-3. The calculated mean chord length is based on the raw data prior to normalization.

From these measurements an estimate of the average particle radius of ~172  $\mu\text{m}$  has been determined. All column assessment and column design analyses presented in this report use this particle radius value when columns packed with IE-911 material are being considered.

Table 6-1. Particle size distributions<sup>a</sup> of CST material in its engineered-form (batch number not recorded) based on MicroTrac<sup>®</sup> Laser Technology.

Particle diameter range [channels] (μm)	Particle diameter midpoint (μm)	Sample 1 volume % [normalized]
< 22.00 <sup>b</sup>	-	0.00
22.00 - 31.11	26.6	0.29
31.11 - 44.00	37.6	0.70
44.00 - 62.23	53.1	1.37
62.23 - 88.00	75.1	2.31
88.00 - 124.50	106.3	4.15
124.50 - 176.00	150.3	5.19
176.00 - 248.90	212.5	13.21
248.90 - 352.00	300.5	30.63
352.00 - 497.80	424.9	35.87
497.80 - 704.00	600.9	6.28
Mean Radius (μm) =		162.6

<sup>a</sup> Laser analysis performed on "as received" CST material.

<sup>b</sup> No particles detected where operating channels as low as ~1 μm were employed.

Table 6-2. Chord size distributions<sup>a</sup> of CST material in its engineered-form (Baseline Lot #9090-76) based on Lasentec<sup>®</sup> Laser Technology.

Chord length lower channel bound (μm)	Chord length upper channel bound (μm)	Chord length channel midpoint (μm)	Sample 1 chord % [normalized]
1	1.08	1.0400	0.001
1.08	1.166	1.1230	0.001
1.166	1.259	1.2125	0.001
1.259	1.359	1.3090	0.002
1.359	1.468	1.4135	0.003
1.468	1.585	1.5265	0.003
1.585	1.711	1.6480	0.003
1.711	1.848	1.7795	0.004
1.848	1.995	1.9215	0.005
1.995	2.154	2.0745	0.006
2.154	2.326	2.2400	0.007
2.326	2.512	2.4190	0.008
2.512	2.712	2.6120	0.017
2.712	2.929	2.8205	0.013
2.929	3.162	3.0455	0.023
3.162	3.415	3.2885	0.029
3.415	3.687	3.5510	0.033
3.687	3.981	3.8340	0.033
3.981	4.299	4.1400	0.043
4.299	4.642	4.4705	0.046
4.642	5.012	4.8270	0.055
5.012	5.412	5.2120	0.066
5.412	5.844	5.6280	0.068
5.844	6.31	6.0770	0.065
6.31	6.813	6.5615	0.07

Chord length lower channel bound ( $\mu\text{m}$ )	Chord length upper channel bound ( $\mu\text{m}$ )	Chord length channel midpoint ( $\mu\text{m}$ )	Sample 1 chord % [normalized]
6.813	7.357	7.0850	0.077
7.357	7.944	7.6505	0.088
7.944	8.578	8.2610	0.097
8.578	9.262	8.9200	0.123
9.262	10.001	9.6315	0.13
10.001	10.799	10.4000	0.143
10.799	11.66	11.2295	0.136
11.66	12.59	12.1250	0.173
12.59	13.595	13.0925	0.179
13.595	14.679	14.1370	0.195
14.679	15.85	15.2645	0.191
15.85	17.115	16.4825	0.221
17.115	18.48	17.7975	0.228
18.48	19.954	19.2170	0.235
19.954	21.546	20.7500	0.245
21.546	23.265	22.4055	0.268
23.265	25.121	24.1930	0.273
25.121	27.125	26.1230	0.314
27.125	29.289	28.2070	0.365
29.289	31.626	30.4575	0.33
31.626	34.149	32.8875	0.388
34.149	36.873	35.5110	0.376
36.873	39.815	38.3440	0.355
39.815	42.991	41.4030	0.347
42.991	46.421	44.7060	0.338
46.421	50.125	48.2730	0.317
50.125	54.123	52.1240	0.327
54.123	58.441	56.2820	0.36
58.441	63.104	60.7725	0.356
63.104	68.138	65.6210	0.37
68.138	73.574	70.8560	0.414
73.574	79.443	76.5085	0.457
79.443	85.781	82.6120	0.491
85.781	92.624	89.2025	0.569
92.624	100.014	96.3190	0.635
100.014	107.993	104.0035	0.677
107.993	116.608	112.3005	0.863
116.608	125.911	121.2595	0.948
125.911	135.956	130.9335	1.188
135.956	146.802	141.3790	1.317
146.802	158.513	152.6575	1.692
158.513	171.159	164.8360	1.919
171.159	184.814	177.9865	2.314
184.814	199.558	192.1860	2.934
199.558	215.478	207.5180	3.313
215.478	232.668	224.0730	4.057
232.668	251.23	241.9490	4.989
251.23	271.273	261.2515	5.996
271.273	292.914	282.0935	6.972
292.914	316.282	304.5980	7.876
316.282	341.514	328.8980	8.268
341.514	368.759	355.1365	7.978
368.759	398.178	383.4685	7.039
398.178	429.944	414.0610	5.847
429.944	464.244	447.0940	4.454
464.244	501.28	482.7620	3.219
501.28	541.271	521.2755	2.111

Chord length lower channel bound ( $\mu\text{m}$ )	Chord length upper channel bound ( $\mu\text{m}$ )	Chord length channel midpoint ( $\mu\text{m}$ )	Sample 1 chord % [normalized]
541.271	584.452	562.8615	1.3
584.452	631.079	607.7655	0.774
631.079	681.425	656.2520	0.487
681.425	735.787	708.6060	0.294
735.787	794.486	765.1365	0.205
794.486	857.869	826.1775	0.127
857.869	926.307	892.0880	0.063
926.307	1000.206	963.2565	0.039
1000.206	1080	1040.1030	0.023
<b>Mean Radius (<math>\mu\text{m}</math>)<sup>b</sup> =</b>		156.0	

<sup>a</sup> Laser analysis performed on "as received" CST material.

<sup>b</sup> No chord lengths below  $\sim 73.5 \mu\text{m}$  were employed in computing mean radius value.

Table 6-3. Estimated average particle radius of CST material in its engineered-form (Baseline Lot #9090-76) based on Lasentec<sup>®</sup> Laser Technology.

	Statistic 1	Statistic 2	Statistic 3
Parameter	Chord Mean (No Wt)	Chord Mean (Sqr Wt)	Chord Mode (No Wt)
Micron range (lower)	73.574	73.574	73.574
Micron range (upper)	1000.206	1000.206	1000.206
Chord Statistic (micron)	311.576	402.171	328.656
Diameter to chord factor (Typical value)	1.1	1.1	1.1
Diameter Statistic (micron)	342.7	442.4	361.5
Avg Radius Statistic (micron)	$\sim 172^a$	$\sim 221$	$\sim 181$

<sup>a</sup> Value used for all column assessment and design analysis for CST IE-911 material.

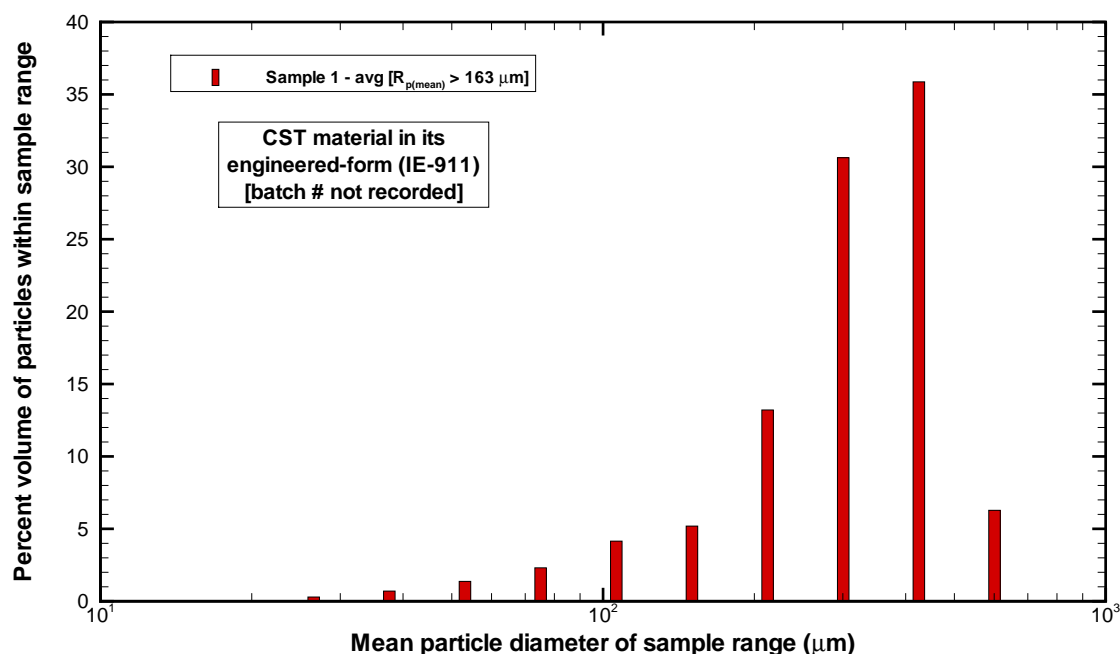


Figure 6-1. Volume percent of particles as a function of particle size for one sample of the CST material in its IE-911 engineered-form (batch # not recorded) based on MicroTrac<sup>®</sup> laser technology (data from Qureshi, 1999).

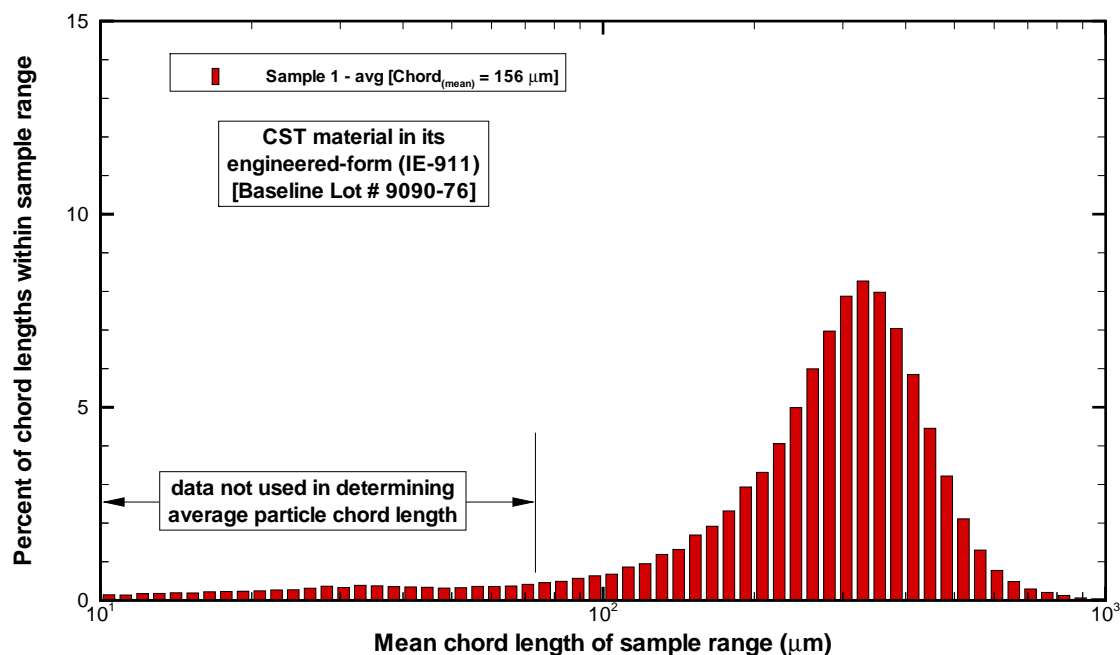


Figure 6-2. Chord length percent of particles as a function of chord size for one sample of the CST material in its IE-911 engineered-form (Baseline Lot # 9090-76) based on Lasentec<sup>®</sup> laser technology.

## 7.0 Pore Diffusion

As mentioned earlier we assume that the local rate of chemical adsorption (i.e., exchange of ions at a surface site) is very fast when compared to the rates of diffusion within the pore fluid and mass transfer across the liquid film at the outer boundary of the solid particles. In this section we discuss the “effective” binary molecular (Brownian motion) diffusion and pore diffusion coefficients for cesium used in the column models. In general the molecular diffusion coefficient depends upon the ionic composition of the surrounding fluid and its temperature, while the pore diffusion coefficient depends upon the internal structure of the porous solid. Here, our approach is to compute molecular diffusion coefficients based on key ionic species and then to compute pore diffusion coefficients assuming that a fixed ratio of molecular-to-pore diffusion exists. This molecular-to-pore diffusion ratio is typically referred to as a particle tortuosity factor, and for our purposes the value chosen is considered to be a true constant (i.e., in practice this is a geometric factor that probably varies depending upon which engineered-form is being considered). We also assumed that the rates of mass transfer within the CST particles are direction independent (i.e., incoming or outgoing).

In summary, we see inconsistencies among the available batch contact test data and deficiencies with using the homogeneous particle concept (and perhaps without addressing surface diffusion) currently within VERSE-LC. As such the particle tortuosity factor chosen (i.e., 5.0) for our design efforts is not based on these batch kinetics tests, but rather is based on the assessment of available column tests as discussed in Chapter 9. Future efforts to determine the important diffusional aspects of CST in its most common engineered-forms are recommended.

After writing this chapter the work of Anthony et al. (2001) was provided to the authors. Anthony et al. (2001) attempt to estimate an average value of the pore diffusivity coefficient for cesium based on their simple simulant (i.e. contains ~5.7 M sodium). The average value given is  $1.9 \times 10^{-4}$  cm<sup>2</sup>/min. This value is approximately a factor of two greater than the values estimated for the Phase 1 LAW feeds, but is within the uncertainty of the method and compositional differences of the solutions. It is interesting to note that their basic approach was to estimate a tortuosity factor of 4 (versus our value of 5) and to use viscosity corrections similar to our method. Both approaches are very similar in nature.

Future CST efforts should focus on determining a better particle diffusion model where pore heterogeneity (i.e., pore size distribution) and surface migration are accounted for along with pore diffusion.

### 7.1 Waste Solution Density and Viscosity

Waste solution density and viscosity varies depending primarily on temperature, sodium content, and composition. As discussed in Appendix A, a modified HTWOS density model is presented that estimates waste solution density typically within a few percent. This correlation is verified by comparison to measured values. For fluid dynamic viscosity few measurements exist and for the Phase 1 LAW batch feeds a constant value is employed based on a measurement of a

Envelope A simulant. The fluid properties for this Envelope A simulated waste were measured and reported by Steimke et al. (2000). The measured values of density and dynamic viscosity for the simulated waste and for pure water are listed in Table 7-1 at 20 °C. Dynamic viscosity values for the waste at 25 °C were estimated based on the measured pure water values also provided in Table 7-1.

Column transport assessments are also considered for various other waste solutions and their fluid properties are required. For the SRS solutions considered measured density and viscosity values are provided in Table 7-2.

## 7.2 Molecular Diffusion Coefficients

Binary diffusion (sometimes referred to as free stream or Brownian motion) coefficients of electrolytes originating from a single salt in solution under dilute conditions can be reasonably estimated by the Nernst-Haskell equation (Reid et al., 1977):

$$D_{\pm}^{\infty} = \left( \frac{RT}{F^2} \right) \left[ \frac{\frac{1}{z_+} + \frac{1}{z_-}}{\frac{1}{\lambda_+^0} + \frac{1}{\lambda_-^0}} \right], \quad (7-1)$$

where

- $D_{\pm}^{\infty}$  - binary diffusion coefficient at infinite dilution, cm<sup>2</sup>/s
- $\lambda_+^0, \lambda_-^0$  - limiting ionic conductance for cation and anion, mhos/equivalent
- $z_+, z_-$  - valences of cation and anion, respectively
- $F$  - Faraday constant, 96,500 C/g-equivalent
- $R$  - gas constant, 8.314 J/gmole-K
- $T$  - absolute temperature, K

Limiting ionic conductance for the various ions of interest are tabulated in Table 7-3 (Reid et al., 1977; Perry, 1973). Using Eq. (7-1) and the limiting ionic conductances provided in Table 7-3, the binary molecular diffusion coefficient for certain single salts within an aqueous phase can be computed. To account for fluid property differences between a waste solution and pure water, a correction factor is applied. Based on a hydrodynamical theory the following expression typically referred to as the Stokes-Einstein equation is obtained (Bird et al., 1960, page 514):

$$\frac{D_{AB}\mu_B}{\kappa T} = \frac{1}{6\pi R_A}, \quad (7-2)$$

where

- $D_{AB}$  - binary diffusion coefficient for A diffusing through solvent B
- $\mu_B$  - dynamic viscosity of solvent mixture
- $R_A$  - radius of diffusing particle
- $\kappa$  - Boltzmann's constant



Based on Eq. (7-2), the ratio of dynamic viscosities (i.e., pure water versus waste solution) is a correction factor that can be applied to the computed molecular diffusion coefficients from Eq. (7-1).

Binary pairs for the dominant cation-anion pairs (i.e., cesium paired with an individual anion) where the anions considered are based on the composition of the various wastes, and their computed binary molecular diffusion coefficients are listed in Table 7-4 at 25 C. The viscosity corrected values are also provided in Table 7-4. In Cussler (1984) the “effective” binary ionic diffusion coefficient of cesium in essentially pure water is  $1.236 \times 10^{-3} \text{ cm}^2/\text{min}$  at 25 °C, which is within 16% of the estimated value computed from Eq. (7-1). Some other values based on Cussler (1984) at 25 C are  $7.98 \times 10^{-4} \text{ cm}^2/\text{min}$  for  $\text{Na}^+$ ,  $1.176 \times 10^{-3} \text{ cm}^2/\text{min}$  for  $\text{K}^+$ , and  $5.586 \times 10^{-3} \text{ cm}^2/\text{min}$  for  $\text{H}^+$ .

The ionic radii of sodium and potassium are 0.95 and 1.33 angstroms with average hydration numbers of 4 and 3, respectively. All metal cations are hydrated in aqueous media, where, for example, sodium migrates perhaps in the form  $\text{Na}(\text{H}_2\text{O})_4^+$ . Reasonable values for the radii of the hydrated alkali metal ions sodium and potassium are  $\sim 2.76$  and  $\sim 2.32$  angstroms (Peters et al., 1974), respectively. Therefore, sodium is bigger and slower moving than potassium in aqueous solutions consistent with the predictions listed in Table 7-3. Anions are characteristically less heavily hydrated, suggesting that the cations set the overall diffusional pace.

Molecular diffusion coefficients are important in determining key dimensionless numbers (e.g., Schmidt Number, Sc) used in various constitutive law correlations pertinent to column transport modeling. They also provide an upper bound for pore diffusion coefficients.

### 7.3 Pore Diffusion Coefficients

Within the complicated pore structure of the CST particles we assume that net fluid motion is approximately zero resulting in equal-molar counter-diffusion. “Effective” binary diffusion coefficients based on Fick’s law are assumed where surface migration is considered negligible. Surface migration generally becomes increasingly more important as the migrating ions increase in size relative to the pore aperture (Froment and Bishoff, 1979). Knudsen diffusion occurs when the molecular dimensions of the ions approach their mean free path lengths.

#### 7.3.1 CST Conceptual Model

CST in its engineered-forms is made up of CST powder (i.e., very fine particles on the order of  $0.8 \text{ }\mu\text{m}$  in diameter) packed together using an inert binder (i.e., 20% to 30% by mass) to form much larger particles (e.g., the Baseline material has an average particle diameter of  $344 \text{ }\mu\text{m}$ ). The pore porosity of the CST powder has been estimated to be  $\sim 0.1$  by ? (), while for CST in its engineered-forms a typical value of  $\sim 0.24$  has been recommended by ? (). The fabrication process itself would suggest that the engineered particles are heterogeneous, potentially containing two pore size distributions. The diffusional rates within each pore distribution could be significantly different. For example, in the larger pores created by the binding material diffusion rates might be larger than the diffusional rates within the smaller pores contained

within the CST powder itself. Below, kinetics tests comparisons suggest that this may in fact be happening.

It has been observed by Ma et al. (1996) and Robinson et al. (1994) that for ion exchange materials with high capacities and affinities for certain ions (who generally have non-linear isotherms), parallel pore and surface diffusion is occurring. Based on equilibrium ion-exchange, Ma et. al. (1996) have derived an expression for an apparent pore diffusion coefficient that handles both pore and surface diffusion given as:

$$D_{p,app} = D_p + \left[ \frac{1 - \varepsilon_p}{\varepsilon_p} \right] D_s \left\{ \frac{\partial q}{\partial c_p} \right\}, \quad (7-3)$$

where the equilibrium isotherm is  $q=f(c_p)$ .

For linear isotherms Eq. (7-3) shows that a constant apparent pore diffusion coefficient can be used to model the parallel mechanisms. Unfortunately, when the isotherms are non-linear this apparent diffusion coefficient becomes concentration dependent. For the favorable isotherms exhibited by CST material and at low cesium concentrations the isotherm is nearly linear where the apparent diffusion coefficient is nearly constant. In this concentration range a pore diffusion model using a constant apparent diffusion coefficient value can adequately model parallel diffusion. However, at higher cesium concentrations the apparent pore diffusion coefficient decreases with increasing concentration. Surface diffusion can play a significant part when high affinity for an ion exists and the intra-particle diffusion cannot be adequately described by a constant apparent diffusion coefficient.

The VERSE-LC code is conceptually based on homogeneous particles where only a single averaged sized homogenous particle is modeled. Heterogeneity within the engineered CST particles can not be directly addressed. The VERSE-LC does have a surface migration option, but on several attempts to use this more recent option the results appeared to be in error. Therefore, for CST column modeling we have chosen to attempt to fit an average apparent diffusion coefficient to the available batch kinetics data. Below the results of this fitting effort are discussed.

### 7.3.2 The Tortuosity Factor

Specific information on the actual pore sizes was not available at the time of this report. Pore sizes within the CST powder are believed to be much smaller than pores within the binding matrix. UOP vendor information suggests that the pore sizes are large relative to the size of migrating ions of interest and that pore diffusion coefficients should not be significantly lower than their molecular values. However, some level of reduction is expected resulting from bends along the pore paths that are generally accounted for by a particle tortuosity factor (Smith, 1981; Froment and Bishoff, 1979) defined as:

$$D_{pi} \cong \frac{1}{\tau_p} D_{oi}, \quad (7-3)$$

Typical values for catalyst particle tortuosity are between 2 and 8. For large pore diameters the tortuosity values range as low as from near 1 to 3. For small ions Mackie and Meares (1955) suggest that the intra-particle pore diffusion coefficient can be estimated from

$$D_{pi} \cong \left[ \frac{\epsilon_p}{(2 - \epsilon_p)^2} \right] D_{oi} \quad (7-4)$$

Based on the available particle porosity values for CST powder and engineered forms, Eq. (7-4) yields particle tortuosity factors of ~8.1 and ~2.4, respectively. These particle tortuosity factors suggest pore diffusion coefficients of ~12% (for powder-form) and ~42% (for engineered-forms) of the molecular value. Given the heterogeneous nature of the actual engineered-forms the average percentage value probably lies within this 12% to 42% range.

For larger molecules pore diffusion coefficient experiments are generally required. Ideally, pore diffusion coefficients can be derived from batch kinetics distribution studies where the mass transfer resistance associated with film diffusion is minimized through significant mechanical mixing (note that, mixing techniques must be limited such that physical grinding of the particles does not become excessive). Various time-dependent cesium distribution studies have been performed using both CST powder and several of its engineered forms.

Batch kinetics tests, where inadequate mixing is achieved between the solid and solution, result in overall diffusion coefficients that are in effect smaller than the actual pore diffusion coefficient. Therefore, the use of the batch kinetics data can provide us with a lower bound estimate of pore diffusion, while molecular diffusion becomes our upper bound. Sufficient mechanical mixing during these tests is assumed, such that the kinetics data measured represent only the mass transfer resistance associated with pore diffusion (i.e., mass transfer resistance due to film diffusion is assumed to be small).

### 7.3.3 Comparison to Previous Studies

Pretest predictions for three SRS column experiments (Walker et al., 1998) were performed by Texas A&M University (see Appendix B of Walker et al., 1998). An available “effective” cesium pore diffusion coefficient value of  $2.7 \times 10^{-11} \text{ m}^2/\text{s}$  (i.e.,  $1.62 \times 10^{-5} \text{ cm}^2/\text{min}$ ) based on standard simulant was assumed to be acceptable for use with the actual SRS-averaged simulant. The “effective” diffusion coefficient is related to the pore diffusion coefficient by:

$$(D_{pi})_{\text{effective}} \equiv \epsilon_p D_{pi} \quad (7-5)$$

For application to CST material in its engineered forms a typical pore porosity of 24% is assumed. Based on a 24% pore porosity, the Texas A&M pore diffusion coefficient becomes  $6.75 \times 10^{-5} \text{ cm}^2/\text{min}$  as compared to the estimated value of  $\sim 10.0 \times 10^{-5} \text{ cm}^2/\text{min}$  based on the approach presented in this report (see SRS simulant values in Table 7-9). Texas A&M have also reported pore diffusion coefficient values of up to  $8.75 \times 10^{-5} \text{ cm}^2/\text{min}$  for standard simulants (with 0.5 M K added) based on column studies.

## 7.4 VERSE-LC Simulations for Batch Kinetics Tests

To estimate a cesium diffusion coefficient using batch kinetics test data, VERSE-LC models were set up consistent with the experimental conditions specified by their investigators:

- Initially CST material is placed into contact with liquid solution at a specified cesium concentration ;
- Initially the CST material is assumed to be fresh containing no cesium cations at its ion exchange sites;
- VERSE-LC geometry parameters is set consistent with the experimental setup, while other parameters are set consistent with the parameters discussed in the column modeling section of this report;
- The film mass transfer and axial dispersion coefficients are set to high values in order to appropriately model the experimental behavior using VERSE-LC (i.e., experimentally the liquid-sample remains well-mixed throughout the contact period resulting from the mechanical mixing);
- A binary transport simulation, along with a binary isotherm model, are chosen to model the cesium isotherm;
- Transient cesium concentrations are computed using VERSE-LC, while experimental values are computed from the various batch contact test data (i.e., contact tests with varying contact times were performed as discussed in Appendix E) and associated information contained within their report (and summarized in Appendix E); and
- Cesium equilibrium isotherms are used consistent with the late time (i.e., longest contact time batch kinetics test) measured  $K_d$  value where complete equilibrium is assumed to have been reached given this amount of contact time.

Sample VERSE-LC input and output decks are provided in Appendix E. The measured liquid cesium concentration for various contact tests (which approximate the transient values at various times during a single contact test) and various key parameters used in this analysis are also provided in Appendix E.

To model the transient behavior occurring during a single batch contact test, special VERSE-LC parameter settings are required. To simulate a well-mixed beaker of liquid-sample one finite element representing the bed is chosen where the axial dispersion coefficient is set to a very large value to ensure negligible concentration gradients exist throughout the bed volume (i.e., liquid region outside the particles). The flowrate through this “artificial” column is set to zero (i.e., actually a very small value is necessary since the superficial velocity is used to compute various dimensionless numbers). Initially, in VERSE-LC the pore spaces are assumed to be filled with liquid free of the various ions of interest (i.e., cesium). The ionic concentrations of the liquid in the bed space are increased to account for the dilution effect (i.e., ratio of total liquid volume to liquid bed volume) where the total liquid volume (i.e., pore plus liquid bed volumes) is set to the test’s initial liquid-sample volume. While the pore porosity is set to the

CST material value, the bed porosity is based on the quantities of materials used (i.e., the majority of volume is occupied by bed liquid).

#### **7.4.1 PNNL Kinetics Studies**

A limited amount of batch kinetics test data was found within the literature for the Cesium-CST system. Early on Brown et al. (1996) performed a series of batch kinetics tests as part of an assessment effort. They measured cesium time-dependent  $K_d$  values for a powder-form and for two early on engineered-forms (batches 08 and 38b). At 25 C and for initial concentrations of  $1.0 \times 10^{-4}$  M [Cs] and 5 M [Na], Brown et al. (1996) performed their tests using a 70% AW-101 DSSF composite liquid simulant. Their experimental contact times range from 1 minute up to 120 hours. The measured  $K_d$  values are shown in Figure 7-1 where impact of a dilution factor effect can clearly be seen. Their database and details are provided in Appendix E.

The adequacy in the level of mixing (i.e., agitation) used during these sets of tests is unknown. As discussed in Hamm et al. (2000a, see Chapter 7) and by Brown et al. (1996), for short contact times film diffusion resistance to mass transfer can begin to have an increased impact on the overall mass transfer resistance. However, since CST material is considered to be significantly pore diffusion limited, it will be assumed here that the mass transfer resistance inferred from these batch kinetics tests is primarily due to pore diffusion alone. The powder-form CST material has an average particle diameter of  $\sim 0.8$   $\mu\text{m}$ , while for the engineered-forms the particle diameters nominally range from 250  $\mu\text{m}$  to 600  $\mu\text{m}$ . Given the drastically larger particle sizes of engineered-forms when compared to its powder-forms, a significant reduction in ion pore diffusion coefficients is expected. The results shown in Figure 7-1 confirm this expectation.

To estimate the pore diffusion coefficient several VERSE-LC simulations were run where the pore diffusion coefficient was varied. The details associated with the VERSE-LC simulations are provided in Appendix E. For the CST power data significantly reduced pore diffusion coefficients (lower than 0.001% of its molecular value) would be required to fit the cesium uptake data, as shown in Figure 7-2. Similar sets of VERSE-LC runs were made for the two engineered forms of CST. The results of these simulations and comparison to the data are shown in Figures 7-3 and 7-4. The solid curves in Figures 7-3 and 7-4 represent VERSE-LC results when a pore diffusion coefficient of 5% of its molecular value is chosen. The data appears to exhibit two different decay time constants, one for early contact times (i.e.,  $< 2$  hours) and one for later contact times (i.e.,  $> 2$  hours). This sort of behavior may be the result of the heterogeneity present within the engineered-form particles or a shift in the effectiveness of the mechanical mixing being achieved.

#### **7.4.2 SRS Kinetics Studies**

More recently, Fondeur et al. (2000) measured timed  $K_d$  values for a more recent engineered-form (Baseline Lot 9090-76; average particle diameter of  $\sim 344$   $\mu\text{m}$ ). At 25 C and for initial concentrations of  $1.4 \times 10^{-4}$  M [Cs] and 5.6 M [Na], Fondeur et al. (2000) performed their tests using a SRS average liquid simulant. The results of their tests are shown in Figure 7-5, while the

details of their database are provided in Appendix E. Their experimental contact times range from 24 to 192 hours. Unfortunately, no short contact time data were recorded.

A rough estimate (i.e., using VERSE-LC simulation assistance) of the earlier contact time behavior is also shown in Figure 7-5 by the dashed line and open symbols. This early contact time estimate is based on the Brown et al. (1996) data for their engineered-forms. An overlay of the two data sets is provided in Figure 7-6 where it can be seen that the kinetic behavior (i.e., time rate of increase in relative  $K_d$  value) of the three engineered-forms appears quite similar. The Baseline engineered-form CST data was extended to early times using the approximate average behavior of the 08 and 38b engineered-form CST data.

As shown in Figure 7-6 a composite of these three data sets was chosen for establishing an “average” cesium pore diffusion coefficient value. Based on the experimental setup by Fondeur et al. (2000), VERSE-LC simulations of the batch kinetics of the Baseline CST material were performed. The VERSE-LC simulation details are provided in Appendix E. Several VERSE-LC simulations were run where the pore diffusion coefficient was varied. The results of these simulations are shown in Figure 7-7. As can be seen in Figure 7-7, a pore diffusion coefficient value of ~5% of its molecular value appears to “fit” the experimental data (i.e., solid circles). The open circles in Figure 7-7 represent the estimated data points as shown in Figures 7-5 and 7-6. The sensitivity of the cesium uptake curves with respect to pore diffusion is also shown in Figure 7-7. The degree of mechanical mixing that might have been achieved is unknown; therefore, the 5% value probably represents an lower bound value due to possible film resistances present within the test as well. The approach to equilibrium can also be plotted as shown in Figure 7-8.

### 7.4.3 Particle Size Impact on Kinetics

The effect of particle size on the rate of cesium uptake has been measured by Anthony et al. (1996) based on TAM5 generated forms (i.e., average particle diameters of ~112  $\mu\text{m}$  and ~334  $\mu\text{m}$ ). Miller and Brown (1997) also performed cesium uptake measured on TAM5 powder (i.e., average particle diameter of ~0.8  $\mu\text{m}$ ). At 25 C and for initial concentrations of  $1.0 \times 10^{-4}$  M [Cs] and 5.0 M [Na], these tests were performed using a DSSF5 liquid simulant. The results of their tests are shown in Figure 7-9, while the details of their database are provided in Appendix E.

VERSE-LC simulations were performed and are plotted in Figure 7-9 for comparison. A particle tortuosity factor of 10.0 was used (i.e., pore diffusion coefficient of 10% of its molecular value). Two items can be seen from the data itself. First, as expected particle size has a large impact on the kinetics but this effect appears to greatly diminish with smaller particles. No simple explanation for the diminishing impact can be given at this time, other than to suspect the data. Second, the shape of the cesium uptake (decay) curves appear to have two difference time constants. One explanation for the differing time constants is the possibility that more rapid diffusion occurs through the larger binding material pores early on, followed by much slower diffusion rates through the smaller powder pores.

#### 7.4.4 ORNL Kinetics Studies

The series of tests measuring the rate of cesium uptake have been taken by Davidson et al. (1998) based on CST powder. Tests at 25 C and an initial concentration of  $1.418 \times 10^{-6}$  M [Cs] were performed for four different phase ratios (i.e., 100, 200, 400, and 1000) using a W-27 supernate solution. The results of their tests are shown in Figure 7-10, while the details of their database are provided in Appendix E. Also shown in Figure 7-10 are VERSE-LC runs based on a phase ratio of 100.

Table 7-1. Fluid density and dynamic viscosity for water and simulated Envelope A 5 M sodium waste solution.

Fluid property	Pure water	Simulated 5 M Na <sup>+</sup> waste solution <sup>a</sup>
<b>For 20 °C</b>		
Density, g/ml	0.99823	1.225 <sup>a</sup>
Dynamic viscosity, cp	1.002	2.94 <sup>a</sup>
<b>For 25 °C</b>		
Density, g/ml	0.9970479	1.22355 <sup>b</sup>
Dynamic viscosity, cp	0.8904	2.61255 <sup>b</sup>

<sup>a</sup> A 5 M sodium simulated waste consistent with Envelope A where properties were measured at 20 °C (Steimke et al., 2000).

<sup>b</sup> Measured properties were adjusted to new temperature based on pure water value ratios.

Table 7-2. Measured fluid density and dynamic viscosity for various SRS waste solutions.

Specific solution	Fluid temperature (C)	Fluid Density (g/ml)	Dynamic viscosity (cp)
SRS Avg	25	1.253	2.78
SRS High OH <sup>-</sup>	25	1.244	3.1
SRS Tank 44	31	1.2015	2.6
UOP	25	1.276	-

Table 7-3. Limiting ionic conductances in water at 25 °C (Reid et al., 1977; Perry, 1973, Glasstone and Lewis, 1960).

Ion	Ionic valance	Limiting ionic conductance MHOS/equivalent
<b>Cations</b>		
Cs <sup>+</sup>	1	77.3
K <sup>+</sup>	1	73.5
Na <sup>+</sup>	1	50.1
H <sup>+</sup>	1	349.8
<b>Anions</b>		
OH <sup>-</sup>	-1	198.6
Cl <sup>-</sup>	-1	76.35
NO <sub>3</sub> <sup>-</sup>	-1	71.46
NO <sub>2</sub> <sup>-</sup>	-1	72.0
I <sup>-</sup>	-1	76.8
F <sup>-</sup>	-1	55.4
CO <sub>3</sub> <sup>-2</sup>	-2	69.3
SO <sub>4</sub> <sup>-2</sup>	-2	80.02
PO <sub>4</sub> <sup>-2</sup>	-2	75.0 <sup>a</sup>
Al(OH) <sub>4</sub> <sup>-</sup>	-1	70.0 <sup>a</sup>

<sup>a</sup> Value estimated.



Table 7-4. Best estimate binary molecular<sup>a</sup> diffusion coefficients at 25 °C for a solution containing essentially only cesium cations and anion of one particular species.

Ion Pair	Molecular diffusion coef. in water (cm <sup>2</sup> /min)	Molecular diffusion coef. in simulated 5M Na waste <sup>b</sup> (cm <sup>2</sup> /min)
<b>For cesium</b>		
Cs <sup>+</sup> - OH <sup>-</sup>	1.778E-03	6.047E-04
Cs <sup>+</sup> - Cl <sup>-</sup>	1.227E-03	4.175E-04
Cs <sup>+</sup> - NO <sub>3</sub> <sup>-</sup>	1.187E-03	4.036E-04
Cs <sup>+</sup> - NO <sub>2</sub> <sup>-</sup>	1.191E-03	4.052E-04
Cs <sup>+</sup> - I <sup>-</sup>	1.231E-03	4.187E-04
Cs <sup>+</sup> - F <sup>-</sup>	1.031E-03	3.507E-04
Cs <sup>+</sup> - CO <sub>3</sub> <sup>-2</sup>	8.757E-04	2.979E-04
Cs <sup>+</sup> - SO <sub>4</sub> <sup>-2</sup>	9.423E-04	3.205E-04
Cs <sup>+</sup> - PO <sub>4</sub> <sup>-2</sup>	9.123E-04	3.103E-04
Cs <sup>+</sup> - Al(OH) <sub>4</sub> <sup>-</sup>	1.174E-03	3.992E-04

<sup>a</sup> The molecular diffusion coefficient is sometimes referred to as the “free” or “Brownian” motion diffusion coefficient.

<sup>b</sup> Fluid viscosity correction ratio applied based on a measured simulated waste viscosity of 2.94 cp at 20 °C (Steimke et al., 2000).

Table 7-5. Phase 1 LAW feed anion concentrations and relative mole fractions<sup>a</sup> for Envelope A used in determining “effective” binary molecular diffusion coefficients with cesium.

Anion considered	Charge	ZAM ID	LAW-1	LAW-5	LAW-6	LAW-8	LAW-9	LAW-10	LAW-11	LAW-12	LAW-13	LAW-14	LAW-15
OH (free) [M]	-1	13	1.553E+00	8.643E-01	9.543E-01	1.343E+00	5.733E-01	8.697E-01	9.307E-01	1.543E+00	1.542E+00	1.748E+00	2.141E+00
Cl [M]	-1	2	4.982E-02	1.034E-01	1.031E-01	1.246E-01	1.272E-01	1.400E-01	1.365E-01	8.623E-02	8.517E-02	8.426E-02	6.978E-02
NO <sub>3</sub> [M]	-1	9	1.868E+00	1.377E+00	1.359E+00	1.278E+00	1.408E+00	1.431E+00	1.200E+00	1.222E+00	1.222E+00	1.325E+00	1.299E+00
NO <sub>2</sub> [M]	-1	27	8.096E-01	1.188E+00	1.192E+00	1.197E+00	1.208E+00	1.312E+00	1.387E+00	1.127E+00	1.127E+00	1.063E+00	1.015E+00
I <sub>29</sub> -I [M]	-1	4	3.145E-06	8.115E-06	8.475E-06	2.189E-05	1.028E-05	1.308E-05	7.391E-06	7.415E-06	6.992E-06	9.391E-06	9.142E-06
F [M]	-1	1	1.335E-01	1.471E-02	1.336E-02	1.654E-02	4.472E-02	2.496E-02	3.109E-02	1.847E-02	1.856E-02	4.061E-02	3.937E-02
CO <sub>3</sub> [M]	-2	19	4.804E-01	3.927E-01	3.588E-01	2.014E-01	5.472E-01	2.785E-01	3.609E-01	1.614E-01	1.604E-01	2.530E-01	1.537E-01
SO <sub>4</sub> [M]	-2	15	3.737E-02	4.843E-02	4.492E-02	2.170E-02	3.667E-02	3.727E-02	2.391E-02	1.138E-02	1.108E-02	1.721E-02	1.062E-02
PO <sub>4</sub> [M]	-2	20	9.786E-03	2.065E-02	1.980E-02	1.084E-02	2.669E-02	4.346E-02	3.652E-02	9.386E-03	9.343E-03	1.099E-02	5.672E-03
Al(OH) <sub>4</sub> [M]	-1	28	2.338E-01	5.707E-01	5.761E-01	6.375E-01	4.533E-01	5.150E-01	4.913E-01	7.536E-01	7.600E-01	4.891E-01	5.013E-01
Conc. sum [M]	-	-	5.176E+00	4.580E+00	4.621E+00	4.831E+00	4.426E+00	4.651E+00	4.598E+00	4.933E+00	4.936E+00	5.031E+00	5.235E+00
OH (free) [fraction]	-1	13	3.00E-01	1.89E-01	2.07E-01	2.78E-01	1.30E-01	1.87E-01	2.02E-01	3.13E-01	3.12E-01	3.47E-01	4.09E-01
Cl [fraction]	-1	2	9.63E-03	2.26E-02	2.23E-02	2.58E-02	2.87E-02	3.01E-02	2.97E-02	1.75E-02	1.73E-02	1.67E-02	1.33E-02
NO <sub>3</sub> [fraction]	-1	9	3.61E-01	3.01E-01	2.94E-01	2.65E-01	3.18E-01	3.08E-01	2.61E-01	2.48E-01	2.48E-01	2.63E-01	2.48E-01
NO <sub>2</sub> [fraction]	-1	27	1.56E-01	2.59E-01	2.58E-01	2.48E-01	2.73E-01	2.82E-01	3.02E-01	2.28E-01	2.28E-01	2.11E-01	1.94E-01
I <sub>29</sub> -I [fraction]	-1	4	6.08E-07	1.77E-06	1.83E-06	4.53E-06	2.32E-06	2.81E-06	1.61E-06	1.50E-06	1.42E-06	1.87E-06	1.75E-06
F [fraction]	-1	1	2.58E-02	3.21E-03	2.89E-03	3.42E-03	1.01E-02	5.37E-03	6.76E-03	3.74E-03	3.76E-03	8.07E-03	7.52E-03
CO <sub>3</sub> [fraction]	-2	19	9.28E-02	8.57E-02	7.76E-02	4.17E-02	1.24E-01	5.99E-02	7.85E-02	3.27E-02	3.25E-02	5.03E-02	2.94E-02
SO <sub>4</sub> [fraction]	-2	15	7.22E-03	1.06E-02	9.72E-03	4.49E-03	8.28E-03	8.01E-03	5.20E-03	2.31E-03	2.24E-03	3.42E-03	2.03E-03
PO <sub>4</sub> [fraction]	-2	20	1.89E-03	4.51E-03	4.29E-03	2.24E-03	6.03E-03	9.34E-03	7.94E-03	1.90E-03	1.89E-03	2.18E-03	1.08E-03
Al(OH) <sub>4</sub> [fraction]	-1	28	4.52E-02	1.25E-01	1.25E-01	1.32E-01	1.02E-01	1.11E-01	1.07E-01	1.53E-01	1.54E-01	9.72E-02	9.58E-02

<sup>a</sup> The relative mole fractions refer to mole fractions for each anion where the their values are normalized to the sum of anions considered and listed in this table. The anions considered are based on the available limiting ionic conductances found within the literature as listed in Table 7-3.

Table 7-6. Phase 1 LAW feed anion concentrations and relative mole fractions<sup>a</sup> for Envelopes B and C used in determining “effective” binary molecular diffusion coefficients with cesium.

Anion considered	Charge	ZAM ID	LAW-1	LAW-5	LAW-6	LAW-8	LAW-9
OH (free) [M]	-1	13	1.599E-01	2.720E-01	1.033E+00	1.033E+00	7.943E-01
Cl [M]	-1	2	5.834E-03	4.725E-04	4.794E-02	4.794E-02	2.784E-02
NO <sub>3</sub> [M]	-1	9	1.277E+00	6.736E-01	1.737E+00	1.737E+00	1.967E+00
NO <sub>2</sub> [M]	-1	27	1.481E+00	1.182E+00	7.959E-01	7.959E-01	6.953E-01
I <sub>29</sub> -I [M]	-1	4	3.975E-02	3.503E-02	1.582E-05	1.582E-05	1.273E-05
F [M]	-1	1	1.029E-01	9.867E-02	4.345E-02	4.345E-02	9.387E-02
CO <sub>3</sub> [M]	-2	19	5.907E-01	1.035E+00	5.101E-01	5.101E-01	6.555E-01
SO <sub>4</sub> [M]	-2	15	1.967E-01	3.369E-01	7.274E-02	7.274E-02	4.693E-02
PO <sub>4</sub> [M]	-2	20	1.61E-02	2.54E-03	2.286E-02	2.286E-02	2.036E-02
Al(OH) <sub>4</sub> [M]	-1	28	4.364E-01	1.342E-01	2.610E-01	2.610E-01	1.391E-01
Conc. sum [M]	-	-	4.306E+00	3.770E+00	4.524E+00	4.524E+00	4.440E+00
OH (free) [fraction]	-1	13	3.71E-02	7.21E-02	2.28E-01	2.28E-01	1.79E-01
Cl [fraction]	-1	2	1.35E-03	1.25E-04	1.06E-02	1.06E-02	6.27E-03
NO <sub>3</sub> [fraction]	-1	9	2.96E-01	1.79E-01	3.84E-01	3.84E-01	4.43E-01
NO <sub>2</sub> [fraction]	-1	27	3.44E-01	3.13E-01	1.76E-01	1.76E-01	1.57E-01
I <sub>29</sub> -I [fraction]	-1	4	9.23E-03	9.29E-03	3.50E-06	3.50E-06	2.87E-06
F [fraction]	-1	1	2.39E-02	2.62E-02	9.61E-03	9.61E-03	2.11E-02
CO <sub>3</sub> [fraction]	-2	19	1.37E-01	2.75E-01	1.13E-01	1.13E-01	1.48E-01
SO <sub>4</sub> [fraction]	-2	15	4.57E-02	8.94E-02	1.61E-02	1.61E-02	1.06E-02
PO <sub>4</sub> [fraction]	-2	20	3.74E-03	6.73E-04	5.05E-03	5.05E-03	4.59E-03
Al(OH) <sub>4</sub> [fraction]	-1	28	1.01E-01	3.56E-02	5.77E-02	5.77E-02	3.13E-02

<sup>a</sup> The relative mole fractions refer to mole fractions for each anion where the their values are normalized to the sum of anions considered and listed in this table. The anions considered are based on the available limiting ionic conductances found within the literature as listed in Table 7-3.

Table 7-7. Simulant or sample anion concentrations and relative mole fractions<sup>a</sup> for various solutions<sup>b</sup> used in determining “effective” binary molecular diffusion coefficients with cesium.

Anion considered	Charge	ZAM ID	SRS Avg	SRS High OH <sup>-</sup>	SRS Tank 44	Brown AW-101	ORNL W27	Sandia DSSF5	Texas A&M Exp1	Hendrickson AW-101
			Walker et al. (?)	Walker et al. (?)	Walker et al. (?)	Brown et al. (1996)	Lee (1997)	Texas A&M slides (?)	Texas A&M report (?)	Hendrickson report (?)
OH (free) [M]	-1	13	1.910E+00	3.050E+00	4.300E+00	2.170E+00	7.080E-02	2.170E+00	6.000E-01	2.541E+00
Cl [M]	-1	2	2.500E-02	3.637E-02	9.000E-03	6.500E-02	9.000E-02	2.576E-01	-	8.830E-02
NO <sub>3</sub> [M]	-1	9	2.180E+00	1.100E+00	3.700E-01	1.490E+00	5.194E+00	1.490E+00	5.100E+00	1.530E+00
NO <sub>2</sub> [M]	-1	27	5.100E-01	7.400E-01	3.500E-01	9.400E-01	-	9.400E-01	-	1.130E+00
129-I [M]	-1	4	-	-	-	-	-	-	-	-
F [M]	-1	1	3.200E-02	1.000E-02	-	4.330E-02	-	4.330E-02	-	3.340E-02
-	-2	19	1.600E-01	1.700E-01	1.412E-01	-	-	-	-	1.100E-01
SO <sub>4</sub> [M]	-2	15	1.500E-01	3.000E-02	1.000E-03	1.260E-02	1.600E-02	1.260E-02	-	3.280E-03
PO <sub>4</sub> [M]	-2	20	1.000E-02	8.000E-03	4.000E-03	1.750E-02	-	1.750E-02	-	5.530E-03
Al(OH) <sub>4</sub> [M]	-1	28	3.100E-01	2.700E-01	1.260E-01	4.970E-01	3.140E-05	4.970E-01	-	5.740E-01
Conc. sum [M]	-	-	5.287E+00	5.414E+00	5.301E+00	5.235E+00	5.371E+00	5.428E+00	5.700E+00	6.016E+00
OH (free) [fraction]	-1	13	3.61E-01	5.63E-01	8.11E-01	4.14E-01	1.32E-02	4.00E-01	1.05E-01	4.22E-01
Cl [fraction]	-1	2	4.73E-03	6.72E-03	1.70E-03	1.24E-02	1.68E-02	4.75E-02	-	1.47E-02
NO <sub>3</sub> [fraction]	-1	9	4.12E-01	2.03E-01	6.98E-02	2.85E-01	9.67E-01	2.75E-01	8.95E-01	2.54E-01
NO <sub>2</sub> [fraction]	-1	27	9.65E-02	1.37E-01	6.60E-02	1.80E-01	-	1.73E-01	-	1.88E-01
129-I [fraction]	-1	4	-	-	-	-	-	-	-	-
F [fraction]	-1	1	6.05E-03	1.85E-03	-	8.27E-03	-	7.98E-03	-	5.55E-03
CO <sub>3</sub> [fraction]	-2	19	3.03E-02	3.14E-02	2.66E-02	-	-	-	-	1.83E-02
SO <sub>4</sub> [fraction]	-2	15	2.84E-02	5.54E-03	1.89E-04	2.41E-03	2.98E-03	2.32E-03	-	5.45E-04
PO <sub>4</sub> [fraction]	-2	20	1.89E-03	1.48E-03	7.55E-04	3.34E-03	-	3.22E-03	-	9.19E-04
Al(OH) <sub>4</sub> [fraction]	-1	28	5.86E-02	4.99E-02	2.38E-02	9.49E-02	5.85E-06	9.16E-02	-	9.54E-02

<sup>a</sup> The relative mole fractions refer to mole fractions for each anion where the their values are normalized to the sum of anions considered and listed in this table. The anions considered are based on the available limiting ionic conductances found within the literature as listed in Table 7-3.

<sup>b</sup> These are solutions used in various CST column tests which were considered in the column transport assessment efforts.

Table 7-8. Best estimate cesium effective molecular and pore diffusion coefficients at 25 °C for each Phase 1 LAW batch feed.

Envelope	Mole averaged Ion Pair <sup>a</sup> (Cs – anion)	Molecular Diffusion coef. in water (cm <sup>2</sup> /min)	Molecular diffusion coef. in simulated 5M Na waste <sup>b</sup> (cm <sup>2</sup> /min)	Pore diffusion coef. in simulated 5M Na waste <sup>c</sup> (cm <sup>2</sup> /min)
<b>A</b>	LAW-1	1.329E-03	4.522E-04	9.044E-05
	LAW-5	1.268E-03	4.312E-04	8.624E-05
	LAW-6	1.281E-03	4.357E-04	8.715E-05
	LAW-8	1.336E-03	4.545E-04	9.090E-05
	LAW-9	1.221E-03	4.152E-04	8.303E-05
	LAW-10	1.274E-03	4.334E-04	8.669E-05
	LAW-11	1.279E-03	4.349E-04	8.698E-05
	LAW-12	1.360E-03	4.624E-04	9.248E-05
	LAW-13	1.359E-03	4.624E-04	9.247E-05
	LAW-14	1.374E-03	4.674E-04	9.347E-05
	LAW-15	1.418E-03	4.822E-04	9.643E-05
<b>B</b>	LAW-2a	1.151E-03	3.914E-04	7.828E-05
	LAW-2b	1.119E-03	3.807E-04	7.614E-05
<b>C</b>	LAW-3	1.280E-03	4.354E-04	8.709E-05
	LAW-4	1.280E-03	4.354E-04	8.709E-05
	LAW-7	1.240E-03	4.217E-04	8.435E-05

<sup>a</sup> Relative anion mole fractions of each LAW candidate feed solution used based on compositions provided in Appendix Table A-5 and A-6 (and computed relative mole fractions listed in Tables 7-4 and 7-5).

<sup>b</sup> Fluid viscosity correction ratio applied based on a measured simulated waste viscosity of 2.94 cp at 20 °C (Steimke et al., 2000).

<sup>c</sup> The cesium pore diffusion value is based on 20% of its molecular diffusion value where the tortuosity of the engineered-form of CST is assumed to independent of liquid composition.

Table 7-9. Best Estimate cesium effective molecular and pore diffusion coefficients at 25 °C for various solutions used in column transport assessments.

Mole averaged Ion Pair <sup>a</sup> (Cs – anion)	Molecular Diffusion coef. in water (cm <sup>2</sup> /min)	Molecular diffusion coef. in simulated 5M Na waste (cm <sup>2</sup> /min)	Pore diffusion coef. in simulated 5M Na waste <sup>d</sup> (cm <sup>2</sup> /min)
SRS Avg	1.382E-03	4.972E-04 <sup>b</sup>	9.944E-05
SRS High OH <sup>-</sup>	1.508E-03	5.425E-04 <sup>b</sup>	1.085E-04
SRS Tank 44	1.658E-03	5.963E-04 <sup>b</sup>	1.193E-04
Brown AW-101	1.429E-03	4.861E-04 <sup>c</sup>	9.721E-05
ORNL W27	1.194E-03	4.062E-04 <sup>c</sup>	8.124E-05
Sandia DSSF5	1.422E-03	4.836E-04 <sup>c</sup>	9.672E-05
Texas A&M Exp1	2.212E-03	7.524E-04 <sup>c</sup>	1.505E-04
Hendrickson AW-101	1.430E-03	4.863E-04 <sup>c</sup>	9.726E-05

<sup>a</sup> Relative anion mole fractions of each solution used based on compositions and computed relative mole fractions provided in Table 7-7.

<sup>b</sup> Fluid viscosity correction ratio applied based on a measured simulated waste viscosity of 2.94 cp at 20 °C (Steimke et al., 2000).

<sup>c</sup> Fluid viscosity correction ratio applied based on a measured simulated waste viscosity of 2.78 cp at 20 °C (Walker et al., ?).

<sup>d</sup> The cesium pore diffusion value is based on 20% of its molecular diffusion value where the tortuosity of the engineered-form of CST is assumed to independent of liquid composition.

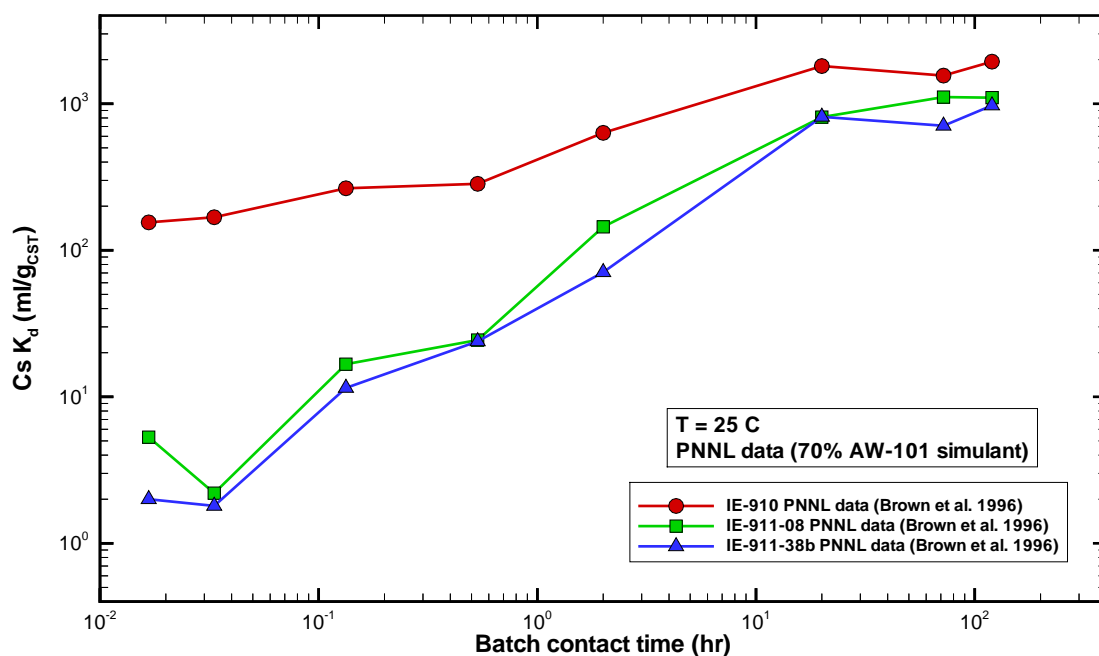


Figure 7-1. Cesium  $K_d$  measurements obtained from batch kinetics tests performed by Brown et al. (1996) at 25 C and in a 70% AW-101 DSSF simulant liquid at  $1 \times 10^{-4}$  M Cs and 5 M Na.

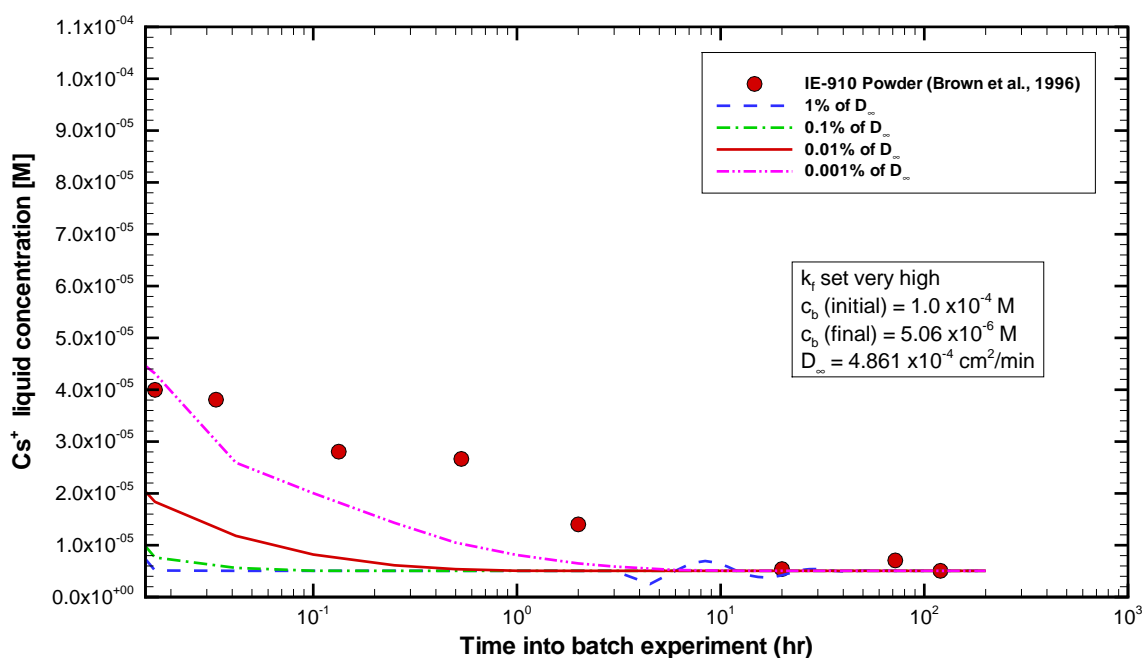


Figure 7-2. Estimation of the cesium pore diffusion coefficient based on batch kinetics tests performed by Brown et al. (1996) at 25 C for cesium uptake on IONSIV® IE-910 CST (powder-form).

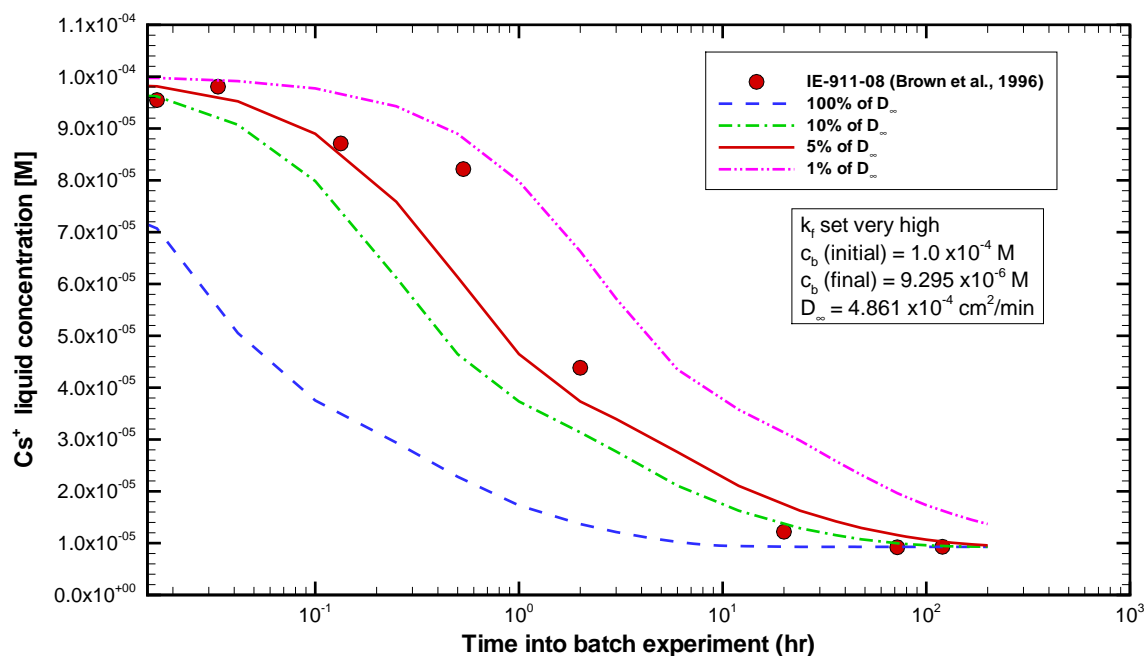


Figure 7-3. Estimation of the cesium pore diffusion coefficient based on batch kinetics tests performed by Brown et al. (1996) at 25 C for cesium uptake on IONSIV® IE-911 CST (engineered-form 08).

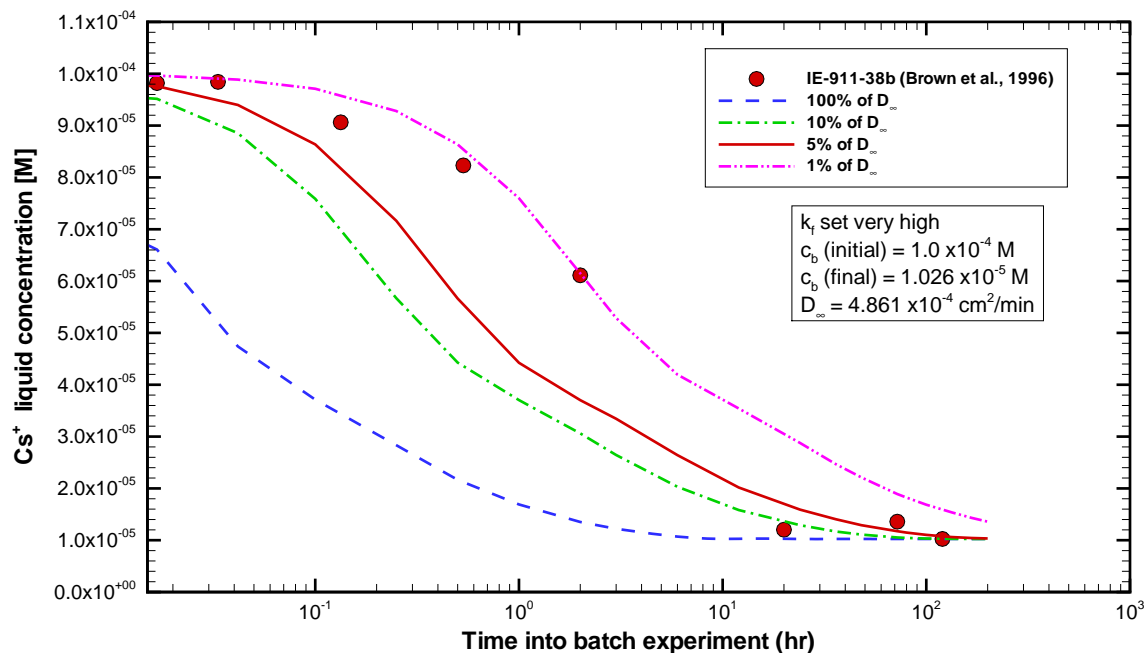


Figure 7-4. Estimation of the cesium pore diffusion coefficient based on batch kinetics tests performed by Brown et al. (1996) at 25 C for cesium uptake on IONSIV® IE-911 CST (engineered-form 38b).



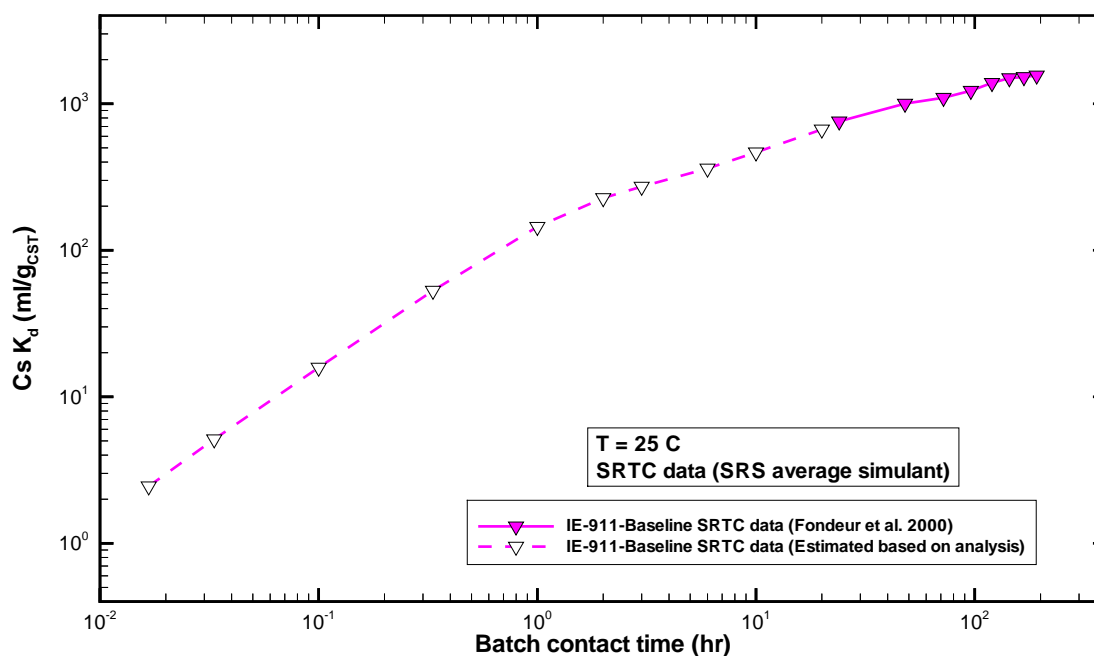


Figure 7-5. Cesium  $K_d$  measurements obtained from batch kinetics tests performed by Fondeur et al. (2000) at 25 C and in a SRS average simulant liquid at  $1.4 \times 10^{-4}$  M Cs and 5.6 M Na. Also shown is an estimated behavior at early times for the Fondeur et al. (2000) data.

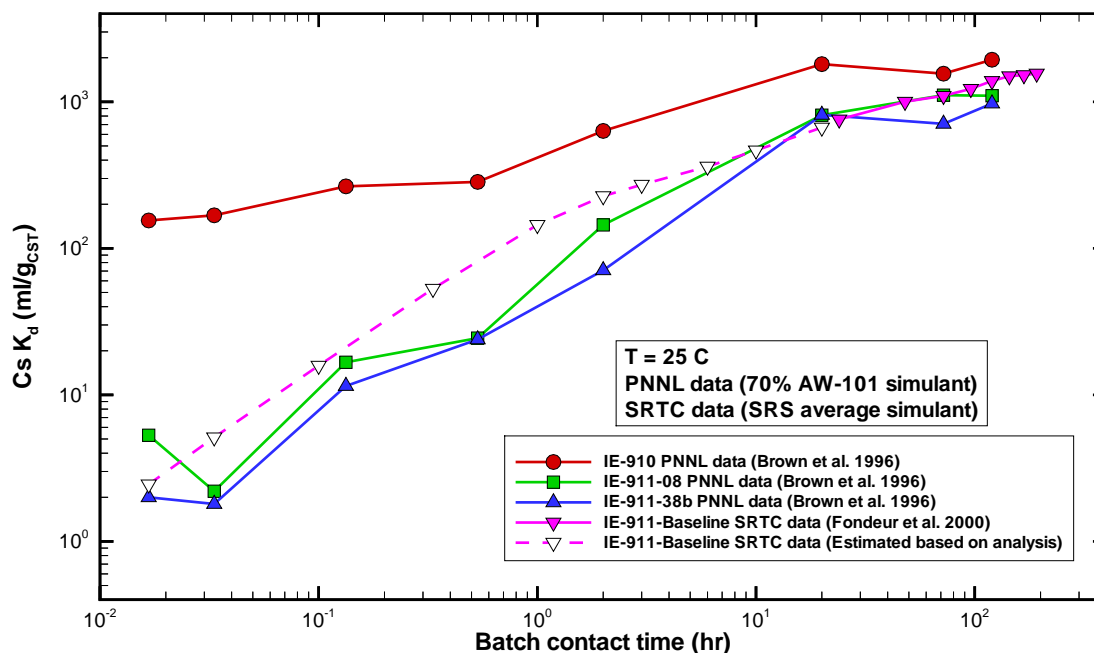


Figure 7-6. A comparison of the cesium  $K_d$  measurements obtained from batch kinetics tests performed by Brown et al. (1996) and Fondeur et al. (2000) on various CST materials at 25 C.

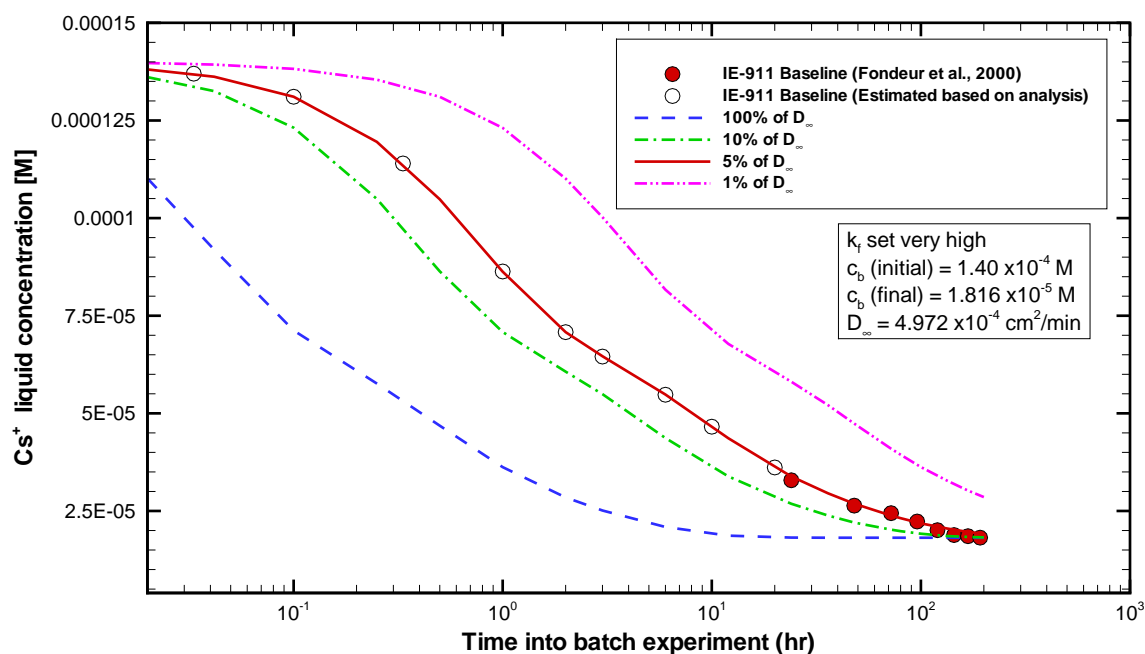


Figure 7-7. Estimation of the cesium pore diffusion coefficient based on batch kinetics tests performed by Fondeur et al. (2000) at 25 C for cesium uptake on IONSIV® IE-911 CST (engineered-form Baseline).

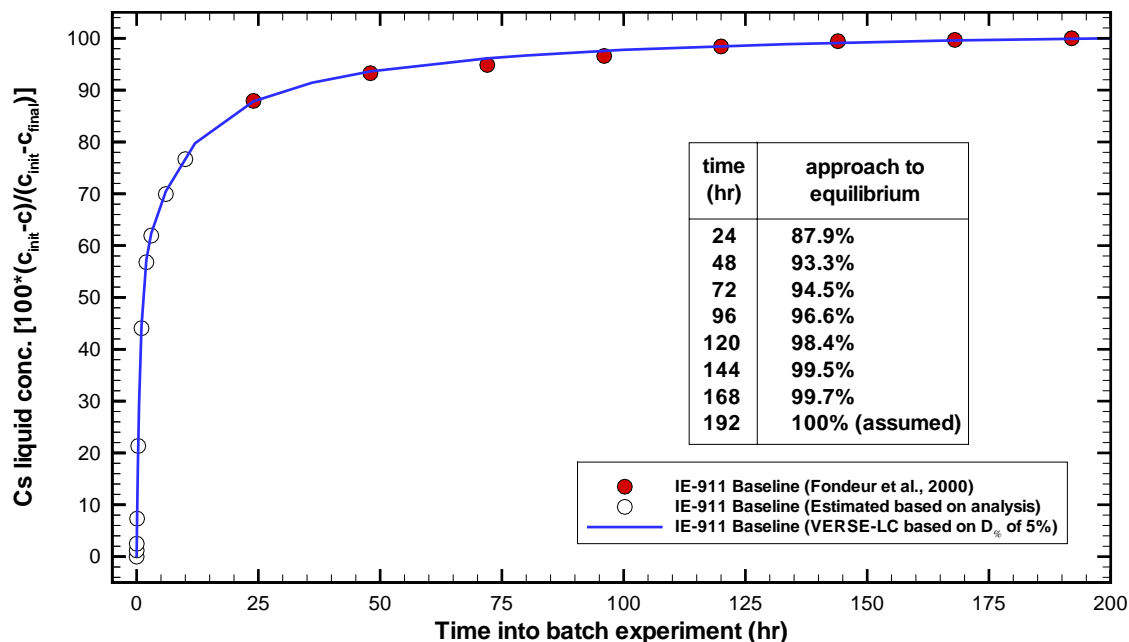


Figure 7-8. Comparison of VERSE-LC predictions to measured cesium concentrations during approach to equilibrium based on batch kinetics tests performed by Fondeur et al. (2000) at 25 C for the Baseline form of CST material (IONSIV® IE-911).

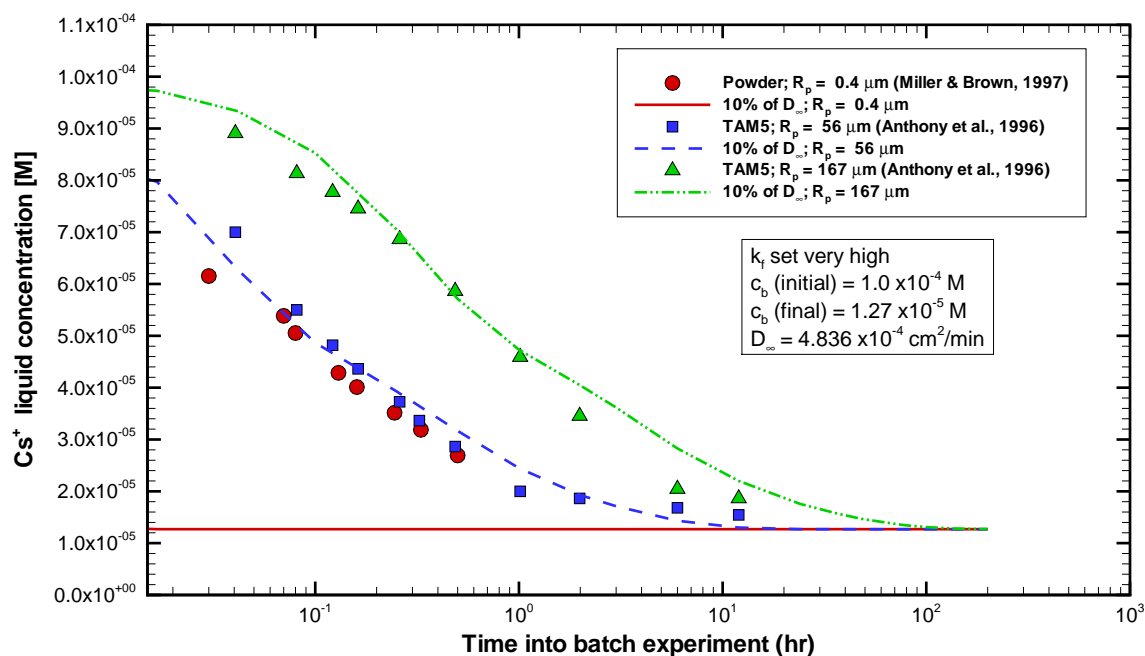


Figure 7-9. The effect particle size has on rates of cesium uptake by IONSIV® IE-910 (Miller and Brown, 1997) and by IONSIV® IE-911 (Anthony et al., 1996) CST materials based on transient cesium uptake testing.

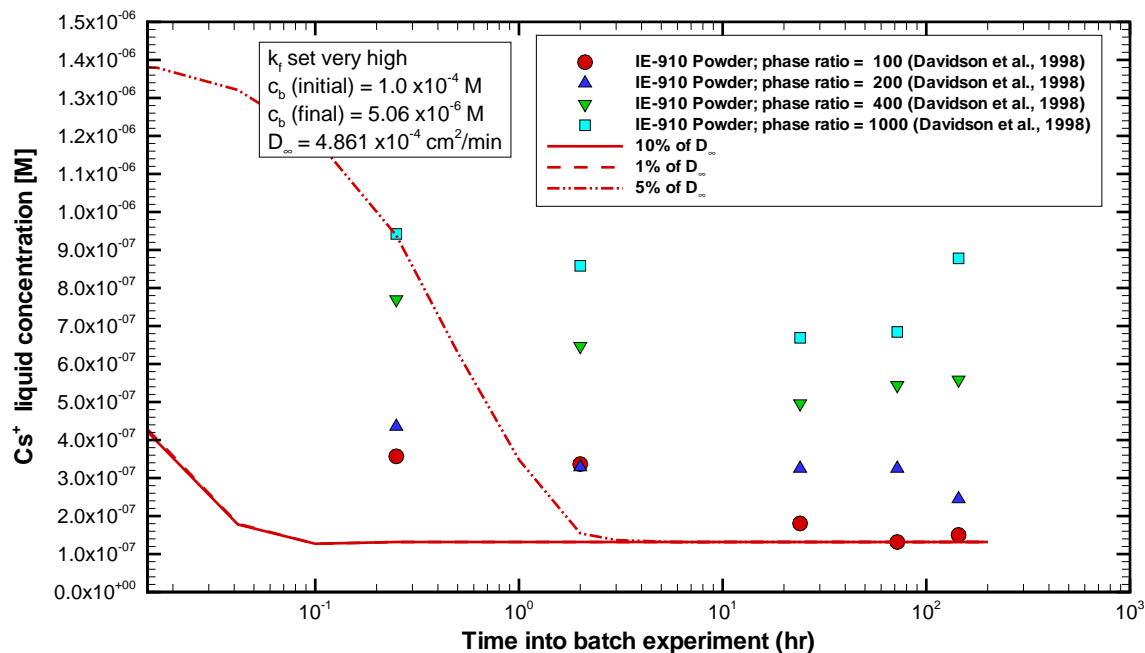


Figure 7-10. The effect phase ratio has on rates of cesium uptake by IONSIV® IE-910 CST material (Davidson et al., 1998) based on batch kinetics testing.

(This Page Intentionally Left Blank)

## 8.0 Axial Dispersion and Film Diffusion

In this section we present the correlations used to define: (1) axial dispersion along the bed length and (2) mass transfer across the liquid film separating the bed fluid from its neighboring particle pore fluid.

### 8.1 Film Diffusion

For the laboratory-scale column tests and proposed full-scale facility, with the IONSIV® IE-911 CST particle size distributions, the Reynolds number range is approximately 0.1 to 1.0. With respect to published literature this is a very low Reynolds number range. Numerous mass transfer correlations exist as discussed by Foo and Rice (1975, see their Figure 2). One of the correlations compared in Foo and Rice (1975) is one developed by Wilson and Geankoplis (1966) based on low Reynolds number data. Large variations between correlations can be seen; however, sensitivity to the film coefficient is low as shown in Hamm et al. (2000a and 2000b). Since VERSE-LC has the Wilson and Geankoplis (1966) correlation as an option and this correlation falls somewhat within the spread of available low Reynolds number data we have chosen it for all the column simulations in this report. For each ion species considered, the Wilson and Geankoplis (1966) correlation is expressed as:

$$J \equiv \left[ \frac{k_{fi}}{u\varepsilon_b} \right] Sc_i^{2/3} = \frac{1.09}{\varepsilon_b} Re^{-2/3}, \quad (8-1)$$

where the Reynolds number is defined as

$$Re \equiv \frac{2R_p \rho_w u \varepsilon_b}{\mu_w},$$

and the Schmidt number for each species is defined as

$$Sc_i \equiv \frac{\mu_w}{\rho_w D_i^\infty}.$$

A standard deviation of approximately 25% is reported for Eq. (8-1) by Wilson and Geankoplis (1966), while from comparison to the various correlations presented by Foo and Rice (1975) a standard deviation of 100% to 200% is observed.

### 8.2 Axial Dispersion

Axial dispersion in packed columns is the result of mechanical dispersion added onto molecular diffusion. For practical flowrates mechanical dispersion dominates. For well-packed columns of sufficient diameter such that wall effects (i.e., channeling) are minimal a variety of correlations exist for long column performance. A brief discussion of minimum column sizing is presented in Brooks (1994).

In the low Reynolds number range of interest the Chung and Wen (1968) correlation is applicable for sufficiently large columns (i.e., large diameter and length) and is expressed as:

$$E_b = \frac{2R_p u \varepsilon_b}{0.2 + 0.011 Re^{0.48}}, \quad (8-2)$$

where the standard deviation of this correlation based on all available data points was reported to be 46%. Equation (8-2) applies for only sufficiently large columns and correction factors must be considered for columns with small diameters and/or short active bed lengths.

### 8.2.1 Radial Flow Maldistribution

Flow maldistribution is caused by packing irregularities. As such the bed porosity varies over the cross-section of a column and increases as the outer wall is approached (even for well-packed columns). “Channeling” near the wall becomes more serious for smaller column diameters and larger particle sizes. As a “rule of thumb” Helfferich (1962) states that this effect becomes significant when the bed diameter is less than thirty times the particle diameter.

The experimental and mathematical basis for this rule of thumb stems from the work of Schwartz and Smith (1953) and Morales et al. (1951). For further discussion on the basis and potential impacts due to flow maldistribution see Hamm et al. (2000b, Chapter 8).

The impact associated with non-uniform radial velocity profiles manifests itself in spreading out the exit breakthrough curves in a manner similar to increased axial dispersion. As listed in Table 9.1 of Section 9, all of the column experiments considered have column-to-particle diameter ratios of ~30 or greater. In the simulations performed in this report no explicit account was made for any apparent increase in axial dispersion.

### 8.2.2 Headspace and Short Column Impacts

The proposed carousel column configurations (i.e., two or three column arrangements) are composed of ion exchange columns that contain headspaces. Each column in the carousel is geometrically identical where above the active bed height is a headspace void. For the design calculations presented in Chapter 10 these inlet headspaces are modeled as CSTRs whose volumes are 25% of the active bed volumes.

Liles and Geankoplis (1960) conducted experiments to ascertain the impact short column lengths and void headspaces have on axial dispersion in packed bed columns. When end effects were eliminated they concluded that no effects of length on axial dispersion were observed. However, in the presence of end effects such as void headspaces significant effects of length can result. For further discussion on the basis and potential impacts due to end effects see Hamm et al. (2000b, Chapter 8).

In the simulations performed in this report no explicit account was made for this apparent increase in axial dispersion based on end effects. For long columns exceeding 60 cm these effects are generally small.

## 9.0 Laboratory-Scale Column Assessments

To perform column transport analyses for sizing the CST columns, a method of estimating an “effective” cesium pore diffusion coefficient value is required. We had hoped that available batch kinetics test data would provide us the appropriate values. Unfortunately, the pore diffusion values based on existing kinetics data did not compare favorably when used in laboratory-scale column performance assessments. Given this situation, we are now estimating the pore diffusion coefficient values based on the laboratory-scale column data directly. Originally, we had planned to use the laboratory-scale column tests in a benchmark fashion but are no longer able to do so. In this chapter the results from our pore diffusion coefficient study are discussed. Note that a pore diffusion coefficient is computed as the product of a free molecular diffusion coefficient divided by a tortuosity factor. The molecular diffusion coefficient is based on the feed solution’s composition, while the tortuosity factor is based on the solid structure of the CST material. It is this tortuosity factor that is being estimated in this chapter. A brief assessment to pilot-scale experiments is also provided.

For the various column tests considered in this chapter no direct measurements were made as to the amount of CST mass that was actually packed into the columns. Unfortunately, only the bed volumes were measured. The amount of ion exchanger within the bed is the dominant factor not the space that it occupies. All future column studies should measure the amount of ion exchanger present within the test column. In the VERSE-LC simulations a constant bed density of 1.0 g/ml is assumed. This is an average observed value for several measured packed columns.

Numerous laboratory-scale column experiments have been performed to measure the cesium removal capability of the IONSIV<sup>®</sup> IE-911 CST material for feed conditions typical for a range of SRS and Hanford waste types. A listing of the laboratory-scale and pilot-scale column studies considered in this chapter is provided in Table 9-1. Key features associated with each column are also given in Table 9-1.

VERSE-LC was used to model 15 of these column experiments where cesium breakthrough curves were experimentally measured for column packed with IONSIV<sup>®</sup> IE-911 CST material. Several differing batch IDs were tested and in some cases corresponding equilibrium contact tests were available. Comparisons of these model calculations to the corresponding experimental data are provided in the following subsections. The VERSE-LC input files for each of the 15 simulations are listed in Appendix H. The transport properties were established by means other than fitting to the column data directly, except for the cesium pore diffusion coefficient. Binary isotherm models for cesium were created for each unique batch ID and waste type (i.e., differing total ionic strengths and compositions) based on ZAM generated databases. A modest shifting of breakthrough prediction versus measured was observed with respect to superficial velocity and future efforts should attempt to investigate this effect.

To briefly summarize our assessments, the exit breakthrough curve model predictions for cesium are generally reasonable when compared to the available data sets. Even for sequential column tests, where the lag column in a previous test is used as the lead column in a follow-on test. No

effort to improve these predictions, by altering the initial estimates of the various transport parameters excluding the tortuosity factor, was attempted.

A summary of recommended nominal transport parameter settings for the Cesium-IONSIV<sup>®</sup> IE-911 CST system column modeling is provided in Table 9-2. The parameters in Table 9-2 are ordered into groups based on their level of importance with respect to the determination of cesium exit breakthrough curves. The ordering of these parameters is based on the numerous simulation runs made during this assessment effort and our sensitivity study for the full-scale facility as discussed in Chapter 10 and earlier modeling efforts with SuperLig<sup>®</sup> resins.

## **9.1 CST Pore Diffusion Coefficient**

CST packed columns are said to be mass transfer limited giving rise to relatively slow “kinetics”. Therefore, in predicting cesium breakthrough behavior for CST packed columns the pore diffusion coefficient should be an important parameter. The “effective” cesium pore diffusion coefficient can be normalized with respect to the free stream “Brownian” diffusion coefficient. The inverse of this ratio is referred to as a tortuosity factor that is primarily dependent upon the internal structure of the porous material. For materials with very large pores a tortuosity factor approaching unity is observed, while for very small pores factors approaching zero can result. The rate of “kinetics” is inversely related to the tortuosity factor. Below the “best estimate” value of this ratio, and the basis of its creation, is discussed. This value was used in all the CST design analysis presented in this report.

### **9.1.1 Tortuosity Factor Optimization Strategy**

It is assumed that this ratio (i.e., pore to free stream) is independent of the aqueous phase composition. The following limited optimization strategy to determine an appropriate value for this ratio was undertaken.

- The exit breakthrough data for several representative column performance tests were utilized (i.e., 9 SRTC tests and 1 PNNL test were considered). Some of the details for each case are provided in subsequent subsections below.
- For each test 5 VERSE-LC simulations were run varying this ratio (i.e., ratio values of 10%, 20%, 26%, 30%, and 35%). Preliminary assessments indicated that this range would bracket the parameter. The dilution factor was fixed to 68% for every simulation used in the optimization.
- For each ratio value an overall residual in calculated breakthrough versus measured (i.e., residual in  $c/c_0$ ) in the form of a root-mean-square was computed. The minimum of this residual curve provided us with a “best estimate” value of this ratio.

The performance of a column is predominately impacted by the isotherm’s dilution factor and the pore diffusion coefficient value. A two-parameter optimization study (i.e., dilution and ratio factors) was not undertaken. The dilution factor was set to 68% during this optimization study. Future efforts to better estimate the cesium pore diffusion coefficients (i.e., tortuosity) is



recommended. However, VERSE-LC simulations are shown below where a dilution factor of both 68% and 100% were used.

The cost function that was chosen to be minimized is given by:

$$\Phi(\eta) \equiv \Phi\left(\frac{1}{\tau}\right) = \sqrt{\frac{1}{n_{\text{tests}}} \sum_{i=1}^{n_{\text{tests}}} \left[ \frac{1}{n_{\text{data},i}} \sum_{j=1}^{n_{\text{data},i}} \left\{ \left( \frac{c}{c_o} \right)_{i,j}^{\text{calc}} - \left( \frac{c}{c_o} \right)_{i,j}^{\text{exp}} \right\}^2 \right]}, \quad (9-1)$$

where

$$\eta \equiv \frac{1}{\tau} = \frac{D_p}{D_\infty}. \quad (9-2)$$

Since the data points within a given test are used to primarily specify the shape of each breakthrough curve, the overall residual based on several column tests,  $n_{\text{tests}}$ , should be computed where equal weighting of each column test is achieved. Equation (9-1) represents a weighted root-mean-square (rms) of individual column test residuals where each set of data from a given column test is weighted by the number of data points taken during the test,  $n_{\text{data}}$ . In this way, uniform weighting on a column test basis is maintained. Since the cesium feed concentration can vary greatly from test to test, the data point residuals are normalized to each test's feed concentration (i.e.,  $c/c_o$ ). Note that a value of say 0.1 for the cost function, Eq. (9-1), indicates that the VERSE-LC's predictive capability would be on average within 10% of the measured curve.

### 9.1.2 Tortuosity Factor Optimization Results

The residuals of the ten various simulations considered are plotted in Figure 9-1, along with the composite rms. The composite results of the simulations are also summarized in Figure 9-2. In Figure 9-2 the solid circles represent the computed composite rms (root-mean-square) values, the solid curve is a spline-fit through the points, and the dashed curves represent estimated behavior outside the tested range. Only 8 of the 10 data sets were used in generating the composite results. After our initial runs, two of the data sets were omitted (i.e., test SRS-Avg-Test5 contained only limited early time breakthrough data, while test PNNL-AW101-Test1 had questionable feed composition values). As shown in Figure 9-1, the rms curves for these two tests do not exhibit minima within the ratio range shown.

For theoretical considerations, as pore diffusion approaches zero the predicted breakthrough curve approaches unity at all times, resulting in a rms of  $\sim 0.5$ . As pore diffusion approaches infinity the predicted breakthrough curve approaches the curve dictated by film diffusion only. At some intermediate value a minimum in the rms curve is expected. For a given column performance, the area between unity and the breakthrough curve represents the total amount of cesium stored within a column as a function of time and at long times this area will be identical for any pore diffusion coefficient value assumed (i.e., capacity depend only). Due to this mass balance constraint placed on the entire exit breakthrough curve, we would expect to see a rather shallow minimum in the rms curve as seen in Figure 9-2. Based on uncertainties the minimum in

the rms curve shown in Figure 9-2 probably exists within the range of 20% to 30%. Using the data (and their individual spline-fits), as shown in Figure 9-1, an overall minimum value of ~22% is computed with an ~4.4% standard deviation. The individual rms values for all ten tests is given in Table 9-3.

The origin of this can further be seen in the comparison of exit breakthrough curves for one specific column study as shown in Figures 9-3 and 9-4 (SRTC data by Wilmarth et al., 1999). The total area for each VERSE-LC simulation curve will be equal. For lower pore diffusion coefficient values (e.g., 10% in Figure 9-3) we see earlier than measured breakthrough at short process times, while for higher pore diffusion coefficient values (e.g., 35% in Figure 9-3) we see later than measured breakthrough. For this case study the average deviations of the VERSE-LC predictions from measurement are approximately the same for ratio values between 20% to 30%. Basically, values between 20% to 30% result in equally acceptable predictions when viewed on an integrated basis. However, in sizing the CST columns and holding all other parameters fixed, lower pore diffusion coefficient values result in larger column sizes.

### 9.1.3 Tortuosity Factor Coefficient Recommendation

Observable predictive improvement is obtained between ratio values of 20% and 30% as shown in Figure 9-2. Looking at one specific case study (SRTC data by Wilmarth et al., 1999), the cesium breakthrough predictions based on both the 20% and 30% ratio values are shown in Figure 9-4. Consistent with the overall rms values shown in Figure 9-2, the two breakthrough predictions in Figure 9-4 are approximately of equal quality. However, with all other parameters being fixed the lower the pore diffusion coefficient the earlier the breakthrough. From a design perspective, lower pore diffusion coefficient values provide more conservative design estimates.

Based on this, it is our recommendation that we use the lower estimated limit of the rms minimum (i.e., ratio value of 20%). It is believed that a value lower than ~20% would significantly impact column size due to its impact on the leading edge of the concentration wave and a clear systematic (on average) departure from the breakthrough data is seen for values lower than this.

## 9.2 Column Assessment Studies

Below we discuss the 15 different column tests listed in Table 9-1. Eight of these tests were used in the tortuosity factor estimation, while the remaining are provided for assessment purposes. The tests are grouped into subsections based on the feed composition type, (SRS simulant, Hanford sample, etc.).

### 9.2.1 SRS Tank 44 Tests

Walker et al. (1999) performed batch contact and column tests at 31 C using CST IE-911 (Lot number 98-05) with actual diluted Tank 44 supernate. A single long bed column of 160 cm in length and 1.5 cm in diameter was tested where cesium concentrations at three axial sampling points were recorded (i.e., 10 cm –lead, 85 cm –lag, and 160 cm –guard column locations). The sampling point at 10 cm represents a lead column, at 85 cm a lag column, and at 160 cm a guard

column. The inlet feed concentration of cesium was set to  $3.51 \times 10^{-4}$  M with a volumetric flowrate of 9.4 ml/min (i.e., superficial velocity of 5.319 cm/min). The cesium breakthrough data for the lead and lag column sampling points are provided in Appendix H.

At a sodium concentration of 5.4 M the beta value for a cesium algebraic model was computed to be  $2.0486 \times 10^{-4}$  M. A comparison of algebraic model to the batch contact test data based on CST engineered-form material is provided in Figure 9-5. The solid-curve represent the model's prediction for CST powder-form behavior, while the dashed-curve represents the prediction for CST engineered-form behavior. Unfortunately, for the Tank 44 solution we see that the data crosses over from the powder-form predictions at lower concentrations to the engineered-form predictions at higher concentrations. This particular behavior is unique with respect to the various other data sets considered and no explanation can be given for it at this time.

VERSE-LC simulations were run based on the column test parameters provided by Walker et al. (1999). Numerous simulations varying both the cesium isotherm (i.e., the dilution factor from 0.68 to 1.0) and cesium pore diffusion coefficient (i.e., tortuosity factor from 10% to 30%). A comparison of breakthrough predictions to the data is provided in Figure 9-6 for four of the cases considered (i.e., dilution factors of 0.68 and 1.0 with tortuosity factors of 10% and 26%). This data was used in the determination of the statistically based tortuosity factor as discussed earlier.

### 9.2.2 SRS Average Simulant Tests

Numerous column studies using CST packed columns and SRS average simulant have been performed. As one of three possible salt alternatives for processing SRS salt waste, these studies were performed over a several year timeframe. Here only a subset of these experiments is addressed. Several differing engineered-forms of CST were considered, both lab-scale and production-scale forms have been tested. In most cases some level of batch contact testing was performed for each series of column tests. The feed composition of the SRS-Avg simulant used in these tests is provided in Table C-1 of Appendix C and a discussion of their preparation is provided by Walker (1999b). The cesium isotherm models used in the VERSE-LC simulations are based on fits to ZAM code generated data at a temperature of 25 C. The resulting beta parameter used is  $2.4145 \times 10^{-4}$  M. Some of the test details and measured breakthrough data for these tests are provided in Appendix H. Example VERSE-LC input files are also provided in Appendix H.

Wilmarth et al. (1999) performed a series of column tests at ~25 C where the effects of CST pretreatment, superficial velocity, and the presence of organic constituents were considered. Four of these column tests are considered here and their test details are provided in Appendix H, along with the VERSE-LC input files. Key parameters for each column are listed in Table 9-1. For the same size column, packed with CST material taken from the same batch, the effect of superficial velocity was varied in tests SRS-Avg-Test1, SRS-Avg-Test2, and SRS-Avg-Test3 (i.e., 5.5, 7.0, and 4.1 cm/min, respectively). A comparison of the data to VERSE-LC simulations is given in Figures 9-7, 9-8, and 9-9, respectively. The VERSE-LC predictions for Test1 and Test2 are reasonably consistent; however, for the two Test3 runs (i.e., Test3a was conducted with CST material having prior exposure to humid air, while Test3b did not) the predictions vary significantly. The test conditions for the Test3 column is very similar to an

earlier test performed by Walker et al. (1998), (i.e., test labeled SRS-Avg-Test7 in Table 9-1). A comparison of these three tests (i.e., Test3a, Test3b, and Test7) is shown in Figure 9-10.

The primary difference between Test3(a and b) and Test7 is the CST Lot numbers. From the measured breakthrough data the earlier CST material (Lot number 96-04) appears to have less ion-exchange capacity than the newer CST material (Lot number 98-05). Wilmarth et al. (1999) repeated the Walker et al. (1998) test using the older CST material (Lot number 96-04). Their measured breakthrough curve was very similar to the earlier Walker et al. (1998) test data. Variability between Lots of this magnitude is seen throughout the CST development history (i.e., especially when a comparison of batch contact data is viewed). At the nominal superficial velocity of 4.1 cm/min, the impact of using a larger diameter column was tested in SRS-Avg-Test4 and a comparison to VERSE-LC predictions is given in Figure 9-11. Even though we see batch variability within this work, all four tests by Wilmarth et al. (1999) were used in the tortuosity factor estimation. Some of the column test variability may be the result of bed density differences due to the manner in which these columns were originally packed. In the VERSE-LC simulations a constant bed density of 1.0 g/ml was assumed.

Walker et al. (1998) performed several batch contact tests and three column tests using CST IE-911 (Lot numbers 96-02 and 96-04) with SRS-Avg simulant. The column tests were performed at ~22 C and the key features of these three tests are listed in Table 9-1 (i.e., tests labeled SRS-Avg-Test5, SRS-Avg-Test6, and SRS-Avg-Test7). The sizes of each column are approximately the same, while the CST packing was changed for the last column test. The volumetric flowrate (i.e., thus superficial velocity) was varied to exceed the expected operating range of the proposed full-scale SRS facility. Comparisons of the data to VERSE-LC simulations are shown in Figures 9-12, 9-13, and 9-14, respectively. Several VERSE-LC simulations are shown for each test. The cesium breakthrough data for the lead and lag column locations are provided in Appendix H.

For test SRS-Avg-Test5 the slow flowrate resulted in only a small portion of the cesium breakthrough curve being measured. This data set was considered to be insufficient for our purposes in estimating a tortuosity factor and the results shown here are for completeness. The three VERSE-LC results shown predict earlier than measured breakthrough.

For test SRS-Avg-Test6 an intermediate flowrate was used. As Figure 9-13 illustrates, significant data scatter was observed in the form of oscillations. On average the data does exhibit a reasonable breakthrough curve and was included in the database for tortuosity factor estimation. The VERSE-LC prediction of breakthrough appears to be sensitive to the dilution factor and pore diffusion coefficient at this flowrate.

For test SRS-Avg-Test7 a fast flowrate was used. As Figure 9-14 illustrates, much smaller data scatter was observed in the form of oscillations. A complete cesium breakthrough curve was achieved and this data set was included in the database for tortuosity factor estimation. The VERSE-LC prediction of breakthrough appears to be less sensitive to the dilution factor and pore diffusion coefficient at this high flowrate.

When comparing the VERSE-LC predictions based on one specific set of input parameter values, we see a systematic shifting of the results from earlier-than to later-than breakthrough

relative to the three data sets. This suggests that a functional superficial velocity dependence of one or more of the VERSE-LC modeling parameters is not being handled adequately (e.g., axial dispersion or film diffusion coefficient) at this time. However, no attempt to pursue this issue was undertaken.

### **9.2.3 SRS High OH Simulant Tests**

Walker et al. (1999) also performed batch contact and column tests using CST IE-911 (Lot number 98-05) with SRS high OH simulant. The column test is basically a repeat of one of the earlier SRS Tank44 studies performed at ~31 C and the key features of this test is listed in Table 9-1 (i.e., test labeled SRS-High-OH-Test1). The size of each column is approximately the same, while the CST packing was based on Lot 98-05 material. Comparisons of the data to VERSE-LC simulations are shown in Figure 9-15. Several VERSE-LC simulations are shown for this test. The beta parameter used for the cesium isotherm is  $2.0987 \times 10^{-4}$  M based on a fit of data generated using the ZAM code at 31 C. No appreciable cesium breakthrough is observed at the 85 cm axial location. This data set was included in the database for tortuosity factor estimation.

### **9.2.4 PNNL Hanford Sample Tests**

Hendrickson (1997) performed a column test using CST IE-911 (Lot number 96-01) with a diluted AW-101 sample. Lee et al. (1997a) also contains a brief description of this test along with several other CST packed column tests. The column test was performed at ~25 C and the key features of these tests are listed in Table 9-1 (i.e., test labeled PNNL-AW101-Test1). Comparisons of the data to VERSE-LC simulations are shown in Figures 9-16. Several VERSE-LC simulations are shown. The beta parameter used for the cesium isotherm is  $4.7414 \times 10^{-4}$  M based on a fit of data generated using the ZAM code at 25 C. Unfortunately, the report was somewhat unclear as to the composition of the AW-101 simulant actually used in the column test. Therefore, this data set was not included in the tortuosity factor estimation.

### **9.2.5 ORNL MVST Sample Tests**

During the mid-90s ORNL performed a “Cesium Removal Demonstration” (CsRD) project where cesium was removed from Melton Valley Storage Tank (MVST) waste using CST packed ion-exchange technology. Approximately 114,000 L (30,000 gal) of supernate was successfully processed. The final report for the CsRD project was issued by Walker, Jr., et al. (1998). Prior to testing the actual pilot-scale facility, various small-scale columns were tested. Below we will look at one of the small-scale tests and then take a look at the performance of the pilot-scale CsRD facility. In some cases due to the older CST batches used or the uncertainties we had in defining feed composition, none of the data sets discussed below were included in the tortuosity factor estimation. This data is primarily shown for completeness and for assessment purposes.

Lee et al. (1997b) performed column tests using CST IE-911 (Lot number –38b) with a MVST W-27 simulant (stored at ORNL). CST Lot number –38b was a developmental sample of CST supplied by UOP. In a summary report Davidson et al. (1998) also discusses these tests along with batch contact testing. The two column tests were performed at ~25 C and the key features

of these tests are listed in Table 9-1 (i.e., tests labeled ORNL-W27-Test1 and ORNL-W27-Test2). Test data and details are provided in Appendix H. These two tests use the same column being operated at different flowrates (i.e., 3 CV/hr and 6 CV/hr). Comparisons of the data to VERSE-LC simulations are shown in Figures 9-17 and 9-18, respectively. Several VERSE-LC simulations are shown. The beta parameter used for the cesium isotherm is  $9.3232 \times 10^{-4}$  M based on a fit of data generated using the ZAM code at 25 C and a measured bed density of 1.15 g/ml.

For the CsRD facility CST Lot number -38b (note that this might also be called 96-01) was used. A two column carousel arrangement was used where both the lead and lag columns were always the same size (i.e., 30.6 cm in diameter and 51.67 cm in length). The breakthrough data and test details are provided by Walker, Jr., et al. (1998) and are also provided in Appendix H. Four basic processing operations were performed (i.e., referred to as runs). The first run (Run1) was limited in terms of the amount of cesium loading allowed and was performed primarily for assessing the radiation exposure risks. Here Run1 (i.e., constituted only a single lead column) is not considered. The feed compositions for the four CsRD runs were not well defined; therefore, cesium isotherms were generated based on the limited  $K_d$  values for the feeds given by Walker, Jr., et al. (1998).

For Run2 a MVST W-29 supernate flowing at ~3 CV/hr was processed where again only one freshly packed lead column was used. A total of ~18,000 L were processed (i.e., ~480 CVs). A comparison of VERSE-LC predictions to the data is shown in Figure 9-19.

For Run3 both freshly packed lead and lag columns were used. The flowrate was doubled over Run2's value (i.e., 6 CV/hr). Approximately 11,600 L were processed (i.e., ~1040 CVs) where significant cesium breakthrough was achieved in both the lead and lag columns as shown in Figure 9-20. VERSE-LC predictions are also shown in Figure 9-20.

The fourth and final CsRD run (i.e., Run4) involved one carousel cycle where a total of 3 columns were utilized. During the first cycle ~28,500 L (i.e., ~750 CVs) of feed was processed and approximately the same amount was processed during the second cycle. During the process run the flowrate was increased from its starting value of 3 CV/hr up to 6 CV/hr. For simplicity the VERSE-LC simulations (i.e., cycle 1 named Run4a and cycle 2 Run4b) were generated using a constant flowrate of 6 CV/hr. The results based on varying the flowrate would only be slightly different. For cycle 1 a comparison of VERSE-LC predictions to the data is shown in Figure 9-21 and for cycle 2 is shown in Figure 9-22. The lag column in cycle 1 becomes the lead column during cycle 2. Reasonably accurate predictions for cycle 1 are seen in Figure 9-21 for both columns. However, as shown in Figure 9-22, the third column sitting in the lag position during cycle 2 experienced much earlier breakthrough than predicted. Given the acceptable predictions made for the first two columns, the discrepancies for the third column suggests that this column were either poorly packed or contained low capacity CST material.

Table 9-1. Key features of Cesium-CST IE-911 fixed bed small-scale columns considered.

Column ID <sup>a</sup>	CST IE-911 Lot Number	Liquid feed type	Active bed volume (ml)	Diameter (cm)	Length (cm)	Column-to-particle diameter ratio	Superficial velocity (cm/min)	CV/hr	Feed conc.: total Cs [M]	Comments
SRS-Avg-Test1 (Wilmarth et al., 1999)	98-05	SRS average simulant	17.7	1.5	10.0	43.6	5.5	33.0	1.30x10 <sup>-4</sup> M	Test designed to study increased flowrate. Data used in tortuosity factor estimation.
SRS-Avg-Test2 (Wilmarth et al., 1999)	98-05	SRS average simulant	17.7	1.5	10.0	43.6	7.0	42.0	1.24x10 <sup>-4</sup> M	Test designed to study increased flowrate. Data used in tortuosity factor estimation.
SRS-Avg-Test3 (Wilmarth et al., 1999)	98-05	SRS average simulant	17.7	1.5	10.0	43.6	4.1	24.6	1.43x10 <sup>-4</sup> M	Two tests were run, Test3a used CST material with prior exposure to humid air, while Test3b did not. Data used in tortuosity factor estimation.
SRS-Avg-Test4 (Wilmarth et al., 1999)	98-05	SRS average simulant	49.1	2.5	10.0	72.7	4.1	24.6	1.366x10 <sup>-4</sup> M	Same conditions as for Test3 but using a larger diameter column. Data used in tortuosity factor estimation.
SRS-Avg-Test5 (Walker et al., 1998)	96-02	SRS average simulant	17.7	1.5	10.0	43.6	0.27	1.59	1.40x10 <sup>-4</sup> M	Only small portion of breakthrough curve seen due to low flowrate. Not used in tortuosity factor estimation.
SRS-Avg-Test6 (Walker et al., 1998)	96-02	SRS average simulant	17.7	1.5	10.0	43.6	0.98	5.88	1.40x10 <sup>-4</sup> M	Significant oscillation seen in breakthrough data, but still used in tortuosity factor estimation.
SRS-Avg-Test7 (Walker et al., 1998)	96-04	SRS average simulant	17.7	1.43	11.0	41.6	4.1	22.1	1.40x10 <sup>-4</sup> M	Complete breakthrough achieved. Data used in tortuosity factor estimation.
SRS-High-OH-Test1 (Walker et al., 1999)	98-05	SRS high OH simulant	17.7 & 150.2	1.5	10.0 & 85.0	43.6	5.43	32.6 & 3.8	3.70x10 <sup>-4</sup> M	Two breakthrough locations sampled. Data used in tortuosity factor estimation.
SRS-Tank44-Test1 (Walker et al., 1999)	98-05	Diluted SRS Tank 44 supernate	17.7 & 150.2	1.5	10.0 & 85.0	43.6	5.32	32.6 & 3.8	3.51x10 <sup>-4</sup> M	Two breakthrough locations sampled. Data used in tortuosity factor estimation.
PNNL-AW101-Test1 (Hendrickson, 1997)	96-01	Envelope A diluted AW-101 sample	7.9	1.0	10.0	29.1	1.06	6.3	7.26x10 <sup>-5</sup> M	Actual feed composition unclear within report. Data not used in tortuosity factor estimation.
ORNL-W27-Test1 (Lee et al., 1997b)	-38b	MVST W-27 sample	10.0	1.5	5.659	43.6	0.283	3.0	7.04x10 <sup>-6</sup> M	Preliminary study for Cs removal demonstration facility. Data for assessment purposes only.

Column ID <sup>a</sup>	CST IE-911 Lot Number	Liquid feed type	Active bed volume (ml)	Diameter (cm)	Length (cm)	Column-to-particle diameter ratio	Superficial velocity (cm/min)	CV/hr	Feed conc.: total Cs [M]	Comments
ORNL-W27-Test2 (Lee et al., 1997b)	-38b	MVST W-27 sample	10.0	1.5	5.659	43.6	0.566	6.0	$7.04 \times 10^{-6}$ M	Preliminary study for Cs removal demonstration facility. Data for assessment purposes only.
ORNL-CsRD-Run2 (Walker, Jr., et al., 1998)	-38b	MVST W-29 sample	1,581.2	30.6	51.672	889.5	2.58	3.0	$1.35 \times 10^{-5}$ M	Part of a Cs removal demonstration facility. Data for assessment purposes only.
ORNL-CsRD-Run3 (Walker, Jr., et al., 1998)	-38b	MVST W-29 sample	1,581.2	30.6	51.672	889.5	5.17	6.0	$1.35 \times 10^{-5}$ M	Part of a Cs removal demonstration facility. Data for assessment purposes only.
ORNL-CsRD-Run4a,b (Walker, Jr., et al., 1998)	-38b	MVST W-29 sample	1,581.2	30.6	51.672	889.5	5.17	6.0	$5.10 \times 10^{-6}$ M	Part of a Cs removal demonstration facility. Data for assessment purposes only.

<sup>a</sup> In some cases more than one column was used in a carousel arrangement.



Table 9-2. Summary of recommended nominal parameter settings for Cesium-IONSIV® IE-911 CST system column modeling.

Key parameter	Definition	Priority for predicting break-through curve	Recommended B. E. settings	Comments
$m_{\text{resin}}$	mass of resin in column	1	column specific	Key quantity generally assumed to be a constant during a series of column runs.
$\eta_{\text{df}}$	Dilution factor of CST when placed in its engineered-form	1	0.68 (Baseline material value while conservative for most batches)	Batch specific, and based on comparisons of available equilibrium contact $K_d$ data powder versus engineered forms.
$\bar{C}_T$	Cesium total ionic capacity of resin	1	0.58 (mmole/g <sub>resin</sub> )	Batch and feed specific, and based on available equilibrium contact $K_d$ data when available.
$\rho_b$	bed density	1	1.0 (g <sub>resin</sub> /ml <sub>bed</sub> )	Ideally measured for each column. Batch average generic value used otherwise.
$\beta$	$\text{XO}_4^-$ to $\text{NO}_3^-$ selectivity coefficient	1	composition dependent (fit to ZAM generated database)	Based on conc's not activities and total ionic strength and composition dependent
$L, D, V_b$	Length, diameter, & volume of column	1	column specific	Does not vary significantly with total ionic strength.
$\langle R_p \rangle$	avg. effective radius of resin	2	172 $\mu\text{m}$ (mean value)	Impacts both film and pore diffusion. Averaging process remains in question.
$U, Q$	superficial velocity & volumetric flow rate	2	column specific	For mass transfer limited columns flow perturbation dependent.
$C_o$	$\text{Cs}^+$ inlet conc	2	column specific	For favorable isotherms higher inlet conc's sharpen breakthru curves. Only a modest favorable isotherm over expected feed ranges.

Table 9-2. Summary of recommended nominal parameter settings for Cesium-IONSIV<sup>®</sup> IE-911 CST system column modeling (continued).

Key parameter	Definition	Priority for predicting break-through curve	Recommended B. E. settings	Comments
$\varepsilon_b, \varepsilon_p$	bed & particle porosities	3	0.50 & 0.24 (average values)	Porosity data very limited and these numbers at Texas A&M recommended values.
$D_p$	pore diffusion coefficient	3	20% of Brownian diffusion value	Based on tortuosity factor optimization using several more recent column studies.
$k_f$	liquid film mass transfer coefficient	3	Wilson and Geankoplis (1966) correlation	This correlation spans the velocity & particle sizes of the CST material.
$D_\infty$	Brownian motion diffusion coefficient	3	Computed based on feed ionic composition	Based on Nernst-Haskell eqn. & published ionic conductances at 25 °C.
$E_b$	axial longitudinal dispersion coefficient	4	Chung & Wen (1968) correlation	This correlation based on long column data for wide range of column conditions.
$E_b(L)/E_b(\infty)$	short column impact ratio	4	Liles & Geankoplis (1960) data	Power law fit to limited short column tests with end effects.
$V_{CSTR}$	CSTR volumes at entrance/exit of columns	4	column specific	Estimated based on specified volumes for each test series or assumed 25% if not available.

Table 9-3. Root-mean-square residuals for each column study as a function of the ratio of pore to free diffusion coefficients ( $\eta$ ).

Test ID	$\eta = 10\%$	$\eta = 20\%$	$\eta = 26\%$	$\eta = 30\%$	$\eta = 35\%$
SRS-Avg-Test1	8.777E-02	6.083E-02	5.623E-02	5.612E-02	5.839E-02
SRS-Avg-Test2	6.026E-02	2.640E-02	3.088E-02	3.894E-02	4.895E-02
SRS-Avg-Test3	1.933E-01	1.677E-01	1.663E-01	1.675E-01	1.700E-01
SRS-Avg-Test4	1.415E-01	1.309E-01	1.368E-01	1.418E-01	1.475E-01
SRS-Avg-Test5	1.505E-01	7.063E-02	5.474E-02	4.634E-02	3.871E-02
SRS-Avg-Test6	1.768E-01	1.746E-01	1.795E-01	1.836E-01	1.882E-01
SRS-Avg-Test7	6.457E-02	4.343E-02	5.865E-02	7.102E-02	8.435E-02
SRS-High-OH-Test1	1.758E-01	1.311E-01	1.289E-01	1.319E-01	1.376E-01
SRS-Tank44-Test1	1.095E-01	6.564E-02	6.050E-02	6.191E-02	6.638E-02
PNNL-AW101-Test1	1.924E-01	1.055E-01	7.756E-02	6.366E-02	4.985E-02
Overall rms <sup>a</sup> =	1.357E-01	1.094E-01	1.075E-01	1.091E-01	1.124E-01

<sup>a</sup> The overall rms value is based on only 8 out of the 10 column tests considered. Tests SRS-Avg-Test5 and PNNL-AW101-Test1 were omitted in the estimation of a "best estimate" tortuosity factor.

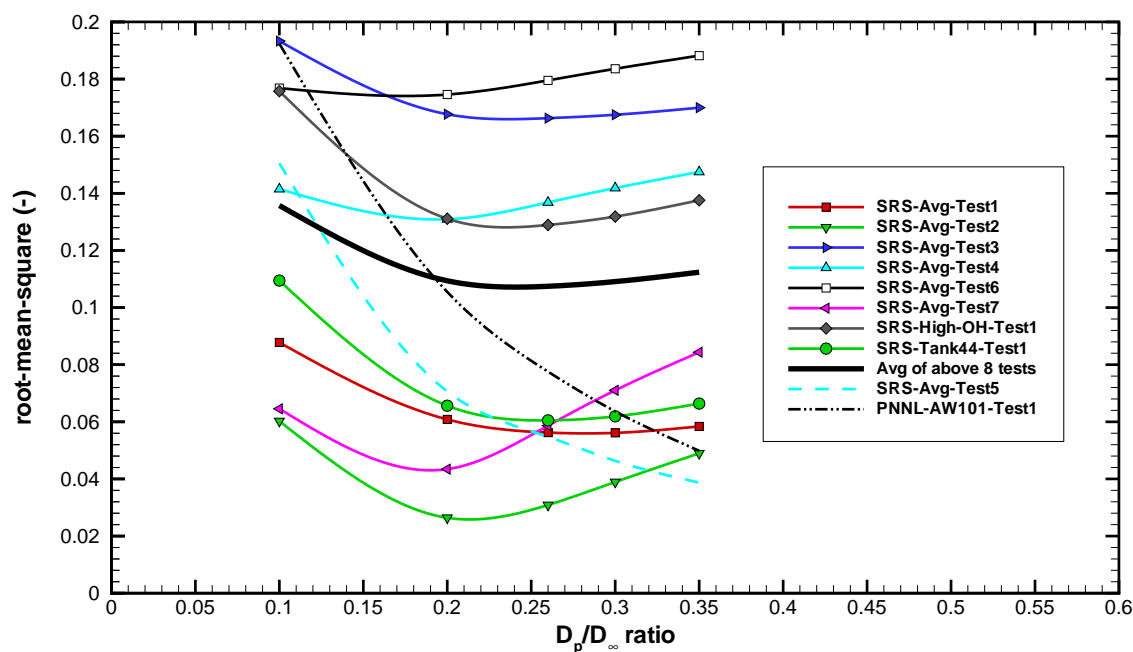


Figure 9-1. Measure of error for individual tests in predicting column exit cesium breakthrough as a function of the ratio of pore to free stream diffusion coefficients. Average behavior of the top eight tests is also plotted.

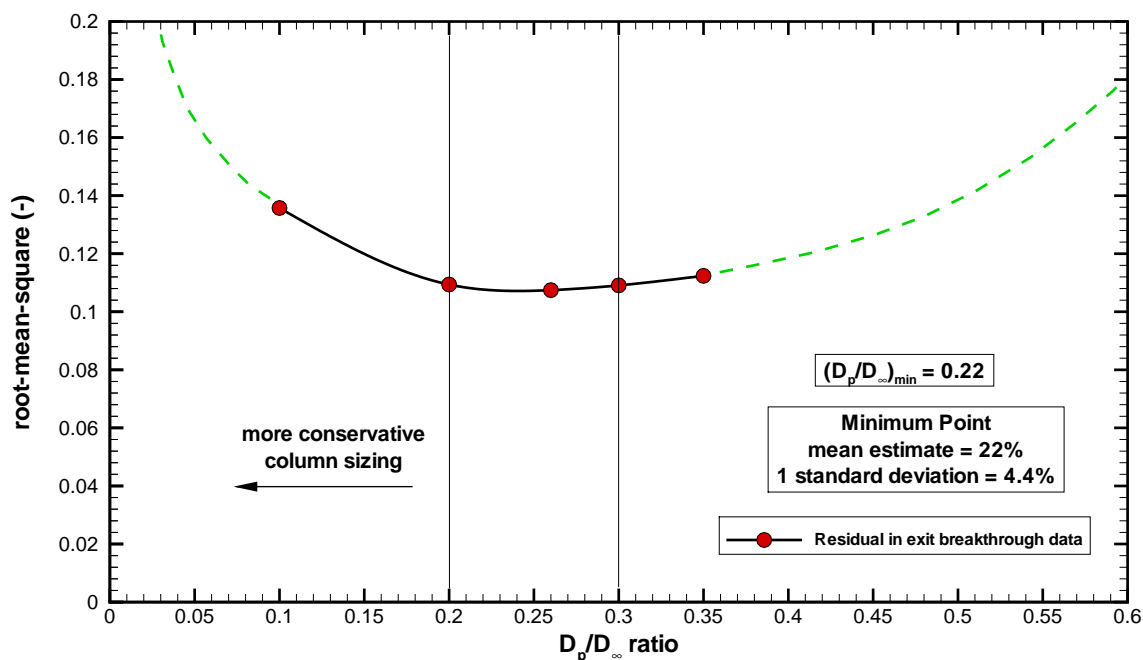


Figure 9-2. Overall measure of error in predicting column exit cesium breakthrough as a function of the pore to free stream diffusion coefficient ratio (8 column tests considered in summation).

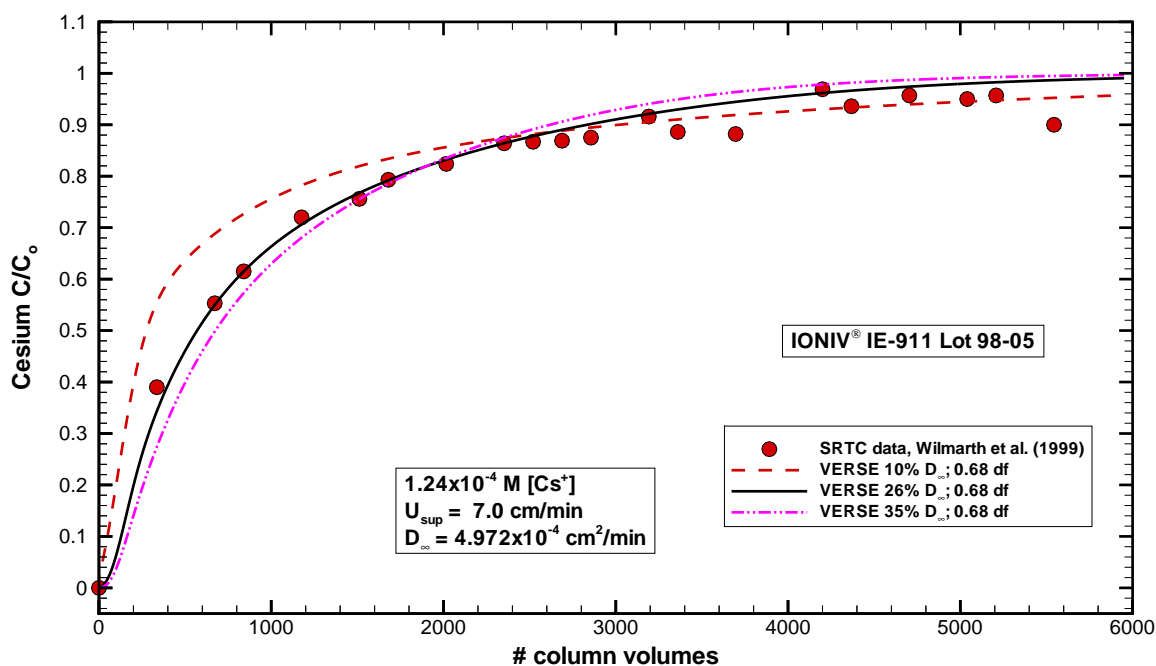


Figure 9-3. Measured versus predicted cesium column exit breakthrough for three assumed pore diffusion coefficient values (test SRS-Avg-Test2 performed by Wilmarth et al. (1999) in a SRS Average simulant liquid at  $1.24 \times 10^{-4}$  M Cs and at 25 C).

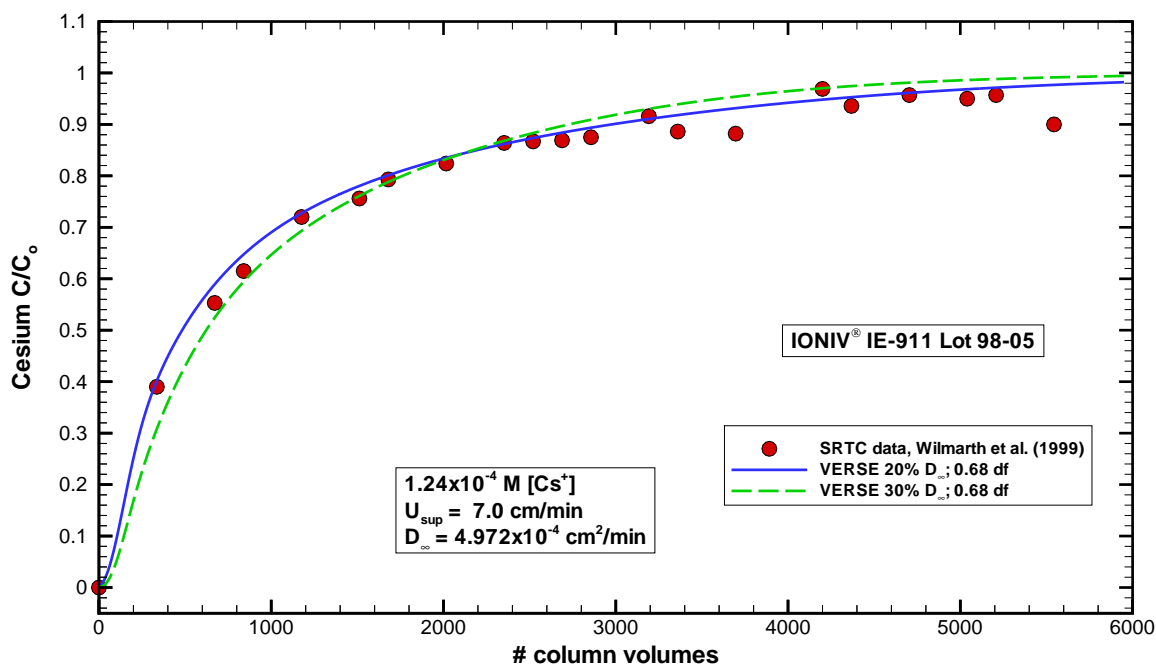


Figure 9-4. Measured versus predicted cesium column exit breakthrough for two assumed pore diffusion coefficient values (test SRS-Avg-Test2 performed by Wilmarth et al. (1999) in a SRS Average simulant liquid at  $1.24 \times 10^{-4}$  M Cs and at 25 C).

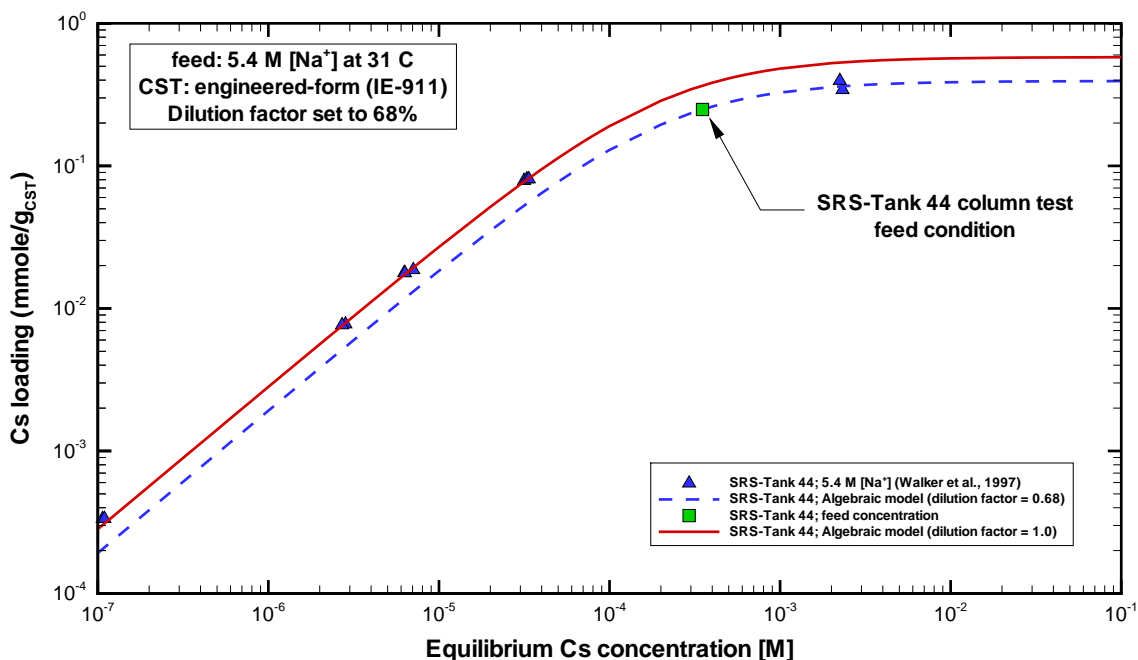


Figure 9-5. A direct comparison of predicted versus measured cesium loadings on IONSIV® IE-911 CST material for diluted SRS Tank 44 waste (Walker et al., 1999). The algebraic model is plotted for both the powder (solid-curve) and engineered (dashed-curve) forms.

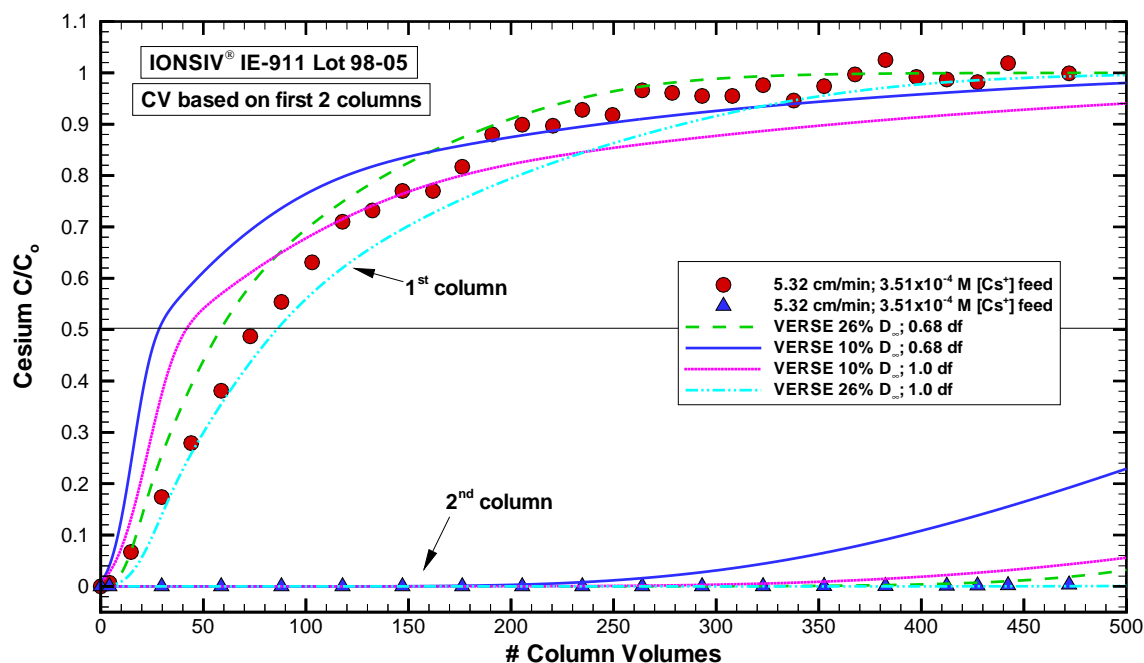


Figure 9-6. VERSE-LC cesium exit breakthrough curves compared to data from Walker et al. (1999) for SRS Tank 44 waste:  $D = 1.59$  cm,  $L = 10$  cm and 85 cm,  $U = 5.319$  cm/min,  $T = 31$  °C.

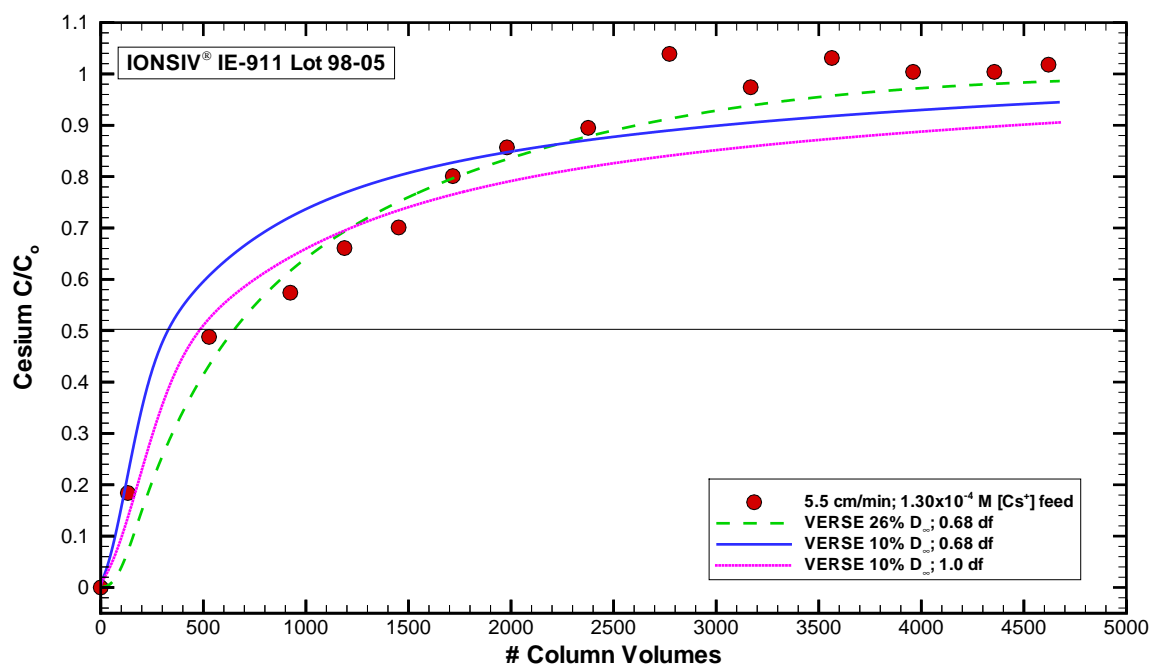


Figure 9-7. VERSE-LC cesium exit breakthrough curve compared to data from SRS-Avg-Test1 (Wilmarth et al., 1999):  $D = 1.5$  cm,  $L = 10$  cm,  $U = 5.5$  cm/min,  $T = \sim 25$  °C.

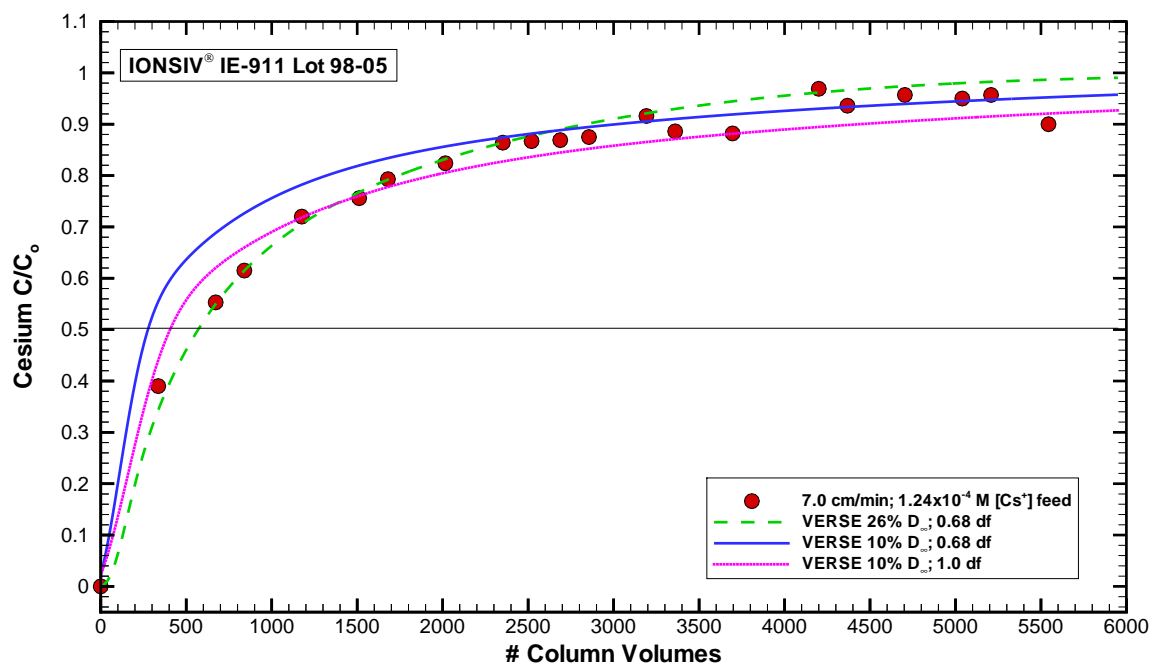


Figure 9-8. VERSE-LC cesium exit breakthrough curve compared to data from SRS-Avg-Test2 (Wilmarth et al., 1999):  $D = 1.5$  cm,  $L = 10$  cm,  $U = 7.0$  cm/min,  $T = \sim 25$  °C.

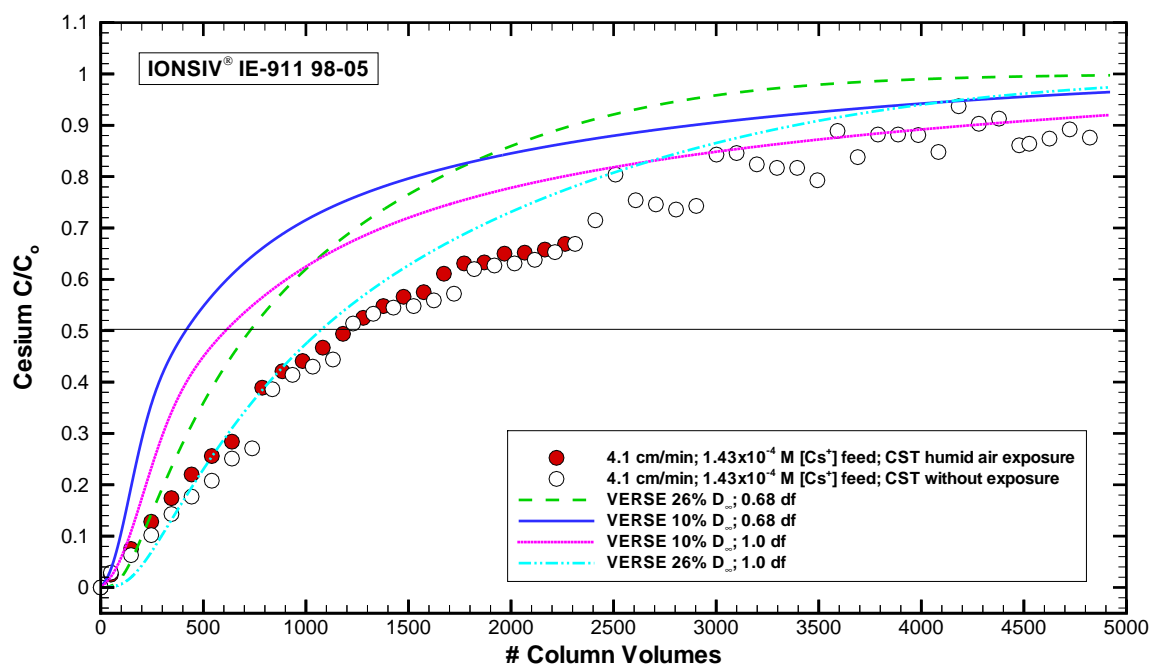


Figure 9-9. VERSE-LC cesium exit breakthrough curve compared to data from SRS-Avg-Test3a and Test3b (Wilmarth et al., 1999):  $D = 1.5$  cm,  $L = 10$  cm,  $U = 4.1$  cm/min,  $T = \sim 25$  °C.

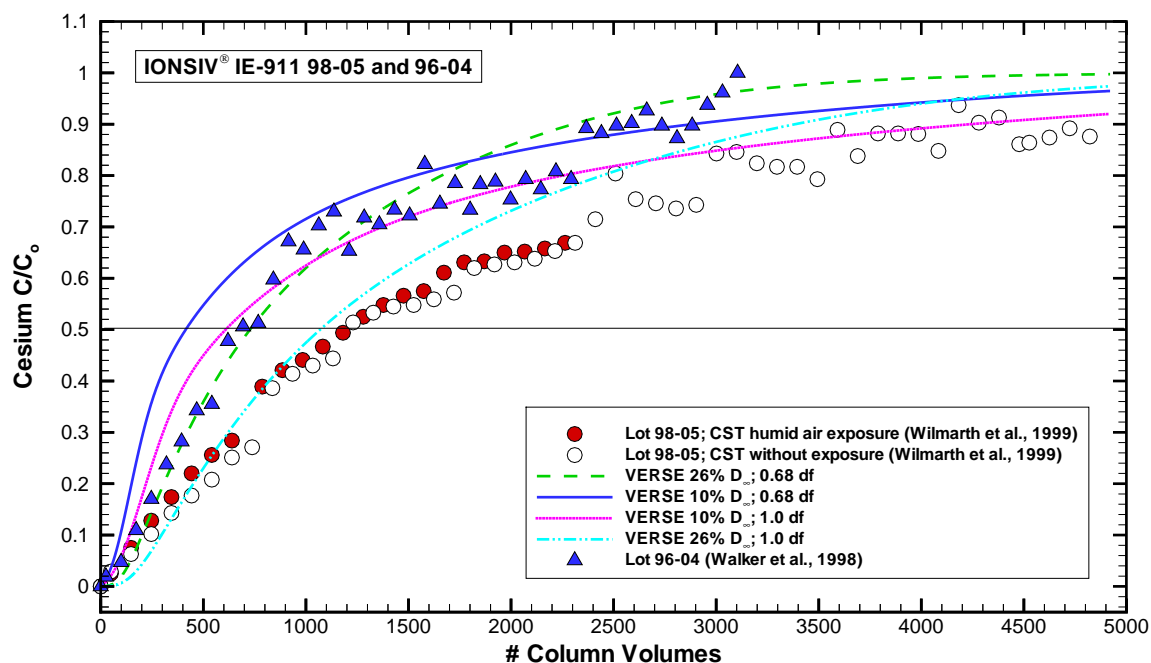


Figure 9-10. VERSE-LC cesium exit breakthrough curve compared to data from Wilmarth et al. (1999) for 98-05 CST material and Walker et al. (1998) for 96-04 CST material:  $D = 1.5$  cm,  $L = 10$  cm,  $U = \sim 4.1$  cm/min,  $T = \sim 25$  °C.

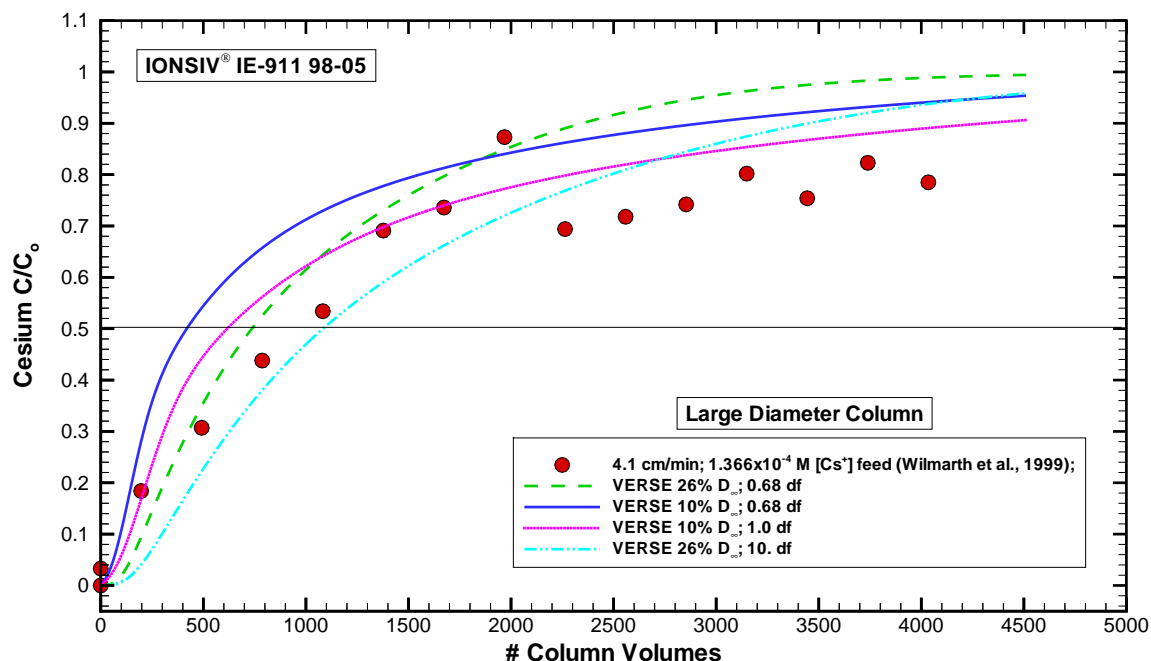


Figure 9-11. VERSE-LC cesium exit breakthrough curve compared to data from SRS-Avg-Test4 (Wilmarth et al., 1999):  $D = 2.5$  cm,  $L = 10$  cm,  $U = 4.1$  cm/min,  $T = \sim 25$  °C.



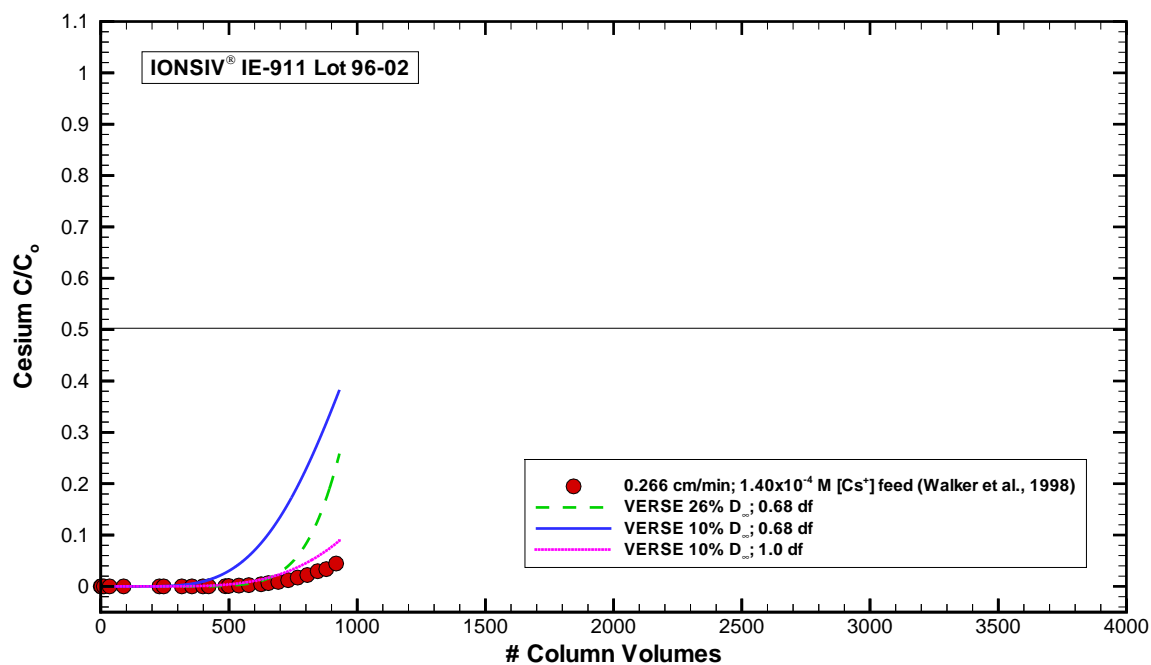


Figure 9-12. VERSE-LC cesium exit breakthrough curve compared to data from SRS-Avg-Test5 (Walker et al., 1998):  $D = 1.5$  cm,  $L = 10$  cm,  $U = 0.47$  cm/min,  $T = \sim 22$  °C.

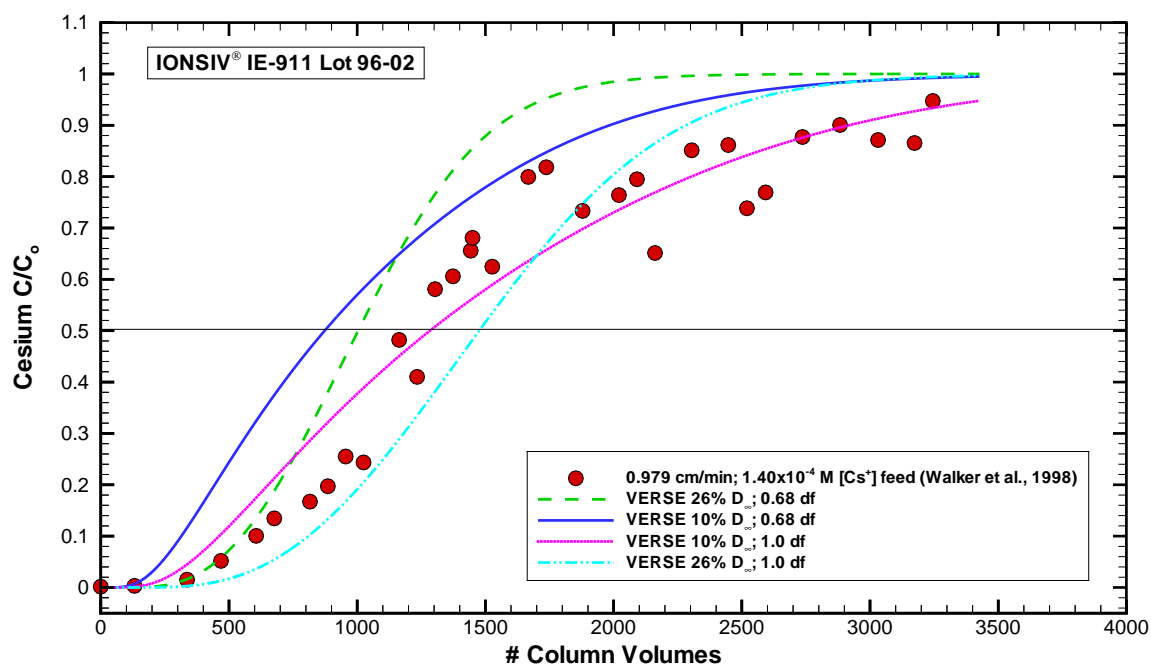


Figure 9-13. VERSE-LC cesium exit breakthrough curve compared to data from SRS-Avg-Test6 (Walker et al., 1998):  $D = 1.5$  cm,  $L = 10$  cm,  $U = 0.98$  cm/min,  $T = \sim 22$  °C.

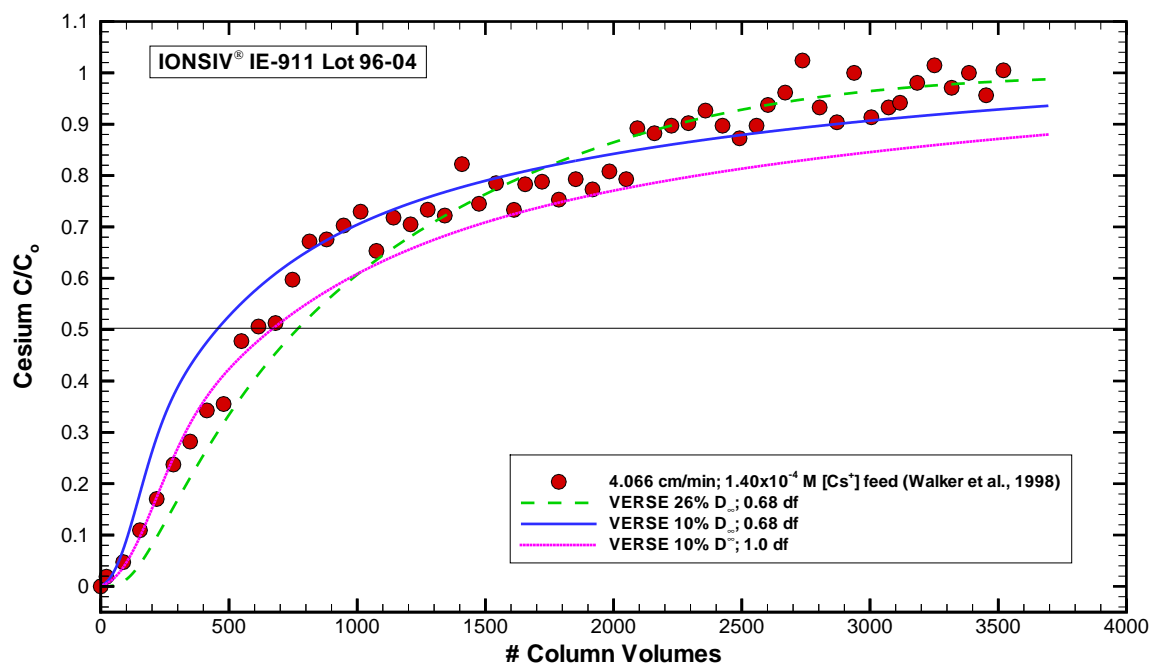


Figure 9-14. VERSE-LC cesium exit breakthrough curve compared to data from SRS-Avg-Test7 (Walker et al., 1998):  $D = 1.43$  cm,  $L = 11$  cm,  $U = 4.1$  cm/min,  $T = \sim 22$  °C.

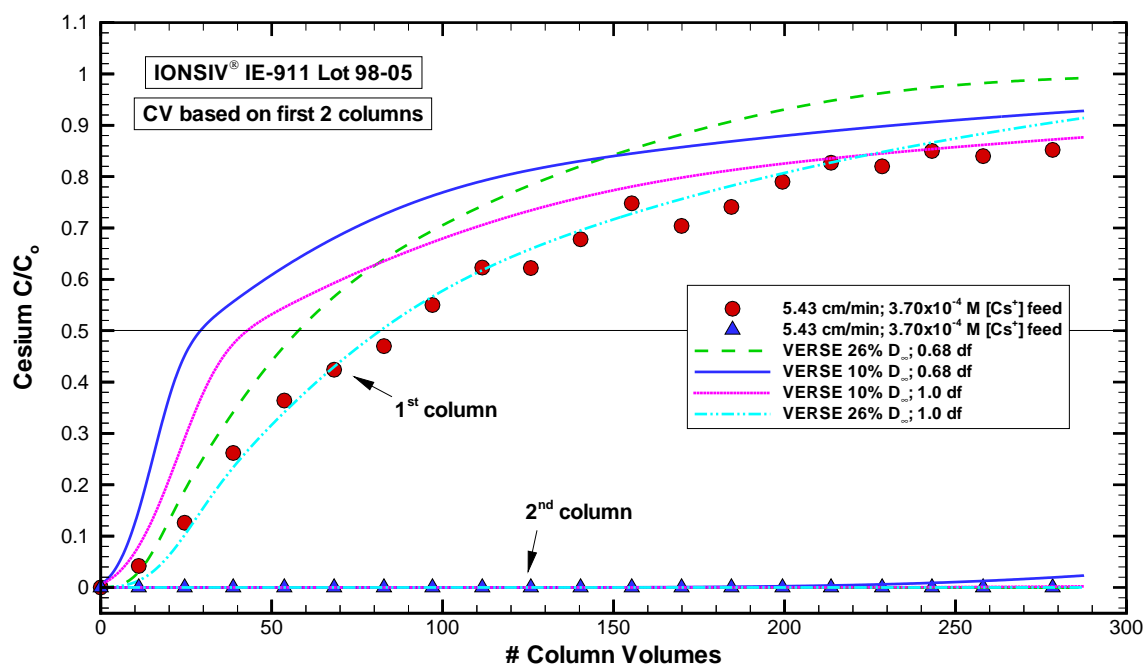


Figure 9-15. VERSE-LC cesium exit breakthrough curve compared to data from SRS-High-OH-Test1 (Walker et al., 1999):  $D = 1.5$  cm,  $L = 10$  cm and 85 cm,  $U = 5.43$  cm/min,  $T = \sim 31$  °C.

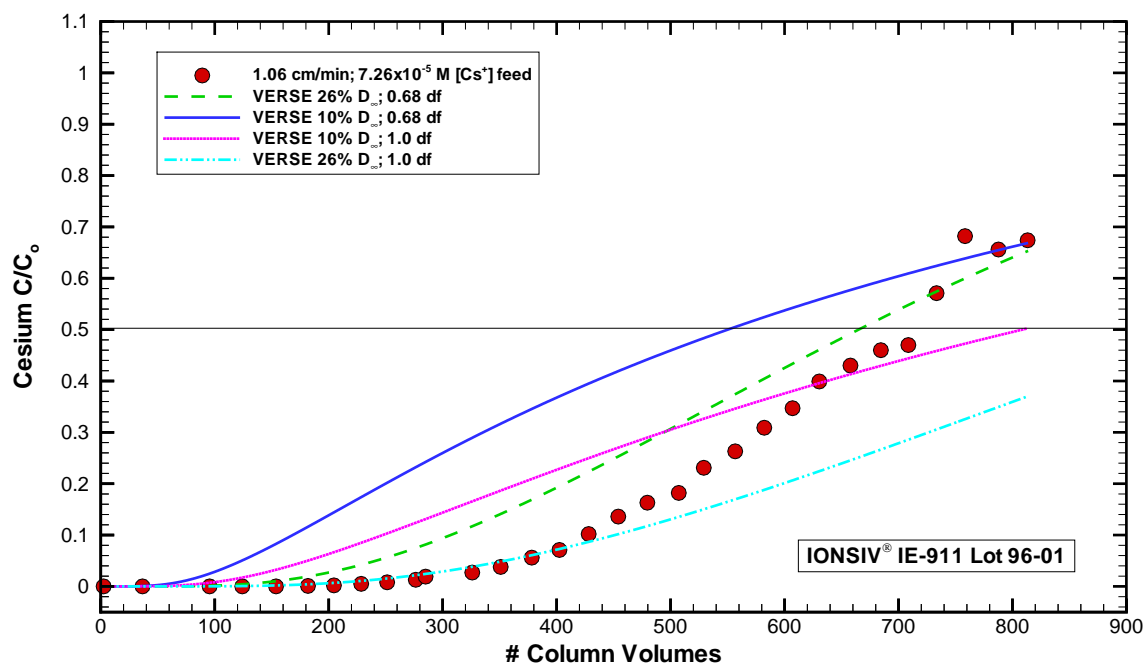


Figure 9-16. VERSE-LC cesium exit breakthrough curve compared to data from PNNL-AW101-Test1 (Hendrickson, 1997): D = 1.5 cm, L = 10 cm and 85 cm, U = 5.43 cm/min, T = ~31 °C.

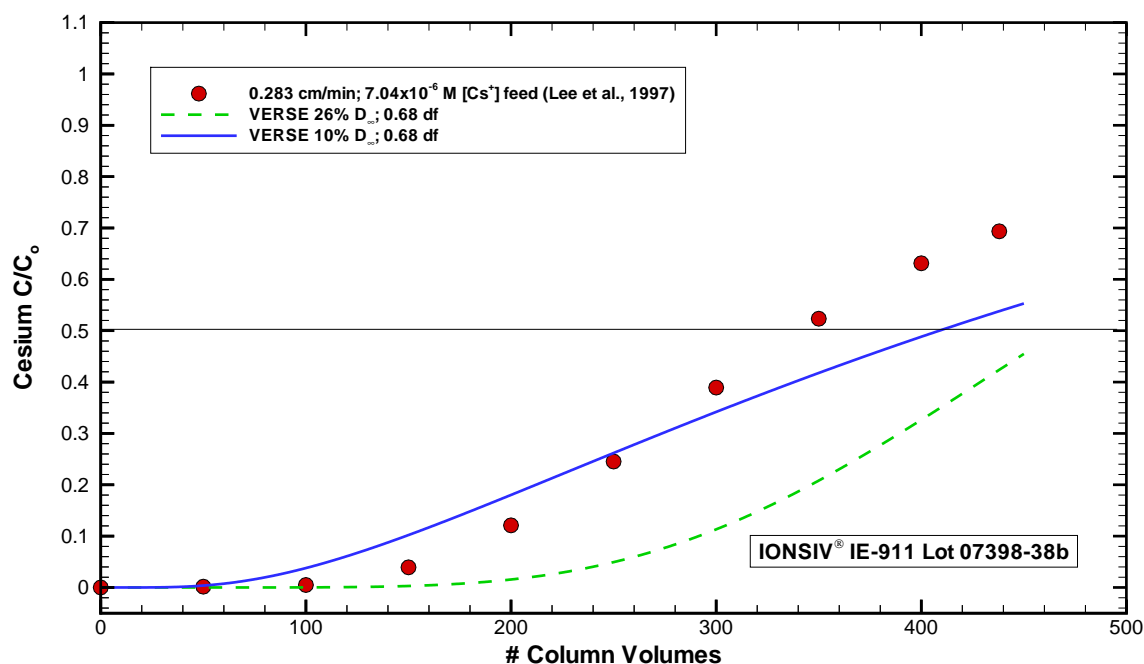


Figure 9-17. VERSE-LC cesium exit breakthrough curve compared to data from ORNL-W27-Test1 (Lee et al., 1997b): D = 1.5 cm, L = 5.659 cm, U = 0.283 cm/min, T = ~25 °C.

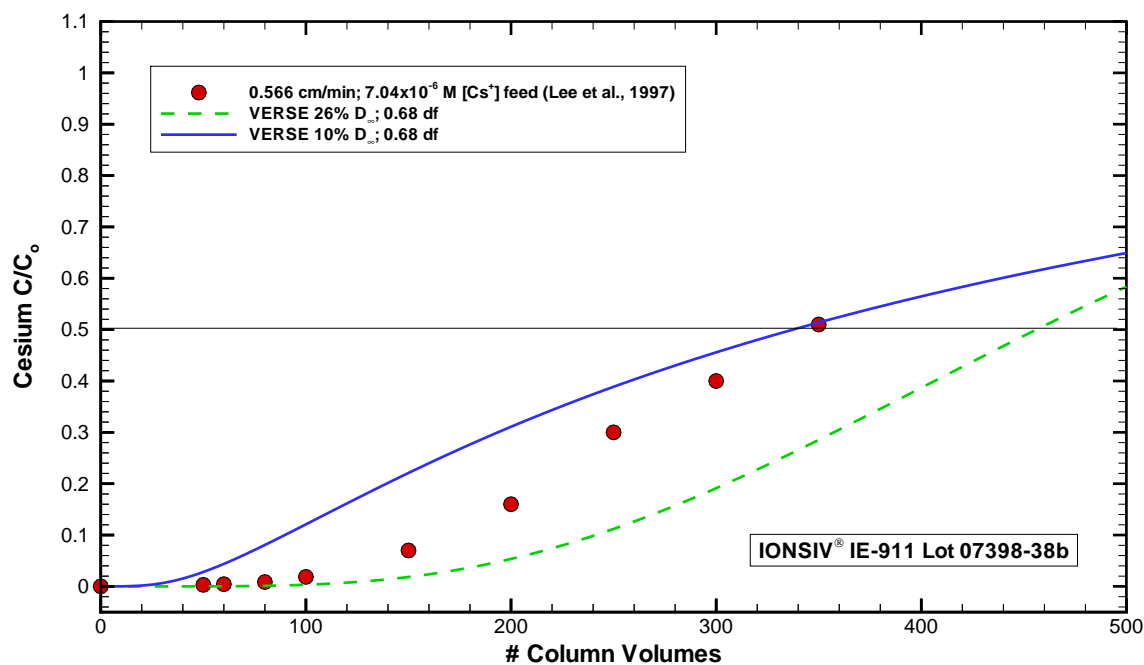


Figure 9-18. VERSE-LC cesium exit breakthrough curve compared to data from ORNL-W27-Test2 (Lee et al., 1997b):  $D = 1.5$  cm,  $L = 5.659$  cm,  $U = 0.566$  cm/min,  $T = \sim 25$  °C.

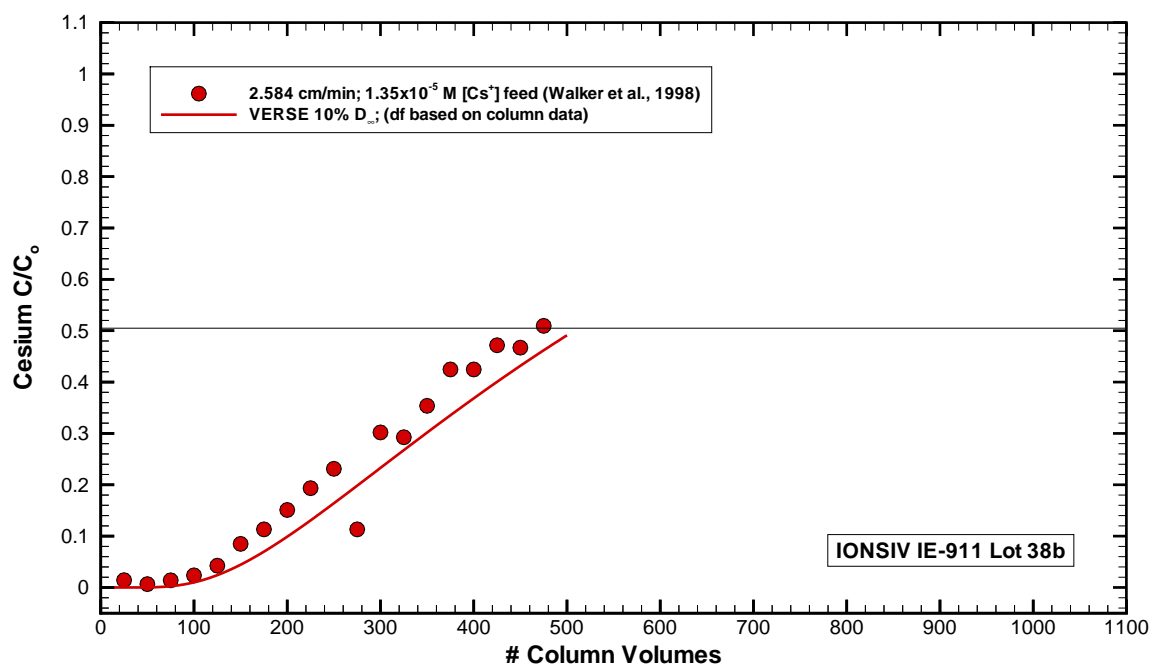


Figure 9-19. VERSE-LC cesium exit breakthrough curve compared to data from ORNL-CsRD-Run2 (Walker, Jr., et al., 1998):  $D = 30.6$  cm,  $L = 51.67$  cm per column,  $U = 2.584$  cm/min,  $T = \sim 25$  °C.

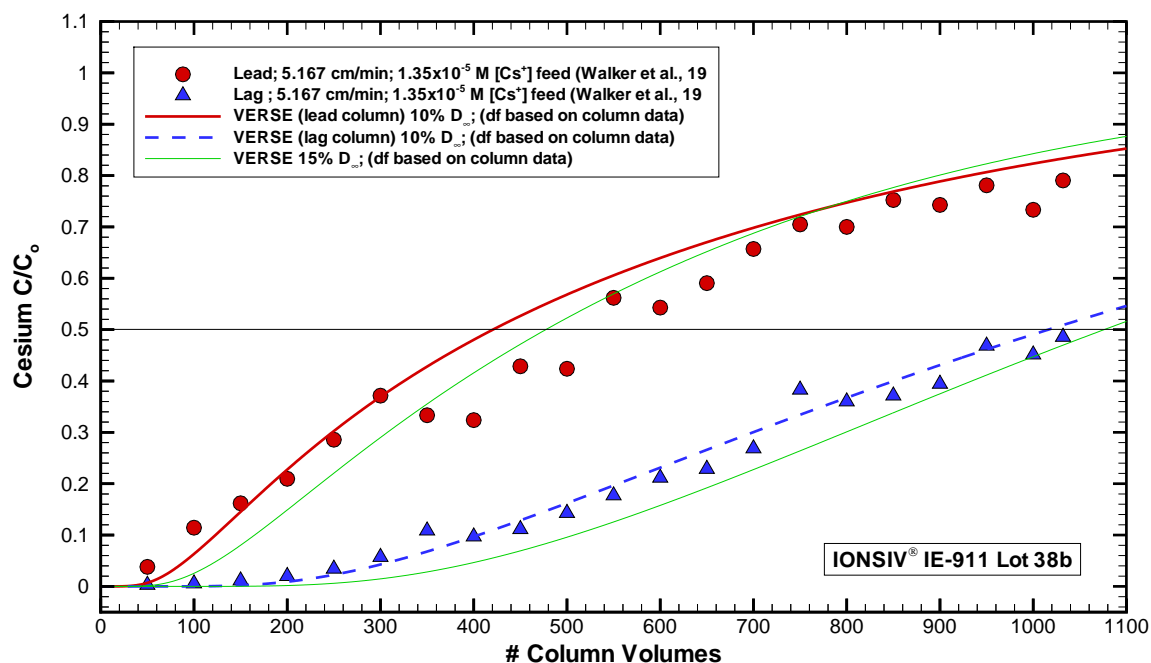


Figure 9-20. VERSE-LC cesium exit breakthrough curve compared to data from ORNL-CsRD-Run3 (Walker, Jr., et al., 1998):  $D = 30.6$  cm,  $L = 51.67$  cm per column,  $U = 5.167$  cm/min,  $T = \sim 25$  °C.

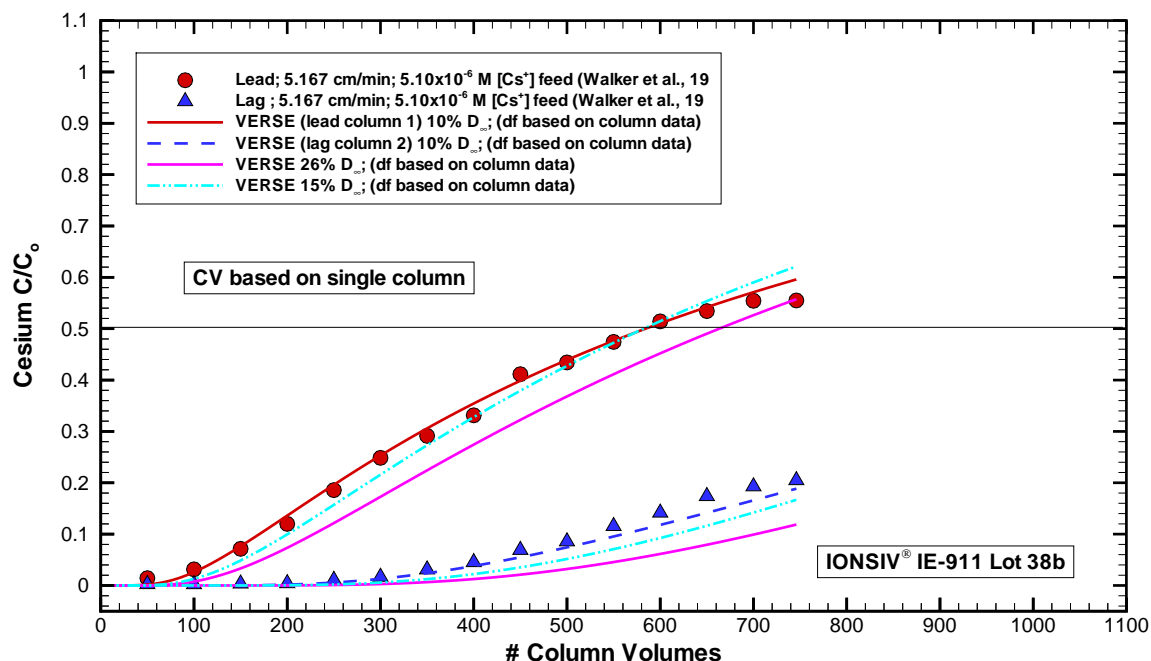


Figure 9-21. VERSE-LC cesium exit breakthrough curve compared to data from ORNL-CsRD-Run4a (Walker, Jr., et al., 1998):  $D = 30.6$  cm,  $L = 51.67$  cm per column,  $U = 5.167$  cm/min,  $T = \sim 25$  °C.

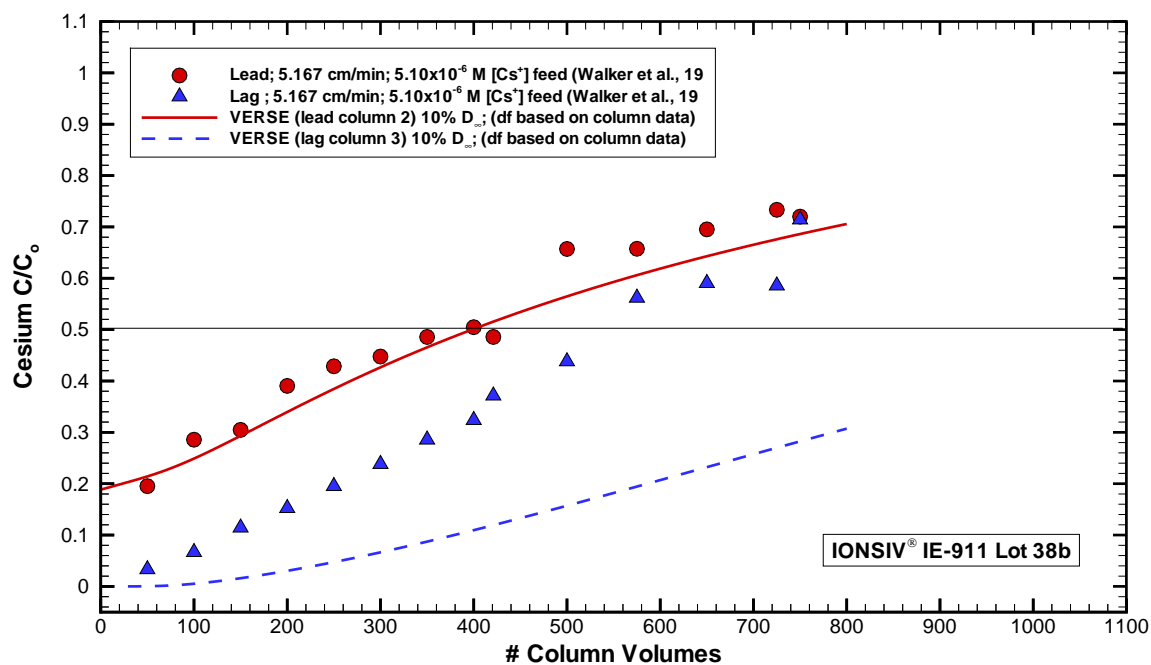


Figure 9-22. VERSE-LC cesium exit breakthrough curve compared to data from ORNL-CsRD-Run4b (Walker, Jr., et al., 1998): D = 30.6 cm, L = 51.67 cm per column, U = 5.167 cm/min, T = ~25 °C.

## 10.0 Full-Scale Column Predictions and Design

Under “nominal” conditions, the predicted performance of a proposed full-scale ion-exchange facility using CST material is discussed in this section. Nominal conditions imply that the majority of parameter settings chosen are our “best estimate” of their values. It is assumed that the majority of properties associated with CST material (e.g., porosities, bed density, and diffusion coefficients) does not vary significantly between batches and can be adequately defined by their averaged behavior. However, due to batch variability observed in the manufacturing of CST material in its engineered-form, a statistically conservative cesium isotherm is used to accommodate the production range of expected CST material. This is accomplished by using a 68% dilution factor.

For column sizing purposes a global optimization strategy is employed where the total amount of spent CST material required to process the entire Phase 1 LAW inventory is minimized. Both 2-column and 3-column carousel configurations are considered, along with a range of possible L/D geometries. All simulations were performed at an operating temperature of 25 C where best estimate feed conditions for the 16 Phase 1 batch feeds in their scheduled order of processing were applied. Based on very limited analyses, variations in the order of batch feed processing had only small impacts on the total computed spent CST required.

The simulations are based on a VERSE-LC model of the lead and lag columns (and guard column for the 3-column configuration) where the parameter settings are consistent with the values used during the assessment of the available laboratory-scale column experiments. The feed concentrations and flowrates chosen are based on the current best estimate of their values consistent with available data and design objectives.

### 10.1 IONSIV® IE-911 CST versus SuperLig® 644 Ion-Exchanger Performance

The CST material is being considered as a potential backup to SuperLig® 644 resin for removal of cesium from the Phase 1 LAW inventory. The two main objectives within this chapter are to (1) determine an optimum column design based on CST that meets the facility’s exit criteria given its input feeds and (2) determine the performance of CST when used in the current facility’s column design. These performance objectives focus only on the loading phase of operation. The broader issues associated with changing over to CST in the overall waste treatment plant (WTP) is not addressed within this report. Since CST is considered to be a non-elutable ion exchange material, the operation within the ion-exchange facility would be impacted, as well as impacts to many other WTP unit operations. Some of the other potential impact issues not addressed are:

- Shielding and heat removal;
- Loaded CST storage;
- Handling and transport;
- HLW glass chemistry;
- Flowsheet compatibility;

- Gas generation and removal; and
- Schedule impact.

The facility's column design as of when these analyses were being performed had an active bed diameter of 77 cm and bed length of 225 cm. This design is ~1000 L in bed volume per column, with a bed L/D of ~2.92. The available headspace above the active bed was designed such that an increased bed height of ~50% was acceptable. This is the design specifications used within this effort for comparison purposes. However, note that more recent design changes now have the bed diameter at 107 cm and the bed height at 119 cm (i.e., an L/D of ~1.1), while the total bed volume remains the same. The shorter columns (i.e., ~50% shorter) help to reduce overall pressure drop concerns, as well as other operational items.

The impact on loading performance (i.e., removal of cesium from LAW streams) of replacing the SuperLig<sup>®</sup> 644 resin with CST material can be qualitatively summarized by comparing some of the key properties of each ion exchanger. A list of key properties for both ion exchangers is provided in Table 10-1. Geometrically, we see that bed porosities are similar which lead to similar superficial velocities within the columns. Since the average particle size of CST IE-911 is about half that of SuperLig<sup>®</sup> 644 and given similar superficial velocities, we would expect the pressure drop across the beds to be approximately double for CST IE-911 versus SuperLig<sup>®</sup> 644. However, experimentally we see that CST IE-911 particles are much more rigid than SuperLig<sup>®</sup> 644 particles. The softer SuperLig<sup>®</sup> 644 particles deform more under applied stresses and can result in significant pressure drops across the beds.

The smaller particle sizes also result in higher bed densities for CST IE-911 (i.e., on average a factor of 5 increase in bed density). This density difference becomes significant when considering the cesium loading capacity of a column. As listed in Table 10-1, the total ionic capacity of CST IE-911 versus SuperLig<sup>®</sup> 644 on a mass basis is very similar. However, when comparing the same amount of exchanger on a bed volume basis, CST IE-911's total capacity is ~6 times that of SuperLig<sup>®</sup> 644. A comparison of cesium loading curves for LAW-12 (AN-103) in contact with CST IE-911 material and SuperLig<sup>®</sup> 644 resin at 25 C is shown in Figure 10-1. The CST IE-911 material curves are based on the algebraic models discussed in section 4, while the SuperLig<sup>®</sup> 644 resin curves were computed using the algebraic model presented by Hamm et al. (2000a). Cesium loading curves on a mass of exchanger and bed volume basis are plotted. The cesium feed concentration for the LAW-12 batch feed is also shown. Over the operating range of interest, the increased cesium loading capacity for CST columns when compared to SuperLig<sup>®</sup> 644 columns is ~30% by mass and ~640% by volume. Basically, CST columns can hold a significantly larger amount of cesium.

The selectivity for Cs<sup>+</sup> cations versus either K<sup>+</sup> or Na<sup>+</sup> cations is very similar between CST IE-911 material and SuperLig<sup>®</sup> 644 resin, as shown in Table 10-1. Again, the ionic capacity of CST IE-911 material is much larger when compared on a bed volume basis.

With respect to column "kinetics" (i.e., mass transfer rates), pore diffusion within the CST IE-911 particles is ~3.5 times slower than for SuperLig<sup>®</sup> 644 particles. The slower kinetics of CST



IE-911 material increases its sensitivity to changes in feed flowrate. This in turn impacts the “Mass Transfer Zone (MTZ)” length, which will be further discussed in a subsection below.

To see the overall impact in loading performance of replacing SuperLig<sup>®</sup> 644 resin with CST IE-911 material, two VERSE-LC simulations were performed where the only difference between the two simulations was the ion-exchange material chosen. The two simulations are based on the current ion-exchange facility column design and under its 2-column carousel configuration operating at 25 C (i.e., 1000 L column beds, bed L/D of ~3). The cesium isotherms shown in Figure 10-1 were used that represent the isotherms for LAW-12 feed (AN-103). The same feed cesium concentration, flowrate, and exit criteria were employed. A comparison of the lead columns exit breakthrough curves is plotted in Figure 10-2 (i.e., the plain solid-curve representing CST IE-911 packed columns and the solid-curve with solid circles representing SuperLig<sup>®</sup> 644 packed columns). The number of column (i.e., “bed”) volumes (CV) of feed that can be processed prior to reaching the cesium exit criterion is ~270 CV for SuperLig<sup>®</sup> 644 columns and ~720 CV for CST IE-911 columns. The degree of cesium loading on the lead columns (i.e., percent of saturation) is ~40% for SuperLig<sup>®</sup> 644 columns and ~20% for CST IE-911 columns. Some of the key properties associated with each exchanger, as discussed above and listed in Table 10-1, can be seen in Figure 10-2. The greater capacity of the CST IE-911 packed columns allow them to process more feed solution, while reduced kinetics of the CST IE-911 packed columns limit the level of cesium loading achieved prior to cycling (i.e., reaching the exit cesium criterion).

## 10.2 Basic Flowsheet

The basic flowsheet for the full-scale ion-exchange columns is shown in Figure 10-1 for a 2-column carousel configuration. The key parameters defining the full-scale facility are provided in Tables D-2 and D-3 for the Phase 1 LAW inventory. Two identically sized columns in series (i.e., a lead and a lag column) are used where an exit cesium concentration criterion (i.e., an envelope dependent value) is imposed on the lag column. Each column has a void headspace that is approximately the same size as each column. Prior to loading both columns are pretreated and contain an aqueous native solution with an ionic strength of approximately 0.25 M sodium (i.e., essentially zero cesium and potassium are present). During the loading phase the feed solution’s ionic strength increases significantly to approximately 5 M sodium and 0 to 1 M potassium. Inlet feed concentration of cesium can vary from 0 to  $5 \times 10^{-4}$  M. A design flowrate of ~3 CV/hr is used during the cesium loading phase. Upon reaching the lag column exit concentration criterion, the cesium loading phase is terminated and for subsequent loading cycles the lag column is placed in the lead column position with a fresh column being placed in the lag position. For SuperLig<sup>®</sup> 644 packed columns the loaded lead column is eluted and pretreated for future use, while for CST IE-911 packed columns the loaded lead column is stored for future disposal. Fresh column implies a cesium free bed. It is assumed that the isotopic feed concentrations of total cesium is made up of <sup>137</sup>Cs and <sup>133</sup>Cs, where their isotopic fractions are envelope dependent.

The cesium, potassium, and sodium concentration profiles along the column train varies with time. Due to the significant selectivity for cesium by SuperLig<sup>®</sup> 644 resin or by CST IE-911

material, the column exit breakthrough for potassium and sodium occurs very early (i.e., within 5-10 column volumes) with cesium's breakthrough significantly retarded. Key concentration points along the facility are numbered from 0 through 4 as shown in Figure 10-1. The inlet conditions correspond to point 0 while the exit product criterion is imposed at point 4. Points 1 and 3 represent the locations where the headspace ends and the active bed begins.

A similar discuss applies for 3-column carousel operation where the first column in series is referred to as the lead column, the second column as the middle column, and the third column as the lag column.

### 10.3 VERSE-LC Modeling of the Full-Scale Facility

The VERSE-LC model representing the full-scale flowsheet is shown in Figure 10-2 for both the 2-column and 3-column carousel configurations. To model the full-scale facility using VERSE-LC the headspaces are considered to be continuous stirred tank reactors (CSTRs). In these CSTRs perfect mixing is assumed where no chemical reactions are taking place. During a VERSE-LC 2-column configuration simulation exit breakthrough curves at points 2 and 4 are generated (and point 6 for 3-column configuration simulations) along with concentration profiles over both columns at key points in time.

Since the selectivity for  $\text{Cs}^+$  is two orders in magnitude greater than either competitor of interest (i.e.,  $\text{K}^+$  or  $\text{Na}^+$ , see Table 10-1), the "effective" single component cesium system is acceptable for transport analysis. The VERSE-LC input parameters are listed for the 11 Envelope A batch feeds, 2 Envelope B batch feeds, and 3 Envelope C batch feeds (i.e., nominal case studies) in Tables D-2 and D-3 of Appendix D. The VERSE-LC input files for typical (nominal) runs are also provided in Appendix D.

During the loading phase for modeling purposes time invariant flowrate and inlet feed conditions are assumed for each LAW batch feed. For one specified carousel configuration and input parameter settings, to compute the total amount of spent CST requires running VERSE-LC 16 times (i.e., once for each batch feed) in sequence. The cesium concentration profiles within the columns (i.e., in the fluid and on the solid) at the end of processing each batch feed are stored and are used as the initial state of the carousel for processing the next batch feed. To automate this process of handling many VERSE-LC runs and I/O files in series, a make utility called "NMAKE" was used. See Appendix D for further discussion on the use of NMAKE for this application.

#### 10.3.1 Volumetric Flowrate on an Envelope Basis

The volumetric flowrate of the LAW stream passing through the ion-exchange facility during the loading phase is envelope dependent. The maximum loadings for waste sodium oxide currently planned for ILAW glass forms are provided in Table 10-2. The flowrates used in the VERSE-LC design calculations are listed in Table 10-3 for the 16 batch feeds. The basis for the flowrates centers on the production goals of glass and the allowable limits of waste sodium oxide ( $\text{Na}_2\text{O}$ ) loading within the glass matrix. Below the basis for each envelope is discussed.

### **Envelope A:**

The maximum waste sodium oxide loading currently planned for LAW Envelope A waste solutions is ~19.6 wt%. In order to support production of 60 MT/day of ILAW glass that contains 19.56 wt% sodium oxide, 8.71 MT/day of sodium must be feed to the ILAW melters. Assuming the LAW feed solution to the cesium ion exchange process is a 5 M sodium solution, the volume of LAW processed through the Cs ion exchange process must be ~75,773 L/day (52.62 L/min) to support the ILAW glass production rate.

### **Envelope B:**

The LAW Envelope B wastes contained in tanks 241-AZ-101 and 241-AZ-102 will be processed during the first ten years of operation at the RPP-WTP. During the first ten years of operation, the ILAW glass production rate is nominally 30 MT/day. The maximum waste sodium oxide loading currently planned for LAW Envelope B waste solutions is 7.0 wt%. In order to support production of 30 MT/day of ILAW glass that contains 7.0 wt% sodium oxide, 1.56 MT/day of sodium must be feed to the ILAW melters. Assuming the LAW feed solution to the cesium ion exchange process is a 5 M sodium solution, the volume of LAW processed through the Cs ion exchange process must be ~13,536 L/day (9.40 L/min) to support the ILAW glass production rate.

After processing the AZ-101 and AZ-102 supernates, the RPP-WTP will receive other Envelope B solutions that will need to be processed at a rate to support production of 60 MT/day ILAW glass. However, these other Envelope B solutions will not contain the relatively high concentration of cesium that is present in the AZ-101 and AZ-102 supernates. Future Envelope B solutions will have cesium, sodium, and potassium concentrations similar to Envelope A solutions.

### **Envelope C:**

The LAW Envelope C wastes contained in tanks 241-AN-102 and 241-AN-107 will be processed during the first ten years of operation at the RPP-WTP. During the first ten years of operation, the ILAW glass production rate is nominally 30 MT/day. The maximum waste sodium oxide loading currently planned for LAW Envelope C waste solutions is 12.0 wt%. In order to support production of 30 MT/day of ILAW glass that contains 12.0 wt% sodium oxide, 2.68 MT/day of sodium must be feed to the ILAW melters. Assuming the LAW feed solution to the cesium ion exchange process is a 5 M sodium solution, the volume of LAW processed through the Cs ion exchange process must be ~23,328 L/day (16.2 L/min) to support the ILAW glass production rate.

## **10.3.2 Cesium-137 Exit Concentration Criterion on an Envelope Basis**

The LAW stream exiting the ion-exchange facility during the loading phase has a  $^{137}\text{Cs}$  concentration criterion that is envelope dependent. Based on a  $^{137}\text{Cs}$  content not to exceed 0.3 Ci/m<sup>3</sup> for the glass product made from the ILAW melters, overall (i.e. bucket) average cesium concentrations in the LAW exiting stream can be computed for each envelope. Based on the maximum allowable waste sodium oxide content of the glass and the 0.3 Ci/m<sup>3</sup> limit of  $^{137}\text{Cs}$  within the glass product,  $^{137}\text{Cs}$  exit criterion can be computed on a Ci/gmole of sodium basis. Table 10-2 lists these values, along with the values based on a 5 M sodium feed solution in terms

of  $\mu\text{Ci/ml}$ . To convert these  $^{137}\text{Cs}$  exit criteria values into total Cs concentration limits, assumed isotopic fractions of  $^{137}\text{Cs}$  to total cesium are used (i.e., for calculational purposes the total Cs is assumed to be made up of  $^{133}\text{Cs}$  and  $^{137}\text{Cs}$  isotopes only). The isotopic fractions assumed for each envelope waste stream is listed in Table 10-2. For each envelope the total cesium exit concentration criterion computed is listed in Table 10-4, where the normalized to the inlet feed concentration is also provided on a batch feed basis.

These exit concentration criteria place limits on the cumulative cesium concentration of the effluent exiting the ion-exchange facility (i.e., the “bucket” average value), not on the instantaneous values during its operation. To perform the carousel operation in an automatic fashion within the VERSE-LC simulations, we impose these cumulative concentration criteria on the VERSE-LC computed instantaneous exit concentrations. No accounting for integration of the breakthrough curve is made. This represents an embedded conservatism within the analysis methodology used.

### 10.3.3 Input Concentration and Flowrate Boundary Conditions

The scheduled sequence of batch feeds is listed in Table 10-3 along with the source tank that it originated from. The volumetric flowrates chosen are envelope dependent. The volumetric flowrates are based on the Phase 1 30 MT/day operation schedule for Envelopes B and C and on the expanded capability (beyond Phase 1) of 60 MT/day operation for Envelope A, as discussed above. Using these flowrates and the estimated solution volumes of each batch feed, batch-processing times were computed and are also provided in Table 10-3. With these batch processing times, time dependent inlet cesium concentration and flowrate boundary conditions for use in VERSE-LC simulations were generated (i.e., note that these boundary conditions are stationary values within a given batch feed, but step change between the batch feeds). These boundary conditions are shown in the barchart plotted in Figure 10-5. The total process time required to process the entire Phase 1 inventory is  $\sim 4.2$  years of operation. If the Envelope A feeds are processed at the lower 30 MT/day glass production rate, then the total process time becomes  $\sim 5.8$  years.

## 10.4 Mass Transfer Zone Concept for Column Design

One approach typically used to size ion-exchange columns is based on the mass transfer zone (MTZ) concept. As discussed in Helfferich and Carr (1993), wave theory indicates that for ion-exchange processes under favorable isotherm conditions the shape of the axial concentration profile becomes stationary at long distances down the column. Axial dispersion tends to spread the profile out, while a favorable isotherm tends to sharpen the profile. These two forces become balanced at sufficiently long distances down a column. The stationary shape is an asymptote that is only approached for finite size columns, where the practical distance required is a function of how nonlinear the isotherm is over its operating range.

The approach is based on the following key assumptions:

- Constant inlet feed conditions (concentration  $c_0$ , flowrate  $Q_0$ , and temperature  $T_0$ );

- Stationary profile achieved within practical lengths;
- Length of MTZ based on stationary conc. profile; and
- Insensitive to carousel process (i.e., cycle number).

For application to a specific carousel configuration (e.g., 2-column case), a lag column exit concentration criterion and a lead column loading criterion must be established. For a conservative design a worst case isotherm must also be chosen where the inlet flowrate and concentration become time invariant. Given these items the length of the MTZ can be estimated as shown by the cartoon illustrated in Figure 10-6. The breakthrough curve shown in Figure 10-6 represents the stationary concentration profile obtained at long distances down a single virtual column. The downstream half of the MTZ length is established by the criteria chosen, where it is assumed that finite profile development length and carousel cycling have a negligible impact.

To estimate the MTZ length for CST packed columns processing Phase 1 LAW solutions, three VERSE-LC column transport simulations were run based on a long single column (i.e., actual runs were performed using a 2000L 2-column carousel arrangement with cycling turned off). The three feed solutions chosen are LAW-1 (Envelope A, AP-101), LAW-2a (Envelope B, AZ-101), and LAW-3 (Envelope C, AN-102). All three LAW feeds have potential worst case isotherms for their respective envelopes.

The normalized axial cesium concentration profile at a point in time prior to when the exit criterion would have been exceeded is plotted in Figure 10-7 for each feed solution. As Figure 10-7 indicates, the MTZ length for each envelope is quite different. Based on this design strategy, the longest MTZ length would be specified (i.e., value corresponding to Envelope A feed). The large differences in MTZ length observed are a direct result of (1) higher flowrates tend to spread out the axial profile, while (2) higher inlet concentrations tend to sharpen the axial profile (i.e., more nonlinear behavior operative).

Based on the envelope dependent results shown in Figure 10-7 and variability seen in isotherms within a given envelope, the MTZ design approach was abandoned. In its place a global optimization strategy was chosen which can directly account for variability of flowrate, feed concentration, and isotherm behavior among the 16 Phase 1 LAW batch feeds. This strategy is recommended for future SuperLig<sup>®</sup> 644 and 639 modeling efforts, too.

## 10.5 The Global Optimization Strategy

To design a CST based ion-exchange facility operating in a carousel manner, the traditional MTZ approach discussed above appeared to be inadequate. The inadequacies were primarily:

- A fairly long virtual column was required to establish a stationary profile, which weakens the assumptions of negligible impact due to finite length columns and carousel cycling; and
- Significant flowrate, feed concentration, exit criterion, and isotherm variability exists between the 16 LAW batch feeds, which make it difficult to obtain a unique worst case scenario for designing to.

To eliminate these difficulties, a global optimization strategy based on simulating the entire processing of the Phase 1 inventory in its schedule sequence was undertaken. Here, the analysis approach chosen is primarily based on “best estimate” parameter values; however, the chosen isotherms for each batch feed are based on a dilution factor of 68% to account of the variability observed in the production of CST in its engineered-form.

The assumption is made that once a batch feed has been completely processed, the next batch feed scheduled will begin without starting with fresh columns (i.e., the batch feeds are stacked inline where the carousel cycling only occurs when the exit lag column criterion is reached). The optimization parameter that was chosen to be tracked is the amount of spent CST material used to process each batch feed. Since the original basic concern was over the amount of CST ultimately having to be placed in the glass product, this appeared to be the obvious choice for our optimization parameter.

The carousel operations are discrete events that take place when the exit cesium concentration reaches its criterion at the exit of a lag column. Initially, both the first lead and lag columns are cesium free. Upon reaching the point where the last drop of LAW feed within the inventory is processed, the process is stopped. At this point both the lead and lag columns present are partially loaded, but contributed as full columns to the total spent CST required. In this way, the computed total spent CST becomes a discrete value based on the number of cycles required.

Based on this concept, the total amount of spent CST material required to process the entire Phase 1 LAW inventory can be computed by:

$$m_{\text{CST}} = \rho_{\text{bed}} V_{\text{bed}} (n_{\text{carousel}} + n_{\text{cycles}}) \quad , \quad (10-1)$$

where the bed density is in terms of g/ml (i.e., an average value of 1.0 g/ml is used), the bed volume per column is given in liters (i.e., this is the key variable for optimization),  $n_{\text{carousel}}$  is the number of columns within a carousel (i.e., 2-column or 3-column arrangements), and  $n_{\text{cycles}}$  is the total number of carousel cycles required. The total number of columns given in Eq. (10-1) has two terms since the carousel initially starts out with  $n_{\text{carousel}}$  fresh columns and then adds one new column to the carousel every cycle.

As demonstrated in a following subsection for CST packed columns, variation in the bed L/D geometry, while holding the bed volume of a column constant, has very little impact on spent CST material based on its computed value using Eq. (10-1). Therefore, the spent CST value is a discrete variable that depends primarily on the bed volume of a column. In this way, we are addressing approximately a single-variable optimization problem.

## 10.6 Theoretical Minimum Spent CST Material

A theoretical minimum in spent CST material can be computed based on the assumption that for each batch feed variably sized columns are available that become fully loaded (i.e., saturated) with respect to the feed’s cesium concentration. For the  $i^{\text{th}}$  batch the maximum CST loading for cesium ( $\text{mmole}_{\text{Cs}}/\text{g}_{\text{CST}}$ ) can be computed based on the cesium isotherm and its cesium inlet concentration using:

$$Q_{Cs,i} = \frac{\eta_{df} \bar{C}_T c_{Cs,i}}{c_{Cs,i} + \beta_i} \quad (10-2)$$

The amount of total cesium present within a given batch feed can be expressed in units of  $\text{mmole}_{Cs}$  as:

$$n_{Cs,i} = 1000 c_{Cs,i} V_i \quad (10-3)$$

Using Eqs. (10-2) and (10-3), the theoretical minimum in spent CST material (kg) for each batch feed becomes:

$$m_{CST,i} = \frac{c_{Cs,i} V_i}{Q_{Cs,i}} \quad (10-4)$$

where the total amount of spent CST material then becomes:

$$m_{CST} = \sum_{i=1}^{16} \left[ \frac{c_{Cs,i} V_i}{Q_{Cs,i}} \right] \quad (10-5)$$

For the 16 batch feeds contained within Phase 1, the theoretical minimum amount of spent CST was computed to be 55,360 kg and is tabulated in Table 10-5. This value is useful for seeing how efficient a given actual column design might be and is plotted as a dashed-horizontal line in the various spent CST figures to be addressed below.

## 10.7 Spent CST Material Dependency on Geometry

Within a given carousel design, each column is geometrically the same (i.e., the same volume and shape). The two key geometric parameters that define a unique column design are its bed volume and length-to-diameter ratio (L/D). For loading phase considerations, to a much lesser extent the headspace volume above the bed is also needed. The length, L, referred to above represents the height of the active resin bed during the 5 M sodium loading phase.

From a theoretical perspective for fixed boundary conditions (i.e., feed composition and volumetric flowrate), we find that the performance of a column during the loading phase depends upon the overall mass transfer in a unique way. The overall mass transfer limitations result from two components: (1) mass transfer resistance across the liquid film present at each particle's outer surface and (2) mass transfer resistance due to diffusion through each particle's pores. For a fixed volumetric flowrate and bed volume design, when varying the cross-sectional area of the column (i.e., its diameter) varies the bed's liquid superficial velocity. The superficial velocity only impacts the mass transfer film coefficient, not the pore diffusivity coefficient.

For CST IE-911 material we find that the overall mass transfer resistance is dominated by pore diffusion, while the resistance due to film diffusion is relatively negligible under the range of flowing conditions of importance in CST column design here. Given this information, we would

expect that the estimated amount of spent CST required to process the entire Phase 1 LAW inventory would be insensitive to geometric variations such as L/D.

To confirm this expected insensitivity to L/D, VERSE-LC simulations were run for L/D values of 1, 2, 3, 4, and 5. The entire Phase 1 LAW inventory was processed in these simulations. Other than the changes in geometry, all other input parameters were kept at their nominal settings (e.g., 25 C operation, 2-column carousel configuration, 2000 L bed column size, 500 L head-space). The results of these five simulation runs are tabulated in Table 10-6. For each L/D test case Table 10-6 provides the column geometry considered, the number of process cycles occurring during each batch feed, the total number of process cycles required, and the total amount of spent CST material required to process the entire Phase 1 LAW inventory. The total amount of spent CST is computed based on the number of cycles required (plus 2 to account for the 2-column configuration and startup), the bed density of the CST material, and the bed volume of a column. These results are also shown in Figure 10-8 where we see that the computed spent CST is very insensitive to L/D.

The degree of sensitivity resulting from the L/D variations considered, is less than the amount required to cause a change in the total number of cycles required. Therefore, as shown in Table 10-6 and in Figure 10-8 no effect on spent CST is observed.

Given the fact that the estimated amount of spent CST required to process the entire Phase 1 LAW inventory is insensitive to variations in L/D (i.e., under constant bed volume conditions), from a design perspective the L/D can be established based on other design considerations (e.g., based on required superficial velocity to sweep out gas bubbles). In the various simulations to be discussed below, typically a L/D=3 is studied; however, for convenience in some cases the L/D is varied (i.e. L/D=2 for most of the 3-column carousel cases).

In the various VERSE-LC design simulations performed, the geometry of each column design considered was computed based on the following approach. For the 2-column carousel cases a total bed volume for the column design and a L/D are specified. Given these two values the diameter, then length, of the column design can be computed using:

$$D_{\text{bed}} = \sqrt[3]{\frac{4V_{\text{bed}}}{\pi\left(\frac{L}{D}\right)}} , \quad (10-6)$$

and

$$L_{\text{bed}} = \left(\frac{L}{D}\right)D_{\text{bed}} . \quad (10-7)$$

For the 3-column carousel designs that are used for direct comparison to their 2-column design counterparts, the total bed volume and computed bed diameter based on Eq. (10-6) above is used. The bed length then becomes two-thirds of the 2-column bed length based on Eq. (10-7). In this way, when comparing a 2-column versus a 3-column carousel configuration, we are looking only at how many subdivisions are being made in a total bed (i.e., both have the same



bed diameter and total bed length). Application of the above approach over a range of column volumes and L/D ratios were considered. For the 2-column carousel configurations considered, the resulting geometries are listed in Table 10-7. Table 10-8 contains the geometries considered for the 3-column carousel configurations.

## **10.8 CST Column Design and Performance**

Numerous VERSE-LC simulations were run in order to study the behavior of CST packed column operating in a carousel fashion and to provide results for establishing a base design. All of the VERSE-LC simulations were performed at 25 C. Both 2-column and 3-column carousel configurations are addressed, where for design purposes a range of potential column volumes was considered. The parameter settings provided in Tables D-2 and D-3 represent our nominal conditions for each batch feed (e.g., at dilution factor of 68% and a cesium pore diffusivity coefficient of 20% of its free diffusion value). Sensitivity studies were performed to estimate the impact that potentially “slow kinetics” might have on the performance of a given design. The results of these simulations are discussed below.

### **10.8.1 Nominal Case Results for 2-Column Carousels**

Under nominal parameter settings, numerous VERSE-LC simulations were performed where the bed volume of a column was varied from 500 L up to 9,000 L. The dilution factor was set to 68% and the cesium pore diffusivity coefficient was set to 20% of its free diffusion value. Both 2-column and some limited 3-column carousel were considered. These nominal case runs were performed to study the loading behavior of a CST packed column carousel and to estimate a near optimal design size.

The cases where the column volume was set to 1000 L and with a L/D=3 represent runs that demonstrate the CST performance when used in the current ion-exchange facility design based on the SuperLig<sup>®</sup> 644 packed columns. For a 2-column carousel configuration the cesium breakthrough curve at history point 2 in Figure 10-4 is plotted in Figure 10-9. The lead column's cesium concentration is plotted versus process time in months for the entire processing period required to process the entire Phase 1 LAW inventory. Also shown in Figure 10-9 are slightly shaded vertical lines that segregate out the individual batch feed processing periods. At the top of the xy frame each batch feed operating period has been labeled. During the processing numerous carousel cycles were performed within each of the 16 batch feed periods. The point in time where a carousel cycle is performed can clearly be seen by the sudden drop to near zero cesium concentration. The actual number of carousel cycles performed per batch feed is tabulated in Table 10-9. The total number of cycles (78) and the total amount of spent CST material required (80,000 kg = 80 MT) are also listed in Table 10-9.

As Figure 10-9 illustrates, the high cesium feed concentrations of the Envelope B LAW feeds have a profound impact on cesium concentrations throughout the carousel well beyond their process periods. Plotting this breakthrough curve in its normalized form (i.e., exit cesium concentration divided by the current inlet feed value), one can better see the impact. In Figure 10-10 the normalized breakthrough curve is plotted where the percentage of column loading can be quickly approximately determined. For the Envelope A feeds the lead columns are ~20%

upon cycling, while for Envelope B feeds the lead columns are ~100% loaded. For the LAW-3 and LAW-4 Envelope C feeds we see them experiencing loadings greater than 100% based on their inlet feed concentrations, with final loadings of ~80%.

For example, during the processing of LAW-3 cesium that was originally stored during LAW-2b is being redistributed from the lead column to the lag column for several carousel cycles. This represents loading and unloading of the ion exchange material where in the VERSE-LC model used we are assuming that:

- The ion exchange isotherm is unique and truly represents the solid-liquid equilibrium state regardless of which side it is being approached from; and
- The mass transfer resistances within the CST particles are not directionally dependent, such that incoming and outgoing pore diffusion rates are the same if the same concentration gradient in each direction were applied.

Limited experimental data exist indicated that the isotherms are probably unique, at least for CST material that has not been heated up to significantly. It is suspected that the diffusion rate leaving the CST particles will be much slower than entering. Under these conditions the assumption of similar rates is conservative.

The cesium breakthrough curves at history point 2 in Figure 10-4 are also plotted for three other larger column designs (i.e., 2000 L, 3000 L, and 4000 L). The breakthrough curve pairs (i.e., concentration and then its normalized value) for the 2000 L case are shown in Figures 10-11 and 10-12. The breakthrough curves for the 3000 L case are shown in Figures 10-13 and 10-14. The breakthrough curves for the 4000 L case are shown in Figures 10-15 and 10-16. The effect of going to increased column volumes beyond the current facility design can clearly be seen in these plots. As one would expect, as the column volume is increased the total number of process cycles drops and lead column loadings rise. For example, when looking at the 4000 L column volume case shown in Figure 10-16, lead column loadings for Envelope A, B, and C feeds are ~70%, ~100%, and +100%, respectively.

The number of carousel cycles and spent CST required for these cases and several other volumes considered are tabulated in Table 10-9. The spent CST results listed in Table 10-9 are plotted in Figure 10-17. Theoretically, the minimum amount of CST required would correspond to the column size where the lag column exit criterion is reached just when the last drop of feed inventory enters the lead column (i.e., just prior to the need to perform the first carousel operation resulting only in a total of two columns used). Note that this minimum point is much greater than the upper limit plotted of 9000 L. For columns larger than this the two columns would be under-loaded. For smaller columns the carousel process occurs at increasing frequency also resulting in reduced loading. The oscillation seen in the data is due to the discrete nature of the computed spent CST required. If numerous data points were to be plotted in Figure 10-17, we would see a shark-tooth pattern forming where a distinct step would occur at the point where the last lead column was nearly full or fresh when the process inventory was consumed. These swings grow in magnitude for larger column volumes. The solid-curve shown in Figure 10-17 is provided only to highlight the general behavior of the data.

Also shown in Figure 10-17, for the VERSE predictions, we see that the shape of this spent CST curve is rather flat over a large range of column volumes, becoming steep only at small column sizes. The optimal column size over the flat portion of this curve can be based on capital and operational costs for the facility and its carouseling needs. A near optimal column design is achieved at 2000 L where ~66 MT of spent CST is generated. During Phase 1 the IHLW glass melter will be generating an estimated 2651 MT of glass product based on the Tank Farm COUP report (Kirkbride et al., 2000, see Table 4.1-1). 66 MT of spent CST adds approximately 2.5 wt% sodium oxide to the IHLW glass melter product. Based on the current column design of a bed volume of 1000 L, the estimated spent CST material increases by ~20% to 80 MT. If the bed volume of CST was to be increased in the current design to ~1500 L (i.e., the upper limit of bed volumes in the current design), the estimated spent CST material increases by ~10% to 72 MT.

### **10.8.2 Nominal Case Results for 3-Column Carousels**

Three-column carousel configurations were considered to determine the potential benefit associated with more column stages. Similar results using a 3-column carousel configuration are tabulated in Table 10-10 for a smaller range of column volumes (i.e., 333 L, 467 L, 667 L, 1333 L, 2000 L, 2667 L, and 3333 L). These particular column volumes yield total bed volumes of the carousel that are equal to similar total volumes used in the 2-column carousel runs. The spent CST results of these 3-column carousel configurations are tabulated in Table 10-10 and are plotted in Figure 10-18, along with the results of the 2-column carousel runs. To put the 2-column and 3-column cases on a common basis for plotting, the computed spent CST is plotted in Figure 10-18 as a function of total carousel bed volume.

As Figure 10-18 shows, only marginal gains can be achieved when a 3-column versus 2-column carousel facility is considered. For example, an ~1% decrease in spent CST is achieved when going from a 2-column to a 3-column carousel based on a total bed volume of 4000 L (i.e., 2000 L beds for the 2-column arrangement and 1333 L for the 3-column arrangement). Theoretically, increased column stages will reduce the amount of spent CST generated; however, the predicted gains are well within the expected accuracy of the methodology and the increased staging is not warranted.

### **10.8.3 Impact of Slow Kinetics on Design**

It is well known that CST overall has relatively slow kinetics. From the standpoint of the VERSE-LC model used, the overall kinetics that we are referring to is controlled by the rates of mass transfer across the particle-bed interface (i.e., the film coefficient) followed by mass transfer through the particle pores (i.e., the cesium binary pore diffusion coefficient). In the modeling options chosen we are assuming that the ion exchange process that occurs locally at a CST exchange site is instantaneous. For the range of design conditions of interest to us, we also through sensitivity studies found that pore diffusion is the limiting mass transfer step. One method to increase the CST kinetics is the use of smaller size particles that reduced the diffusion path lengths. Unfortunately, this also increases the pressure drop across the bed. To reduce the increased pressure drop a reduction in the bed L/D could then be considered.

To assess the overall impact resulting from overall mass transfer resistances (i.e., the “kinetics”), three different column sizes were investigated based on a 2-column carousel configuration where the mass transfer resistances were essentially eliminated. The results of these VERSE-LC simulations are provided in Table 10-11, along with the nominal case runs for comparison. By setting the film and pore diffusivity coefficients to very high values, the impacts due to mass transfer resistances can be eliminated.

To assess the sensitivity pore diffusion has on computed spent CST requirements, additional VERSE-LC simulations were generated based on pore diffusivity coefficients of 10% and 30% of its free diffusion value (see Tables 10-12 and 10-13, respectively). The nominal setting for the cesium pore diffusivity coefficient is 20% of its free diffusion value, whose results were discussed earlier.

The computed spent CST results of these sensitivity runs are all plotted in Figure 10-19 for comparison to the nominal 2-column carousel results. For the 2000 L bed volume design, the resistances associated with mass transfer only increases the computed spent CST by ~14% when compared to the nominal result. Impacts of this magnitude would suggest that further reduction in particle size or in bed L/D is not warranted based on improving the “kinetics” alone. However, uncertainty in the actual value of the pore diffusivity coefficient can result in larger impacts.

We see in Figure 10-19, for a fixed column volume design, that as the pore diffusivity coefficient is increased (i.e., infinity, 10%, 20%, 30%, ...) its impact on spent CST becomes more aggressive. Future efforts should be focused on obtaining better confidence in the magnitude of this diffusivity coefficient. The impact of pore diffusion also increases for decreasing column volume designs where the more dispersed wave-fronts breakthrough much earlier. In general, as the column volume is increased the impacts associated with “kinetics” diminish and ultimately are lost as shown in Figure 10-19.

Also the theoretical minimum in spent CST required is plotted in Figure 10-19. This value can not be reached using practical designs, but is shown to help gage how efficient or inefficient the current CST material and carousel designs are. For the 2000 L bed volume design (i.e., 4000 L total bed volume condition), the actual/practical design only increases the computed spent CST by ~19%.

## 10.9 Cesium Column Inventory

In order to bound the IONSIV<sup>®</sup> IE-911 CST material’s radioactive exposure levels associated with radioactive decay of cesium-137, cesium inventories within the column (i.e., cesium content in the liquid-phase plus adsorbed onto the solid-phase) must be computed during the loading cycle corresponding to the worst case conditions. This bounding inventory calculation is based on the VERSE-LC results described above. This inventory estimate can be used in subsequent analyses (beyond the scope of this report) for estimating conservative exposure levels.

During a loading cycle, cesium is continually being adsorbed onto the IONSIV<sup>®</sup> IE-911 CST material. At any point in time the total column inventory of cesium is made up of: absorbed

cesium on the solid resin typically referred to as the cesium loading, cesium contained within the interstitial voids of the bed, and cesium contained within the pores of the resin particles. The sum total of cesium contained within a column is referred to as its column inventory. Due to the high affinity IONSIV<sup>®</sup> IE-911 CST material has for cesium, after several column volumes of feed has past through the column, the majority of cesium column inventory will reside on the resin.

In order to compute the cumulative cesium inventories along the column, breakthrough curves at various axial locations are used. The molar balance of total cesium for a specified section of the lead column (i.e., from its inlet to a given axial location  $z$ ) can be expressed as:

$$\frac{dn_{oz}}{dt} = \dot{n}_o - \dot{n}_z(t) . \quad (10-8)$$

Integration of Eq. (10-8) from an initial condition (i.e., assuming a fresh lead column and a fixed rate of feed input and concentration) up to some specified point in time,  $t$ , yields:

$$n_{oz}(t) = \dot{n}_o t - \int_0^t \dot{n}_z(t') dt' . \quad (10-9)$$

Given the definition of a breakthrough curve, Eq. (10-9) can be rearranged to:

$$n_{oz}(t) = Qc_o t - Q \int_0^t c_b(z, t') dt' . \quad (10-10)$$

Equation (10-10) can be further simplified by making use of the normalized time quantity expressed in terms of column volume (sometimes referred to as bed volume):

$$n_{oz}(t) \equiv n_{oz}(\tau) = c_o V_{CV} \int_0^\tau \left[ 1 - \frac{c_b(z, \tau')}{c_o} \right] d\tau' , \quad (10-11)$$

where

$$\tau = \frac{tQ}{V_{CV}} .$$

The integral in Eq. (10-11) represents the area above the normalized breakthrough curve up to the specified point in time. For the case where step changes in flowrate and feed concentration occur (i.e., LAW batch feed changes), Eq. (10-11) applies for each process segment where the cumulative inventory becomes the sum of the computed inventories for all process segments within the given cycle of interest.

Typically, in order to compute the cumulative cesium inventory contained within the lead column, the exit breakthrough curve is used. Envelope B LAW feeds provide the bounding case since their cesium feed concentrations are almost one order larger in magnitude than the other envelopes and due to their lower volumetric flowrate have the longest process time (i.e.,

exposure time). Their lower flowrate also results in much sharper concentration fronts along the column where a plug-flow assumption may be adequate for estimating inventories. As shown in Figure 10-11, which presents the results for the two-column carousel configuration at a 2 m<sup>3</sup> column volume design, the 4<sup>th</sup> and 5<sup>th</sup> loading cycles experience the largest cesium concentration levels within the lead columns. From an exposure perspective, the 4<sup>th</sup> loading cycle is larger since its lead column remains at a higher cesium level for a longer duration. It is this 4<sup>th</sup> loading cycle, where the Envelope B LAW-2a feed is being processed, which represents our bounding case for a 2 m<sup>3</sup> column volume design. As shown in Figures 10-9 and 10-13 for 1 m<sup>3</sup> and 3 m<sup>3</sup> column volume design cases, cycle 9 and cycle 2 are bounding, respectively.

Based on the integration of Eq. (10-11) for a two-column carousel configuration at the column sizes of 1, 2, and 3 m<sup>3</sup>, the lead column cesium inventories over the process time of their most bounding cycles are shown in Figure 10-20. The cesium inventories plotted in Figure 10-20 are expressed in terms of the total amount of cesium in gmoles contained within the lead column per liter of column (i.e. bed) volume. This cesium inventory concentration increases fairly linearly up to the point where the lead column becomes saturated at its feed value over the entire length of the column (i.e., no additional accumulation within the column can occur). Since the volumetric flowrate for each case shown is identical (i.e., Envelope B's flowrate is 9,400 ml/min), the column saturation point occurs earlier the smaller the column size.

At the end of the process cycle, all three cases shown are processing Envelope B's LAW-2a feed and have the same saturation point. A cesium concentration level of ~0.25 gmoles/L<sub>column</sub> is the saturation conditions corresponding to the LAW-2a feed. The initial portion of the larger column's inventory curve is at a different slope than the remainder. This is a result of the fact that the process cycle is initially being fed by Envelope A's LAW-1 feed and then converts over to Envelope B's LAW-2a.

Table 10-1. Comparison of key parameters <sup>a</sup> between IONSIV<sup>®</sup> IE-911 CST material and SuperLig<sup>®</sup> 644 resin for removal of cesium from LAW by ion exchange.

Parameter	IONSIV <sup>®</sup> IE-911 CST	SuperLig <sup>®</sup> 644
Bed porosity, (-)	0.50	0.45
Particle porosity, (-)	0.24	0.61
Avg. particle diameter, (μm)	345	660
Bed density, (g <sub>solid</sub> /ml <sub>bed</sub> )	1.0	0.2
Total Cs capacity, mass basis (mmole <sub>Cs</sub> /g <sub>solid</sub> ) volume basis (mmole <sub>Cs</sub> /ml <sub>bed</sub> )	0.3944 0.3944	0.3333 0.0667
Pore diffusion coef., (cm <sup>2</sup> /min)	0.925x10 <sup>-5</sup>	3.395x10 <sup>-5</sup>
Cs <sup>+</sup> to K <sup>+</sup> selectivity, (-)	1,400:1	1,200:1
Cs <sup>+</sup> to Na <sup>+</sup> selectivity, (-)	26,000:1	23,000:1

<sup>a</sup> These are approximate values based on available data and analyses.

Table 10-2. Ion-exchange facility cesium exit concentration criterion on an envelope basis.

Envelope	<sup>137</sup> Cs exit criterion <sup>a</sup> (Ci/gmole of Na)	<sup>137</sup> Cs exit criterion on a 5 M Na <sup>+</sup> basis (μCi/ml)	Isotopic fraction ( <sup>137</sup> Cs/ <sup>total</sup> Cs)	Basis <sup>b</sup>
A	1.75x10 <sup>-5</sup>	0.088	25%	~19.6 wt% sodium oxide (Na <sub>2</sub> O) at the 60 MT/day operation
B	5.00x10 <sup>-5</sup>	0.250	30%	~7.0 wt% sodium oxide (Na <sub>2</sub> O) at the 30 MT/day operation
C	2.90x10 <sup>-5</sup>	0.150	25%	~12.0 wt% sodium oxide (Na <sub>2</sub> O) at the 30 MT/day operation

<sup>a</sup> The actual cesium exit concentration criterion is a bucket average value exiting the lag columns and for VERSE-LC simulations this criterion is converted into total cesium concentrations in molar units. The values listed limit the Ci/m<sup>3</sup> content in the glass matrix due to <sup>137</sup>Cs.

<sup>b</sup> A different operating basis is used for Envelope A (60 MT/d) than for Envelopes B and C (30 MT/d) since Envelopes B and C will be completely processed during the Phase 1 campaign. To meet DOE's requirement of an expanded capability beyond Phase 1, the remaining LAWs, all Envelope A wastes, are potentially handled at twice the Phase 1 flowrate.

Table 10-3. Processing information on the Phase 1 Low activity waste (LAW) feeds listed in their scheduled order to be processed.

Envelope	Source Tank	LAW batch feed (id)	Flowrate <sup>b</sup> (L/min)	Cesium feed conc. [M]	Batch volume to be processed <sup>a</sup> (m <sup>3</sup> )	Batch process time <sup>b,c</sup> at 30 MT/d (day)	Batch process time <sup>b,c</sup> at 60 MT/day (day)
A	AP-101	LAW-1	52.62	3.598E-05	4,626	122	61
B	AZ-101	LAW-2a	9.4	4.676E-04	2,906	215	-
B	AZ-102	LAW-2b	9.4	4.311E-04	1,755	130	-
C	AN-102	LAW-3	16.2	3.967E-05	4,200	180	-
C	AN-102	LAW-4	16.2	3.779E-05	4,200	180	-
A	AN-104	LAW-5	52.62	6.283E-05	3,820	101	50
A	AN-104	LAW-6	52.62	6.328E-05	3,540	93	47
C	AN-107	LAW-7	16.2	4.455E-05	5,498	236	-
A	AN-105	LAW-8	52.62	4.324E-05	3,700	98	49
A	AN-105	LAW-9	52.62	4.444E-05	3,600	95	48
A	SY-101	LAW-10	52.62	3.692E-05	2,600	69	34
A	SY-101	LAW-11	52.62	3.739E-05	4,600	121	61
A	AN-103	LAW-12	52.62	4.831E-05	4,720	125	62
A	AN-103	LAW-13	52.62	4.831E-05	4,720	125	62
A	AW-101	LAW-14	52.62	4.569E-05	3,940	104	52
A	AW-101	LAW-15	52.62	4.552E-05	5,360	141	71

<sup>a</sup> The volume of each batch feed represents the volume of solution entering the ion-exchange facility at a 5 M sodium basis and includes the volume changes that occur upstream to this facility (i.e., pretreatment activities).

<sup>b</sup> The volumetric flowrates and batch process times are based on the 30 MT/day operation schedule for Envelopes B and C and on the expanded capability of 60 MT/day operation for Envelope A.

<sup>c</sup> The total amount of processing time is ~4.2 years. If the Envelope A feeds are processed at 30 MT/day, then the total amount of processing time is ~5.8 years.



Table 10-4. Ion-exchange facility total cesium exit concentration criterion on a batch feed basis.

Envelope	Isotopic fraction ( $^{137}\text{Cs}/^{137}\text{Cs}+^{133}\text{Cs}$ )	$^{137}\text{Cs}$ exit criterion <sup>a</sup> (Ci/gmole of Na)	LAW batch feed (id)	Cesium feed concentration ( $c_o$ ) [M]	Total Cs exit criterion <sup>b</sup> [M]	Total Cs exit criterion ( $c/c_o$ )
<b>A</b>	25%	$1.75 \times 10^{-5}$	LAW-1	3.598E-05	2.953E-08	8.208E-04
			LAW-5	6.283E-05	2.953E-08	4.701E-04
			LAW-6	6.328E-05	2.953E-08	4.667E-04
			LAW-8	4.324E-05	2.953E-08	6.830E-04
			LAW-9	4.444E-05	2.953E-08	6.645E-04
			LAW-10	3.692E-05	2.953E-08	7.999E-04
			LAW-11	3.739E-05	2.953E-08	7.899E-04
			LAW-12	4.831E-05	2.953E-08	6.114E-04
			LAW-13	4.831E-05	2.953E-08	6.114E-04
			LAW-14	4.569E-05	2.953E-08	6.465E-04
			LAW-15	4.552E-05	2.953E-08	6.488E-04
<b>B</b>	30%	$5.00 \times 10^{-5}$	LAW-2a	4.676E-04	7.032E-08	1.504E-04
			LAW-2b	4.311E-04	7.032E-08	1.631E-04
<b>C</b>	25%	$2.90 \times 10^{-5}$	LAW-3	3.967E-05	4.894E-08	1.234E-03
			LAW-4	3.779E-05	4.894E-08	1.295E-03
			LAW-7	4.455E-05	4.894E-08	1.099E-03

<sup>a</sup> During the loading cycle the solution entering the ion-exchange facility is at a 5 M sodium concentration.<sup>b</sup> The  $^{137}\text{Cs}$  criterion is computed based on the  $^{137}\text{Cs}$  exit criterion, its isotopic fraction (assumes the total is made up only of the isotopes  $^{133}\text{Cs}$  and  $^{137}\text{Cs}$ ), and the conversion factor of 1  $\mu\text{Ci}/\text{ml}$  of  $^{137}\text{Cs}$  equals  $8.43820142 \times 10^{-8}$  M of  $^{137}\text{Cs}$ . A radioactive half-life of 30.17 years for  $^{137}\text{Cs}$  is used taken from GE Nuclear Energy (1996).

Table 10-5. Estimate of the theoretical minimum amount of spent CST material required to process each Phase 1 LAW batch feed.

Envelope	LAW batch feed (id)	Batch volume to be processed <sup>a</sup> (m <sup>3</sup> )	Cesium feed concentration [M]	Max cesium loading <sup>b</sup> (mmole <sub>Cs</sub> /g <sub>CST</sub> )	Total Cs to be processed (gmole)	Theoretical minimum spent CST (kg)
<b>A</b>	LAW-1	4,626	3.598E-05	3.375E-02	166.4	4,931
	LAW-5	3,820	6.283E-05	8.339E-02	240.0	2,878
	LAW-6	3,540	6.328E-05	8.320E-02	224.0	2,692
	LAW-8	3,700	4.324E-05	5.787E-02	160.0	2,765
	LAW-9	3,600	4.444E-05	6.517E-02	160.0	2,455
	LAW-10	2,600	3.692E-05	5.638E-02	96.0	1,703
	LAW-11	4,600	3.739E-05	6.073E-02	172.0	2,832
	LAW-12	4,720	4.831E-05	5.599E-02	228.0	4,072
	LAW-13	4,720	4.831E-05	5.577E-02	228.0	4,088
	LAW-14	3,940	4.569E-05	4.411E-02	180.0	4,081
	LAW-15	5,360	4.552E-05	4.169E-02	244.0	5,853
<b>B</b>	LAW-2a	2,906	4.676E-04	2.527E-01	1,358.5	5,377
	LAW-2b	1,755	4.311E-04	2.640E-01	756.6	2,866
<b>C</b>	LAW-3	4,200	3.967E-05	6.080E-02	166.6	2,741
	LAW-4	4,200	3.779E-05	5.833E-02	158.7	2,721
	LAW-7	5,498	4.455E-05	7.409E-02	244.9	3,306
<b>Total</b>	All LAW's	63,784	-	-	-	55,360

<sup>a</sup> The volume of each batch feed represents the volume of solution entering the ion-exchange facility at a 5 M sodium basis and includes the volume changes that occur upstream to this facility (i.e., pretreatment activities).

<sup>b</sup> The maximum cesium loading evaluation is based on the feed concentration using the appropriate cesium isotherm (i.e., algebraic model and appropriate beta value).

Table 10-6. Impact of L/D geometry on estimated amount of total spent CST material generated to process the Phase 1 LAW inventory and the number of cycles required per batch of feed (i.e., based on a 2000 L 2-column carousel facility operating at 25 C under nominal parameter settings <sup>a</sup>, except for those parameters explicitly listed in this table).

Column L/D	1.0	2.0	3.0	4.0	5.0
Column length (cm)	136.6	216.8	284.0	344.1	399.3
Column diameter (cm)	136.6	108.4	94.7	86.0	79.9
Bed volume of one column (L) <sup>b</sup>	2,000.0	2,000.0	2,000.0	2,000.0	2,000.0
Total bed volume of columns (L) <sup>b</sup>	4,000	4,000	4,000	4,000	4,000
LAW-1	2	2	2	2	2
LAW-2a	2	2	2	2	2
LAW-2b	1	1	1	1	1
LAW-3	3	3	3	3	3
LAW-4	2	2	2	2	2
LAW-5	2	2	2	2	2
LAW-6	2	2	2	2	2
LAW-7	1	1	1	1	1
LAW-8	1	1	1	1	1
LAW-9	2	2	2	2	2
LAW-10	1	1	1	1	1
LAW-11	1	1	1	1	1
LAW-12	3	3	3	3	3
LAW-13	2	2	2	2	2
LAW-14	3	3	3	3	3
LAW-15	3	3	3	3	3
Total cycles for all 16 feeds	31	31	31	31	31
Total spent CST (kg)	66,000	66,000	66,000	66,000	66,000

<sup>a</sup> The dilution factor set to 68% and the cesium pore diffusion coefficient to 20% of its “free” diffusion value.

<sup>b</sup> Column volumes here refer to the actual volume containing the CST beds and does not include head space volume. Headspace volume set to 25% of bed volume (i.e., 500 L).

Table 10-7. Geometric L/D ratios and resulting geometries considered in CST column design simulations using VERSE-LC based on a 2-column carousel configuration.

Individual column bed volume (L)	Bed (L/D) ratio	Bed diameter (cm)	Bed column length (cm)	Head-space volume (L)	Total bed length (L)	Total bed volume (L)
500	3.0	59.6	178.9	125	357.9	1000
700	3.0	66.7	200.2	175	400.4	1400
1000 <sup>a</sup>	3.0	75.2	225.5	250	450.9	2000
1500	3.0	86.0	258.1	375	516.2	3000
2000 <sup>b</sup>	3.0	94.7	284.0	500	568.1	4000
3000	3.0	108.4	325.2	750	650.3	6000
4000	3.0	119.3	357.9	1000	715.8	8000
5000	3.0	128.5	385.5	1250	771.0	10000
6000	3.0	136.6	409.7	1500	819.3	12000
7000	3.0	143.8	431.3	1750	862.5	14000
8000	3.0	150.3	450.9	2000	901.8	16000
9000	3.0	156.3	469.0	2250	937.9	18000
2000	1.0	136.6	136.6	500	273.1	4000
2000	2.0	108.4	216.8	500	433.5	4000
2000	4.0	86.0	344.1	500	688.2	4000
2000	5.0	79.9	399.3	500	798.6	4000

<sup>a</sup> At the time these analyses were being performed, this represented the current ion-exchange facility column design for use with SuperLig<sup>®</sup> 644 resin. More recent design efforts have changed the L/D to ~1.1 (i.e., 119 cm in length and 107 cm in diameter).

<sup>b</sup> This represents the nominal (and near optimum) ion-exchange facility column design for use with IONSIV<sup>®</sup> IE-911 CST material.

Table 10-8. Geometric L/D ratios and resulting geometries considered in CST column design simulations using VERSE-LC based on a 3-column carousel configuration.<sup>a</sup>

Individual column (in 2-column carousel) bed volume (L)	Bed diameter (cm)	Individual column bed volume (L)	Bed column length (cm)	Bed (L/D) ratio	Head-space volume (L)	Total bed length (L)	Total bed volume (L)
500	59.6	333.3	119.3	2.0	83	357.9	1000
700	66.7	466.7	133.5	2.0	117	400.4	1400
1000	75.2	666.7	150.3	2.0	167	450.9	2000
2000	94.7	1333.3	189.4	2.0	333	568.1	4000
3000	108.4	2000.0	216.8	2.0	500	650.3	6000
4000	119.3	2666.7	238.6	2.0	667	715.8	8000
5000	128.5	3333.3	257.0	2.0	833	771.0	10000

<sup>a</sup> The use of a third (i.e., “guard”) column in the carousel configuration was not intended to be a normal operating mode, but was a backup column in the original facility design.

Table 10-9. Estimated amount of total spent CST material generated to process the Phase 1 LAW inventory and the number of cycles required per batch of feed (i.e., based on a 2-column carousel facility operating at 25 C under nominal parameter settings <sup>a</sup>).

Column L/D	3.0	3.0	3.0	3.0	3.0	3.0	3.0	3.0	3.0	3.0	3.0	3.0
Column length (cm)	178.9	200.2	225.5	258.1	284.0	325.2	357.9	385.5	409.7	431.3	450.9	469.0
Column diameter (cm)	59.6	66.7	75.2	86.0	94.7	108.4	119.3	128.5	136.6	143.8	150.3	156.3
Bed volume of one column (L) <sup>b</sup>	500	700	1,000	1,500	2,000	3,000	4,000	5,000	6,000	7,000	8,000	9,000
Total bed volume of columns (L) <sup>b</sup>	1,000	1,400	2,000	3,000	4,000	6,000	8,000	10,000	12,000	14,000	16,000	18,000
LAW-1 cycles	24	14	7	4	2	1	0	0	0	0	0	0
LAW-2a cycles	10	6	4	2	2	1	1	0	0	0	0	0
LAW-2b cycles	6	5	3	2	1	0	0	1	0	0	0	0
LAW-3 cycles	8	5	5	4	3	2	2	1	1	1	1	0
LAW-4 cycles	6	5	3	2	2	2	1	1	1	1	0	1
LAW-5 cycles	15	8	5	3	2	1	1	1	1	0	1	1
LAW-6 cycles	13	7	4	2	2	1	1	0	1	1	0	0
LAW-7 cycles	8	5	3	2	1	1	1	1	0	0	1	0
LAW-8 cycles	13	8	4	2	1	1	1	1	0	1	1	0
LAW-9 cycles	13	7	4	3	2	1	1	1	1	0	0	1
LAW-10 cycles	8	5	3	1	1	1	0	0	0	0	1	0
LAW-11 cycles	14	8	4	3	1	1	1	1	1	1	0	1
LAW-12 cycles	20	11	7	3	3	2	1	1	1	1	1	0
LAW-13 cycles	20	11	6	4	2	1	1	0	0	0	0	1
LAW-14 cycles	20	11	6	3	3	2	1	1	1	1	1	0
LAW-15 cycles	28	17	10	6	3	2	2	2	1	1	1	1
Total cycles for all 16 feeds	226	133	78	46	31	20	15	12	9	8	8	6
Total spent CST (kg)	114,000	94,500	80,000	72,000	66,000	66,000	68,000	70,000	66,000	70,000	80,000	72,000

<sup>a</sup> The dilution factor set to 68% and the cesium pore diffusion coefficient to 20% of its "free" diffusion value.

<sup>b</sup> Column volumes here refer to the actual volume containing the CST beds and does not include head space volume. Headspace volume set to 25% of bed volume.

Table 10-10. Estimated amount of total spent CST material generated to process the Phase 1 LAW inventory and the number of cycles required per batch of feed (i.e., based on a 3-column carousel facility operating at 25 C under nominal parameter settings <sup>a</sup>).

Column L/D	2.0	2.0	2.0	2.0	2.0	2.0	2.0
Column length (cm)	119.3	133.5	150.3	189.4	216.8	238.6	257.0
Column diameter (cm)	59.6	66.7	75.2	94.7	108.4	119.3	128.5
Bed volume of one column (L) <sup>b</sup>	333.3	466.7	666.7	1,333.3	2,000.0	2,666.7	3,333.3
Total bed volume of columns (L) <sup>b</sup>	1,000	1,400	2,000	4,000	6,000	8,000	10,000
LAW-1 cycles	31	18	10	3	1	0	0
LAW-2a cycles	14	9	6	2	1	1	0
LAW-2b cycles	9	7	4	2	1	0	1
LAW-3 cycles	12	9	7	4	3	3	1
LAW-4 cycles	10	7	5	3	3	2	2
LAW-5 cycles	18	10	7	4	2	1	1
LAW-6 cycles	16	9	5	2	2	2	1
LAW-7 cycles	11	8	5	2	1	1	1
LAW-8 cycles	17	10	6	3	1	1	2
LAW-9 cycles	16	9	5	2	2	1	1
LAW-10 cycles	10	7	4	1	1	1	0
LAW-11 cycles	18	10	6	3	1	1	1
LAW-12 cycles	25	14	8	3	3	2	2
LAW-13 cycles	25	15	9	3	2	2	1
LAW-14 cycles	25	15	9	4	2	2	2
LAW-15 cycles	37	21	12	5	3	2	2
Total cycles for all 16 feeds	294	178	108	46	29	22	18
Total spent CST (kg)	99,000	84,467	74,000	65,333	64,000	66,667	70,000

<sup>a</sup> The dilution factor set to 68% and the cesium pore diffusion coefficient to 20% of its “free” diffusion value.

<sup>b</sup> Column volumes here refer to the actual volume containing the CST beds and does not include head space volume. Headspace volume set to 25% of bed volume.

Table 10-11. Impact of mass transfer limitations on estimated amount of total spent CST material generated to process the Phase 1 LAW inventory and the number of cycles required per batch of feed (i.e., based on a 2-column carousel facility operating at 25 C under nominal parameter settings <sup>a</sup>, except for those parameters explicitly listed in this table).

Column L/D	3.0		3.0		3.0	
Column length (cm)	225.5		284.0		325.2	
Column diameter (cm)	75.2		94.7		108.4	
Bed volume of one column (L) <sup>b</sup>	1,000.0		2,000.0		3,000.0	
Total bed volume of columns (L) <sup>b</sup>	2,000		4,000		6,000	
State of mass transfer limits <sup>c</sup>	Nominal conditions	No MTL	Nominal conditions	No MTL	Nominal conditions	No MTL
LAW-1	7	4	2	1	1	0
LAW-2a	4	4	2	2	1	1
LAW-2b	3	3	1	1	0	1
LAW-3	5	5	3	3	2	2
LAW-4	3	3	2	2	2	1
LAW-5	5	3	2	1	1	1
LAW-6	4	2	2	2	1	1
LAW-7	3	4	1	1	1	1
LAW-8	4	3	1	1	1	1
LAW-9	4	3	2	1	1	1
LAW-10	3	2	1	1	1	1
LAW-11	4	3	1	2	1	1
LAW-12	7	4	3	2	2	1
LAW-13	6	4	2	2	1	2
LAW-14	6	4	3	2	2	1
LAW-15	10	5	3	3	2	2
Total cycles for all 16 feeds	78	56	31	27	20	18
Total spent CST (kg)	80,000	58,000	66,000	58,000	66,000	60,000

<sup>a</sup> The dilution factor set to 68% and the cesium pore diffusion coefficient to 20% of its “free” diffusion value.

<sup>b</sup> Column volumes here refer to the actual volume containing the CST beds and does not include head space volume. Head space volume set to 25% of bed volume.

<sup>c</sup> The mass transfer parameters (i.e., pore diffusivity and film coefficients) are set either to their nominal settings (MTL on) or to very large values to eliminate mass transfer resistance (no MTL).

Table 10-12. Estimated amount of total spent CST material generated to process the Phase 1 LAW inventory and the number of cycles required per batch of feed (i.e., based on a 2-column carousel facility operating at 25 C under nominal parameter settings <sup>a</sup>, except for the cesium pore diffusivity coefficient).

Column L/D	3.0	3.0	3.0	3.0	3.0	3.0	3.0	3.0
Column length (cm)	178.9	200.2	225.5	258.1	284.0	325.2	357.9	385.5
Column diameter (cm)	59.6	66.7	75.2	86.0	94.7	108.4	119.3	128.5
Bed volume of one column (L) <sup>b</sup>	500	700	1,000	1,500	2,000	3,000	4,000	5,000
Total bed volume of columns (L) <sup>b</sup>	1,000	1,400	2,000	3,000	4,000	6,000	8,000	10,000
LAW-1 cycles	42	22	12	6	3	2	1	0
LAW-2a cycles	10	7	4	2	2	0	0	1
LAW-2b cycles	6	4	3	2	1	0	1	0
LAW-3 cycles	10	7	5	4	3	2	1	1
LAW-4 cycles	9	5	3	2	2	2	1	1
LAW-5 cycles	24	13	7	4	2	2	2	1
LAW-6 cycles	23	12	7	3	2	1	1	1
LAW-7 cycles	11	7	4	2	2	1	1	0
LAW-8 cycles	23	12	6	4	2	1	0	1
LAW-9 cycles	22	12	6	3	2	1	1	1
LAW-10 cycles	14	8	4	2	1	1	1	0
LAW-11 cycles	24	13	7	3	3	1	1	1
LAW-12 cycles	34	18	10	5	3	2	1	1
LAW-13 cycles	34	18	10	5	3	2	1	1
LAW-14 cycles	34	19	10	5	3	1	1	1
LAW-15 cycles	48	26	13	7	5	3	2	1
Total cycles for all 16 feeds	368	203	111	59	39	22	16	12
Total spent CST (kg)	185,000	143,500	113,000	91,500	82,000	72,000	72,000	70,000

<sup>a</sup> The dilution factor set to 68% and the cesium pore diffusion coefficient to 10% of its “free” diffusion value.

<sup>b</sup> Column volumes here refer to the actual volume containing the CST beds and does not include head space volume. Headspace volume set to 25% of bed volume.



Table 10-13. Estimated amount of total spent CST material generated to process the Phase 1 LAW inventory and the number of cycles required per batch of feed (i.e., based on a 2-column carousel facility operating at 25 C under nominal parameter settings <sup>a</sup>, except for the cesium pore diffusivity coefficient).

Column L/D	3.0	3.0	3.0	3.0	3.0	3.0	3.0	3.0
Column length (cm)	178.9	200.2	225.5	258.1	284.0	325.2	357.9	385.5
Column diameter (cm)	59.6	66.7	75.2	86.0	94.7	108.4	119.3	128.5
Bed volume of one column (L) <sup>b</sup>	500	700	1,000	1,500	2,000	3,000	4,000	5,000
Total bed volume of columns (L) <sup>b</sup>	1,000	1,400	2,000	3,000	4,000	6,000	8,000	10,000
LAW-1 cycles	19	11	6	3	2	1	0	0
LAW-2a cycles	10	6	4	2	1	1	1	0
LAW-2b cycles	5	4	3	2	2	0	0	1
LAW-3 cycles	8	6	5	4	3	2	2	1
LAW-4 cycles	6	5	3	2	1	2	1	1
LAW-5 cycles	11	6	4	3	3	1	1	0
LAW-6 cycles	10	6	3	2	1	1	1	1
LAW-7 cycles	7	5	4	2	1	1	1	1
LAW-8 cycles	10	6	4	2	2	1	1	1
LAW-9 cycles	10	5	3	2	1	1	0	0
LAW-10 cycles	6	4	2	1	1	1	1	1
LAW-11 cycles	11	7	4	2	1	1	1	1
LAW-12 cycles	15	9	5	3	3	1	1	0
LAW-13 cycles	15	9	6	4	2	2	1	1
LAW-14 cycles	16	9	5	3	2	1	1	1
LAW-15 cycles	22	13	8	4	3	2	2	2
Total cycles for all 16 feeds	181	111	69	41	29	19	15	12
Total spent CST (kg)	91,500	79,100	71,000	64,500	62,000	63,000	68,000	70,000

<sup>a</sup> The dilution factor set to 68% and the cesium pore diffusion coefficient to 30% of its “free” diffusion value.

<sup>b</sup> Column volumes here refer to the actual volume containing the CST beds and does not include head space volume. Headspace volume set to 25% of bed volume.

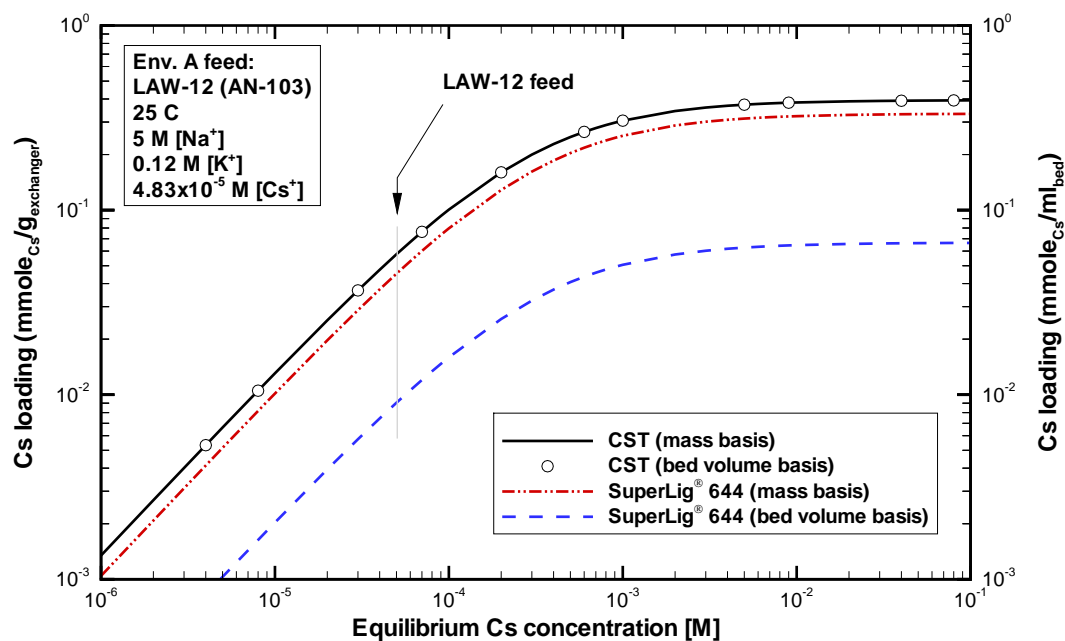


Figure 10-1. Comparison of cesium loading curves for IONSIV® IE-911 CST material and SuperLig® 644 resin in contact with LAW-12 feed solution (241-AN-103) both on a mass and bed volume basis.

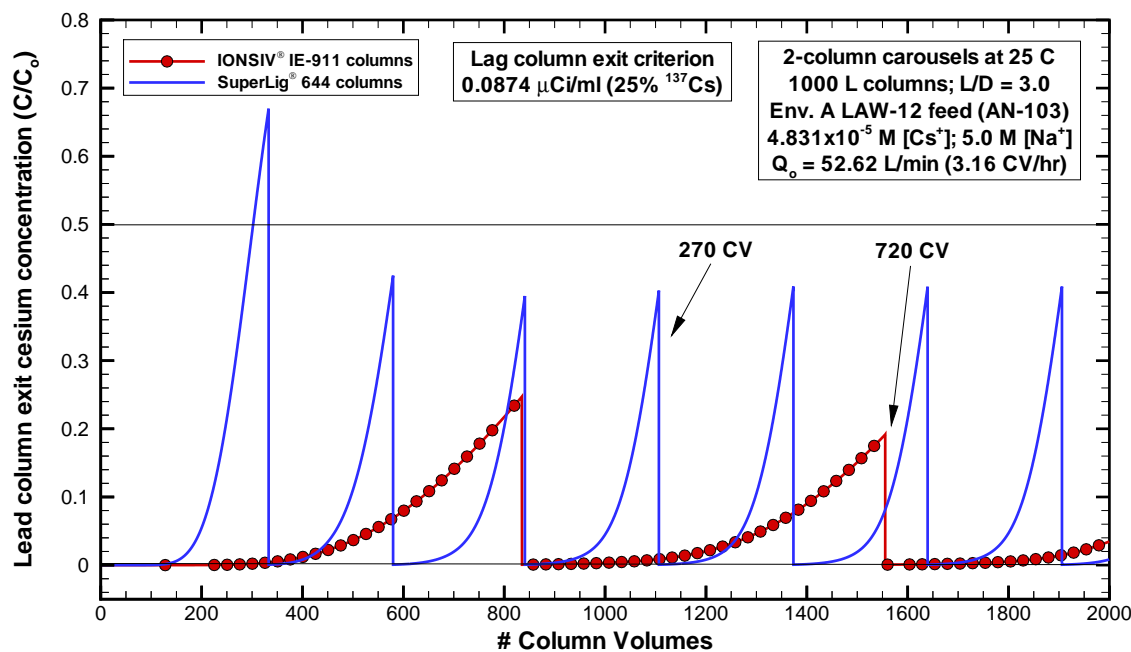


Figure 10-2. Comparison of normalized cesium breakthrough curves for IONSIV® IE-911 CST packed and SuperLig® 644 packed columns at 25 C using LAW-12 feed solution (i.e., 241-AN-103, identical 2-column carousel configuration, 1000 L columns, L/D=3).

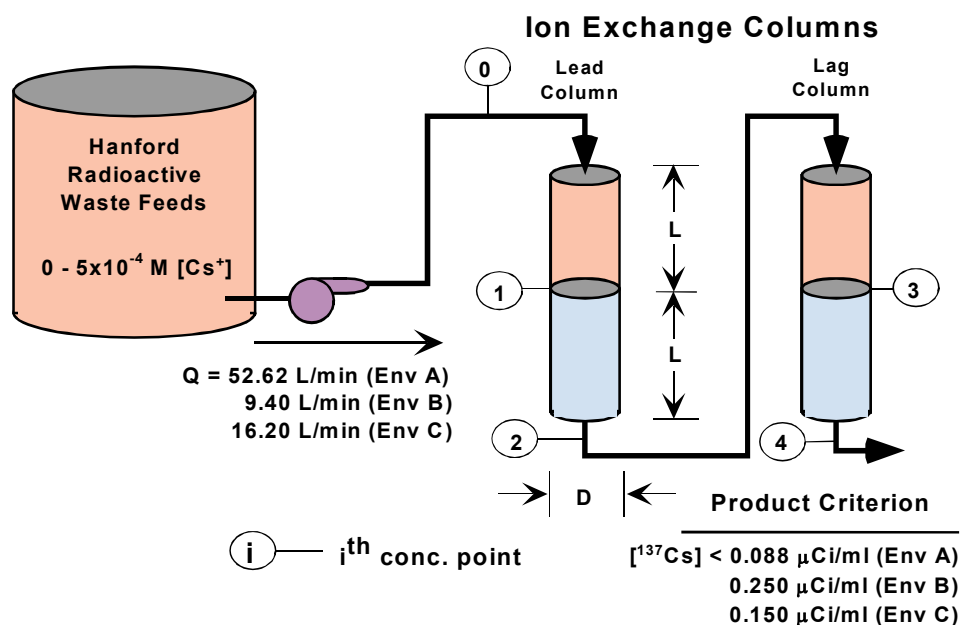


Figure 10-3. Basic flowsheet for a full-scale (two-column carousel configuration) ion-exchange facility for removal of cesium using IONSIV® IE-911 CST material.

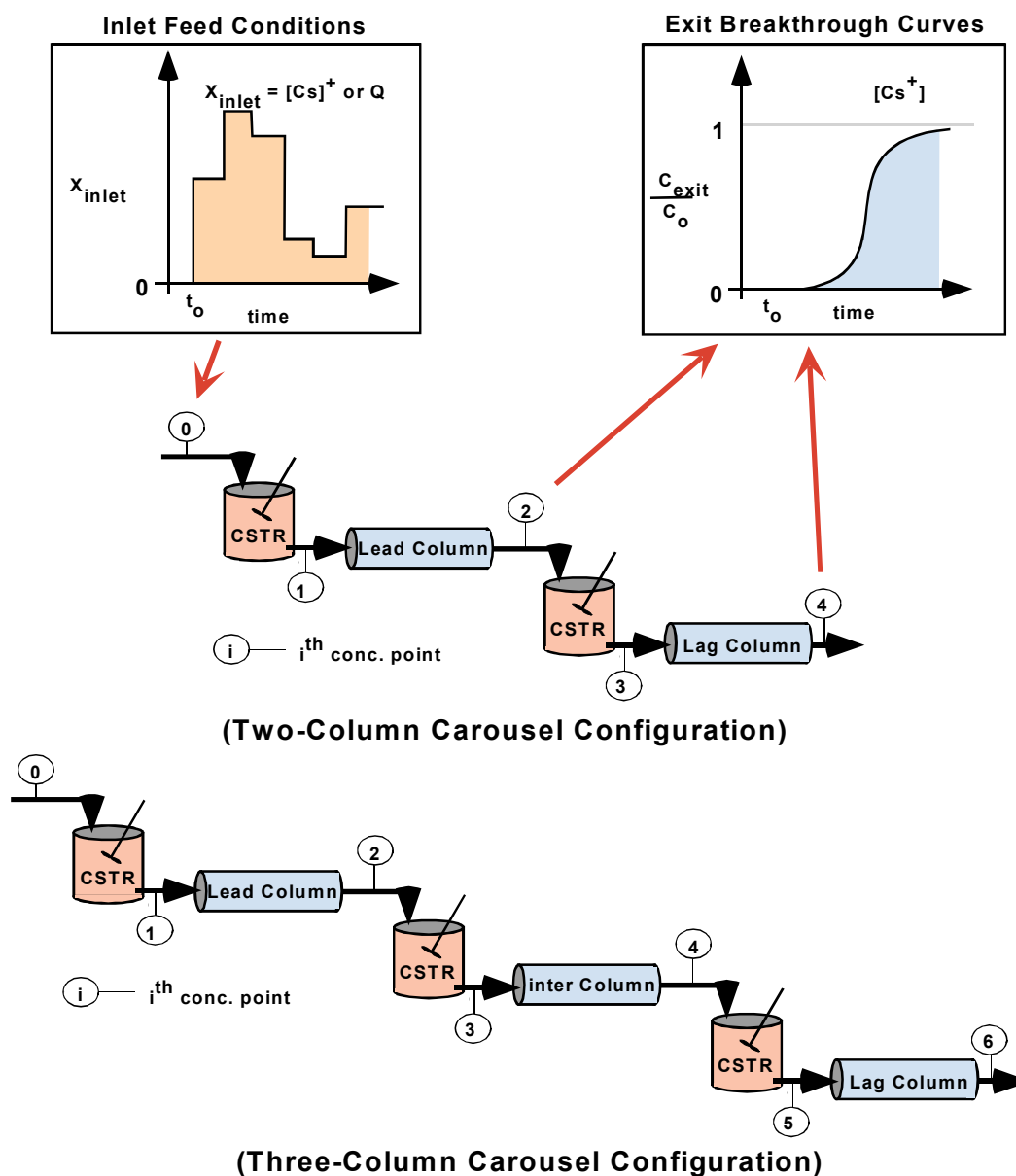


Figure 10-4. VERSE-LC model representing a (two-column or three-column carousel configuration) full-scale facility for removal of cesium using IONSIV® IE-911 CST material. The locations where the inlet feed conditions are applied and the exit breakthrough curves are monitored is shown.

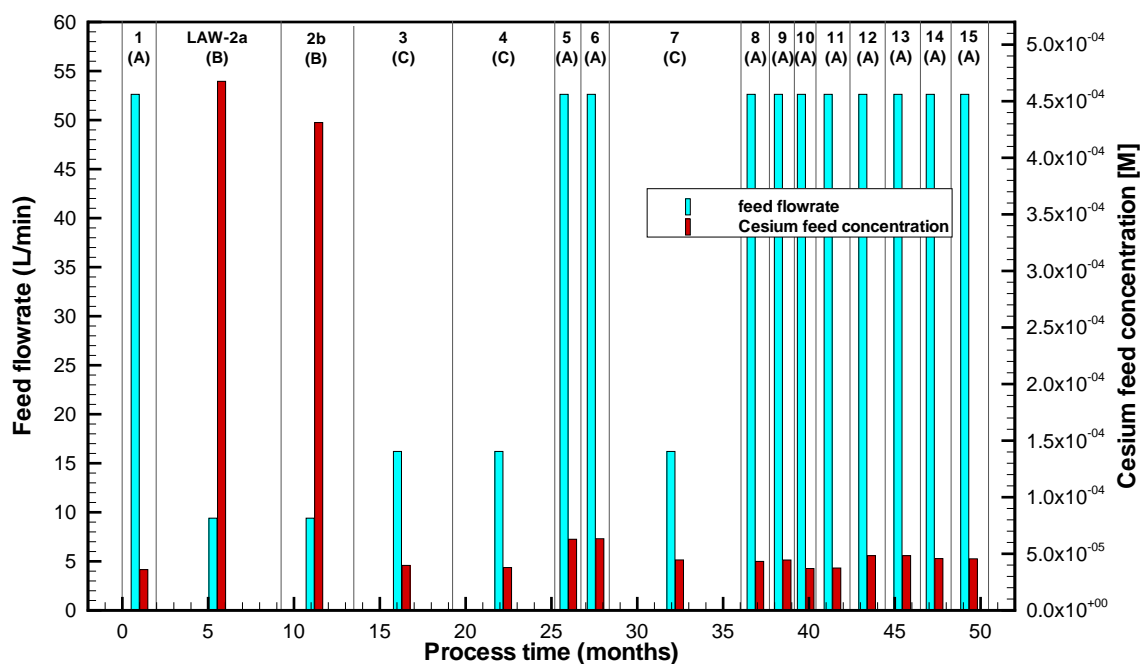


Figure 10-5. Phase 1 LAW batch feed inlet flowrates and cesium concentrations used as input boundary conditions for VERSE-LC CST column design simulations. Constant values are applied over each batch process period.

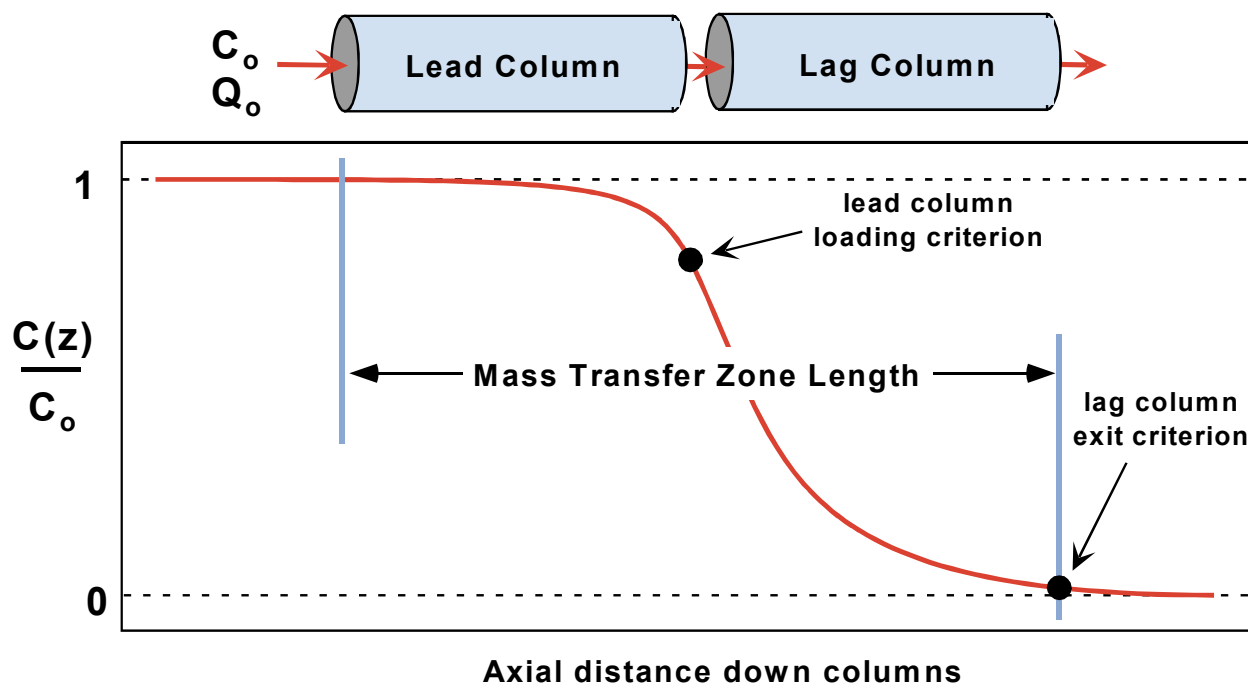


Figure 10-6. The conceptual model defining the length of the mass transfer zone based on a 2-column carousel configuration with specified exit criteria for both columns.

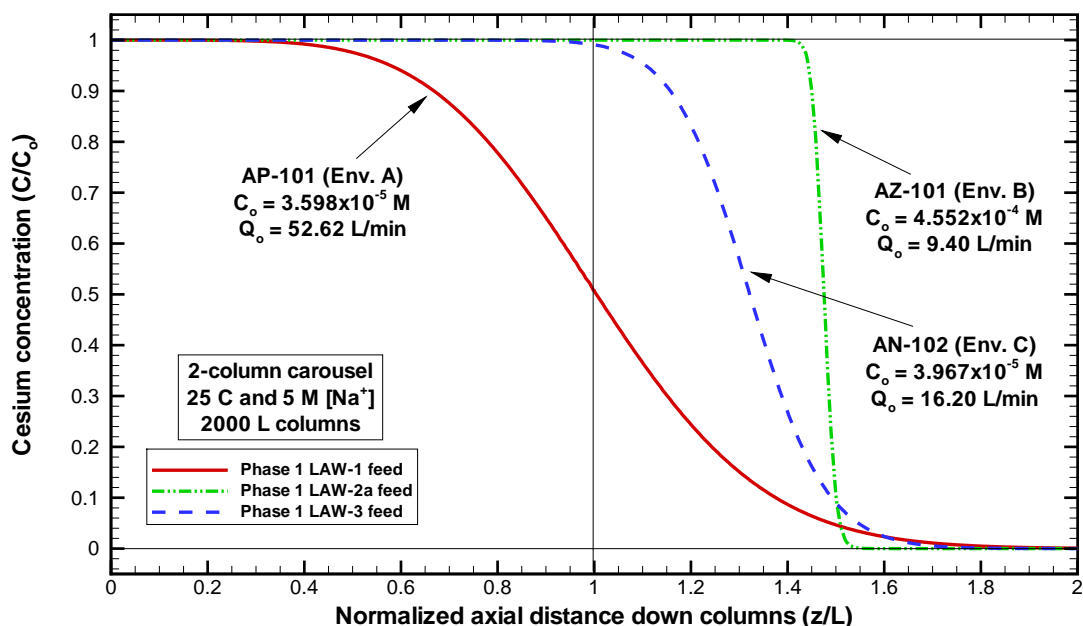


Figure 10-7. Typical impact on mass transfer zone length (i.e., concentration profiles) due to envelope cesium concentration and flowrate differences based on VERSE-LC model predictions when using the IONSIV® IE-911 material.

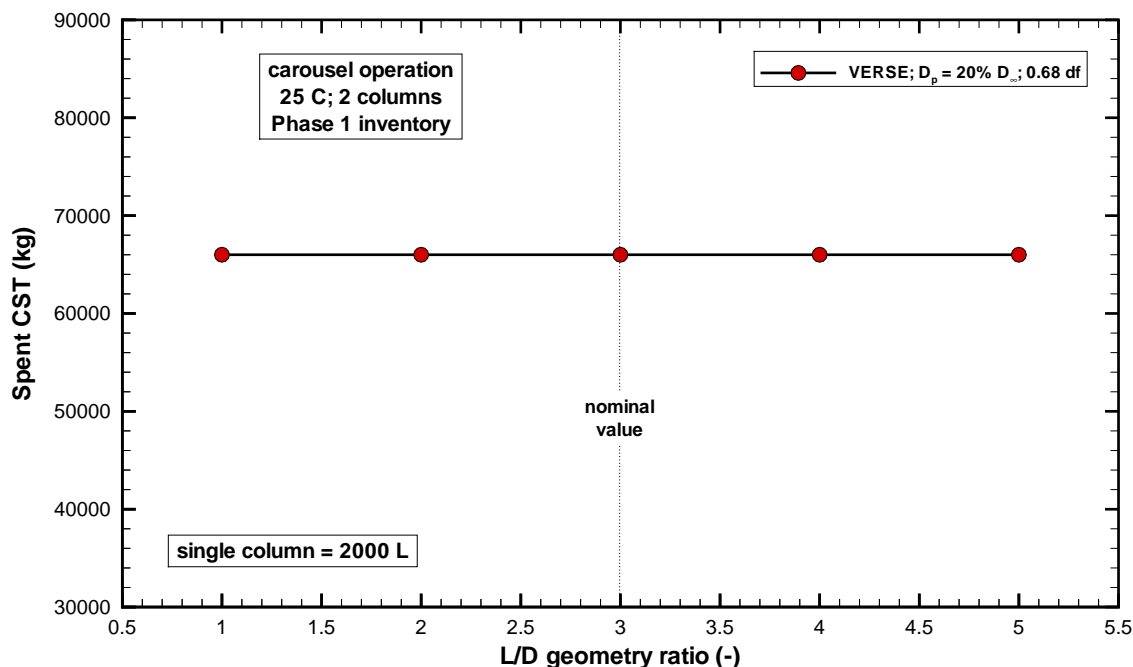


Figure 10-8. Sensitivity of spent CST to the bed L/D geometric ratio for the total processing of the Phase 1 LAW inventory (i.e., a 2-column carousel configuration operating at 25 C with 2000 L columns of varying L/D geometries).

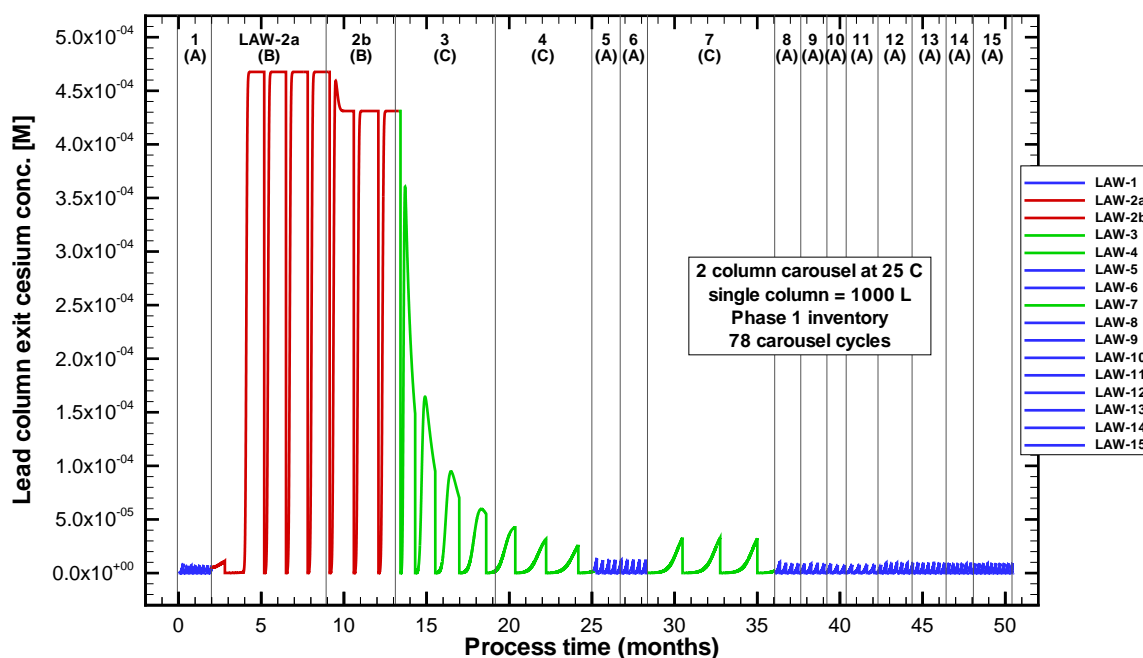


Figure 10-9. VERSE-LC cesium concentration predictions at the exit of the lead column based on CST and the Phase 1 LAW inventory (i.e., a 2-column carousel configuration operating at 25 C with 1000 L columns for a total of 78 carousel cycles performed).

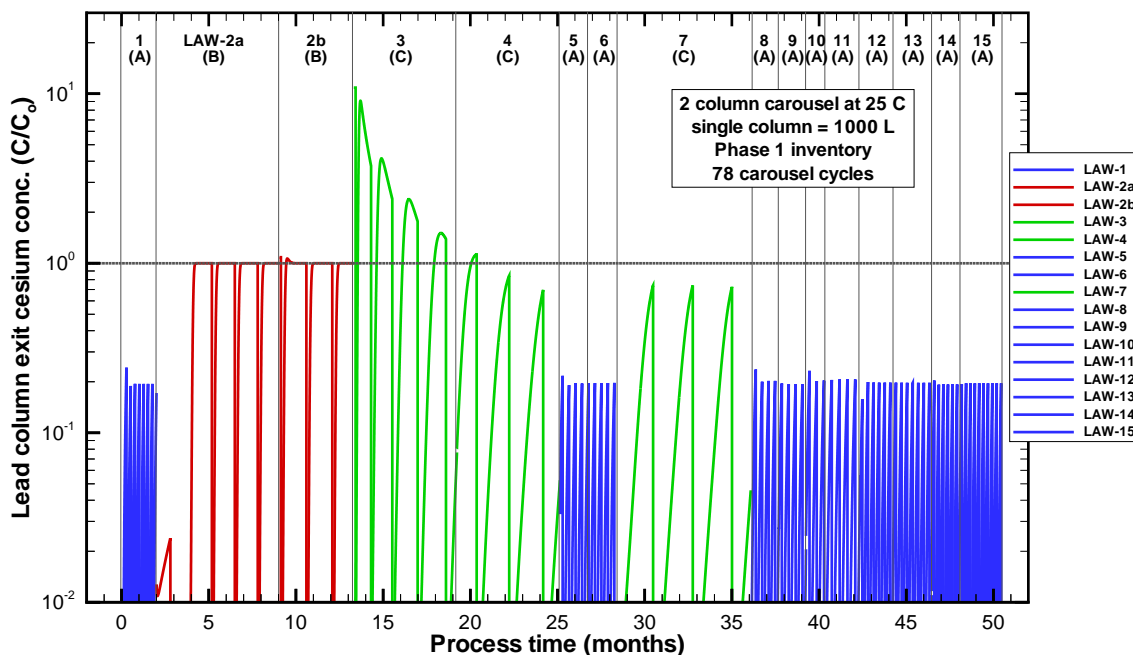


Figure 10-10. VERSE-LC normalized cesium concentration predictions at the exit of the lead column based on CST and the Phase 1 LAW inventory (i.e., a 2-column carousel configuration operating at 25 C with 1000 L columns for a total of 78 carousel cycles performed).

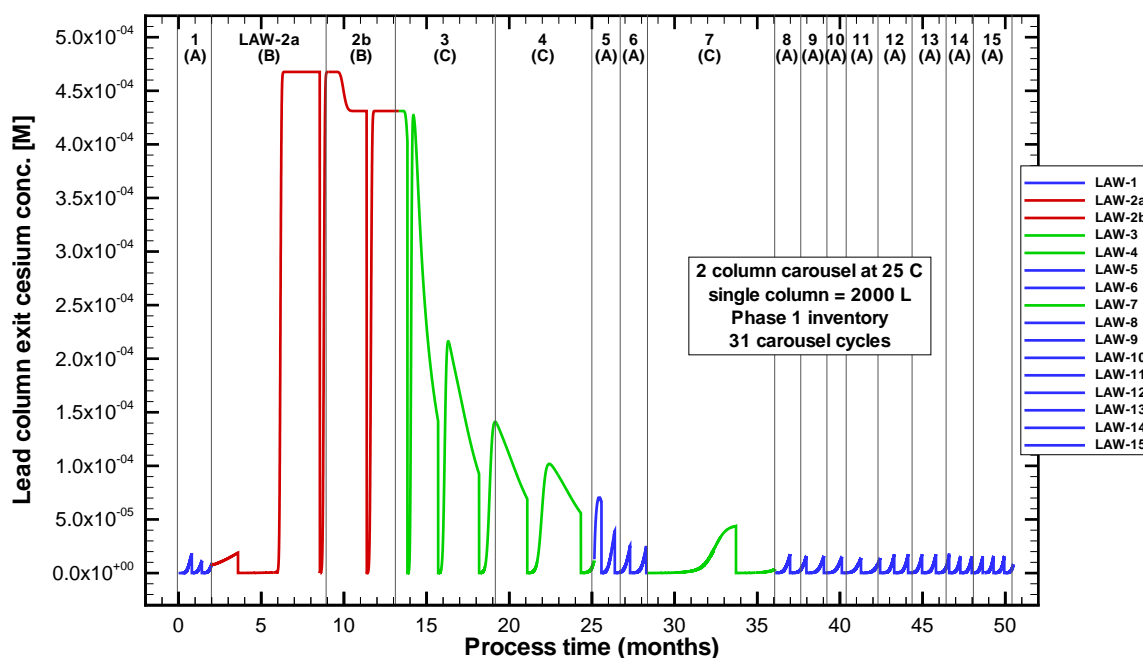


Figure 10-11. VERSE-LC cesium concentration predictions at the exit of the lead column based on CST and the Phase 1 LAW inventory (i.e., a 2-column carousel configuration operating at 25 C with 2000 L columns for a total of 31 carousel cycles performed).

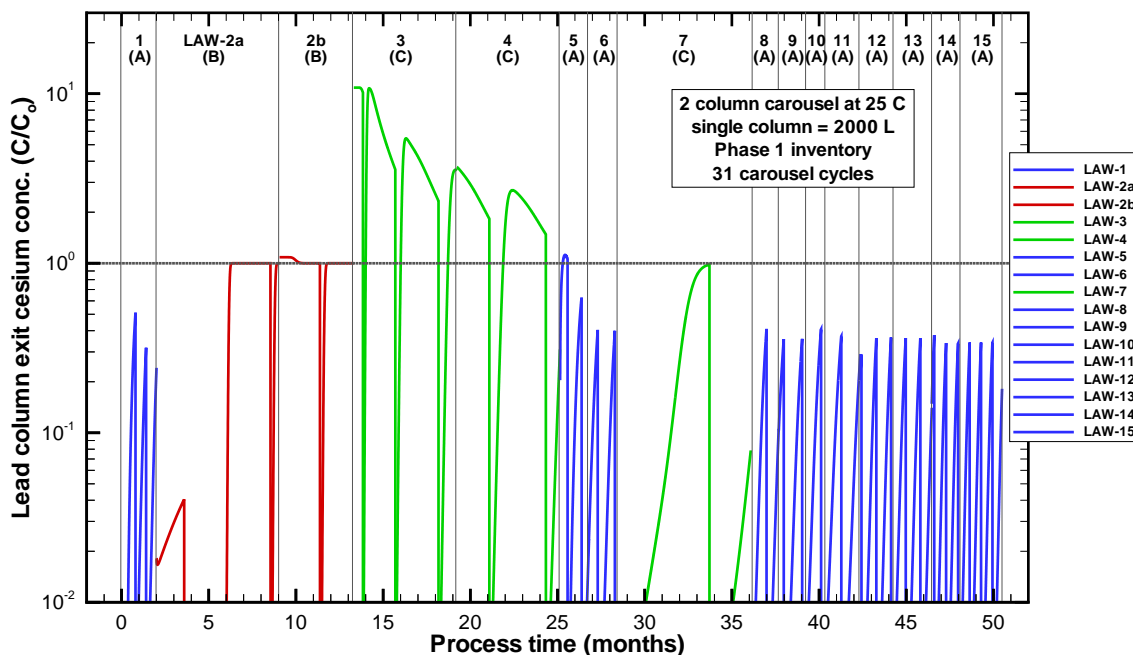


Figure 10-12. VERSE-LC normalized cesium concentration predictions at the exit of the lead column based on CST and the Phase 1 LAW inventory (i.e., a 2-column carousel configuration operating at 25 C with 2000 L columns for a total of 31 carousel cycles performed).



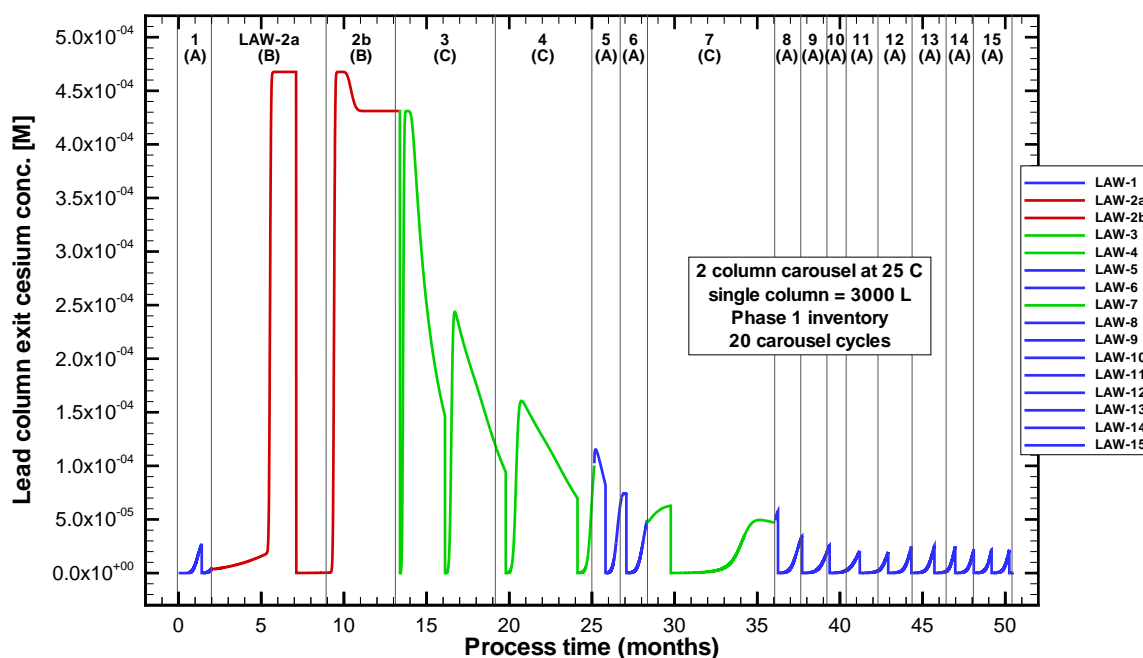


Figure 10-13. VERSE-LC normalized cesium concentration predictions at the exit of the lead column based on CST and the Phase 1 LAW inventory (i.e., a 2-column carousel configuration operating at 25 C with 3000 L columns for a total of 20 carousel cycles performed).

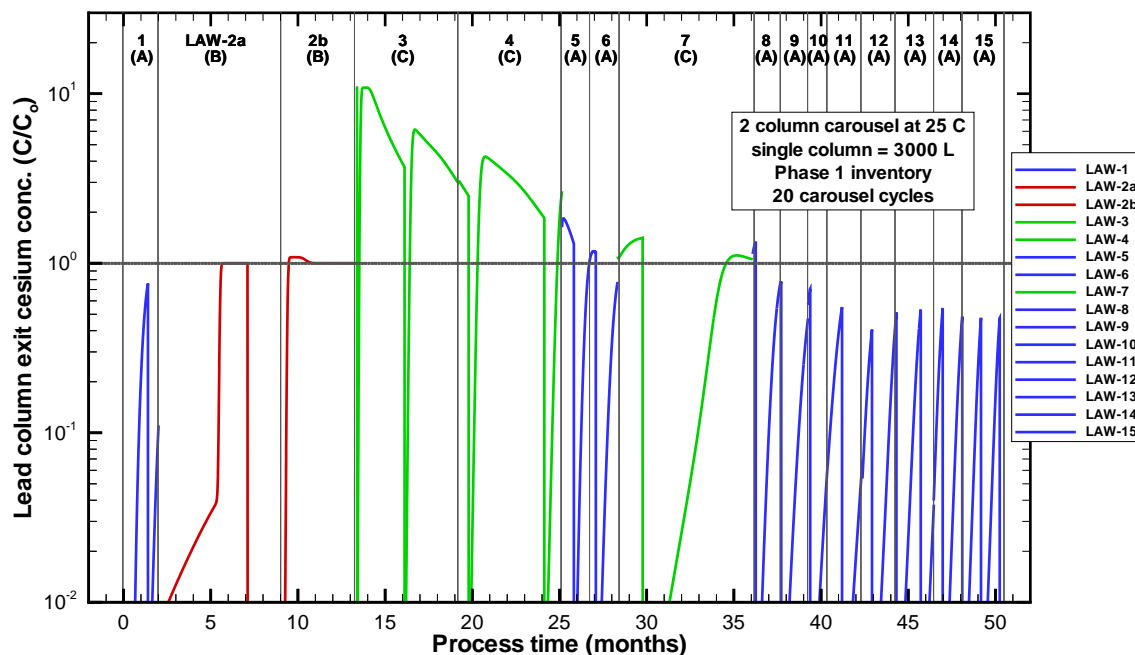


Figure 10-14. VERSE-LC cesium concentration predictions at the exit of the lead column based on CST and the Phase 1 LAW inventory (i.e., a 2-column carousel configuration operating at 25 C with 3000 L columns for a total of 20 carousel cycles performed).

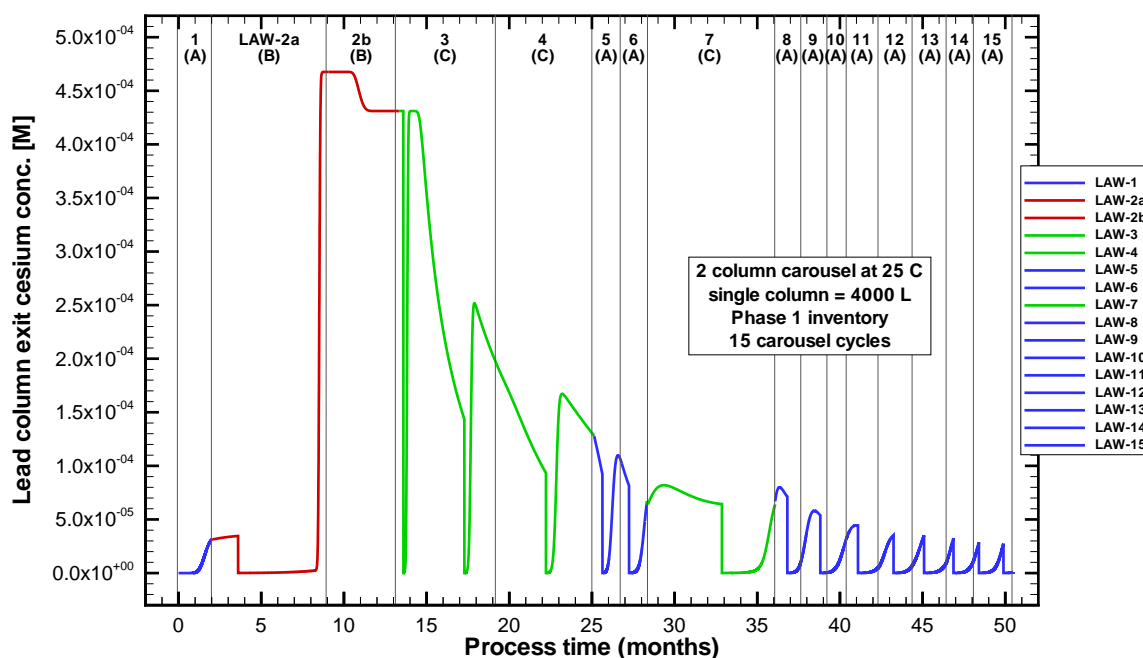


Figure 10-15. VERSE-LC cesium concentration predictions at the exit of the lead column based on CST and the Phase 1 LAW inventory (i.e., a 2-column carousel configuration operating at 25 C with 4000 L columns for a total of 15 carousel cycles performed).

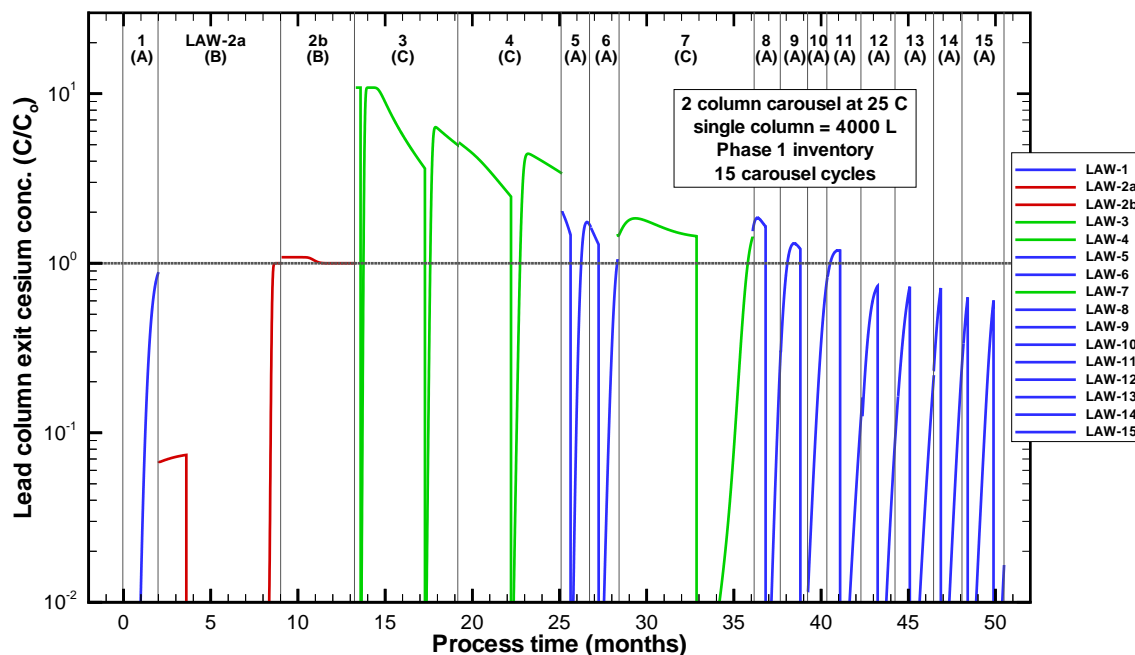


Figure 10-16. VERSE-LC normalized cesium concentration predictions at the exit of the lead column based on CST and the Phase 1 LAW inventory (i.e., a 2-column carousel configuration operating at 25 C with 4000 L columns for a total of 15 carousel cycles performed).

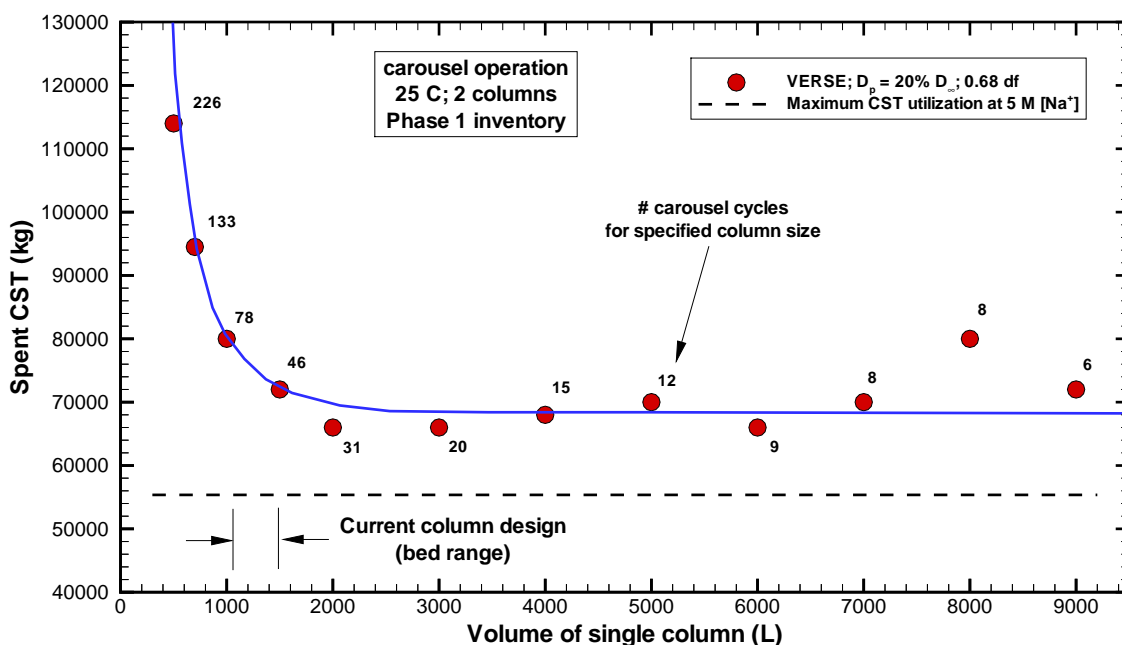


Figure 10-17. Computed total spent CST material required to process the entire Phase 1 LAW inventory based on a two-column carousel configuration at 25 C and nominal parameter settings (solid circles are VERSE-LC results while the solid line represents its average behavior).

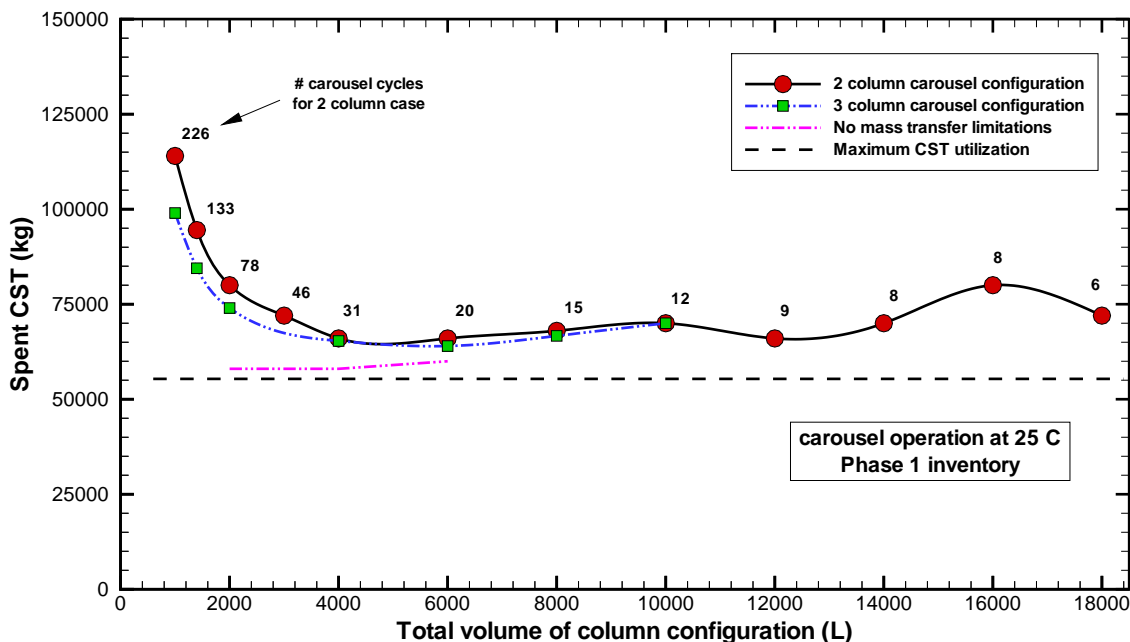


Figure 10-18. Computed total spent CST material required to process the entire Phase 1 LAW inventory at 25 C and nominal parameter settings (VERSE-LC results for 2-column and 3-column carousels and limiting cases).

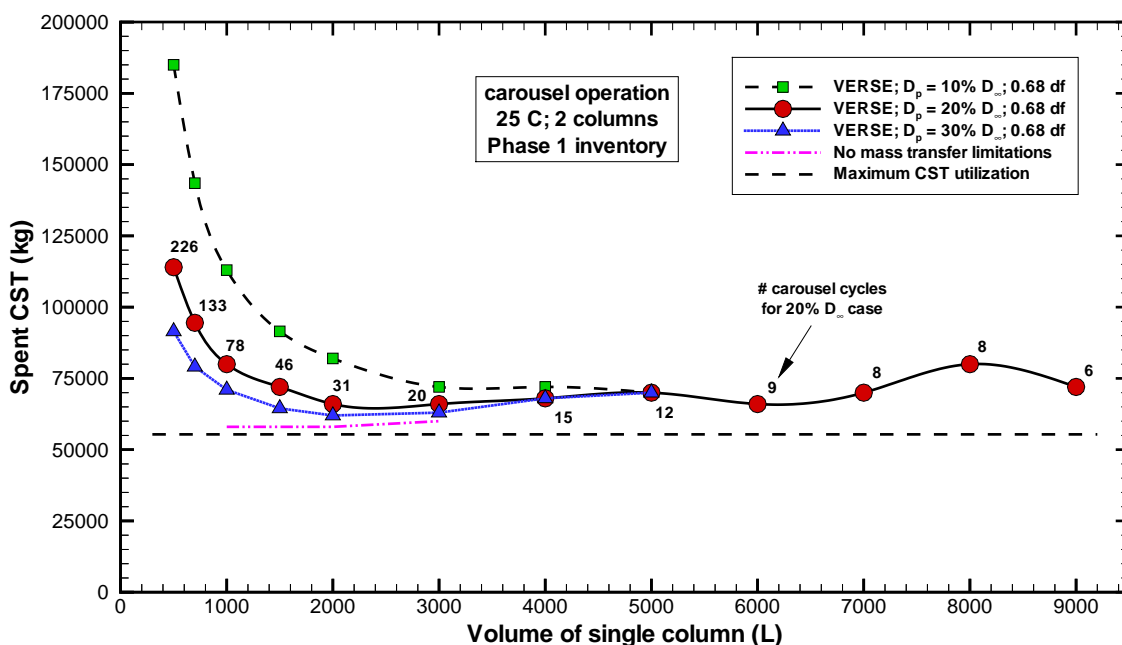


Figure 10-19. Computed total spent CST material required to process the entire Phase 1 LAW inventory based on a two-column carousel configuration at 25 C and nominal parameter settings (VERSE-LC results for various pore diffusivity coefficients and limiting cases).

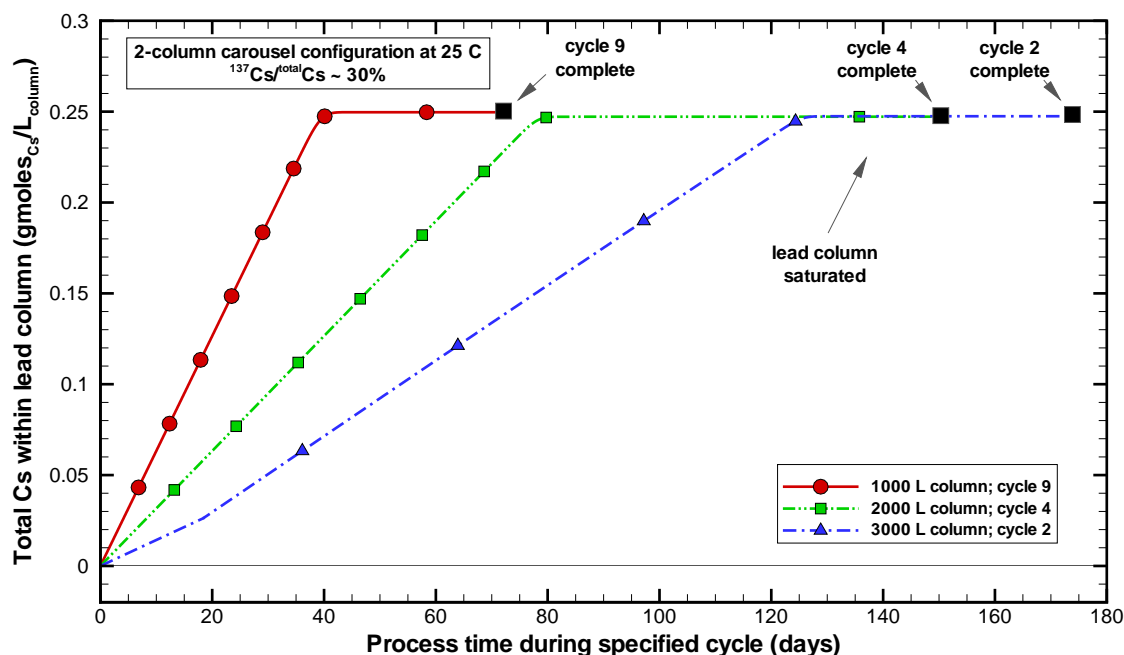


Figure 10-20. Estimated total cesium inventory contained within a lead column during the worst case process cycle for a two-column carousel configuration (results for 3 differing column sizes are shown; worst case cycles occur primarily in the LAW-2a processing period).

## 11.0 References

- Anderson, T. F., D. S. Abrams, and E. A. Grens, II, 1978. "Evaluation of Parameters for Nonlinear Thermodynamic Models," *AIChE Journal*, Vol. 24, No. 1, pp. 20-29.
- Anthony, R. T., C. V. Philip, and S. H. Kim, 2001. "Crystalline Silicotitanate Ion Exchange Support for Salt Alternatives: Final Report," Department of Chemical Engineering, Texas A&M University, Final report KF-90594-O, August 15.
- Berninger, J. A., R. D. Whitley, X. Zhang, and L. N.-H. Wang, 1991. "A Versatile Model for Simulation of Reaction and Nonequilibrium Dynamics in Multicomponent Fixed-Bed Adsorption Processes," *Computers Chem. Engr.*, Vol. 15, No. 11, pp. 749-768.
- Bray, L. A., J. E. Amonette, G. N. Brown, T. M. Kafka, and S. F. Yates, 1995. "Efficient Separations and Processing Crosscutting Program: Develop and Test Sorbents," a FY 1995 Annual Progress Report, PNL-10750 (UC-2030), Battelle PNL, September.
- Brooks, K. P., 1994. "Cesium Ion Exchange using Actual Waste: Column Size Considerations," TWRSP-94-091, PNNL, September.
- Brown, G. N., L. A. Bray, C. D. Carlson, K. J. Carson, J. R. DesChane, R. J. Elovich, F. V. Hoopes, D. E. Kurath, L. L. Nenninger, and P. K. Tanaka, 1996. "Comparison of Organic and Inorganic Ion Exchangers for Removal of Cesium and Strontium from Simulated and Actual Hanford 241-AW-101 DSSF Tank Waste," PNL-10920 (UC-2030), Battelle PNL, January.
- Chung, S. F. and C. Y. Wen, 1968. "Longitudinal Dispersion of Liquid Flowing Through Fixed and Fluidized Beds," *AIChE Journal*, Vol. 14, No. 6, pp. 857-866.
- Clift, R., J. R. Grace, and M. E. Weber, 1978. Bubbles, Drops, and Particles, Academic Press, Inc., Boston.
- Collins, J. L., B. Z. Egan, K. K. Anderson, C. W. Chase, J. T. Bell, and G. E. Jernigan, 1998. "Evaluation of Selected Ion Exchangers for the Removal of Cesium and Strontium from MVST W-25 Supernate," Chemical Technology Division, ORNL, (no report number given), August 27.
- Cussler, E. L., 1984. Diffusion: Mass Transfer in Fluid Systems, Cambridge University Press, Cambridge.
- Davidson, D. J., J. L. Collins, K. K. Anderson, C. W. Chase, and B. Z. Egan, 1998. "Removal of Cesium, Technetium, and Strontium from Tank Waste Supernatant," ORNL/TM-13612, Lockheed Martin ORNL, August.
- Ernest, M. V., Jr., R. D. Whitley, Z. Ma., and N.-H. L. Wang, 1997. "Effects of Mass Action Equilibria on Fixed-Bed Multicomponent Ion-Exchange Dynamics," *Ind. Eng. Chem. Res.*, Vol. 36, No. 1, pp. 212-226.
- Ernest, M. V., Jr., J. P. Bibler, R. D. Whitley, and N.-H. L. Wang, 1997. "Development of a Carousel Ion-Exchange Process for Removal of Cesium-137 from Alkaline Waste," *Ind. Eng. Chem. Res.*, Vol. 36, No. 7, pp. 2775-2788.
- Foo, S. C. and R. G. Rice, 1975. "On the Predication of Ultimate Separation in Parametric Pumps," *AIChE Journal*, Vol. 21, No. 6, pp. 1149-1158.
- GE Nuclear Energy, 1996. Nuclides and Isotopes, General Electric Company, Nuclear Energy Operations, 15<sup>th</sup> Edition, pp.31.

- German, R. M., 1989. Particle Packing Characteristics, Metal Powder Industries Federation, Princeton, New Jersey.
- Glasstone, S., and D. Lewis, 1960. Elements of Physical Chemistry, D. Van Nostrand Company, Inc., Princeton, N.J.
- Fiskum, S. K., ?, and ??????, 2000. "Inorganic, Radioisotopic, and Organic Analysis of 241-AP-101 Tank Waste," PNNL-13354, Battelle PNNL, October.
- Fondeur, F. F., T. Hang, M. P. Bussey, W. R. Wilmarth, D. D. Walker, and S. D. Fink, 2000. "The Effect of Carbonate, Oxalate, and Peroxide on the Cesium Loading of IONSIV® IE-910 and IE-911," WSRC-TR-2000-00344, October, 30.
- Freund, J. E., 1971. Mathematical Statistics, 2<sup>nd</sup> Edition, Prentice-Hall, Inc., N.J.
- Hamm, L. L., F. G. Smith, III, and A. M. Shadday, 1999. "QA Verification Package for VERSE-LC Version 7.80," WSRC-TR-99-00238, November.
- Hamm, L. L., F. G. Smith, III, and D. J. McCabe, 2000a. "Preliminary Ion Exchange Modeling for Removal of Cesium from Hanford Waste Using SuperLig® 644 Resin," BNF-003-98-0220, June 16.
- Hamm, L. L., F. G. Smith, III, and D. J. McCabe, 2000b. "Preliminary Ion Exchange Modeling for Removal of Technetium from Hanford Waste Using SuperLig® 639 Resin," WSRC-TR-2000-00305 (SRT-RPP-2000-00011), August.
- Hang, T., L. L. Hamm, and D. J. McCabe, 2001. "Estimating Effects of IONSIV IE-911 (Crystalline Silicotitanate) for Treating Hanford Phase 1 Low-Activity Waste Solutions (U)," WSRC-TR-2001-00033 (SRT-RPP-2001-00016), January 18.
- Hay, M. S. and M. G. Bronikowski, 2000. "Chemical Characterization of an Envelope B/D Sample from Hanford Tank 241-AZ-102," BNF-003-98-0249, July 31, revision 0.
- Hay, M. S., M. G. Bronikowski, and N. H. Hassan, 2000a. "Chemical Characterization of an Envelope A Sample from Hanford Tank 241-AN-103," BNF-003-98-0248, July 31, revision 0.
- Hay, M. S., M. G. Bronikowski, C. W. Hsu, and T. L. White, 2000b. "Chemical Characterization of an Envelope C Sample from Hanford Tank 241-AN-102," BNF-003-98-0250, July 31, revision 0.
- Hay, M. S., and T. B. Edwards, 1994. "Statistical Analysis of ESP Verification Test Samples," WSRC-RP-94-1224, November 4, revision 0.
- Helferich, 1962. Ion Exchange, McGraw-Hill series in advanced chemistry, McGraw-Hill Book Company, Inc., New York.
- Helferich, F. G. and P. W. Carr, 1993. The review paper "Non-linear Waves in Chromatography, I. Waves, Shocks, and Shapes," Journal of Chromatography, Vol 627, pp. 97-122.
- Hendrickson, D. W., 1997. "Hanford Salt Cake Cesium Removal Using Crystalline Silicotitanate," SGN Eurisys Services Corporation, SESC-EN-RPT-006. Revision 0, September.
- Hritzko, B. J., D. D. Walker, and N. H. L. Wang, 1998. "Design of a Carousel Process for Removing Cesium from SRS Waste Using Crystalline Silicotitanate Ion Exchanger," Progress report from School of Chemical Engineering, Purdue University, October 15.

- Huckman, M. E., I. M. Latheef, and R. G. Anthony, 1998. "Treating Savannah River Waste Using UOP IONSIV IE-911: revised Design Based on Laboratory Column Experiments," Kinetics, Catalysis, and Reaction Engineering Laboratory, Department of Chemical Engineering, Texas A&M University, October 18.
- Huckman, M. E., I. M. Latheef, and R. G. Anthony, 1999. "Ion Exchange of Several Radionuclides on the Hydrous Crystalline Silicotitanate, UOP IONSIV IE-911," Separation Science and Technology, Vol. 34, pp. 1145-1166.
- Johnson, M. E., 2000. "Estimating Effects of IONSIV IE-911 (Crystalline Silicotitanate) for Treating Hanford Phase 1 Low-Activity Waste Solutions: Test Specification," TSP-W375-00-00029, Revision 0, November 27.
- Kirkbride, R. A., G. K. Allen, B. A. Higley, R. M. Orme, R. S. Wittman, J. H. Baldwin, T. W. Crawford, J. Jo, J. N. Strode, T. M. Hohl, S. L. Lambert, D. E. Place, and J. A. Seidl, 2000. "Tank Farm Contractor Operation and Utilization Plan," HNF-SD-WM-SP-012 (Revision 2), April.
- Lee, D. D., J. F. Walker, Jr., P. A. Taylor, and D. W. Hendrickson, 1997a. "Cesium-Removal Flow Studies using Ion Exchange," Environmental Progress, Vol. 16, No. 4 pp. 251-262.
- Lee, D. D., J. R. Travis, and M. R. Gibson, 1997b. "Hot Demonstration of Proosed Commerical Cesium Removal Technology," ORNL/TM-13169, December.
- Liles, A. W. and C. J. Geankoplis, 1960. "Axial Diffusion of Liquids in Packed Beds and End Effects," AIChE Journal, Vol. 6, No. 4, pp. 591-595.
- Ma, Z., R. D. Whitley, and N.-H. L. Wang, 1996. "Pore and Surface Diffusion in Multicomponent Adsorption and Liquid Chromatography Systems," AIChE Journal, Vol. 42, No. 5, pp. 1244-1262.
- McCabe, D. J., 1995. "Crystalline Silicotitanate Examination Results (U)," WSRC-RP-94-1123, Revision 0, May 18.
- McCabe, D. J., 1997. "Examination of Crystalline Silicotitanate Applicability in Removal of Cesium from SRS High Level Waste (U)," WSRC-TR-97-0016, Revision 0, April 25.
- Miller, J. E., and N. E. Brown, 1997. "Development and Properties of Crystalline Silicotitanate (CST) Ion Exchangers for Radioactive Waste Applications," Sandia National Laboratories, SAND97-0771, April.
- Morales, M., C. W. Spinn, and J. M. Smith, 1951. "Velocities and Effective Thermal Conductivities in Packed Beds," Industrial and Engr. Chemistry, Vol. 43, No. 1, pp. 225-232.
- Philip, C. V. and R. G. Anthony, 2000. "Crystalline Silicotitanate Ion Exchange Support for Salt Alternatives," Department of Chemical Engineering, Texas A&M University, Final report KE-49242-0, September 30.
- Qureshi, Z. H., 1999. "Mixing and Sampling of Sludge-Frit-CST Slurries (U)," WSRC-TR-99-00309, September.
- Reynolds, D. A. and D. L. Herting, 1984. "Solubilities of Sodium Nitrate, Sodium Nitrite, and Sodium Aluminate in Simulated Nuclear Waste," RHO-RE-ST-14P, Rockwell International, Rockwell Hanford Operations, September.
- Robinson, S. M., W. D. Arnold, and C. H. Byers, 1994. "Mass-Transfer Mechanisms for Zeolite Ion Exchange in Wastewater Treatment," AIChE Journal, Vol. 40, No. 1, pp. 2045.
- Schwartz, C. E. and J. M. Smith, 1953. "Flow Distribution in Packed Beds," Industrial and Engr. Chemistry, Vol. 45, No. 6, pp. 1209-1218.

- Steimke, J. L., M. A. Norato, T. J. Steeper, and D. J. McCabe, 2000. "Summary of Testing of SuperLig® 639 at the TFL Ion Exchange Facility," WSRC-TR-2000-00302 (SRT-RPP-2000-00008), Rev. 0, August 24.
- Thibaud-Erkey, C. and R. G. Anthony, 1999. "Mathematical Modeling of an Ion-Exchange Column for Nuclear Waste Remediation," Department of Chemical Engineering, Texas A&M University, Special report RF-8761-#2.
- Walker, D. D. and C. J. Coleman, 1991. "Densities and Weight % Solids of Simulated Salt Solutions (U)," WSRC-TR-91-176, April 17.
- Walker, D. D., 1998. "Modeling of Crystalline Silicotitanate Ion Exchange Columns," WSRC-TR-98-00343, Revision 0, October 12.
- Walker, D. D., W. D. King, D. P. Diprete, L. L. Tovo, D. T. Hobbs, and W. L. Wilmarth, 1998a. "Cesium Removal from Simulated SRS High-Level Waste using Crystalline Silicotitanate," WSRC-TR-98-00344, Revision 1, October 16.
- Walker, J. F., Jr., P. A. Taylor, R. L. Cummins, B. S. Evans, S. D. Heath, J. D. Hewitt, R. D. Hunt, H. L. Jennings, J. A. Kilby, D. D. Lee, S. Lewis-Lambert, S. A. Richardson, and R. F. Utrera, 1998b. "Cesium-Removal Demonstration Utilizing Crystalline Silicotitanate Sorbent for Processing Melton Valley Storage Tank supernate: Final Report," ORNL/TM-13503, March.
- Walker, D. D., 1999a. "Modeling of Crystalline Silicotitanate Ion Exchange Columns using Experimental Data from Simulated SRS Waste," WSRC-TR-98-00396, Revision 0, January 6.
- Walker, D. D., 1999b. "Preparation of Simulated Waste Solutions," WSRC-TR-98-00116, Revision 0, April 15.
- Walker, D. D., D. J. Adamson, T. D. Allen, R. W. Blessing, W. T. Boyce, B. H. Croy, R. A. ewberry, D. P. Diprete, S. D. Fink, T. Hang, J. C. Hart, M. C. Lee, J. J. Olson, and M. J. Whitaker, 1999. "Cesium Removal from Savannah River Site Radioactive Waste using Crystalline Silicotitanate (IONSIV® IE-911)," WSRC-TR-99-00308, Revision 0, September 18.
- Walker, D. D., W. R. Wilmarth, S. D. Fink, M. Nymar, J. Krumhansel, J. T. Mills, V. H. Dukes, and B. H. Croy, 2001. "Examination of Pre-production Samples of UOP IONSIV® IE-910 and IE-911," WSRC-TR-2001-00221, Revision 0, April 18.
- Washburn, E. W., C. J. West, N. E. Dorsey, F. R. Bichowsky, and A. K. Klemenc, 1928. International Critical Tables of Numerical Data, Physics, Chemistry and Technology, Volume IV, by the National Research Council of U.S.A., McGraw-Hill Book Company, Inc., New York.
- Wilmarth, W. L., T. Hang, J. T. Mills, V. H. Dukes, and S. D. Fink, 1999. "The Effect of Pretreatment, Superficial Velocity, and Presence of Organic Constituents on IONSIV® IE-911 Column Performance," WSRC-TR-99-00313, August 31.
- Wilson, E. J. and C. J. Geankoplis, 1966. "Liquid Mass Transfer at Very Low Reynolds Numbers in Packed Beds," *Industrial and Engineering Chemistry Fundamentals*, Vol. 5, No. 1, pp. 9-14.
- UOP, 1996, "IONSIV Ion Exchangers: Crystalline Silicotitanates – Novel Commerical Cesium Ion Exchangers," a product information/specification advertisement brochure.
- Zheng, Z., D. Gu, and R. G. Anthony, 1995. "Estimation of Cesium Ion Exchange Distribution Coefficients for Concentrated Electrolytic Solutions When Using Crystalline Silicotitanates," *Ind. Eng. Chem. Res.*, Vol. 34, No. 6, pp. 2142-2147.



Zheng, Z., C. V. Philip, R. G. Anthony, J. L. Krumhansl, D. E. Trudell, and J. E. Miller, 1996. "Ion Exchange of Group I Metals by Hydrous Crystalline Silicotitanates," Ind. Eng. Chem. Res., Vol. 35, No. 11, pp. 4246-4256.

Zheng, Z., R. G. Anthony, and J. E. Miller, 1997. "Modeling Multicomponent Ion Exchange Equilibrium Utilizing Hydrous Crystalline Silicotitanates by a Multiple Interactive Ion Exchange Site Model," Ind. Eng. Chem. Res., Vol. 36, No. 6, pp. 2427-2434.

(This Page Intentionally Left Blank)

## Appendix A (BBI Phase 1 LAW Feed Solution Definitions)

For evaluation and sizing of ion-exchange columns based on CST resin, candidate batch feed compositions for each Envelope (i.e., Envelopes A, B, and C) must be considered. The 16 candidate batch feeds are determined based on available Best Basis Inventory (BBI) Phase 1 LAW feed solution data. Alterations and adjustments were necessary to the raw BBI data in order for it to conform to current pretreatment plans and for overall charge balancing. The alterations and adjustments made focused on only those ionic species who have a direct impact on cesium loading (i.e., those ionic species considered in the cesium isotherm modeling – ZAM code input options). No attempt was made to adjust or correct all species inventories provided in the test specification document; however, for comparative purposes the concentrations of these species are provided.

No recent equilibrium batch contact testing is available for establishing or verifying the batch feed isotherms. Instead, cesium adsorption isotherms are estimated based on the ZAM equilibrium model developed at Texas A&M for CST powder material. In order to successfully use the ZAM equilibrium model, charge balancing is required for the species chosen as input to the algorithm. Below, the various alterations/adjustments, and the reasoning behind them, are provided. A brief description and user's guide to ZAM is provided in Appendix F where some limited validation of ZAM for Hanford waste feeds is provided (based on earlier AW-101 contact data).

The planned waste treatment processing of the Phase 1 LAW tank inventory consists of processing 16 separate batches of feeds from the ten targeted waste tanks in a sequential fashion (based on a current schedule). The sequence chosen is reflected in the numbering sequence used to label each batch feed (i.e., LAW-1, LAW-2a, LAW-2b, LAW-3, ..., LAW-15). Each batch represents a fixed amount of liquid waste volume whose volume includes all planned dilution processes. Decay corrections for the various radioisotopes listed are also considered, based on the scheduled time of processing.

### A.1 Altered Tank Solutions

BBI Phase 1 LAW feed solution data (i.e., 11 Envelope A's, 2 Envelope B's, and 3 Envelope C's) for the following tanks were provided within the test specification document by Johnson (2000):

- Envelope A (AP-101, AN-104, AN-105, SY-101, AN-103, AW-101);
- Envelope B (AZ-101 and AZ-102); and
- Envelope C (AN-102, AN-107).

The following alterations were made to these candidate feed solutions to establish our starting point for performing isotherm modeling:

- The “bound”  $\text{OH}^-$  inventory for Envelope C’s AN-107 (i.e., LAW-7) appeared to be off by one order of magnitude (i.e.,  $3.48 \times 10^{+7}$  gmoles provided and assumed to be  $3.48 \times 10^{+6}$  gmoles). The inventory value was reduced by one order of magnitude based on charge balance considerations.
- Inconsistencies between total cesium and cesium-137 (i.e., in some cases more  $^{137}\text{Cs}$  present than total cesium) existed. For Envelope A and C wastes, total cesium was estimated by assuming that  $^{137}\text{Cs}$  inventories are correct and that the isotopic fraction of  $^{137}\text{Cs}$  to total is 25%. For Envelope B wastes the test specification contains cesium values based on the project baseline assumption that the AZ tanks are pretreated and waste is then returned to the double-shell tanks (DSTs) for storage and vitrification to occur at a later date. However, a revised baseline assumes that the supernate in the AZ tanks is pretreated and vitrified all at once. Therefore, new values for the original cesium content in the AZ tanks will be based on the Tank Farm COUP report (Kirkbride et al., 2000, see Table 3.1-2) where for tanks AZ-101 and AZ-102 the  $^{137}\text{Cs}$  inventories were reported as  $1.23 \times 10^{10}$  and  $1.33 \times 10^{10}$  Bq/gmole of Na, respectively. This results out to 1.662 and 1.797 Ci/L at 5.0 M Na. For Envelope B wastes the  $^{137}\text{Cs}$  total cesium fraction is set to 30%.
- “Free”  $\text{OH}^-$  inventory was estimated by first summing up the tabulated values for  $\text{OH}^-$  and “bound”  $\text{OH}^-$ . Then, this sum was reduced to account for the amount used to form  $\text{Al}(\text{OH})_4^-$  and  $\text{Cr}(\text{OH})_4^-$ , where listed inventories for total Al and total Cr were assumed to be correct. For one feed solution (i.e., Envelope B LAW-2b) the computed free  $\text{OH}^-$  inventory, based on this logic, would result in a negative value given the total amount of Al and Cr reported. Even when total  $\text{OH}^-$  was used (i.e., not reduced by either the Al or Cr terms), a negative charge balance would result, indicating that an increase in the cations was needed. The reported tank concentration for  $\text{Na}^+$  was 2.36 M, while measurements taken by Hay and Bronikowski (2000) for a sample of Tank AZ-102 gave a concentration for  $\text{Na}^+$  of 2.77 M. A negligible difference is seen for the  $\text{K}^+$  concentration between the two data sources. Using this sodium value eliminated the negative  $\text{OH}^-$  concentration upon reaching an ionic charge balance and was considered an acceptable value to use.
- The  $\text{H}^+$  inventory was zero. For modeling purposes the concentration was computed based on the estimated “free”  $\text{OH}^-$  concentration for every feed solution (i.e., this is not a sensitive parameter under these highly alkaline conditions).
- Numerous species listed in the Phase 1 LAW feed solution data provided in the test specification document contained zero inventories for all 16 waste feed solutions. These species were omitted from further calculational processing.
- The species inventories were provided by Johnson (2000) in gmole units along with estimated total liquid volumes. Molar concentrations were computed based on the above alterations to the data set and then dividing by the specified total liquid volume for each candidate feed solution to convert to molarity units. Note that the total liquid volumes provided are the actual tank liquid inventories including estimated increases associated with the necessary dilution processes used during tank retrieval and pipeline transport activities.

- It is assumed that no liquid-phase or surface reactions are occurring at a kinetic rate of importance where species are being created or destroyed. Potential liquid-phase and precipitation reactions that may occur during a dilution or concentration process have not been considered.
- For waste tank AP-101 (LAW-1) the Tank Farm COUP report (Kirkbride et al., 2000) contains errors in its estimates for inventories of K, Na, and  $^{137}\text{Cs}$  (based on recent information provided by Mike Johnson). As such, more recent analytical analyses performed by Fiskum et al. (2000) on an AP-101 sample are used. The  $^{137}\text{Cs}$  inventory provided by Fiskum et al. (2000) was decay adjusted by 8 years to account for the expected time duration between the measurements and LAW-1 pretreatment processing.
- All  $^{137}\text{Cs}$  inventories are decay corrected from ~1999 to the date of waste processing in the Waste Treatment Plant (WTP) and all concentrations computed are based on total tank volumes plus any additional liquid processing volumes necessary.

Based on the above stated alterations/processing, the Phase 1 LAW feed solution data in terms of molarity are provided in Tables A-1 and A-2. The assumed valence state, of only those species used in the equilibrium isotherm modeling, is provided.

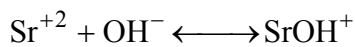
In computing the “free”  $\text{OH}^-$  concentration levels for each candidate feed batch, a three-step process was used:

- First, “total”  $\text{OH}^-$  concentration levels were computed from the available inventory database;
- Next, “free”  $\text{OH}^-$  concentration levels were estimated by subtracting off from the “total”  $\text{OH}^-$  four times the amount of total Al and total Cr present (i.e., assumed to be in the  $\text{Al}^{\text{III}}(\text{OH})_4^-$  and  $\text{Cr}^{\text{III}}(\text{OH})_4^-$  forms);
- Finally, the “free”  $\text{OH}^-$  concentration levels were then adjusted to establish a neutral solution (i.e., to maintain an ionic charge balance based only on those species available in ZAM).

If some fraction of the total Cr is in the  $\text{Cr}^{\text{VI}}$  state, it would probably be in the species form of  $\text{Cr}^{\text{VI}}\text{O}_4^{2-}$ . Under these conditions the second step above should be change to only subtract off the  $\text{Al}^{\text{III}}(\text{OH})_4^-$  species. Separate analyses were made where all of the total Cr was assumed to be in the  $\text{Cr}^{\text{VI}}$  state. The final “free”  $\text{OH}^-$  concentration levels were generally within 3% (for Envelope A and B feeds) and 10% (for Envelope C feeds) when compared to the above approach, indicating that either method would be acceptable for our purposes within this report.

## A.2 Isotopic Dilution Process for Strontium-90

Strontium is present in high quantities within Envelope C feed solutions. The current pretreatment plan for the Envelope C waste solutions (i.e., tanks AN-102 and AN-107) is to perform an isotopic dilution process to reduce  $^{90}\text{Sr}^{+2}$  within the feed solutions entering the ion-exchange facility by adding strontium (in natural abundance) and precipitating out  $\text{SrCO}_3$ . Within the liquid phase an equilibrium reaction involving  $\text{Sr}^{+2}$ ,  $\text{OH}^-$ , and  $\text{SrOH}$  exists:



The actual amount of  $\text{Sr}^{+2}$  present within a liquid solution, that is available for CST ion exchange in the form  $\text{SrOH}^{+}$ , is currently unknown due to the various reactions occurring and the formation of  $\text{Sr}^{+2}$  based complexants (e.g., EDTA). Even though the ZAM equilibrium model can estimate the competitive adsorption rate of  $\text{SrOH}^{+}$  onto CST, we shall assume that no  $\text{SrOH}^{+}$  species are present in the isotherm modeling for Envelope A, B, and C solutions. To remove transuranic (TRU) elements (e.g.,  $^{241}\text{Am}$ ),  $\text{Na}(\text{MnO}_4)$  is added where TRUs are co-precipitated out of solution along with manganese dioxide.

However, in order to obtain the correct amounts of  $\text{Na}^{+}$  and  $\text{NO}_3^{-}$  within a feed solution, adjustments are made consistent with the current isotopic dilution process for the Envelope C solutions (i.e., only done for Envelope C feeds). The processes used to make these adjustments are:

- First, the candidate feed solutions (see batches LAW-3, LAW-4, and LAW-7 in Table A-2) are diluted to 6 M  $\text{Na}^{+}$  by the addition of water;
- 18 M  $\text{NaOH}$  is then added to the above diluted solution until the free  $\text{OH}^{-}$  concentration reaches  $\sim 1$  M (i.e., in some cases free  $\text{OH}^{-}$  concentration already greater than 1 M and no addition was made);
- Assuming zero initial  $\text{Sr}^{+2}$  present in the feed solutions,  $\text{Sr}(\text{NO}_3)_2$  is added until its concentration reaches  $\sim 0.075$  M; and
- Finally,  $\text{Na}(\text{MnO}_4)$  is added until its concentration reaches  $\sim 0.05$  M.
- A significant amount of the strontium added forms precipitates that are separated out from the feed solution leaving behind a saturated (at the solubility limits) feed solution isotopically diluted with respect to  $^{90}\text{Sr}^{+2}$ .

Table A-3 contains the species concentrations for the Envelope C feed solutions after application of the above pretreatment process steps.

### A.3 Adjusted Tank Solutions for $K_d$ Modeling

The ZAM equilibrium model for CST (i.e., CSTIEXV#, version #, # = 4 and 5) was chosen to compute the ion exchange characteristics of CST material in the powder-form when exposed to various Hanford waste solutions. An estimated correction factor must then be applied to the powder-form results when estimating the performance behavior of the CST engineered-form exchangers. In order to compute the equilibrium cesium loading (and its  $K_d$  value), and final cesium liquid concentration for a specific liquid sample, the liquid sample must be defined such that the important ionic species are specified. Also, the overall charge balance for these specific species must be very close to being neutral (i.e., a net misbalance in charge less than  $\sim 5 \times 10^{-4}$ ). The ionic concentrations in the above 16 candidate feed solutions (see Tables A-1 and A-3) were adjusted to meet the restrictions/limitations imposed by ZAM based on the following:

- Due to pretreatment issues associated with what “free”  $\text{Sr}^{2+}$  would be available within the liquid solutions, it was assumed that no  $\text{Sr}^{2+}$  would be present. Since a reaction equilibrium between  $\text{Sr}^{2+}$  and  $\text{SrOH}^+$  exists within the liquid phase, no  $\text{SrOH}^+$  will be present to compete for exchange sites. Therefore, Cs loadings are over-predicted based on this assumption and its impact should be reconsidered in future efforts.
- Only those cation and anion species available as input to ZAM are considered (see Table A-4 for listing of available ionic species). ZAM does allow the limited input of other special species (i.e., IDs 37-39 for cations and IDs 24-26 for anions, but the current list appeared adequate for our purposes.
- To arrive at a neutral charge balance, based only on those species available to ZAM, the ‘free’  $\text{OH}^-$  concentration was adjusted up or down, if necessary.
- In order to determine which feed solution represents a worst case feed for each Envelope, every feed solution was diluted/evaporated to a 5.0 M  $\text{Na}^+$  state. Therefore, the identification of an Envelope’s worst feed composition is based on a common  $\text{Na}^+$  basis where sensitivity studies are then performed on each worst case solution where  $\text{Na}^+$  concentrations are varied by evaporation/dilution.
- Since the species  $\text{Cr}(\text{OH})_4^-$  is not available for use in ZAM, species  $\text{Al}(\text{OH})_4^-$  represents the total concentration of both species. Sensitivity studies indicated that this would have a small effect on ZAM predicted cesium loadings.

The final “best estimate” concentrations used to model the CST ion-exchange process for each candidate feed solution is listed in Tables A-5 and A-6 where only those input species available as input to ZAM are listed.

ZAM addresses the surface adsorption (i.e., ion-exchange) competition between  $\text{Na}^+$ ,  $\text{K}^+$ ,  $\text{Cs}^+$ ,  $\text{H}^+$ ,  $\text{Rb}^+$ , and  $\text{SrOH}^+$ . For this set of analyses it is assumed that  $\text{Rb}^+$  and  $\text{SrOH}^+$  cations are negligible in the liquid feed (i.e., their concentrations are set to zero).

#### A.4 Feed Solution Densities

The ZAM equilibrium model for CST computes a point on the cesium adsorption isotherm by performing a simulated batch equilibrium contact experiment. In order to compute the necessary liquid-phase activity coefficients, the ZAM code must have as input the liquid density of the feed sample of interest. The liquid-phase density is used to convert the inputted concentration of ionic species from molarity to molality units. Molality units (gmole/kg-water) are used by the activity coefficient correlation (i.e., Bromley’s) and in computing the mixture total ionic strength. Based on several ZAM runs, predicted cesium loadings are not very sensitive to solution density.

Polynomial based correlations exist based on the fitting of available experimentally measured liquid density for a range of LAW samples and simulants. For SRS wastes the Walker correlation (Walker and Coleman, 1991) has been used. For Hanford wastes the Reynolds-

Herting correlation (Reynolds and Herting, 1984) and more recently the HTWOS Density model (Kirkbride et al., 2000), have been used. Kirkbride et al. (2000) recommends the use of the HTWOS density model due to its flexibility of adding future components. A subset of the available liquid density data is provided in Table A-7.

For Hanford LAWs the functional form of the two correlations (based on molarity concentration and degree C temperature units) are:

$$\rho_{RH} = 1.017 + 0.0587c_{AlO_2} - 0.01943c_{OH} - 0.000883c_{NO_2}c_{NO_3} + 0.0459(c_{AlO_2} + c_{OH} + c_{NO_3} + c_{NO_2}) - 0.000505T \quad (A-1)$$

for the Reynolds-Herting correlation and

$$\rho_{HTWOS} = 1.0 + 0.2 \left( \begin{array}{l} -0.0955c_{Al}^2 + 0.383c_{Al} - 0.0054c_{Na}^2 + 0.1096c_{Na} \\ -0.073c_{NO_2}^2 + 0.373c_{NO_2} + 0.00046c_{NO_3}^2 \\ + 0.201c_{NO_3} + 0.0197c_{OH}^2 + 0.0077c_{OH} \end{array} \right) \quad (A-2)$$

for the HTWOS density model. Both correlations are limited in what species are accounted for. For waste solutions containing significant quantities of other species it is expected that these correlations will generally under predict liquid density. One simple way to approximate the impact associated with other ionic species is to add their mass to the total mass present assuming that zero volume of mixing occurs as a result of their presence. For example, the HTWOS density model can be modified to account for the added species by the expression:

$$\rho_{HTWOS}^{Mod} = \rho_{HTWOS} + \frac{\theta}{1000} \sum_j c_j M_j \quad (A-3)$$

where the liquid density is in g/ml, ionic concentrations in molarity,  $M_j$  the ionic molecular weight, the summation is over all ionic species excluding Al, Na,  $NO_2$ ,  $NO_3$ , OH, and a correction factor  $\theta$ . The correction factor would be one if zero volume of mixing occurred upon addition of other species and if the original HTWOS density model was based on samples containing only Al, Na,  $NO_2$ ,  $NO_3$ , OH. Based on the data provided in Table A-7, a correction factor ( $\theta$  in Eq. (A-3)) of ~0.6 is required.

Date taken from several sources [i.e., Hay and Bronikowski (2000), Hay et al. (2000a), Hay et al. (2000b), PNNL PNWD-3001, PNNL PNWD-3039, Steimke et al. (2000), and Walker and Coleman (1991)] are provided in Table A-7. A comparison to the Hanford waste data is made between the Reynolds-Herting correlation, the HTWOS density model, and the modified HTWOS density model. The results of the comparison are shown in Table A-8. Based on computed mean bias and root mean square indicators, as expected, the HTWOS density model out performs the Reynolds-Herting correlation. Also, the simple modification to the HTWOS density model provides additional improvements.



For the creation of cesium adsorption isotherms using the ZAM model, the modified HTWOS density model is chosen (i.e., Eq. (A-3)) where the summation is over all species other than those directly accounted for by the original HTWOS density model. The corresponding “best estimate” liquid densities for the various candidate feed solutions are provided in Tables A-5 and A-6. Liquid density based on both the original HTWOS density model and its modification are listed, along with the percent difference in the estimates.

Table A-1. Best Basis Inventory (BBI) Phase 1 LAW feed solution data for Envelope A where stated alterations were made to minimize inventory inconsistencies and to establish an ionic charge balance (a value of zero implies that no information was provided on species).

Batch Name		LAW-1	LAW-5	LAW-6	LAW-8	LAW-9	LAW-10	LAW-11	LAW-12	LAW-13	LAW-14	LAW-15
Staging (Source) Tank		AP-101	AN-104	AN-104	AN-105	AN-105	SY-101	SY-101	AN-103	AN-103	AW-101	AW-101
Total Volume of Liquid (L)		4.12E+06	2.77E+06	2.57E+06	2.66E+06	2.57E+06	2.83E+06	3.37E+06	3.49E+06	3.52E+06	2.82E+06	3.84E+06
Species	Concentration Units	[M]	[M]	[M]	[M]	[M]	[M]	[M]	[M]	[M]	[M]	[M]
Charge	LAW Envelope	A	A	A	A	A	A	A	A	A	A	A
-1	129-I	3.53E-06	1.12E-05	1.17E-05	3.05E-05	1.44E-05	1.20E-05	1.01E-05	1.00E-05	9.38E-06	1.31E-05	1.28E-05
	137-Cs	1.01E-05	2.17E-05	2.18E-05	1.50E-05	1.56E-05	8.48E-06	1.28E-05	1.63E-05	1.62E-05	1.60E-05	1.59E-05
1	Total Cs (137-Cs/iso fraction)	4.04E-05	8.66E-05	8.72E-05	6.02E-05	6.23E-05	3.39E-05	5.10E-05	6.53E-05	6.48E-05	6.38E-05	6.35E-05
	232-Th	0.00E+00	7.94E-05	7.16E-05	5.83E-05	1.05E-05	5.41E-05	4.15E-06	1.14E-04	1.15E-04	5.99E-04	7.97E-04
	238-U	2.31E-04	4.15E-05	3.85E-05	3.80E-05	6.23E-06	6.78E-05	5.82E-05	8.02E-06	7.10E-06	4.08E-04	5.47E-04
	99-Tc	2.92E-05	6.86E-05	6.89E-05	1.03E-04	1.11E-04	8.69E-05	8.93E-05	5.73E-05	5.54E-05	7.94E-05	6.90E-05
3	Al	0.00E+00	0.00E+00	0.00E+00	0.00E+00	0.00E+00	0.00E+00	0.00E+00	0.00E+00	0.00E+00	0.00E+00	0.00E+00
-1	Al(OH) <sub>4</sub>	2.60E-01	7.83E-01	7.90E-01	8.83E-01	6.30E-01	4.52E-01	6.35E-01	1.01E+00	1.01E+00	6.81E-01	6.98E-01
	As	0.00E+00	0.00E+00	0.00E+00	0.00E+00	0.00E+00	0.00E+00	0.00E+00	0.00E+00	0.00E+00	0.00E+00	0.00E+00
	B	0.00E+00	0.00E+00	0.00E+00	0.00E+00	0.00E+00	0.00E+00	0.00E+00	0.00E+00	0.00E+00	0.00E+00	0.00E+00
2	Ba	2.40E-06	8.23E-05	8.75E-05	1.26E-04	5.80E-05	0.00E+00	2.67E-06	7.54E-05	7.33E-05	1.45E-05	0.00E+00
	Bi	0.00E+00	2.27E-05	2.02E-05	1.34E-04	9.92E-05	6.11E-05	1.48E-06	8.22E-05	8.01E-05	3.01E-05	6.77E-06
2	Ca	1.90E-04	6.61E-04	6.85E-04	1.48E-03	1.47E-03	1.50E-03	3.03E-03	4.53E-04	4.20E-04	1.27E-03	1.20E-03
2	Cd	1.70E-05	1.01E-05	1.05E-05	3.42E-05	5.84E-06	0.00E+00	2.97E-07	1.29E-05	1.22E-05	1.42E-06	0.00E+00
3	Ce	0.00E+00	2.19E-19	2.39E-19	0.00E+00	0.00E+00	2.37E-05	5.93E-07	0.00E+00	0.00E+00	0.00E+00	0.00E+00
-1	Cl	5.60E-02	1.43E-01	1.42E-01	1.73E-01	1.78E-01	1.29E-01	1.86E-01	1.17E-01	1.14E-01	1.18E-01	9.74E-02
-2	CO <sub>3</sub>	5.40E-01	5.42E-01	4.94E-01	2.80E-01	7.67E-01	2.56E-01	4.93E-01	2.18E-01	2.15E-01	3.54E-01	2.15E-01
3	Cr	0.00E+00	0.00E+00	0.00E+00	0.00E+00	0.00E+00	0.00E+00	0.00E+00	0.00E+00	0.00E+00	0.00E+00	0.00E+00
-1	Cr(OH) <sub>4</sub>	2.80E-03	3.57E-03	3.61E-03	3.23E-03	4.55E-03	2.08E-02	3.56E-02	4.87E-03	4.89E-03	2.53E-03	1.85E-03
-1	F	1.50E-01	2.03E-02	1.84E-02	2.30E-02	6.26E-02	2.29E-02	4.24E-02	2.50E-02	2.49E-02	5.67E-02	5.49E-02
2	Fe	4.50E-05	2.22E-04	2.33E-04	3.91E-04	1.30E-04	1.60E-03	4.21E-03	1.30E-04	1.21E-04	3.28E-04	3.96E-04
1	H	5.73E-15	8.39E-15	7.61E-15	5.35E-15	1.25E-14	1.25E-14	7.87E-15	4.79E-15	4.84E-15	4.10E-15	3.35E-15
	H <sub>2</sub> O	0.00E+00	4.69E+01	4.67E+01	4.44E+01	4.67E+01	4.91E+01	4.84E+01	8.19E+01	9.06E+01	4.54E+01	4.51E+01
	Hg	2.00E-07	0.00E+00	0.00E+00	0.00E+00	0.00E+00	1.07E-07	2.97E-08	0.00E+00	0.00E+00	0.00E+00	0.00E+00
1	K	8.00E-01	8.38E-02	8.60E-02	1.00E-01	8.44E-02	3.85E-02	5.67E-02	1.67E-01	1.68E-01	4.47E-01	5.68E-01

	Batch Name	LAW-1	LAW-5	LAW-6	LAW-8	LAW-9	LAW-10	LAW-11	LAW-12	LAW-13	LAW-14	LAW-15
	Staging (Source) Tank	AP-101	AN-104	AN-104	AN-105	AN-105	SY-101	SY-101	AN-103	AN-103	AW-101	AW-101
	Total Volume of Liquid (L)	4.12E+06	2.77E+06	2.57E+06	2.66E+06	2.57E+06	2.83E+06	3.37E+06	3.49E+06	3.52E+06	2.82E+06	3.84E+06
Species	Concentration Units	[M]	[M]	[M]	[M]	[M]	[M]	[M]	[M]	[M]	[M]	[M]
Charge	LAW Envelope	A	A	A	A	A	A	A	A	A	A	A
3	La	9.40E-06	8.30E-06	8.95E-06	4.36E-13	2.39E-12	1.87E-05	2.97E-07	2.29E-06	2.56E-06	6.67E-12	8.10E-12
2	Mn	0.00E+00	4.73E-05	4.94E-05	1.11E-04	3.07E-05	6.15E-05	1.15E-04	2.72E-05	2.47E-05	7.06E-05	8.41E-05
1	Na	5.62E+00	6.90E+00	6.89E+00	6.95E+00	7.00E+00	4.59E+00	6.82E+00	6.76E+00	6.70E+00	6.99E+00	6.98E+00
	NH <sub>3</sub>	0.00E+00	1.35E-01	1.44E-01	1.12E-01	5.33E-02	7.74E-02	5.91E-02	2.31E-01	2.33E-01	4.18E-01	5.42E-01
2	Ni	1.40E-04	8.48E-05	8.91E-05	3.70E-04	1.09E-04	7.67E-04	2.00E-03	5.64E-05	4.69E-05	1.40E-04	1.51E-04
-1	NO <sub>2</sub>	9.10E-01	1.64E+00	1.64E+00	1.67E+00	1.69E+00	1.20E+00	1.89E+00	1.52E+00	1.51E+00	1.49E+00	1.42E+00
-1	NO <sub>3</sub>	2.10E+00	1.90E+00	1.87E+00	1.78E+00	1.97E+00	1.31E+00	1.64E+00	1.65E+00	1.64E+00	1.85E+00	1.81E+00
	OH(BOUND)	5.40E-01	1.94E+00	2.06E+00	3.24E+00	1.53E+00	8.90E-01	3.74E-01	3.32E-01	2.43E-01	1.91E+00	2.04E+00
	OH-	1.86E+00	3.32E+00	3.24E+00	2.08E+00	2.05E+00	1.66E+00	3.62E+00	6.22E+00	6.31E+00	3.34E+00	3.78E+00
-1	OH- (Bound+Free-4Al-4Cr)	1.75E+00	1.19E+00	1.31E+00	1.87E+00	8.03E-01	7.99E-01	1.27E+00	2.09E+00	2.07E+00	2.44E+00	2.99E+00
2	Pb	7.20E-05	1.29E-04	1.35E-04	1.84E-04	1.01E-04	1.39E-03	2.37E-04	1.58E-04	1.56E-04	1.93E-04	2.24E-04
-3	PO <sub>4</sub>	1.10E-02	2.85E-02	2.73E-02	1.51E-02	3.74E-02	3.99E-02	4.99E-02	1.27E-02	1.25E-02	1.54E-02	7.92E-03
	Si	0.00E+00	5.67E-03	5.64E-03	4.55E-03	3.02E-03	5.30E-03	1.19E-02	6.56E-03	6.59E-03	4.79E-03	5.39E-03
-2	SO <sub>4</sub>	4.20E-02	6.68E-02	6.19E-02	3.02E-02	5.14E-02	3.42E-02	3.26E-02	1.54E-02	1.49E-02	2.40E-02	1.48E-02
	Sr (w/o 90 Sr)	0.00E+00	1.78E-07	1.77E-07	3.27E-05	2.18E-05	1.38E-05	1.19E-06	2.18E-05	2.13E-05	6.03E-06	5.21E-07
	Sr (inc. 90Sr)	0.00E+00	1.83E-07	1.83E-07	3.29E-05	2.19E-05	1.39E-05	1.36E-06	2.18E-05	2.13E-05	6.13E-06	6.17E-07
	TOC	1.60E-01	1.68E-01	1.67E-01	3.91E-01	3.17E-01	2.84E-01	6.02E-01	9.17E-02	8.24E-02	2.06E-01	1.69E-01
	U (w/o 232, 3, 4, 5, 6, and 8)	0.00E+00	1.73E-08	1.55E-08	3.04E-08	3.32E-09	8.23E-08	4.51E-08	8.74E-10	0.00E+00	3.55E-07	5.21E-07
2	U (inc. all U isotopes)	2.60E-04	4.19E-05	3.88E-05	3.83E-05	6.26E-06	6.82E-05	5.85E-05	8.08E-06	7.16E-06	4.11E-04	5.52E-04
2	Zn	0.00E+00	0.00E+00	0.00E+00	0.00E+00	0.00E+00	0.00E+00	0.00E+00	0.00E+00	0.00E+00	0.00E+00	0.00E+00
	Zr	0.00E+00	4.01E-05	4.12E-05	5.90E-05	2.22E-05	2.12E-05	1.69E-05	2.12E-05	1.99E-05	1.07E-04	1.36E-04
	Cations =	6.4215	6.9817	6.9759	7.0608	7.0922	4.6431	6.9009	6.9311	6.8742	7.4375	7.5521
	Anions =	-6.4215	-6.9817	-6.9759	-7.0608	-7.0922	-4.6431	-6.9010	-6.9311	-6.8742	-7.4375	-7.5521
	Sum =	0.000	0.000	0.000	0.000	0.000	0.000	0.000	0.000	0.000	0.000	0.000
	Na/Cs	1.39E+05	7.96E+04	7.90E+04	1.16E+05	1.13E+05	1.35E+05	1.34E+05	1.04E+05	1.04E+05	1.09E+05	1.10E+05
	K/Cs	1.98E+04	9.67E+02	9.87E+02	1.67E+03	1.36E+03	1.14E+03	1.11E+03	2.56E+03	2.59E+03	7.00E+03	8.93E+03

	Batch Name	LAW-1	LAW-5	LAW-6	LAW-8	LAW-9	LAW-10	LAW-11	LAW-12	LAW-13	LAW-14	LAW-15
	Staging (Source) Tank	AP-101	AN-104	AN-104	AN-105	AN-105	SY-101	SY-101	AN-103	AN-103	AW-101	AW-101
	Total Volume of Liquid (L)	4.12E+06	2.77E+06	2.57E+06	2.66E+06	2.57E+06	2.83E+06	3.37E+06	3.49E+06	3.52E+06	2.82E+06	3.84E+06
Species	Concentration Units	[M]	[M]	[M]	[M]	[M]	[M]	[M]	[M]	[M]	[M]	[M]
Charge	LAW Envelope	A	A	A	A	A	A	A	A	A	A	A
	137-Cs/Total Cs	0.25	0.25	0.25	0.25	0.25	0.25	0.25	0.25	0.25	0.25	0.25

Table A-2. Best Basis Inventory (BBI) Phase 1 LAW feed solution data for Envelopes B and C where stated alterations were made to minimize inventory inconsistencies and to establish an ionic charge balance (a value of zero implies that no information was provided on species).

	Batch Name	LAW-2a	LAW-2b	LAW-3	LAW-4	LAW-7
	Staging (Source) Tank	AZ-101	AZ-102	AN-102	AN-102	AN-107
	Total Volume of Liquid (L)	3.02E+06	3.17E+06	2.34E+06	2.34E+06	3.62E+06
Species	Concentration Units	[M]	[M]	[M]	[M]	[M]
Charge	LAW Envelope	B	B	C	C	C
-1	129-I	3.83E-02	1.94E-02	2.86E-05	2.86E-05	2.21E-05
	137-Cs	1.35E-04	7.16E-05	1.79E-05	1.71E-05	1.93E-05
1	Total Cs (137-Cs/iso fraction)	4.50E-04	2.39E-04	7.18E-05	6.84E-05	7.73E-05
	232-Th	1.00E-09	5.31E-09	1.17E-03	1.17E-03	1.85E-03
	238-U	2.12E-02	6.35E-01	6.11E-04	6.11E-04	5.36E-04
	99-Tc	1.80E-03	1.04E-03	6.75E-05	6.75E-05	4.45E-05
3	Al	0.00E+00	0.00E+00	0.00E+00	0.00E+00	0.00E+00
-1	Al(OH) <sub>3</sub>	4.05E-01	5.52E-02	4.66E-01	4.66E-01	2.36E-01
	As	0.00E+00	0.00E+00	0.00E+00	0.00E+00	0.00E+00
	B	0.00E+00	0.00E+00	0.00E+00	0.00E+00	0.00E+00
2	Ba	1.97E-05	3.10E-13	1.81E-04	1.81E-04	0.00E+00
	Bi	0.00E+00	0.00E+00	0.00E+00	0.00E+00	2.42E-04
2	Ca	1.22E-05	1.09E-04	1.25E-02	1.25E-02	1.31E-02
2	Cd	4.19E-05	6.60E-13	4.70E-04	4.66E-04	0.00E+00
3	Ce	0.00E+00	0.00E+00	0.00E+00	0.00E+00	0.00E+00
-1	Cl	5.62E-03	2.62E-04	8.68E-02	8.68E-02	4.83E-02

	Batch Name	LAW-2a	LAW-2b	LAW-3	LAW-4	LAW-7
	Staging (Source) Tank	AZ-101	AZ-102	AN-102	AN-102	AN-107
	Total Volume of Liquid (L)	3.02E+06	3.17E+06	2.34E+06	2.34E+06	3.62E+06
Species	Concentration Units	[M]	[M]	[M]	[M]	[M]
Charge	LAW Envelope	B	B	C	C	C
-2	CO <sub>3</sub>	5.69E-01	5.73E-01	9.23E-01	9.23E-01	1.14E+00
3	Cr	0.00E+00	0.00E+00	0.00E+00	0.00E+00	0.00E+00
-1	Cr(OH) <sub>4</sub>	1.49E-02	1.91E-02	6.54E-03	6.54E-03	5.36E-03
-1	F	9.91E-02	5.47E-02	7.86E-02	7.86E-02	1.63E-01
2	Fe	2.01E-04	1.89E-04	3.15E-03	3.15E-03	4.61E-02
1	H	6.50E-14	6.64E-14	5.34E-15	5.34E-15	8.06E-15
	H <sub>2</sub> O	4.95E+01	5.31E+01	2.08E+02	2.07E+02	1.17E+02
	Hg	0.00E+00	0.00E+00	0.00E+00	0.00E+00	1.66E-06
1	K	1.20E-01	7.92E-02	7.95E-02	7.95E-02	3.87E-02
3	La	2.25E-10	1.95E-05	0.00E+00	0.00E+00	2.29E-04
2	Mn	2.46E-07	1.30E-05	1.26E-03	1.26E-03	9.92E-03
1	Na	4.82E+00	2.77E+00	8.97E+00	8.97E+00	8.45E+00
	NH <sub>3</sub>	1.76E-02	7.88E-03	7.01E-02	7.01E-02	4.09E-02
2	Ni	8.92E-07	3.56E-05	5.56E-03	5.56E-03	7.71E-03
-1	NO <sub>2</sub>	1.43E+00	6.55E-01	1.44E+00	1.44E+00	1.21E+00
-1	NO <sub>3</sub>	1.23E+00	3.73E-01	2.92E+00	2.92E+00	3.20E+00
	OH(BOUND)	9.92E-01	1.40E-02	2.83E+00	2.83E+00	9.61E-01
	OH-	1.01E+00	1.26E-01	3.80E-01	3.80E-01	1.54E+00
-1	OH- (Bound+Free-4Al-4Cr)	1.54E-01	1.51E-01	1.87E+00	1.87E+00	1.24E+00
2	Pb	0.00E+00	0.00E+00	7.78E-04	7.78E-04	1.76E-03
-3	PO <sub>4</sub>	1.55E-02	1.41E-03	4.14E-02	4.14E-02	3.54E-02
	Si	1.31E-02	1.89E-02	4.53E-03	4.53E-03	2.18E-03
-2	SO <sub>4</sub>	1.89E-01	1.87E-01	1.32E-01	1.32E-01	8.15E-02
	Sr (w/o 90 Sr)	1.03E-05	2.11E-06	3.42E-05	3.42E-05	6.69E-05
	Sr (inc. 90Sr)	1.33E-05	2.13E-06	3.85E-05	3.80E-05	7.38E-05
	TOC	1.20E-01	1.31E-01	1.78E+00	1.78E+00	2.93E+00
	U (w/o 232, 3, 4, 5, 6, and 8)	2.84E-08	2.14E-07	4.27E-07	4.27E-07	0.00E+00
2	U (inc. all U isotopes)	2.14E-05	6.42E-04	6.15E-04	6.15E-04	5.39E-04

Batch Name		LAW-2a	LAW-2b	LAW-3	LAW-4	LAW-7
Staging (Source) Tank		AZ-101	AZ-102	AN-102	AN-102	AN-107
Total Volume of Liquid (L)		3.02E+06	3.17E+06	2.34E+06	2.34E+06	3.62E+06
Species	Concentration Units	[M]	[M]	[M]	[M]	[M]
Charge	LAW Envelope	B	B	C	C	C
2	Zn	0.00E+00	0.00E+00	0.00E+00	0.00E+00	0.00E+00
	Zr	0.00E+00	4.53E-05	5.77E-04	5.77E-04	1.00E-03
	cations =	4.9364	2.8513	9.1030	9.1030	8.6508
	anions =	-4.9364	-2.8513	-9.1030	-9.1030	-8.6508
	sum =	0.000	0.000	0.000	0.000	0.000
	Na/Cs	1.07E+04	1.16E+04	1.25E+05	1.31E+05	1.09E+05
	K/Cs	2.67E+02	3.32E+02	1.11E+03	1.16E+03	5.00E+02
	137-Cs/Total Cs	0.30	0.30	0.25	0.25	0.25

Table A-3. Best Basis Inventory (BBi) Phase 1 LAW feed solution data for Envelope C where the impact from the isotopic dilution pretreatment process for Strontium-90 and permanganate addition for TRUs separation have been taken into account.

Batch Name		LAW-3	LAW-4	LAW-7
Staging (Source) Tank		AN-102	AN-102	AN-107
Total Volume of Liquid (L)		3.47E+06	3.47E+06	4.46E+06
Species	Concentration Units	[M]	[M]	[M]
Charge	LAW Envelope	C	C	C
-1	129-I	1.91E-05	1.91E-05	1.57E-05
	137-Cs	1.20E-05	1.14E-05	1.37E-05
1	Total Cs (137-Cs/iso fract)	4.80E-05	4.57E-05	5.49E-05
	232-Th	7.83E-04	7.83E-04	1.31E-03
	238-U	4.09E-04	4.09E-04	3.80E-04
	99-Tc	4.51E-05	4.51E-05	3.16E-05
3	Al	0.00E+00	0.00E+00	0.00E+00

	Batch Name	LAW-3	LAW-4	LAW-7
	Staging (Source) Tank	AN-102	AN-102	AN-107
	Total Volume of Liquid (L)	3.47E+06	3.47E+06	4.46E+06
Species	Concentration Units	[M]	[M]	[M]
Charge	LAW Envelope	C	C	C
-1	Al(OH <sub>4</sub>	3.11E-01	3.11E-01	1.68E-01
	As	0.00E+00	0.00E+00	0.00E+00
	B	0.00E+00	0.00E+00	0.00E+00
2	Ba	1.21E-04	1.21E-04	0.00E+00
	Bi	0.00E+00	0.00E+00	1.72E-04
2	Ca	8.37E-03	8.37E-03	9.31E-03
2	Cd	3.14E-04	3.11E-04	0.00E+00
3	Ce	0.00E+00	0.00E+00	0.00E+00
-1	Cl	5.80E-02	5.80E-02	3.43E-02
-2	CO <sub>3</sub>	6.17E-01	6.17E-01	8.08E-01
3	Cr	0.00E+00	0.00E+00	0.00E+00
-1	Cr(OH) <sub>4</sub>	4.37E-03	4.37E-03	3.80E-03
-1	F	5.26E-02	5.26E-02	1.16E-01
2	Fe	2.11E-03	2.11E-03	3.27E-02
1	H	8.00E-15	8.00E-15	1.02E-14
	H <sub>2</sub> O	1.39E+02	1.38E+02	8.27E+01
	Hg	0.00E+00	0.00E+00	1.18E-06
1	K	5.31E-02	5.31E-02	2.75E-02
3	La	0.00E+00	0.00E+00	1.62E-04
2	Mn	5.00E-02	5.00E-02	5.00E-02
1	Na	6.05E+00	6.05E+00	6.16E+00
	NH <sub>3</sub>	4.69E-02	4.69E-02	2.90E-02
2	Ni	3.71E-03	3.71E-03	5.47E-03
-1	NO <sub>2</sub>	9.63E-01	9.63E-01	8.57E-01
-1	NO <sub>3</sub>	2.10E+00	2.10E+00	2.42E+00
	OH(BOUND)	1.89E+00	1.89E+00	6.82E-01
	OH-	2.54E-01	2.54E-01	1.09E+00
-1	OH- (Bound+Free-4Al-4Cr)	1.25E+00	1.25E+00	9.79E-01

Batch Name		LAW-3	LAW-4	LAW-7
Staging (Source) Tank		AN-102	AN-102	AN-107
Total Volume of Liquid (L)		3.47E+06	3.47E+06	4.46E+06
Species	Concentration Units	[M]	[M]	[M]
Charge	LAW Envelope	C	C	C
2	Pb	5.20E-04	5.20E-04	1.25E-03
-3	PO <sub>4</sub>	2.77E-02	2.77E-02	2.51E-02
	Si	3.03E-03	3.03E-03	1.55E-03
-2	SO <sub>4</sub>	8.80E-02	8.80E-02	5.78E-02
	Sr (w/o 90 Sr)	2.29E-05	2.29E-05	4.75E-05
	Sr (inc. 90Sr)	7.50E-02	7.50E-02	7.51E-02
	TOC	1.19E+00	1.19E+00	2.08E+00
	U (w/o 232, 3, 4, 5, 6, and 8)	2.86E-07	2.86E-07	0.00E+00
2	U (inc. all U isotopes)	4.11E-04	4.11E-04	3.82E-04
2	Zn	0.00E+00	0.00E+00	0.00E+00
	Zr	3.86E-04	3.86E-04	7.10E-04
	cations =	6.2335	6.2335	6.3884
	anions =	-6.2335	-6.2335	-6.3884
	sum =	0.000	0.000	0.000
	Na/Cs	1.26E+05	1.32E+05	1.12E+05
	K/Cs	1.11E+03	1.16E+03	5.00E+02
	137-Cs/Total Cs	0.25	0.25	0.25



Table A-4. Ionic species available within the ZAM CST ion-exchange equilibrium model.

ID	Cations	Anions	ID	Cations	Anions
1	H <sup>+</sup>	F <sup>-</sup>	21	Cd <sup>2+</sup>	AsO <sub>4</sub> <sup>3-</sup>
2	Li <sup>+</sup>	Cl <sup>-</sup>	22	Pb <sup>2+</sup>	Fe(CN) <sub>6</sub> <sup>3-</sup>
3	Na <sup>+</sup>	Br <sup>-</sup>	23	UO <sub>2</sub> <sup>2+</sup>	Mo(CN) <sub>8</sub> <sup>3-</sup>
4	K <sup>+</sup>	I <sup>-</sup>	24	Cr <sup>3+</sup>	User defined <sup>a</sup>
5	Rb <sup>+</sup>	ClO <sub>3</sub> <sup>-</sup>	25	Al <sup>3+</sup>	User defined
6	Cs <sup>+</sup>	ClO <sub>4</sub> <sup>-</sup>	26	Sc <sup>3+</sup>	User defined
7	NH <sub>4</sub> <sup>+</sup>	BrO <sub>3</sub> <sup>-</sup>	27	Y <sup>3+</sup>	NO <sub>2</sub> <sup>-</sup>
8	Tl <sup>+</sup>	IO <sub>3</sub> <sup>-</sup>	28	La <sup>3+</sup>	Al(OH) <sub>4</sub> <sup>-</sup>
9	Ag <sup>+</sup>	NO <sub>3</sub> <sup>-</sup>	29	Ce <sup>3+</sup>	na <sup>b</sup>
10	Be <sup>2+</sup>	H <sub>2</sub> PO <sub>4</sub> <sup>-</sup>	30	Pr <sup>3+</sup>	na
11	Mg <sup>2+</sup>	H <sub>2</sub> AsO <sub>4</sub> <sup>-</sup>	31	Nd <sup>3+</sup>	na
12	Ca <sup>2+</sup>	CNS <sup>-</sup>	32	Sm <sup>3+</sup>	na
13	Sr <sup>2+</sup>	OH <sup>-</sup>	33	Eu <sup>3+</sup>	na
14	Ba <sup>2+</sup>	CrO <sub>4</sub> <sup>2-</sup>	34	Ga <sup>3+</sup>	na
15	Mn <sup>2+</sup>	SO <sub>4</sub> <sup>2-</sup>	35	Co <sup>3+</sup>	na
16	Fe <sup>2+</sup>	S <sub>2</sub> O <sub>3</sub> <sup>2-</sup>	36	Th <sup>4+</sup>	na
17	Co <sup>2+</sup>	HPO <sub>4</sub> <sup>2-</sup>	37	User defined <sup>a</sup>	na
18	Ni <sup>2+</sup>	HAsO <sub>4</sub> <sup>2-</sup>	38	User defined	na
19	Cu <sup>2+</sup>	CO <sub>3</sub> <sup>2-</sup>	39	User defined	na
20	Zn <sup>2+</sup>	PO <sub>4</sub> <sup>3-</sup>	40	SrOH <sup>+</sup>	na

<sup>a</sup> Array locations in storage that are available for user to specify additional species.<sup>b</sup> Array locations in storage that are currently unused.

Table A-5. Best estimate Phase 1 LAW feed solution data for Envelope A adjusted to 5 M Na<sup>a</sup> and used as input to the CST equilibrium model.

Batch Name		LAW-1	LAW-5	LAW-6	LAW-8	LAW-9	LAW-10	LAW-11	LAW-12	LAW-13	LAW-14	LAW-15
Staging (Source) Tank		AP-101	AN-104	AN-104	AN-105	AN-105	SY-101	SY-101	AN-103	AN-103	AW-101	AW-101
Total Volume of Liquid (L)		4.63E+06	3.82E+06	3.54E+06	3.70E+06	3.60E+06	2.60E+06	4.60E+06	4.72E+06	4.72E+06	3.94E+06	5.36E+06
Species	Concentration Units	[M]	[M]	[M]	[M]	[M]	[M]	[M]	[M]	[M]	[M]	[M]
Charge	LAW Envelope	A	A	A	A	A	A	A	A	A	A	A
Cations												
1	Na	5.00E+00	5.00E+00	5.00E+00	5.00E+00	5.00E+00	5.00E+00	5.00E+00	5.00E+00	5.00E+00	5.00E+00	5.00E+00
1	Cs (total)	3.60E-05	6.28E-05	6.33E-05	4.32E-05	4.44E-05	3.69E-05	3.74E-05	4.83E-05	4.83E-05	4.57E-05	4.55E-05
1	H	6.44E-15	1.16E-14	1.05E-14	7.44E-15	1.74E-14	1.15E-14	1.07E-14	6.48E-15	6.48E-15	5.72E-15	4.67E-15
1	Rb	0.00E+00	0.00E+00	0.00E+00	0.00E+00	0.00E+00	0.00E+00	0.00E+00	0.00E+00	0.00E+00	0.00E+00	0.00E+00
1	K	7.12E-01	6.07E-02	6.24E-02	7.22E-02	6.03E-02	4.19E-02	4.15E-02	1.24E-01	1.25E-01	3.20E-01	4.07E-01
1	SrOH	0.00E+00	0.00E+00	0.00E+00	0.00E+00	0.00E+00	0.00E+00	0.00E+00	0.00E+00	0.00E+00	0.00E+00	0.00E+00
2	Sr (total)	0.00E+00	0.00E+00	0.00E+00	0.00E+00	0.00E+00	0.00E+00	0.00E+00	0.00E+00	0.00E+00	0.00E+00	0.00E+00
2	Ba	2.14E-06	5.97E-05	6.36E-05	9.08E-05	4.14E-05	0.00E+00	1.96E-06	5.57E-05	5.47E-05	1.04E-05	0.00E+00
2	Ca	1.69E-04	4.79E-04	4.97E-04	1.06E-03	1.05E-03	1.63E-03	2.22E-03	3.35E-04	3.14E-04	9.09E-04	8.60E-04
2	Cd	1.51E-05	7.33E-06	7.63E-06	2.46E-05	4.17E-06	0.00E+00	2.17E-07	9.53E-06	9.11E-06	1.02E-06	0.00E+00
2	Mn	0.00E+00	3.43E-05	3.59E-05	7.95E-05	2.19E-05	6.69E-05	8.41E-05	2.01E-05	1.84E-05	5.05E-05	6.03E-05
2	Ni	1.25E-04	6.15E-05	6.47E-05	2.66E-04	7.78E-05	8.35E-04	1.46E-03	4.17E-05	3.50E-05	1.00E-04	1.08E-04
2	U (total)	2.31E-04	3.04E-05	2.82E-05	2.76E-05	4.47E-06	7.42E-05	4.28E-05	5.97E-06	5.34E-06	2.94E-04	3.96E-04
2	Zn	0.00E+00	0.00E+00	0.00E+00	0.00E+00	0.00E+00	0.00E+00	0.00E+00	0.00E+00	0.00E+00	0.00E+00	0.00E+00
2	Fe	4.00E-05	1.61E-04	1.69E-04	2.81E-04	9.25E-05	1.74E-03	3.09E-03	9.60E-05	9.05E-05	2.35E-04	2.84E-04
2	Pb	6.41E-05	9.37E-05	9.77E-05	1.32E-04	7.22E-05	1.52E-03	1.74E-04	1.17E-04	1.16E-04	1.38E-04	1.61E-04
3	Al	0.00E+00	0.00E+00	0.00E+00	0.00E+00	0.00E+00	0.00E+00	0.00E+00	0.00E+00	0.00E+00	0.00E+00	0.00E+00
3	Cr	0.00E+00	0.00E+00	0.00E+00	0.00E+00	0.00E+00	0.00E+00	0.00E+00	0.00E+00	0.00E+00	0.00E+00	0.00E+00
3	La	8.36E-06	6.02E-06	6.50E-06	3.14E-13	1.71E-12	2.04E-05	2.17E-07	1.69E-06	1.91E-06	4.77E-12	5.80E-12
3	Ce	0.00E+00	1.59E-19	1.73E-19	0.00E+00	0.00E+00	2.58E-05	4.35E-07	0.00E+00	0.00E+00	0.00E+00	0.00E+00
Anions												
-1	OH (free)	1.55E+00	8.64E-01	9.54E-01	1.34E+00	5.73E-01	8.70E-01	9.31E-01	1.54E+00	1.54E+00	1.75E+00	2.14E+00
-1	NO <sub>3</sub>	1.87E+00	1.38E+00	1.36E+00	1.28E+00	1.41E+00	1.43E+00	1.20E+00	1.22E+00	1.22E+00	1.32E+00	1.30E+00
-1	NO <sub>2</sub>	8.10E-01	1.19E+00	1.19E+00	1.20E+00	1.21E+00	1.31E+00	1.39E+00	1.13E+00	1.13E+00	1.06E+00	1.01E+00
-1	Cl	4.98E-02	1.03E-01	1.03E-01	1.25E-01	1.27E-01	1.40E-01	1.37E-01	8.62E-02	8.52E-02	8.43E-02	6.98E-02

	Batch Name	LAW-1	LAW-5	LAW-6	LAW-8	LAW-9	LAW-10	LAW-11	LAW-12	LAW-13	LAW-14	LAW-15
	Staging (Source) Tank	AP-101	AN-104	AN-104	AN-105	AN-105	SY-101	SY-101	AN-103	AN-103	AW-101	AW-101
	Total Volume of Liquid (L)	4.63E+06	3.82E+06	3.54E+06	3.70E+06	3.60E+06	2.60E+06	4.60E+06	4.72E+06	4.72E+06	3.94E+06	5.36E+06
Species	Concentration Units	[M]	[M]	[M]	[M]	[M]	[M]	[M]	[M]	[M]	[M]	[M]
Charge	LAW Envelope	A	A	A	A	A	A	A	A	A	A	A
-1	F	1.33E-01	1.47E-02	1.34E-02	1.65E-02	4.47E-02	2.50E-02	3.11E-02	1.85E-02	1.86E-02	4.06E-02	3.94E-02
-1	Al(OH) <sub>4</sub>	2.31E-01	5.68E-01	5.73E-01	6.35E-01	4.50E-01	4.92E-01	4.65E-01	7.50E-01	7.56E-01	4.87E-01	5.00E-01
-1	Cr(OH) <sub>4</sub>	2.49E-03	2.59E-03	2.62E-03	2.32E-03	3.25E-03	2.27E-02	2.61E-02	3.60E-03	3.64E-03	1.81E-03	1.32E-03
-1	I <sup>29</sup> -I	3.14E-06	8.12E-06	8.47E-06	2.19E-05	1.03E-05	1.31E-05	7.39E-06	7.42E-06	6.99E-06	9.39E-06	9.14E-06
-2	CO <sub>3</sub>	4.80E-01	3.93E-01	3.59E-01	2.01E-01	5.47E-01	2.78E-01	3.61E-01	1.61E-01	1.60E-01	2.53E-01	1.54E-01
-2	SO <sub>4</sub>	3.74E-02	4.84E-02	4.49E-02	2.17E-02	3.67E-02	3.73E-02	2.39E-02	1.14E-02	1.11E-02	1.72E-02	1.06E-02
-3	PO <sub>4</sub>	9.79E-03	2.07E-02	1.98E-02	1.08E-02	2.67E-02	4.35E-02	3.65E-02	9.39E-03	9.34E-03	1.10E-02	5.67E-03
	Best estimate density based on HTWOS model (g/ml) =	1.237	1.210	1.211	1.212	1.210	1.217	1.211	1.209	1.209	1.214	1.217
	Best estimate density based on modified HTWOS model (g/ml) =	1.277	1.232	1.231	1.225	1.238	1.237	1.232	1.221	1.221	1.234	1.235
	% difference in density estimate =	3.2	1.8	1.7	1.1	2.3	1.6	1.7	1.0	1.0	1.7	1.5
	Cations =	5.7131	5.0626	5.0644	5.0761	5.0630	5.0538	5.0557	5.1249	5.1265	5.3233	5.4105
	Anions =	-5.7131	-5.0626	-5.0644	-5.0761	-5.0630	-5.0538	-5.0557	-5.1249	-5.1265	-5.3233	-5.4105
	Sum =	0.000	0.000	0.000	0.000	0.000	0.000	0.000	0.000	0.000	0.000	0.000
	Ionic strength (gmole/kg)	6.304	6.727	6.652	6.304	6.951	6.553	6.618	6.324	6.327	6.617	6.487
	Na/Cs	1.39E+05	7.96E+04	7.90E+04	1.16E+05	1.13E+05	1.35E+05	1.34E+05	1.04E+05	1.04E+05	1.09E+05	1.10E+05
	K/Cs	1.98E+04	9.67E+02	9.87E+02	1.67E+03	1.36E+03	1.14E+03	1.11E+03	2.56E+03	2.59E+03	7.00E+03	8.93E+03
	Na/K	7.0	82.3	80.1	69.3	82.9	119.3	120.4	40.5	39.9	15.6	12.3
	137-Cs/Total Cs	0.25	0.25	0.25	0.25	0.25	0.25	0.25	0.25	0.25	0.25	0.25

<sup>a</sup> For analysis at other Na<sup>+</sup> concentration levels, such as 4 M or 6 M feeds, the concentrations of each species provided in this table is computed based on a simple ratio. No shifts in molar ratios due to potential liquid-phase or precipitation reactions are considered.

Table A-6. Best estimate Phase 1 LAW feed solution data for Envelopes B and C adjusted to 5 M Na<sup>a</sup> and used as input to the CST equilibrium model.

Batch Name		LAW-2a	LAW-2b	LAW-3	LAW-4	LAW-7
Staging (Source) Tank		AZ-101	AZ-102	AN-102	AN-102	AN-107
Total Volume of Liquid (L)		2.91E+06	1.76E+06	4.20E+06	4.20E+06	5.50E+06
Species	Concentration Units	[M]	[M]	[M]	[M]	[M]
Charge	LAW Envelope	B	B	C	C	C
Cations						
1	Na	5.00E+00	5.00E+00	5.00E+00	5.00E+00	5.00E+00
1	Cs (total)	4.68E-04	4.31E-04	3.97E-05	3.78E-05	4.45E-05
1	H	6.26E-14	3.68E-14	9.68E-15	9.68E-15	1.26E-14
1	Rb	0.00E+00	0.00E+00	0.00E+00	0.00E+00	0.00E+00
1	K	1.25E-01	1.43E-01	4.39E-02	4.39E-02	2.23E-02
1	SrOH	0.00E+00	0.00E+00	0.00E+00	0.00E+00	0.00E+00
2	Sr (total)	0.00E+00	0.00E+00	0.00E+00	0.00E+00	0.00E+00
2	Ba	2.04E-05	5.60E-13	1.00E-04	1.00E-04	0.00E+00
2	Ca	1.27E-05	1.98E-04	6.92E-03	6.92E-03	7.56E-03
2	Cd	4.35E-05	1.19E-12	2.60E-04	2.57E-04	0.00E+00
2	Mn	2.55E-07	2.34E-05	4.13E-02	4.13E-02	4.06E-02
2	Ni	9.26E-07	6.43E-05	3.07E-03	3.07E-03	4.44E-03
2	U (total)	2.23E-05	1.16E-03	3.40E-04	3.40E-04	3.10E-04
2	Zn	0.00E+00	0.00E+00	0.00E+00	0.00E+00	0.00E+00
2	Fe	2.09E-04	3.41E-04	1.74E-03	1.74E-03	2.66E-02
2	Pb	0.00E+00	0.00E+00	4.30E-04	4.30E-04	1.02E-03
3	Al	0.00E+00	0.00E+00	0.00E+00	0.00E+00	0.00E+00
3	Cr	0.00E+00	0.00E+00	0.00E+00	0.00E+00	0.00E+00
3	La	2.33E-10	3.52E-05	0.00E+00	0.00E+00	1.32E-04
3	Ce	0.00E+00	0.00E+00	0.00E+00	0.00E+00	0.00E+00
anions						
-1	OH (free)	1.60E-01	2.72E-01	1.03E+00	1.03E+00	7.94E-01
-1	NO <sub>3</sub>	1.28E+00	6.74E-01	1.74E+00	1.74E+00	1.97E+00
-1	NO <sub>2</sub>	1.48E+00	1.18E+00	7.96E-01	7.96E-01	6.95E-01

	Batch Name	LAW-2a	LAW-2b	LAW-3	LAW-4	LAW-7
	Staging (Source) Tank	AZ-101	AZ-102	AN-102	AN-102	AN-107
	Total Volume of Liquid (L)	2.91E+06	1.76E+06	4.20E+06	4.20E+06	5.50E+06
Species	Concentration Units	[M]	[M]	[M]	[M]	[M]
Charge	LAW Envelope	B	B	C	C	C
-1	Cl	5.83E-03	4.72E-04	4.79E-02	4.79E-02	2.78E-02
-1	F	1.03E-01	9.87E-02	4.35E-02	4.35E-02	9.39E-02
-1	Al(OH) <sub>4</sub>	4.21E-01	9.97E-02	2.57E-01	2.57E-01	1.36E-01
-1	Cr(OH) <sub>4</sub>	1.55E-02	3.45E-02	3.61E-03	3.61E-03	3.09E-03
-1	I <sub>29</sub> -I	3.97E-02	3.50E-02	1.58E-05	1.58E-05	1.27E-05
-2	CO <sub>3</sub>	5.91E-01	1.03E+00	5.10E-01	5.10E-01	6.55E-01
-2	SO <sub>4</sub>	1.97E-01	3.37E-01	7.27E-02	7.27E-02	4.69E-02
-3	PO <sub>4</sub>	1.61E-02	2.54E-03	2.29E-02	2.29E-02	2.04E-02
	Best estimate density based on HTWOS model (g/ml) =	1.213	1.178	1.209	1.209	1.211
	Best estimate density based on modified HTWOS model (g/ml) =	1.254	1.242	1.237	1.237	1.243
	% difference in density estimate =	3.4	5.5	2.3	2.3	2.7
	cations =	5.1256	5.1467	5.1523	5.1523	5.1836
	anions =	-5.1256	-5.1467	-5.1524	-5.1524	-5.1836
	sum =	0.000	0.000	0.000	0.000	0.000
	Ionic strength (gmole/kg)	7.361	8.171	6.995	6.995	7.209
	Na/Cs	1.07E+04	1.16E+04	1.26E+05	1.32E+05	1.12E+05
	K/Cs	2.67E+02	3.32E+02	1.11E+03	1.16E+03	5.00E+02
	Na/K	40.0	35.0	113.8	113.8	224.5
	137-Cs/Total Cs	0.30	0.30	0.25	0.25	0.25

<sup>a</sup> For analysis at other Na<sup>+</sup> concentration levels, such as 4 M or 6 M feeds, the concentrations of each species provided in this table is computed based on a simple ratio. No shifts in molar ratios due to potential liquid-phase or precipitation reactions are considered.

Table A-7. Hanford and SRS measured liquid-phase densities for several LAW liquid samples and simulants considered.

LAW Sample	Envelope	Temperature (C)	Na [M]	NO <sub>2</sub> [M]	NO <sub>3</sub> [M]	Al total [M]	OH (free) [M]	K [M]	CO <sub>3</sub> [M]	SO <sub>4</sub> [M]	Measured density (g/ml)	Reference
AN-103; as received	A sample	20 <sup>a</sup>	11.700	2.318	3.499	1.556	4.836	0.270	0.568	0.017	1.490	Hay and Bronikowski, 2000
AN-103, diluted	A sample	20 <sup>a</sup>	5.250	1.040	1.570	0.698	2.170	0.121	0.255	0.008	1.260	Hay and Bronikowski, 2000
AZ-102, as received	B sample	20 <sup>a</sup>	2.770	0.659	0.273	0.0279	0.109	0.081	0.392	0.172	1.150	Hay et al., 2000a
AN-102, as received	C sample	20 <sup>a</sup>	10.200	1.795	3.082	0.543	1.298	0.056	0.777	0.135	1.470	Hay et al., 2000b
AN-102, diluted	C sample	20 <sup>a</sup>	6.420	1.130	1.940	0.342	0.817	0.035	0.489	0.085	1.330	Hay et al., 2000b
TFL Simulant	A simulant	20 <sup>a</sup>	5.000	1.132	1.247	0.690	1.627	0.089	0.069	0.004	1.225	Steimke et al., 2000
AW-101; PNNL	A sample	?	4.590	1.010	1.500	0.410	2.170	0.390	?	?	1.228	PNWD-3001
AN-107, PNNL	C sample	?	4.840	0.620	1.820	0.087	0.800	0.019	?	?	1.241	PNWD-3039
High OH <sup>b</sup>	SRS simulant	25	5.000	0.500	1.429	0.500	2.457	0.000	0.018	0.018	1.217	Walker and Coleman, 1991
Average <sup>b</sup>	SRS simulant	25	5.000	0.707	1.907	0.300	1.393	0.000	0.164	0.136	1.229	Walker and Coleman, 1991
High NO <sub>3</sub> <sup>b</sup>	SRS simulant	25	5.000	0.300	2.586	0.164	0.664	0.000	0.321	0.300	1.244	Walker and Coleman, 1991

<sup>a</sup> These tests were performed in hot-cells where the ambient temperature of the cells were not controlled or closely measured. Historically, measured temperatures on the order of 20 C is assumed.

<sup>b</sup> For SRS wastes simulants are typically studied that reflect the average tank compositions and also the upper OH and NO<sub>3</sub> expected conditions. These specific destinations (i.e., average, high OH, high NO<sub>3</sub>) have been in use for many years and their specific species compositions have varied slightly over the years. The concentrations listed are consistent with those at the time of the listed measurement.

Table A-8. Comparison of measured to predicted liquid-phase densities for several Hanford LAW liquid samples and simulants based on available correlations.

LAW Sample	Envelope	Measured density (g/ml)	Reynolds-Herting calc. density (g/ml)	% Error	HTWOS calc. density (g/ml)	% Error	Modified <sup>a</sup> HTWOS calc. density (g/ml)	% Error
AN-103; as received	A sample	1.490	1.557	4.5	1.517	1.8	1.545	3.7
AN-103, diluted	A sample	1.260	1.256	-0.3	1.277	1.3	1.289	2.3
AZ-102, as received	B sample	1.150	1.055	-8.2	1.109	-3.6	1.134	-1.3
AN-102, as received	C sample	1.470	1.317	-10.4	1.367	-7.0	1.405	-4.5
AN-102, diluted	C sample	1.330	1.203	-9.5	1.268	-4.7	1.291	-2.9
TFL Simulant	A simulant	1.225	1.230	0.4	1.255	2.5	1.260	2.9
AW-101; PNNL	A sample	1.228	1.221	-0.6	1.249	1.7	1.258	2.4
AN-107, PNNL	C sample	1.241	1.148	-7.5	1.205	-2.9	1.206	-2.9
Mean bias (%)				-3.95		-1.35		-0.03
Root mean square (%)				2.32		1.29		1.06
High OH <sup>b</sup>	SRS simulant	1.217	1.210	-0.6	1.235	1.5	1.237	1.6
Average <sup>b</sup>	SRS simulant	1.229	1.191	-3.1	1.236	0.6	1.250	1.7
High NO <sub>3</sub> <sup>b</sup>	SRS simulant	1.244	1.171	-5.9	1.223	-1.7	1.252	0.6

<sup>a</sup> The modification results shown only account for the additional species K, CO<sub>3</sub>, and SO<sub>4</sub>. For the candidate feed solutions all additional species are accounted for based on Eq. (A-3) approach where the correction factor was set to 0.6.

(This Page Intentionally Left Blank)



## Appendix B (Cesium Isotherms for LAW Phase 1 Batch Feeds)

In column sizing one of two possible design strategies are typically considered: (1) bounding analysis where “worst case” feed compositions are used or (2) global optimization where best estimate feed compositions for each individual batch are used. Each approach has its on advantages and disadvantages. For example, the bounding approach requires less analysis overall but it may be difficult to establish a reasonable bound that is not too excessive. Since the amount of waste to be processed, flowrate, and key feed compositions depend significantly on which envelope is being considered, the global optimization strategy is taken. However, in this appendix the isotherms required by either design approach are determined. The least favorable isotherm for each envelope is determined by comparison of all batch feed isotherms within each envelope.

For the CST exchanger material, individual and least favorable isotherms for each batch feed and Envelope (i.e., Envelopes A, B, and C) are determined, respectively. The isotherms corresponding to the 16 batch feeds are determined based on available BBI Phase 1 LAW feed solution data. For each envelope class, worst case here implies the largest amount of CST material necessary to achieve the same level of decontamination factor for operating columns, while least favorable represents a lower cesium loading curve. For linear isotherms this can easily be established based on the lowest  $K_d$  value (note: for a linear isotherm its  $K_d$  value is a constant). However, for the Cesium-CST system the isotherm is slightly non-linear over the region of interest and in general differing isotherms could cross each other. Therefore, a definitive determination of the worst case isotherm requires consideration over the entire operating range for cesium. One additional complication is the fact that for each candidate feed within a given envelope its cesium concentration varies. The least favorable isotherm is easily determined by inspection of all isotherms within a given envelope. To determine which isotherm is the worst case requires consideration of the feed cesium concentration as well.

Appendix A contains the BBI data set and discusses the various alterations and adjustments that were necessary. In order to successfully use the ZAM equilibrium model, a tight charge balance (i.e., less than  $5 \times 10^{-4}$  mismatch) is required for the species chosen as input to the algorithm. Tables A-5 and A-6 contain the best estimate BBI feed solutions (i.e., 16 in total) all adjusted to a common  $\text{Na}^+$  concentration of 5 M. This common  $\text{Na}^+$  concentration is chosen for establishing the individual isotherms based on the current feed design to the ion-exchange facilities for cesium then technetium removal.

In order to generate an isotherm using ZAM, the input  $\text{Cs}^+$  concentration must be varied over the region of interest (i.e., zero up to the maximum expected  $\text{Cs}^+$  feed concentration). To maintain a tight charge balance, the best estimate feed compositions provided in Tables A-5 and A-6 were adjusted by adding/subtracting  $\text{CsCl}$  to the solutions. All other species were kept at their tabulated values. For fitting an appropriate algebraic isotherm model to this data, alterations such as concentrating or diluting were also considered. For example, feed solutions having a 4 M  $\text{Na}^+$  concentration were generated by dilution of the 5 M feeds (i.e., an 80% dilution was applied to each constituent). Also, to obtain a higher degree of confidence in the estimated

parameters to the algebraic models several additional equilibrium data points were generated (e.g., variations in the Na/K and Na/SrOH ratios were considered).

Table B-1 contains some of the key parameter values for CST in its powder-form and three of its engineered-forms. For comparison purposes, SuperLig<sup>®</sup> 644 properties are also provided.

### B.1 Molar Ratios of Na/Cs, K/Cs, and SrOH/Cs

As stated earlier, ZAM addresses the surface ion-exchange competition between  $\text{Na}^+$ ,  $\text{K}^+$ ,  $\text{Cs}^+$ ,  $\text{H}^+$ ,  $\text{Rb}^+$ , and  $\text{SrOH}^+$ . For this set of analyses it is assumed that  $\text{Rb}^+$  cations are not present in the liquid feed (i.e., their concentrations are set to zero since only trace amounts are typically present) and under loading conditions the  $\text{H}^+$  concentration levels are extremely small (i.e.,  $<1 \times 10^{-14}$  M). Under these assumptions, only the species  $\text{Na}^+$ ,  $\text{K}^+$ ,  $\text{SrOH}^+$ , and  $\text{Cs}^+$  are competing for surface sites. The molar feed ratios of  $[\text{Na}^+/\text{Cs}^+]$ ,  $[\text{K}^+/\text{Cs}^+]$ , and  $[\text{SrOH}^+/\text{Cs}^+]$  provide us with some initial indication of which candidate feed solutions will be less favorable. For the nominal set of analyses performed within this report,  $\text{SrOH}^+$  is assumed to be zero within the feed solutions; therefore, only the other two molar ratios are considered. The impact of  $\text{SrOH}^+$  within the feed is addressed as a sensitivity parameter. For each envelope class the molar ratios provided in Tables A-5 and A-6 are plotted in Figures B-1, B-2, and B-3 for Envelopes A, B, and C, respectively. The higher a ratio becomes the more competition for surface sites will occur. Based on this simple indicator (i.e., maximum number of  $\text{Na}^+$  plus  $\text{K}^+$  competitors versus  $\text{Cs}^+$ ) the following feed solutions should ultimately result in the least favorable isotherms (see Table B-2):

- For Envelope A Figure B-1 indicates feed solution LAW-1 is the least favorable, but the worst case isotherm may be one with a higher cesium feed concentration such as LAW-15;
- For Envelope B Figure B-2 indicates feed solution LAW-2b is both the least favorable and worst case isotherm; and
- For Envelope C Figure B-3 indicates feed solutions LAW-3 and LAW-4 are the least favorable isotherms, but the worst case isotherm may be LAW-7 who has the highest cesium feed concentration.

For comparison purposes, the molar ratios for all feed solutions are plotted together in Figure B-4. Also in Figure B-4, for each envelope the least favorable isotherm is highlighted. To see how representative the Phase 1 LAW batch feeds are when compared to the entire LAW inventory, Figure B-5 contains the molar ratios for all 177 Hanford waste tank inventories (10 of which define the Phase 1 campaign).

### B.2 Isotherm Predictions using the ZAM Model

The ZAM code performs a simulated batch contact test producing one point on a given isotherm curve. To establish an entire isotherm curve, for each feed solution of interest the ZAM equilibrium isotherm model was run for a range of 14 initial total  $\text{Cs}^+$  concentrations (i.e.,  $0.0$ ,  $1.0 \times 10^{-6}$ ,  $1.0 \times 10^{-5}$ ,  $5.0 \times 10^{-5}$ ,  $1.0 \times 10^{-4}$ ,  $5.0 \times 10^{-4}$ ,  $1.0 \times 10^{-3}$ ,  $2.0 \times 10^{-3}$ ,  $3.0 \times 10^{-3}$ ,  $5.0 \times 10^{-3}$ ,  $1.0 \times 10^{-2}$ ,  $3.0 \times 10^{-2}$ ,  $5.0 \times 10^{-2}$ ,  $1.0 \times 10^{-1}$  in units of M). In order to maintain liquid concentrations nearly

constant a high value for the phase ratio (i.e., liquid volume to solid mass) of  $1.0 \times 10^5$  ml/g was chosen. All calculations were performed at 25 °C with a liquid solution density set to the modified HTWOS model estimates provided in Tables A-5 and A-6. The initial form of the resin was set to the Na-form. Cesium and potassium loadings, along with their  $K_d$  and final equilibrium liquid concentration values, were recorded. Note that the isotherm curve created is not dependent upon the choice of phase ratio or initial CST form, but does depend upon temperature and solution density.

The total cation exchange capacity of the CST material in its powder-form (batch IE-910) is species dependent. Two types of exchange sites exist on the CST solid. The total ion exchange capacity is stated to be  $\sim 4.6$  mmole/g<sub>CST</sub>, but the cesium exchange capacity is much less indicating that not all sites are available for cesium exchange (see, Zheng et al., 1996). In the ideal solid region (i.e., prior to the first step of the isotherm), the apparent total capacities are  $\sim 0.58$  mmole/g<sub>CST</sub> for Cs<sup>+</sup>,  $\sim 1.2$  mmole/g<sub>CST</sub> for K<sup>+</sup>,  $\sim 1.18$  mmole/g<sub>CST</sub> for Rb<sup>+</sup>, and  $\sim 1.0$  mmole/g<sub>CST</sub> for SrOH<sup>+</sup>. For the expected feed concentrations it is anticipated that the entire columns will be operating within this ideal solid region. The ZAM algorithm employs the above stated total exchange capacities that apply only to the CST in its powder-form (IE-910). A brief discussion about ZAM, along with limited verification/validation assessments, is provided in Appendix F.

For each of the 16 batch feeds defined in Table A-5 and Table A-6, and for each of the 14 cesium concentration values chosen, a simulated batch contact test was performed using the ZAM code. The results of these ZAM runs are tabulated in Tables B-3 through B-18 where:

- for Envelope A feeds Table B-3 through Table B-13 correspond to batch feeds LAW-1, LAW-5, LAW-6, LAW-8, LAW-9, LAW-10, LAW-11, LAW-12, LAW-13, LAW-14, and LAW-15, respectively;
- for Envelope B feeds Table B-14 and Table B-15 correspond to batch feeds LAW-2a and LAW-2b, respectively; and
- for Envelope C feeds Table B-16 through Table B-18 correspond to batch feeds LAW-3, LAW-4, and LAW-7, respectively.

In each table the equilibrium cesium concentration, cesium  $K_d$ , and cesium loading are given for each ZAM simulated batch contact test, along with similar information for potassium. The ionic strength of each solution is also provided. The ZAM input files used to generate the data corresponding to the cesium concentration of the 16 batch feeds are provided in Appendix G (along with some of the sensitivity input files). For each batch feed condition, the remaining 13 input files can be obtained by adding or removing CsCl from the concentration levels given in input files listed in Appendix G. The database provided in Tables B-4 through B-18 constitutes our cesium isotherm database for 5 M sodium adjusted feeds.

### B.3 Isotherm Model for VERSE-LC Application

In order to perform column transport simulations, the ZAM generated batch contact test data, presented above, must be correlated using one of the VERSE-LC isotherm modeling options. As

demonstrated by Hamm et al. (2000a, Figure 3-3), for ion exchange competitors with affinities significantly less than the value for cesium, a single-component transport modeling approach is adequate for the cesium loading phase. To perform single-component transport simulations, an “effective” binary isotherm model in an algebraic form must be available for use in the VERSE-LC code. Based on our previous experience using VERSE-LC for modeling SuperLig<sup>®</sup> 644 and SuperLig<sup>®</sup> 639 resins (Hamm et al., 2000a and 2000b), the VERSE-LC Freundlich/Langmuir Hybrid isotherm model was chosen. As described by Hamm et al. (2000a, see Chapter 4), the cations cesium, potassium, sodium, and strontium hydroxide form a 4-component homovalent system where the surface loading for cesium on the CST material can be expressed as:

$$Q_{Cs^+} = \frac{\eta_{df} \bar{C}_T c_{pCs^+}}{c_{pCs^+} + \tilde{K}_{21} c_{pK^+} + \tilde{K}_{31} c_{pNa^+} + \tilde{K}_{41} c_{pSrOH^+}} , \quad (B-1a)$$

or as

$$Q_{Cs^+} = \frac{\eta_{df} \bar{C}_T c_{pCs^+}}{c_{pCs^+} + \beta} \quad (B-1b)$$

where

$$\beta = \tilde{K}_{21} c_{pK^+} + \tilde{K}_{31} c_{pNa^+} + \tilde{K}_{41} c_{pSrOH^+} .$$

It has been assumed that the binary selectivity coefficients are not composition dependent, but are true constants (i.e., note that the selectivity coefficients actually contain the true equilibrium constants and liquid/solid phase activity coefficients). This assumption appears to be somewhat adequate when considering different feeds within the same envelope (i.e., generally only small variations are observed in selectivity coefficients within a given envelope), but should not be used between envelopes. The composite impact on cesium loading from the other cation competitors is summed up in the beta parameter shown. Equation (B-1a) can be rearranged into a more convenient form where liquid concentrations are expressed as molar ratios by:

$$Q_{Cs^+} = \frac{\eta_{df} \bar{C}_T}{1 + \tilde{K}_{21} \left[ \frac{c_{pK^+}}{c_{pCs^+}} \right] + \tilde{K}_{31} \left[ \frac{c_{pNa^+}}{c_{pCs^+}} \right] + \tilde{K}_{41} \left[ \frac{c_{pSrOH^+}}{c_{pCs^+}} \right]} = \frac{\eta_{df} \bar{C}_T}{1 + \frac{\beta}{c_{pCs^+}}} . \quad (B-2)$$

Under the simple assumption of constant binary selectivity coefficients, we see that the cesium loading isotherm is only a function of the molar ratios  $[K^+/Cs^+]$ ,  $[Na^+/Cs^+]$ , and  $[SrOH^+/Cs^+]$  where the total cesium exchange capacity is a constant value within the ideal solid region (i.e., depends only on the exchange material properties and for the powder-form its value has been determined to be  $\bar{C}_T = 0.58$  mmole/g<sub>CST</sub>). Equation (B-2) also indicates that the larger the beta value the less favorable the cesium isotherm.

The VERSE-LC Freundlich/Langmuir Hybrid model is expressed as:

$$\bar{C}_{pi} = \frac{a_i c_{pi}^{M_{ai}}}{\beta_i + b_1 c_{pl}^{M_{b1}} + b_2 c_{p2}^{M_{b2}} + b_3 c_{p3}^{M_{b3}} + b_4 c_{p4}^{M_{b4}}} \quad \text{for } i = 1, 4 , \quad (B-3)$$

where the model parameters ( $a_i$ ,  $b_i$ ,  $M_{ai}$ ,  $M_{bi}$ , and  $\beta_i$  for  $i=1,4$ ) can be determined from the parameter values associated with the 4-component homovalent model.

The Freundlich/Langmuir Hybrid model can also be used for an “effective” single-component case as well. Here the potassium, sodium, and strontium hydroxide concentrations throughout the column are assumed to be at their feed concentration levels. For an “effective” single-component total cesium isotherm, Eq. (B-3) under these conditions reduces to:

$$\bar{C}_{p1} = \frac{a_1 c_{p1}^{M_{a1}}}{[\beta_i + b_2 c_{p2}^{M_{b2}} + b_3 c_{p3}^{M_{b3}} + b_4 c_{p4}^{M_{b4}}] + b_1 c_{p1}^{M_{b1}}} \Rightarrow \frac{a_1 c_{p1}^{M_{a1}}}{\hat{\beta}_i + b_1 c_{p1}^{M_{b1}}} , \quad (B-4)$$

where the beta parameter for cesium becomes dependent upon the potassium, sodium, and strontium hydroxide feed concentrations. The relationship between the two models expressed by Eqs. (B-3) and (B-4) (i.e., 4-component homovalent and “effective” single-component isotherm models, respectively) is provided in Table B-19. The dilution factor,  $\eta_{df}$ , is set to unity when CST in its powder-form is being considered.

Since ZAM can be used directly to generate cesium isotherms for each candidate feed, we shall develop cesium isotherms based on the “effective” single-component model and not explicitly rely on the selectivity coefficients ( $K_{i1}$ ,  $i=2,4$ ) required by the 4-component homovalent model. In this way, the propagation of errors will be minimized.

#### B.4 Isotherm Parameter Estimation Technique

To establish a cesium isotherm, three independent binary selectivity coefficient parameters (or depending upon the model chosen a single beta parameter directly) must be determined based on equilibrium contact test data or ZAM generated data. As seen by Eq. (B-2), based on the functional form chosen the fitting parameter(s) can be obtained from equilibrium contact tests where only one of the cations solid-phase concentration (or surface loading) is known.

A non-linear regression analysis based on the maximum likelihood principle (see Anderson et al., 1978) was chosen consistent with earlier work (Hamm et al., 2000a and 2000b). The maximum likelihood approach minimizes a cost function based on the sum of squares of weighted residuals. Special attention must be given to the choice of weights. Due to the broad range of cesium concentrations considered (i.e.,), a logarithmic weighting criterion for parameter estimation was found to be superior (i.e., more uniform weighting over several orders of magnitude in cesium concentration was achieved). The cost function being minimized is

$$\Phi(\tilde{K}_{21}, \tilde{K}_{31}, \tilde{K}_{41}) = \sum_{i=1}^n [R_i^2], \quad (B-5a)$$

where the chosen weighted residual function is

$$R_i = \ln(Q_{Cs^+}^{ZAM}) - \ln(Q_{Cs^+}^{algebraic}). \quad (B-5b)$$

Equation (B-5) results in uniform weighting among all of the data points. Application of the maximum likelihood algorithm (using logarithmic weighting) to the algebraic model (Eq. B-2) results in “best estimate” values for the three selectivity coefficients (or beta parameter directly), as discussed below for each envelope. The various other binary selectivity coefficients (i.e., combinations of the three primary ones) can be computed based on reciprocity identities. The confidence levels, covariance matrix, and correlation coefficient matrix for the fitted parameters are also computed during the optimization process.

## B.5 The Least Favorable Isotherm

As Eq. (B-2) indicates, along with the excellent agreement achieved in fitting this algebraic model to the various isotherms created using the ZAM model, the dominant factors affecting an isotherm are the molar ratios. Over the range of candidate feed solutions considered, their compositional variations within the liquid-phase play only a secondary role. Therefore, the determination of a least favorable isotherm for each set of candidate feed solutions within a given envelope can be directly determined by Eq. (B-2) once the three binary selectivity coefficients are known. Using Eq. (B-2), the following criterion can be derived that establishes conditions under which the least favorable isotherm can be determined:

$$\left( \tilde{K}_{21} \left[ \frac{c_{pK^+}}{c_{pCs^+}} \right] + \tilde{K}_{31} \left[ \frac{c_{pNa^+}}{c_{pCs^+}} \right] + \tilde{K}_{41} \left[ \frac{c_{pSrOH^+}}{c_{pCs^+}} \right] \right)_{\text{least favorable}} \geq \left( \tilde{K}_{21} \left[ \frac{c_{pK^+}}{c_{pCs^+}} \right] + \tilde{K}_{31} \left[ \frac{c_{pNa^+}}{c_{pCs^+}} \right] + \tilde{K}_{41} \left[ \frac{c_{pSrOH^+}}{c_{pCs^+}} \right] \right)_{\text{candidate feed solution}} \quad (B-6)$$

Table B-1 lists the numerical value of Eq. (B-6) for each candidate feed solution where it is assumed that the [SrOH/Cs] ratio is zero. For example, as shown in Table B-1 for Envelope A, the worst case isotherm results from the feed solution corresponding to LAW-1. Overall estimates (Envelope A only) for the three binary selectivity coefficients were obtained using the non-linear regression analysis scheme described above. The overall regression results for the 11 Envelope A feeds is provided in Tables B-20 and B-21. The estimated binary selectivity coefficients obtained are (see Table B-20):

- for ( SrOH<sup>+</sup> versus Cs<sup>+</sup> )  $K_{14} \approx 6.9 \rightarrow K_{41} \approx 1.443 \times 10^{-1}$ ;
- for ( K<sup>+</sup> versus Cs<sup>+</sup> )  $K_{12} \approx 1,400 \rightarrow K_{21} \approx 7.143 \times 10^{-4}$ ; and
- for ( Na<sup>+</sup> versus Cs<sup>+</sup> )  $K_{13} \approx 26,000 \rightarrow K_{31} \approx 3.846 \times 10^{-5}$ .

The parameter estimation results for Envelope A (i.e., 11 batch fees) are provided in Table B-20 where the various possible binary selectivity coefficients for this 4-component isotherm are provided. Also provided are the approximate standard errors for each coefficient. The correlation coefficient matrix for the fitting process is given in Table B-21. As Table B-21 indicates, the degree of cross-correlation between SrOH<sup>+</sup> versus K<sup>+</sup> and SrOH<sup>+</sup> versus Na<sup>+</sup> is

high (i.e., 0.1118 and -0.2493; where a good indication would have been near 1.0 or -1.0). Even though the  $\text{SrOH}^+$  selectivity coefficient,  $K_{14}$ , is not uniquely defined, comparison of predicted versus ZAM generated data remains excellent. These results support the need to handle each batch feed separately, in order to increase our predictive capability.

Note that Eq. (B-2) is based on the assumption of constant binary selectivity coefficients which implies that for the range of feed solutions considered, compositional variations have only a minor impact on the isotherm. However, compositional variations between envelopes are significant enough to warrant, in general, different estimates for the three binary selectivity coefficients. However, due to the poor parameter confidence levels achieved, the binary selectivity coefficients for Envelopes B and C are not presented here.

## B.6 “Effective” Single-Component Isotherm Models

As discussed above, an effective single-component total cesium isotherm can be expressed as:

$$Q_{\text{Cs}} = \frac{\eta_{\text{df}} \bar{C}_{\text{T}} c_{\text{Cs}}}{c_{\text{Cs}} + [\tilde{K}_{21} c_{\text{K}} + \tilde{K}_{31} c_{\text{Na}} + \tilde{K}_{41} c_{\text{SrOH}} + \cdots]} \Rightarrow \frac{\eta_{\text{df}} \bar{C}_{\text{T}} c_{\text{Cs}}}{c_{\text{Cs}} + \beta}, \quad (\text{B-7})$$

where the beta parameter for cesium becomes dependent upon the other ionic competitors for CST adsorption (i.e.,  $\text{K}^+$ ,  $\text{Na}^+$ ,  $\text{SrOH}^+$ , and  $\text{Rb}^+$ ). The beta parameter contains the selectivity coefficients making it dependent upon temperature and liquid composition of all of the ionic species in solution. The dilution factor ( $\eta_{\text{df}}$ ) is unity when considering a specific power-form and is less than one upon addition of an inert binder. Based on analyses discussed in Appendix C the best estimate dilution factor for the engineered-form is set to 0.68. The total cesium capacity term is only a function of which batch of powder-form material is being considered and is set to 0.58 mmole<sub>Cs</sub>/g<sub>CST</sub>.

For each candidate feed solution the ZAM model was run to obtain a database for determining a beta value for that particular feed. This database is generated by varying the cesium and chloride concentrations, while holding all other ionic concentrations at their best estimate values. Using the database generated for each batch feed and Eq. (B-7) above, a “best estimate” of the beta parameter for each batch feed was computed. The summary results from the non-linear regression analyses are listed in Table B-22 for all 16 batch feeds, along with the overall average for each envelope. As shown in Table B-22, the root-mean-square error in predicting the cesium loading over the entire cesium concentration range is excellent. Based on the results shown in Table B-22, the Freundlich/Langmuir Hybrid modeling parameters for the 16 batch feeds are tabulated in Table B-23. The leading coefficient,  $a_i$ , varies depending upon which form of the CST material is to be considered.

Using the algebraic model, predictions for comparison to the ZAM model were generated for each batch feed and are tabulated in Tables B-24 through B-39. Tables B-24 through B-39 contain the algebraic model predictions for both the powder-form and the engineered-form. Residual plots of the algebraic model predictions of cesium loading versus the ZAM model predictions of cesium loading are provided in Figures B-6 through B-8 for the Envelope A, B,

and C feeds, respectively. In all cases the algebraic model provides an excellent fit to the ZAM generated databases. A bar-chart of the beta values for each batch feed is illustrated in Figure B-9 where the various beta values have been grouped according to envelope. As Eq. (B-7) indicates, the higher the beta value the less favorable the isotherm.

### **B.6.1 PHASE 1 Envelope A LAW Isotherms**

As Figure B-9 illustrates, a wide variation in isotherms is seen for the Envelope A batch feeds. In Figure B-10 a log-log plot of the cesium loading isotherms for all 11 Envelope A batch feeds is shown. Also shown, is the location where the column inlet cesium concentration of each feed would be. The least favorable isotherm can be easily seen in Figure B-10 to be LAW-1. However, since LAW-1's cesium concentration is not also the highest value, LAW-1 may not be the worst case isotherm, as well. Column transport analyses would be required to determine which of these isotherms would generate more total spent CST material to process the LAW solutions.

### **B.6.2 PHASE 1 Envelope B LAW Isotherms**

As Figure B-9 illustrates, a modest variation in isotherms is seen for the Envelope B batch feeds. In Figure B-11 a log-log plot of the cesium loading isotherms for both Envelope B batch feeds is shown. Also shown, is the location where the column inlet cesium concentration of each feed would be. The least favorable isotherm can be easily seen in Figure B-11 to be LAW-2a. Since LAW-2a also contains the higher cesium feed concentration, it is also the worst case isotherm.

### **B.6.3 PHASE 1 Envelope C LAW Isotherms**

As Figure B-9 illustrates, a small variation in isotherms is seen for the Envelope C batch feeds. In Figure B-12 a log-log plot of the cesium loading isotherms for all 3 Envelope C batch feeds is shown. Also shown, is the location where the column inlet cesium concentration of each feed would be. The least favorable isotherm can be easily seen in Figure B-12 to be LAW-3 and LAW-4. However, since neither LAW-3's nor LAW-4's cesium concentration is also the highest value, LAW-7 may be the worst case isotherm. Column transport analyses would be required to determine which of these isotherms would generate more total spent CST material to process the LAW solutions.

### **B.6.4 Comparison of Least Favorable Isotherms**

In Figures B-10, B-11, and B-12, the least favorable isotherms were seen to be LAW-1 for Envelope A, LAW-2a for Envelope B, and LAW-3 (or LAW-4) for Envelope C. A direct comparison of these three isotherms is given in Figure B-13. The least favorable isotherm among these is LAW-1; however, LAW-1 also has the lowest cesium feed concentration. To determine which isotherm would be the worst case isotherm again requires separate column transport analyses. Based on issues such as these and others (i.e., envelope dependent cesium exit criteria, waste volumes, flowrates, and cesium feed concentrations), a global strategy for



CST column design was chosen where the overall worst case isotherm is not considered; instead, all 16 best estimate isotherms are employed directly.

### **B.6.5 LAW-1 Feed (KNO<sub>3</sub> precipitation Issue)**

The best estimate feed composition for LAW-1 (i.e., Tank AP-101) presented a unique problem when the 5.0 M sodium feed was used in developing its isotherm using the ZAM model. For this feed composition ZAM predicts that some KNO<sub>3</sub> will precipitate out indicating that the KNO<sub>3</sub> solubility limit had been exceeded. Based on experience with making Hanford and SRS simulants, KNO<sub>3</sub> precipitation at these concentrations (i.e., for LAW-1 at 5.0 M Na<sup>+</sup> and 25 C, K<sup>+</sup> is at 0.712 M and NO<sub>3</sub><sup>-</sup> is at 1.87 M) had not been observed.

For a simple solution, a comparison of the ZAM prediction versus measured data (Washburn et al., 1928) for the solubility limit of KNO<sub>3</sub> is shown in Figure B-14. The results shown are for an aqueous solution of Na<sup>+</sup>, K<sup>+</sup>, OH<sup>-</sup>, and NO<sub>3</sub><sup>-</sup> where a fixed amount of K<sup>+</sup> and NO<sub>3</sub><sup>-</sup> (i.e., at two different molar ratios) were considered over a wide range of varying NaOH. The decreasing solubility upon increasing ionic strength clearly shows the expected “salt-effect”. Unfortunately, for the case of pure K<sup>+</sup> and NO<sub>3</sub><sup>-</sup> (i.e., no NaOH present) the ZAM prediction of ~1.1 M is significantly lower than the measured value of ~3.3 M. It would appear that either the KNO<sub>3</sub> Bromley activity coefficient or the KNO<sub>3</sub> solubility product being used is incorrect.

Once KNO<sub>3</sub> precipitation is encountered within the ZAM model, ZAM performs mass balance calculations to appropriately reduce the initial feed concentrations of K<sup>+</sup> and NO<sub>3</sub><sup>-</sup> to account for the level of KNO<sub>3</sub> precipitation predicted to occur and then performs the solid-liquid equilibrium calculation using the new adjusted feed composition. Unfortunately, we are unable to turn off this feature directly within ZAM through input and must through the following extrapolation procedure to estimate the cesium loadings consistent with the initial feed compositions.

For the Phase 1 LAW-1 feed the nominal nitrate to nitrite concentration ratio is lowered such that the point where KNO<sub>3</sub> precipitation starts to occur is located (i.e., an equal amount of nitrite is added in place of nitrate). The cesium loading curve resulting from this analysis is shown in Figure B-15, where the input nitrate to nitrite concentration ratio into ZAM is varied on both sides of this solubility point. The solid line represents the ZAM results where a clear discontinuity in slope is experienced at the point of reaching the predicted KNO<sub>3</sub> solubility limit. Prior to reaching this solubility limit, increased nitrate to nitrite concentration ratio results in a decreased cesium loading primarily due to the increased ionic strength. Without KNO<sub>3</sub> precipitation occurring, further increase in the nitrate to nitrite concentration ratio would follow the linear extrapolation shown as a dashed line in Figure B-15. With KNO<sub>3</sub> precipitation occurring, the decreased quantity of liquid-phase K<sup>+</sup> and NO<sub>3</sub><sup>-</sup> present (K<sup>+</sup> as a competitor and both as contributors to ionic strength) reduces this trend. In generating the entire cesium isotherm for the Phase 1 LAW-1 feed, the above extrapolation technique is used at every cesium concentration point considered. The database generated is tabulated in Table B-3.

After writing this chapter the work of Anthony et al. (2001) was provided to the authors. Anthony et al. (2001) updated the ZAM code where the solubility product for KNO<sub>3</sub> would be inputted through the input. As stated within their report, a solubility product fixed to 0.19 M

was in the earlier version of ZAM. This value was based on the presence of salt formation induced by TAM5 during a 1.6 M NaKNO<sub>3</sub> step change experiment and looking at the potassium isotherms. For solutions without TAM5 no such low solubility product is observed (even in the presence of CST in its engineered-forms).

### B.6.6 Impact of Strontium on Envelope C Isotherms

There are three candidate feed solutions to be considered for Envelope C. The total strontium concentration estimates available were:

- $<2.28 \times 10^{-6}$  M total Sr<sup>2+</sup> for tank AN-103
- $<2.85 \times 10^{-6}$  M total Sr<sup>2+</sup> for tank AZ-102
- $2.04 \times 10^{-5}$  M total Sr<sup>2+</sup> for tank AN-102
- $1.633 \times 10^{-3}$  M total Sr<sup>2+</sup> for tank AN-102 post Sr/TRU
- $5.0 \times 10^{-4}$  M total Sr<sup>2+</sup> for tank AN-107 post Sr/TRU

The value of  $1.633 \times 10^{-3}$  M total strontium in solution was chosen as an upper bound value for free strontium in solution based on the currently available analytical analyses listed above. Based on complexants (e.g., EDTA) the free strontium available to form strontium hydroxide should be much smaller. The following liquid-phase equilibrium reaction is being modeled within the ZAM code:



where the equilibrium constant is  $\sim 197$ . Based on ZAM equilibrium calculations using this mass-action equation and equilibrium constant, the majority of free Sr<sup>2+</sup> initially assumed in solution (i.e.,  $1.633 \times 10^{-3}$  M) is converted into SrOH<sup>+</sup>, approximately  $1.625 \times 10^{-3}$  M, which competes for CST surface sites.

In fitting the algebraic isotherm model the following data sets were considered:

- LAW-3 candidate feed at 5 M Na<sup>+</sup> whose species concentrations are specified in Table A-6 where free Sr<sup>2+</sup> concentration was set to zero (i.e., the nominal case); and
- LAW-3 candidate feed at 5 M Na<sup>+</sup> whose species concentrations are specified in Table A-6, except for free strontium which was set to  $1.633 \times 10^{-3}$  M Sr<sup>2+</sup>.

As shown in Table B-22, the beta value for the nominal LAW-3 batch feed is  $2.1769 \times 10^{-4}$  M. When the free strontium concentration is increased from zero to  $1.633 \times 10^{-3}$  M Sr<sup>2+</sup> (i.e., zero to  $1.625 \times 10^{-3}$  M SrOH<sup>+</sup>) the computed beta value increases to  $3.8445 \times 10^{-4}$  M (i.e., an increase of  $\sim 77\%$ ). A comparison of the two LAW-3 isotherms is shown in Figure B-16.

As Figure B-16 suggests, the presence of free strontium in solution can have a significant impact on the cesium isotherm. In this bounding case approximately 50% reduction in cesium loading is observed over the operating range of the isotherm. Prior to final CST column design,

additional investigations are warranted to determine the expected levels of free strontium in solution and its ultimate impact on the cesium isotherms.

## **B.7 Cesium Isotherm Sensitivity Study and Error Analysis**

Our cesium isotherm is based on the ZAM model multiplied by a bias term (referred to in this report as a dilution factor). The ZAM model solves the appropriate liquid-solid equilibrium equations for the Cesium-CST system where its modeling parameters were determined based on CST powder batch and kinetic contact tests. The dilution factor is based on the measured deviations of engineered contact test data when compared to ZAM predicted powder behavior. In this section we discuss the uncertainties associated with our cesium isotherm model.

To evaluate the impact on the cesium isotherms associated with uncertainties in the composition of the various batch feeds, a sensitivity analysis was performed. The Envelope A LAW-15 batch feed was chosen where various species composition values, along with temperature and feed density, were individually altered from their “nominal” settings. The results of this sensitivity study are provided in Tables B-40 and B-41. These tables list the sensitivity variables considered and their impact on cesium loading (i.e., Table B-40 for the nominal state set to 100% of the cesium feed concentration and Table B-41 for 50% of the cesium feed concentration). A simple star-pattern approach to the sensitivity analysis was considered to be adequate (i.e., for each parameter considered its value was varied while all other parameters were kept at their nominal settings).

Using the sensitivity results, a “simplified” error analysis is performed where an estimate of the overall uncertainty in the cesium isotherm is computed. Much of this effort is based on a good engineering judgement approach where errors in various variables are stated based on an assumed/implied confidence level of approximately 2-sigma. Where available, supporting data are used in establishing these error estimates.

### **B.7.1 The Uncertainty Approach Taken**

For estimating our level of confidence in the predicted cesium isotherms, a best estimate plus quantified uncertainty approach is being attempted. A rough measure of uncertainty in a cesium isotherm can be estimated based on the following approach.

The ZAM model solves a set of equations describing the liquid-solid equilibrium behavior for the Cesium-CST system. At an equilibrium state the cesium loading can be functionally expressed as:

$$Q = \eta_{df} F(\bar{c}, T, \rho_{soln}, c_{Cs}) , \quad (B-9)$$

where the concentration vector represents all cations and anions (excluding cesium) within the candidate feed that is considered within the ZAM model. Equation (B-9) represents a nonlinear cesium isotherm that can be linearized about some nominal cesium concentration (e.g., its feed value) yielding:

$$Q - Q_o = \left( \frac{\partial Q}{\partial \eta_{df}} \right)_o [\eta_{df} - \eta_{df,o}] + \left( \frac{\partial Q}{\partial T} \right)_o [T - T_o] + \left( \frac{\partial Q}{\partial \rho_{so\ln}} \right)_o [\rho_{so\ln} - \rho_{so\ln,o}] + \sum_{i \neq Cs} \left( \frac{\partial Q}{\partial c_i} \right)_o [c_i - c_{i,o}] \quad , \quad (B-10)$$

where the subscript o implies that the variable is evaluated at its nominal value. If we consider these variables to be random variables that are independent, then the propagation of errors approach (Freund, 1971) provides us with a simple method of combining in a statistical way the uncertainty associated with each of these variables to produce a composite impact.

To make use of the propagation of errors approach the linear equation Eq. (B-10) must be used, where an overall variance results in:

$$\sigma_Q^2 = \left( \frac{\partial Q}{\partial \eta_{df}} \right)_o^2 \sigma_{\eta_{df}}^2 + \left( \frac{\partial Q}{\partial T} \right)_o^2 \sigma_T^2 + \left( \frac{\partial Q}{\partial \rho_{so\ln}} \right)_o^2 \sigma_{\rho_{so\ln}}^2 + \sum_{i \neq Cs} \left( \frac{\partial Q}{\partial c_i} \right)_o^2 \sigma_{c_i}^2 \quad , \quad (B-11)$$

and due to the actual nonlinear behavior of the isotherm, the overall variance becomes dependent upon the choice of the nominal state (i.e., the variance varies with respect to cesium concentration). By defining an error estimate in terms of percentage and dividing through by Q, Eq. (B-11) can be expressed as:

$$E_Q^2 = E_{\eta_{df}}^2 + E_T^2 + E_{\rho_{so\ln}}^2 + \sum_{i \neq Cs} E_{c_i}^2 \quad , \quad (B-12)$$

where the error estimates in terms of percentages are:

$$E_x = 100 \left( \frac{\partial Q}{\partial x} \right)_o \sigma_x^2 \quad . \quad (B-13)$$

## B.7.2 Feed Composition Uncertainties

In order to estimate uncertainty levels in the feed composition a comparison must be made between the candidate feed batches provided in Tables A-1 and A-2 and actual measured samples. Recent characterization data of three waste tank samples have been performed by Hay et al. (2000a) for Envelope A's AN-103 (sample size of 1.2 L), by Hay and Bronikowski (2000) for Envelope B's AZ-102 (sample size of 14.25 L), and by Hay et al. (2000b) for Envelope C's AN-102 (sample size of 3.75 L). In their reports they state that "recent experience at SRS indicates the combined sampling and analytical error associated with obtaining small samples from a well mixed waste tank is on the order of 15-20%" (Hay and Edwards, 1994). In Table B-42 a comparison is made between the measured feed compositions and the candidate feeds listed in Table A-1 and A-2. The percent difference in measured versus LAW candidate feed compositions are listed for each envelope, along with a root-mean-square value for the key species of interest. The majority of error values listed are greater than 20%. These tanks are probably not well mixed. The degree of uncertainty in tank variability due to lack of

homogeneity will be highly tank and time dependent. We shall implicitly account for tank non-homogeneity, and our lack of knowledge, by setting our error estimates for each species to 50% (except for sodium). Since the sodium level of the pretreatment feed will be adjusted to a target concentration of ~5.0 M, for sodium we shall set our error estimate to back 20%.

Free  $\text{OH}^-$  concentrations appear to be difficult to pin down since analytical methods typically used to determine this quantity actually measure total  $\text{OH}^-$  and then compute the free  $\text{OH}^-$  by assuming certain chemical reactions (e.g., aluminate or carbonate formations) have consumed (bound)  $\text{OH}^-$ . In these analyses presented here we allow the free  $\text{OH}^-$  to vary in order to achieve a charge balance for all candidate feed solutions (i.e., both nominal compositions, as well as compositions used in the sensitivity studies). For sensitivity studies species concentration variations can not be arbitrarily chosen, but must adhere to the overall ionic charge balance. For each species variation considered, the  $\text{OH}^-$  concentration is adjusted to maintain the charge balance. Table B-43 provides the species concentrations for each sensitivity study performed. In reality a more complex variation of several species concentrations would be occurring. However, for our purposes this more limited star-pattern approach was considered to be adequate.

As stated elsewhere within this report, no account is taken both nominally or statistically for the loading of  $\text{SrOH}^+$  onto the CST material. It is assumed that the total Sr present is not available to form the  $\text{SrOH}^+$  species (i.e., zero free strontium). This assumption should be addressed in any future considerations of CST columns since the loading capacity for  $\text{SrOH}^+$  is on the same order as or greater than for  $\text{Cs}^+$ .

### **B.7.3 Feed Density and Process Temperature Uncertainties**

As discussed in Appendix A, a modified HTWOS density model was chosen for estimating the liquid-phase density of the various candidate feed solutions. A comparison of predicted versus measure densities are shown in Table A-8 where the overall root-mean-square is ~1% for the available Hanford data and ~1.4% for available SRS waste. For our purposes will shall assume an error estimate of ~3% to be acceptable (i.e., two times 1.5%). Note that a decreased solution density only marginally decreases the cesium loadings as can be seen in Figure B-17.

Current column designs assume an operating temperature of ~25 C. To take into account potential non-uniform temperatures within the columns and CST material itself, due to  $^{137}\text{Cs}$  decay and possible operational upsets, a 5 C variation (i.e., 1.68%) is considered. Note that increased temperature decreases the cesium loadings.

### **B.7.4 Dilution Factor Uncertainty**

In Appendix C the dilution factor (i.e., ratio of total cesium capacity for an engineered-form versus total cesium capacity for its powder-form) is discussed. Based on the various engineered forms tested a range of dilution factors were observed. A mean value of 0.76 was computed; however, for more recent engineered forms a mean value of 0.68 appeared to be more appropriate. Based on this lower value for dilution factor an ~15% error estimate seems reasonable.

### **B.7.5 Sensitivity Results and Error Estimates**

A sensitivity study was performed using the candidate feed LAW-15. Batch LAW-15 was chosen since Envelope A constitutes the major amount of LAW tank waste to be process (i.e., 71% by volume Envelope A, 7% Envelope B, and 22% Envelope C when adjusted to a common 5.0 M sodium basis) and among the Envelope A feed candidates it demonstrates a potentially worst case isotherm.

To determine the impact of each variable listed in Table B-40 or Table B-41, a ZAM model run was made. The results of the ZAM model runs are listed in Tables B-40 and B-41 for the nominal cesium feed concentration value of  $4.552 \times 10^{-5}$  M and for 50% of this value, respectively. The input concentrations used for each sensitivity case are provided in Table B-43.

During the sensitivity runs, the ZAM code predicted that  $\text{KNO}_3$  would start to precipitate out of solution, reducing the amount of  $\text{K}^+$  in solution for competition with  $\text{Cs}^+$  for CST sites. At approximately 41.5% increase in  $\text{K}^+$  above its nominal value, precipitation started. To estimate the cesium loading impact associated with a 50% increase in  $\text{K}^+$ , an extrapolation of results were made. The extrapolation performed is shown in Figure B-18 as the dashed line, while the solid curve shown represents the unaltered results from ZAM over the 0% to 60% increase in  $\text{K}^+$  concentration inputs. At a 50% increase in  $\text{K}^+$  the extrapolation yields a 5.8% decrease in cesium loading.

As the entries in Tables B-40 and B-41 indicate, an overall error for the cesium isotherm is ~28% and is not sensitive to the chosen nominal value for cesium concentration. Except for the dilution factor, which exhibits a one-for-one impact as expected, all the other variables have a reduced impact (i.e., a smaller % change in loading than the % change in the variable itself).

Table B-1. Key CST exchange properties taken from literature.

Resin Form	Batch Name	F Factor <sup>a</sup> (-)	Bulk Dry Density <sup>a</sup> (g/ml <sub>bed</sub> )	Dilution Factor <sup>c</sup> (-)	Cesium Total Ion- Exchange Capacity <sup>b</sup> (mmole/g <sub>solid</sub> )	Cesium Total Ion- Exchange Capacity <sup>b</sup> (mmole/ml <sub>bed</sub> )
SuperLig® 644	10-SM-171	0.9751	0.2238	1.0	0.3333	0.0746
Powder	IE-910	0.9680	0.7738	1.0	0.580	0.4488
Engineered	IE-911 (38b)	0.8870	1.1300	not reported	not reported	not reported
Engineered	IE-911 (08)	0.8990	0.8999	not reported	not reported	not reported
Engineered	Nominal <sup>d</sup>	0.80	1.00	0.68 (estimated)	0.3944 (estimated)	0.3944 (estimated)

<sup>a</sup> Data obtained from Brown et al. (1996, Table 3.1).

<sup>b</sup> Data obtained from Zheng et al. (1996) and confirmed by running ZAM at very large liquid cesium concentrations.

<sup>c</sup> During the manufacturing production process of IONSIV® IE-911 resin, an inert binder is added to CST powder to create an engineered form that is useable in ion-exchange columns. The additional inert binding material reduces the total Cs ion-exchange capacity and this reduction factor is referred to as its “dilution factor”.

<sup>d</sup> The average properties of IONSIV® IE-911 exchanger as stated by UOP (1996).

Table B-2. Key molar ratios for the various LAW batch feed solutions.

Envelope	Batch Name	Staging (Source) Tank	Na/Cs	K/Cs	(Na+K)/Cs	Na/K	High (Na+K) Level Ranking <sup>a</sup>	Worst Case Indicator <sup>b</sup>
A	LAW-1	AP-101	1.39E+05	1.98E+04	1.59E+05	7.0	1	19.5
A	LAW-5	AN-104	7.96E+04	9.67E+02	8.06E+04	82.3	9	3.8
A	LAW-6	AN-104	7.90E+04	9.87E+02	8.00E+04	80.1	10	3.7
A	LAW-8	AN-105	1.16E+05	1.67E+03	1.17E+05	69.3	5	5.6
A	LAW-9	AN-105	1.13E+05	1.36E+03	1.14E+05	82.9	7	5.3
A	LAW-10	SY-101	1.35E+05	1.14E+03	1.37E+05	119.3	2	6.0
A	LAW-11	SY-101	1.34E+05	1.11E+03	1.35E+05	120.4	3	5.9
A	LAW-12	AN-103	1.04E+05	2.56E+03	1.06E+05	40.5	8	5.8
A	LAW-13	AN-103	1.04E+05	2.59E+03	1.06E+05	39.9	8	5.8
A	LAW-14	AW-101	1.09E+05	7.00E+03	1.16E+05	15.6	6	9.2
A	LAW-15	AW-101	1.10E+05	8.93E+03	1.19E+05	12.3	4	10.6
B	LAW-2a	Pretreated AZ-101/AZ-102	1.07E+04	2.67E+02	1.10E+04	40.0	2	-
B	LAW-2b	Pretreated AZ-101/AZ-102	1.16E+04	3.32E+02	1.19E+04	35.0	1	-
C	LAW-3	AN-102	1.26E+05	1.11E+03	1.27E+05	113.8	2	-
C	LAW-4	AN-102	1.32E+05	1.16E+03	1.33E+05	113.8	1	-
C	LAW-7	AN-107	1.12E+05	5.00E+02	1.13E+05	224.5	3	-

<sup>a</sup> Ranking was performed over each envelope where the highest (Na<sup>+</sup> + K<sup>+</sup>) level is ranked number 1. However, the higher the concentration of K<sup>+</sup> relative to Na<sup>+</sup> in a feed solution, the more competition for surface sites experienced since the CST material has a much stronger affinity for K<sup>+</sup> than for Na<sup>+</sup>.

<sup>b</sup> The worst case indicator is based on Eq. (B-2) and the appropriate binary selectivity coefficients. The higher the number the worst (i.e., lower cesium adsorption) the isotherm. Here, appropriate Envelope A weighting between K<sup>+</sup> (K<sub>12</sub>=1,400) and Na<sup>+</sup> (K<sub>13</sub>=26,000,) levels due to affinity differences is achieved.

Table B-3. "Extrapolated" ZAM equilibrium isotherm model predictions for CST material in the powder form (IE-910) in contact with Envelope A's LAW-1 feed solution at 5 M  $[\text{Na}^+]$ .<sup>a</sup>

Cs (initial)	Cs (final) <sup>b</sup>	Na/Cs	Ionic strength <sup>c</sup>	Cs $K_d$	Cs loading	K $K_d$ <sup>c</sup>	K loading <sup>c</sup>
[M]	[M]	[molar ratio]	[gmole/kg]	[ml/g]	[mmole/g]	[ml/g]	[mmole/g]
0	same as initial	infinity	-	0.0	0.000E+00	-	-
0.000001	same as initial	5.000E+06	-	1326.5	1.326E-03	-	-
0.00001	same as initial	5.000E+05	-	1300.3	1.300E-02	-	-
0.00005	same as initial	1.000E+05	-	1197.8	5.989E-02	-	-
0.0001	same as initial	5.000E+04	-	1089.6	1.090E-01	-	-
0.0005	same as initial	1.000E+04	-	625.8	3.129E-01	-	-
0.001	same as initial	5.000E+03	-	407.3	4.073E-01	-	-
0.002	same as initial	2.500E+03	-	239.4	4.788E-01	-	-
0.003	same as initial	1.667E+03	-	169.5	5.084E-01	-	-
0.005	same as initial	1.000E+03	-	107.0	5.348E-01	-	-
0.01	same as initial	5.000E+02	-	55.7	5.565E-01	-	-
0.03	same as initial	1.667E+02	-	19.1	5.719E-01	-	-
0.05	same as initial	1.000E+02	-	11.5	5.751E-01	-	-
0.1	same as initial	5.000E+01	-	5.8	5.775E-01	-	-
3.598E-05 (feed conc.)	same as initial	1.390E+05	-	1238.0	4.455E-02	-	-

<sup>a</sup> At a 5.0 M sodium concentration level the solution density is estimated to be 1.277 g/ml and at 0.712 M  $[\text{K}^+]$ .<sup>b</sup> Final cesium equilibrium concentrations are approx. equal to initial values due to extrapolation scheme used.<sup>c</sup> These quantities were not computed during the application of the extrapolation scheme chosen to correct ZAM model output due to its unwarranted prediction of  $\text{KNO}_3$  precipitation.Table B-4. ZAM equilibrium isotherm model predictions for CST material in the powder form (IE-910) in contact with Envelope A's LAW-5 feed solution at 5 M  $[\text{Na}^+]$ .<sup>a</sup>

Cs (initial)	Cs (final) <sup>b</sup>	Na/Cs	Ionic strength	Cs $K_d$	Cs loading	K $K_d$	K loading
[M]	[M]	[molar ratio]	[gmole/kg]	[ml/g]	[mmole/g]	[ml/g]	[mmole/g]
0	0.000E+00	infinity	6.727	0.0	0.000E+00	5.548	3.369E-01
0.000001	9.759E-07	5.123E+06	6.727	2465.0	2.406E-03	5.539	3.364E-01
0.00001	9.768E-06	5.119E+05	6.727	2376.0	2.321E-02	5.455	3.313E-01
0.00005	4.900E-05	1.020E+05	6.727	2047.0	1.003E-01	5.146	3.125E-01
0.0001	9.829E-05	5.087E+04	6.727	1744.0	1.714E-01	4.861	2.952E-01
0.0005	4.961E-04	1.008E+04	6.728	794.0	3.939E-01	3.969	2.410E-01
0.001	9.953E-04	5.024E+03	6.729	471.6	4.694E-01	3.666	2.226E-01
0.002	1.995E-03	2.506E+03	6.732	260.2	5.191E-01	3.467	2.106E-01
0.003	2.995E-03	1.669E+03	6.734	179.6	5.379E-01	3.391	2.059E-01
0.005	4.994E-03	1.001E+03	6.739	110.9	5.538E-01	3.326	2.020E-01
0.01	9.994E-03	5.003E+02	6.751	56.7	5.667E-01	3.273	1.988E-01
0.03	2.999E-02	1.667E+02	6.801	19.2	5.755E-01	3.229	1.961E-01
0.05	4.999E-02	1.000E+02	6.851	11.6	5.774E-01	3.213	1.951E-01
0.1	9.999E-02	5.001E+01	6.979	5.8	5.785E-01	3.185	1.934E-01
6.283E-05 (feed conc.)	6.162E-05	8.114E+04	6.727	1960.0	1.208E-01	5.064	3.075E-01

<sup>a</sup> At a 5.0 M sodium concentration level the solution density is estimated to be 1.232 g/ml and at 0.06073 M  $[\text{K}^+]$ .<sup>b</sup> Final cesium equilibrium concentrations are only slightly less than initial values due to large phase ratio used.



Table B-5. ZAM equilibrium isotherm model predictions for CST material in the powder form (IE-910) in contact with Envelope A's LAW-6 feed solution at 5 M [Na<sup>+</sup>].<sup>a</sup>

Cs (initial)	Cs (final) <sup>b</sup>	Na/Cs	Ionic strength	Cs K <sub>d</sub>	Cs loading	K K <sub>d</sub>	K loading
[M]	[M]	[molar ratio]	[gmole/kg]	[ml/g]	[mmole/g]	[ml/g]	[mmole/g]
0	0.000E+00	infinity	6.652	0.0	0.000E+00	5.505	3.437E-01
0.000001	9.762E-07	5.122E+06	6.652	2441.0	2.383E-03	5.496	3.431E-01
0.00001	9.770E-06	5.118E+05	6.652	2353.0	2.299E-02	5.414	3.380E-01
0.00005	4.901E-05	1.020E+05	6.652	2030.0	9.949E-02	5.113	3.192E-01
0.0001	9.830E-05	5.086E+04	6.652	1731.0	1.702E-01	4.834	3.018E-01
0.0005	4.961E-04	1.008E+04	6.653	791.5	3.927E-01	3.957	2.470E-01
0.001	9.953E-04	5.024E+03	6.654	470.7	4.685E-01	3.657	2.283E-01
0.002	1.995E-03	2.506E+03	6.657	259.9	5.185E-01	3.460	2.160E-01
0.003	2.995E-03	1.669E+03	6.659	179.5	5.376E-01	3.385	2.113E-01
0.005	4.994E-03	1.001E+03	6.664	110.9	5.538E-01	3.320	2.073E-01
0.01	9.994E-03	5.003E+02	6.677	56.7	5.665E-01	3.267	2.040E-01
0.03	2.999E-02	1.667E+02	6.726	19.2	5.752E-01	3.223	2.012E-01
0.05	4.999E-02	1.000E+02	6.776	11.6	5.774E-01	3.207	2.002E-01
0.1	9.999E-02	5.001E+01	6.902	5.8	5.785E-01	3.180	1.985E-01
6.328E-05 (feed conc.)	6.207E-05	8.055E+04	6.652	1941.0	1.205E-01	5.030	3.140E-01

<sup>a</sup> At a 5.0 M sodium concentration level the solution density is estimated to be 1.231 g/ml and at 0.06243 M [K<sup>+</sup>].<sup>b</sup> Final cesium equilibrium concentrations are only slightly less than initial values due to large phase ratio used.Table B-6. ZAM equilibrium isotherm model predictions for CST material in the powder form (IE-910) in contact with Envelope A's LAW-8 feed solution at 5 M [Na<sup>+</sup>].<sup>a</sup>

Cs (initial)	Cs (final) <sup>b</sup>	Na/Cs	Ionic strength	Cs K <sub>d</sub>	Cs loading	K K <sub>d</sub>	K loading
[M]	[M]	[molar ratio]	[gmole/kg]	[ml/g]	[mmole/g]	[ml/g]	[mmole/g]
0	0.000E+00	infinity	6.304	0.0	0.000E+00	5.231	3.775E-01
0.000001	9.775E-07	5.115E+06	6.304	2297.0	2.245E-03	5.223	3.769E-01
0.00001	9.783E-06	5.111E+05	6.304	2220.0	2.172E-02	5.153	3.718E-01
0.00005	4.905E-05	1.019E+05	6.304	1930.0	9.467E-02	4.891	3.529E-01
0.0001	9.837E-05	5.083E+04	6.304	1658.0	1.631E-01	4.646	3.353E-01
0.0005	4.962E-04	1.008E+04	6.305	775.7	3.849E-01	3.851	2.779E-01
0.001	9.954E-04	5.023E+03	6.307	465.1	4.630E-01	3.571	2.577E-01
0.002	1.995E-03	2.506E+03	6.309	258.2	5.151E-01	3.384	2.442E-01
0.003	2.995E-03	1.669E+03	6.311	178.7	5.352E-01	3.312	2.390E-01
0.005	4.994E-03	1.001E+03	6.316	110.5	5.518E-01	3.250	2.345E-01
0.01	9.994E-03	5.003E+02	6.328	56.6	5.657E-01	3.199	2.308E-01
0.03	2.999E-02	1.667E+02	6.376	19.2	5.749E-01	3.157	2.278E-01
0.05	4.999E-02	1.000E+02	6.424	11.5	5.769E-01	3.141	2.267E-01
0.1	9.999E-02	5.001E+01	6.547	5.8	5.784E-01	3.115	2.248E-01
4.324E-05 (feed conc.)	4.241E-05	1.179E+05	6.304	1974.0	8.372E-02	4.931	3.558E-01

<sup>a</sup> At a 5.0 M sodium concentration level the solution density is estimated to be 1.225 g/ml and at 0.07216 M [K<sup>+</sup>].<sup>b</sup> Final cesium equilibrium concentrations are only slightly less than initial values due to large phase ratio used.

Table B-7. ZAM equilibrium isotherm model predictions for CST material in the powder form (IE-910) in contact with Envelope A's LAW-9 feed solution at 5 M [Na<sup>+</sup>].<sup>a</sup>

Cs (initial)	Cs (final) <sup>b</sup>	Na/Cs	Ionic strength	Cs K <sub>d</sub>	Cs loading	K K <sub>d</sub>	K loading
[M]	[M]	[molar ratio]	[gmole/kg]	[ml/g]	[mmole/g]	[ml/g]	[mmole/g]
0	0.000E+00	infinity	6.951	0.0	0.000E+00	5.626	3.391E-01
0.000001	9.749E-07	5.129E+06	6.951	2573.0	2.508E-03	5.616	3.385E-01
0.00001	9.758E-06	5.124E+05	6.951	2476.0	2.416E-02	5.528	3.332E-01
0.00005	4.896E-05	1.021E+05	6.951	2121.0	1.038E-01	5.205	3.137E-01
0.0001	9.823E-05	5.090E+04	6.951	1797.0	1.765E-01	4.910	2.960E-01
0.0005	4.960E-04	1.008E+04	6.952	805.0	3.993E-01	4.008	2.416E-01
0.001	9.953E-04	5.024E+03	6.954	475.5	4.733E-01	3.708	2.235E-01
0.002	1.995E-03	2.506E+03	6.956	261.3	5.213E-01	3.512	2.117E-01
0.003	2.995E-03	1.669E+03	6.959	180.2	5.397E-01	3.438	2.072E-01
0.005	4.994E-03	1.001E+03	6.964	111.1	5.548E-01	3.375	2.034E-01
0.01	4.994E-03	1.001E+03	6.964	111.1	5.548E-01	3.375	2.034E-01
0.03	2.999E-02	1.667E+02	7.026	19.2	5.755E-01	3.280	1.977E-01
0.05	4.999E-02	1.000E+02	7.077	11.6	5.774E-01	3.264	1.968E-01
0.1	9.999E-02	5.001E+01	7.206	5.8	5.786E-01	3.237	1.951E-01
4.444E-05 (feed conc.)	4.350E-05	1.149E+05	6.951	2164.0	9.413E-02	5.244	3.161E-01

<sup>a</sup> At a 5.0 M sodium concentration level the solution density is estimated to be 1.238 g/ml and at 0.06027 M [K<sup>+</sup>].<sup>b</sup> Final cesium equilibrium concentrations are only slightly less than initial values due to large phase ratio used.Table B-8. ZAM equilibrium isotherm model predictions for CST material in the powder form (IE-910) in contact with Envelope A's LAW-10 feed solution at 5 M [Na<sup>+</sup>].<sup>a</sup>

Cs (initial)	Cs (final) <sup>b</sup>	Na/Cs	Ionic strength	Cs K <sub>d</sub>	Cs loading	K K <sub>d</sub>	K loading
[M]	[M]	[molar ratio]	[gmole/kg]	[ml/g]	[mmole/g]	[ml/g]	[mmole/g]
0	0.000E+00	infinity	6.553	0.0	0.000E+00	6.011	2.520E-01
0.000001	9.746E-07	5.130E+06	6.553	2609.0	2.543E-03	5.999	2.515E-01
0.00001	9.755E-06	5.126E+05	6.553	2509.0	2.448E-02	5.894	2.471E-01
0.00005	4.895E-05	1.021E+05	6.553	2146.0	1.050E-01	5.508	2.309E-01
0.0001	9.822E-05	5.091E+04	6.553	1815.0	1.783E-01	5.158	2.162E-01
0.0005	4.960E-04	1.008E+04	6.554	808.5	4.010E-01	4.092	1.715E-01
0.001	9.953E-04	5.024E+03	6.555	476.7	4.745E-01	3.741	1.568E-01
0.002	1.995E-03	2.506E+03	6.558	261.7	5.221E-01	3.512	1.472E-01
0.003	2.995E-03	1.669E+03	6.560	180.3	5.400E-01	3.426	1.436E-01
0.005	4.994E-03	1.001E+03	6.565	111.2	5.553E-01	3.352	1.405E-01
0.01	9.994E-03	5.003E+02	6.577	56.8	5.674E-01	3.291	1.380E-01
0.03	2.999E-02	1.667E+02	6.626	19.2	5.755E-01	3.242	1.359E-01
0.05	4.999E-02	1.000E+02	6.675	11.6	5.774E-01	3.224	1.352E-01
0.1	9.999E-02	5.001E+01	6.799	5.8	5.786E-01	3.193	1.339E-01
3.692E-05 (feed conc.)	3.611E-05	1.385E+05	6.553	2253.0	8.136E-02	5.622	2.357E-01

<sup>a</sup> At a 5.0 M sodium concentration level the solution density is estimated to be 1.237 g/ml and at 0.04192 M [K<sup>+</sup>].<sup>b</sup> Final cesium equilibrium concentrations are only slightly less than initial values due to large phase ratio used.

Table B-9. ZAM equilibrium isotherm model predictions for CST material in the powder form (IE-910) in contact with Envelope A's LAW-11 feed solution at 5 M  $[\text{Na}^+]$ .<sup>a</sup>

Cs (initial)	Cs (final) <sup>b</sup>	Na/Cs	Ionic strength	Cs $K_d$	Cs loading	K $K_d$	K loading
[M]	[M]	[molar ratio]	[gmole/kg]	[ml/g]	[mmole/g]	[ml/g]	[mmole/g]
0	0.000E+00	infinity	6.618	0.0	0.000E+00	6.323	2.625E-01
0.000001	9.727E-07	5.140E+06	6.618	2810.0	2.733E-03	6.309	2.619E-01
0.00001	9.737E-06	5.135E+05	6.618	2696.0	2.625E-02	6.192	2.571E-01
0.00005	4.889E-05	1.023E+05	6.618	2281.0	1.115E-01	5.768	2.395E-01
0.0001	9.813E-05	5.095E+04	6.618	1911.0	1.875E-01	5.389	2.238E-01
0.0005	4.959E-04	1.008E+04	6.619	827.0	4.101E-01	4.281	1.777E-01
0.001	9.952E-04	5.024E+03	6.620	483.0	4.807E-01	3.930	1.632E-01
0.002	1.995E-03	2.506E+03	6.622	263.6	5.259E-01	3.705	1.538E-01
0.003	2.995E-03	1.669E+03	6.625	181.2	5.427E-01	3.620	1.503E-01
0.005	4.994E-03	1.001E+03	6.630	111.5	5.568E-01	3.548	1.473E-01
0.01	9.994E-03	5.003E+02	6.642	56.9	5.683E-01	3.490	1.449E-01
0.03	2.999E-02	1.667E+02	6.691	19.2	5.758E-01	3.442	1.429E-01
0.05	4.999E-02	1.000E+02	6.740	11.6	5.774E-01	3.424	1.422E-01
0.1	9.999E-02	5.001E+01	6.864	5.8	5.787E-01	3.395	1.410E-01
3.739E-05 (feed conc.)	3.652E-05	1.369E+05	6.618	2397.0	8.754E-02	5.887	2.444E-01

<sup>a</sup> At a 5.0 M sodium concentration level the solution density is estimated to be 1.232 g/ml and at 0.04152 M  $[\text{K}^+]$ .<sup>b</sup> Final cesium equilibrium concentrations are only slightly less than initial values due to large phase ratio used.Table B-10. ZAM equilibrium isotherm model predictions for CST material in the powder form (IE-910) in contact with Envelope A's LAW-12 feed solution at 5 M  $[\text{Na}^+]$ .<sup>a</sup>

Cs (initial)	Cs (final) <sup>b</sup>	Na/Cs	Ionic strength	Cs $K_d$	Cs loading	K $K_d$	K loading
[M]	[M]	[molar ratio]	[gmole/kg]	[ml/g]	[mmole/g]	[ml/g]	[mmole/g]
0	0.000E+00	infinity	6.324	0.0	0.000E+00	4.207	5.196E-01
0.000001	9.806E-07	5.099E+06	6.324	1980.0	1.942E-03	4.203	5.191E-01
0.00001	9.811E-06	5.096E+05	6.324	1922.0	1.886E-02	4.164	5.143E-01
0.00005	4.916E-05	1.017E+05	6.324	1700.0	8.357E-02	4.015	4.959E-01
0.0001	9.854E-05	5.074E+04	6.324	1485.0	1.463E-01	3.871	4.781E-01
0.0005	4.963E-04	1.007E+04	6.325	735.7	3.651E-01	3.367	4.158E-01
0.001	9.955E-04	5.023E+03	6.327	450.5	4.485E-01	3.176	3.922E-01
0.002	1.995E-03	2.506E+03	6.329	253.6	5.059E-01	3.043	3.758E-01
0.003	2.995E-03	1.669E+03	6.331	176.5	5.286E-01	2.991	3.694E-01
0.005	4.995E-03	1.001E+03	6.336	109.7	5.480E-01	2.945	3.637E-01
0.01	9.994E-03	5.003E+02	6.348	56.4	5.635E-01	2.908	3.591E-01
0.03	2.999E-02	1.667E+02	6.397	19.2	5.743E-01	2.876	3.552E-01
0.05	4.999E-02	1.000E+02	6.446	11.5	5.764E-01	2.865	3.538E-01
0.1	9.999E-02	5.001E+01	6.570	5.8	5.782E-01	2.844	3.512E-01
4.831E-05 (feed conc.)	4.749E-05	1.053E+05	6.324	1709.0	8.116E-02	4.021	4.966E-01

<sup>a</sup> At a 5.0 M sodium concentration level the solution density is estimated to be 1.221 g/ml and at 0.1235 M  $[\text{K}^+]$ .<sup>b</sup> Final cesium equilibrium concentrations are only slightly less than initial values due to large phase ratio used.

Table B-11. ZAM equilibrium isotherm model predictions for CST material in the powder form (IE-910) in contact with Envelope A's LAW-13 feed solution at 5 M  $[\text{Na}^+]$ .<sup>a</sup>

Cs (initial)	Cs (final) <sup>b</sup>	Na/Cs	Ionic strength	Cs $K_d$	Cs loading	K $K_d$	K loading
[M]	[M]	[molar ratio]	[gmole/kg]	[ml/g]	[mmole/g]	[ml/g]	[mmole/g]
0	0.000E+00	infinity	6.327	0.0	0.000E+00	4.177	5.230E-01
0.000001	9.807E-07	5.098E+06	6.327	1971.0	1.933E-03	4.173	5.225E-01
0.00001	9.812E-06	5.096E+05	6.327	1914.0	1.878E-02	4.135	5.177E-01
0.00005	4.917E-05	1.017E+05	6.327	1694.0	8.329E-02	3.988	4.993E-01
0.0001	9.854E-05	5.074E+04	6.327	1480.0	1.458E-01	3.846	4.815E-01
0.0005	4.964E-04	1.007E+04	6.328	734.4	3.646E-01	3.350	4.194E-01
0.001	9.955E-04	5.023E+03	6.330	450.0	4.480E-01	3.161	3.958E-01
0.002	1.995E-03	2.506E+03	6.332	253.4	5.055E-01	3.029	3.792E-01
0.003	2.995E-03	1.669E+03	6.334	176.4	5.283E-01	2.978	3.728E-01
0.005	4.995E-03	1.001E+03	6.339	109.7	5.480E-01	2.933	3.672E-01
0.01	9.994E-03	5.003E+02	6.351	56.4	5.634E-01	2.896	3.626E-01
0.03	2.999E-02	1.667E+02	6.400	19.2	5.743E-01	2.864	3.586E-01
0.05	4.999E-02	1.000E+02	6.449	11.5	5.764E-01	2.853	3.572E-01
0.1	9.999E-02	5.001E+01	6.573	5.8	5.782E-01	2.832	3.546E-01
4.831E-05 (feed conc.)	4.750E-05	1.053E+05	6.327	1702.0	8.085E-02	3.994	5.000E-01

<sup>a</sup> At a 5.0 M sodium concentration level the solution density is estimated to be 1.221 g/ml and at 0.1252 M  $[\text{K}^+]$ .<sup>b</sup> Final cesium equilibrium concentrations are only slightly less than initial values due to large phase ratio used.Table B-12. ZAM equilibrium isotherm model predictions for CST material in the powder form (IE-910) in contact with Envelope A's LAW-14 feed solution at 5 M  $[\text{Na}^+]$ .<sup>a</sup>

Cs (initial)	Cs (final) <sup>b</sup>	Na/Cs	Ionic strength	Cs $K_d$	Cs loading	K $K_d$	K loading
[M]	[M]	[molar ratio]	[gmole/kg]	[ml/g]	[mmole/g]	[ml/g]	[mmole/g]
0	0.000E+00	infinity	6.617	0.0	0.000E+00	2.444	7.816E-01
0.000001	9.843E-07	5.080E+06	6.617	1594.0	1.569E-03	2.443	7.813E-01
0.00001	9.847E-06	5.078E+05	6.617	1557.0	1.533E-02	2.433	7.781E-01
0.00005	4.931E-05	1.014E+05	6.617	1407.0	6.938E-02	2.396	7.662E-01
0.0001	9.876E-05	5.063E+04	6.617	1257.0	1.241E-01	2.359	7.544E-01
0.0005	4.966E-04	1.007E+04	6.618	674.8	3.351E-01	2.215	7.084E-01
0.001	9.957E-04	5.022E+03	6.619	426.9	4.251E-01	2.154	6.888E-01
0.002	1.995E-03	2.506E+03	6.622	246.0	4.908E-01	2.109	6.745E-01
0.003	2.995E-03	1.669E+03	6.624	172.7	5.172E-01	2.091	6.687E-01
0.005	4.995E-03	1.001E+03	6.629	108.2	5.405E-01	2.075	6.636E-01
0.01	9.994E-03	5.003E+02	6.641	56.0	5.596E-01	2.061	6.591E-01
0.03	2.999E-02	1.667E+02	6.690	19.1	5.728E-01	2.049	6.553E-01
0.05	4.999E-02	1.000E+02	6.739	11.5	5.759E-01	2.045	6.540E-01
0.1	9.999E-02	1.000E+02	6.739	11.5	5.759E-01	2.045	6.540E-01
4.569E-05 (feed conc.)	4.504E-05	1.110E+05	6.617	1422.0	6.405E-02	2.400	7.675E-01

<sup>a</sup> At a 5.0 M sodium concentration level the solution density is estimated to be 1.234 g/ml and at 0.3198 M  $[\text{K}^+]$ .<sup>b</sup> Final cesium equilibrium concentrations are only slightly less than initial values due to large phase ratio used.

Table B-13. ZAM equilibrium isotherm model predictions for CST material in the powder form (IE-910) in contact with Envelope A's LAW-15 feed solution at 5 M  $[\text{Na}^+]$ .<sup>a</sup>

Cs (initial)	Cs (final) <sup>b</sup>	Na/Cs	Ionic strength	Cs $K_d$	Cs loading	K $K_d$	K loading
[M]	[M]	[molar ratio]	[gmole/kg]	[ml/g]	[mmole/g]	[ml/g]	[mmole/g]
0	0.000E+00	infinity	6.487	0.0	0.000E+00	2.068	8.411E-01
0.000001	9.852E-07	5.075E+06	6.487	1502.0	1.480E-03	2.067	8.406E-01
0.00001	9.855E-06	5.074E+05	6.487	1468.0	1.447E-02	2.061	8.382E-01
0.00005	4.934E-05	1.013E+05	6.487	1335.0	6.587E-02	2.038	8.289E-01
0.0001	9.882E-05	5.060E+04	6.487	1198.0	1.184E-01	2.014	8.191E-01
0.0005	4.967E-04	1.007E+04	6.488	657.7	3.267E-01	1.918	7.801E-01
0.001	9.958E-04	5.021E+03	6.489	420.0	4.182E-01	1.876	7.630E-01
0.002	1.995E-03	2.506E+03	6.491	243.6	4.860E-01	1.845	7.504E-01
0.003	2.995E-03	1.669E+03	6.494	171.6	5.139E-01	1.832	7.451E-01
0.005	4.995E-03	1.001E+03	6.498	107.8	5.385E-01	1.821	7.406E-01
0.01	9.994E-03	5.003E+02	6.510	55.9	5.584E-01	1.811	7.365E-01
0.03	2.999E-02	1.667E+02	6.559	19.1	5.725E-01	1.803	7.333E-01
0.05	4.999E-02	1.000E+02	6.607	11.5	5.754E-01	1.799	7.317E-01
0.1	9.999E-02	5.001E+01	6.730	5.8	5.776E-01	1.794	7.296E-01
4.552E-05 (feed conc.)	4.492E-05	1.113E+05	6.487	1349.0	6.060E-02	2.040	8.297E-01

<sup>a</sup> At a 5.0 M sodium concentration level the solution density is estimated to be 1.235 g/ml and at 0.4067 M  $[\text{K}^+]$ .<sup>b</sup> Final cesium equilibrium concentrations are only slightly less than initial values due to large phase ratio used.Table B-14. ZAM equilibrium isotherm model predictions for CST material in the powder form (IE-910) in contact with Envelope B's LAW-2a feed solution at 5 M  $[\text{Na}^+]$ .<sup>a</sup>

Cs (initial)	Cs (final) <sup>b</sup>	Na/Cs	Ionic strength	Cs $K_d$	Cs loading	K $K_d$	K loading
[M]	[M]	[molar ratio]	[gmole/kg]	[ml/g]	[mmole/g]	[ml/g]	[mmole/g]
0	0.000E+00	infinity	7.360	0.0	0.000E+00	4.143	5.179E-01
0.000001	9.784E-07	5.110E+06	7.360	2203.0	2.155E-03	4.138	5.173E-01
0.00001	9.791E-06	5.107E+05	7.360	2132.0	2.087E-02	4.095	5.119E-01
0.00005	4.909E-05	1.019E+05	7.360	1863.0	9.145E-02	3.935	4.919E-01
0.0001	9.842E-05	5.080E+04	7.360	1608.0	1.583E-01	3.783	4.729E-01
0.0005	4.962E-04	1.008E+04	7.361	764.6	3.794E-01	3.280	4.100E-01
0.001	9.954E-04	5.023E+03	7.362	461.1	4.590E-01	3.099	3.874E-01
0.002	1.995E-03	2.506E+03	7.365	256.9	5.125E-01	2.977	3.721E-01
0.003	2.995E-03	1.669E+03	7.368	178.1	5.334E-01	2.930	3.663E-01
0.005	4.994E-03	1.001E+03	7.373	110.3	5.508E-01	2.889	3.611E-01
0.01	9.994E-03	5.003E+02	7.386	56.5	5.651E-01	2.855	3.569E-01
0.03	2.999E-02	1.667E+02	7.438	19.2	5.749E-01	2.826	3.533E-01
0.05	4.999E-02	1.000E+02	7.490	11.5	5.769E-01	2.815	3.519E-01
0.1	9.999E-02	5.001E+01	7.624	5.8	5.784E-01	2.795	3.494E-01
4.676E-04 (feed conc.)	4.638E-04	1.078E+04	7.361	798.7	3.704E-01	3.301	4.126E-01

<sup>a</sup> At a 5.0 M sodium concentration level the solution density is estimated to be 1.254 g/ml and at 0.1250 M  $[\text{K}^+]$ .<sup>b</sup> Final cesium equilibrium concentrations are only slightly less than initial values due to large phase ratio used.

Table B-15. ZAM equilibrium isotherm model predictions for CST material in the powder form (IE-910) in contact with Envelope B's LAW-2b feed solution at 5 M  $[Na^+]$ .<sup>a</sup>

Cs (initial)	Cs (final) <sup>b</sup>	Na/Cs	Ionic strength	Cs $K_d$	Cs loading	K $K_d$	K loading
[M]	[M]	[molar ratio]	[gmole/kg]	[ml/g]	[mmole/g]	[ml/g]	[mmole/g]
0	0.000E+00	infinity	8.170	0.0	0.000E+00	4.453	6.363E-01
0.000001	9.736E-07	5.136E+06	8.170	2711.0	2.639E-03	4.448	6.356E-01
0.00001	9.746E-06	5.130E+05	8.170	2604.0	2.538E-02	4.405	6.295E-01
0.00005	4.892E-05	1.022E+05	8.170	2215.0	1.084E-01	4.247	6.069E-01
0.0001	9.817E-05	5.093E+04	8.170	1864.0	1.830E-01	4.106	5.867E-01
0.0005	4.959E-04	1.008E+04	8.171	818.1	4.057E-01	3.683	5.263E-01
0.001	9.952E-04	5.024E+03	8.172	480.0	4.777E-01	3.546	5.067E-01
0.002	1.995E-03	2.506E+03	8.175	262.7	5.241E-01	3.458	4.941E-01
0.003	2.995E-03	1.669E+03	8.178	180.8	5.415E-01	3.424	4.893E-01
0.005	4.994E-03	1.001E+03	8.183	111.4	5.563E-01	3.396	4.853E-01
0.01	9.994E-03	5.003E+02	8.197	56.8	5.679E-01	3.373	4.820E-01
0.03	2.999E-02	1.667E+02	8.251	19.2	5.758E-01	3.354	4.793E-01
0.05	4.999E-02	1.000E+02	8.305	11.6	5.774E-01	3.346	4.781E-01
0.1	9.999E-02	5.001E+01	8.444	5.8	5.786E-01	3.334	4.764E-01
4.311E-04 (feed conc.)	4.272E-04	1.170E+04	8.171	905.9	3.870E-01	3.718	5.313E-01

<sup>a</sup> At a 5.0 M sodium concentration level the solution density is estimated to be 1.242 g/ml and at 0.1429 M  $[K^+]$ .<sup>b</sup> Final cesium equilibrium concentrations are only slightly less than initial values due to large phase ratio used.Table B-16. ZAM equilibrium isotherm model predictions for CST material in the powder form (IE-910) in contact with Envelope C's LAW-3 feed solution at 5 M  $[Na^+]$ .<sup>a</sup>

Cs (initial)	Cs (final) <sup>b</sup>	Na/Cs	Ionic strength	Cs $K_d$	Cs loading	K $K_d$	K loading
[M]	[M]	[molar ratio]	[gmole/kg]	[ml/g]	[mmole/g]	[ml/g]	[mmole/g]
0	0.000E+00	infinity	6.995	0.0	0.000E+00	6.339	2.784E-01
0.000001	9.742E-07	5.132E+06	6.995	2653.0	2.585E-03	6.326	2.778E-01
0.00001	9.751E-06	5.128E+05	6.995	2550.0	2.487E-02	6.217	2.731E-01
0.00005	4.894E-05	1.022E+05	6.995	2175.0	1.064E-01	5.817	2.555E-01
0.0001	9.820E-05	5.092E+04	6.995	1836.0	1.803E-01	5.455	2.396E-01
0.0005	4.960E-04	1.008E+04	6.996	812.7	4.031E-01	4.362	1.916E-01
0.001	9.952E-04	5.024E+03	6.997	478.1	4.758E-01	4.005	1.759E-01
0.002	1.995E-03	2.506E+03	7.000	262.1	5.229E-01	3.774	1.658E-01
0.003	2.995E-03	1.669E+03	7.002	180.5	5.406E-01	3.686	1.619E-01
0.005	4.994E-03	1.001E+03	7.007	111.3	5.558E-01	3.611	1.586E-01
0.01	9.994E-03	5.003E+02	7.019	56.8	5.676E-01	3.551	1.560E-01
0.03	2.999E-02	1.667E+02	7.069	19.2	5.758E-01	3.502	1.538E-01
0.05	4.999E-02	1.000E+02	7.120	11.6	5.774E-01	3.484	1.530E-01
0.1	9.999E-02	5.001E+01	7.247	5.8	5.786E-01	3.455	1.517E-01
3.967E-05 (feed conc.)	3.880E-05	1.289E+05	6.995	2261.0	8.773E-02	5.909	2.595E-01

<sup>a</sup> At a 5.0 M sodium concentration level the solution density is estimated to be 1.237 g/ml and at 0.04393 M  $[K^+]$ .<sup>b</sup> Final cesium equilibrium concentrations are only slightly less than initial values due to large phase ratio used.

Table B-17. ZAM equilibrium isotherm model predictions for CST material in the powder form (IE-910) in contact with Envelope C's LAW-4 feed solution at 5 M  $[\text{Na}^+]$ .<sup>a</sup>

Cs (initial)	Cs (final) <sup>b</sup>	Na/Cs	Ionic strength	Cs $K_d$	Cs loading	K $K_d$	K loading
[M]	[M]	[molar ratio]	[gmole/kg]	[ml/g]	[mmole/g]	[ml/g]	[mmole/g]
0	0.000E+00	infinity	6.995	0.0	0.000E+00	6.339	2.784E-01
0.000001	9.742E-07	5.132E+06	6.995	2653.0	2.585E-03	6.326	2.778E-01
0.00001	9.751E-06	5.128E+05	6.995	2550.0	2.487E-02	6.217	2.731E-01
0.00005	4.894E-05	1.022E+05	6.995	2175.0	1.064E-01	5.817	2.555E-01
0.0001	9.820E-05	5.092E+04	6.995	1836.0	1.803E-01	5.455	2.396E-01
0.0005	4.960E-04	1.008E+04	6.996	812.7	4.031E-01	4.362	1.916E-01
0.001	9.952E-04	5.024E+03	6.997	478.1	4.758E-01	4.005	1.759E-01
0.002	1.995E-03	2.506E+03	7.000	262.1	5.229E-01	3.774	1.658E-01
0.003	2.995E-03	1.669E+03	7.002	180.5	5.406E-01	3.686	1.619E-01
0.005	4.994E-03	1.001E+03	7.007	111.3	5.558E-01	3.611	1.586E-01
0.01	9.994E-03	5.003E+02	7.019	56.8	5.676E-01	3.551	1.560E-01
0.03	2.999E-02	1.667E+02	7.069	19.2	5.758E-01	3.502	1.538E-01
0.05	4.999E-02	1.000E+02	7.120	11.6	5.774E-01	3.484	1.530E-01
0.1	9.999E-02	5.001E+01	7.247	5.8	5.786E-01	3.455	1.517E-01
3.779E-05 (feed conc.)	3.694E-05	1.354E+05	6.995	2278.0	8.415E-02	5.926	2.603E-01

<sup>a</sup> At a 5.0 M sodium concentration level the solution density is estimated to be 1.237 g/ml and at 0.04393 M  $[\text{K}^+]$ .<sup>b</sup> Final cesium equilibrium concentrations are only slightly less than initial values due to large phase ratio used.Table B-18. ZAM equilibrium isotherm model predictions for CST material in the powder form (IE-910) in contact with Envelope C's LAW-7 feed solution at 5 M  $[\text{Na}^+]$ .<sup>a</sup>

Cs (initial)	Cs (final) <sup>b</sup>	Na/Cs	Ionic strength	Cs $K_d$	Cs loading	K $K_d$	K loading
[M]	[M]	[molar ratio]	[gmole/kg]	[ml/g]	[mmole/g]	[ml/g]	[mmole/g]
0	0.000E+00	infinity	7.209	0.0	0.000E+00	7.316	1.629E-01
0.000001	9.709E-07	5.150E+06	7.209	2997.0	2.910E-03	7.297	1.625E-01
0.00001	9.721E-06	5.144E+05	7.209	2867.0	2.787E-02	7.139	1.590E-01
0.00005	4.883E-05	1.024E+05	7.209	2403.0	1.173E-01	6.572	1.464E-01
0.0001	9.804E-05	5.100E+04	7.210	1996.0	1.957E-01	6.075	1.353E-01
0.0005	4.958E-04	1.008E+04	7.211	842.5	4.177E-01	4.666	1.039E-01
0.001	9.951E-04	5.025E+03	7.212	488.3	4.859E-01	4.234	9.429E-02
0.002	1.995E-03	2.506E+03	7.214	265.1	5.289E-01	3.961	8.821E-02
0.003	2.995E-03	1.669E+03	7.217	182.0	5.451E-01	3.859	8.594E-02
0.005	4.994E-03	1.001E+03	7.222	111.8	5.583E-01	3.772	8.400E-02
0.01	9.994E-03	5.003E+02	7.234	56.9	5.690E-01	3.703	8.247E-02
0.03	2.999E-02	1.667E+02	7.285	19.2	5.761E-01	3.646	8.120E-02
0.05	4.999E-02	1.000E+02	7.336	11.6	5.779E-01	3.627	8.077E-02
0.1	9.999E-02	5.001E+01	7.465	5.8	5.788E-01	3.594	8.004E-02
4.455E-05 (feed conc.)	4.348E-05	1.150E+05	7.209	2457.0	1.068E-01	6.638	1.478E-01

<sup>a</sup> At a 5.0 M sodium concentration level the solution density is estimated to be 1.243 g/ml and at 0.02227 M  $[\text{K}^+]$ .<sup>b</sup> Final cesium equilibrium concentrations are only slightly less than initial values due to large phase ratio used.

Table B-19. Parameter identities between a 4-component VERSE-LC Freundlich/Langmuir Hybrid equilibrium isotherm model and the “effective” single-component homovalent isotherm model.

Parameter <sup>a</sup>	Total Cesium (component 1)	Potassium (component 2)	Sodium (component 3)	Strontium hydroxide (component 4)	Total Cesium (effective single component)
$a_i$ (gmoles/L <sub>CV</sub> )	$\eta_{df} \rho_b \bar{C}_T$	$\eta_{df} \rho_b \bar{C}_T \tilde{K}_{21}$	$\eta_{df} \rho_b \bar{C}_T \tilde{K}_{31}$	$\eta_{df} \rho_b \bar{C}_T \tilde{K}_{41}$	$\eta_{df} \rho_b \bar{C}_T$
$b_i$ (M <sup>-1</sup> )	1.0	$\tilde{K}_{21}$	$\tilde{K}_{31}$	$\tilde{K}_{41}$	1.0
$M_{ai}$ (-)	1.0	1.0	1.0	1.0	1.0
$M_{bi}$ (-)	1.0	1.0	1.0	1.0	1.0
$\beta_i$ (-)	0.0	0.0	0.0	0.0	$\tilde{K}_{21} c_{p2}^{M_{b2}} + \tilde{K}_{31} c_{p3}^{M_{b3}} + \tilde{K}_{41} c_{p4}^{M_{b4}}$

<sup>a</sup> The parameters for components 1, 2, 3, and 4 refer to total cesium, potassium, sodium, and strontium hydroxide, respectively, when the ion-exchange system of interest is the Cesium-CST system.



Table B-20. Estimated selectivity coefficients for the Cesium-CST system based on ZAM predictions and the 4-component homovalent isotherm model for the Envelope A feed solutions.

Selectivity Coefficient	Definition	Parameter Estimate	Approx. Standard Error	Relative Error (%)
$\tilde{K}_{21}$	K <sup>+</sup> to Cs <sup>+</sup> selectivity	7.0665x10 <sup>-4</sup>	3.9835x10 <sup>-5</sup>	5.6%
$\tilde{K}_{31}$	Na <sup>+</sup> to Cs <sup>+</sup> selectivity	3.7897x10 <sup>-5</sup>	6.4175x10 <sup>-7</sup>	1.7%
$\tilde{K}_{41}$	SrOH <sup>+</sup> to Cs <sup>+</sup> selectivity	1.4432x10 <sup>-1</sup>	4.3031x10 <sup>-2</sup>	29.8%
$\tilde{K}_{12}$	Cs <sup>+</sup> to K <sup>+</sup> selectivity	1,415.1	79.2	5.6%
$\tilde{K}_{13}$	Cs <sup>+</sup> to Na <sup>+</sup> selectivity	26,387.3	448.6	1.7%
$\tilde{K}_{14}$	Cs <sup>+</sup> to SrOH <sup>+</sup> selectivity	6.9	2.1	29.8%
$\tilde{K}_{23}$	K <sup>+</sup> to Na <sup>+</sup> selectivity	18.6	-	-
$\tilde{K}_{42}$	SrOH <sup>+</sup> to K <sup>+</sup> selectivity	204.2	-	-
$\tilde{K}_{43}$	SrOH <sup>+</sup> to Na <sup>+</sup> selectivity	3,808.2	-	-

Table B-21. The resulting correlation coefficient matrix for the fit of the selectivity coefficients for the Cesium-CST system, ZAM produced data, and the 4-component homovalent isotherm model for the Envelope A feed solutions.

Selectivity Coefficient (species)	$\tilde{K}_{21}$ (K <sup>+</sup> )	$\tilde{K}_{31}$ (Na <sup>+</sup> )	$\tilde{K}_{41}$ (SrOH <sup>+</sup> )
$\tilde{K}_{21}$ (K <sup>+</sup> )	1.0000	-0.7984	0.1118
$\tilde{K}_{31}$ (Na <sup>+</sup> )	-0.7984	1.0000	-0.2493
$\tilde{K}_{41}$ (SrOH <sup>+</sup> )	0.1118	-0.2493	1.0000

Table B-22. Estimated beta parameter values and error estimate for a one-component (total cesium) homovalent algebraic isotherm model based on CST in its powder-form (IE-910) where the data sets used were created using the ZAM code.

Feed Solution	"Best Estimate" $\beta_i$ [M]	Standard Error in $\beta_i$ [M]	Root Mean Square in Cs loading <sup>a</sup> (% difference)
<b>Envelope A</b>			
LAW-1	4.3376E-04	± 8.3713E-07	0.3912
LAW-5	2.3431E-04	± 2.0648E-08	0.0137
LAW-6	2.3668E-04	± 2.2931E-08	0.0202
LAW-8	2.5147E-04	± 3.8060E-08	0.0270
LAW-9	2.2453E-04	± 2.8251E-08	0.0220
LAW-10	2.2135E-04	± 2.2209E-08	0.0161
LAW-11	2.0543E-04	± 2.4697E-08	0.0229
LAW-12	2.9196E-04	± 3.2849E-08	0.0177
LAW-13	2.9328E-04	± 3.2820E-08	0.0184
LAW-14	3.6283E-04	± 4.0017E-08	0.0262
LAW-15	3.8513E-04	± 3.7129E-08	0.0219
Overall avg.	2.8552E-04	± 1.0334E-07	0.0543
<b>Envelope B</b>			
LAW-2a	2.6230E-04	± 2.9902E-08	0.0173
LAW-2b	2.1296E-04	± 2.3999E-08	0.0138
Overall avg.	2.3763E-04	± 2.6951E-08	0.0156
<b>Envelope C</b>			
LAW-3	2.1769E-04	± 2.4699E-08	0.0135
LAW-4	2.1769E-04	± 2.4646E-08	0.0132
LAW-7	1.9258E-04	± 2.0511E-08	0.0166
Overall avg.	2.0932E-04	± 2.3285E-08	0.0144

<sup>a</sup> Based on a percent difference in Cs loading [i.e., 100(algebraic-ZAM)/ZAM].

Table B-23. Parameter settings for an “effective” single component Freundlich/Langmuir Hybrid equilibrium isotherm model for total cesium on CST based on the 1-component homovalent model.

Feed Solution	“Powder-form” (IE-910) $a_i$ (gmoles/L <sub>CV</sub> )	“Engineered-form” (IE-911) <sup>a</sup> $a_i$ (gmoles/L <sub>CV</sub> )	$b_i$ (M <sup>-1</sup> )	$M_{ai}$ (-)	$M_{bi}$ (-)	“Effective” <sup>b</sup> $\beta_i$ (-)
<b>Envelope A</b>						
LAW-1	0.580	0.3944	1.0	1.0	1.0	4.3376E-04
LAW-5	0.580	0.3944	1.0	1.0	1.0	2.3431E-04
LAW-6	0.580	0.3944	1.0	1.0	1.0	2.3668E-04
LAW-8	0.580	0.3944	1.0	1.0	1.0	2.5147E-04
LAW-9	0.580	0.3944	1.0	1.0	1.0	2.2453E-04
LAW-10	0.580	0.3944	1.0	1.0	1.0	2.2135E-04
LAW-11	0.580	0.3944	1.0	1.0	1.0	2.0543E-04
LAW-12	0.580	0.3944	1.0	1.0	1.0	2.9196E-04
LAW-13	0.580	0.3944	1.0	1.0	1.0	2.9328E-04
LAW-14	0.580	0.3944	1.0	1.0	1.0	3.6283E-04
LAW-15	0.580	0.3944	1.0	1.0	1.0	3.8513E-04
<b>Envelope B</b>						
LAW-2a	0.580	0.3944	1.0	1.0	1.0	2.6230E-04
LAW-2b	0.580	0.3944	1.0	1.0	1.0	2.1296E-04
<b>Envelope C</b>						
LAW-3	0.580	0.3944	1.0	1.0	1.0	2.1769E-04
LAW-4	0.580	0.3944	1.0	1.0	1.0	2.1769E-04
LAW-7	0.580	0.3944	1.0	1.0	1.0	1.9258E-04

<sup>a</sup> A dilution factor of 68% is assumed when going from the powder-form to the engineered-form and a bed density of 1.0 g/ml assumed.

<sup>b</sup> These are “best estimate” values based on the maximum likelihood algorithm.

Table B-24. “Extrapolated” ZAM equilibrium model versus algebraic model cesium loading predictions for CST material in contact with Envelope A’s LAW-1 feed solution at 5 M [Na<sup>+</sup>].<sup>a</sup>

Cs (initial)	Cs (final) <sup>b</sup>	Powder form			Engineered form <sup>c</sup>
		Cs loading (ZAM model)	Cs loading (Algebraic model)	Loading difference	Cs loading (Algebraic model)
[M]	[M]	[mmole/g]	[mmole/g]	[%]	[mmole/g]
0	same as initial	0.000E+00	0.000E+00	na	0.000E+00
0.000001	same as initial	1.326E-03	1.334E-03	0.5744	9.072E-04
0.00001	same as initial	1.300E-02	1.307E-02	0.5132	8.888E-03
0.00005	same as initial	5.989E-02	5.995E-02	0.0975	4.076E-02
0.0001	same as initial	1.090E-01	1.087E-01	-0.2698	7.389E-02
0.0005	same as initial	3.129E-01	3.106E-01	-0.7442	2.112E-01
0.001	same as initial	4.073E-01	4.045E-01	-0.6848	2.751E-01
0.002	same as initial	4.788E-01	4.766E-01	-0.4595	3.241E-01
0.003	same as initial	5.084E-01	5.067E-01	-0.3200	3.446E-01
0.005	same as initial	5.348E-01	5.337E-01	-0.2110	3.629E-01
0.01	same as initial	5.565E-01	5.559E-01	-0.1156	3.780E-01
0.03	same as initial	5.719E-01	5.717E-01	-0.0356	3.888E-01
0.05	same as initial	5.751E-01	5.750E-01	-0.0218	3.910E-01

Cs (initial)	Cs (final) <sup>b</sup>	Powder form			Engineered form <sup>c</sup>
		Cs loading (ZAM model)	Cs loading (Algebraic model)	Loading difference	Cs loading (Algebraic model)
[M]	[M]	[mmole/g]	[mmole/g]	[%]	[mmole/g]
0.1	same as initial	5.775E-01	5.775E-01	0.0050	3.927E-01
3.598E-05 (feed conc.)	same as initial	4.455E-02	4.443E-02	-0.2663	3.021E-02
				rms =	0.3912

<sup>a</sup> At a 5.0 M sodium concentration level the solution density is estimated to be 1.277 g/ml and at 0.712 M [K<sup>+</sup>].

<sup>b</sup> Final cesium equilibrium concentrations are approx. equal to initial values due to extrapolation scheme used.

<sup>c</sup> To estimate isotherm for engineered form a dilution factor of 0.68 is employed.

Table B-25. ZAM equilibrium model versus algebraic model cesium loading predictions for CST material in contact with Envelope A's LAW-5 feed solution at 5 M [Na<sup>+</sup>].<sup>a</sup>

Cs (initial)	Cs (final) <sup>b</sup>	Powder form			Engineered form <sup>c</sup>
		Cs loading (ZAM model)	Cs loading (Algebraic model)	Loading difference	Cs loading (Algebraic model)
[M]	[M]	[mmole/g]	[mmole/g]	[%]	[mmole/g]
0	0.000E+00	0.000E+00	0.000E+00	na	0.000E+00
0.000001	9.759E-07	2.406E-03	2.406E-03	0.0035	1.636E-03
0.00001	9.768E-06	2.321E-02	2.321E-02	0.0122	1.578E-02
0.00005	4.900E-05	1.003E-01	1.003E-01	0.0111	6.821E-02
0.0001	9.829E-05	1.714E-01	1.714E-01	-0.0094	1.166E-01
0.0005	4.961E-04	3.939E-01	3.939E-01	0.0094	2.679E-01
0.001	9.953E-04	4.694E-01	4.695E-01	0.0200	3.192E-01
0.002	1.995E-03	5.191E-01	5.190E-01	-0.0115	3.529E-01
0.003	2.995E-03	5.379E-01	5.379E-01	0.0027	3.658E-01
0.005	4.994E-03	5.538E-01	5.540E-01	0.0311	3.767E-01
0.01	9.994E-03	5.667E-01	5.667E-01	0.0095	3.854E-01
0.03	2.999E-02	5.755E-01	5.755E-01	-0.0008	3.913E-01
0.05	4.999E-02	5.774E-01	5.773E-01	-0.0156	3.926E-01
0.1	9.999E-02	5.785E-01	5.786E-01	0.0176	3.935E-01
6.283E-05 (feed conc.)	6.162E-05	1.208E-01	1.208E-01	-0.0039	8.212E-02
				root mean square =	0.0137

<sup>a</sup> At a 5.0 M sodium concentration level the solution density is estimated to be 1.232 g/ml and at 0.06073 M [K<sup>+</sup>].

<sup>b</sup> Final cesium equilibrium concentrations are only slightly less than initial values due to large phase ratio used.

<sup>c</sup> To estimate isotherm for engineered form a dilution factor of 0.68 is employed.

Table B-26. ZAM equilibrium model versus algebraic model cesium loading predictions for CST material in contact with Envelope A's LAW-6 feed solution at 5 M [Na<sup>+</sup>].<sup>a</sup>

Cs (initial)	Cs (final) <sup>b</sup>	Powder form			Engineered form <sup>c</sup>
		Cs loading (ZAM model)	Cs loading (Algebraic model)	Loading difference	Cs loading (Algebraic model)
[M]	[M]	[mmole/g]	[mmole/g]	[%]	[mmole/g]
0	0.000E+00	0.000E+00	0.000E+00	na	0.000E+00
0.000001	9.762E-07	2.383E-03	2.382E-03	-0.0205	1.620E-03
0.00001	9.770E-06	2.299E-02	2.299E-02	0.0178	1.564E-02
0.00005	4.901E-05	9.949E-02	9.950E-02	0.0085	6.766E-02

Cs (initial)	Cs (final) <sup>b</sup>	Powder form			Engineered form <sup>c</sup>
		Cs loading (ZAM model)	Cs loading (Algebraic model)	Loading difference	Cs loading (Algebraic model)
[M]	[M]	[mmole/g]	[mmole/g]	[%]	[mmole/g]
0.0001	9.830E-05	1.702E-01	1.702E-01	0.0258	1.157E-01
0.0005	4.961E-04	3.927E-01	3.927E-01	0.0008	2.670E-01
0.001	9.953E-04	4.685E-01	4.686E-01	0.0185	3.186E-01
0.002	1.995E-03	5.185E-01	5.185E-01	-0.0024	3.526E-01
0.003	2.995E-03	5.376E-01	5.375E-01	-0.0149	3.655E-01
0.005	4.994E-03	5.538E-01	5.538E-01	-0.0142	3.766E-01
0.01	9.994E-03	5.665E-01	5.666E-01	0.0216	3.853E-01
0.03	2.999E-02	5.752E-01	5.755E-01	0.0435	3.913E-01
0.05	4.999E-02	5.774E-01	5.773E-01	-0.0204	3.925E-01
0.1	9.999E-02	5.785E-01	5.786E-01	0.0152	3.935E-01
6.328E-05 (feed conc.)	6.207E-05	1.205E-01	1.205E-01	0.0218	8.194E-02
root mean square =				0.0202	

<sup>a</sup> At a 5.0 M sodium concentration level the solution density is estimated to be 1.231 g/ml and at 0.06243 M [K<sup>+</sup>].

<sup>b</sup> Final cesium equilibrium concentrations are only slightly less than initial values due to large phase ratio used.

<sup>c</sup> To estimate isotherm for engineered form a dilution factor of 0.68 is employed.

Table B-27. ZAM equilibrium model versus algebraic model cesium loading predictions for CST material in contact with Envelope A's LAW-8 feed solution at 5 M [Na<sup>+</sup>].<sup>a</sup>

Cs (initial)	Cs (final) <sup>b</sup>	Powder form			Engineered form <sup>c</sup>
		Cs loading (ZAM model)	Cs loading (Algebraic model)	Loading difference	Cs loading (Algebraic model)
[M]	[M]	[mmole/g]	[mmole/g]	[%]	[mmole/g]
0	0.000E+00	0.000E+00	0.000E+00	na	0.000E+00
0.000001	9.775E-07	2.245E-03	2.246E-03	0.0221	1.527E-03
0.00001	9.783E-06	2.172E-02	2.172E-02	0.0032	1.477E-02
0.00005	4.905E-05	9.467E-02	9.467E-02	-0.0006	6.437E-02
0.0001	9.837E-05	1.631E-01	1.631E-01	-0.0060	1.109E-01
0.0005	4.962E-04	3.849E-01	3.849E-01	0.0056	2.617E-01
0.001	9.954E-04	4.630E-01	4.630E-01	0.0139	3.149E-01
0.002	1.995E-03	5.151E-01	5.151E-01	-0.0066	3.503E-01
0.003	2.995E-03	5.352E-01	5.351E-01	-0.0249	3.638E-01
0.005	4.994E-03	5.518E-01	5.522E-01	0.0648	3.755E-01
0.01	9.994E-03	5.657E-01	5.658E-01	0.0183	3.847E-01
0.03	2.999E-02	5.749E-01	5.752E-01	0.0467	3.911E-01
0.05	4.999E-02	5.769E-01	5.771E-01	0.0368	3.924E-01
0.1	9.999E-02	5.784E-01	5.785E-01	0.0178	3.934E-01
4.324E-05 (feed conc.)	4.241E-05	8.372E-02	8.370E-02	-0.0205	5.692E-02
root mean square =				0.0270	

<sup>a</sup> At a 5.0 M sodium concentration level the solution density is estimated to be 1.225 g/ml and at 0.07216 M [K<sup>+</sup>].

<sup>b</sup> Final cesium equilibrium concentrations are only slightly less than initial values due to large phase ratio used.

<sup>c</sup> To estimate isotherm for engineered form a dilution factor of 0.68 is employed.

Table B-28. ZAM equilibrium model versus algebraic model cesium loading predictions for CST material in contact with Envelope A's LAW-9 feed solution at 5 M  $[\text{Na}^+]$ .<sup>a</sup>

Cs (initial)	Cs (final) <sup>b</sup>	Powder form			Engineered form <sup>c</sup>
		Cs loading (ZAM model)	Cs loading (Algebraic model)	Loading difference	Cs loading (Algebraic model)
[M]	[M]	[mmole/g]	[mmole/g]	[%]	[mmole/g]
0	0.000E+00	0.000E+00	0.000E+00	na	0.000E+00
0.000001	9.749E-07	2.508E-03	2.507E-03	-0.0386	1.705E-03
0.00001	9.758E-06	2.416E-02	2.416E-02	-0.0167	1.643E-02
0.00005	4.896E-05	1.038E-01	1.038E-01	-0.0125	7.061E-02
0.0001	9.823E-05	1.765E-01	1.765E-01	0.0000	1.200E-01
0.0005	4.960E-04	3.993E-01	3.993E-01	-0.0046	2.715E-01
0.001	9.953E-04	4.733E-01	4.732E-01	-0.0050	3.218E-01
0.002	1.995E-03	5.213E-01	5.213E-01	0.0063	3.545E-01
0.003	2.995E-03	5.397E-01	5.396E-01	-0.0275	3.669E-01
0.005	4.994E-03	5.548E-01	5.550E-01	0.0382	3.774E-01
0.01	4.994E-03	5.548E-01	5.550E-01	0.0382	3.774E-01
0.03	2.999E-02	5.755E-01	5.757E-01	0.0316	3.915E-01
0.05	4.999E-02	5.774E-01	5.774E-01	0.0038	3.926E-01
0.1	9.999E-02	5.786E-01	5.787E-01	0.0101	3.935E-01
4.444E-05 (feed conc.)	4.350E-05	9.413E-02	9.413E-02	-0.0029	6.401E-02
root mean square =				0.0220	

<sup>a</sup> At a 5.0 M sodium concentration level the solution density is estimated to be 1.238 g/ml and at 0.06027 M  $[\text{K}^+]$ .<sup>b</sup> Final cesium equilibrium concentrations are only slightly less than initial values due to large phase ratio used.<sup>c</sup> To estimate isotherm for engineered form a dilution factor of 0.68 is employed.Table B-29. ZAM equilibrium model versus algebraic model cesium loading predictions for CST material in contact with Envelope A's LAW-10 feed solution at 5 M  $[\text{Na}^+]$ .<sup>a</sup>

Cs (initial)	Cs (final) <sup>b</sup>	Powder form			Engineered form <sup>c</sup>
		Cs loading (ZAM model)	Cs loading (Algebraic model)	Loading difference	Cs loading (Algebraic model)
[M]	[M]	[mmole/g]	[mmole/g]	[%]	[mmole/g]
0	0.000E+00	0.000E+00	0.000E+00	na	0.000E+00
0.000001	9.746E-07	2.543E-03	2.543E-03	-0.0077	1.729E-03
0.00001	9.755E-06	2.448E-02	2.448E-02	0.0272	1.665E-02
0.00005	4.895E-05	1.050E-01	1.050E-01	-0.0110	7.142E-02
0.0001	9.822E-05	1.783E-01	1.783E-01	-0.0034	1.212E-01
0.0005	4.960E-04	4.010E-01	4.010E-01	0.0039	2.727E-01
0.001	9.953E-04	4.745E-01	4.745E-01	0.0040	3.226E-01
0.002	1.995E-03	5.221E-01	5.221E-01	-0.0032	3.550E-01
0.003	2.995E-03	5.400E-01	5.401E-01	0.0159	3.673E-01
0.005	4.994E-03	5.553E-01	5.554E-01	0.0092	3.777E-01
0.01	9.994E-03	5.674E-01	5.674E-01	0.0129	3.859E-01
0.03	2.999E-02	5.755E-01	5.758E-01	0.0421	3.915E-01
0.05	4.999E-02	5.774E-01	5.774E-01	0.0102	3.927E-01
0.1	9.999E-02	5.786E-01	5.787E-01	0.0133	3.935E-01
3.692E-05 (feed conc.)	3.611E-05	8.136E-02	8.135E-02	-0.0099	5.532E-02

Cs (initial)	Cs (final) <sup>b</sup>	Powder form			Engineered form <sup>c</sup>
		Cs loading (ZAM model)	Cs loading (Algebraic model)	Loading difference	Cs loading (Algebraic model)
[M]	[M]	[mmole/g]	[mmole/g]	[%]	[mmole/g]
				root mean square =	0.0161

<sup>a</sup> At a 5.0 M sodium concentration level the solution density is estimated to be 1.237 g/ml and at 0.04192 M [K<sup>+</sup>].

<sup>b</sup> Final cesium equilibrium concentrations are only slightly less than initial values due to large phase ratio used.

<sup>c</sup> To estimate isotherm for engineered form a dilution factor of 0.68 is employed.

Table B-30. ZAM equilibrium model versus algebraic model cesium loading predictions for CST material in contact with Envelope A's LAW-11 feed solution at 5 M [Na<sup>+</sup>].<sup>a</sup>

Cs (initial)	Cs (final) <sup>b</sup>	Powder form			Engineered form <sup>c</sup>
		Cs loading (ZAM model)	Cs loading (Algebraic model)	Loading difference	Cs loading (Algebraic model)
[M]	[M]	[mmole/g]	[mmole/g]	[%]	[mmole/g]
0	0.000E+00	0.000E+00	0.000E+00	na	0.000E+00
0.000001	9.727E-07	2.733E-03	2.733E-03	0.0015	1.859E-03
0.00001	9.737E-06	2.625E-02	2.625E-02	-0.0156	1.785E-02
0.00005	4.889E-05	1.115E-01	1.115E-01	-0.0179	7.582E-02
0.0001	9.813E-05	1.875E-01	1.875E-01	-0.0178	1.275E-01
0.0005	4.959E-04	4.101E-01	4.101E-01	0.0000	2.789E-01
0.001	9.952E-04	4.807E-01	4.808E-01	0.0165	3.269E-01
0.002	1.995E-03	5.259E-01	5.259E-01	-0.0057	3.576E-01
0.003	2.995E-03	5.427E-01	5.428E-01	0.0142	3.691E-01
0.005	4.994E-03	5.568E-01	5.571E-01	0.0455	3.788E-01
0.01	9.994E-03	5.683E-01	5.683E-01	0.0104	3.865E-01
0.03	2.999E-02	5.758E-01	5.761E-01	0.0427	3.917E-01
0.05	4.999E-02	5.774E-01	5.776E-01	0.0419	3.928E-01
0.1	9.999E-02	5.787E-01	5.788E-01	0.0119	3.936E-01
3.739E-05 (feed conc.)	3.652E-05	8.754E-02	8.755E-02	0.0079	5.953E-02
				root mean square =	0.0229

<sup>a</sup> At a 5.0 M sodium concentration level the solution density is estimated to be 1.232 g/ml and at 0.04152 M [K<sup>+</sup>].

<sup>b</sup> Final cesium equilibrium concentrations are only slightly less than initial values due to large phase ratio used.

<sup>c</sup> To estimate isotherm for engineered form a dilution factor of 0.68 is employed.

Table B-31. ZAM equilibrium model versus algebraic model cesium loading predictions for CST material in contact with Envelope A's LAW-12 feed solution at 5 M [Na<sup>+</sup>].<sup>a</sup>

Cs (initial)	Cs (final) <sup>b</sup>	Powder form			Engineered form <sup>c</sup>
		Cs loading (ZAM model)	Cs loading (Algebraic model)	Loading difference	Cs loading (Algebraic model)
[M]	[M]	[mmole/g]	[mmole/g]	[%]	[mmole/g]
0	0.000E+00	0.000E+00	0.000E+00	na	0.000E+00
0.000001	9.806E-07	1.942E-03	1.942E-03	-0.0039	1.320E-03
0.00001	9.811E-06	1.886E-02	1.886E-02	-0.0007	1.282E-02
0.00005	4.916E-05	8.357E-02	8.359E-02	0.0166	5.684E-02
0.0001	9.854E-05	1.463E-01	1.464E-01	0.0185	9.952E-02
0.0005	4.963E-04	3.651E-01	3.652E-01	0.0133	2.483E-01

Cs (initial)	Cs (final) <sup>b</sup>	Powder form			Engineered form <sup>c</sup>
		Cs loading (ZAM model)	Cs loading (Algebraic model)	Loading difference	Cs loading (Algebraic model)
[M]	[M]	[mmole/g]	[mmole/g]	[%]	[mmole/g]
0.001	9.955E-04	4.485E-01	4.485E-01	-0.0001	3.050E-01
0.002	1.995E-03	5.059E-01	5.060E-01	0.0046	3.440E-01
0.003	2.995E-03	5.286E-01	5.285E-01	-0.0256	3.594E-01
0.005	4.995E-03	5.480E-01	5.480E-01	0.0035	3.726E-01
0.01	9.994E-03	5.635E-01	5.635E-01	0.0134	3.832E-01
0.03	2.999E-02	5.743E-01	5.744E-01	0.0173	3.906E-01
0.05	4.999E-02	5.764E-01	5.766E-01	0.0429	3.921E-01
0.1	9.999E-02	5.782E-01	5.783E-01	0.0120	3.933E-01
4.831E-05 (feed conc.)	4.749E-05	8.116E-02	8.114E-02	-0.0207	5.518E-02
root mean square =				0.0177	

<sup>a</sup> At a 5.0 M sodium concentration level the solution density is estimated to be 1.221 g/ml and at 0.1235 M [K<sup>+</sup>].

<sup>b</sup> Final cesium equilibrium concentrations are only slightly less than initial values due to large phase ratio used.

<sup>c</sup> To estimate isotherm for engineered form a dilution factor of 0.68 is employed.

Table B-32. ZAM equilibrium model versus algebraic model cesium loading predictions for CST material in contact with Envelope A's LAW-13 feed solution at 5 M [Na<sup>+</sup>].<sup>a</sup>

Cs (initial)	Cs (final) <sup>b</sup>	Powder form			Engineered form <sup>c</sup>
		Cs loading (ZAM model)	Cs loading (Algebraic model)	Loading difference	Cs loading (Algebraic model)
[M]	[M]	[mmole/g]	[mmole/g]	[%]	[mmole/g]
0	0.000E+00	0.000E+00	0.000E+00	na	0.000E+00
0.000001	9.807E-07	1.933E-03	1.933E-03	0.0021	1.314E-03
0.00001	9.812E-06	1.878E-02	1.878E-02	-0.0204	1.277E-02
0.00005	4.917E-05	8.329E-02	8.328E-02	-0.0190	5.663E-02
0.0001	9.854E-05	1.458E-01	1.459E-01	0.0183	9.919E-02
0.0005	4.964E-04	3.646E-01	3.646E-01	0.0102	2.479E-01
0.001	9.955E-04	4.480E-01	4.480E-01	0.0084	3.046E-01
0.002	1.995E-03	5.055E-01	5.057E-01	0.0258	3.439E-01
0.003	2.995E-03	5.283E-01	5.283E-01	-0.0091	3.592E-01
0.005	4.995E-03	5.480E-01	5.478E-01	-0.0214	3.725E-01
0.01	9.994E-03	5.634E-01	5.635E-01	0.0183	3.832E-01
0.03	2.999E-02	5.743E-01	5.744E-01	0.0130	3.906E-01
0.05	4.999E-02	5.764E-01	5.766E-01	0.0403	3.921E-01
0.1	9.999E-02	5.782E-01	5.783E-01	0.0107	3.932E-01
4.831E-05 (feed conc.)	4.750E-05	8.085E-02	8.084E-02	-0.0013	5.497E-02
root mean square =				0.0184	

<sup>a</sup> At a 5.0 M sodium concentration level the solution density is estimated to be 1.221 g/ml and at 0.1252 M [K<sup>+</sup>].

<sup>b</sup> Final cesium equilibrium concentrations are only slightly less than initial values due to large phase ratio used.

<sup>c</sup> To estimate isotherm for engineered form a dilution factor of 0.68 is employed.

Table B-33. ZAM equilibrium model versus algebraic model cesium loading predictions for CST material in contact with Envelope A's LAW-14 feed solution at 5 M [Na<sup>+</sup>].<sup>a</sup>

Powder form				Engineered form <sup>c</sup>
-------------	--	--	--	------------------------------



Cs (initial)	Cs (final) <sup>b</sup>	Cs loading (ZAM model)	Cs loading (Algebraic model)	Loading difference	Cs loading (Algebraic model)
[M]	[M]	[mmole/g]	[mmole/g]	[%]	[mmole/g]
0	0.000E+00	0.000E+00	0.000E+00	na	0.000E+00
0.000001	9.843E-07	1.569E-03	1.569E-03	0.0138	1.067E-03
0.00001	9.847E-06	1.533E-02	1.532E-02	-0.0445	1.042E-02
0.00005	4.931E-05	6.938E-02	6.939E-02	0.0205	4.719E-02
0.0001	9.876E-05	1.241E-01	1.241E-01	-0.0377	8.438E-02
0.0005	4.966E-04	3.351E-01	3.351E-01	0.0098	2.279E-01
0.001	9.957E-04	4.251E-01	4.251E-01	0.0075	2.891E-01
0.002	1.995E-03	4.908E-01	4.907E-01	-0.0045	3.337E-01
0.003	2.995E-03	5.172E-01	5.173E-01	0.0177	3.518E-01
0.005	4.995E-03	5.405E-01	5.407E-01	0.0488	3.677E-01
0.01	9.994E-03	5.596E-01	5.597E-01	0.0209	3.806E-01
0.03	2.999E-02	5.728E-01	5.731E-01	0.0450	3.897E-01
0.05	4.999E-02	5.759E-01	5.758E-01	-0.0111	3.916E-01
0.1	4.999E-02	5.759E-01	5.758E-01	-0.0111	3.916E-01
4.569E-05 (feed conc.)	4.504E-05	6.405E-02	6.405E-02	0.0015	4.355E-02
root mean square =				0.0262	

<sup>a</sup> At a 5.0 M sodium concentration level the solution density is estimated to be 1.234 g/ml and at 0.3198 M [K<sup>+</sup>].

<sup>b</sup> Final cesium equilibrium concentrations are only slightly less than initial values due to large phase ratio used.

<sup>c</sup> To estimate isotherm for engineered form a dilution factor of 0.68 is employed.

Table B-34. ZAM equilibrium model versus algebraic model cesium loading predictions for CST material in contact with Envelope A's LAW-15 feed solution at 5 M [Na<sup>+</sup>].<sup>a</sup>

Cs (initial)	Cs (final) <sup>b</sup>	Powder form			Engineered form <sup>c</sup>
		Cs loading (ZAM model)	Cs loading (Algebraic model)	Loading difference	Cs loading (Algebraic model)
[M]	[M]	[mmole/g]	[mmole/g]	[%]	[mmole/g]
0	0.000E+00	0.000E+00	0.000E+00	na	0.000E+00
0.000001	9.852E-07	1.480E-03	1.480E-03	0.0095	1.006E-03
0.00001	9.855E-06	1.447E-02	1.447E-02	0.0279	9.840E-03
0.00005	4.934E-05	6.587E-02	6.587E-02	-0.0030	4.479E-02
0.0001	9.882E-05	1.184E-01	1.184E-01	0.0393	8.053E-02
0.0005	4.967E-04	3.267E-01	3.267E-01	0.0035	2.221E-01
0.001	9.958E-04	4.182E-01	4.182E-01	0.0016	2.844E-01
0.002	1.995E-03	4.860E-01	4.861E-01	0.0346	3.306E-01
0.003	2.995E-03	5.139E-01	5.139E-01	-0.0052	3.495E-01
0.005	4.995E-03	5.385E-01	5.385E-01	0.0038	3.662E-01
0.01	9.994E-03	5.584E-01	5.585E-01	0.0204	3.798E-01
0.03	2.999E-02	5.725E-01	5.726E-01	0.0239	3.894E-01
0.05	4.999E-02	5.754E-01	5.756E-01	0.0314	3.914E-01
0.1	9.999E-02	5.776E-01	5.778E-01	0.0229	3.929E-01
4.552E-05 (feed conc.)	4.492E-05	6.060E-02	6.058E-02	-0.0237	4.120E-02
root mean square =				0.0219	

<sup>a</sup> At a 5.0 M sodium concentration level the solution density is estimated to be 1.235 g/ml and at 0.4067 M [K<sup>+</sup>].

<sup>b</sup> Final cesium equilibrium concentrations are only slightly less than initial values due to large phase ratio used.

<sup>c</sup> To estimate isotherm for engineered form a dilution factor of 0.68 is employed.

Table B-35. ZAM equilibrium model versus algebraic model cesium loading predictions for CST material in contact with Envelope B's LAW-2a feed solution at 5 M  $[\text{Na}^+]$ .<sup>a</sup>

Cs (initial)	Cs (final) <sup>b</sup>	Powder form			Engineered form <sup>c</sup>
		Cs loading (ZAM model)	Cs loading (Algebraic model)	Loading difference	Cs loading (Algebraic model)
[M]	[M]	[mmole/g]	[mmole/g]	[%]	[mmole/g]
0	0.000E+00	0.000E+00	0.000E+00	na	0.000E+00
0.000001	9.784E-07	2.155E-03	2.155E-03	-0.0004	1.466E-03
0.00001	9.791E-06	2.087E-02	2.087E-02	-0.0169	1.419E-02
0.00005	4.909E-05	9.145E-02	9.144E-02	-0.0206	6.218E-02
0.0001	9.842E-05	1.583E-01	1.582E-01	-0.0065	1.076E-01
0.0005	4.962E-04	3.794E-01	3.794E-01	0.0088	2.580E-01
0.001	9.954E-04	4.590E-01	4.590E-01	0.0129	3.121E-01
0.002	1.995E-03	5.125E-01	5.126E-01	0.0172	3.486E-01
0.003	2.995E-03	5.334E-01	5.333E-01	-0.0216	3.626E-01
0.005	4.994E-03	5.508E-01	5.511E-01	0.0397	3.747E-01
0.01	9.994E-03	5.651E-01	5.652E-01	0.0188	3.843E-01
0.03	2.999E-02	5.749E-01	5.750E-01	0.0109	3.910E-01
0.05	4.999E-02	5.769E-01	5.770E-01	0.0153	3.923E-01
0.1	9.999E-02	5.784E-01	5.785E-01	0.0070	3.934E-01
4.676E-04 (feed conc.)	4.638E-04	3.704E-01	3.705E-01	0.0110	2.519E-01
root mean square =				0.0173	

<sup>a</sup> At a 5.0 M sodium concentration level the solution density is estimated to be 1.254 g/ml and at 0.1250 M  $[\text{K}^+]$ .<sup>b</sup> Final cesium equilibrium concentrations are only slightly less than initial values due to large phase ratio used.<sup>c</sup> To estimate isotherm for engineered form a dilution factor of 0.68 is employed.Table B-36. ZAM equilibrium model versus algebraic model cesium loading predictions for CST material in contact with Envelope B's LAW-2b feed solution at 5 M  $[\text{Na}^+]$ .<sup>a</sup>

Cs (initial)	Cs (final) <sup>b</sup>	Powder form			Engineered form <sup>c</sup>
		Cs loading (ZAM model)	Cs loading (Algebraic model)	Loading difference	Cs loading (Algebraic model)
[M]	[M]	[mmole/g]	[mmole/g]	[%]	[mmole/g]
0	0.000E+00	0.000E+00	0.000E+00	na	0.000E+00
0.000001	9.736E-07	2.639E-03	2.640E-03	0.0045	1.795E-03
0.00001	9.746E-06	2.538E-02	2.538E-02	0.0127	1.726E-02
0.00005	4.892E-05	1.084E-01	1.083E-01	-0.0111	7.368E-02
0.0001	9.817E-05	1.830E-01	1.830E-01	0.0093	1.244E-01
0.0005	4.959E-04	4.057E-01	4.058E-01	0.0141	2.759E-01
0.001	9.952E-04	4.777E-01	4.778E-01	0.0143	3.249E-01
0.002	1.995E-03	5.241E-01	5.241E-01	-0.0054	3.564E-01
0.003	2.995E-03	5.415E-01	5.415E-01	0.0001	3.682E-01
0.005	4.994E-03	5.563E-01	5.563E-01	-0.0095	3.783E-01
0.01	9.994E-03	5.679E-01	5.679E-01	0.0070	3.862E-01
0.03	2.999E-02	5.758E-01	5.759E-01	0.0178	3.916E-01
0.05	4.999E-02	5.774E-01	5.775E-01	0.0269	3.927E-01
0.1	9.999E-02	5.786E-01	5.788E-01	0.0216	3.936E-01
4.311E-04 (feed conc.)	4.272E-04	3.870E-01	3.871E-01	0.0136	2.632E-01

Cs (initial)	Cs (final) <sup>b</sup>	Powder form			Engineered form <sup>c</sup>
		Cs loading (ZAM model)	Cs loading (Algebraic model)	Loading difference	Cs loading (Algebraic model)
[M]	[M]	[mmole/g]	[mmole/g]	[%]	[mmole/g]
				root mean square =	0.0138

<sup>a</sup> At a 5.0 M sodium concentration level the solution density is estimated to be 1.242 g/ml and at 0.1429 M [K<sup>+</sup>].

<sup>b</sup> Final cesium equilibrium concentrations are only slightly less than initial values due to large phase ratio used.

<sup>c</sup> To estimate isotherm for engineered form a dilution factor of 0.68 is employed.

Table B-37. ZAM equilibrium model versus algebraic model cesium loading predictions for CST material in contact with Envelope C's LAW-3 feed solution at 5 M [Na<sup>+</sup>].<sup>a</sup>

Cs (initial)	Cs (final) <sup>b</sup>	Powder form			Engineered form <sup>c</sup>
		Cs loading (ZAM model)	Cs loading (Algebraic model)	Loading difference	Cs loading (Algebraic model)
[M]	[M]	[mmole/g]	[mmole/g]	[%]	[mmole/g]
0	0.000E+00	0.000E+00	0.000E+00	na	0.000E+00
0.000001	9.742E-07	2.585E-03	2.584E-03	-0.0200	1.757E-03
0.00001	9.751E-06	2.487E-02	2.487E-02	0.0044	1.691E-02
0.00005	4.894E-05	1.064E-01	1.065E-01	0.0138	7.239E-02
0.0001	9.820E-05	1.803E-01	1.803E-01	0.0045	1.226E-01
0.0005	4.960E-04	4.031E-01	4.031E-01	-0.0027	2.741E-01
0.001	9.952E-04	4.758E-01	4.759E-01	0.0202	3.236E-01
0.002	1.995E-03	5.229E-01	5.229E-01	0.0093	3.556E-01
0.003	2.995E-03	5.406E-01	5.407E-01	0.0189	3.677E-01
0.005	4.994E-03	5.558E-01	5.558E-01	-0.0105	3.779E-01
0.01	9.994E-03	5.676E-01	5.676E-01	0.0135	3.860E-01
0.03	2.999E-02	5.758E-01	5.758E-01	0.0021	3.916E-01
0.05	4.999E-02	5.774E-01	5.775E-01	0.0174	3.927E-01
0.1	9.999E-02	5.786E-01	5.787E-01	0.0169	3.935E-01
3.967E-05 (feed conc.)	3.880E-05	8.773E-02	8.774E-02	0.0131	5.966E-02
				root mean square =	0.0135

<sup>a</sup> At a 5.0 M sodium concentration level the solution density is estimated to be 1.237 g/ml and at 0.04393 M [K<sup>+</sup>].

<sup>b</sup> Final cesium equilibrium concentrations are only slightly less than initial values due to large phase ratio used.

<sup>c</sup> To estimate isotherm for engineered form a dilution factor of 0.68 is employed.

Table B-38. ZAM equilibrium model versus algebraic model cesium loading predictions for CST material in contact with Envelope C's LAW-4 feed solution at 5 M [Na<sup>+</sup>].<sup>a</sup>

Cs (initial)	Cs (final) <sup>b</sup>	Powder form			Engineered form <sup>c</sup>
		Cs loading (ZAM model)	Cs loading (Algebraic model)	Loading difference	Cs loading (Algebraic model)
[M]	[M]	[mmole/g]	[mmole/g]	[%]	[mmole/g]
0	0.000E+00	0.000E+00	0.000E+00	na	0.000E+00
0.000001	9.742E-07	2.585E-03	2.584E-03	-0.0200	1.757E-03
0.00001	9.751E-06	2.487E-02	2.487E-02	0.0044	1.691E-02
0.00005	4.894E-05	1.064E-01	1.065E-01	0.0138	7.239E-02
0.0001	9.820E-05	1.803E-01	1.803E-01	0.0045	1.226E-01
0.0005	4.960E-04	4.031E-01	4.031E-01	-0.0027	2.741E-01

Cs (initial)	Cs (final) <sup>b</sup>	Powder form			Engineered form <sup>c</sup>
		Cs loading (ZAM model)	Cs loading (Algebraic model)	Loading difference	Cs loading (Algebraic model)
[M]	[M]	[mmole/g]	[mmole/g]	[%]	[mmole/g]
0.001	9.952E-04	4.758E-01	4.759E-01	0.0202	3.236E-01
0.002	1.995E-03	5.229E-01	5.229E-01	0.0093	3.556E-01
0.003	2.995E-03	5.406E-01	5.407E-01	0.0189	3.677E-01
0.005	4.994E-03	5.558E-01	5.558E-01	-0.0105	3.779E-01
0.01	9.994E-03	5.676E-01	5.676E-01	0.0135	3.860E-01
0.03	2.999E-02	5.758E-01	5.758E-01	0.0021	3.916E-01
0.05	4.999E-02	5.774E-01	5.775E-01	0.0174	3.927E-01
0.1	9.999E-02	5.786E-01	5.787E-01	0.0169	3.935E-01
3.779E-05 (feed conc.)	3.694E-05	8.415E-02	8.414E-02	-0.0081	5.722E-02
root mean square =				0.0132	

<sup>a</sup> At a 5.0 M sodium concentration level the solution density is estimated to be 1.237 g/ml and at 0.04393 M [K<sup>+</sup>].

<sup>b</sup> Final cesium equilibrium concentrations are only slightly less than initial values due to large phase ratio used.

<sup>c</sup> To estimate isotherm for engineered form a dilution factor of 0.68 is employed.

Table B-39. ZAM equilibrium model versus algebraic model cesium loading predictions for CST material in contact with Envelope C's LAW-7 feed solution at 5 M [Na<sup>+</sup>].<sup>a</sup>

Cs (initial)	Cs (final) <sup>b</sup>	Powder form			Engineered form <sup>c</sup>
		Cs loading (ZAM model)	Cs loading (Algebraic model)	Loading difference	Cs loading (Algebraic model)
[M]	[M]	[mmole/g]	[mmole/g]	[%]	[mmole/g]
0	0.000E+00	0.000E+00	0.000E+00	Na	0.000E+00
0.000001	9.709E-07	2.910E-03	2.909E-03	-0.0124	1.978E-03
0.00001	9.721E-06	2.787E-02	2.787E-02	0.0005	1.895E-02
0.00005	4.883E-05	1.173E-01	1.173E-01	-0.0187	7.978E-02
0.0001	9.804E-05	1.957E-01	1.957E-01	-0.0134	1.330E-01
0.0005	4.958E-04	4.177E-01	4.177E-01	0.0069	2.841E-01
0.001	9.951E-04	4.859E-01	4.860E-01	0.0096	3.304E-01
0.002	1.995E-03	5.289E-01	5.289E-01	0.0125	3.597E-01
0.003	2.995E-03	5.451E-01	5.450E-01	-0.0241	3.706E-01
0.005	4.994E-03	5.583E-01	5.585E-01	0.0242	3.798E-01
0.01	9.994E-03	5.690E-01	5.690E-01	0.0135	3.869E-01
0.03	2.999E-02	5.761E-01	5.763E-01	0.0332	3.919E-01
0.05	4.999E-02	5.779E-01	5.778E-01	-0.0191	3.929E-01
0.1	9.999E-02	5.788E-01	5.789E-01	0.0074	3.936E-01
4.455E-05 (feed conc.)	4.348E-05	1.068E-01	1.068E-01	0.0001	7.264E-02
root mean square =				0.0166	

<sup>a</sup> At a 5.0 M sodium concentration level the solution density is estimated to be 1.243 g/ml and at 0.02227 M [K<sup>+</sup>].

<sup>b</sup> Final cesium equilibrium concentrations are only slightly less than initial values due to large phase ratio used.

<sup>c</sup> To estimate isotherm for engineered form a dilution factor of 0.68 is employed.

Table B-40. Cesium isotherm (engineered-form) sensitivity results based on the ZAM model for deviations about the nominal settings for the Phase 1 LAW-15 feed solution at 5.0 M Na<sup>+</sup>, 25 C, and 4.552x10<sup>-5</sup> M Cs<sup>+</sup> (100% of feed value).

Sensitivity Case	Variable change (%)	Ionic Strength (gmole/kg)	Cs Kd (ml/g)	Cs loading (mmole/g)	Cs loading change (%)	Comments
Nominal	0%	6.49	917	4.121E-02	0.0	Nominal settings at 5.0 M Na <sup>+</sup> and 25 C.
Dilution factor	-15%	6.49	780	3.503E-02	-15.0	Dilution factor (engineered to powder capacity ratio) was reduced to 0.578.
H <sup>+</sup>	no impact	6.49	917	4.121E-02	0.0	Has no impact since hydroxyl ion is used to set solution pH level in ZAM model directly.
Density	-3.0%	6.77	906	4.069E-02	-1.3	Liquid-phase density was decreased by 3%.
Temperature	+1.7%	6.49	838	3.770E-02	-8.5	Temperature was increased by 5 C.
K <sup>+</sup>	+50%	6.74	874	3.927E-02	-5.8	Potassium was increased by 50% and OH <sup>-</sup> adjusted appropriately. Compensating effects minimize its overall impact. Extrapolated value where no KNO <sub>3</sub> is allowed to precipitate out of solution.
Na <sup>+</sup>	+20.0%	7.99	800	3.601E-02	-12.6	Sodium was increased by 20% and OH <sup>-</sup> adjusted appropriately..
NO <sub>2</sub> <sup>-</sup>	+50%	6.60	896	4.024E-02	-2.4	Nitrite was increased by 50% and OH <sup>-</sup> adjusted appropriately.
NO <sub>3</sub> <sup>-</sup>	+50%	6.71	782	3.519E-02	-14.6	Nitrate was increased by 50% and OH <sup>-</sup> adjusted appropriately.
Al(OH) <sub>4</sub> <sup>-</sup>	+50%	6.63	890	3.999E-02	-2.9	Aluminate was increased by 50% and OH <sup>-</sup> adjusted appropriately. All Al within the feed inventory is assumed to be converted into the Al(OH) <sub>4</sub> <sup>-</sup> species. The total amount of OH <sup>-</sup> inventory is reduced by the appropriate amount for this reaction.
Cl <sup>-</sup>	+50%	6.49	913	4.099E-02	-0.5	Chloride was increased by 50% and OH <sup>-</sup> adjusted appropriately.
CO <sub>3</sub> <sup>-2</sup>	-50%	6.33	905	4.066E-02	-1.3	Carbonate was decreased by 50% and OH <sup>-</sup> adjusted appropriately. Carbonate levels increase over time within a waste tank due to a liquid-phase reaction between OH <sup>-</sup> and CO <sub>2</sub> (present in the vent gas space).
CrO <sub>4</sub> <sup>-2</sup> or Cr(OH) <sub>4</sub> <sup>-</sup>	+50%	8.10	886	3.982E-02	-3.4	Chromate was increased by 50% and OH <sup>-</sup> adjusted appropriately. The chromate CrO <sub>4</sub> <sup>-2</sup> anion has chromium(VI), while for the Cr(OH) <sub>4</sub> <sup>-</sup> anion has chromium(III). The impact of total Cr using ZAM can only be checked using the chromate anion since ZAM currently only handles the chromate species in the aqueous solution. The total amount of OH <sup>-</sup> inventory is reduced by the appropriate amount for these reactions.
OH <sup>-</sup>	varies	-	-	-	-	No explicit sensitivity results are listed for the hydroxyl ion since its impact is accounted for automatically for in the other results (i.e., OH <sup>-</sup> is varied to maintain charge balance).
Overall error estimate at 100% cesium feed concentration (%)					27%	Represents an overall error estimate in the cesium loading curve due to the various uncertainties listed above.

Table B-41. Cesium isotherm (engineered-form) sensitivity results based on the ZAM model for deviations about the nominal settings for the Phase 1 LAW-15 feed solution at 5.0 M Na<sup>+</sup>, 25 C, and 2.276x10<sup>-5</sup> M Cs<sup>+</sup> (50% of feed value).

Sensitivity Case	Variable change (%)	Ionic Strength (gmole/kg)	Cs Kd (ml/g)	Cs loading (mmole/g)	Cs loading change (%)	Comments
Nominal	0%	6.49	968	2.171E-02	0.0	Nominal settings at 5.0 M Na <sup>+</sup> and 25 C.
Dilution factor	-15%	6.49	822	1.846E-02	-15.0	Dilution factor (engineered to powder capacity ratio) was reduced to 0.578.
H <sup>+</sup>	no impact	6.49	968	2.171E-02	0.0	Has no impact since hydroxyl ion is used to set solution pH level in ZAM model directly.
Density	-3.0%	6.77	955	2.143E-02	-1.3	Liquid-phase density was decreased by 3%.
Temperature	+1.7%	6.49	881	1.979E-02	-8.9	Temperature was increased by 5 C.
K <sup>+</sup>	+50%	6.74	920	2.066E-02	-6.0	Potassium was increased by 50% and OH <sup>-</sup> adjusted appropriately. Compensating effects minimize its overall impact. Extrapolated value where no KNO <sub>3</sub> is allowed to precipitate out of solution.
Na <sup>+</sup>	+20.0%	7.99	839	1.886E-02	-13.1	Sodium was increased by 20% and OH <sup>-</sup> adjusted appropriately..
NO <sub>2</sub> <sup>-</sup>	+50%	6.60	944	2.119E-02	-2.4	Nitrite was increased by 50% and OH <sup>-</sup> adjusted appropriately.
NO <sub>3</sub> <sup>-</sup>	+50%	6.71	819	1.841E-02	-15.2	Nitrate was increased by 50% and OH <sup>-</sup> adjusted appropriately.
Al(OH) <sub>4</sub> <sup>-</sup>	+50%	6.63	938	2.105E-02	-3.0	Aluminate was increased by 50% and OH <sup>-</sup> adjusted appropriately. All Al within the feed inventory is assumed to be converted into the Al(OH) <sub>4</sub> <sup>-</sup> species. The total amount of OH <sup>-</sup> inventory is reduced by the appropriate amount for this reaction.
Cl <sup>-</sup>	+50%	6.49	963	2.161E-02	-0.5	Chloride was increased by 50% and OH <sup>-</sup> adjusted appropriately.
CO <sub>3</sub> <sup>-2</sup>	-50%	6.33	955	2.143E-02	-1.3	Carbonate was decreased by 50% and OH <sup>-</sup> adjusted appropriately. Carbonate levels increase over time within a waste tank due to a liquid-phase reaction between OH <sup>-</sup> and CO <sub>2</sub> (present in the vent gas space).
CrO <sub>4</sub> <sup>-2</sup> or Cr(OH) <sub>4</sub> <sup>-</sup>	+50%	8.10	933	2.094E-02	-3.5	Chromate was increased by 50% and OH <sup>-</sup> adjusted appropriately. The chromate CrO <sub>4</sub> <sup>-2</sup> anion has chromium(VI), while for the Cr(OH) <sub>4</sub> <sup>-</sup> anion has chromium(III). The impact of total Cr using ZAM can only be checked using the chromate anion since ZAM currently only handles the chromate species in the aqueous solution. The total amount of OH <sup>-</sup> inventory is reduced by the appropriate amount for these reactions.
OH <sup>-</sup>	varies	-	-	-	-	No explicit sensitivity results are listed for the hydroxyl ion since its impact is accounted for automatically for in the other results (i.e., OH <sup>-</sup> is varied to maintain charge balance).
Overall error estimate at 50% of cesium feed concentration (%)					28%	Represents an overall error estimate in the cesium loading curve due to the various uncertainties listed above.

Table B-42. Error estimates associated with feed compositions for the key species of interest.

AN-103 (Env-A [Hay et al., 2000a]; LAW-12 and 13)					AZ-102 (Env-B [Hay and Bronikowski, 2000]; LAW-2b)				AN-102 (Env-A [Hay et al., 2000b]; LAW-3 and 4)				Summary
	data	LAW-12 feed	Adjusted data	Difference	Data	LAW-2b feed	Adjusted data	Difference	data	LAW-3 feed	Adjusted data	Difference	rms difference
Species	[M]	[M]	[M]	(%)	[M]	[M]	[M]	(%)	[M]	[M]	[M]	(%)	(%)
	-	factor =	1.29	-	-	factor =	8.53	-	-	factor =	1.40	-	-
Na <sup>+</sup>	5.25	6.76E+00	6.76E+00	0.0	2.77	2.36E+00	2.36E+00	0.0	6.42	8.97E+00	8.97E+00	0.0	0.0
K <sup>+</sup>	1.21E-01	1.67E-01	1.56E-01	7.2	8.07E-02	7.92E-02	6.88E-02	15.1	3.52E-02	7.95E-02	4.92E-02	61.5	36.8
Total Cr	1.41E-03	4.87E-03	1.82E-03	168.2	1.48E-02	2.17E-05	1.26E-02	-99.8	3.06E-03	6.54E-03	4.28E-03	52.9	117.0
Total Al	6.98E-01	1.01E+00	8.99E-01	12.8	2.79E-02	5.52E-02	2.38E-02	132.1	3.42E-01	4.66E-01	4.78E-01	-2.6	76.7
NO <sub>3</sub> <sup>-</sup>	1.57E+00	1.65E+00	2.02E+00	-18.2	2.73E-01	3.73E-01	2.33E-01	60.3	1.94E+00	2.92E+00	2.71E+00	7.6	36.7
NO <sub>2</sub> <sup>-</sup>	1.04E+00	1.52E+00	1.34E+00	13.8	6.59E-01	6.55E-01	5.62E-01	16.5	1.13E+00	1.44E+00	1.58E+00	-8.8	13.4
CO <sub>3</sub> <sup>-</sup>	2.55E-01	2.18E-01	3.28E-01	-33.5	3.92E-01	5.73E-01	3.34E-01	71.6	4.89E-01	9.23E-01	6.84E-01	35.0	49.9
Cl <sup>-</sup>	6.15E-02	1.17E-01	7.92E-02	47.7	1.41E-03	2.62E-04	1.20E-03	-78.2	6.76E-02	8.68E-02	9.45E-02	-8.1	53.1
SO <sub>4</sub> <sup>-2</sup>	7.73E-03	1.54E-02	9.96E-03	54.5	1.72E-01	1.87E-01	1.47E-01	27.3	8.48E-02	1.32E-01	1.19E-01	11.0	35.8
Total Sr <sup>b</sup>	2.33E-06	2.18E-05	3.00E-06	626.4	2.85E-06	2.13E-06	2.43E-06	-12.3	2.04E-05	3.85E-05	2.85E-05	35.0	362.3
OH <sup>-</sup> (free)	2.81E+00 <sup>a</sup>	6.22E+00	3.62E+00	71.8	1.09E-01	1.26E-01	9.29E-02	35.2	8.17E-01	2.83E+00	1.14E+00	147.7	97.0
OH <sup>-</sup> (bound)	-	3.32E-01	3.60E+00	-90.8	-	1.40E-02	1.46E-01	-90.4	-	3.80E-01	1.93E+00	-80.3	87.3
OH <sup>-</sup> (total)	-	6.55E+00	7.22E+00	-9.3	-	1.40E-01	2.39E-01	-41.5	-	3.21E+00	3.07E+00	4.5	24.7

<sup>a</sup> For AN-103 data the OH<sup>-</sup> (free) is based on a simple dilution factor and not the data since significant dissolution of solids occurred during dilution process.

<sup>b</sup> CST has a strong affinity for SrOH<sup>+</sup>; however, the actual amount of total Sr available in solution to form SrOH<sup>+</sup> is currently believed to be small but is unknown at this time. In this report the Sr concentration has been set to zero. Future work will need to address this issue.

Table B-43. Phase 1 LAW-15 feed solution data used as input to the CST equilibrium model sensitivity study.

[illegible]

Species	Sensitivity Case	Nominal	Al(OH) <sub>4</sub> <sup>-</sup>	CrO <sub>4</sub> <sup>-2</sup>	pH	NO <sub>3</sub> <sup>-</sup>	NO <sub>2</sub> <sup>-</sup>	CO <sub>3</sub> <sup>-2</sup>	Cl <sup>-</sup>	K <sup>+</sup>	SrOH <sup>-</sup>	Na <sup>+</sup>
Charge	Concentration Units	[M]	[M]	[M]	[M]	[M]	[M]	[M]	[M]	[M]	[M]	[M]
1	H+	1.07E-15	1.07E-15	1.07E-15	4.67E-15	1.07E-15	1.07E-15	1.07E-15	1.07E-15	1.07E-15	1.07E-15	1.07E-15
1	Rb	0.00E+00	0.00E+00	0.00E+00	0.00E+00	0.00E+00	0.00E+00	0.00E+00	0.00E+00	0.00E+00	0.00E+00	0.00E+00
1	K	4.07E-01	4.07E-01	4.07E-01	4.07E-01	4.07E-01	4.07E-01	4.07E-01	4.07E-01	6.10E-01	4.07E-01	4.07E-01
1	SrOH	0.00E+00	0.00E+00	0.00E+00	0.00E+00	0.00E+00	0.00E+00	0.00E+00	0.00E+00	0.00E+00	0.00E+00	0.00E+00
2	Sr	0.00E+00	0.00E+00	0.00E+00	0.00E+00	0.00E+00	0.00E+00	0.00E+00	0.00E+00	0.00E+00	2.28E-05	0.00E+00
2	Ba	0.00E+00	0.00E+00	0.00E+00	0.00E+00	0.00E+00	0.00E+00	0.00E+00	0.00E+00	0.00E+00	0.00E+00	0.00E+00
2	Ca	8.60E-04	8.60E-04	8.60E-04	8.60E-04	8.60E-04	8.60E-04	8.60E-04	8.60E-04	8.60E-04	8.60E-04	8.60E-04
2	Cd	0.00E+00	0.00E+00	0.00E+00	0.00E+00	0.00E+00	0.00E+00	0.00E+00	0.00E+00	0.00E+00	0.00E+00	0.00E+00
2	Mn	6.03E-05	6.03E-05	6.03E-05	6.03E-05	6.03E-05	6.03E-05	6.03E-05	6.03E-05	6.03E-05	6.03E-05	6.03E-05
2	Ni	1.08E-04	1.08E-04	1.08E-04	1.08E-04	1.08E-04	1.08E-04	1.08E-04	1.08E-04	1.08E-04	1.08E-04	1.08E-04
2	U (total)	3.96E-04	3.96E-04	3.96E-04	3.96E-04	3.96E-04	3.96E-04	3.96E-04	3.96E-04	3.96E-04	3.96E-04	3.96E-04
2	Zn	0.00E+00	0.00E+00	0.00E+00	0.00E+00	0.00E+00	0.00E+00	0.00E+00	0.00E+00	0.00E+00	0.00E+00	0.00E+00
2	Fe	2.84E-04	2.84E-04	2.84E-04	2.84E-04	2.84E-04	2.84E-04	2.84E-04	2.84E-04	2.84E-04	2.84E-04	2.84E-04
2	Pb	1.61E-04	1.61E-04	1.61E-04	1.61E-04	1.61E-04	1.61E-04	1.61E-04	1.61E-04	1.61E-04	1.61E-04	1.61E-04
3	Al	0.00E+00	0.00E+00	0.00E+00	0.00E+00	0.00E+00	0.00E+00	0.00E+00	0.00E+00	0.00E+00	0.00E+00	0.00E+00
3	Cr	0.00E+00	0.00E+00	0.00E+00	0.00E+00	0.00E+00	0.00E+00	0.00E+00	0.00E+00	0.00E+00	0.00E+00	0.00E+00
3	La	5.80E-12	5.80E-12	5.80E-12	5.80E-12	5.80E-12	5.80E-12	5.80E-12	5.80E-12	5.80E-12	5.80E-12	5.80E-12
3	Ce	0.00E+00	0.00E+00	0.00E+00	0.00E+00	0.00E+00	0.00E+00	0.00E+00	0.00E+00	0.00E+00	0.00E+00	0.00E+00
<b>Anions</b>												
-1	OH- (free)	2.14E+00	1.89E+00	1.14E+00	2.14E+00	1.49E+00	1.63E+00	2.29E+00	2.11E+00	2.34E+00	2.14E+00	3.14E+00
-1	NO3	1.30E+00	1.30E+00	1.30E+00	1.30E+00	1.95E+00	1.30E+00	1.30E+00	1.30E+00	1.30E+00	1.30E+00	1.30E+00
-1	NO2	1.01E+00	1.01E+00	1.01E+00	1.01E+00	1.01E+00	1.52E+00	1.01E+00	1.01E+00	1.01E+00	1.01E+00	1.01E+00
-1	Cl	6.98E-02	6.98E-02	6.98E-02	6.98E-02	6.98E-02	6.98E-02	6.98E-02	1.05E-01	6.98E-02	6.98E-02	6.98E-02
-1	F	3.94E-02	3.94E-02	3.94E-02	3.94E-02	3.94E-02	3.94E-02	3.94E-02	3.94E-02	3.94E-02	3.94E-02	3.94E-02
-1	Al(OH)4	5.01E-01	7.52E-01	0.00E+00	5.01E-01	5.01E-01	5.01E-01	5.01E-01	5.01E-01	5.01E-01	5.01E-01	5.01E-01
-1	129-I	9.14E-06	9.14E-06	9.14E-06	9.14E-06	9.14E-06	9.14E-06	9.14E-06	9.14E-06	9.14E-06	9.14E-06	9.14E-06
-2	CrO4	0.00E+00	0.00E+00	7.52E-01	0.00E+00	0.00E+00	0.00E+00	0.00E+00	0.00E+00	0.00E+00	0.00E+00	0.00E+00
-2	CO3	1.54E-01	1.54E-01	1.54E-01	1.54E-01	1.54E-01	1.54E-01	7.69E-02	1.54E-01	1.54E-01	1.54E-01	1.54E-01
-2	SO4	1.06E-02	1.06E-02	1.06E-02	1.06E-02	1.06E-02	1.06E-02	1.06E-02	1.06E-02	1.06E-02	1.06E-02	1.06E-02
-3	PO4	5.67E-03	5.67E-03	5.67E-03	5.67E-03	5.67E-03	5.67E-03	5.67E-03	5.67E-03	5.67E-03	5.67E-03	5.67E-03
	cations =	5.4105	5.4105	5.4105	5.4105	5.4105	5.4105	5.4105	5.4105	5.6139	5.4105	6.4105
	anions =	-5.4105	-5.4105	-5.4105	-5.4105	-5.4105	-5.4105	-5.4105	-5.4105	-5.6138	-5.4105	-6.4105



[illegible]

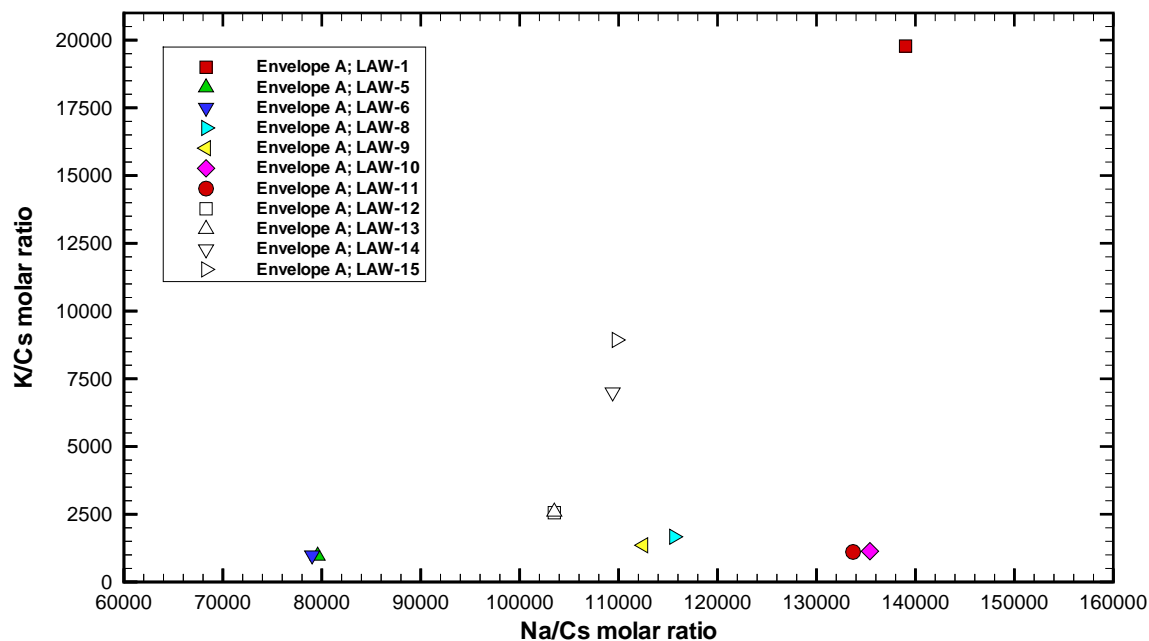


Figure B-1. Molar ratios of Na/Cs versus K/Cs for the Envelope A candidate feed solutions.

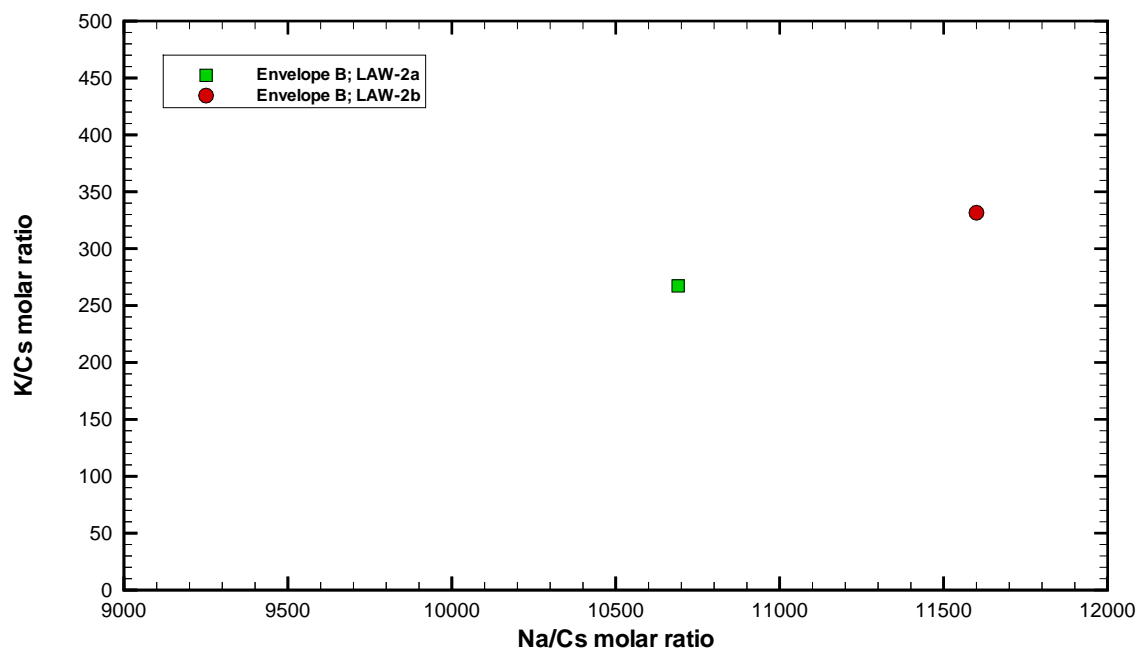


Figure B-2. Molar ratios of Na/Cs versus K/Cs for the Envelope B candidate feed solutions.

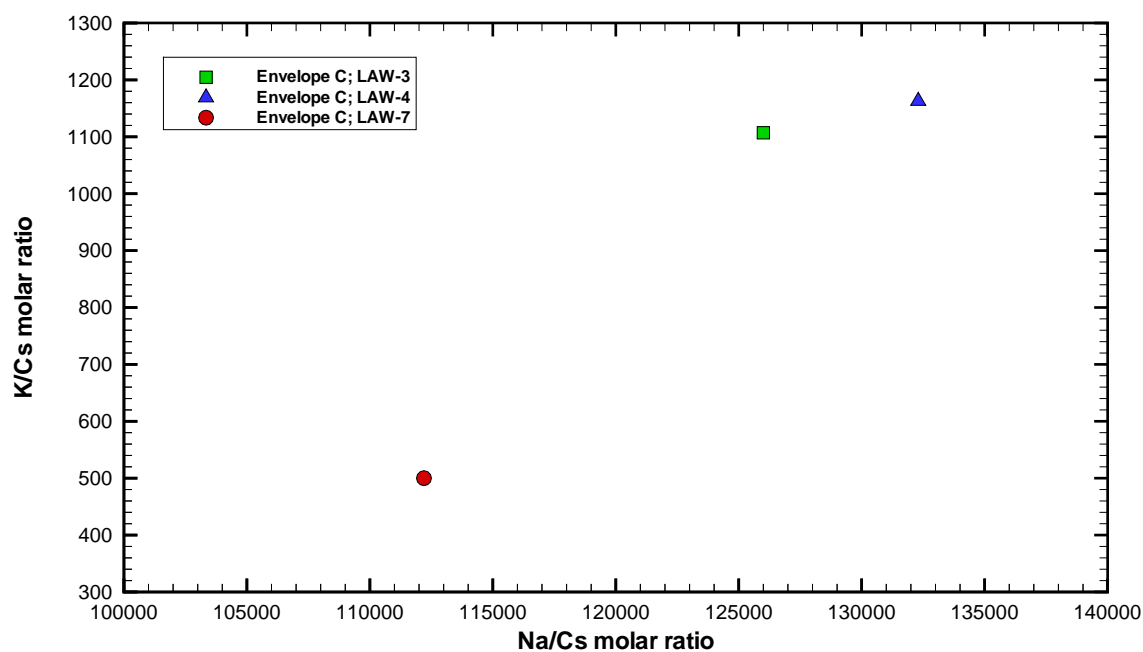


Figure B-3. Molar ratios of Na/Cs versus K/Cs for the Envelope C candidate feed solutions.

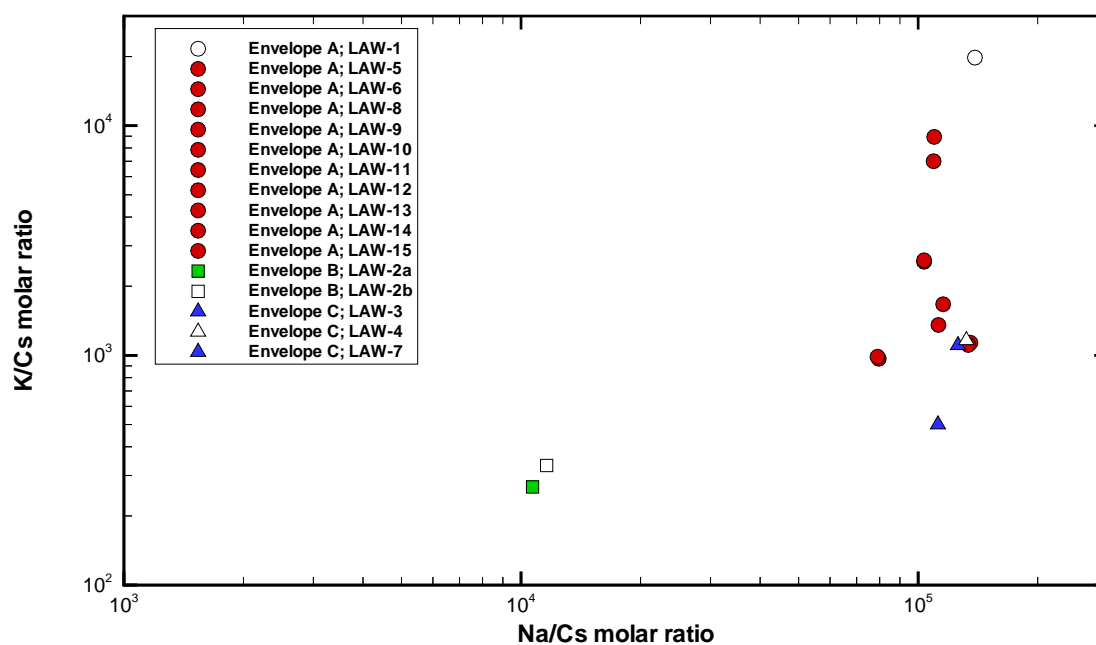


Figure B-4. Molar ratios of Na/Cs versus K/Cs for all Envelope A, B, and C candidate feed solutions. The least favorable feed solutions for each envelope are highlighted by open symbols.

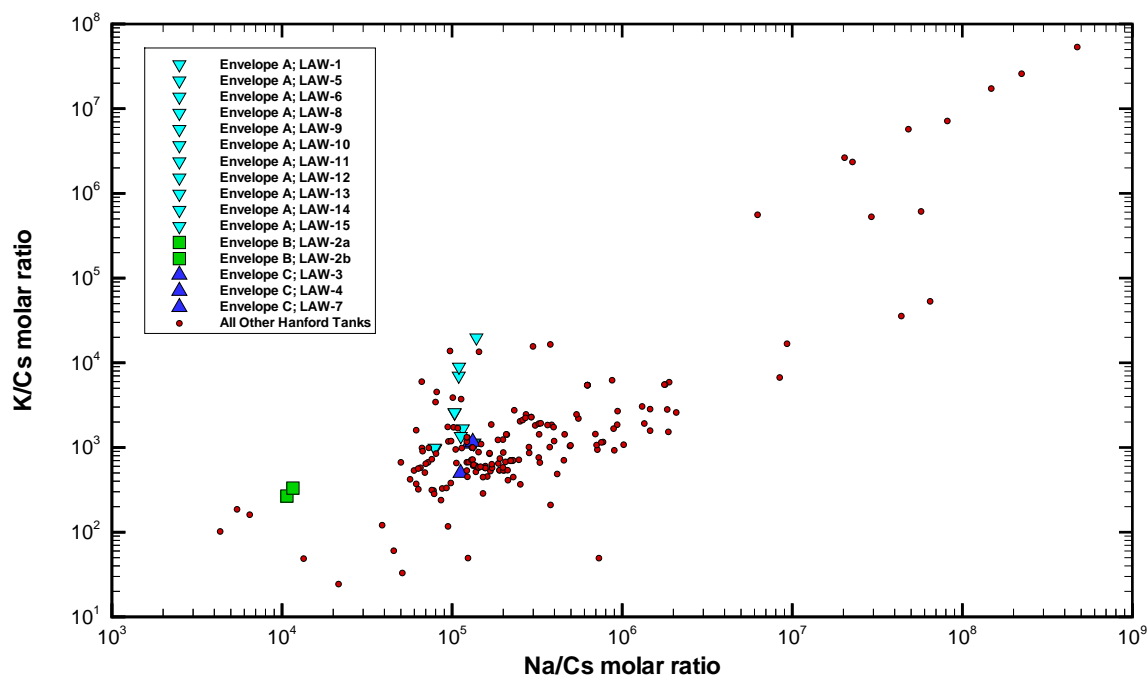


Figure B-5. LAW molar ratios of Na/Cs versus K/Cs for all 177 Hanford waste tanks. The Phase 1 LAW batch feeds are highlighted using larger symbols.

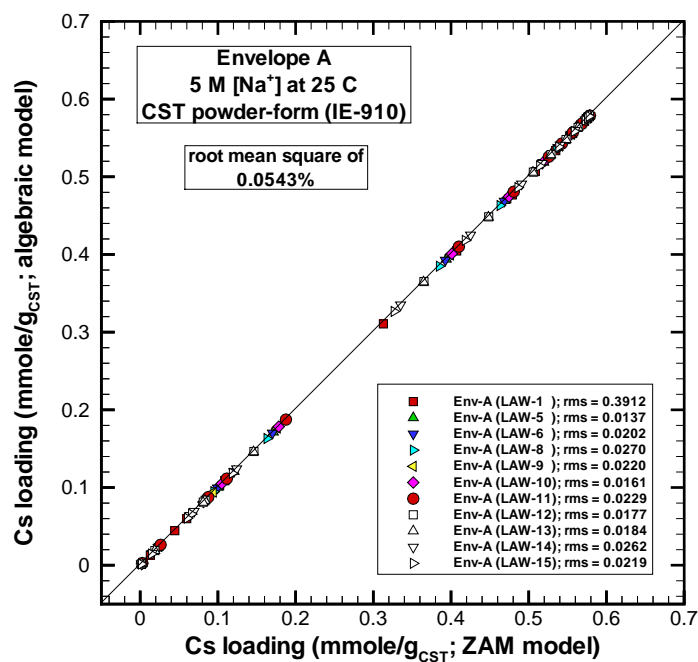


Figure B-6. Comparison of ZAM model versus “effective” single-component Freundlich/Langmuir Hybrid isotherm model predictions for cesium loadings on CST material in the powder-form (IE-910) for the eleven Envelope A candidate feed solutions.

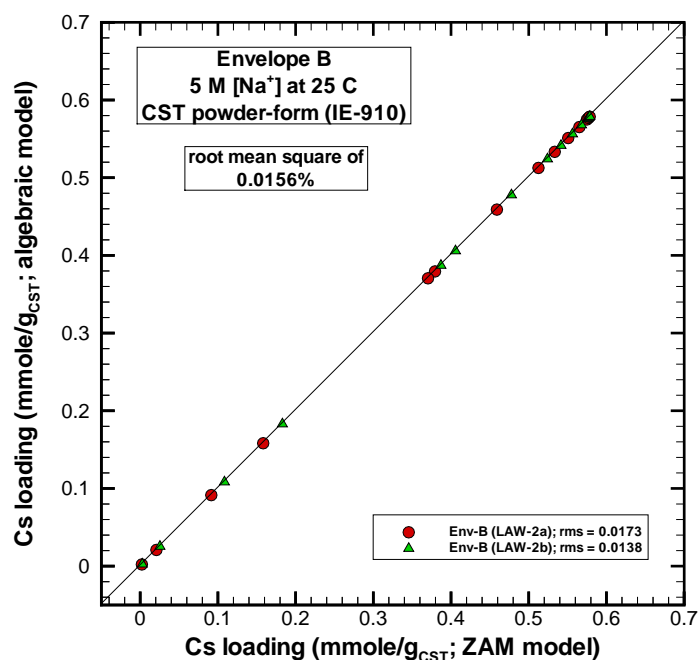


Figure B-7. Comparison of ZAM model versus “effective” single-component Freundlich/Langmuir Hybrid isotherm model predictions for cesium loadings on CST material in the powder-form (IE-910) for the two Envelope B candidate feed solutions.

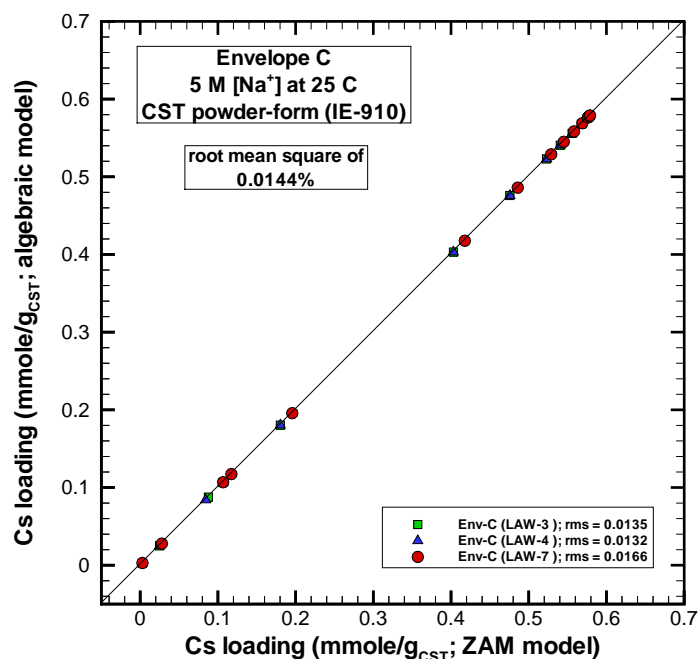


Figure B-8. Comparison of ZAM model versus “effective” single-component Freundlich /Langmuir Hybrid isotherm model predictions for cesium loadings on CST material in the powder-form (IE-910) for the three Envelope C candidate feed solutions.

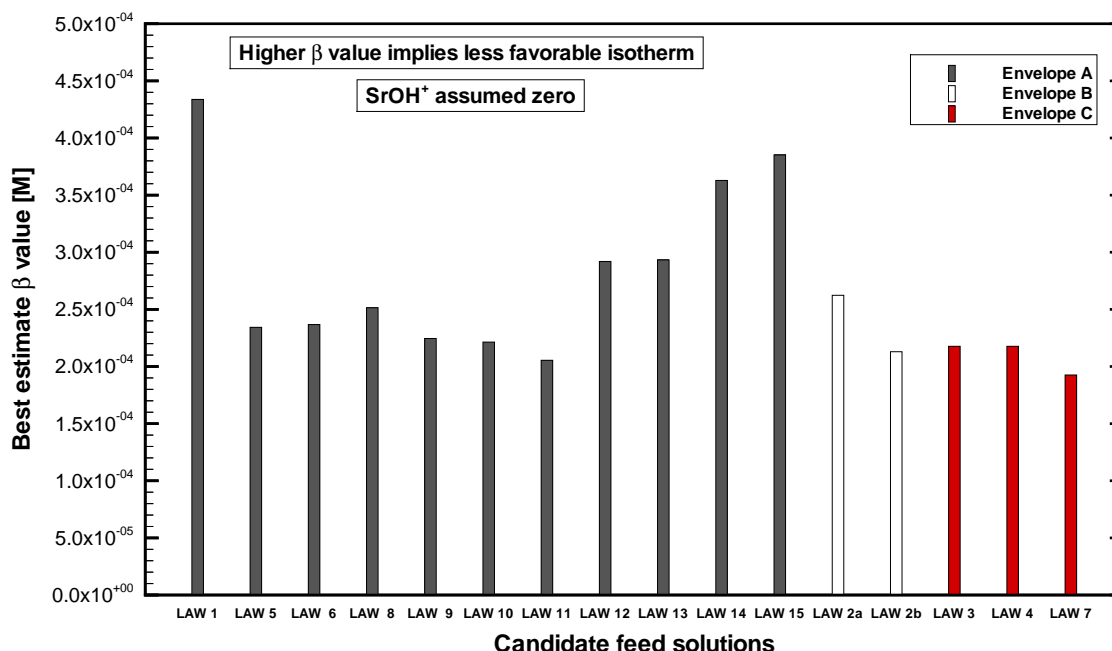


Figure B-9. The estimated Phase 1 feed beta values used in the cesium effective single-component isotherm model for CST powder-form and engineered-form materials. The beta values are grouped by envelope and are based on feeds assuming zero  $\text{Rb}^+$  and  $\text{SrOH}^+$  present.

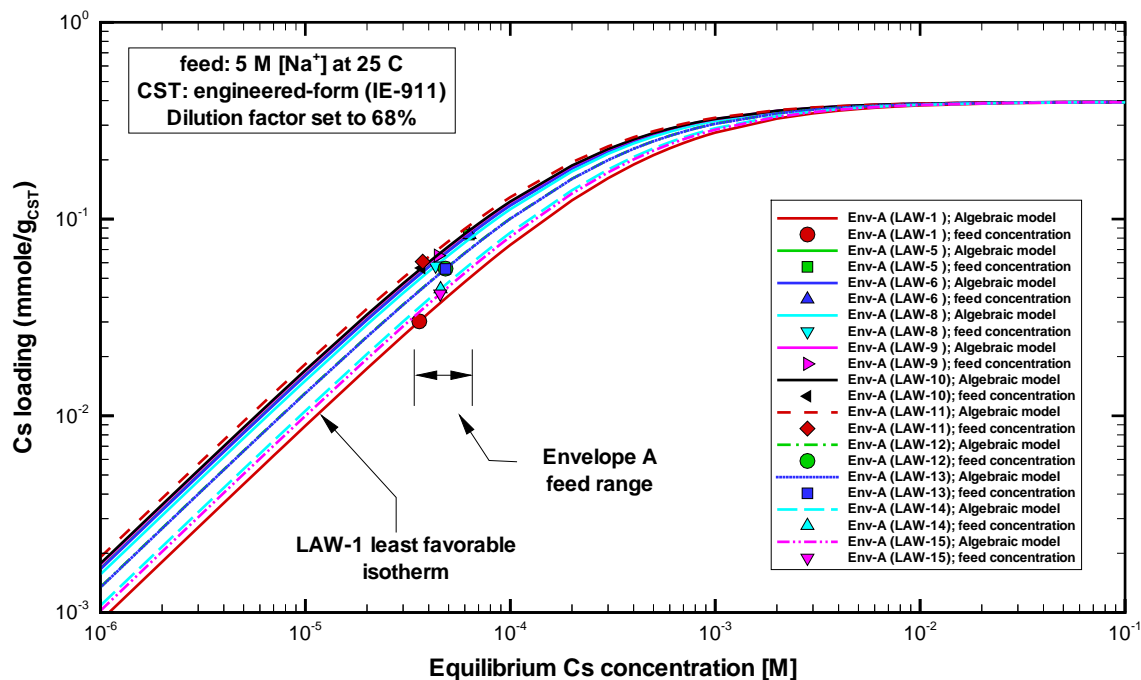


Figure B-10. Comparison of Envelope A isotherms for the CST material in its engineered-form (IE-911). The lines represent predictions based on the “effective” single-component Freundlich/Langmuir Hybrid isotherm model and symbols indicate the feed concentrations of cesium.

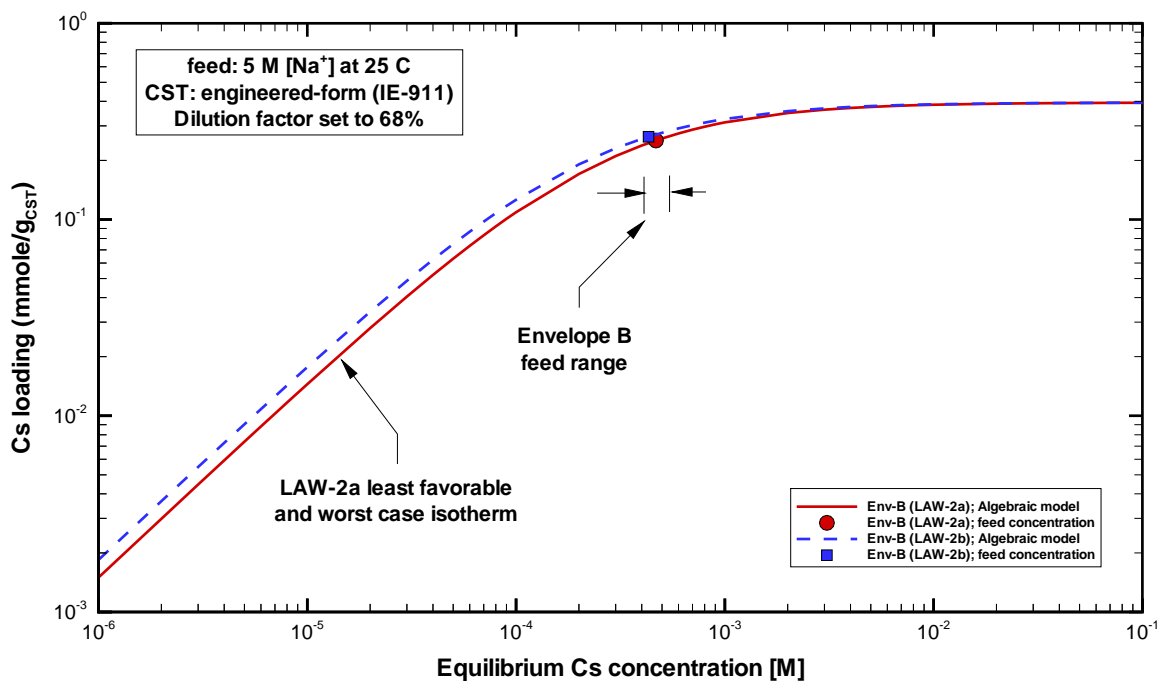


Figure B-11. Comparison of Envelope B isotherms for the CST material in its engineered-form (IE-911). The lines represent predictions based on the “effective” single-component Freundlich/Langmuir Hybrid isotherm model and symbols indicate cesium feed concentrations.

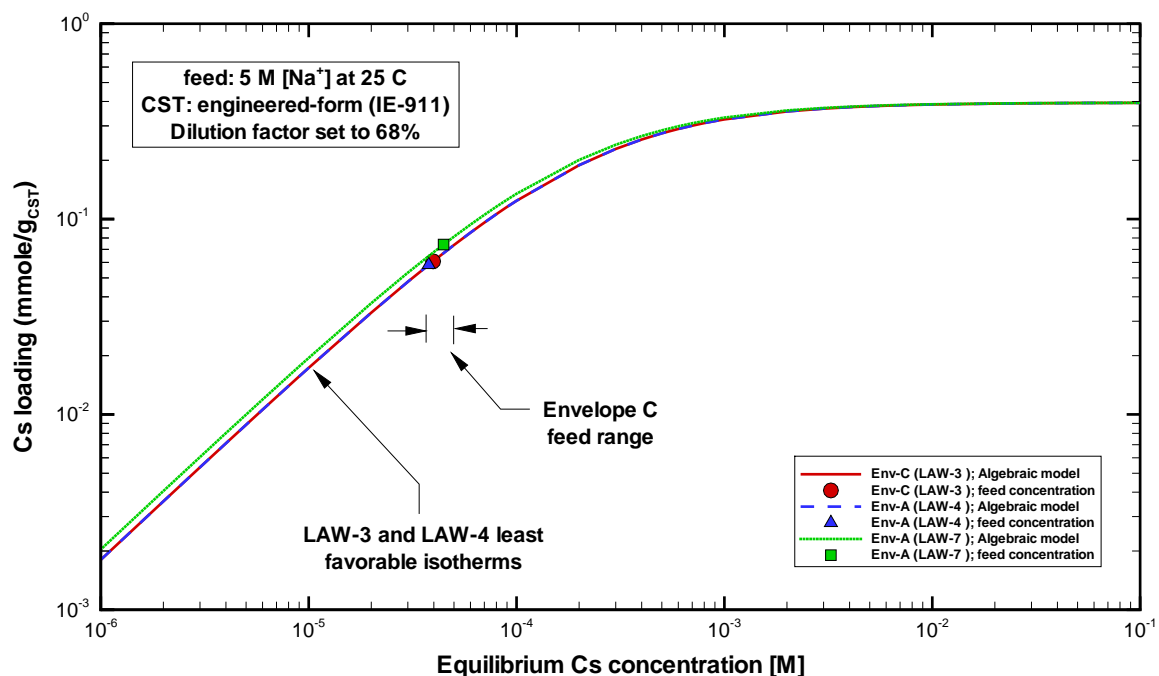


Figure B-12. Comparison of Envelope C isotherms for the CST material in its engineered-form (IE-911). The lines represent predictions based on the “effective” single-component Freundlich/Langmuir Hybrid isotherm model and symbols indicate cesium feed concentrations.

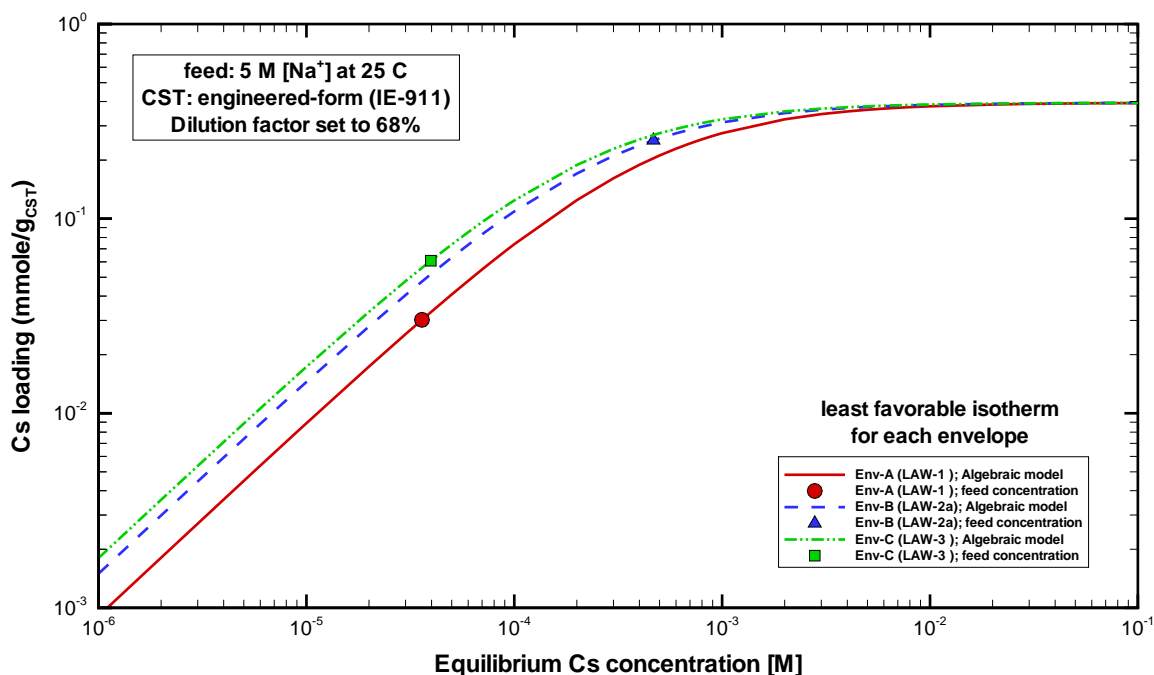


Figure B-13. Comparison of the least favorable isotherms for Envelope A, B, and C feeds for the CST material in its engineered-form (IE-911). The lines represent predictions based on the “effective” single-component Freundlich/Langmuir Hybrid isotherm model.

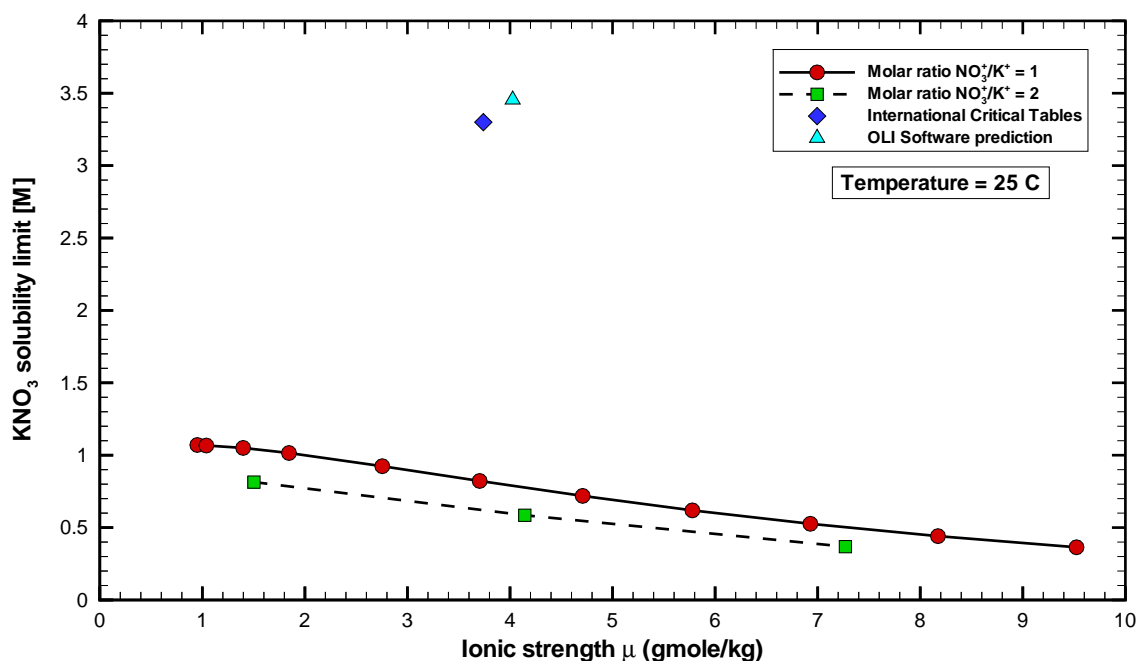


Figure B-14. Comparison of ZAM model predicted versus experimental (Washburn et al., 1928) KNO<sub>3</sub> solubility limit at 25 C (also shown is OLI version 6.5 prediction). For ZAM predictions NaOH was added to see the ionic strength effect.



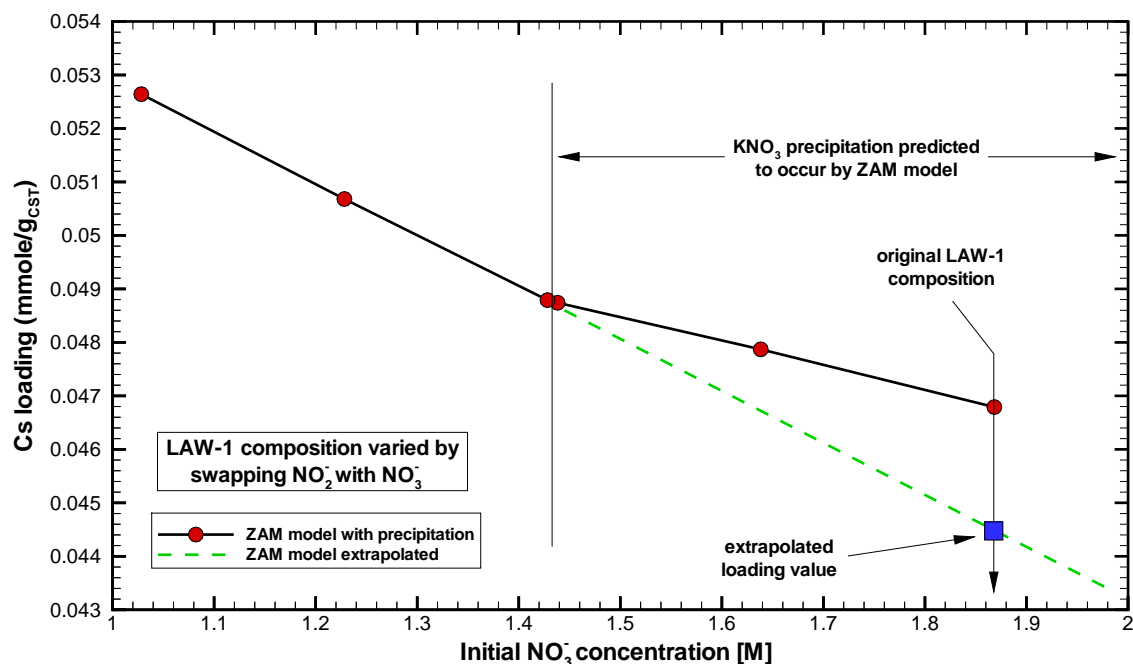


Figure B-15. Predicted impact for cesium loading on CST engineered-form material upon a swapping of nitrate with nitrite starting with a nominal solution of LAW-1 feed at 5.0 M  $\text{Na}^+$  and 25 C (the effect with [solid line] and without [dashed line]  $\text{KNO}_3$  precipitation is shown).

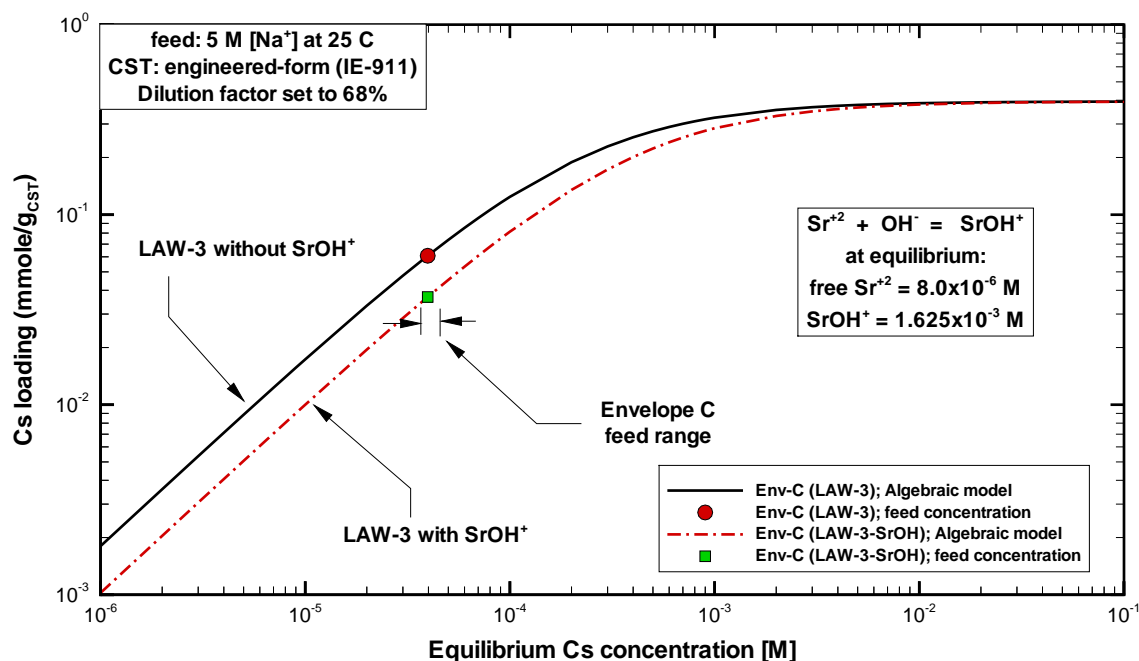


Figure B-16. Estimated impact of aqueous strontium hydroxide on cesium loadings for CST engineered-form material starting with a nominal solution of LAW-3 feed at 5.0 M  $\text{Na}^+$  and 25 C (zero  $\text{SrOH}^+$  present [solid line] and upper bound of  $\text{SrOH}^+$  present [dashed line]).

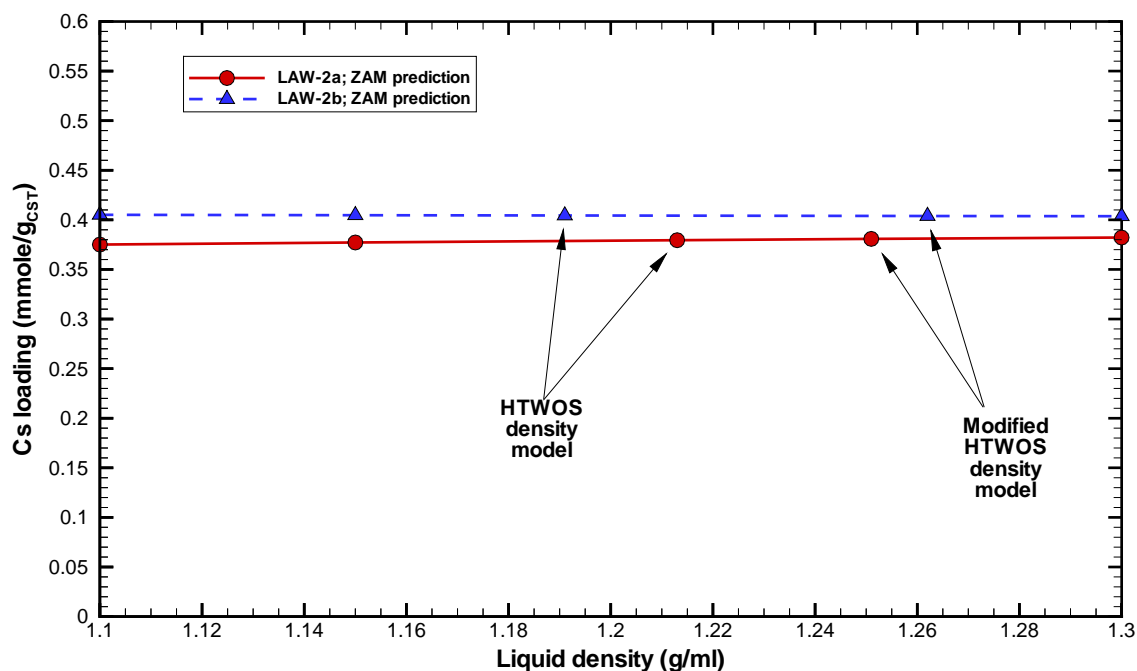


Figure B-17. Predicted impact of solution density on ZAM prediction of cesium loading on CST material based on LAW-2a and LAW-2b feeds at 5.0 M Na<sup>+</sup> and 25 C (the modified HTWOS density model values represent nominal conditions).

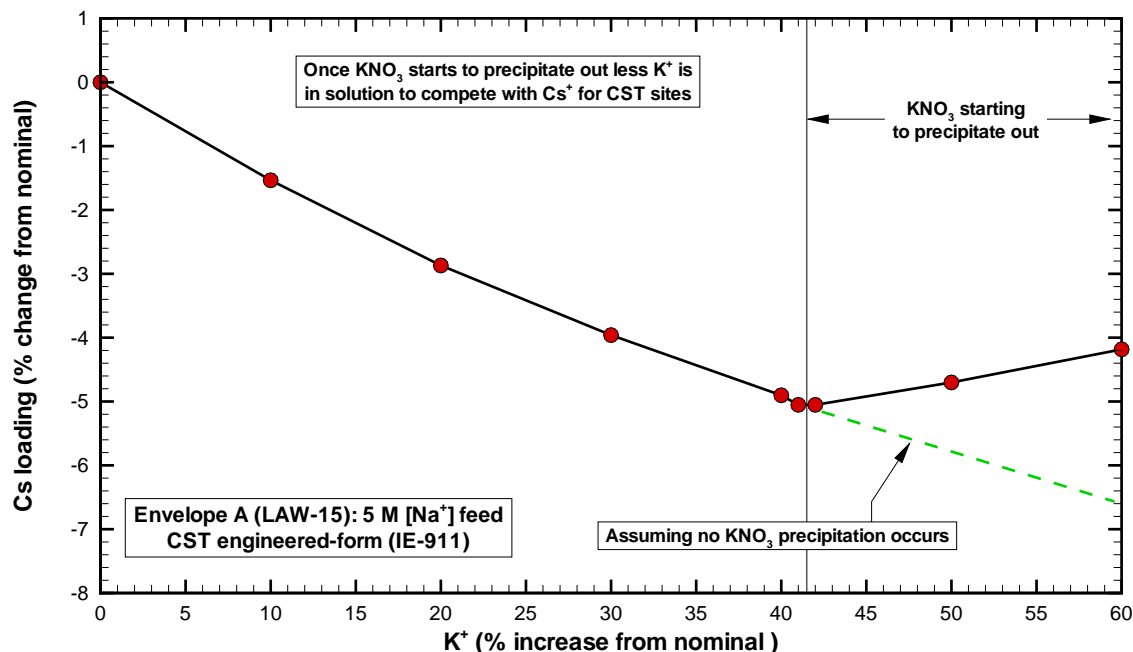


Figure B-18. Predicted impact for cesium loading on CST engineered-form material upon an increase in potassium concentration starting with a nominal solution of LAW-15 feed at 5.0 M Na<sup>+</sup> and 25 C (the effect with [solid line] and without [dashed line] KNO<sub>3</sub> precipitation is shown).

## Appendix C (Dilution Factor for IONSIV® IE-911)

The basic ion exchange material is originally in a powder-form (i.e., very fine particles) and is referred to by UOP as IE-910 (and earlier on in its development phase by Texas A&M University as TAM-5). In order to make use of this ion exchanger an “engineered-form” must be generated and ultimately processed at a production level. The selectivity and capacity characteristics of the ion exchanger are addressed primarily from the powder-form perspective. The smaller the particles the more improved the mass transfer rates will be, while in contrast, the larger the flow resistance (pressure drop) through a packed bed. Therefore, an optimal size particle potentially exists for the engineered-forms.

The IE-910 material is too fine for optimal use in large-scale ion-exchange columns. Commercial development of an engineered-form referred to by UOP as IE-911 has been underway during the later part of the 90’s focusing on achieving optimal mass transfer efficiency within optimally sized particles. During the manufacturing production process of IONSIV® IE-911 material, an inert binder is added to IE-910 powder to create an engineered form that consists of larger sized particles made up from binding together numerous fine particles of IE-910. The additional inert binding material reduces the total “effective” Cs ion-exchange capacity on a per weight basis and this reduction factor is referred to as its “dilution factor”.

Typically, the engineered forms of IE-911 contain approximately 25-to-30% by mass inert binder. If during the production process, the inert binder does not chemically alter the CST or block off assessable surface adsorption sites; then, the resulting total cesium capacity of the IE-911 resin would simply be 70-to-75% of its original IE-910 powder value. For an engineered-form this is probably its upper limit. For example, for an engineered-form containing 30% binder this would result in a total Cs<sup>+</sup> exchange capacity of:

$$[\bar{C}_T]_{Cs}^{Engineered-Form} = \left( 0.58 \frac{\text{mmole}_{Cs}}{g_{\text{powder}}} \right) \left( 0.70 \frac{g_{\text{powder}}}{g_{CST}} \right) \Rightarrow 0.406 \frac{\text{mmole}_{Cs}}{g_{CST}}, \quad (C-1a)$$

and for SrOH<sup>+</sup>:

$$[\bar{C}_T]_{SrOH}^{Engineered-Form} = \left( 1.00 \frac{\text{mmole}_{SrOH}}{g_{\text{powder}}} \right) \left( 0.70 \frac{g_{\text{powder}}}{g_{CST}} \right) \Rightarrow 0.700 \frac{\text{mmole}_{SrOH}}{g_{CST}}, \quad (C-1b)$$

where it is assumed that the dilution factor is not species dependent.

The powder-form total ionic capacities used in Eqs. (C-1) are those based on the original development of TAM-5 and reported by Zheng et al. (1996). During the crystal growth process in making CST powder several solid-phases can result. One particular solid-phase produces a material with superior Cs selectivity. The current manufacturer (i.e., UOP) states that their process improvements result in CST powder that is “better” than earlier batches by optimizing the growth of this particular solid-phase. This implies that the newer powder-form batches should have higher total ionic capacities than the values stated above.

To obtain a better estimate and basis for the dilution factor, comparisons are made between ion-exchange data for the more recent engineered-forms versus its original powder-forms. During the mid-90's the CST materials were tested using Hanford waste solutions. More recently, the SRS has been testing the CST materials using SRS waste solutions and newer engineered-forms. Below, analyses are presented that establish our "best estimate" of this dilution factor. The value ultimately chosen, 68%, represents our best estimate of its value for the Baseline engineered-form and based on the various other engineered-forms this value appears to be conservative (i.e., ~85% confidence level, mean minus one sigma). The use of 68% for the dilution factor sets a CST material acceptance criterion that should be reasonably achieved by the manufacturer of the CST engineered-forms.

After writing this appendix the work of Anthony et al. (2001) was provided to the authors. Anthony et al. (2001) upgraded the ZAM model to take into account the effect of the binder used to make CST in its engineered-forms. Based on SRS average simulant at 25 C, the improved ZAM predictions for IE-911 granules when compared to the ZAM predictions for CST powder yield a dilution factor of ~73%. This value is very consistent with the data provided in this report where the conservative value of 68% is used.

### C.1 Cesium loading on IONSIV® IE-911 versus IONSIV® IE-910

Recently, using SRS-average simulant,  $K_d$  equilibrium contact tests were performed by Walker et al. (2001) at SRTC. The composition of the SRS-average simulant is given in Table C-1, along with the composition of various other simulants studied. A comparison of the cesium  $K_d$  data at 36.2 C is shown in Figure C-1 and the data is tabulated in Table C-2. This data set contains one set of data using the powder-form and three using engineered-forms. Similar data by Walker et al. (2001) taken at other temperatures are provided in Table C-3 and by Fondeur et al. (2000) in Table C-4. The powder-form data provided corresponds to the same batch of powder-form used in the creation of the Baseline and New IE-911 batches. The engineered-form Old IE-911 was made using an older powder-form not listed here. Figure C-2 presents the same data sets in terms of the cesium loading.

Figures C-1 and C-2 indicate that the engineered-forms have consistently less selectivity than the powder-form when viewed on a per mass basis. The engineered-forms Baseline IE-911 and Old IE-911 are production level batches, while New IE-911 is a smaller lab-scale batch. The variability between the three engineered-forms result from:

- Two different powder-forms were used in creating the three batches;
- The fraction of inert binder added may have been different for the three batches; and
- The production techniques were different (e.g., lab-scale versus production-scale).

For determining an appropriate "best estimate" dilution factor we restrict our analysis to comparing the Baseline IE-911 to its New IE-910 powder. In this way, we are comparing only the impact of adding inert binder at the production-scale level to a specific powder-form. To estimate the level of variability observed between differing batches of engineered-form CST material, dilution factors are computed and compared for the more recent data sets available.

## C.2 Averaged Dilution Factor for Baseline IE-911 CST Material

In order to establish cesium isotherms for Envelopes A, B, and C, the Texas A&M equilibrium isotherm model (i.e., ZAM) is being used. The ZAM model is based on CST in its powder-form (i.e., actually TAM-5 powder-form from an earlier state around 1995). To make use of the ZAM model, adjustments must be made to its predictions when being applied to CST in its engineered-forms. Below we discuss a proposed way in which to make such adjustments. Typically, the engineered forms of IE-911 contain inert binder at approximately 25-to-30% by mass. If during the production process, the inert binder does not chemically alter the CST or block off assessable surface adsorption sites; then, the resulting total cesium capacity of the IE-911 resin would simply be 70-to-75% of its original IE-910 powder value. For an engineered-form this is probably its upper limit.

At any given equilibrium cesium concentration a dilution factor between IE-911 and IE-910 can be computed based on:

$$\eta_{df}(c_{Cs}) \equiv \left( \frac{Q_{Cs}^{IE-911}}{Q_{Cs}^{IE-910}} \right) . \quad (C-2)$$

Over the range of the data being considered the cesium loading curve can be expressed as:

$$Q_{Cs}^{IE-91x} = a^{IE-91x} [c_{Cs}]^{b^{IE-91x}} , \quad (C-3)$$

which represents a linear line on a log-log plot (i.e., linearity is observed at lower cesium concentrations with nonlinear behavior beginning to occur at higher concentrations). Substitution of Eq. (C-3) into Eq. (C-2) results in an expression for the dilution factor given by:

$$\eta_{df}(c_{Cs}) = \left[ \frac{a^{IE-911}}{a^{IE-910}} \right] [c_{Cs}]^{(b^{IE-911} - b^{IE-910})} . \quad (C-4)$$

In principle the dilution factor should be a true constant; however, due to analytical uncertainties the value computed using Eq. (C-4) will vary some. To eliminate the variation an algebraically averaged value over the entire cesium data range is computed using:

$$\langle \eta_{df} \rangle = \left[ \frac{1}{c_{Cs}^{max} - c_{Cs}^{min}} \right] \left[ \int_{c_{Cs}^{min}}^{c_{Cs}^{max}} \eta_{df}(c'_{Cs}) dc'_{Cs} \right] , \quad (C-5)$$

where upon substitution of Eq. (C-4) into Eq. (C-5a) and integrating yields

$$\langle \eta_{df} \rangle = \frac{a^{IE-911}}{a^{IE-910} (c_{Cs}^{max} - c_{Cs}^{min}) (b^{IE-911} - b^{IE-910} + 1)} . \quad (C-6)$$

The cesium loading data at 36.2 C by Walker et al. (2001) for the Baseline IE-911 and its New IE-910 powder are shown in Figure C-3. The data correspond to newer powder-form CST (i.e.,

solid circles), along with a production version baseline of engineered-form CST made using the new powder-form (i.e., solid triangles). As shown in Figure C-3, the equilibrium cesium concentration ranges from  $\sim 3 \times 10^{-7}$  to  $\sim 7 \times 10^{-5}$  M. Also shown in Figure C-3 are the power-law (i.e., Eq. (C-3)) fits to the cesium loading data (i.e., solid-line representing the powder-form fit and dashed-line representing the engineered-form fit). The power-law fits represent the data well over the range being considered. For comparison purposes the power-law Eq. (C-3) was fitted to all of the CST material presented in Table C-2. The a and b coefficients to the power-law equation for each material is listed in Table C-5, along with their integral average dilution factor estimate.

Making use of Eq. (C-4), point values of the dilution factor can be computed as tabulated in Table C-5. For example, for the Baseline IE-911 material we see the dilution factor varying from 75.5% at its lowest cesium concentration to 61.0% at its highest value. Using the power-law fits, the average deviation over the entire cesium concentration range was computed to be  $\sim 68\%$  based on Eq. (C-6). Also shown in Figure C-3, are the ranges of inlet cesium feed concentrations for each Hanford LAW envelope and the lag column exit cesium criterion.

Conservatively, for our current column transport efforts we shall set the total  $\text{Cs}^+$  exchange capacity to:

$$[\overline{C}_T]_{\text{Cs}}^{\text{Engineered-Form}} = \left( 0.58 \frac{\text{mmole}_{\text{Cs}}}{g_{\text{powder}}} \right) \left( 0.68 \frac{g_{\text{powder}}}{g_{\text{CST}}} \right) \Rightarrow 0.3944 \frac{\text{mmole}_{\text{Cs}}}{g_{\text{CST}}} , \quad (\text{C-7a})$$

and for  $\text{SrOH}^+$  to:

$$[\overline{C}_T]_{\text{SrOH}}^{\text{Engineered-Form}} = \left( 1.00 \frac{\text{mmole}_{\text{SrOH}}}{g_{\text{powder}}} \right) \left( 0.68 \frac{g_{\text{powder}}}{g_{\text{CST}}} \right) \Rightarrow 0.680 \frac{\text{mmole}_{\text{SrOH}}}{g_{\text{CST}}} . \quad (\text{C-7b})$$

In Figure C-4 the same set of data as shown in Figure C-3 is re-plotted. However, the power-law fits as shown in Figure C-3 are now replaced with ZAM predictions. The solid-curve represents the ZAM predictions for the powder-form material. Using as a constant dilution factor, 68%, the adjusted ZAM predictions are shown as a dashed-curve. Also shown in Figure C-4, are the ranges of inlet cesium feed concentrations for each envelope and the lag column exit criterion.

In the log-log plot shown in Figure C-4, both sets of data exhibit approximately linear behavior, while the ZAM model shows slight curvature at increasing cesium concentrations due to the finite/fixed amount of exchange sites available within the model. The current manufacturer (i.e., UOP) states that their process improvements result in CST powder that is “better” than earlier batches. The data sets at the high cesium concentration test conditions, show slight up-turns in loading. This might indicate that a slightly increased total cesium exchange capacity may exist or a varying capacity exists at higher cesium concentration levels; however, no explicit attempts to take credit for this is proposed. From an overall perspective the two predictions appear reasonable and the estimated dilution factor falls below its expected maximum bound of 70-to-75%.

Based on these simple analyses we propose to use this dilution factor for the CST column simulations. Above an average dilution factor was computed based on equilibrium contact tests performed at 36.2 C. Below we shall address the impact on the isotherm when at lower operating temperatures and its variation dependence on cesium concentration.

### C.3 Dilution Factor Variability

As stated above, the expectation is that for a specific batch of the engineered-form the dilution factor is a true constant and not a function of temperature or liquid composition. Unfortunately, the currently available batch contact data produces dilution factors with a modest variation in magnitude. Below we shall show the computed variation and compare it to the earlier average value of 0.68 for the Baseline IE-911 material (i.e., estimated using a power-law/integration method).

#### C.3.1 Impact of Cesium Concentration

As discussed in Appendix B, an effective single-component total cesium isotherm can be expressed as:

$$Q_{Cs} = \frac{\eta_{DF} \bar{C}_T c_{Cs}}{c_{Cs} + [\tilde{K}_{21} c_K + \tilde{K}_{31} c_{Na} + \tilde{K}_{41} c_{SrOH} + \dots]} \Rightarrow \frac{\eta_{DF} \bar{C}_T c_{Cs}}{c_{Cs} + \beta}, \quad (C-8)$$

where the beta parameter for cesium becomes dependent upon the other ionic competitors for CST exchange (i.e.,  $K^+$ ,  $Na^+$ ,  $SrOH^+$ , and  $Rb^+$ ). The beta parameter contains the selectivity coefficients making it dependent upon temperature and liquid composition. The dilution factor ( $\eta_{DF}$ ) is unity when considering a specific powder-form and is less than one upon addition of an inert binder. The total cesium capacity term is only a function of which batch of powder-form material is being considered.

Assuming that the New IE-910 powder-form material has the total cesium capacity of 0.58 mmole/g<sub>CST</sub>, Eq. (C-8) was fitted to various available batch contact data to estimate beta values for different liquid compositions and temperatures. The results of the fitting process are listed in Table C-6. For each batch contact data point obtained for each engineered-form, the appropriate beta value was used and a dilution factor was estimated. Averaged values (i.e., original plus duplicate measurement values) for the equilibrium cesium concentration and cesium loading were used in computing these parameters. These results are also listed in Table C-6. Here we are making the reasonable assumption that the beta value for the engineered-form is the same as the value for its powder-form when considering data at the same temperature and nearly the same liquid composition.

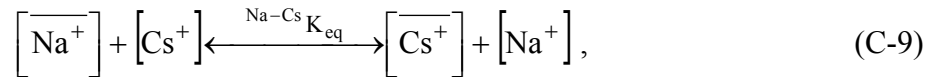
The calculated variation observed in dilution factor is shown in Figure C-5 with respect to equilibrium cesium concentration. Three different batches of engineered-forms are provided, with each batch represented by a different symbol. No apparent explanation can be provided at this time for the level of variation observed. Also provided is the sample mean and one standard deviation values for the dilution factor estimates shown as horizontal lines (i.e., mean the solid-

line and the mean minus one standard deviation the dashed-line). The mean minus one standard deviation value of  $\sim 0.66$  is very close to the computed average value of 0.68 for the Baseline material.

Given the variability within the estimated dilution factors, partly stemming from data uncertainties and actual batch variability, the average value of 0.68 still appears acceptable.

### C.3.2 Impact of Temperature

During the loading phase of column operation cesium ions are replacing sodium ions at surface sites. This is the dominant ion-exchange reaction occurring when the more selective cesium ion takes a surface site as expressed by the mass-action relation:



where the bar over a species implies that it resides on a surface site. Ion exchange is not a chemical reaction and generally occurs with little evolution or uptake of heat (see Helfferich, 1962). Therefore, the temperature dependence of ion-exchange equilibria is usually minor. For the mass-action relationship expressed by Eq. (C-9) when using CST material we have an exothermic heat of ion-exchange (i.e.,  $\Delta H_{\text{IX}} < 0$ ). The temperature dependence of ion-exchange equilibria is given by the thermodynamic relation:

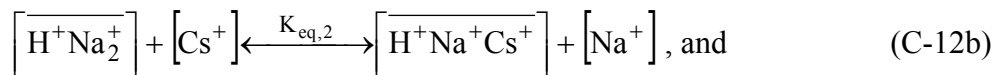
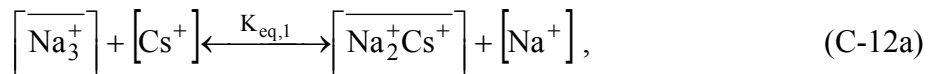
$$\left( \frac{d \ln K_{\text{eq}}}{dT} \right)_p = \frac{\Delta H_{\text{IX}}}{RT^2}. \quad (\text{C-10})$$

Assuming that the heat of ion-exchange is constant, Eq. (C-10) can be integrated resulting in:

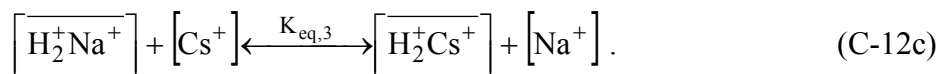
$$\ln \left( \frac{K_{\text{eq},2}}{K_{\text{eq},1}} \right) = -\frac{\Delta H_{\text{IX}}}{R} \left[ \frac{1}{T_2} - \frac{1}{T_1} \right]. \quad (\text{C-11})$$

When considering an exothermic reaction, Eq. (C-11) states that a rise in temperature will reduce the thermodynamic equilibrium constant. For our ion-exchange process, this results in reduced cesium adsorption at higher temperatures.

In the ZAM model, Zheng et al. (1997) are using a triple-site (i.e., super-site) concept that can be justified based on the differences measured in total ionic capacities for the various competitors. Ion exchange of cesium with a super-site on the CST material is represented by the set of mass-action relations:







The estimated values of the heat of ion-exchange for Eqs. (C-12) are reported by Zheng et al. (1997) to be:

- Eq. (C-12a)  $\Delta H_{\text{IX}} = -2.18 \times 10^4$  J/gmole;
- Eq. (C-12b)  $\Delta H_{\text{IX}} = 1.46 \times 10^4$  J/gmole; and
- Eq. (C-12c)  $\Delta H_{\text{IX}} =$  not recorded (probably small).

For cesium removal during the loading cycle the feed will be under very high pH conditions where the CST material will be predominately in its sodium form. Therefore, under these conditions the dominant mass-action reaction expected to be occurring is expressed by Eq. (C-12a) resulting in an overall exothermic reaction. The above ZAM modeling parameters are based on batch contact data over a broad pH range covering a temperature range of 25 to 44 C (see Zheng et al. (1996,1997)). In the ZAM model the total ionic capacity values are constants, not a direct function of temperature.

Walker et al. (2001) have recently measured the temperature dependence of several CST materials for cesium loading. Their data are tabulated in Table C-3. For the new powder-form IE-910 material, a comparison of the measured to ZAM predicted cesium loadings is provided in Figure C-6 (also showing the data point by Fondeur et al. (2000)). As can be seen in Figure C-6, both the measured and the predicted loading curves show reduced cesium loadings at higher temperatures, consistent with the above arguments. As observed earlier the ZAM model under-predicts the cesium loading measured for the new powder-form material at these liquid cesium concentrations. However, the ZAM model shifts the isotherms approximately the same amount as indicated by the data.

The temperature dependence of the computed point values for the dilution factor is shown in Figure C-7 based on the data provided in Table C-6. Similar to the comments made for the cesium concentration dependence observed, no apparent explanation can be provided at this time for the level of variation observed.

#### C.4 Cesium Loading Curve Comparisons

Using the ZAM code to predict CST powder-form behavior and the average dilution factor value of 68% to adjust the ZAM results to predict CST engineered-form behavior, several other data sets are compared. Walker et al. (2001) also measured cesium loadings using same standard simulant composition typical used by UOP for their performance testing (i.e., see Table C-1 for UOP simulant composition). Their data is tabulated in Table C-6 and is plotted in Figures C-8 and C-9. Figure C-8 contains the only the Baseline data and its powder-form data similar to the plot shown in Figure C-4 for direct comparison. The shift in the data (i.e., powder-form to engineered-form) is consistent with the shift computed with ZAM. However, as seen in Figure C-4, ZAM under-predicts the cesium loadings at these higher cesium concentration levels. To

see the variability in cesium loading due to batch differences among engineered-forms, Figure C-9 is a close-up of Figure C-8 where the data for the other two engineered-forms has been added.

Similar data was taken by Fondeur et al. (2000) at 25 C using SRS-average simulant. This data is listed in Table C-4 and is plotted in Figure C-10. Excellent agreement is seen between the powder-form and Baseline engineered-form data and their corresponding ZAM predictions.

Cesium loadings were also measured for the Baseline CST material (IE-911) using actual waste samples taken from SRS Tank 44 by Walker et al. (1997). The composition of the SRS Tank 44 samples is given in Table C-1 and the data obtained from the batch contact testing is listed in Table C-7. A comparison of the data to the ZAM predictions is shown in Figure C-11. The data is for the Baseline engineered-form of CST, while the dashed-curve represents the ZAM prediction of the engineered-form of CST. Unfortunately, the data follows the powder-form predictions of ZAM at the lower tested cesium concentrations and then falls on the engineered-form predictions of ZAM at the highest tested cesium concentration. This behavior can not be explained at this time, but does indicate to some extent why there has been a lot of confusion historically over the issue of whether or not a dilution factor is required. The low concentration data would suggest that no dilution effects occur (i.e., a dilution factor of unity), while the highest concentration indicates a dilution effect of 68% occurs.

Batch contact tests based on some of the earlier CST forms was performed by McCabe (1995) for powder-form CST (DG-112) and by McCabe (1997) for engineered-form CST (38b). Both sets of tests were done at ~25 C using the same SRS simulant. The composition of the SRS simulant used is given in Table C-1 and the test data is listed in Table C-8. A comparison of the data to ZAM predictions is shown in Figure C-12. The ZAM predictions compare favorably to the data, where the data supports the use of a constant dilution factor of ~68%.

Some of the key properties for the various CST materials considered above is provided in Table C-9.

## C.5 Strontium Loading Curve Comparisons

Walker et al. (2001) also performed a series of batch contact tests at 36.2 C using the SRS-average simulant spiked with  $\text{Sr}^{+2}$  at an initial concentration of  $1.141 \times 10^{-5}$  M. Measured strontium  $K_d$  and loading values are listed in Table C-10. ZAM predictions for both the powder-form and engineered-form were also computed and a comparison to the experimental data is provided in Figure C-13. As shown in Figure C-13, the three different engineered-forms have similar strontium loading values; however, the powder-form values appear to be inconsistent when compared to the engineered-form values.

In general the ZAM predictions have similar behavior when viewed with the engineered-form data (i.e., loading values are somewhat in the same ballpark). However, overall the comparisons between the data and/or predictions are poor.

Table C-1. Ionic species molar concentrations for simulated waste solutions used in ZAM batch contact simulations for estimating the dilution factor.

Species ID	SRS Average simulant [M]	SRS High OH <sup>-</sup> simulant [M]	SRS Tank 44 sample [M]	UOP simulant [M]	McCabe simulant [M]	TAM Exp1 [M]
<b>Cations</b>						
Na <sup>+</sup>	5.6	5.6	5.4	5.7	5.55	5.7
Cs <sup>+</sup> <sup>a</sup>	1.4x10 <sup>-4</sup>	3.7x10 <sup>-4</sup>	3.51x10 <sup>-4</sup>	7.4403x10 <sup>-4</sup>	2.4x10 <sup>-4</sup>	1.0x10 <sup>-4</sup>
K <sup>+</sup>	0.015	0.03	0.051	-	0.015	-
H <sup>+</sup>	5.2x10 <sup>-15</sup>	3.3x10 <sup>-15</sup>	2.3x10 <sup>-15</sup>	1.7x10 <sup>-15</sup>	3.4x10 <sup>-15</sup>	1.7x10 <sup>-14</sup>
<b>Anions</b>						
NO <sub>3</sub> <sup>-</sup>	2.14	1.1	0.37	5.1	1.2152	5.1
NO <sub>2</sub> <sup>-</sup>	0.52	0.74	0.35	-	0.71	-
Cl <sup>-</sup>	0.025	3.637x10 <sup>-2</sup>	0.009	7.4403x10 <sup>-4</sup>	-	-
F <sup>-</sup>	0.032	0.01	-	-	-	-
OH <sup>-</sup> (free)	1.938	3.05	4.3	0.6	2.9	0.6
Al(OH) <sub>4</sub> <sup>-</sup>	0.31	0.27	0.126	-	-	-
CO <sub>3</sub> <sup>2-</sup>	0.16	0.17	0.1412	-	0.2	-
SO <sub>4</sub> <sup>2-</sup>	0.15	0.03	0.001	-	0.17	-
PO <sub>4</sub> <sup>3-</sup>	0.01	0.008	0.0001	-	-	-
Cations =	5.615	5.630	5.451	5.701	5.565	5.700
Anions =	-5.615	-5.630	-5.451	-5.701	-5.565	-5.700
Sum =	0.000	0.000	0.000	0.000	0.000	0.000

<sup>a</sup> For varying Cs the nominal SRS-average value for 1x10<sup>-4</sup> M is adjusted where the total concentration of Cs plus Na is maintained constant. No variation in liquid sample composition occurred for the UOP experiments.

Table C-2. Cesium batch contact test data taken by Walker et al. (2001) for various batches of CST material in contact with SRS-average simulated waste samples at 36.2 C.

CST Form	Batch Name <sup>a</sup>	Na Concentration [M]	Cs Equilibrium Concentration [M]	Cs K <sub>d</sub> (ml/g <sub>CST</sub> )	Cs loading (mmole/g <sub>CST</sub> )
powder	New IE-910 (?)	5.59939	3.8557E-05	2040.98	7.8695E-02
		5.59939	4.0307E-05	2038.93	8.2183E-02
		5.59999	9.0107E-06	1747.32	1.5745E-02
		5.59999	8.9799E-06	1762.20	1.5824E-02
		5.60011	1.8895E-06	1682.41	3.1789E-03
		5.60011	1.6621E-06	1937.59	3.2204E-03
		5.60013	3.7494E-07	1689.98	6.3365E-04
		5.60013	3.5027E-07	1758.94	6.1610E-04
Engineered	Baseline (9090-76)	5.59939	5.7745E-05	1508.1	8.7083E-02
		5.59939	6.2271E-05	1370.2	8.5321E-02
		5.59999	1.3578E-05	1231.9	1.6727E-02
		5.59999	1.5117E-05	1098.2	1.6602E-02
		5.60011	2.6678E-06	1233.5	3.2906E-03
		5.60011	2.6514E-06	1207.3	3.2010E-03
		5.60013	6.5170E-07	1000.3	6.5189E-04
		5.60013	5.8351E-07	1105.9	6.4530E-04
Engineered	New IE-911 (30950-49)	5.59939	5.6684E-05	1373.3	7.7847E-02
		5.59939	6.3489E-05	1248.8	7.9283E-02
		5.59999	1.4273E-05	1072.8	1.5311E-02
		5.59999	1.3657E-05	1131.7	1.5456E-02
		5.60011	2.6940E-06	1133.6	3.0540E-03
		5.60011	2.7748E-06	1109.0	3.0773E-03
		5.60013	6.1033E-07	980.1	5.9819E-04
		5.60013	5.8064E-07	1045.8	6.0726E-04
Engineered	Old IE-911 (99-9)	5.59939	5.3253E-05	1539.0	8.1956E-02
		5.59939	5.3145E-05	1514.0	8.0462E-02
		5.59999	1.1487E-05	1424.0	1.6357E-02
		5.59999	1.1315E-05	1416.6	1.6028E-02
		5.60011	2.1228E-06	1523.7	3.2345E-03
		5.60011	2.0731E-06	1555.5	3.2246E-03
		5.60013	4.3556E-07	1486.6	6.4750E-04
		5.60013	4.3003E-07	1465.8	6.3033E-04

<sup>a</sup> The engineered-forms Baseline IE-911 and New IE-911 were made using the power-form New IE-910 material. The Old IE-911 engineered-form material was made using an earlier batch of power-form IE-910.

Table C-3. Cesium batch contact test data taken by Walker et al. (2001) for various batches of CST material in contact with SRS-average simulated waste samples at different temperatures.

CST Form	Batch Name <sup>a</sup>	Temperature (C)	Na Equilibrium Concentration [M]	Cs Equilibrium Concentration [M]	Cs K <sub>d</sub> (ml/g <sub>CST</sub> )	Cs loading (mmole/g <sub>CST</sub> )
powder	New IE-910 (?)	36.2	5.59939	3.8557E-05	2040.98	7.8695E-02
		36.2	5.59939	4.0307E-05	2038.93	8.2183E-02
		30.2	5.59939	4.0075E-05	2056.68	8.2420E-02
		30.2	5.59939	3.8060E-05	2175.98	8.2817E-02
		26.7	5.59940	3.4254E-05	2246.30	7.6944E-02
		26.7	5.59940	3.4254E-05	2369.63	8.1169E-02
Engineered	Baseline (9090-76)	36.2	5.59939	5.7745E-05	1508.07	8.7083E-02
		36.2	5.59939	6.2271E-05	1370.16	8.5321E-02
		30.2	5.59939	4.9254E-05	1807.22	8.9012E-02
		30.2	5.59939	5.0075E-05	1773.76	8.8820E-02
		26.7	5.59940	4.7239E-05	1839.95	8.6917E-02
		26.7	5.59940	4.3881E-05	1933.33	8.4836E-02
Engineered	New IE-911 (30950-49)	36.2	5.59939	5.6684E-05	1373.34	7.7847E-02
		36.2	5.59939	6.3489E-05	1248.78	7.9283E-02
		30.2	5.59939	5.0821E-05	1576.51	8.0120E-02
		30.2	5.59939	5.1493E-05	1571.19	8.0905E-02
		26.7	5.59940	4.6343E-05	1748.13	8.1014E-02
		26.7	5.59940	4.6791E-05	1698.47	7.9473E-02
Engineered	Old IE-911 (99-9)	36.2	5.59939	5.3253E-05	1538.99	8.1956E-02
		36.2	5.59939	5.3145E-05	1514.02	8.0462E-02
		30.2	5.59939	4.2985E-05	1875.92	8.0637E-02
		30.2	5.59939	4.1418E-05	1945.68	8.0586E-02
		26.7	5.59940	4.1418E-05	1982.71	8.2120E-02
		26.7	5.59940	3.8955E-05	2101.12	8.1850E-02

<sup>a</sup> The engineered-forms Baseline IE-911 and New IE-911 were made using the power-form New IE-910 material. The Old IE-911 engineered-form material was made using an earlier batch of power-form IE-910.

Table C-4. Cesium batch contact test data taken by Fondeur et al. (2000) for two batches of CST material in contact with SRS-average simulated waste samples at 25 C.

CST Form	Batch Name <sup>a</sup>	Temperature (C)	Na Equilibrium Concentration [M]	Cs Equilibrium Concentration [M]	Cs K <sub>d</sub> (ml/g <sub>CST</sub> )	Cs loading (mmole/g <sub>CST</sub> )
powder	New IE-910 (?)	25.0	5.6	1.2243E-05	2087.0	2.5551E-02
Engineered	Baseline (9090-76)	25.0	5.6	1.5909E-05	1560.0	2.4818E-02

<sup>a</sup> The engineered-form Baseline IE-911 was made using the power-form New IE-910 material.

Table C-5. Power-law coefficients based on cesium loading data taken by Walker et al. (2001) for various batches of CST material in contact with SRS-average simulated waste samples at 36.2 C.

CST Form	Batch Name	Power-law coefficient a	Power-law coefficient b	Integral average dilution factor <sup>a</sup>
powder	New IE-910 (?)	2631.6	1.0293	1.0 (reference)
Engineered	Baseline (9090-76)	2370.5	1.0560	0.680
Engineered	New IE-911 (30950-49)	2011.7	1.0479	0.628
Engineered	Old IE-911 (99-9)	1506.8	1.0009	0.772

<sup>a</sup> The integrated average dilution factor, based on Eq. (C-5b), was obtained using as the lower and upper cesium concentration integration limits,  $3 \times 10^{-7}$  M and  $7 \times 10^{-5}$  M, respectively. The power-law fit for the New IE-910 powder is used for each dilution factor estimate.

Table C-6. Estimated dilution factors based on an “effective” single component homovalent isotherm model of the cesium loading curve computed for selected SRS batch contact data <sup>a</sup>.

CST Form	Batch Name	Liquid sample	T (C)	Equilibrium Cs <sup>c</sup> [M]	Cs loading <sup>c</sup> (mmole/g <sub>CST</sub> )	Beta parameter <sup>d</sup>	Total capacity parameter	Dilution Factor
Powder	New-IE-910 (?)	SRS-Avg	36.2	-	-	3.057E-04 <sup>b</sup>	0.580 (specified)	1.000 (reference)
			30.2			2.352E-04		
			26.7			2.170E-04		
			25.0			2.657E-04		
		UOP	36.2			5.3290E-04		
Engineered	Baseline-IE-911 (9090-76)	SRS-Avg	36.2	6.0008E-05	8.6202E-02	2.4489E-04	0.438	0.755
		SRS-Avg	36.2	1.4347E-05	1.6664E-02	3.2154E-04	0.390	0.673
		SRS-Avg	36.2	2.6596E-06	3.2458E-03	3.2012E-04	0.394	0.679
		SRS-Avg	36.2	6.1761E-07	6.4860E-04	3.3620E-04	0.354	0.610
		UOP	36.2	1.1555E-04	7.7318E-02	5.3290E-04	0.434	0.748
		SRS-Avg	30.2	4.9664E-05	8.8916E-02	2.3519E-04	0.510	0.879
		SRS-Avg	26.7	4.5560E-05	8.5876E-02	2.1705E-04	0.495	0.853
		SRS-Avg	25.0	1.5909E-05	2.4818E-02	2.6567E-04	0.439	0.757
Engineered	New-IE-911 (30950-49)	SRS-Avg	36.2	6.0087E-05	7.8565E-02	2.4489E-04	0.399	0.688
		SRS-Avg	36.2	1.3965E-05	1.5383E-02	3.2154E-04	0.370	0.637
		SRS-Avg	36.2	2.7344E-06	3.0656E-03	3.2012E-04	0.362	0.624
		SRS-Avg	36.2	5.9549E-07	6.0272E-04	3.3620E-04	0.341	0.588
		UOP	36.2	1.2488E-04	7.1069E-02	5.3290E-04	0.374	0.645
		SRS-Avg	30.2	5.1157E-05	8.0512E-02	2.3519E-04	0.451	0.777
		SRS-Avg	26.7	4.6567E-05	8.0244E-02	2.1705E-04	0.454	0.783
Engineered	Old-IE-911 (99-9)	SRS-Avg	36.2	5.3199E-05	8.1209E-02	2.4489E-04	0.455	0.785
		SRS-Avg	36.2	1.1401E-05	1.6193E-02	3.2154E-04	0.473	0.815
		SRS-Avg	36.2	2.0979E-06	3.2296E-03	3.2012E-04	0.496	0.855
		SRS-Avg	36.2	4.3279E-07	6.3892E-04	3.3620E-04	0.497	0.857
		UOP	36.2	9.6517E-05	7.4439E-02	5.3290E-04	0.485	0.837
		SRS-Avg	30.2	4.2201E-05	8.0611E-02	2.3519E-04	0.530	0.914

CST Form	Batch Name	Liquid sample	T (C)	Equilibrium Cs <sup>c</sup> [M]	Cs loading <sup>c</sup> (mmole/g <sub>CST</sub> )	Beta parameter <sup>d</sup>	Total capacity parameter	Dilution Factor
		SRS-Avg	26.7	4.0187E-05	8.1985E-02	2.1705E-04	0.525	0.905
							Mean =	0.76
							Standard deviation =	0.10

<sup>a</sup> Data obtained from Walker et al. (2001) and Fondeur et al. (2000).

<sup>b</sup> Beta parameter value averaged over the cesium concentration range of  $3 \times 10^{-7}$  to  $7 \times 10^{-5}$  M, but is not used in calculating point dilution factor estimates.

<sup>c</sup> The cesium concentration and loading values are averages of the two tests performed for each data point (i.e., original sample plus its duplicate).

<sup>c</sup> The beta parameter value used for each dilution factor estimate is based on powder-form data at the temperature of interest and the nearest cesium concentration available.

Table C-7. Cesium batch contact test data taken by Walker et al. (1997) for the Baseline CST material in contact with SRS Tank 44 actual waste samples at 31 C. <sup>a</sup>

CST Form	Batch Name	Na Concentration [M]	Cs Equilibrium Concentration [M]	Cs K <sub>d</sub> (ml/g <sub>CST</sub> )	Cs loading (mmole/g <sub>CST</sub> )
Engineered	Baseline (9090-76)	5.40	2.3239E-03	147.1	3.4187E-01
		5.40	2.2409E-03	176.9	3.9642E-01
		5.40	3.1525E-05	2497.3	7.8727E-02
		5.40	3.2742E-05	2470.0	8.0873E-02
		5.40	3.3638E-05	2404.4	8.0879E-02
		5.40	6.2606E-06	2848.2	1.7831E-02
		5.40	7.0744E-06	2637.1	1.8656E-02
		5.40	6.3195E-06	2805.8	1.7731E-02
		5.40	2.8309E-06	2743.0	7.7653E-03
		5.40	2.7029E-06	2831.9	7.6545E-03
		5.40	1.0667E-07	3135.1	3.3444E-04
		5.40	1.0940E-07	3066.2	3.3543E-04

<sup>a</sup> The solution density was 1.2015 g/ml and its viscosity was 2.6 cP at 31 C.

Table C-8. Cesium batch contact test data taken by McCabe (1995 & 1997) for two CST materials in contact with a SRS simulant at 25 C. <sup>a</sup>

CST Form	Batch Name <sup>a</sup>	Temperature (C)	Na Equilibrium Concentration [M]	Cs Equilibrium Concentration [M]	Cs K <sub>d</sub> (ml/g <sub>CST</sub> )	Cs loading (mmole/g <sub>CST</sub> )
Powder	TAM-5 (DG-112)	25.0	5.599	3.8557E-05	2041.0	7.8695E-02
		25.0	5.599	4.0307E-05	2038.9	8.2183E-02
		25.0	5.600	9.0107E-06	1747.3	1.5745E-02
		25.0	5.600	8.9799E-06	1762.2	1.5824E-02
		25.0	5.600	1.8895E-06	1682.4	3.1789E-03
		25.0	5.600	1.6621E-06	1937.6	3.2204E-03
		25.0	5.600	3.7494E-07	1690.0	6.3365E-04
		25.0	5.600	3.5027E-07	1758.9	6.1610E-04
Engineered	Early batch (38B)	25.0	5.5500	3.6343E-05	1503.6	5.4646E-02
		25.0	5.5497	7.2761E-05	1770.0	1.2879E-01
		25.0	5.5495	1.1358E-04	1281.9	1.4560E-01
		25.0	5.5492	2.2881E-04	850.9	1.9470E-01
		25.0	5.5490	3.5940E-04	641.7	2.3062E-01
		25.0	5.5488	4.9321E-04	491.4	2.4235E-01
		25.0	5.5486	6.7448E-04	367.6	2.4793E-01

<sup>a</sup> These are CST materials early on in their development history.

Table C-9. Key CST exchange properties taken from literature.

CST Form	Batch Name	F Factor <sup>a</sup> (-)	Bulk Dry Density <sup>a</sup> (g/ml)	Dilution Factor <sup>c</sup> (-)	Cesium Total Ion-Exchange Capacity <sup>b</sup> (mmole/g)
SuperLig <sup>®</sup> 644	10-SM-171	0.9751	0.2238	Na	0.3333
powder	IE-910	0.9680	0.7738	1.0	0.580
powder	New-IE-910	0.8573	-	1.0	0.580
Engineered	IE-911 (38b)	0.8870	1.1300	not reported	not reported
Engineered	IE-911 (08)	0.8990	0.8999	not reported	not reported
Engineered	Baseline	0.7875	1.00	0.68	0.3944
Engineered	New-IE-911	0.8493	1.00	0.63	0.3654
Engineered	Old-IE-911	0.8331	1.00	0.77	0.4466

<sup>a</sup> Data obtained from Brown et al. (1996, Table 3.1) or Walker et al. (2001).

<sup>b</sup> Data obtained from Zheng et al. (1996) and confirmed by running ZAM at a very large liquid cesium concentration for the powder-form and estimated for the engineered-forms.

<sup>c</sup> During the manufacturing production process of IONSIV<sup>®</sup> IE-911 resin, an inert binder is added to CST powder to create an engineered form that is useable in ion-exchange columns. The additional inert binding material reduces the total Cs ion-exchange capacity and this reduction factor is referred to as its “dilution factor”.



Table C-10. Strontium batch contact test data taken by Walker et al. (2001) for various batches of CST material in contact with SRS-average simulated waste samples at 36.2 C.

CST Form	Batch Name <sup>a</sup>	Na Concentration [M]	Sr Equilibrium Concentration <sup>b</sup> [M]	Sr K <sub>d</sub> (ml/g <sub>CST</sub> )	Sr loading (mmole/g <sub>CST</sub> )
powder	New IE-910 (?)	5.60	1.297E-07	20096.5	2.606E-03
		5.60	1.235E-07	20545.1	2.537E-03
		5.60	7.608E-08	8682.3	6.605E-04
		5.60	6.577E-08	9952.4	6.546E-04
		5.60	5.527E-08	4781.3	2.643E-04
		5.60	5.694E-08	4629.6	2.636E-04
Engineered	Baseline (9090-76)	5.60	2.519E-07	11074.7	2.790E-03
		5.60	2.499E-07	11124.0	2.779E-03
		5.60	1.241E-07	5626.8	6.982E-04
		5.60	1.085E-07	6554.1	7.110E-04
		5.60	4.781E-08	5991.8	2.865E-04
		5.60	4.849E-08	5933.9	2.878E-04
Engineered	New IE-911 (30950-49)	5.60	2.261E-07	11445.2	2.588E-03
		5.60	2.419E-07	10144.2	2.454E-03
		5.60	1.057E-07	6215.3	6.571E-04
		5.60	1.052E-07	6266.2	6.594E-04
		5.60	4.840E-08	5520.3	2.672E-04
		5.60	5.272E-08	5062.5	2.669E-04
Engineered	Old IE-911 (99-9)	5.60	2.659E-07	9337.2	2.482E-03
		5.60	2.560E-07	10000.9	2.561E-03
		5.60	1.222E-07	5448.4	6.660E-04
		5.60	1.094E-07	6114.2	6.687E-04
		5.60	4.663E-08	5794.6	2.702E-04
		5.60	4.791E-08	5674.2	2.719E-04

<sup>a</sup> The engineered-forms Baseline IE-911 and New IE-911 were made using the power-form New IE-910 material. The Old IE-911 engineered-form material was made using an earlier batch of power-form IE-910.

<sup>b</sup> The initial Sr<sup>+2</sup> concentrations were all experimentally set to 1.141x10<sup>-5</sup> M. The actual free Sr<sup>+2</sup> concentrations available for forming aqueous SrOH<sup>+</sup> are unknown, but were assumed to be equal to the total Sr<sup>+2</sup> present.

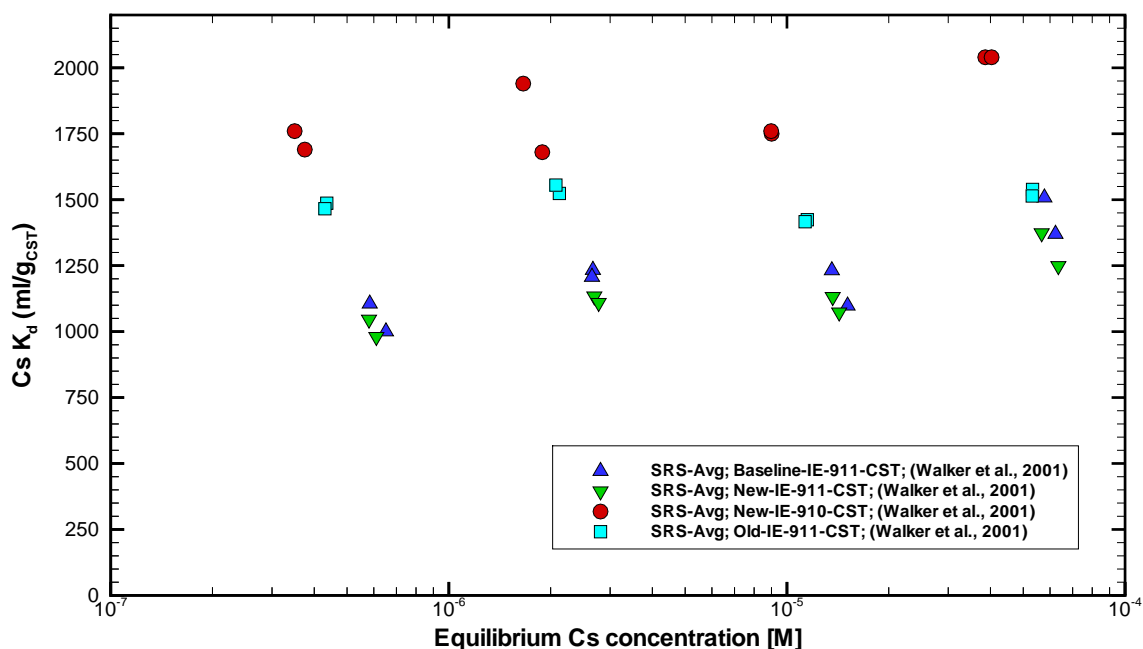


Figure C-1. Comparison of measured cesium  $K_d$  values for several CST batches taken by Walker et al. (2001) in contact with a SRS-average simulated waste sample at 36.2 C.

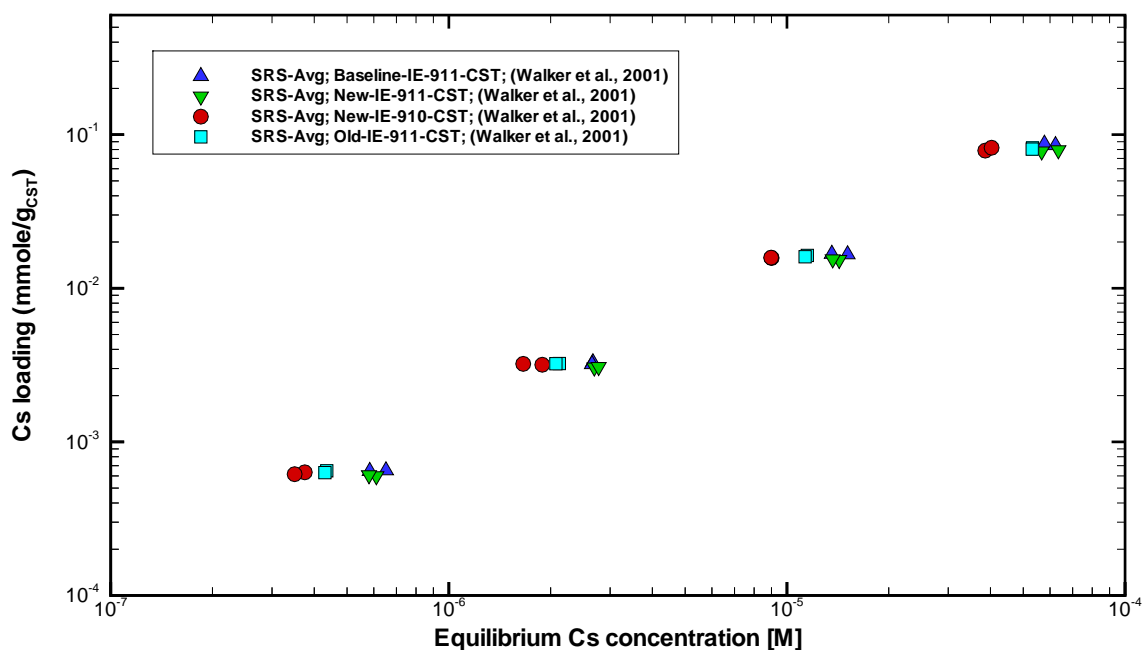


Figure C-2. Comparison of measured cesium loading values for several CST batches taken by Walker et al. (2001) in contact with a SRS-average simulated waste sample at 36.2 C.

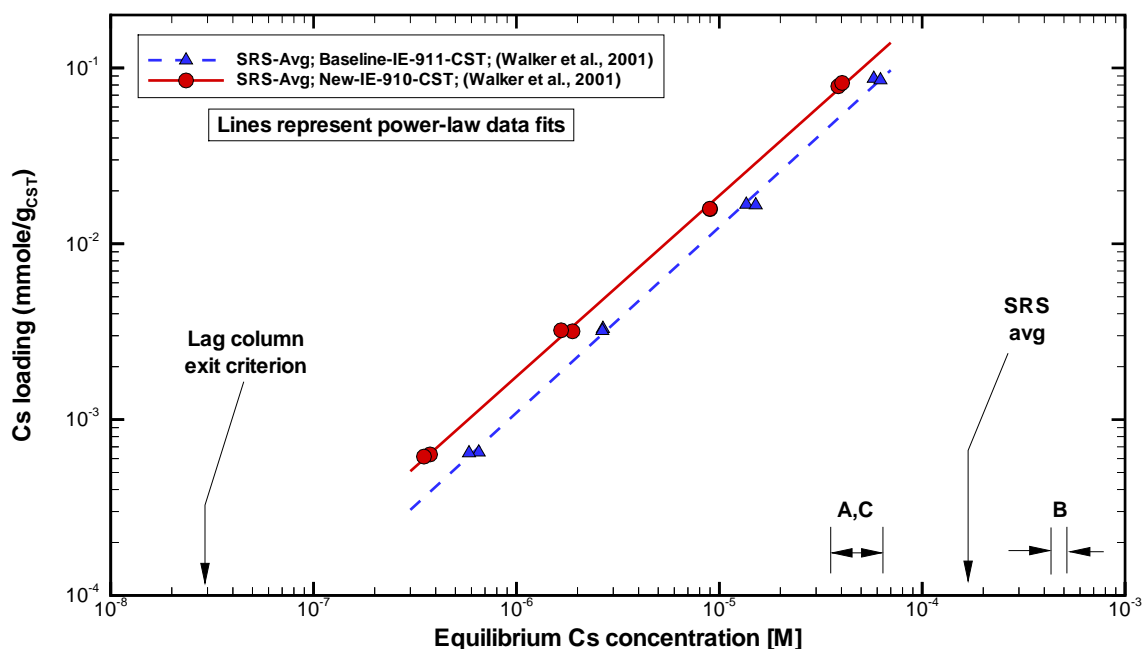


Figure C-3. Comparison of SRS-Avg simulant cesium CST loading data recently taken by Walker et al. (2001) to power-law fits through the data sets at 36.2 C.

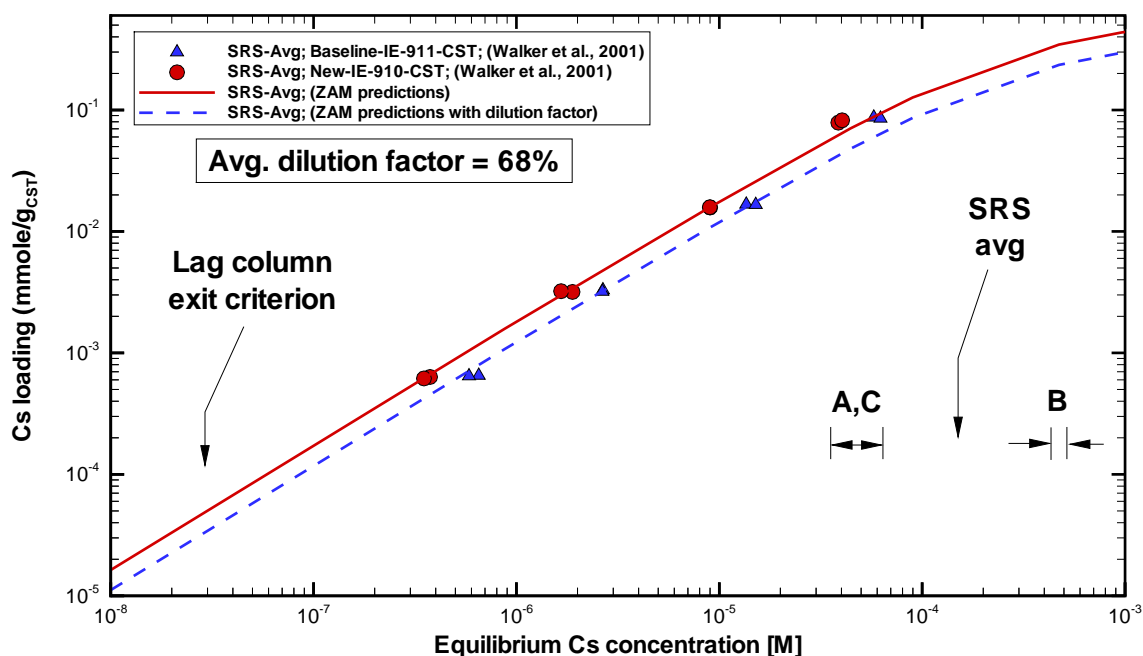


Figure C-4. Comparison of SRS-Avg simulant cesium CST loading data recently taken by Walker et al. (2001) to both best estimate and adjusted ZAM predictions at 36.2 C.

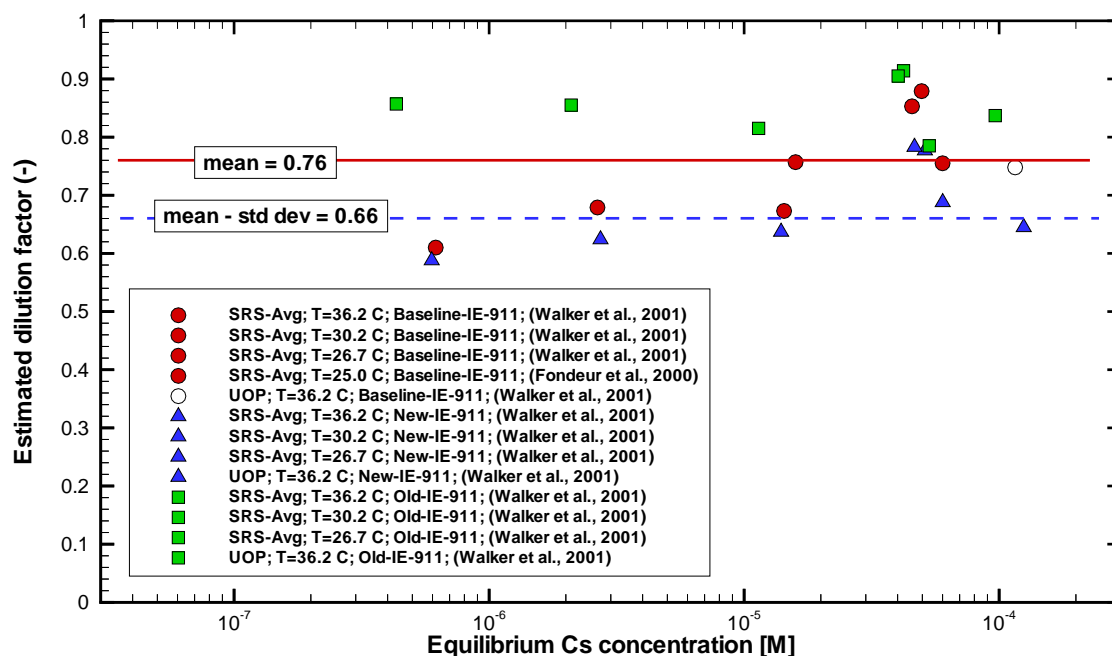


Figure C-5. Comparison of dilution factor for several CST batch contact data sets with respect to equilibrium cesium concentration.

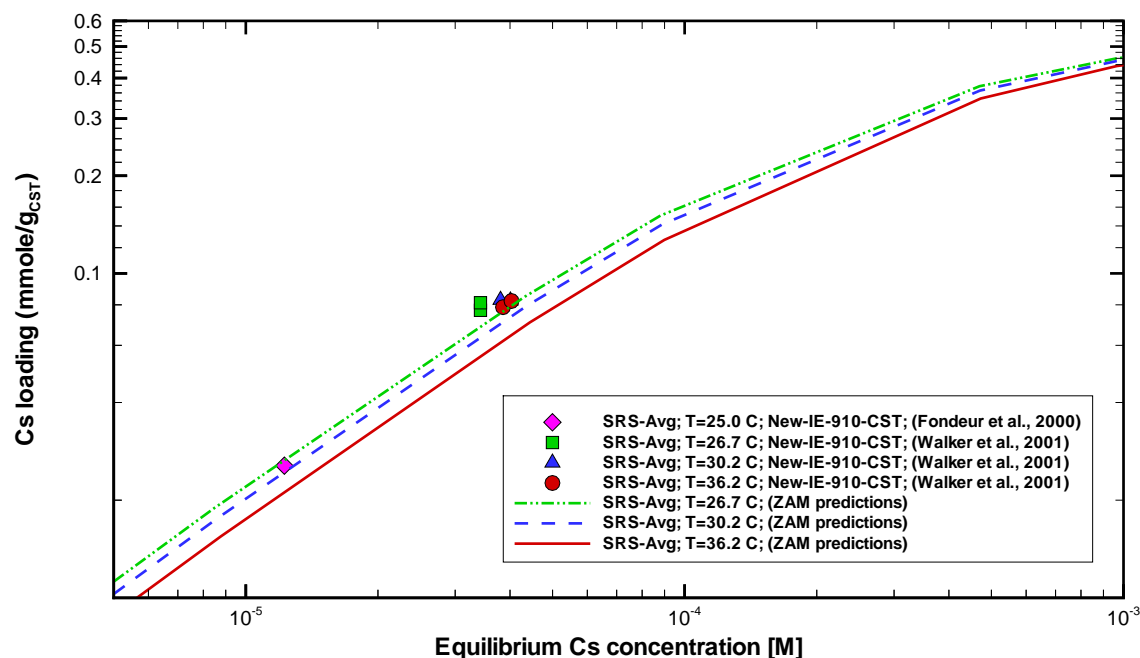


Figure C-6. Comparison of SRS-Avg simulant cesium CST (new powder-form) loading data taken by Fondeur et al. (2000) and Walker et al. (2001) to best estimate ZAM predictions at 26.7, 30.2, and 36.2 C.

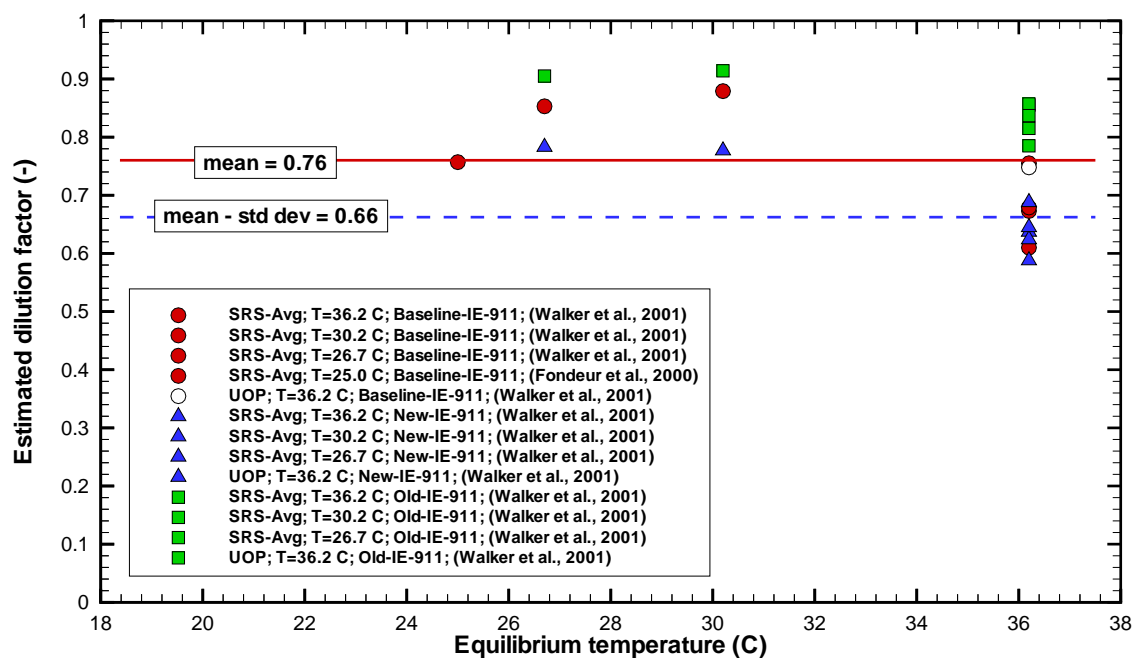


Figure C-7. Comparison of dilution factor for several CST batch contact data sets with respect to equilibrium contact temperature.

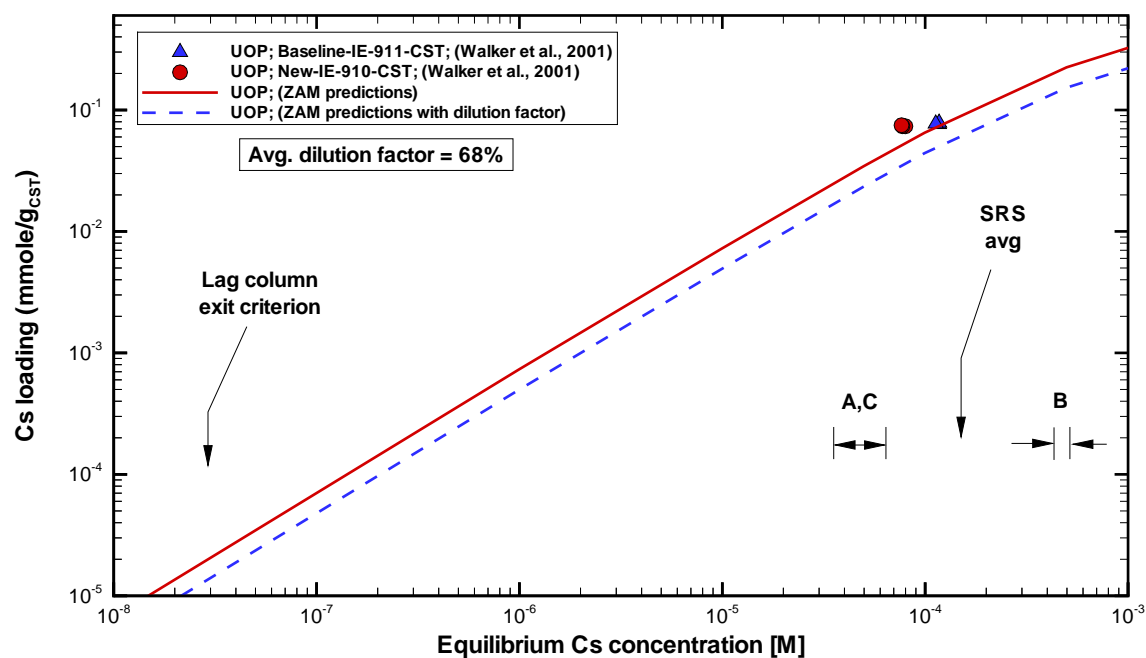


Figure C-8. Comparison of UOP simulant cesium CST loading data recently taken by Walker et al. (2001) to both best estimate and adjusted ZAM predictions at 36.2 C.

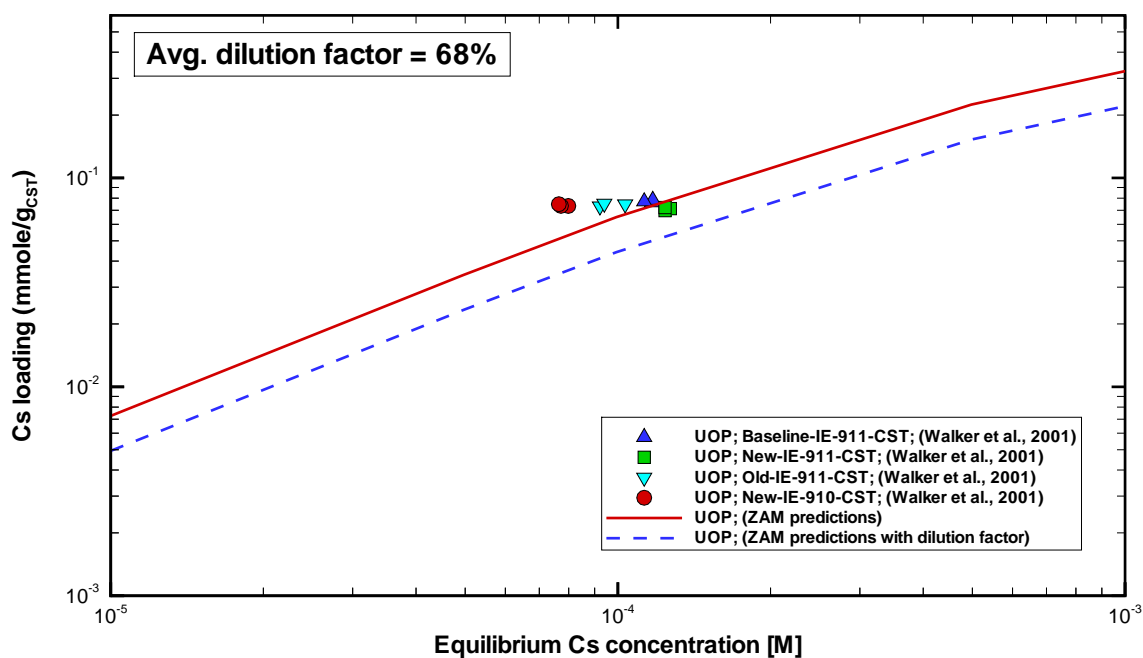


Figure C-9. A close-up comparison of UOP simulant cesium CST loading data recently taken by Walker et al. (2001) to both best estimate and adjusted ZAM predictions at 36.2 C.

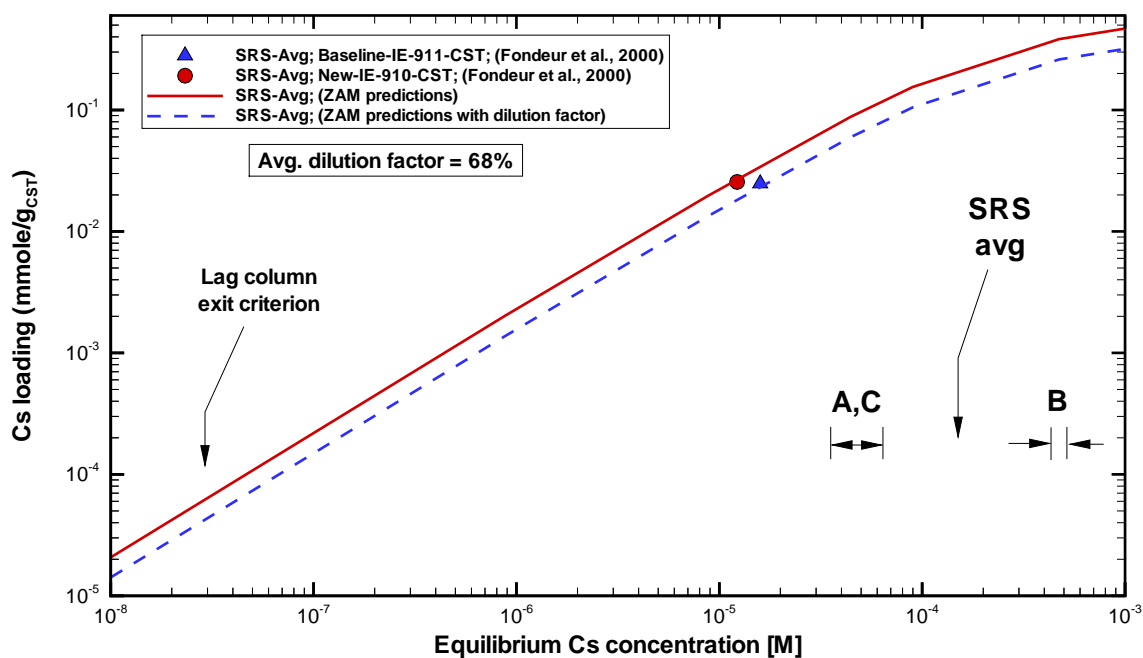


Figure C-10. Comparison of SRS-Avg simulant cesium CST loading data taken by Fondeur et al. (2000) to both best estimate and adjusted ZAM predictions at ~25 C.

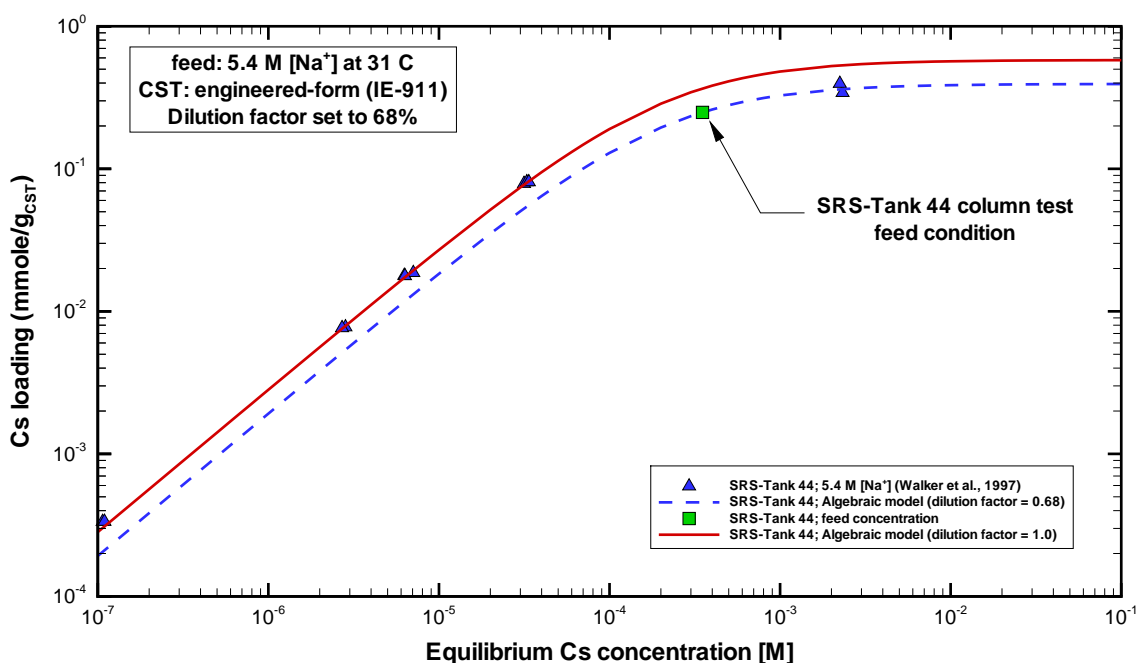


Figure C-11. Comparison of SRS-Tank 44 sample cesium CST loading data taken by Walker et al. (1997) to both best estimate and adjusted ZAM predictions at 31 C.

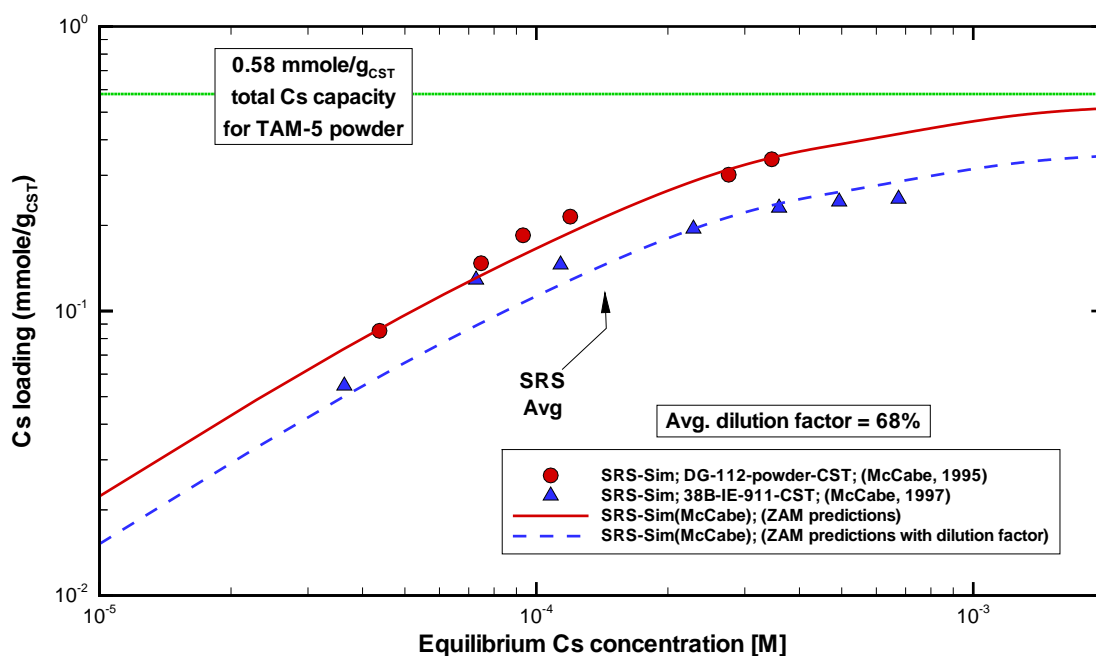


Figure C-12. Comparison of SRS simulant cesium loading data on CST powder and an early on engineered-form material taken by McCabe (1995 [powder data] and 1997 [engineered-form data]) to both best estimate and adjusted ZAM predictions at ~25 C.

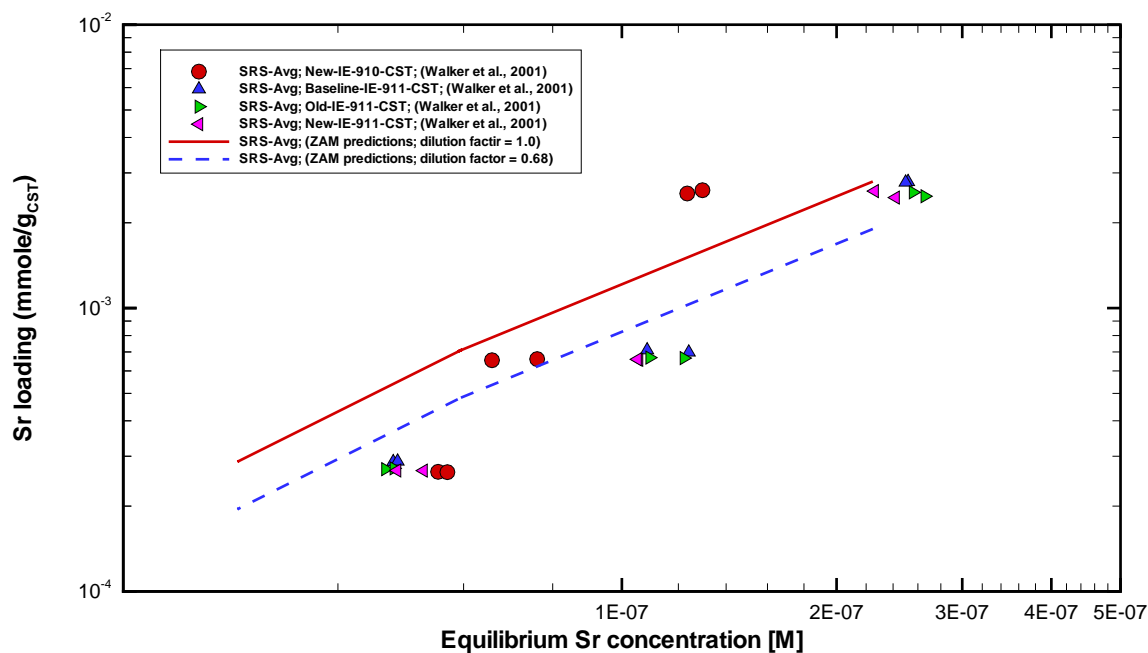


Figure C-13. Comparison of SRS-Avg simulant strontium CST loading data recently taken by Walker et al. (2001) to both best estimate and adjusted ZAM predictions at 36.2 C.



## Appendix D (VERSE-LC Input Files for Phase 1 Batch Feeds)

VERSE-LC column transport simulations were performed to estimate the total amount of spent CST material required to process the entire Phase 1 inventory. Various column sizes and carousel configurations (i.e., 2-column and 3-column cases) were considered. For reference the VERSE-LC input files for 16 Phase 1 batch feeds are provided in this appendix. Only the input files for the nominal VERSE-LC runs are provided (i.e., 2-column carousel configuration, 2000 L column volume, L/D=3 geometry, cesium pore diffusivity equal to 20% of its free diffusion value). The other input files can be obtained by changing those specific parameter settings as discussed in Chapter 10. One representative VERSE-LC main output file is provided for each of the envelopes (i.e., LAW-1 for Envelope A, LAW-2b for Envelope B, and LAW-3 for Envelope C).

For one specified carousel configuration and input parameter settings, to compute the total amount of spent CST requires running VERSE-LC 16 times (i.e., once for each batch feed) in sequence. Table D-1 provides the run sequence used and the necessary I/O options used in VERSE-LC. Basically, once the total volume of a given batch feed was processed the cesium concentration profiles contained within the lead and lag columns (and intermediate column if present) were stored on an output file (i.e., bed and pore concentrations throughout the two or three columns). On the subsequent batch feed, the previous batch feed output file was read into the current run as its initial cesium concentration profiles. The VERSE-LC simulations were performed on a PC-based Windows-95 machine.

To automate this process of handling many VERSE-LC runs and I/O files in series, a make utility called "NMAKE" was used. A sample input file to NMAKE (i.e., Makefile) is also provided below within this appendix where two cases (vol\_a and vol\_b) are being executed. In this example, directories were created to hold the files for each of the two case studies (Dir\_a and Dir\_b). Within each directory subdirectories containing the VERSE-LC input file for each of the 16 batch feeds was created (e.g., ...\\Dir\_a\\LAW\_1, ...\\Dir\_a\\LAW-2a, etc.). Using copy and directory change commands, the above file sequencing was achieved.

The nominal settings for key VERSE-LC input parameters are tabulated in Table D-2 for the Envelope A batch feeds and in Table D-3 for the Envelope B and C batch feeds. At the bottom of the three example VERSE-LC main output files, the process time(s) when a carousel cycle occurred is written out. This provides the number of cycles required on a batch by batch basis as tabulated in Chapter 10.

Table D-1. Listing of batch feed sequence and VERSE-LC I/O transferring.

Envelope	Phase 1 LAW batch feed sequence	VERSE-LC input	VERSE-LC output
A	LAW-1	Initially fresh columns	yio file of LAW-1
B	LAW-2a	yio file of LAW-1	yio file of LAW-2a
B	LAW-2b	yio file of LAW-2a	yio file of LAW-2b
C	LAW-3	yio file of LAW-2b	yio file of LAW-3
C	LAW-4	yio file of LAW-3	yio file of LAW-4
A	LAW-5	yio file of LAW-4	yio file of LAW-5
A	LAW-6	yio file of LAW-5	yio file of LAW-6
A	LAW-7	yio file of LAW-6	yio file of LAW-7
A	LAW-8	yio file of LAW-7	yio file of LAW-8
A	LAW-9	yio file of LAW-8	yio file of LAW-9
A	LAW-10	yio file of LAW-9	yio file of LAW-10
A	LAW-11	yio file of LAW-10	yio file of LAW-11
A	LAW-12	yio file of LAW-11	yio file of LAW-12
A	LAW-13	yio file of LAW-12	yio file of LAW-13
A	LAW-14	yio file of LAW-13	yio file of LAW-14
A	LAW-15	yio file of LAW-14	-

Table D-2. VERSE-LC nominal input parameters settings used in the Envelope A batch feed simulations at 25 C.

Feed Batch Name	LAW-1	LAW-5	LAW-6	LAW-8	LAW-9	LAW-10	LAW-11	LAW-12	LAW-13	LAW-14	LAW-15
Tank source	AP-101	AN-104	AN-104	AN-105	AN-105	SY-101	SY-101	AN-103	AN-103	AW-101	AW-101
<b>Input Parameters</b>											
Flow rate (L/min)	52.62	52.62	52.62	52.62	52.62	52.62	52.62	52.62	52.62	52.62	52.62
Feed <sup>total</sup> Cs conc. (M)	3.598E-05	6.283E-05	6.328E-05	4.324E-05	4.444E-05	3.692E-05	3.739E-05	4.831E-05	4.831E-05	4.569E-05	4.552E-05
Fluid viscosity (Poise)	2.6125	2.6125	2.6125	2.6125	2.6125	2.6125	2.6125	2.6125	2.6125	2.6125	2.6125
Fluid density (g/ml) <sup>a</sup>	1.277	1.232	1.231	1.225	1.238	1.237	1.232	1.221	1.221	1.234	1.235
Particle radius (μm)	172.0	172.0	172.0	172.0	172.0	172.0	172.0	172.0	172.0	172.0	172.0
Bed porosity	0.50	0.50	0.50	0.50	0.50	0.50	0.50	0.50	0.50	0.50	0.50
Particle porosity	0.24	0.24	0.24	0.24	0.24	0.24	0.24	0.24	0.24	0.24	0.24
Pore diffusivity (cm <sup>2</sup> /min) <sup>b</sup>	9.044E-05	8.624E-05	8.715E-05	9.090E-05	8.303E-05	8.669E-05	8.698E-05	9.248E-05	9.247E-05	9.347E-05	9.643E-05
Brownian diffusivity (cm <sup>2</sup> /min)	4.522E-04	4.312E-04	4.357E-04	4.545E-04	4.152E-04	4.334E-04	4.349E-04	4.624E-04	4.624E-04	4.674E-04	4.822E-04
Fr/La Hybrid a (moles/L B.V.) <sup>b</sup>	0.3944	0.3944	0.3944	0.3944	0.3944	0.3944	0.3944	0.3944	0.3944	0.3944	0.3944
Fr/La Hybrid b (1/M)	1.0	1.0	1.0	1.0	1.0	1.0	1.0	1.0	1.0	1.0	1.0
Fr/La Hybrid M <sub>a</sub>	1.0	1.0	1.0	1.0	1.0	1.0	1.0	1.0	1.0	1.0	1.0
Fr/La Hybrid M <sub>b</sub>	1.0	1.0	1.0	1.0	1.0	1.0	1.0	1.0	1.0	1.0	1.0
Fr/La Hybrid beta	3.8445E-04	2.3431E-04	2.3668E-04	2.5147E-04	2.2453E-04	2.2135E-04	2.0543E-04	2.9196E-04	2.9328E-04	3.6283E-04	3.8513E-04
Total Cs exit criterion [M]	2.9534E-08	2.9534E-08	2.9534E-08	2.9534E-08	2.9534E-08	2.9534E-08	2.9534E-08	2.9534E-08	2.9534E-08	2.9534E-08	2.9534E-08

<sup>a</sup> The bed density used represents a typical average value of measured engineered-form CST material where swelling due to feed ionic strength variations have negligible effects.

<sup>a</sup> The dilution factor is nominally set to 68% and the cesium pore diffusion coefficient to 20% of its “free” diffusion value.

Table D-3. VERSE-LC nominal input parameters settings used in the Envelopes B and C batch feed simulations at 25 C.

Envelope	B	B	C	C	C
Feed Batch Name	LAW-2a	LAW-2b	LAW-3	LAW-4	LAW-7
Tank source	AZ-101	AZ-102	AN-102	AN-102	AN-107
Input Parameters					
Flow rate (L/min)	9.4	9.4	16.2	16.2	16.2
Feed <sup>total</sup> Cs conc. (M)	4.676E-04	4.311E-04	3.967E-05	3.779E-05	4.455E-05
Fluid viscosity (Poise)	2.6125	2.6125	2.6125	2.6125	2.6125
Fluid density (g/ml) <sup>a</sup>	1.254	1.242	1.237	1.237	1.243
Particle radius (μm)	172.0	172.0	172.0	172.0	172.0
Bed porosity	0.50	0.50	0.50	0.50	0.50
Particle porosity	0.24	0.24	0.24	0.24	0.24
Pore diffusivity (cm <sup>2</sup> /min) <sup>b</sup>	7.828E-05	7.614E-05	8.709E-05	8.709E-05	8.435E-05
Brownian diffusivity (cm <sup>2</sup> /min)	3.914E-04	3.807E-04	4.354E-04	4.354E-04	4.217E-04
Fr/La Hybrid a (moles/L B.V.) <sup>b</sup>	0.3944	0.3944	0.3944	0.3944	0.3944
Fr/La Hybrid b (1/M)	1.0	1.0	1.0	1.0	1.0
Fr/La Hybrid M <sub>a</sub>	1.0	1.0	1.0	1.0	1.0
Fr/La Hybrid M <sub>b</sub>	1.0	1.0	1.0	1.0	1.0
Fr/La Hybrid beta	2.6230E-04	2.1296E-04	2.1769E-04	2.1769E-04	1.9258E-04
Total Cs exit criterion [M]	7.0318E-08	7.0318E-08	4.8942E-08	4.8942E-08	4.8942E-08

<sup>a</sup> The bed density used represents a typical average value of measured engineered-form CST material where swelling due to feed ionic strength variations have negligible effects.

<sup>a</sup> The dilution factor is nominally set to 68% and the cesium pore diffusion coefficient to 20% of its “free” diffusion value.

## Makefile for NMAKE Utility (2 nominal case runs of VERSE-LC)

---

```
CODE                = E:\CST2_20\Verse.exe

DESTDIR = E:\CST2_20

DIRS              = vol_a vol_b
all:               $(DIRS)

clean:  vol_a.clean vol_b.clean

#####
vol_a:
    cd $(DESTDIR)\LAW_1\Dir_a
    dir/B | $(CODE)
    copy case.yio case.output
    copy case.yio ..\..\LAW_2a\Dir_a
    cd $(DESTDIR)\LAW_2a\Dir_a
    copy case.yio case.input
    dir/B | $(CODE)
    copy case.yio case.output
    copy case.yio ..\..\LAW_2b\Dir_a
    cd $(DESTDIR)\LAW_2b\Dir_a
    copy case.yio case.input
    dir/B | $(CODE)
    copy case.yio case.output
    copy case.yio ..\..\LAW_3\Dir_a
    cd $(DESTDIR)\LAW_3\Dir_a
    copy case.yio case.input
    dir/B | $(CODE)
    copy case.yio case.output
    copy case.yio ..\..\LAW_4\Dir_a
    cd $(DESTDIR)\LAW_4\Dir_a
    copy case.yio case.input
    dir/B | $(CODE)
    copy case.yio case.output
    copy case.yio ..\..\LAW_5\Dir_a
    cd $(DESTDIR)\LAW_5\Dir_a
    copy case.yio case.input
    dir/B | $(CODE)
    copy case.yio case.output
    copy case.yio ..\..\LAW_6\Dir_a
    cd $(DESTDIR)\LAW_6\Dir_a
    copy case.yio case.input
    dir/B | $(CODE)
    copy case.yio case.output
    copy case.yio ..\..\LAW_7\Dir_a
    cd $(DESTDIR)\LAW_7\Dir_a
    copy case.yio case.input
    dir/B | $(CODE)
    copy case.yio case.output
    copy case.yio ..\..\LAW_8\Dir_a
    cd $(DESTDIR)\LAW_8\Dir_a
    copy case.yio case.input
    dir/B | $(CODE)
    copy case.yio case.output
    copy case.yio ..\..\LAW_9\Dir_a
    cd $(DESTDIR)\LAW_9\Dir_a
    copy case.yio case.input
    dir/B | $(CODE)
    copy case.yio case.output
    copy case.yio ..\..\LAW_10\Dir_a
    cd $(DESTDIR)\LAW_10\Dir_a
    copy case.yio case.input
    dir/B | $(CODE)
    copy case.yio case.output
    copy case.yio ..\..\LAW_11\Dir_a
    cd $(DESTDIR)\LAW_11\Dir_a
    copy case.yio case.input
    dir/B | $(CODE)
    copy case.yio case.output
```

```
copy case.yio ..\..\LAW_12\Dir_a
cd $(DESTDIR)\LAW_12\Dir_a
copy case.yio case.input
dir/B | $(CODE)
copy case.yio case.output
copy case.yio ..\..\LAW_13\Dir_a
cd $(DESTDIR)\LAW_13\Dir_a
copy case.yio case.input
dir/B | $(CODE)
copy case.yio case.output
copy case.yio ..\..\LAW_14\Dir_a
cd $(DESTDIR)\LAW_14\Dir_a
copy case.yio case.input
dir/B | $(CODE)
copy case.yio case.output
copy case.yio ..\..\LAW_15\Dir_a
cd $(DESTDIR)\LAW_15\Dir_a
copy case.yio case.input
dir/B | $(CODE)

vol_b:
cd $(DESTDIR)\LAW_1\Dir_b
dir/B | $(CODE)
copy case.yio case.output
copy case.yio ..\..\LAW_2a\Dir_b
cd $(DESTDIR)\LAW_2a\Dir_b
copy case.yio case.input
dir/B | $(CODE)
copy case.yio case.output
copy case.yio ..\..\LAW_2b\Dir_b
cd $(DESTDIR)\LAW_2b\Dir_b
copy case.yio case.input
dir/B | $(CODE)
copy case.yio case.output
copy case.yio ..\..\LAW_3\Dir_b
cd $(DESTDIR)\LAW_3\Dir_b
copy case.yio case.input
dir/B | $(CODE)
copy case.yio case.output
copy case.yio ..\..\LAW_4\Dir_b
cd $(DESTDIR)\LAW_4\Dir_b
copy case.yio case.input
dir/B | $(CODE)
copy case.yio case.output
copy case.yio ..\..\LAW_5\Dir_b
cd $(DESTDIR)\LAW_5\Dir_b
copy case.yio case.input
dir/B | $(CODE)
copy case.yio case.output
copy case.yio ..\..\LAW_6\Dir_b
cd $(DESTDIR)\LAW_6\Dir_b
copy case.yio case.input
dir/B | $(CODE)
copy case.yio case.output
copy case.yio ..\..\LAW_7\Dir_b
cd $(DESTDIR)\LAW_7\Dir_b
copy case.yio case.input
dir/B | $(CODE)
copy case.yio case.output
copy case.yio ..\..\LAW_8\Dir_b
cd $(DESTDIR)\LAW_8\Dir_b
copy case.yio case.input
dir/B | $(CODE)
copy case.yio case.output
copy case.yio ..\..\LAW_9\Dir_b
cd $(DESTDIR)\LAW_9\Dir_b
copy case.yio case.input
dir/B | $(CODE)
copy case.yio case.output
copy case.yio ..\..\LAW_10\Dir_b
cd $(DESTDIR)\LAW_10\Dir_b
copy case.yio case.input
dir/B | $(CODE)
copy case.yio case.output
```

```
copy case.yio ../../LAW_11\Dir_b
cd $(DESTDIR)\LAW_11\Dir_b
copy case.yio case.input
dir/B | $(CODE)
copy case.yio case.output
copy case.yio ../../LAW_12\Dir_b
cd $(DESTDIR)\LAW_12\Dir_b
copy case.yio case.input
dir/B | $(CODE)
copy case.yio case.output
copy case.yio ../../LAW_13\Dir_b
cd $(DESTDIR)\LAW_13\Dir_b
copy case.yio case.input
dir/B | $(CODE)
copy case.yio case.output
copy case.yio ../../LAW_14\Dir_b
cd $(DESTDIR)\LAW_14\Dir_b
copy case.yio case.input
dir/B | $(CODE)
copy case.yio case.output
copy case.yio ../../LAW_15\Dir_b
cd $(DESTDIR)\LAW_15\Dir_b
copy case.yio case.input
dir/B | $(CODE)

vol_a.clean:
cd $(DESTDIR)\LAW_1\Dir_a
-@erase *.run
-@erase *.h*
-@erase *.p*
-@erase *.yio*
-@erase *.output
cd $(DESTDIR)\LAW_5\Dir_a
-@erase *.run
-@erase *.h*
-@erase *.p*
-@erase *.yio*
-@erase *.input
-@erase *.output
cd $(DESTDIR)\LAW_6\Dir_a
-@erase *.run
-@erase *.h*
-@erase *.p*
-@erase *.yio*
-@erase *.input
-@erase *.output
cd $(DESTDIR)\LAW_8\Dir_a
-@erase *.run
-@erase *.h*
-@erase *.p*
-@erase *.yio*
-@erase *.input
-@erase *.output
cd $(DESTDIR)\LAW_9\Dir_a
-@erase *.run
-@erase *.h*
-@erase *.p*
-@erase *.yio*
-@erase *.input
-@erase *.output
cd $(DESTDIR)\LAW_10\Dir_a
-@erase *.run
-@erase *.h*
-@erase *.p*
-@erase *.yio*
-@erase *.input
-@erase *.output
cd $(DESTDIR)\LAW_11\Dir_a
-@erase *.run
-@erase *.h*
-@erase *.p*
-@erase *.yio*
-@erase *.input
-@erase *.output
```

```
cd $(DESTDIR)\LAW_12\Dir_a
-@erase *.run
-@erase *.h*
-@erase *.p*
-@erase *.yio*
-@erase *.input
-@erase *.output
cd $(DESTDIR)\LAW_13\Dir_a
-@erase *.run
-@erase *.h*
-@erase *.p*
-@erase *.yio*
-@erase *.input
-@erase *.output
cd $(DESTDIR)\LAW_14\Dir_a
-@erase *.run
-@erase *.h*
-@erase *.p*
-@erase *.yio*
-@erase *.input
-@erase *.output
cd $(DESTDIR)\LAW_15\Dir_a
-@erase *.run
-@erase *.h*
-@erase *.p*
-@erase *.yio*
-@erase *.input
-@erase *.output
cd $(DESTDIR)\LAW_2a\Dir_a
-@erase *.run
-@erase *.h*
-@erase *.p*
-@erase *.yio*
-@erase *.input
-@erase *.output
cd $(DESTDIR)\LAW_2b\Dir_a
-@erase *.run
-@erase *.h*
-@erase *.p*
-@erase *.yio*
-@erase *.input
-@erase *.output
cd $(DESTDIR)\LAW_3\Dir_a
-@erase *.run
-@erase *.h*
-@erase *.p*
-@erase *.yio*
-@erase *.input
-@erase *.output
cd $(DESTDIR)\LAW_4\Dir_a
-@erase *.run
-@erase *.h*
-@erase *.p*
-@erase *.yio*
-@erase *.input
-@erase *.output
cd $(DESTDIR)\LAW_7\Dir_a
-@erase *.run
-@erase *.h*
-@erase *.p*
-@erase *.yio*
-@erase *.input

vol_b.clean:
cd $(DESTDIR)\LAW_1\Dir_b
-@erase *.run
-@erase *.h*
-@erase *.p*
-@erase *.yio*
-@erase *.output
cd $(DESTDIR)\LAW_5\Dir_b
-@erase *.run
-@erase *.h*
-@erase *.p*
```



```
-@erase *.yio*
-@erase *.input
-@erase *.output
cd $(DESTDIR)\LAW_6\Dir_b
-@erase *.run
-@erase *.h*
-@erase *.p*
-@erase *.yio*
-@erase *.input
-@erase *.output
cd $(DESTDIR)\LAW_8\Dir_b
-@erase *.run
-@erase *.h*
-@erase *.p*
-@erase *.yio*
-@erase *.input
-@erase *.output
cd $(DESTDIR)\LAW_9\Dir_b
-@erase *.run
-@erase *.h*
-@erase *.p*
-@erase *.yio*
-@erase *.input
-@erase *.output
cd $(DESTDIR)\LAW_10\Dir_b
-@erase *.run
-@erase *.h*
-@erase *.p*
-@erase *.yio*
-@erase *.input
-@erase *.output
cd $(DESTDIR)\LAW_11\Dir_b
-@erase *.run
-@erase *.h*
-@erase *.p*
-@erase *.yio*
-@erase *.input
-@erase *.output
cd $(DESTDIR)\LAW_12\Dir_b
-@erase *.run
-@erase *.h*
-@erase *.p*
-@erase *.yio*
-@erase *.input
-@erase *.output
cd $(DESTDIR)\LAW_13\Dir_b
-@erase *.run
-@erase *.h*
-@erase *.p*
-@erase *.yio*
-@erase *.input
-@erase *.output
cd $(DESTDIR)\LAW_14\Dir_b
-@erase *.run
-@erase *.h*
-@erase *.p*
-@erase *.yio*
-@erase *.input
-@erase *.output
cd $(DESTDIR)\LAW_15\Dir_b
-@erase *.run
-@erase *.h*
-@erase *.p*
-@erase *.yio*
-@erase *.input
-@erase *.output
cd $(DESTDIR)\LAW_2a\Dir_b
-@erase *.run
-@erase *.h*
-@erase *.p*
-@erase *.yio*
-@erase *.input
-@erase *.output
cd $(DESTDIR)\LAW_2b\Dir_b
```

```
-@erase *.run
-@erase *.h*
-@erase *.p*
-@erase *.yio*
-@erase *.input
-@erase *.output
cd $(DESTDIR)\LAW_3\Dir_b
-@erase *.run
-@erase *.h*
-@erase *.p*
-@erase *.yio*
-@erase *.input
-@erase *.output
cd $(DESTDIR)\LAW_4\Dir_b
-@erase *.run
-@erase *.h*
-@erase *.p*
-@erase *.yio*
-@erase *.input
-@erase *.output
cd $(DESTDIR)\LAW_7\Dir_b
-@erase *.run
-@erase *.h*
-@erase *.p*
-@erase *.yio*
-@erase *.input
```

---

**VERSE-LC Input for Phase 1 LAW-1 Batch Feed (nominal case; 2000 L)**


---

```

[Full-Scale] Simulation of Cs removal on Baseline CST material lead/lag columns
1 component (Cs) isotherm (Na 5.0 M) (LAW-1: Envelope A Salt Solution)
1, 100, 3, 6      ncomp, nele, ncol-bed, ncol-part
FCWNA             isotherm,axial-disp,film-coef,surf-diff,BC-col  FCUNA
NNNNY            input-only,perfusable,feed-equil,datafile.yio
MM               comp-conc units
568.1, 94.7, 52620.0, 5.00d+5  Length(cm),Diam(cm),Q-flow(ml/min),CSTR-vol(ml)
172.0, 0.50, 0.240, 0.0      part-rad(um), bed-void, part-void, sorb-cap()
0.0, 0.0            initial concentrations (M)
S                 COMMAND - conc step change
1, 0.0, 3.598d-5, 1, 0.0     spec id, time(min), conc(M), freq, dt(min)
V                 COMMAND - viscosity/density change
0.026125, 1.277          fluid viscosity(posie), density(g/cm^3)
m                 COMMAND - subcolumns
50, 100, 0, 1, 2.9534d-8, 0.0, 900000.0 elem-shift,elem-watch,pp-watch,c-watch,c-thresh,t-e,t-ee
h                 COMMAND - effluent history dump
2, 1.0, 1.0, 0.25, 0.1      unit op#, ptscale(1-4) filtering
h                 COMMAND - effluent history dump
4, 1.0, 1.0, 0.25, 0.1      unit op#, ptscale(1-4) filtering
-                 end of commands
87907.0, 1.0             end time(min), max dt in B.V.s
1.0d-7, 1.0d-4          abs-tol, rel-tol
-                 non-negative conc constraint
1.0d0                size exclusion factor
9.044d-5             part-pore diffusivities(cm^2/min) 20% of free values
4.522d-4             Brownian diffusivities(cm^2/min)
0.3944              Freundlich/Langmuir Hybrid a      (moles/L B.V.) rhob=1.0
1.0                 Freundlich/Langmuir Hybrid b      (1/M)  Batch specific isotherm
1.0                 Freundlich/Langmuir Hybrid Ma     (-)   ccap=0.580
1.0                 Freundlich/Langmuir Hybrid Mb     (-)
3.8445d-4           Freundlich/Langmuir Hybrid beta  (-) "eff" isotherm Na = 5.0 M
-----

```

---

**VERSE-LC Input for Phase 1 LAW-2a Batch Feed (nominal case; 2000 L)**


---

```

[Full-Scale] Simulation of Cs removal on Baseline CST material lead/lag columns
1 component (Cs) isotherm (Na 5.0 M) (LAW-2a: Envelope B Salt Solution)
1, 100, 3, 6      ncomp, nele, ncol-bed, ncol-part
FCWNA             isotherm,axial-disp,film-coef,surf-diff,BC-col  FCUNA
NNNNY            input-only,perfusable,feed-equil,datafile.yio
MM               comp-conc units
568.1, 94.7, 9400.0, 5.00d+5  Length(cm),Diam(cm),Q-flow(ml/min),CSTR-vol(ml)
172.0, 0.50, 0.240, 0.0      part-rad(um), bed-void, part-void, sorb-cap()
0.0, 0.0            initial concentrations (M)
S                 COMMAND - conc step change
1, 0.0, 4.676d-4, 1, 0.0     spec id, time(min), conc(M), freq, dt(min)
V                 COMMAND - viscosity/density change
0.026125, 1.254          fluid viscosity(posie), density(g/cm^3)
m                 COMMAND - subcolumns
50, 100, 0, 1, 7.0318d-8, 0.0, 900000.0 elem-shift,elem-watch,pp-watch,c-watch,c-thresh,t-e,t-ee
h                 COMMAND - effluent history dump
2, 1.0, 1.0, 0.25, 0.1      unit op#, ptscale(1-4) filtering
h                 COMMAND - effluent history dump
4, 1.0, 1.0, 0.25, 0.1      unit op#, ptscale(1-4) filtering
-                 end of commands
309110.0, 1.0           end time(min), max dt in B.V.s
1.0d-7, 1.0d-4          abs-tol, rel-tol
-                 non-negative conc constraint
1.0d0                size exclusion factor
7.828d-5             part-pore diffusivities(cm^2/min) 20% of free values
3.914d-4             Brownian diffusivities(cm^2/min)
0.3944              Freundlich/Langmuir Hybrid a      (moles/L B.V.) rhob=1.0
1.0                 Freundlich/Langmuir Hybrid b      (1/M)  Batch specific isotherm
1.0                 Freundlich/Langmuir Hybrid Ma     (-)   ccap=0.580
1.0                 Freundlich/Langmuir Hybrid Mb     (-)
2.6230d-4           Freundlich/Langmuir Hybrid beta  (-) "eff" isotherm Na = 5.0 M
-----

```

---

**VERSE-LC Input for Phase 1 LAW-2b Batch Feed (nominal case; 2000 L)**


---

```

[Full-Scale] Simulation of Cs removal on Baseline CST material lead/lag columns
1 component (Cs) isotherm (Na 5.0 M) (LAW-2b: Envelope B Salt Solution)
1, 100, 3, 6      ncomp, nelelem, ncol-bed, ncol-part
FCWNA            isotherm,axial-disp,film-coef,surf-diff,BC-col  FCUNA
NNNYY           input-only,perfusable,feed-equil,datafile.yio
MM              comp-conc units
568.1, 94.7, 9400.0, 5.00d+5  Length(cm),Diam(cm),Q-flow(ml/min),CSTR-vol(ml)
172.0, 0.50, 0.240, 0.0      part-rad(um), bed-void, part-void, sorb-cap()
0.0, 0.0              initial concentrations (M)
S                  COMMAND - conc step change
1, 0.0, 4.311d-4, 1, 0.0      spec id, time(min), conc(M), freq, dt(min)
V                  COMMAND - viscosity/density change
0.026125, 1.242          fluid viscosity(posie), density(g/cm^3)
m                  COMMAND - subcolumns
50, 100, 0, 1, 7.0318d-8, 0.0, 900000.0 elem-shift,elem-watch,pp-watch,c-watch,c-thresh,t-e,t-ee
h                  COMMAND - effluent history dump
2, 1.0, 1.0, 0.25, 0.1      unit op#, ptscale(1-4) filtering
h                  COMMAND - effluent history dump
4, 1.0, 1.0, 0.25, 0.1      unit op#, ptscale(1-4) filtering
-                  end of commands
186710.0, 1.0            end time(min), max dt in B.V.s
1.0d-7, 1.0d-4          abs-tol, rel-tol
-                  non-negative conc constraint
1.0d0                size exclusion factor
7.614d-5              part-pore diffusivities(cm^2/min) 20% of free values
3.807d-4              Brownian diffusivities(cm^2/min)
0.3944               Freundlich/Langmuir Hybrid a      (moles/L B.V.) rhob=1.0
1.0                  Freundlich/Langmuir Hybrid b      (1/M) Batch specific isotherm
1.0                  Freundlich/Langmuir Hybrid Ma      (-) ccap=0.580
1.0                  Freundlich/Langmuir Hybrid Mb      (-)
2.1296d-4            Freundlich/Langmuir Hybrid beta (-) "eff" isotherm Na = 5.0 M
-----

```

---

**VERSE-LC Input for Phase 1 LAW-3 Batch Feed (nominal case; 2000 L)**


---

```

[Full-Scale] Simulation of Cs removal on Baseline CST material lead/lag columns
1 component (Cs) isotherm (Na 5.0 M) (LAW-3: Envelope C Salt Solution)
1, 100, 3, 6      ncomp, nelelem, ncol-bed, ncol-part
FCWNA            isotherm,axial-disp,film-coef,surf-diff,BC-col  FCUNA
NNNYY           input-only,perfusable,feed-equil,datafile.yio
MM              comp-conc units
568.1, 94.7, 16200.0, 5.00d+5  Length(cm),Diam(cm),Q-flow(ml/min),CSTR-vol(ml)
172.0, 0.50, 0.240, 0.0      part-rad(um), bed-void, part-void, sorb-cap()
0.0, 0.0              initial concentrations (M)
S                  COMMAND - conc step change
1, 0.0, 3.967d-5, 1, 0.0      spec id, time(min), conc(M), freq, dt(min)
V                  COMMAND - viscosity/density change
0.026125, 1.237          fluid viscosity(posie), density(g/cm^3)
m                  COMMAND - subcolumns
50, 100, 0, 1, 4.8942d-8, 0.0, 900000.0 elem-shift,elem-watch,pp-watch,c-watch,c-thresh,t-e,t-ee
h                  COMMAND - effluent history dump
2, 1.0, 1.0, 0.25, 0.1      unit op#, ptscale(1-4) filtering
h                  COMMAND - effluent history dump
4, 1.0, 1.0, 0.25, 0.1      unit op#, ptscale(1-4) filtering
-                  end of commands
259260.0, 1.0            end time(min), max dt in B.V.s
1.0d-7, 1.0d-4          abs-tol, rel-tol
-                  non-negative conc constraint
1.0d0                size exclusion factor
8.709d-5              part-pore diffusivities(cm^2/min) 20% of free values
4.354d-4              Brownian diffusivities(cm^2/min)
0.3944               Freundlich/Langmuir Hybrid a      (moles/L B.V.) rhob=1.0
1.0                  Freundlich/Langmuir Hybrid b      (1/M) Batch specific isotherm
1.0                  Freundlich/Langmuir Hybrid Ma      (-) ccap=0.580
1.0                  Freundlich/Langmuir Hybrid Mb      (-)
2.1769d-4            Freundlich/Langmuir Hybrid beta (-) "eff" isotherm Na = 5.0 M
-----

```

---

**VERSE-LC Input for Phase 1 LAW-4 Batch Feed (nominal case; 2000 L)**


---

```
[Full-Scale] Simulation of Cs removal on Baseline CST material lead/lag columns
1 component (Cs) isotherm (Na 5.0 M) (LAW-4: Envelope C Salt Solution)
1, 100, 3, 6      ncomp, nelelem, ncol-bed, ncol-part
FCWNA            isotherm,axial-disp,film-coef,surf-diff,BC-col  FCUNA
NNNYY           input-only,perfusable,feed-equil,datafile.yio
MM              comp-conc units
568.1, 94.7, 16200.0, 5.00d+5 Length(cm),Diam(cm),Q-flow(ml/min),CSTR-vol(ml)
172.0, 0.50, 0.240, 0.0      part-rad(um), bed-void, part-void, sorb-cap()
0.0, 0.0                initial concentrations (M)
S                      COMMAND - conc step change
1, 0.0, 3.779d-5, 1, 0.0    spec id, time(min), conc(M), freq, dt(min)
V                      COMMAND - viscosity/density change
0.026125, 1.237          fluid viscosity(posie), density(g/cm^3)
m                      COMMAND - subcolumns
50, 100, 0, 1, 4.8942d-8, 0.0, 900000.0 elem-shift,elem-watch,pp-watch,c-watch,c-thresh,t-e,t-ee
h                      COMMAND - effluent history dump
2, 1.0, 1.0, 0.25, 0.1      unit op#, ptscale(1-4) filtering
h                      COMMAND - effluent history dump
4, 1.0, 1.0, 0.25, 0.1      unit op#, ptscale(1-4) filtering
-                      end of commands
259260.0, 1.0            end time(min), max dt in B.V.s
1.0d-7, 1.0d-4          abs-tol, rel-tol
-                      non-negative conc constraint
1.0d0                  size exclusion factor
8.709d-5              part-pore diffusivities(cm^2/min) 20% of free values
4.354d-4              Brownian diffusivities(cm^2/min)
0.3944               Freundlich/Langmuir Hybrid a      (moles/L B.V.) rhob=1.0
1.0                  Freundlich/Langmuir Hybrid b      (1/M) Batch specific isotherm
1.0                  Freundlich/Langmuir Hybrid Ma     (-) ccap=0.580
1.0                  Freundlich/Langmuir Hybrid Mb     (-)
2.1769d-4            Freundlich/Langmuir Hybrid beta (-) "eff" isotherm Na = 5.0 M
-----
```

---

**VERSE-LC Input for Phase 1 LAW-5 Batch Feed (nominal case; 2000 L)**


---

```
[Full-Scale] Simulation of Cs removal on Baseline CST material lead/lag columns
1 component (Cs) isotherm (Na 5.0 M) (LAW-5: Envelope A Salt Solution)
1, 100, 3, 6      ncomp, nelelem, ncol-bed, ncol-part
FCWNA            isotherm,axial-disp,film-coef,surf-diff,BC-col  FCUNA
NNNYY           input-only,perfusable,feed-equil,datafile.yio
MM              comp-conc units
568.1, 94.7, 52620.0, 5.00d+5 Length(cm),Diam(cm),Q-flow(ml/min),CSTR-vol(ml)
172.0, 0.50, 0.240, 0.0      part-rad(um), bed-void, part-void, sorb-cap()
0.0, 0.0                initial concentrations (M)
S                      COMMAND - conc step change
1, 0.0, 6.283d-5, 1, 0.0    spec id, time(min), conc(M), freq, dt(min)
V                      COMMAND - viscosity/density change
0.026125, 1.232          fluid viscosity(posie), density(g/cm^3)
m                      COMMAND - subcolumns
50, 100, 0, 1, 2.9534d-8, 0.0, 900000.0 elem-shift,elem-watch,pp-watch,c-watch,c-thresh,t-e,t-ee
h                      COMMAND - effluent history dump
2, 1.0, 1.0, 0.25, 0.1      unit op#, ptscale(1-4) filtering
h                      COMMAND - effluent history dump
4, 1.0, 1.0, 0.25, 0.1      unit op#, ptscale(1-4) filtering
-                      end of commands
72596.0, 1.0            end time(min), max dt in B.V.s
1.0d-7, 1.0d-4          abs-tol, rel-tol
-                      non-negative conc constraint
1.0d0                  size exclusion factor
8.624d-5              part-pore diffusivities(cm^2/min) 20% of free values
4.312d-4              Brownian diffusivities(cm^2/min)
0.3944               Freundlich/Langmuir Hybrid a      (moles/L B.V.) rhob=1.0
1.0                  Freundlich/Langmuir Hybrid b      (1/M) Batch specific isotherm
1.0                  Freundlich/Langmuir Hybrid Ma     (-) ccap=0.580
1.0                  Freundlich/Langmuir Hybrid Mb     (-)
2.3431d-4            Freundlich/Langmuir Hybrid beta (-) "eff" isotherm Na = 5.0 M
-----
```

---

**VERSE-LC Input for Phase 1 LAW-6 Batch Feed (nominal case; 2000 L)**


---

```

[Full-Scale] Simulation of Cs removal on Baseline CST material lead/lag columns
1 component (Cs) isotherm (Na 5.0 M) (LAW-6: Envelope A Salt Solution)
1, 100, 3, 6      ncomp, nelelem, ncol-bed, ncol-part
FCWNA             isotherm,axial-disp,film-coef,surf-diff,BC-col  FCUNA
NNNNY            input-only,perfusable,feed-equil,datafile.yio
MM               comp-conc units
568.1,  94.7, 52620.0, 5.00d+5  Length(cm),Diam(cm),Q-flow(ml/min),CSTR-vol(ml)
172.0, 0.50, 0.240,  0.0      part-rad(um), bed-void, part-void, sorb-cap()
      0.0, 0.0                initial concentrations (M)
S                  COMMAND - conc step change
1, 0.0, 6.328d-5, 1, 0.0      spec id, time(min), conc(M), freq, dt(min)
V                  COMMAND - viscosity/density change
0.026125, 1.231            fluid viscosity(posie), density(g/cm^3)
m                  COMMAND - subcolumns
50, 100, 0, 1, 2.9534d-8, 0.0, 900000.0 elem-shift,elem-watch,pp-watch,c-watch,c-thresh,t-e,t-ee
h                  COMMAND - effluent history dump
2, 1.0, 1.0, 0.25, 0.1      unit op#, ptscale(1-4) filtering
h                  COMMAND - effluent history dump
4, 1.0, 1.0, 0.25, 0.1      unit op#, ptscale(1-4) filtering
-                  end of commands
67275.0, 1.0              end time(min), max dt in B.V.s
1.0d-7, 1.0d-4            abs-tol, rel-tol
-                          non-negative conc constraint
1.0d0                    size exclusion factor
8.715d-5                 part-pore diffusivities(cm^2/min) 20% of free values
4.357d-4                 Brownian diffusivities(cm^2/min)
0.3944                  Freundlich/Langmuir Hybrid a      (moles/L B.V.) rhob=1.0
1.0                     Freundlich/Langmuir Hybrid b      (1/M)  Batch specific isotherm
1.0                     Freundlich/Langmuir Hybrid Ma     (-)   ccap=0.580
1.0                     Freundlich/Langmuir Hybrid Mb     (-)
2.3668d-4               Freundlich/Langmuir Hybrid beta  (-) "eff" isotherm Na = 5.0 M
-----

```

---

**VERSE-LC Input for Phase 1 LAW-7 Batch Feed (nominal case; 2000 L)**


---

```

[Full-Scale] Simulation of Cs removal on Baseline CST material lead/lag columns
1 component (Cs) isotherm (Na 5.0 M) (LAW-7: Envelope C Salt Solution)
1, 100, 3, 6      ncomp, nelelem, ncol-bed, ncol-part
FCWNA             isotherm,axial-disp,film-coef,surf-diff,BC-col  FCUNA
NNNNY            input-only,perfusable,feed-equil,datafile.yio
MM               comp-conc units
568.1,  94.7, 16200.0, 5.00d+5  Length(cm),Diam(cm),Q-flow(ml/min),CSTR-vol(ml)
172.0, 0.50, 0.240,  0.0      part-rad(um), bed-void, part-void, sorb-cap()
      0.0, 0.0                initial concentrations (M)
S                  COMMAND - conc step change
1, 0.0, 4.455d-5, 1, 0.0      spec id, time(min), conc(M), freq, dt(min)
V                  COMMAND - viscosity/density change
0.026125, 1.243            fluid viscosity(posie), density(g/cm^3)
m                  COMMAND - subcolumns
50, 100, 0, 1, 4.8942d-8, 0.0, 900000.0 elem-shift,elem-watch,pp-watch,c-watch,c-thresh,t-e,t-ee
h                  COMMAND - effluent history dump
2, 1.0, 1.0, 0.25, 0.1      unit op#, ptscale(1-4) filtering
h                  COMMAND - effluent history dump
4, 1.0, 1.0, 0.25, 0.1      unit op#, ptscale(1-4) filtering
-                  end of commands
339380.0, 1.0              end time(min), max dt in B.V.s
1.0d-7, 1.0d-4            abs-tol, rel-tol
-                          non-negative conc constraint
1.0d0                    size exclusion factor
8.435d-5                 part-pore diffusivities(cm^2/min) 20% of free values
4.217d-4                 Brownian diffusivities(cm^2/min)
0.3944                  Freundlich/Langmuir Hybrid a      (moles/L B.V.) rhob=1.0
1.0                     Freundlich/Langmuir Hybrid b      (1/M)  Batch specific isotherm
1.0                     Freundlich/Langmuir Hybrid Ma     (-)   ccap=0.580
1.0                     Freundlich/Langmuir Hybrid Mb     (-)
1.9258d-4               Freundlich/Langmuir Hybrid beta  (-) "eff" isotherm Na = 5.0 M
-----

```

---

**VERSE-LC Input for Phase 1 LAW-8 Batch Feed (nominal case; 2000 L)**


---

```
[Full-Scale] Simulation of Cs removal on Baseline CST material lead/lag columns
1 component (Cs) isotherm (Na 5.0 M) (LAW-8: Envelope A Salt Solution)
1, 100, 3, 6      ncomp, nelelem, ncol-bed, ncol-part
FCWNA             isotherm,axial-disp,film-coef,surf-diff,BC-col  FCUNA
NNNYY            input-only,perfusable,feed-equil,datafile.yio
MM               comp-conc units
568.1, 94.7, 52620.0, 5.00d+5 Length(cm),Diam(cm),Q-flow(ml/min),CSTR-vol(ml)
172.0, 0.50, 0.240, 0.0      part-rad(um), bed-void, part-void, sorb-cap()
0.0, 0.0              initial concentrations (M)
S                  COMMAND - conc step change
1, 0.0, 4.324d-5, 1, 0.0     spec id, time(min), conc(M), freq, dt(min)
V                  COMMAND - viscosity/density change
0.026125, 1.225          fluid viscosity(posie), density(g/cm^3)
m                  COMMAND - subcolumns
50, 100, 0, 1, 2.9534d-8, 0.0, 900000.0 elem-shift,elem-watch,pp-watch,c-watch,c-thresh,t-e,t-ee
h                  COMMAND - effluent history dump
2, 1.0, 1.0, 0.25, 0.1      unit op#, ptscale(1-4) filtering
h                  COMMAND - effluent history dump
4, 1.0, 1.0, 0.25, 0.1      unit op#, ptscale(1-4) filtering
-                  end of commands
70315.0, 1.0             end time(min), max dt in B.V.s
1.0d-7, 1.0d-4           abs-tol, rel-tol
-                       non-negative conc constraint
1.0d0                  size exclusion factor
9.090d-5               part-pore diffusivities(cm^2/min) 20% of free values
4.545d-4               Brownian diffusivities(cm^2/min)
0.3944                Freundlich/Langmuir Hybrid a      (moles/L B.V.) rhob=1.0
1.0                   Freundlich/Langmuir Hybrid b      (1/M) Batch specific isotherm
1.0                   Freundlich/Langmuir Hybrid Ma     (-) ccap=0.580
1.0                   Freundlich/Langmuir Hybrid Mb     (-)
2.5147d-4              Freundlich/Langmuir Hybrid beta (-) "eff" isotherm Na = 5.0 M
-----
```

---

**VERSE-LC Input for Phase 1 LAW-9 Batch Feed (nominal case; 2000 L)**


---

```
[Full-Scale] Simulation of Cs removal on Baseline CST material lead/lag columns
1 component (Cs) isotherm (Na 5.0 M) (LAW-9: Envelope A Salt Solution)
1, 100, 3, 6      ncomp, nelelem, ncol-bed, ncol-part
FCWNA             isotherm,axial-disp,film-coef,surf-diff,BC-col  FCUNA
NNNYY            input-only,perfusable,feed-equil,datafile.yio
MM               comp-conc units
568.1, 94.7, 52620.0, 5.00d+5 Length(cm),Diam(cm),Q-flow(ml/min),CSTR-vol(ml)
172.0, 0.50, 0.240, 0.0      part-rad(um), bed-void, part-void, sorb-cap()
0.0, 0.0              initial concentrations (M)
S                  COMMAND - conc step change
1, 0.0, 4.444d-5, 1, 0.0     spec id, time(min), conc(M), freq, dt(min)
V                  COMMAND - viscosity/density change
0.026125, 1.238          fluid viscosity(posie), density(g/cm^3)
m                  COMMAND - subcolumns
50, 100, 0, 1, 2.9534d-8, 0.0, 900000.0 elem-shift,elem-watch,pp-watch,c-watch,c-thresh,t-e,t-ee
h                  COMMAND - effluent history dump
2, 1.0, 1.0, 0.25, 0.1      unit op#, ptscale(1-4) filtering
h                  COMMAND - effluent history dump
4, 1.0, 1.0, 0.25, 0.1      unit op#, ptscale(1-4) filtering
-                  end of commands
68415.0, 1.0             end time(min), max dt in B.V.s
1.0d-7, 1.0d-4           abs-tol, rel-tol
-                       non-negative conc constraint
1.0d0                  size exclusion factor
8.303d-5               part-pore diffusivities(cm^2/min) 20% of free values
4.152d-4               Brownian diffusivities(cm^2/min)
0.3944                Freundlich/Langmuir Hybrid a      (moles/L B.V.) rhob=1.0
1.0                   Freundlich/Langmuir Hybrid b      (1/M) Batch specific isotherm
1.0                   Freundlich/Langmuir Hybrid Ma     (-) ccap=0.580
1.0                   Freundlich/Langmuir Hybrid Mb     (-)
2.2453d-4              Freundlich/Langmuir Hybrid beta (-) "eff" isotherm Na = 5.0 M
-----
```

---

**VERSE-LC Input for Phase 1 LAW-10 Batch Feed (nominal case; 2000 L)**


---

```
[Full-Scale] Simulation of Cs removal on Baseline CST material lead/lag columns
1 component (Cs) isotherm (Na 5.0 M) (LAW-10: Envelope A Salt Solution)
1, 100, 3, 6      ncomp, nelelem, ncol-bed, ncol-part
FCWNA            isotherm,axial-disp,film-coef,surf-diff,BC-col  FCUNA
NNNYY           input-only,perfusable,feed-equil,datafile.yio
MM              comp-conc units
568.1, 94.7, 52620.0, 5.00d+5 Length(cm),Diam(cm),Q-flow(ml/min),CSTR-vol(ml)
172.0, 0.50, 0.240, 0.0      part-rad(um), bed-void, part-void, sorb-cap()
0.0, 0.0                initial concentrations (M)
S                      COMMAND - conc step change
1, 0.0, 3.692d-5, 1, 0.0    spec id, time(min), conc(M), freq, dt(min)
V                      COMMAND - viscosity/density change
0.026125, 1.237          fluid viscosity(posie), density(g/cm^3)
m                      COMMAND - subcolumns
50, 100, 0, 1, 2.9534d-8, 0.0, 900000.0 elem-shift,elem-watch,pp-watch,c-watch,c-thresh,t-e,t-ee
h                      COMMAND - effluent history dump
2, 1.0, 1.0, 0.25, 0.1     unit op#, ptscale(1-4) filtering
h                      COMMAND - effluent history dump
4, 1.0, 1.0, 0.25, 0.1     unit op#, ptscale(1-4) filtering
-                      end of commands
49411.0, 1.0             end time(min), max dt in B.V.s
1.0d-7, 1.0d-4          abs-tol, rel-tol
-                      non-negative conc constraint
1.0d0                  size exclusion factor
8.669d-5              part-pore diffusivities(cm^2/min) 20% of free values
4.334d-4              Brownian diffusivities(cm^2/min)
0.3944               Freundlich/Langmuir Hybrid a      (moles/L B.V.) rhob=1.0
1.0                  Freundlich/Langmuir Hybrid b      (1/M) Batch specific isotherm
1.0                  Freundlich/Langmuir Hybrid Ma     (-) ccap=0.580
1.0                  Freundlich/Langmuir Hybrid Mb     (-)
2.2135d-4            Freundlich/Langmuir Hybrid beta (-) "eff" isotherm Na = 5.0 M
-----
```

---

**VERSE-LC Input for Phase 1 LAW-11 Batch Feed (nominal case; 2000 L)**


---

```
[Full-Scale] Simulation of Cs removal on Baseline CST material lead/lag columns
1 component (Cs) isotherm (Na 5.0 M) (LAW-11: Envelope A Salt Solution)
1, 100, 3, 6      ncomp, nelelem, ncol-bed, ncol-part
FCWNA            isotherm,axial-disp,film-coef,surf-diff,BC-col  FCUNA
NNNYY           input-only,perfusable,feed-equil,datafile.yio
MM              comp-conc units
568.1, 94.7, 52620.0, 5.00d+5 Length(cm),Diam(cm),Q-flow(ml/min),CSTR-vol(ml)
172.0, 0.50, 0.240, 0.0      part-rad(um), bed-void, part-void, sorb-cap()
0.0, 0.0                initial concentrations (M)
S                      COMMAND - conc step change
1, 0.0, 3.739d-5, 1, 0.0    spec id, time(min), conc(M), freq, dt(min)
V                      COMMAND - viscosity/density change
0.026125, 1.232          fluid viscosity(posie), density(g/cm^3)
m                      COMMAND - subcolumns
50, 100, 0, 1, 2.9534d-8, 0.0, 900000.0 elem-shift,elem-watch,pp-watch,c-watch,c-thresh,t-e,t-ee
h                      COMMAND - effluent history dump
2, 1.0, 1.0, 0.25, 0.1     unit op#, ptscale(1-4) filtering
h                      COMMAND - effluent history dump
4, 1.0, 1.0, 0.25, 0.1     unit op#, ptscale(1-4) filtering
-                      end of commands
87419.0, 1.0             end time(min), max dt in B.V.s
1.0d-7, 1.0d-4          abs-tol, rel-tol
-                      non-negative conc constraint
1.0d0                  size exclusion factor
8.698d-5              part-pore diffusivities(cm^2/min) 20% of free values
4.349d-4              Brownian diffusivities(cm^2/min)
0.3944               Freundlich/Langmuir Hybrid a      (moles/L B.V.) rhob=1.0
1.0                  Freundlich/Langmuir Hybrid b      (1/M) Batch specific isotherm
1.0                  Freundlich/Langmuir Hybrid Ma     (-) ccap=0.580
1.0                  Freundlich/Langmuir Hybrid Mb     (-)
2.0543d-4            Freundlich/Langmuir Hybrid beta (-) "eff" isotherm Na = 5.0 M
-----
```

---



**VERSE-LC Input for Phase 1 LAW-12 Batch Feed (nominal case; 2000 L)**


---

```

[Full-Scale] Simulation of Cs removal on Baseline CST material lead/lag columns
1 component (Cs) isotherm (Na 5.0 M) (LAW-12: Envelope A Salt Solution)
1, 100, 3, 6      ncomp, nelelem, ncol-bed, ncol-part
FCWNA            isotherm,axial-disp,film-coef,surf-diff,BC-col  FCUNA
NNNYY           input-only,perfusable,feed-equil,datafile.yio
MM              comp-conc units
568.1, 94.7, 52620.0, 5.00d+5  Length(cm),Diam(cm),Q-flow(ml/min),CSTR-vol(ml)
172.0, 0.50, 0.240, 0.0      part-rad(um), bed-void, part-void, sorb-cap()
0.0, 0.0            initial concentrations (M)
S                COMMAND - conc step change
1, 0.0, 4.831d-5, 1, 0.0     spec id, time(min), conc(M), freq, dt(min)
V                COMMAND - viscosity/density change
0.026125, 1.221          fluid viscosity(posie), density(g/cm^3)
m                COMMAND - subcolumns
50, 100, 0, 1, 2.9534d-8, 0.0, 900000.0 elem-shift,elem-watch,pp-watch,c-watch,c-thresh,t-e,t-ee
h                COMMAND - effluent history dump
2, 1.0, 1.0, 0.25, 0.1      unit op#, ptscale(1-4) filtering
h                COMMAND - effluent history dump
4, 1.0, 1.0, 0.25, 0.1      unit op#, ptscale(1-4) filtering
-                end of commands
89700.0, 1.0            end time(min), max dt in B.V.s
1.0d-7, 1.0d-4          abs-tol, rel-tol
-                non-negative conc constraint
1.0d0              size exclusion factor
9.248d-5           part-pore diffusivities(cm^2/min) 20% of free values
4.624d-4           Brownian diffusivities(cm^2/min)
0.3944            Freundlich/Langmuir Hybrid a (moles/L B.V.) rhob=1.0
1.0               Freundlich/Langmuir Hybrid b (1/M) Batch specific isotherm
1.0               Freundlich/Langmuir Hybrid Ma (-) ccap=0.580
1.0               Freundlich/Langmuir Hybrid Mb (-)
2.9196d-4          Freundlich/Langmuir Hybrid beta (-) "eff" isotherm Na = 5.0 M
-----

```

---

**VERSE-LC Input for Phase 1 LAW-13 Batch Feed (nominal case; 2000 L)**


---

```

[Full-Scale] Simulation of Cs removal on Baseline CST material lead/lag columns
1 component (Cs) isotherm (Na 5.0 M) (LAW-13: Envelope A Salt Solution)
1, 100, 3, 6      ncomp, nelelem, ncol-bed, ncol-part
FCWNA            isotherm,axial-disp,film-coef,surf-diff,BC-col  FCUNA
NNNYY           input-only,perfusable,feed-equil,datafile.yio
MM              comp-conc units
568.1, 94.7, 52620.0, 5.00d+5  Length(cm),Diam(cm),Q-flow(ml/min),CSTR-vol(ml)
172.0, 0.50, 0.240, 0.0      part-rad(um), bed-void, part-void, sorb-cap()
0.0, 0.0            initial concentrations (M)
S                COMMAND - conc step change
1, 0.0, 4.831d-5, 1, 0.0     spec id, time(min), conc(M), freq, dt(min)
V                COMMAND - viscosity/density change
0.026125, 1.221          fluid viscosity(posie), density(g/cm^3)
m                COMMAND - subcolumns
50, 100, 0, 1, 2.9534d-8, 0.0, 900000.0 elem-shift,elem-watch,pp-watch,c-watch,c-thresh,t-e,t-ee
h                COMMAND - effluent history dump
2, 1.0, 1.0, 0.25, 0.1      unit op#, ptscale(1-4) filtering
h                COMMAND - effluent history dump
4, 1.0, 1.0, 0.25, 0.1      unit op#, ptscale(1-4) filtering
-                end of commands
89700.0, 1.0            end time(min), max dt in B.V.s
1.0d-7, 1.0d-4          abs-tol, rel-tol
-                non-negative conc constraint
1.0d0              size exclusion factor
9.247d-5           part-pore diffusivities(cm^2/min) 20% of free values
4.624d-4           Brownian diffusivities(cm^2/min)
0.3944            Freundlich/Langmuir Hybrid a (moles/L B.V.) rhob=1.0
1.0               Freundlich/Langmuir Hybrid b (1/M) Batch specific isotherm
1.0               Freundlich/Langmuir Hybrid Ma (-) ccap=0.580
1.0               Freundlich/Langmuir Hybrid Mb (-)
2.9328d-4          Freundlich/Langmuir Hybrid beta (-) "eff" isotherm Na = 5.0 M
-----

```

---

**VERSE-LC Input for Phase 1 LAW-14 Batch Feed (nominal case; 2000 L)**


---

```

[Full-Scale] Simulation of Cs removal on Baseline CST material lead/lag columns
1 component (Cs) isotherm (Na 5.0 M) (LAW-14: Envelope A Salt Solution)
1, 100, 3, 6      ncomp, nelelem, ncol-bed, ncol-part
FCWNA            isotherm,axial-disp,film-coef,surf-diff,BC-col  FCUNA
NNNYY           input-only,perfusable,feed-equil,datafile.yio
MM              comp-conc units
568.1, 94.7, 52620.0, 5.00d+5 Length(cm),Diam(cm),Q-flow(ml/min),CSTR-vol(ml)
172.0, 0.50, 0.240, 0.0      part-rad(um), bed-void, part-void, sorb-cap()
0.0, 0.0                  initial concentrations (M)
S                        COMMAND - conc step change
1, 0.0, 4.569d-5, 1, 0.0    spec id, time(min), conc(M), freq, dt(min)
V                        COMMAND - viscosity/density change
0.026125, 1.234           fluid viscosity(posie), density(g/cm^3)
m                        COMMAND - subcolumns
50, 100, 0, 1, 2.9534d-8, 0.0, 900000.0 elem-shift,elem-watch,pp-watch,c-watch,c-thresh,t-e,t-ee
h                        COMMAND - effluent history dump
2, 1.0, 1.0, 0.25, 0.1     unit op#, ptscale(1-4) filtering
h                        COMMAND - effluent history dump
4, 1.0, 1.0, 0.25, 0.1     unit op#, ptscale(1-4) filtering
-                        end of commands
74876.0, 1.0              end time(min), max dt in B.V.s
1.0d-7, 1.0d-4            abs-tol, rel-tol
-                        non-negative conc constraint
1.0d0                    size exclusion factor
9.347d-5                 part-pore diffusivities(cm^2/min) 20% of free values
4.674d-4                 Brownian diffusivities(cm^2/min)
0.3944                  Freundlich/Langmuir Hybrid a      (moles/L B.V.) rhob=1.0
1.0                     Freundlich/Langmuir Hybrid b      (1/M) Batch specific isotherm
1.0                     Freundlich/Langmuir Hybrid Ma      (-) ccap=0.580
1.0                     Freundlich/Langmuir Hybrid Mb      (-)
3.6283d-4               Freundlich/Langmuir Hybrid beta (-) "eff" isotherm Na = 5.0 M
-----

```

---

**VERSE-LC Input for Phase 1 LAW-15 Batch Feed (nominal case; 2000 L)**


---

```

[Full-Scale] Simulation of Cs removal on Baseline CST material lead/lag columns
1 component (Cs) isotherm (Na 5.0 M) (LAW-15: Envelope A Salt Solution)
1, 100, 3, 6      ncomp, nelelem, ncol-bed, ncol-part
FCWNA            isotherm,axial-disp,film-coef,surf-diff,BC-col  FCUNA
NNNYY           input-only,perfusable,feed-equil,datafile.yio
MM              comp-conc units
568.1, 94.7, 52620.0, 5.00d+5 Length(cm),Diam(cm),Q-flow(ml/min),CSTR-vol(ml)
172.0, 0.50, 0.240, 0.0      part-rad(um), bed-void, part-void, sorb-cap()
0.0, 0.0                  initial concentrations (M)
S                        COMMAND - conc step change
1, 0.0, 4.552d-5, 1, 0.0    spec id, time(min), conc(M), freq, dt(min)
V                        COMMAND - viscosity/density change
0.026125, 1.235           fluid viscosity(posie), density(g/cm^3)
m                        COMMAND - subcolumns
50, 100, 0, 1, 2.9534d-8, 0.0, 900000.0 elem-shift,elem-watch,pp-watch,c-watch,c-thresh,t-e,t-ee
h                        COMMAND - effluent history dump
2, 1.0, 1.0, 0.25, 0.1     unit op#, ptscale(1-4) filtering
h                        COMMAND - effluent history dump
4, 1.0, 1.0, 0.25, 0.1     unit op#, ptscale(1-4) filtering
-                        end of commands
101860.0, 1.0             end time(min), max dt in B.V.s
1.0d-7, 1.0d-4            abs-tol, rel-tol
-                        non-negative conc constraint
1.0d0                    size exclusion factor
9.643d-5                 part-pore diffusivities(cm^2/min) 20% of free values
4.822d-4                 Brownian diffusivities(cm^2/min)
0.3944                  Freundlich/Langmuir Hybrid a      (moles/L B.V.) rhob=1.0
1.0                     Freundlich/Langmuir Hybrid b      (1/M) Batch specific isotherm
1.0                     Freundlich/Langmuir Hybrid Ma      (-) ccap=0.580
1.0                     Freundlich/Langmuir Hybrid Mb      (-)
3.8513d-4               Freundlich/Langmuir Hybrid beta (-) "eff" isotherm Na = 5.0 M
-----

```

---

**VERSE-LC Output for Phase 1 LAW-1 Batch Feed (nominal case; 2000 L)**

```
=====
VERSE v7.80 by R. D. Whitley and N.-H. L. Wang, c1999 PRF
=====
```

```
Input file: case
[Full-Scale] Simulation of Cs removal on Baseline CST material lead/lag col
1 component (Cs) isotherm (Na 5.0 M) (LAW-1: Envelope A Salt Solution)
Begin Run: 12:51:27 on 05-04-2001 running under Windows 95/8
Finite elements - axial:100 particle: 1
Collocation points - axial: 3 particle: 6 => Number of eqns: 3219
Inlet species at equilib.? N Perfusable sorbent? N Feed profile only? N
Use Profile File? N Generate Profile File? Y
Axial dispersion correlation: Chung & Wen (1968)
Film mass transfer correlation: Wilson & Geankoplis (1966)
Sub-Column Boundary Conditions: Axial Dispersion and CSTR
=====
```

## SYSTEM PARAMETERS (at initial conditions):

```
t(stop)      = 87907.00000 min      dtheta max   = 1.00000 BV
abs. tol.    = .10000E-06          rel. tol.    = .10000E-03
Total Length = 568.10000 cm        D            = 94.70000 cm
Tot. Capacity = .00000 eq/L solid  Col. Vol.     = 4001424.51597 mL
F            = 52620.00000 mL/min    Uo (linear)   = 14.94139 cm/min
R            = 172.00000 microns     L/R          = 33029.06977
Bed Void frac. = .50000            Pcl. Porosity = .24000
Spec. Area   = 87.20930 1/cm        Time/BV      = 19.01095 min
Vol CSTRs    = 500000.00000 mL
```

```
Component no. = 1
Ke [-]        = .10000E+01
Eb [cm2/min]  = .12524E+01
Dp [cm2/min]  = .90440E-04
Doo [cm2/min] = .45220E-03
kf [cm/min]   = .23737E+00
Ds [cm2/min]  = .00000E+00
```

## Dimensionless Groups:

```
Re           = .20936E+00
Sc(i)        = .27145E+04
Peb(i)       = .33887E+04
Bi(i)        = .18810E+03
Nf(i)        = .78708E+03
Np(i)        = .13948E+01
Pep(i)       = .11840E+05
```

```
Isotherm     = Freundlich/Langmuir Hybrid
Iso. Const. 1 = .39440E+00
Iso. Const. 2 = .10000E+01
Iso. Const. 3 = .10000E+01
Iso. Const. 4 = .10000E+01
Iso. Const. 5 = .38445E-03
Init. Conc.   = .00000E+00
Conc. at eqb. = .00000E+00
Conc. units   = M
=====
```

## COMMAND LIST:

- 1: Step conc. of component 1 at .0000 min to .3598E-04 M  
Execute 1 times, every .0000 mins.
- 2: User set viscosity to .2612E-01 poise and density to 1.277 g/cm3
- 3: Carousel (conc.). Active between t = .0000 and .9000E+06 min.  
When comp. 1 reaches .2953E-07 M at end of node 100,  
shift 50 axial elements out the feed end
- 4: Monitor conc. history at stream 2. Filename = case.h01  
Output density adjustments:  
1.0 \*default abs conc delta, 1.0 \*default rel conc delta,  
.25 \*default force w/ conc delta, .10 \*default force w/o conc delta
- 5: Monitor conc. history at stream 4. Filename = case.h02  
Output density adjustments:  
1.0 \*default abs conc delta, 1.0 \*default rel conc delta,  
.25 \*default force w/ conc delta, .10 \*default force w/o conc delta

```
=====
Conc. Carousel caused bed shift at t = .3511E+05 min
```

Conc. Carousel caused bed shift at t = .6174E+05 min  
 VERSE-LC finished in 5032 steps. Average step size 17.47 minutes  
 End run: 12:58:15 on 05-04-2001  
 Integrated Areas in History Files:  
 case.h01 .253632  
 case.h02 .206094E-03

## VERSE-LC Output for Phase 1 LAW-2b Batch Feed (nominal case; 2000 L)

=====

VERSE v7.80 by R. D. Whitley and N.-H. L. Wang, c1999 PRF

=====

Input file: case  
 [Full-Scale] Simulation of Cs removal on Baseline CST material lead/lag col  
 1 component (Cs) isotherm (Na 5.0 M) (LAW-2b: Envelope B Salt Solution)  
 Begin Run: 13:04:53 on 05-04-2001 running under Windows 95/8  
 Finite elements - axial:100 particle: 1  
 Collocation points - axial: 3 particle: 6 => Number of eqns: 3219  
 Inlet species at equilib.? N Perfusable sorbent? N Feed profile only? N  
 Use Profile File? Y Generate Profile File? Y  
 Axial dispersion correlation: Chung & Wen (1968)  
 Film mass transfer correlation: Wilson & Geankoplis (1966)  
 Sub-Column Boundary Conditions: Axial Dispersion and CSTR

### =====

#### SYSTEM PARAMETERS (at initial conditions):

t(stop)	= 186710.00000 min	dtheta max	= 1.00000 BV
abs. tol.	= .10000E-06	rel. tol.	= .10000E-03
Total Length	= 568.10000 cm	D	= 94.70000 cm
Tot. Capacity	= .00000 eq/L solid	Col. Vol.	= 4001424.51597 mL
F	= 9400.00000 mL/min	Uo (linear)	= 2.66912 cm/min
R	= 172.00000 microns	L/R	= 33029.06977
Bed Void frac.	= .50000	Pcl. Porosity	= .24000
Spec. Area	= 87.20930 1/cm	Time/BV	= 106.42086 min
Vol CSTRs	= 500000.00000 mL		

Component no.	= 1
Ke [-]	= .10000E+01
Eb [cm2/min]	= .22700E+00
Dp [cm2/min]	= .76140E-04
Doo [cm2/min]	= .38070E-03
kf [cm/min]	= .11919E+00
Ds [cm2/min]	= .00000E+00

#### Dimensionless Groups:

Re	= .36376E-01
Sc(i)	= .33151E+04
Peb(i)	= .33399E+04
Bi(i)	= .11219E+03
Nf(i)	= .22124E+04
Np(i)	= .65735E+01
Pep(i)	= .25123E+04

Isotherm = Freundlich/Langmuir Hybrid

Iso. Const. 1	= .39440E+00
Iso. Const. 2	= .10000E+01
Iso. Const. 3	= .10000E+01
Iso. Const. 4	= .10000E+01
Iso. Const. 5	= .21296E-03
Init. Conc.	= .00000E+00
Conc. at eqb.	= .00000E+00
Conc. units	M

#### =====

#### COMMAND LIST:

- 1: Step conc. of component 1 at .0000 min to .4311E-03 M  
Execute 1 times, every .0000 mins.
- 2: User set viscosity to .2612E-01 poise and density to 1.242 g/cm3
- 3: Carousel (conc.). Active between t = .0000 and .9000E+06 min.  
When comp. 1 reaches .7032E-07 M at end of node 100,  
shift 50 axial elements out the feed end
- 4: Monitor conc. history at stream 2. Filename = case.h01  
Output density adjustments:

```

1.0      *default abs conc delta,      1.0      *default rel conc delta,
.25      *default force w/ conc delta, .10      *default force w/o conc delta
5: Monitor conc. history at stream 4.  Filename = case.h02
Output density adjustments:
1.0      *default abs conc delta,      1.0      *default rel conc delta,
.25      *default force w/ conc delta, .10      *default force w/o conc delta

```

```

=====
Conc. Carousel caused bed shift at t = .1018E+06 min
VERSE-LC finished in 1798 steps. Average step size 103.8      minutes
End run: 13:06:47 on 05-04-2001
Integrated Areas in History Files:
case.h01      77.2638
case.h02      .782044E-04

```

## VERSE-LC Output for Phase 1 LAW-3 Batch Feed (nominal case; 2000 L)

```

=====
VERSE v7.80 by R. D. Whitley and N.-H. L. Wang, c1999 PRF
=====

```

```

Input file: case
[Full-Scale] Simulation of Cs removal on Baseline CST material lead/lag col
1 component (Cs) isotherm (Na 5.0 M) (LAW-3: Envelope C Salt Solution)
Begin Run: 13:06:47 on 05-04-2001 running under Windows 95/8
Finite elements - axial:100 particle: 1
Collocation points - axial: 3 particle: 6 => Number of eqns: 3219
Inlet species at equilib.? N Perfusable sorbent? N Feed profile only? N
Use Profile File? Y Generate Profile File? Y
Axial dispersion correlation: Chung & Wen (1968)
Film mass transfer correlation: Wilson & Geankoplis (1966)
Sub-Column Boundary Conditions: Axial Dispersion and CSTR

```

### SYSTEM PARAMETERS (at initial conditions):

```

t(stop)      = 259260.00000 min      dtheta max    = 1.00000 BV
abs. tol.     = .10000E-06           rel. tol.     = .10000E-03
Total Length  = 568.10000 cm          D             = 94.70000 cm
Tot. Capacity = .00000 eq/L solid    Col. Vol.     = 4001424.51597 mL
F            = 16200.00000 mL/min     Uo (linear)   = 4.59997 cm/min
R            = 172.00000 microns      L/R           = 33029.06977
Bed Void frac. = .50000              Pcl. Porosity = .24000
Spec. Area    = 87.20930 1/cm         Time/BV       = 61.75038 min
Vol CSTRs     = 500000.00000 mL

```

```

Component no. = 1
Ke [-]        = .10000E+01
Eb [cm2/min]  = .38993E+00
Dp [cm2/min]  = .87090E-04
Doo [cm2/min] = .43540E-03
kf [cm/min]   = .15629E+00
Ds [cm2/min]  = .00000E+00

```

### Dimensionless Groups:

```

Re           = .62438E-01
Sc(i)        = .29104E+04
Peb(i)       = .33509E+04
Bi(i)        = .12861E+03
Nf(i)        = .16833E+04
Np(i)        = .43628E+01
Pep(i)       = .37853E+04

```

```

Isotherm      = Freundlich/Langmuir Hybrid

```

```

Iso. Const. 1 = .39440E+00
Iso. Const. 2 = .10000E+01
Iso. Const. 3 = .10000E+01
Iso. Const. 4 = .10000E+01
Iso. Const. 5 = .21769E-03
Init. Conc.   = .00000E+00
Conc. at eqb. = .00000E+00
Conc. units   = M

```

### COMMAND LIST:

```

1: Step conc. of component 1 at .0000 min to .3967E-04 M

```

```
Execute 1 times, every .0000 mins.
2: User set viscosity to .2612E-01 poise and density to 1.237 g/cm3
3: Carousel (conc.). Active between t = .0000 and .9000E+06 min.
   When comp. 1 reaches .4894E-07 M at end of node 100,
   shift 50 axial elements out the feed end
4: Monitor conc. history at stream 2. Filename = case.h01
   Output density adjustments:
   1.0 *default abs conc delta, 1.0 *default rel conc delta,
   .25 *default force w/ conc delta, .10 *default force w/o conc delta
5: Monitor conc. history at stream 4. Filename = case.h02
   Output density adjustments:
   1.0 *default abs conc delta, 1.0 *default rel conc delta,
   .25 *default force w/ conc delta, .10 *default force w/o conc delta
```

```
=====
Conc. Carousel caused bed shift at t = .2286E+05 min
Conc. Carousel caused bed shift at t = .1043E+06 min
Conc. Carousel caused bed shift at t = .2129E+06 min
VERSE-LC finished in 4561 steps. Average step size 56.84 minutes
End run: 13:13:25 on 05-04-2001
Integrated Areas in History Files:
case.h01 46.7109
case.h02 .257035E-03
```

---

## **Appendix E (Batch Kinetics Test Input and Output Files)**

For reference the VERSE-LC input and output files for the batch kinetics test simulations are provided in this appendix. Several simulations were run. This appendix contains the measured transient liquid-phase cesium response corresponding to several batch kinetics tests performed using CST powder and engineered forms. For each CST material a cesium isotherm was created based on the batch  $K_d$  test with the longest contact time. A beta factor was computed where it is assumed that 100% equilibrium is reached once this contact time has occurred. Based on the amounts of CST material and solution used for each batch contact test, material balance calculations were used to estimate the test's bed density and porosity. The various values computed and used in the VERSE-LC simulations are also tabulated in this appendix.

### **E.1 PNNL Kinetics Studies**

The batch kinetics test data taken by Brown et al. (1996) are listed in Table C-1. Table C-2 provides a listing of the key test parameters. Three CST materials were tested where timed  $K_d$  tests were performed. A listing of input VERSE-LC files is also provided in this appendix for all three materials, while only a VERSE-LC output file for the powder form is given.

### **E.2 SRS Kinetics Studies**

The batch kinetics test data taken by Fondeur et al. (2000) are listed in Table C-3. Table C-4 provides a listing of the key test parameters. One CST material was tested (i.e., the Baseline engineered-form of CST) where timed  $K_d$  tests were performed. A listing of an input and its output VERSE-LC files are also provided in this appendix.

### **E.3 Particle Size Impact on Kinetics**

A series of transient cesium uptake tests were performed to investigate the impact that CST particle size has on its kinetics. This was part of an earlier effort to determining an optimum sized engineered-form of CST. The batch kinetics test data taken by Miller and Brown (1997) and by Anthony et al. (1996) are listed in Table C-5. Table C-6 provides a listing of the key test parameters. Three CST materials were tested (i.e., TAM5 powder and two TAM5 generated engineered-forms of CST with average particle diameters of  $\sim 112 \mu\text{m}$  and  $\sim 334 \mu\text{m}$ ) where transient cesium uptake tests were performed. A listing of input VERSE-LC files is also provided in this appendix.

### **E.4 ORNL Kinetics Studies**

The batch kinetics test data taken by Davidson et al. (1998) are listed in Table C-7. Table C-8 provides a listing of the key test parameters. One CST material was tested (i.e., a powder-form of CST) where timed  $K_d$  tests were performed.

Table E-1. Cesium uptake measurements made at 25 C during the batch kinetics tests of Brown et al., 1996 (initial cesium concentration of  $1.0 \times 10^{-4}$  M).

Contact time	Cs $K_d$ value, (ml/g)			Final Liquid Cs <sup>+</sup> conc., [M]		
	Powder-form	Engineered-form (08)	Engineered-form (38b)	Powder-form	Engineered-form (08)	Engineered-form (38b)
1.0 (mins)	155.1	5.3	2.0	3.998E-05	9.548E-05	9.820E-05
2.0 (mins)	168.0	2.2	1.8	3.808E-05	9.807E-05	9.843E-05
8.0 (mins)	264.9	16.7	11.5	2.805E-05	8.712E-05	9.063E-05
32.0 (mins)	284.3	24.4	23.9	2.665E-05	8.218E-05	8.232E-05
2.0 (hrs)	633.2	144.5	70.8	1.403E-05	4.383E-05	6.111E-05
20.0 (hrs)	1809.3	811.2	814.2	5.401E-06	1.220E-05	1.202E-05
72.0 (hrs)	1356.9	1111.2	708.0	7.075E-06	9.211E-06	1.358E-05
120.0 (hrs)	1938.5	1100.1	973.5	5.060E-06	9.295E-06	1.026E-05



Table E-2. Key parameters measured or specified during the batch kinetics tests of Brown et al. (1996) and used to establish the cesium isotherms used in VERSE-LC kinetic modeling.

Parameter	Parameter setting for powder form	Parameter setting for engineered-form (08)	Parameter setting for engineered-form (38b)
CST material	IE-910	IE-911	IE-911
Temperature	25 °C	25 °C	25 °C
Initial liquid Na <sup>+</sup> conc.	5.0 M	5.0 M	5.0 M
Initial liquid Cs <sup>+</sup> conc.	1.0x10 <sup>-4</sup> M	1.0x10 <sup>-4</sup> M	1.0x10 <sup>-4</sup> M
Final liquid Cs <sup>+</sup> conc. (actually at 120 hours)	5.060x10 <sup>-6</sup> M	9.295x10 <sup>-6</sup> M	1.026x10 <sup>-5</sup> M
Initial liquid sample volume	10.0 ml	10.0 ml	10.0 ml
Initial resin mass	0.1 g	0.1 g	0.1 g
Batch ID	na	Lot 08	Lot 38b
Solution composition	70% AW-101 DSSF	70% AW-101 DSSF	70% AW-101 DSSF
Particle porosity	0.1	0.24	0.24
solid density	1.176 g/ml	1.717 g/ml	1.368 g/ml
Solution density	1.409 g/ml	1.409 g/ml	1.409 g/ml
Solution viscosity	na	na	na
F factor	0.968	0.887	0.879
Phase ratio	103.31	112.74	111.23
Bed density	0.009601 g/ml	0.008824 g/ml	0.008931 g/ml
Bed porosity	0.989259	0.993240	0.991409
Estimated beta value for cesium isotherm	2.94143x10 <sup>-4</sup> M	3.49210x10 <sup>-4</sup> M	3.94901x10 <sup>-4</sup> M

Table E-3. Cesium uptake measurements made at 25 C during the batch kinetics tests of Fondeur et al., 2000. Also included are estimated conditions at earlier contact times.

Batch Kinetics Contact Test ID	Contact time (hrs)	Initial Liquid Cs <sup>+</sup> conc. [M]	K <sub>d</sub> value (ml/g)	Final Liquid Cs <sup>+</sup> conc. [M]	Approach to equilibrium (%)
Fondeur	0.0	1.40E-04	-	1.400E-04	0.00
estimated	0.03333	1.40E-04	2.0	1.388E-04	0.98
estimated	0.1	1.40E-04	7.0	1.359E-04	3.36
estimated	0.5	1.40E-04	25.0	1.264E-04	11.15
estimated	1.0	1.40E-04	51.0	1.148E-04	20.67
estimated	3.0	1.40E-04	147.0	8.578E-05	44.50
estimated	6.0	1.40E-04	265.0	6.544E-05	61.20
estimated	12.0	1.40E-04	500.0	4.444E-05	78.43

<b>Fondeur</b>	24.0	1.40E-04	758.13	3.286E-05	87.93
<b>Fondeur</b>	48.0	1.40E-04	1002.34	2.637E-05	93.27
<b>Fondeur</b>	72.0	1.40E-04	1099.57	2.444E-05	94.85
<b>Fondeur</b>	96.0	1.40E-04	1227.15	2.230E-05	96.60
<b>Fondeur</b>	120.0	1.40E-04	1389	2.008E-05	98.43
<b>Fondeur</b>	144.0	1.40E-04	1496	1.884E-05	99.45
<b>Fondeur</b>	168.0	1.40E-04	1523	1.855E-05	99.69
<b>Fondeur</b>	192.0	1.40E-04	1560	1.816E-05	100.00

Table E-4. Key parameters measured or specified during the batch kinetics tests of Fondeur et al. (2000) and used to establish the cesium isotherm used in VERSE-LC kinetic modeling.

<b>Parameter</b>	<b>Parameter setting</b>
CST material	IE-911
Temperature	25 °C
Initial liquid Na <sup>+</sup> conc.	5.6 M
Initial liquid Cs <sup>+</sup> conc.	1.40x10 <sup>-4</sup> M
Final liquid Cs <sup>+</sup> conc. (actually at 192 hours)	1.816x10 <sup>-5</sup> M
Initial liquid sample volume	20.0 ml
Initial resin mass	0.1 g
Batch ID	Lot 9090-76
Solution composition	SRS Avg.
Particle porosity	0.24
solid density	1.520 g/ml
solution density	1.253 g/ml
solution viscosity	2.78 cP
F factor	0.86
Phase ratio	232.56
Bed density	0.004288 g/ml
Bed porosity	0.996288
Estimated beta value for cesium isotherm	3.53632x10 <sup>-4</sup> M

Table E-5. Cesium uptake measurements made at 25 C during the transient cesium uptake tests of Miller and Brown (1997) and Anthony et al., 1996.

Miller and Brown (1997) TAM5 powder avg diameter of 0.8 $\mu\text{m}$		Anthony et al. (1996) Engineered-form avg diameter of 112 $\mu\text{m}$		Anthony et al. (1996) Engineered-form avg diameter of 334 $\mu\text{m}$	
Contact time (hrs)	Liquid Cs <sup>+</sup> conc. [M]	Contact time (hrs)	Liquid Cs <sup>+</sup> conc. [M]	Contact time (hrs)	Liquid Cs <sup>+</sup> conc. [M]
0.0	1.0E-04	0.0	1.0E-04	0.0	1.0E-04
0.030	6.154E-05	0.0405	7.000E-05	0.0405	8.909E-05
0.070	5.385E-05	0.0811	5.500E-05	0.0811	8.136E-05
0.080	5.055E-05	0.1216	4.818E-05	0.1216	7.773E-05
0.130	4.286E-05	0.1622	4.364E-05	0.1622	7.455E-05
0.160	4.011E-05	0.2595	3.727E-05	0.2595	6.864E-05
0.245	3.516E-05	0.3243	3.364E-05	0.3243	6.500E-05
0.330	3.187E-05	0.4865	2.864E-05	0.4865	5.864E-05
0.500	2.692E-05	1.0135	2.000E-05	1.0135	4.591E-05
1.000	1.758E-05	1.9865	1.864E-05	1.9865	3.455E-05
-	-	6.0000	1.682E-05	6.0000	2.046E-05
-	-	12.0000	1.546E-05	12.0000	1.864E-05

Table E-6. Key parameters measured or specified during the transient cesium uptake tests of Miller and Brown (1997) and Anthony et al. (1996) and used to establish the cesium isotherm used in VERSE-LC kinetic modeling.

Parameter	Parameter setting	Parameter setting	Parameter setting
CST material	Avg diameter 0.8 mm	Avg diameter 112 mm	Avg diameter 334 mm
Temperature	25 °C	25 °C	25 °C
Initial liquid Na <sup>+</sup> conc.	5.0 M	5.0 M	5.0 M
Initial liquid Cs <sup>+</sup> conc.	1.0x10 <sup>-4</sup> M	1.0x10 <sup>-4</sup> M	1.0x10 <sup>-4</sup> M
Final liquid Cs <sup>+</sup> conc. (actually at 120 hours)	1.27x10 <sup>-5</sup> M	1.27x10 <sup>-5</sup> M	1.27x10 <sup>-5</sup> M
Initial liquid sample volume	19.0 ml	19.0 ml	19.0 ml
Initial resin mass	0.1 g	0.1 g	0.1 g
Batch ID	TAM5 powder	TAM5 generated	TAM5 generated
Solution composition	DSSF5 simulant	DSSF5 simulant	DSSF5 simulant
Particle porosity	.1	0.24	0.24
solid density	1.520 g/ml	1.520 g/ml	1.520 g/ml
solution density	1.26 g/ml	1.26 g/ml	1.26 g/ml
solution viscosity	na	na	na
F factor	1.0	1.0	1.0
Phase ratio	190.00	190.00	190.00
Bed density	0.005245 g/ml	0.005245 g/ml	0.005245 g/ml
Bed porosity	0.996166	0.995460	0.995460
Estimated beta value for cesium isotherm	2.89276x10 <sup>-4</sup> M	2.89276x10 <sup>-4</sup> M	2.89276x10 <sup>-4</sup> M

Table E-7. Cesium uptake measurements made at 25 C during the batch kinetics tests of Davidson et al., 1998.

Phase ratio	Contact time (hrs)	Initial Liquid Cs <sup>+</sup> conc. [M]	K <sub>d</sub> value (ml/g)	Final Liquid Cs <sup>+</sup> conc. [M]	Approach to equilibrium (%)
100	0.00	1.418E-06	-	1.418E-06	0.00
100	0.25	1.418E-06	297	3.572E-07	83.69
100	2.00	1.418E-06	321	3.368E-07	85.29
100	24.00	1.418E-06	686	1.804E-07	97.63
100	72.00	1.418E-06	976	1.318E-07	101.47
100	144.00	1.418E-06	843	1.504E-07	100.00
200	0.00	1.418E-06	-	1.418E-06	0.00
200	0.25	1.418E-06	451	4.356E-07	83.74
200	2.00	1.418E-06	662	3.290E-07	92.83
200	24.00	1.418E-06	672	3.252E-07	93.15
200	72.00	1.418E-06	672	3.252E-07	93.15
200	144.00	1.418E-06	958	2.449E-07	100.00
400	0.00	1.418E-06	-	1.418E-06	0.00
400	0.25	1.418E-06	337	7.696E-07	70.31
400	2.00	1.418E-06	477	6.468E-07	83.63
400	24.00	1.418E-06	744	4.958E-07	100.00
400	72.00	1.418E-06	643	5.438E-07	94.79
400	144.00	1.418E-06	616	5.583E-07	93.23
1000	0.00	1.418E-06	-	1.418E-06	0.00
1000	0.25	1.418E-06	505	9.422E-07	63.51
1000	2.00	1.418E-06	652	8.584E-07	74.71
1000	24.00	1.418E-06	1120	6.689E-07	100.00
1000	72.00	1.418E-06	1072	6.844E-07	97.93
1000	144.00	1.418E-06	615	8.780E-07	72.08

Table E-8. Key parameters measured or specified during the batch kinetics tests of Davidson et al. (1998) and used to establish the cesium isotherm used in VERSE-LC kinetic modeling.

Parameter	Parameter setting for phase ratio of 100	Parameter setting for phase ratio of 100	Parameter setting for phase ratio of 100	Parameter setting for phase ratio of 100
CST material	IE-910	IE-910	IE-910	IE-910
Temperature	25 °C	25 °C	25 °C	25 °C
Initial liquid Na <sup>+</sup> conc.	? M	? M	? M	? M
Initial liquid Cs <sup>+</sup> conc.	1.418x10 <sup>-4</sup> M	1.418x10 <sup>-4</sup> M	1.418x10 <sup>-4</sup> M	1.418x10 <sup>-4</sup> M
Final liquid Cs <sup>+</sup> conc. (actually at 144 hours)	1.318x10 <sup>-7</sup> M	2.449x10 <sup>-7</sup> M	4.958x10 <sup>-7</sup> M	6.689x10 <sup>-7</sup> M
Initial liquid sample volume	10.0 ml	10.0 ml	10.0 ml	10.0 ml
Initial resin mass	0.1 g	0.05 g	0.025 g	0.01 g
Batch ID	na	na	na	na
Solution composition	W-25 supernate	W-25 supernate	W-25 supernate	W-25 supernate
Particle porosity	0.1	0.1	0.1	0.1
solid density	1.520 g/ml	1.520 g/ml	1.520 g/ml	1.520 g/ml
solution density	1.253 g/ml	1.253 g/ml	1.253 g/ml	1.253 g/ml
solution viscosity	na	na	na	na
F factor	0.86	0.86	0.86	0.86
Phase ratio	100	200	400	1000
Bed density	0.009935 g/ml	0.004984 g/ml	0.002496 g/ml	0.000999 g/ml
Bed porosity	0.991400	0.995686	0.997839	0.999135
Estimated beta value for cesium isotherm	4.03967x10 <sup>-4</sup> M	4.11446x10 <sup>-4</sup> M	5.29612x10 <sup>-4</sup> M	3.51474x10 <sup>-4</sup> M

**VERSE Input for Powder Test (Brown et al., 1996)**

Simulation of PNNL Brown et al. (1996) Cs-CST powder batch kinetic test (AW-101 simulant)

```

1 component (Cs) isotherm (1.0e-4 M initial Cs)
1, 1, 1, 6      ncomp, nelem, ncol-bed, ncol-part
FUUNA          isotherm,axial-disp,film-coef,surf-diff,BC-col  FCUNA
NNNYN          input-only,perfusable,feed-equil,datafile.yio
MM             comp-conc units
1.989769, 2.54, 0.000000001, 0.0 Length(cm),Diam(cm),Q-flow(ml/min),CSTR-vol(ml)
0.4, 0.989259, 0.24, 0.0      part-rad(um), bed-void, part-void, sorb-cap()
0.0              initial concentrations (M)
S              COMMAND - conc step change
1, 0.0, 1.00261d-4, 1, 0.0    spec id, time(min), conc(M), freq, dt(min)
V              COMMAND - viscosity/density change
0.02940, 1.409      fluid viscosity(posie), density(g/cm^3)
h              COMMAND - effluent history dump
2, 1.0, 1.0, 0.25, 0.1      unit op#, ptscale(1-4) filtering
D
-1, 0.016667, 1, 0.0
D
-1, 1.0, 1, 0.0
D
-1, 2.5, 1, 0.0
D
-1, 6, 1, 0.0
D
-1, 15, 1, 0.0
D
-1, 30, 1, 0.0
D
-1, 60, 1, 0.0
D
-1, 120, 1, 0.0
D
-1, 180, 1, 0.0
D
-1, 360, 1, 0.0
D
-1, 720, 1, 0.0
D
-1, 1440, 1, 0.0
D
-1, 2160, 1, 0.0
D
-1, 2880, 1, 0.0
D
-1, 4320, 1, 0.0
D
-1, 4800, 1, 0.0
D
-1, 6000, 1, 0.0
D
-1, 8000, 1, 0.0
D
-1, 10000, 1, 0.0
D
-1, 12000, 1, 0.0
-
-              end of commands
12000.0, 1.0      end time(min), max dt in B.V.s
1.0d-7, 1.0d-4   abs-tol, rel-tol
-              non-negative conc constraint
1.0d0            size exclusion factor
5.0             bed dispersion coefficient (cm^2/min)
4.861d-9        part-pore diffusivities (cm^2/min)
4.861d-4        Brownian diffusivities (cm^2/min)
0.01            specified film coefficient (cm/min)
5.56857d-3      Freundlich/Langmuir Hybrid a      (moles/L B.V.) rhob=0.004288
1.0             Freundlich/Langmuir Hybrid b      (1/M)          ccap=0.580
1.0             Freundlich/Langmuir Hybrid Ma      (-)
1.0             Freundlich/Langmuir Hybrid Mb      (-)
2.94143d-4      Freundlich/Langmuir Hybrid beta    (-)

```

## VERSE Output for Powder Test (Brown et al., 1996)

```
=====
VERSE v7.80 by R. D. Whitley and N.-H. L. Wang, c1999 PRF
=====
Input file: case
Simulation of PNNL Brown et al. (1996) Cs-CST powder batch kinetic test (AW
1 component (Cs) isotherm (1.0e-4 M initial Cs)
Begin Run: 17:04:43 on 03-12-2001 running under Windows 95/8
Finite elements - axial: 1 particle: 1
Collocation points - axial: 1 particle: 6 => Number of eqns: 26
Inlet species at equilib.? N Perfusable sorbent? N Feed profile only? N
Use Profile File? Y Generate Profile File? N
Axial dispersion correlation: User-specified
Film mass transfer correlation: User-specified
=====
SYSTEM PARAMETERS (at initial conditions):

t(stop) = 12000.00000 min dtheta max = 1.00000 BV
abs. tol. = .10000E-06 rel. tol. = .10000E-03
Total Length = 1.98977 cm D = 2.54000 cm
Tot. Capacity = .00000 eq/L solid Col. Vol. = 10.08231 mL
F = .00000 mL/min Uo (linear) = .00000 cm/min
R = .40000 microns L/R = 49744.22500
Bed Void frac. = .98926 Pcl. Porosity = .24000
Spec. Area = 805.57500 1/cm Time/BV = ***** min
Vol CSTRs = .00000 mL

Component no. = 1
Ke [-] = .10000E+01
Eb [cm2/min] = .50000E+01
Dp [cm2/min] = .48610E-08
Doo [cm2/min] = .48610E-03
kf [cm/min] = .10000E-01
Ds [cm2/min] = .00000E+00

Dimensionless Groups:
Re = .12611E-13
Sc(i) = .25755E+04
Peb(i) = .79390E-10
Bi(i) = .34286E+03
Nf(i) = .81221E+11
Np(i) = .72726E+10
Pep(i) = .68400E-05

Isotherm = Freundlich/Langmuir Hybrid
Iso. Const. 1 = .55686E-02
Iso. Const. 2 = .10000E+01
Iso. Const. 3 = .10000E+01
Iso. Const. 4 = .10000E+01
Iso. Const. 5 = .29414E-03
Init. Conc. = .00000E+00
Conc. at eqb. = .00000E+00
Conc. units M
=====
COMMAND LIST:
1: Step conc. of component 1 at .0000 min to .1003E-03 M
Execute 1 times, every .0000 mins.
2: User set viscosity to .2940E-01 poise and density to 1.409 g/cm3
3: Monitor conc. history at stream 2. Filename = case.h01
Output density adjustments:
1.0 *default abs conc delta, 1.0 *default rel conc delta,
.25 *default force w/ conc delta, .10 *default force w/o conc delta
4: Dump full profile file at .1667E-01 min
Execute 1 times, every .0000 mins.
5: Dump full profile file at 1.000 min
Execute 1 times, every .0000 mins.
6: Dump full profile file at 2.500 min
Execute 1 times, every .0000 mins.
```



```

7: Dump full profile file at 6.000 min
   Execute 1 times, every .0000 mins.
8: Dump full profile file at 15.00 min
   Execute 1 times, every .0000 mins.
9: Dump full profile file at 30.00 min
   Execute 1 times, every .0000 mins.
10: Dump full profile file at 60.00 min
   Execute 1 times, every .0000 mins.
11: Dump full profile file at 120.0 min
   Execute 1 times, every .0000 mins.
12: Dump full profile file at 180.0 min
   Execute 1 times, every .0000 mins.
13: Dump full profile file at 360.0 min
   Execute 1 times, every .0000 mins.
14: Dump full profile file at 720.0 min
   Execute 1 times, every .0000 mins.
15: Dump full profile file at 1440. min
   Execute 1 times, every .0000 mins.
16: Dump full profile file at 2160. min
   Execute 1 times, every .0000 mins.
17: Dump full profile file at 2880. min
   Execute 1 times, every .0000 mins.
18: Dump full profile file at 4320. min
   Execute 1 times, every .0000 mins.
19: Dump full profile file at 4800. min
   Execute 1 times, every .0000 mins.
20: Dump full profile file at 6000. min
   Execute 1 times, every .0000 mins.
21: Dump full profile file at 8000. min
   Execute 1 times, every .0000 mins.
22: Dump full profile file at .1000E+05 min
   Execute 1 times, every .0000 mins.
23: Dump full profile file at .1200E+05 min
   Execute 1 times, every .0000 mins.

```

```

=====
VERSE-LC finished in 241 steps. Average step size 49.79 minutes
End run: 17:04:44 on 03-12-2001
Integrated Areas in History Files:
case.h01 .614614E-01

```

## VERSE Input for Engineered -08 Test (Brown et al., 1996)

Simulation of PNNL Brown et al. (1996) Cs-CST engineered -08 batch kinetic test (AW-101 simulant)

```

1 component (Cs) isotherm (1.0e-4 M initial Cs)
1, 1, 1, 6 ncomp, nele, ncol-bed, ncol-part
FUUNA isotherm,axial-disp,film-coef,surf-diff,BC-col FCUNA
NNNYN input-only,perfusable,feed-equil,datafile.yio
MM comp-conc units
1.983719, 2.54, 0.000000001, 0.0 Length(cm),Diam(cm),Q-flow(ml/min),CSTR-vol(ml)
172.0, 0.993240, 0.24, 0.0 part-rad(um), bed-void, part-void, sorb-cap()
0.0 initial concentrations (M)
S COMMAND - conc step change
1, 0.0, 1.00163d-4, 1, 0.0 spec id, time(min), conc(M), freq, dt(min)
V COMMAND - viscosity/density change
0.02940, 1.409 fluid viscosity(posie), density(g/cm^3)
h COMMAND - effluent history dump
2, 1.0, 1.0, 0.25, 0.1 unit op#, ptscale(1-4) filtering
D
-1, 0.016667, 1, 0.0
D
-1, 1.0, 1, 0.0
D
-1, 2.5, 1, 0.0
D
-1, 6, 1, 0.0
D
-1, 15, 1, 0.0
D
-1, 30, 1, 0.0
D
-1, 60, 1, 0.0
D

```

```

-1, 120, 1, 0.0
D
-1, 180, 1, 0.0
D
-1, 360, 1, 0.0
D
-1, 720, 1, 0.0
D
-1, 1440, 1, 0.0
D
-1, 2160, 1, 0.0
D
-1, 2880, 1, 0.0
D
-1, 4320, 1, 0.0
D
-1, 4800, 1, 0.0
D
-1, 6000, 1, 0.0
D
-1, 8000, 1, 0.0
D
-1, 10000, 1, 0.0
D
-1, 12000, 1, 0.0
-
12000.0, 1.0
1.0d-7, 1.0d-4
-
1.0d0
5.0
2.431d-5
4.861d-4
10.0
3.48035d-3
1.0
1.0
1.0
3.4921d-4
end of commands
end time(min), max dt in B.V.s
abs-tol, rel-tol
non-negative conc constraint
size exclusion factor
bed dispersion coefficient (cm^2/min)
part-pore diffusivities (cm^2/min)
Brownian diffusivities (cm^2/min)
specified film coefficient (cm/min)
Freundlich/Langmuir Hybrid a (moles/L B.V.) rhob=0.004288
Freundlich/Langmuir Hybrid b (1/M) ccap=0.580
Freundlich/Langmuir Hybrid Ma (-)
Freundlich/Langmuir Hybrid Mb (-)
Freundlich/Langmuir Hybrid beta (-)

```

## VERSE Input for Engineered -38b Test (Brown et al., 1996)

```

Simulation of PNNL Brown et al. (1996) Cs-CST engineered -38b batch kinetic test(AW-101 simulant)
1 component (Cs) isotherm (1.0e-4 M initial Cs)
1, 1, 1, 6 ncomp, nelemt, ncol-bed, ncol-part
FUUNA isotherm,axial-disp,film-coef,surf-diff,BC-col FCUNA
NNNYN input-only,perfusable,feed-equil,datafile.yio
MM comp-conc units
1.986498, 2.54, 0.000000001, 0.0 Length(cm),Diam(cm),Q-flow(ml/min),CSTR-vol(ml)
172.0, 0.991409, 0.24, 0.0 part-rad(um), bed-void, part-void, sorb-cap()
0.0 initial concentrations (M)
S COMMAND - conc step change
1, 0.0, 1.00208d-4, 1, 0.0 spec id, time(min), conc(M), freq, dt(min)
V COMMAND - viscosity/density change
0.02940, 1.409 fluid viscosity(posie), density(g/cm^3)
h COMMAND - effluent history dump
2, 1.0, 1.0, 0.25, 0.1 unit op#, ptscale(1-4) filtering
D
-1, 0.016667, 1, 0.0
D
-1, 1.0, 1, 0.0
D
-1, 2.5, 1, 0.0
D
-1, 6, 1, 0.0
D
-1, 15, 1, 0.0
D
-1, 30, 1, 0.0

```

```

D
-1, 60, 1, 0.0
D
-1, 120, 1, 0.0
D
-1, 180, 1, 0.0
D
-1, 360, 1, 0.0
D
-1, 720, 1, 0.0
D
-1, 1440, 1, 0.0
D
-1, 2160, 1, 0.0
D
-1, 2880, 1, 0.0
D
-1, 4320, 1, 0.0
D
-1, 4800, 1, 0.0
D
-1, 6000, 1, 0.0
D
-1, 8000, 1, 0.0
D
-1, 10000, 1, 0.0
D
-1, 12000, 1, 0.0
-
12000.0, 1.0
1.0d-7, 1.0d-4
-
1.0d0
5.0
2.431d-5
4.861d-4
10.0
3.52250d-3
1.0
1.0
1.0
3.94901d-4
end of commands
end time(min), max dt in B.V.s
abs-tol, rel-tol
non-negative conc constraint
size exclusion factor
bed dispersion coefficient (cm^2/min)
part-pore diffusivities (cm^2/min)
Brownian diffusivities (cm^2/min)
specified film coefficient (cm/min)
Freundlich/Langmuir Hybrid a (moles/L B.V.) rhob=0.004288
Freundlich/Langmuir Hybrid b (l/M) ccap=0.580
Freundlich/Langmuir Hybrid Ma (-)
Freundlich/Langmuir Hybrid Mb (-)
Freundlich/Langmuir Hybrid beta (-)

```

## VERSE Input for Batch Kinetic Test (Fondeur et al., 2000)

```

Simulation of SRTC Fondeur et al. (2000) Cs-CST Baseline batch kinetic test (SRS avg)
1 component (Cs) isotherm (1.4e-4 M initial Cs)
1, 1, 1, 6 ncomp, nelem, ncol-bed, ncol-part
FUUNA isotherm,axial-disp,film-coef,surf-diff,BC-col FCUNA
NNNYN input-only,perfusable,feed-equil,datafile.yio
MM comp-conc units
3.958220, 2.54, 0.000000001, 0.0 Length(cm),Diam(cm),Q-flow(ml/min),CSTR-vol(ml)
172.0, 0.996288, 0.24, 0.0 part-rad(um), bed-void, part-void, sorb-cap()
0.0 initial concentrations (M)
S COMMAND - conc step change
1, 0.0, 1.40125d-4, 1, 0.0 spec id, time(min), conc(M), freq, dt(min)
V COMMAND - viscosity/density change
0.0278, 1.253 fluid viscosity(posie), density(g/cm^3)
h COMMAND - effluent history dump
2, 1.0, 1.0, 0.25, 0.1 unit op#, ptscale(1-4) filtering
D
-1, 0.016667, 1, 0.0
D
-1, 1.0, 1, 0.0
D
-1, 2.5, 1, 0.0
D
-1, 6, 1, 0.0
D

```

```

-1, 15, 1, 0.0
D
-1, 30, 1, 0.0
D
-1, 60, 1, 0.0
D
-1, 120, 1, 0.0
D
-1, 180, 1, 0.0
D
-1, 360, 1, 0.0
D
-1, 720, 1, 0.0
D
-1, 1440, 1, 0.0
D
-1, 2160, 1, 0.0
D
-1, 2880, 1, 0.0
D
-1, 4320, 1, 0.0
D
-1, 4800, 1, 0.0
D
-1, 6000, 1, 0.0
D
-1, 8000, 1, 0.0
D
-1, 10000, 1, 0.0
D
-1, 12000, 1, 0.0
-
12000.0, 1.0
1.0d-7, 1.0d-4
-
1.0d0
5.0
2.486d-5
4.972d-4
10.00
2.48696d-3
1.0
1.0
1.0
3.53632d-4
end of commands
end time(min), max dt in B.V.s
abs-tol, rel-tol
non-negative conc constraint
size exclusion factor
bed dispersion coefficient (cm^2/min)
part-pore diffusivities (cm^2/min) 5% of free
Brownian diffusivities (cm^2/min)
specified film coefficient (cm/min)
Freundlich/Langmuir Hybrid a (moles/L B.V.) rhob=0.004288
Freundlich/Langmuir Hybrid b (1/M) ccap=0.580
Freundlich/Langmuir Hybrid Ma (-)
Freundlich/Langmuir Hybrid Mb (-)
Freundlich/Langmuir Hybrid beta (-)

```

## VERSE Output for Batch Kinetic Test (Fondeur et al., 2000)

```

=====
VERSE v7.80 by R. D. Whitley and N.-H. L. Wang, c1999 PRF
=====
Input file: case
Simulation of SRTC Fondeur et al. (2000) Cs-CST Baseline batch kinetic test
1 component (Cs) isotherm (1.4e-4 M initial Cs)
Begin Run: 10:00:19 on 08-07-2001 running under Windows 95/8
Finite elements - axial: 1 particle: 1
Collocation points - axial: 1 particle: 6 => Number of eqns: 26
Inlet species at equilib.? N Perfusable sorbent? N Feed profile only? N
Use Profile File? Y Generate Profile File? N
Axial dispersion correlation: User-specified
Film mass transfer correlation: User-specified
=====
SYSTEM PARAMETERS (at initial conditions):

t(stop) = 12000.00000 min dtheta max = 1.00000 BV
abs. tol. = .10000E-06 rel. tol. = .10000E-03
Total Length = 3.95822 cm D = 2.54000 cm
Tot. Capacity = .00000 eq/L solid Col. Vol. = 20.05660 mL
F = .00000 mL/min Uo (linear) = .00000 cm/min
R = 172.00000 microns L/R = 230.12907

```

Bed Void frac. =	.99629	Pcl. Porosity =	.24000
Spec. Area =	.64744 1/cm	Time/BV =	***** min
Vol CSTRs =	.00000 mL		

Component no. =	1
Ke [-] =	.10000E+01
Eb [cm2/min] =	.50000E+01
Dp [cm2/min] =	.24860E-04
Doo [cm2/min] =	.49720E-03
kf [cm/min] =	.10000E+02
Ds [cm2/min] =	.00000E+00

## Dimensionless Groups:

Re	=	.50998E-11
Sc(i)	=	.26774E+04
Peb(i)	=	.15682E-09
Bi(i)	=	.28828E+05
Nf(i)	=	.12985E+12
Np(i)	=	.40299E+09
Pep(i)	=	.57105E-06

Isotherm = Freundlich/Langmuir Hybrid

Iso. Const. 1 =	.24870E-02
Iso. Const. 2 =	.10000E+01
Iso. Const. 3 =	.10000E+01
Iso. Const. 4 =	.10000E+01
Iso. Const. 5 =	.35363E-03
Init. Conc. =	.00000E+00
Conc. at eqb. =	.00000E+00
Conc. units	M

## COMMAND LIST:

```

=====
1: Step conc. of component 1 at .0000 min to .1401E-03 M
   Execute 1 times, every .0000 mins.
2: User set viscosity to .2780E-01 poise and density to 1.253 g/cm3
3: Monitor conc. history at stream 2. Filename = case.h01
   Output density adjustments:
   1.0 *default abs conc delta, 1.0 *default rel conc delta,
   .25 *default force w/ conc delta, .10 *default force w/o conc delta
4: Dump full profile file at .1667E-01 min
   Execute 1 times, every .0000 mins.
5: Dump full profile file at 1.000 min
   Execute 1 times, every .0000 mins.
6: Dump full profile file at 2.500 min
   Execute 1 times, every .0000 mins.
7: Dump full profile file at 6.000 min
   Execute 1 times, every .0000 mins.
8: Dump full profile file at 15.00 min
   Execute 1 times, every .0000 mins.
9: Dump full profile file at 30.00 min
   Execute 1 times, every .0000 mins.
10: Dump full profile file at 60.00 min
   Execute 1 times, every .0000 mins.
11: Dump full profile file at 120.0 min
   Execute 1 times, every .0000 mins.
12: Dump full profile file at 180.0 min
   Execute 1 times, every .0000 mins.
13: Dump full profile file at 360.0 min
   Execute 1 times, every .0000 mins.
14: Dump full profile file at 720.0 min
   Execute 1 times, every .0000 mins.
15: Dump full profile file at 1440. min
   Execute 1 times, every .0000 mins.
16: Dump full profile file at 2160. min
   Execute 1 times, every .0000 mins.
17: Dump full profile file at 2880. min
   Execute 1 times, every .0000 mins.
18: Dump full profile file at 4320. min
   Execute 1 times, every .0000 mins.
19: Dump full profile file at 4800. min
   Execute 1 times, every .0000 mins.
20: Dump full profile file at 6000. min
   Execute 1 times, every .0000 mins.
21: Dump full profile file at 8000. min

```

```

Execute 1 times, every .0000 mins.
22: Dump full profile file at .1000E+05 min
Execute 1 times, every .0000 mins.
23: Dump full profile file at .1200E+05 min
Execute 1 times, every .0000 mins.

```

```

=====
VERSE-LC finished in 239 steps. Average step size 50.21 minutes
End run: 10:00:20 on 08-07-2001
Integrated Areas in History Files:
case.h01 .309182

```

## VERSE Input for Cs Uptake Test (Anthony et al., 1996; 112 $\mu\text{m}$ )

Simulation of Sandia (TAM slide show) Cs-CST TAM5 Engr batch kinetic test (DSSF55 simulant)

```

1 component (Cs) isotherm (1.0e-4 M initial Cs)
1, 1, 1, 6 ncomp, nelem, ncol-bed, ncol-part
FUUNA isotherm,axial-disp,film-coef,surf-diff,BC-col FCUNA
NNNYN input-only,perfusable,feed-equil,datafile.yio
MM comp-conc units
3.762685, 2.54, 0.000000001, 0.0 Length(cm),Diam(cm),Q-flow(ml/min),CSTR-vol(ml)
56.0, 0.995460, 0.24, 0.0 part-rad(um), bed-void, part-void, sorb-cap()
0.0 initial concentrations (M)
S COMMAND - conc step change
1, 0.0, 1.00109d-4, 1, 0.0 spec id, time(min), conc(M), freq, dt(min)
V COMMAND - viscosity/density change
0.02780, 1.26 fluid viscosity(posie), density(g/cm^3)
h COMMAND - effluent history dump
2, 1.0, 1.0, 0.25, 0.1 unit op#, ptscale(1-4) filtering
D
-1, 0.016667, 1, 0.0
D
-1, 1.0, 1, 0.0
D
-1, 2.5, 1, 0.0
D
-1, 6, 1, 0.0
D
-1, 15, 1, 0.0
D
-1, 30, 1, 0.0
D
-1, 60, 1, 0.0
D
-1, 120, 1, 0.0
D
-1, 180, 1, 0.0
D
-1, 360, 1, 0.0
D
-1, 720, 1, 0.0
D
-1, 1440, 1, 0.0
D
-1, 2160, 1, 0.0
D
-1, 2880, 1, 0.0
D
-1, 4320, 1, 0.0
D
-1, 4800, 1, 0.0
D
-1, 6000, 1, 0.0
D
-1, 8000, 1, 0.0
D
-1, 10000, 1, 0.0
D
-1, 12000, 1, 0.0
-
end of commands
12000.0, 1.0 end time(min), max dt in B.V.s
1.0d-7, 1.0d-4 abs-tol, rel-tol
- non-negative conc constraint

```

1.0d0	size exclusion factor	
5.0	bed dispersion coefficient (cm <sup>2</sup> /min)	
1.257d-4	part-pore diffusivities (cm <sup>2</sup> /min)	
4.836d-4	Brownian diffusivities (cm <sup>2</sup> /min)	
10.0	specified film coefficient (cm/min)	
2.06863d-3	Freundlich/Langmuir Hybrid a	(moles/L B.V.) rhob=0.004288
1.0	Freundlich/Langmuir Hybrid b	(1/M) ccap=0.580
1.0	Freundlich/Langmuir Hybrid Ma	(-)
1.0	Freundlich/Langmuir Hybrid Mb	(-)
2.89276d-4	Freundlich/Langmuir Hybrid beta	(-)

## VERSE Input for Cs Uptake Test (Anthony et al., 1996; 334 $\mu$ m)

Simulation of Sandia (TAM slide show) Cs-CST TAM5 Engr batch kinetic test (DSSF55 simulant)

1 component (Cs) isotherm (1.0e-4 M initial Cs)

1, 1, 1, 6 ncomp, nelem, ncol-bed, ncol-part

FUUNA isotherm,axial-disp,film-coef,surf-diff,BC-col FCUNA

NNNYN input-only,perfusable,feed-equil,datafile.yio

MM comp-conc units

3.762685, 2.54, 0.000000001, 0.0 Length(cm),Diam(cm),Q-flow(ml/min),CSTR-vol(ml)

167.0, 0.995460, 0.24, 0.0 part-rad(um), bed-void, part-void, sorb-cap()

0.0 initial concentrations (M)

S COMMAND - conc step change

1, 0.0, 1.00109d-4, 1, 0.0 spec id, time(min), conc(M), freq, dt(min)

V COMMAND - viscosity/density change

0.02780, 1.26 fluid viscosity(posie), density(g/cm<sup>3</sup>)

h COMMAND - effluent history dump

2, 1.0, 1.0, 0.25, 0.1 unit op#, ptscale(1-4) filtering

D

-1, 0.016667, 1, 0.0

D

-1, 1.0, 1, 0.0

D

-1, 2.5, 1, 0.0

D

-1, 6, 1, 0.0

D

-1, 15, 1, 0.0

D

-1, 30, 1, 0.0

D

-1, 60, 1, 0.0

D

-1, 120, 1, 0.0

D

-1, 180, 1, 0.0

D

-1, 360, 1, 0.0

D

-1, 720, 1, 0.0

D

-1, 1440, 1, 0.0

D

-1, 2160, 1, 0.0

D

-1, 2880, 1, 0.0

D

-1, 4320, 1, 0.0

D

-1, 4800, 1, 0.0

D

-1, 6000, 1, 0.0

D

-1, 8000, 1, 0.0

D

-1, 10000, 1, 0.0

D

-1, 12000, 1, 0.0

-

end of commands

12000.0, 1.0 end time(min), max dt in B.V.s

---

1.0d-7, 1.0d-4	abs-tol, rel-tol	
-	non-negative conc constraint	
1.0d0	size exclusion factor	
5.0	bed dispersion coefficient (cm <sup>2</sup> /min)	
1.257d-4	part-pore diffusivities (cm <sup>2</sup> /min)	
4.836d-4	Brownian diffusivities (cm <sup>2</sup> /min)	
10.0	specified film coefficient (cm/min)	
2.06863d-3	Freundlich/Langmuir Hybrid a	(moles/L B.V.) rhob=0.004288
1.0	Freundlich/Langmuir Hybrid b	(1/M) ccap=0.580
1.0	Freundlich/Langmuir Hybrid Ma	(-)
1.0	Freundlich/Langmuir Hybrid Mb	(-)
2.89276d-4	Freundlich/Langmuir Hybrid beta	(-)

---



## Appendix F (ZAM Code Description)

The ZAM code is purchased commercial software developed at Texas A&M University by Rayford G. Anthony and Zhixin Zheng. The ZAM code is a product of over several years development and research in Professor R. G. Anthony's Kinetics, Catalysis and Reaction Engineering Laboratory in the Department of Chemical Engineering Texas A&M University. ZAM is written in FORTRAN 90 using the Microsoft Developer's Workbench. For applications performed at SRTC, PC based versions running under MS-DOS are used. No extensive user guide exists for ZAM; however, a brief user guide is available from Professor Anthony. A description of the current ZAM model is provided by Zheng et al. (1997). Supporting information and earlier modeling are provided by Zheng et al. (1995) and Zheng et al. (1996). Further information on ZAM is available by contacting Rayford G. Anthony at e-mail: RG-ANTHONY@TAMU.edu, Telephone (409)845-3370, or Fax (409)862-3266.

This appendix contains or references the information necessary for using version 4 or 5 of the ZAM code (i.e., executables referred to as CSTIEXV4 or CSTIEXV5; CST Ion Exchange Version 4 or 5). ZAM is commercial software designed to simulate ion-exchange equilibria of electrolytic solutions and crystalline silicotitanate solid in its powdered form (labeled as CST, TAM5, or IONSIV® IE-910).

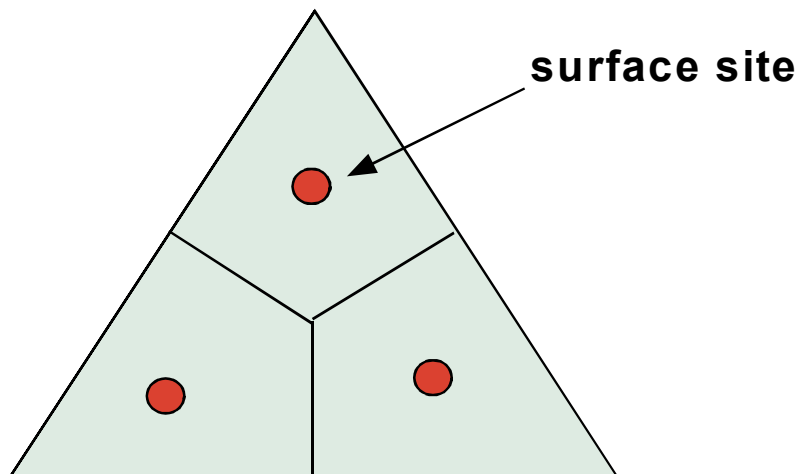
In order to use ZAM for predicting the behavior of CST in its engineered forms, a correction factor accounting for the inert binding material must be considered (i.e., referred to in this report as a dilution factor,  $\eta_{df}$ ). After the writing of this report a recent upgrade to ZAM was report by Anthony et al (2001), where several improvements pertinent to this work should be considered in any future modeling efforts.

### F.1 About the Model

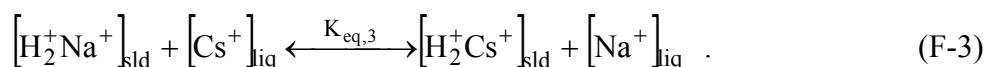
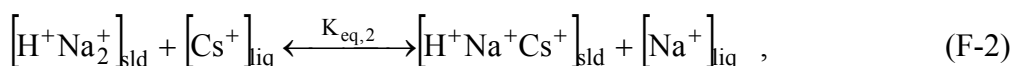
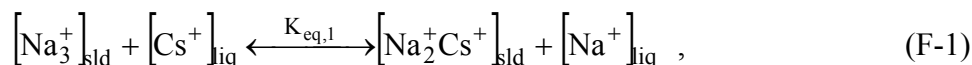
The ZAM model solves a set of equations for solid-liquid equilibrium. This model includes the competitive ion exchange at CST exchange sites between the following homovalent cations:  $\text{Na}^+$ ,  $\text{Cs}^+$ ,  $\text{H}^+$ ,  $\text{Rb}^+$ ,  $\text{K}^+$ , and  $\text{SrOH}^+$ . Non-idealities within the aqueous phase are handled using Bromley's model for calculating activity coefficients of the ions. Since Bromley (1973) only established modeling parameters for some of the most common ions up to an ionic strength of ~6 molal, errors may occur when one uses the ZAM code beyond 6 molal or when addressing solutions containing ions whose Bromley parameters do not exist. However, experience by the developers indicated that even at ionic strengths exceeding 6 molal good results were achieved for DSSF5, DSF7, NCAW, and other Hanford simulants (i.e., for Phase 1 inventories 10 molal and higher need to be addressed). A listing of the currently available ionic species contained within the ZAM database is provided in Table F-1.

Surface non-idealities on the solid phase CST material are handled by a supersite approach (see Zheng et al., 1997). The supersite approach involves three neighboring surface sites as shown below:

## ZAM Supersite



Here, experimental data indicates that a thermodynamically ideal solid phase can be achieved when the CST material is viewed on a supersite basis. Investigations made by Zheng et al. (1996) found step changes in binary ion exchange isotherms and that prior to these step changes, the solid phase was found to be ideal along the isotherms. For example, when viewing the ion exchange process between sodium and cesium we have the following three possible mass-action relationships to consider:



Equations F-1, F-2, and F-3 represents the removal of a  $Na^+$  cation at a surface site with a  $Cs^+$  cation. The three possible cases reflect the three possible states that the supersite might be in prior to the ion exchange (note that a supersite can not hold more than one  $Cs^+$  cation at any point in time). The temperature dependence of the equilibrium constants for each of the above mass-action equations can be approximated by:

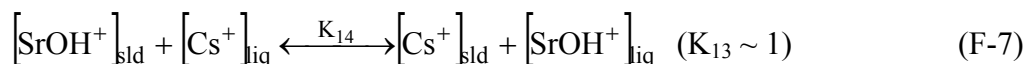
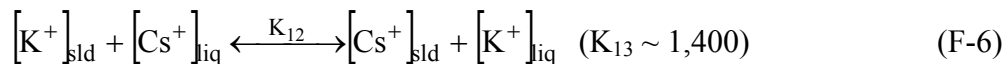
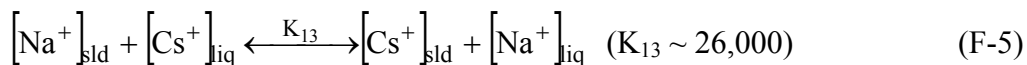
$$\ln\left(\frac{K_{eq}(T_2)}{K_{eq}(T_1)}\right) = -\frac{\Delta H_{IX}}{R} \left[ \frac{1}{T_2} - \frac{1}{T_1} \right] , \quad (F-4)$$

where the heats of ion exchange under high alkaline conditions have been estimated to be:

- (Reaction 1)  $\Delta H_{IX} = -2.18 \times 10^4$  J/gmole
- (Reaction 2)  $\Delta H_{IX} = 1.46 \times 10^4$  J/gmole
- (Reaction 3)  $\Delta H_{IX} =$  (not recorded)

During the loading phase, the CST material will be in its Na-form with only trace amount of H<sup>+</sup> present. Therefore, Eq. (F-1) will be the dominant ion exchange reaction taking place. Under these conditions the overall ion exchange process will be exothermic implying that higher column temperatures yields lower cesium loadings consistent with currently available batch contact data.

Looking at just the overall ion exchange reactions involving Cs<sup>+</sup> we have:



where the selectivity coefficients (K<sub>ij</sub>) listed reflect approximate estimates and provide insight into the selectivity of CST for cesium.

Mass-action relationships similar to those above are also written for each of the potential competitors (Na<sup>+</sup>, Cs<sup>+</sup>, H<sup>+</sup>, Rb<sup>+</sup>, K<sup>+</sup>, and SrOH<sup>+</sup>). Also species material balance equations are written relating the amount of each species within the liquid and solid phases in the initial state to amounts in the final (“equilibrium”) state. To obtain these material balances the mass of CST and mass of liquid (i.e., volume of liquid and its density) must also be specified. Solution of this set of nonlinear algebraic equations is achieved using a modified (“rate-limited”) Newton-Raphson technique.

Two versions of ZAM have been used within SRTC (i.e., Version 4 and Version 5). Both versions model the effect of temperature on the system (Na<sup>+</sup>, Cs<sup>+</sup>, H<sup>+</sup>, Rb<sup>+</sup>, and K<sup>+</sup>) when considering a basic solution of pH>12. The newer version (Version 5) contains the following code improvements:

- Updates to aqueous phase strontium reaction (Sr<sup>+</sup>, OH<sup>-</sup>, and SrOH<sup>+</sup>) in basic solutions of pH>12 has been added;
- Improvements were made in estimating the effect of K<sup>+</sup> on cesium distribution coefficients; and
- Bromley’s parameters for NO<sub>2</sub><sup>-</sup> and Al(OH)<sub>4</sub><sup>-</sup> have been updated.

The actual impact as a result of these updates is small when considering the Phase 1 Law batch feeds as to be demonstrated by example below. For many of the Phase 1 LAW batch feed simulations required Version 5 had difficulty in converging. Since the final results from both versions are very similar, Version 4 was used the majority of the time.

The solid-liquid equilibrium model solves the various mass-action equations involving ion exchange in conjunction with the appropriate material balance equations. At a specified operating temperature (K) and solution density (g/L or kg/m<sup>3</sup>) ZAM performs a simulated batch

contact (“K<sub>d</sub>”) test where the quantity of the following variables at their initial state must be specified:

- Initial composition of aqueous solution (gmole/L);
- Amount of aqueous solution present (L);
- Amount of CST material present (g); and
- Initial form of CST (0 for sodium or 1 for hydrogen).

Upon solving the simulated contact test, ZAM outputs the following final (“at equilibrium”) state values for four of the competing cations (Cs<sup>+</sup>, Rb<sup>+</sup>, SrOH<sup>+</sup>, and K<sup>+</sup>; note Na<sup>+</sup> and H<sup>+</sup> loading numbers are not provided):

- Final CST loading of cation (Q, mmole/g<sub>CST</sub>);
- Final aqueous phase concentration of cation (gmole/L); and
- K<sub>d</sub> value of cation (ml/g<sub>CST</sub>).

Note that the CST loading value is simply the product of the K<sub>d</sub> value times the final concentration for each competitor. Also printed in output is the solutions pH and ionic strength values.

## F.2 I/O Files and Running the ZAM Code

The program is accessed from the MS-DOS prompt. The executables are named “CSTIEXV4” for Version-4 and “CSTIEXV5” for Version-5. The standard input file is named “CSTIEXV.in” and contains all the necessary input to perform a single simulated K<sub>d</sub> test. Scripts can be used when multiple K<sub>d</sub> simulations are desired. The results of the simulated K<sub>d</sub> test are placed in the standard output file named “CSTIEXV.out”.

Assuming that the above executables are located in a directory defined by your PATH or resides within the current directory, at the MS-DOS prompt entering the executable filename will execute the ZAM program if an input file named “CSTIEXV.in” exists within the current directory. The output file named “CSTIEXV.out” is placed into this current directory, as well. During execution ZAM may printout various runtime messages (i.e., progression of solver or error messages). If a KNO<sub>3</sub> precipitation/solubility limit is reached, then ZAM prints out to the active MS-DOS window the new adjusted concentrations for K<sup>+</sup> and NO<sub>3</sub><sup>-</sup>. ZAM is paused under these conditions requiring the user to enter a keystroke to continue the simulation if desired.

For computing several ZAM simulations together, a simple script such as the one below is useful. This script runs a comparison case where Version-4 and Version-5 results are generated based on the same input:

```
copy cstiexv_LAW_1_a.in cstiexv.in
cstiexv4
```

```
move cstiexv.out cst_LAW_1_5M_v4.out
#
copy cstiexv_LAW_1_a.in cstiexv.in
cstiexv5
move cstiexv.out cst_LAW_1_5M_v5.out
#
```

Note that the results of a simulation need to be moved or new results will overwrite the old results.

### F.3 Input File Structure

The standard input file is named “CSTIEXV.in” and contains all the necessary input to perform a single simulated  $K_d$  test. This file contains the information required prior to ion-exchange and the program then calculates the equilibrium based on this initial information. Briefly, you need to specify the choice of activity coefficient model, temperature, the title, the liquid molar density, the number of cations, the number of anions, cation concentrations, anion concentrations, amount of liquid, amount of solid, the initial solid form parameter, and the calculation adjustment parameter. The liquid phase concentrations must be charged balanced (i.e., ZAM assumes the solution to be charged balance to within a small tolerance). If the solution charge miss-balance exceed the tolerance an error message is printed and ZAM execution is terminated. Charge balancing should be performed using a species having a small overall impact like chlorine.

The following is a line-by-line description of the input needs for “CSTIEXV.in”:

- Line 1) **Choice of activity model and temperature:** Option 1 is the only activity model currently available and presents Bromley’s model. Temperature is input in K units. The temperature dependent parameter within the ZAM model are based on experimental data taken within the range 298.15 K to 317.15 K. The temperature effect in neutral to acidic solutions (pH<12) is not included, and the effect of temperature for strontium is not addressed.
- Line 2) **Title:** The title inputted is printed out as a header in the output file and must be less than 33 characters long.
- Line 3) **Number of Cations:** An integer whose number must exceed 6. A minimum of 7 cations is required because  $\text{Na}^+$ ,  $\text{Cs}^+$ ,  $\text{H}^+$ ,  $\text{Rb}^+$ ,  $\text{K}^+$ , and  $\text{SrOH}^+$  are competing cations for CST exchange sites and  $\text{Sr}^{2+}$  is in equilibrium with  $\text{SrOH}^+$  in the aqueous phase.
- Line 4) **Number of Anions:** An integer whose number must exceed 1. A minimum of 2 anions is required because  $\text{OH}^-$  and  $\text{NO}_3^-$  are assumed to be always considered within the aqueous phase solution model formulation.

- Line 5) **Solution Density (g/L or kg/m<sup>3</sup>):** The aqueous phase density is required to convert molar ion concentrations (gmole/L) into molal units (gmole/kg<sub>water</sub>). Bromley's activity coefficient model is based on molal units.
- Line 6) **Cation Code IDs:** These are integer ID numbers specifying which cations are being considered (see Table F-1). The first 7 cations (minimum number required) must be Na<sup>+</sup>, Cs<sup>+</sup>, H<sup>+</sup>, Rb<sup>+</sup>, K<sup>+</sup>, SrOH<sup>+</sup>, and Sr<sup>2+</sup> in this order (i.e., 3, 6, 1, 1, 5, 4, 40, 13). Additional cations can be added to the list starting in the 8<sup>th</sup> position and beyond in any given order. Even under conditions where some of the first 7 cations do not exist within the aqueous phase, they must still be given with zero concentrations inputted.
- Line 7) **Anion Code IDs:** These are integer ID numbers specifying which anions are being considered (see Table F-1). The first 2 anions (minimum number required) must be OH<sup>-</sup> and NO<sub>3</sub><sup>-</sup> in this order (i.e., 13, 9). Additional anions can be added to the list starting in the 3<sup>rd</sup> position and beyond in any given order. Even under conditions where some of the first 2 anions do not exist within the aqueous phase, they must still be given with zero concentrations inputted.
- Line 8) **Formula Weight:** If you have chosen a ion not explicitly listed in Table F-1, then its molecular weight (g/gmole) must be supplied. If you have only requested ions contained within Table F-1, this line can be skipped. Three unlisted cations and three unlisted anions are optional. For cations the possible code IDs are 37, 38, and 39 (see Table F-1). For anions the possible code IDs are 24, 25, and 26 (see Table F-1).
- Line 9) **Cation Concentrations (M):** Here the concentrations should be listed in the same order as the cation code IDs are listed. Zero concentrations can be used. However the concentration of H<sup>+</sup> must be greater than zero. For example, if the solution is basic use [H<sup>+</sup>][OH<sup>-</sup>]=1x10<sup>-14</sup> to estimate the H<sup>+</sup> concentration. The ZAM program will internally correct the H<sup>+</sup> concentration. If the solution is neutral use 1x10<sup>-7</sup>. For strontium considerations, input zero concentration for SrOH<sup>+</sup> (cation #40) and the actual concentration of total strontium as Sr<sup>2+</sup> (cation #13). The program will calculate the liquid-phase equilibrium between SrOH<sup>+</sup> and Sr<sup>2+</sup> based on available free OH<sup>-</sup>.
- Line 10) **Anion Concentrations (M):** Here the concentrations should be listed in the same order as the anion code IDs are listed. Zero concentrations can be used. However the concentration of OH<sup>-</sup> must be greater than zero. For example, if the solution is acidic use [H<sup>+</sup>][OH<sup>-</sup>]=1x10<sup>-14</sup> to estimate the OH<sup>-</sup> concentration. The ZAM program will internally correct the OH<sup>-</sup> concentration. If the solution is neutral use 1x10<sup>-7</sup>.
- Line 11) **Liquid Volume (L) and Solid Mass (g):** Enter the amount of volume of aqueous phase solution being placed in contact with CST. Enter the amount of mass of CST being considered. The phase ratio is the ratio of these two quantities.
- Line 12) **Initial form of solid:** There are two initial forms for the CST material (its Na-form or its H-form). Here it is assumed that all exchange sites are initially occupied by either Na<sup>+</sup> (option 0) or by H<sup>+</sup> (option 1).

Line 13) **Calculational Adjustment Parameter:** Real number ranging from 0.0 to 1.0. This is an under-relaxation iteration parameter used to assist in convergence of the non-linear equation solver. The larger the number the faster (less under-relaxed) convergence is generally achieved (however, the larger the risk of divergence). The best overall value is around 0.7. The program has more difficulty in converging under near neutral conditions. Note that concentration ranges covering 5 to 10 orders in magnitude are typically being computed and the system of equations can become very stiff. This set of equilibrium and material balance equations are a very non-linear set of algebraic equations that can be difficult to solve for most standard solvers. Generally, low values of this adjustment parameter helps convergence but can greatly extend the overall runtime.

#### F.4 Installation, Verification & Validation

The functional requirements placed on ZAM Version 4 or 5 are as follows:

1. Capability to reproduce the total ionic capacities of its cation competitors consistent with experimentally measured values.

Acceptance criterion: Successful prediction of total ionic capacity for  $\text{Cs}^+$ ,  $\text{K}^+$ ,  $\text{Rb}^+$ , and  $\text{SrOH}^+$  (in the judgement of the author(s) and independent technical reviewer).

2. Capability to reproduce the cesium  $K_d$  and loading curves for Hanford AW-101 simulant and samples consistent with the experimentally measured values used in ZAM's original development phase.

Acceptance criterion: Successful prediction of the cesium  $K_d$  and loading curves for Hanford AW-101 simulant and samples (in the judgement of the author(s) and independent technical reviewer).

PC based executable that has the capability to run on the following computer platform:

##### Computer platform chosen:

Platform:	Intel™ based Personal Computer
System:	Microsoft Windows-95 version 4.0 or higher
Compilers:	None required
Options:	Default settings
Acceptance criterion:	Successful installation testing

The ZAM executables for this effort were loaded on an IBM Personal Computer 300PL (with a PII 400 processor). Files corresponding to test cases were placed in shared folders while the ZAM code executables were kept in a protected file due to its proprietary nature.

Full path name: **d:\verse\**

**Cstiexv4.exe** (protected; ZAM version 4)

**Cstiexv5.exe (protected; ZAM version 5)**

The ZAM code was tested by running and comparing its output results to:

1. Isolated competitor to determine that ZAM will approach the appropriate total loading capacity at its limits (i.e., this is a verification activity checking that the version loaded onto the above PC is installed correctly and conforms to the expected behavior as published by its developers); and
2. Simulated and actual Hanford waste solutions that were originally used in ZAM's development (i.e., this is a validation activity checking that the version loaded onto the above PC is providing predictions that are consistent with those published by its developers for use with typical Hanford waste feeds).

**F.4.1 ZAM Verification of Total Ionic Capacities**

The ZAM model solves the solid-liquid equilibrium exchange and material balance equations that describe the ion exchange process between CST in its powdered-form in contact with a finite volume of liquid. In order to appropriately model this process, the number of "surface" sites (i.e., on a per mass basis of CST) that are available ("active") for a given cation competitor must be known and becomes an internally defined parameter within the equation set.

The total cation exchange capacity of the CST resin in its powder-form (batch IE-910) is species dependent. Two types of exchange sites exist on the CST solid. The total ion exchange capacity is stated to be  $\sim 4.6$  mmole/g<sub>resin</sub>, but the cesium exchange capacity is much less indicating that not all sites are available for cesium exchange (see, Zheng et al., 1996). In the ideal solid region (i.e., the prior to the first step of the isotherm), the experimentally measured total capacities are  $\sim 0.58$  mmole/g<sub>resin</sub> for Cs<sup>+</sup>,  $\sim 1.2$  mmole/g<sub>resin</sub> for K<sup>+</sup>,  $\sim 1.18$  mmole/g<sub>resin</sub> for Rb<sup>+</sup>, and  $\sim 1.0$  mmole/g<sub>resin</sub> for SrOH<sup>+</sup>. For the expected feed concentrations it is anticipated that the entire columns will be operating within this ideal solid region.

To numerically compute these asymptotic cation capacities, the ZAM code was run under conditions where each cation competitor was individually set to a very high concentration (i.e., simple 5 M Na<sup>+</sup> and 2 M OH<sup>-</sup> solutions were used where NO<sub>3</sub><sup>-</sup> concentrations were varied along with the given competitor for charge balance). The ZAM predicted results of these tests are:

- Cs<sup>+</sup> total ionic capacity = 0.5797 mmole/g<sub>CST</sub> (experimentally  $\sim 0.58$ ; - 0.05% difference)
- K<sup>+</sup> total ionic capacity = 1.066 mmole/g<sub>CST</sub> (experimentally  $\sim 1.2$ ; - 11.2% difference)
- Rb<sup>+</sup> total ionic capacity = 1.139 mmole/g<sub>CST</sub> (experimentally  $\sim 1.18$ ; - 3.5% difference)
- SrOH<sup>+</sup> total ionic capacity = 1.159 mmole/g<sub>CST</sub> (experimentally  $\sim 1.0$ ; - 15.9% difference)

As shown, the ZAM predicted total ionic capacities are all slightly under-predicting the measured values. However, these differences should be within experimental uncertainties and the ZAM results are considered acceptable.



#### **F.4.2 ZAM Validation to Hanford LAW Solutions**

At the outset of development of ZAM, its intended purpose was to model the solid-liquid equilibrium exchange process of CST in its powdered-form in contact with high alkaline Hanford waste solutions (i.e., Cs removal from LAW solutions). Early on, validation of ZAMs ability to successfully model the ion exchange properties of CST in Hanford LAW was accomplished by direct comparison of ZAM predictions to experimental measurements. Here, we shall compare the ZAM results generated by our PC installed versions of ZAM to the original experimental database used in its creation.

Experimental batch contact tests (“ $K_d$  studies”) by Brown et al. (1996) were performed placing CST (i.e., powder and engineered forms) in contact with both simulated and actual AW-101 Hanford waste solutions. In the simulated AW-101 studies the sodium concentration level was varied from ~2 to ~7 M over a large variation of cesium concentrations. For the smaller set of actual waste samples, a sodium concentration of ~5 M was tested.

A comparison of measured versus ZAM predicted  $K_d$  values for CST in its powder-form in contact with simulated AW-101 solutions is shown in Figure F-1. The measured data is provided in Table F-3. Sodium concentration levels varied from 2 M up to 5 M with all tests run at ~25 C. Overall, good agreement is achieved with ZAM for the  $K_d$  values corresponding to sodium levels of 1 M and above. ZAM consistently under-predicts the measured  $K_d$  values for the 0.2 M sodium solutions. Our current applications focus primarily near 5 M sodium solutions where adequate agreement exists. At 5 M sodium conditions a comparison of measure  $K_d$  values for CST powder in contact with simulated and actual AW-101 solutions is provided in Figure F-2. Also shown in Figure F-2 is the corresponding ZAM prediction. The cesium  $K_d$  values for the actual waste sample are systematically lower than ZAM or the simulated solution at increasing cesium concentrations. This may suggest that other species are present that affect  $Cs^+$  competition. The results shown in Figures F-1 and F-2 are consistent with the results provided by Zheng et al. (1997), indicating that our PC installed version of ZAM is operating consistent with its original release.

Brown et al. (1996) also performed batch contact tests using two CST engineered-form materials labeled as “38b” and “08” (i.e., these are some of the earlier-on engineered-forms made). Their contact data for these engineered-forms are given in Tables F-4 and F-5, respectively. Batch contact data ranging from 0.2 M to 7 M sodium were measured and are compared to ZAM predictions in Figures F-3 and F-4 for the “08” and “38b” engineered-forms, respectively. When comparing Figure F-1 to Figures F-3 and F-4, we see that in general ZAM slightly under-predicts CST powder performance while over-predicts CST engineered-form performance. This is a direct result of the presence of an inert binder (i.e., typically 20% to 30% by mass) used in making an engineered-form starting with CST powder.

For the engineered-form “38b” batch contact tests using actual AW-101 waste samples were performed at 5 M sodium conditions. A comparison of measured cesium  $K_d$  values for engineered-form “38b” in contact with simulant and actual waste samples is shown in Figure F-5, along with the ZAM prediction. Similar to the trend mentioned above, when comparing Figures F-2 and F-5 we see that the engineered-forms have slightly degraded performance.

Cesium loading data and ZAM predictions for the CST powder, engineered-form “08”, and engineered-form “38b” are shown in Figures F-6, F-7, and F-8, respectively. In all three figures significant data scatter is seen at low  $\text{Na}^+/\text{Cs}^+$  ratios (i.e., very high cesium concentrations). In Figure F-6 the data suggests that the total cesium capacity for CST powder varies with sodium concentration. However, at cesium and sodium concentrations levels of interest for Phase 1 inventories the ZAM predictions are reasonably consistent with the data.

Based on the comparisons made in this section of measured versus ZAM predicted cesium  $K_d$  values and Cs loadings, we conclude that the ZAM model provides a reasonable estimate for CST powder (as shown in Figure F-9) but requires an adjustment (i.e., “dilution”) factor when engineered-forms are being considered. For referencing, the ZAM predictions shown in Figures F-1 through F-9 are tabulated in Table F-6. The ZAM generated database is based on the AW-101 compositions provided in Table F-7 where the cesium concentrations were varied from  $1 \times 10^{-6}$  M up to 0.1 M. To maintain charge balance CsCl was added where the original difference between Cs and Cl is maintained. Example AW-101 input and output files for the 5 M sodium conditions are provided in sections F.5 and F.6, respectively.

#### **F.4.3 Version-4 Versus Version-5 Comparison**

To see the impact of the improvements made in Version-5 when compared to results of Version-4, both ZAM versions were run for the LAW-1 batch feed. For all Phase 1 LAW batch feeds, the ionic species considered in ZAM analyses are listed in Table F-2.

The input file for either version has the file structure as shown below in section F.5 for the Phase 1 LAW-1 batch feed. The test case considered for comparison has the CST initially in its sodium form where the equilibrium is calculated at 25 C. The LAW-1 feed adjusted to a 5 M  $\text{Na}^+$  basis with a solution density of 1.255 g/ml. At these conditions the solution has an ionic strength of ~6.3 molal and a pH of ~14.6. For convenience the phase ratio of the solid-liquid system is set to a very high value of  $1 \times 10^5$  ml/g (i.e., 1000 L solution in contact with 0.01 g of CST). This is done so that the equilibrium point of interest will be very close to initial conditions (i.e., final cesium concentration close to its initial concentration).

Using the input file listed in section F.7 (file name: cstiexv.in), the results from Version-4 and Version-5 are provided in sections F.8 and F.9, respectively. The results are identical to within the level of accuracy provided (i.e., within round-off of the printed results; 4 digits for Version-4 and 3 digits for Version-5). As mentioned above, the use of a very high phase ratio resulted in the final  $\text{Cs}^+$  solution concentration (i.e.,  $3.386 \times 10^{-4}$  M) being close to its initial concentration (i.e.,  $3.433 \times 10^{-4}$  M).

Comparisons made for other LAW batch feeds and for varying cesium concentrations (i.e., CsCl variations) show similar behavior. Basically, results based on versions 4 and 5 do not differ in any meaningful way.

Table F-1. Ionic species available within the ZAM CST ion-exchange equilibrium model.

ID	Cations	Anions	ID	Cations	Anions
1	H <sup>+</sup>	F <sup>-</sup>	21	Cd <sup>2+</sup>	AsO <sub>4</sub> <sup>3-</sup>
2	Li <sup>+</sup>	Cl <sup>-</sup>	22	Pb <sup>2+</sup>	Fe(CN) <sub>6</sub> <sup>3-</sup>
3	Na <sup>+</sup>	Br <sup>-</sup>	23	UO <sub>2</sub> <sup>2+</sup>	Mo(CN) <sub>8</sub> <sup>3-</sup>
4	K <sup>+</sup>	I <sup>-</sup>	24	Cr <sup>3+</sup>	User defined <sup>a</sup>
5	Rb <sup>+</sup>	ClO <sub>3</sub> <sup>-</sup>	25	Al <sup>3+</sup>	User defined
6	Cs <sup>+</sup>	ClO <sub>4</sub> <sup>-</sup>	26	Sc <sup>3+</sup>	User defined
7	NH <sub>4</sub> <sup>+</sup>	BrO <sub>3</sub> <sup>-</sup>	27	Y <sup>3+</sup>	NO <sub>2</sub> <sup>-</sup>
8	Tl <sup>+</sup>	IO <sub>3</sub> <sup>-</sup>	28	La <sup>3+</sup>	Al(OH) <sub>4</sub> <sup>-</sup>
9	Ag <sup>+</sup>	NO <sub>3</sub> <sup>-</sup>	29	Ce <sup>3+</sup>	na <sup>b</sup>
10	Be <sup>2+</sup>	H <sub>2</sub> PO <sub>4</sub> <sup>-</sup>	30	Pr <sup>3+</sup>	na
11	Mg <sup>2+</sup>	H <sub>2</sub> AsO <sub>4</sub> <sup>-</sup>	31	Nd <sup>3+</sup>	na
12	Ca <sup>2+</sup>	CNS <sup>-</sup>	32	Sm <sup>3+</sup>	na
13	Sr <sup>2+</sup>	OH <sup>-</sup>	33	Eu <sup>3+</sup>	na
14	Ba <sup>2+</sup>	CrO <sub>4</sub> <sup>2-</sup>	34	Ga <sup>3+</sup>	na
15	Mn <sup>2+</sup>	SO <sub>4</sub> <sup>2-</sup>	35	Co <sup>3+</sup>	na
16	Fe <sup>2+</sup>	S <sub>2</sub> O <sub>3</sub> <sup>2-</sup>	36	Th <sup>4+</sup>	na
17	Co <sup>2+</sup>	HPO <sub>4</sub> <sup>2-</sup>	37	User defined <sup>a</sup>	na
18	Ni <sup>2+</sup>	HAsO <sub>4</sub> <sup>2-</sup>	38	User defined	na
19	Cu <sup>2+</sup>	CO <sub>3</sub> <sup>2-</sup>	39	User defined	na
20	Zn <sup>2+</sup>	PO <sub>4</sub> <sup>3-</sup>	40	SrOH <sup>+</sup>	na

<sup>a</sup> Array locations in storage that are available for user to specify additional species.<sup>b</sup> Array locations in storage that are currently unused.

Table F-2. ZAM ionic species used in CST modeling of Phase 1 LAW batch feeds.

ID	Cations	Anions	ID	Cations	Anions
1	H <sup>+</sup>	F <sup>-</sup>	21	Cd <sup>2+</sup>	-
2	-	Cl <sup>-</sup>	22	Pb <sup>2+</sup>	-
3	Na <sup>+</sup>	-	23	UO <sub>2</sub> <sup>2+</sup>	-
4	K <sup>+</sup>	I <sup>-</sup>	24	Cr <sup>3+</sup>	
5	Rb <sup>+</sup>	-	25	Al <sup>3+</sup>	
6	Cs <sup>+</sup>	-	26	-	
7	-	-	27	-	NO <sub>2</sub> <sup>-</sup>
8	-	-	28	La <sup>3+</sup>	Al(OH) <sub>4</sub> <sup>-</sup>
9	-	NO <sub>3</sub> <sup>-</sup>	29	Ce <sup>3+</sup>	
10	-	-	30	-	
11	-	-	31	-	
12	Ca <sup>2+</sup>	-	32	-	
13	Sr <sup>2+</sup>	OH <sup>-</sup>	33	-	
14	Ba <sup>2+</sup>	-	34	-	
15	Mn <sup>2+</sup>	SO <sub>4</sub> <sup>2-</sup>	35	-	
16	Fe <sup>3+</sup>	-	36	-	
17	-	-	37		
18	Ni <sup>2+</sup>	-	38		
19	-	CO <sub>3</sub> <sup>2-</sup>	39		
20	Zn <sup>2+</sup>	PO <sub>4</sub> <sup>3-</sup>	40	SrOH <sup>+</sup>	

Table F-3. Equilibrium data for cesium on CST powder (IE-910) based on batch contact tests performed at 25 C in simulated and actual AW-101 solutions (Brown et al. (1996), 0.475 M potassium).<sup>a</sup>

Sample Description	Liquid Na <sup>+</sup> [M]	Liquid Cs <sup>+</sup> [M]	Liquid Na <sup>+</sup> /Cs <sup>+</sup> [ratio]	K <sub>d</sub> [ml/g]	Cs <sup>+</sup> loading [mmole/g <sub>CST</sub> ]
POW-SIM-0.2	0.20	4.600E-04	4.348E+02	1857.00	8.542E-01
POW-SIM-0.2	0.20	4.455E-04	4.489E+02	1923.00	8.568E-01
POW-SIM-0.2	0.20	3.419E-06	5.850E+04	80630.00	2.757E-01
POW-SIM-0.2	0.20	3.892E-06	5.139E+04	47780.00	1.860E-01
POW-SIM-0.2	0.20	3.783E-07	5.287E+05	57100.00	2.160E-02
POW-SIM-0.2	0.20	3.783E-07	5.287E+05	61570.00	2.329E-02
POW-SIM-0.2	0.20	3.428E-08	5.834E+06	72750.00	2.494E-03
POW-SIM-0.2	0.20	3.313E-08	6.036E+06	80260.00	2.659E-03
POW-SIM-0.2	0.20	3.810E-09	5.250E+07	70840.00	2.699E-04
POW-SIM-0.2	0.20	3.723E-09	5.372E+07	74930.00	2.790E-04
POW-SIM-1.0	1.00	1.460E-02	6.847E+01	57.33	8.373E-01
POW-SIM-1.0	1.00	1.463E-02	6.836E+01	56.89	8.322E-01
POW-SIM-1.0	1.00	5.672E-05	1.763E+04	6463.00	3.666E-01
POW-SIM-1.0	1.00	5.882E-05	1.700E+04	6243.00	3.672E-01
POW-SIM-1.0	1.00	4.444E-06	2.250E+05	9493.00	4.219E-02

Sample Description	Liquid Na <sup>+</sup> [M]	Liquid Cs <sup>+</sup> [M]	Liquid Na <sup>+</sup> /Cs <sup>+</sup> [ratio]	K <sub>d</sub> [ml/g]	Cs <sup>+</sup> loading [mmole/g <sub>CST</sub> ]
POW-SIM-1.0	1.00	4.521E-06	2.212E+05	9293.00	4.201E-02
POW-SIM-1.0	1.00	4.448E-07	2.248E+06	10100.00	4.493E-03
POW-SIM-1.0	1.00	4.305E-07	2.323E+06	10500.00	4.520E-03
POW-SIM-1.0	1.00	4.715E-08	2.121E+07	8875.00	4.184E-04
POW-SIM-1.0	1.00	4.531E-08	2.207E+07	9296.00	4.212E-04
POW-SIM-3.0	3.00	5.486E-02	5.468E+01	14.91	8.180E-01
POW-SIM-3.0	3.00	5.489E-02	5.465E+01	15.12	8.300E-01
POW-SIM-3.0	3.00	1.569E-03	1.912E+03	340.70	5.346E-01
POW-SIM-3.0	3.00	1.581E-03	1.898E+03	335.50	5.303E-01
POW-SIM-3.0	3.00	3.750E-05	8.000E+04	2709.00	1.016E-01
POW-SIM-3.0	3.00	3.750E-05	8.000E+04	2681.00	1.005E-01
POW-SIM-3.0	3.00	3.750E-06	8.000E+05	2845.00	1.067E-02
POW-SIM-3.0	3.00	3.750E-06	8.000E+05	2735.00	1.026E-02
POW-SIM-3.0	3.00	3.750E-07	8.000E+06	2749.00	1.031E-03
POW-SIM-3.0	3.00	3.750E-07	8.000E+06	2791.00	1.047E-03
POW-SIM-5.0	5.00	9.482E-02	5.273E+01	8.44	8.002E-01
POW-SIM-5.0	5.00	9.562E-02	5.229E+01	7.03	6.722E-01
POW-SIM-5.0	5.00	6.007E-03	8.323E+02	103.60	6.224E-01
POW-SIM-5.0	5.00	5.904E-03	8.469E+02	106.20	6.270E-01
POW-SIM-5.0	5.00	1.089E-04	4.590E+04	1373.00	1.496E-01
POW-SIM-5.0	5.00	1.114E-04	4.489E+04	1305.00	1.454E-01
POW-SIM-5.0	5.00	9.690E-06	5.160E+05	1574.00	1.525E-02
POW-SIM-5.0	5.00	9.705E-06	5.152E+05	1568.00	1.522E-02
POW-SIM-5.0	5.00	9.850E-07	5.076E+06	1545.00	1.522E-03
POW-SIM-5.0	5.00	9.766E-07	5.120E+06	1545.00	1.509E-03
POW-ACT-5.0	5.01	4.246E-02	1.180E+02	18.90	8.024E-01
POW-ACT-5.0	5.01	4.357E-02	1.150E+02	14.50	6.317E-01
POW-ACT-5.0	5.01	1.681E-03	2.980E+03	276.00	4.640E-01
POW-ACT-5.0	5.01	1.710E-03	2.930E+03	269.00	4.600E-01
POW-ACT-5.0	5.01	5.536E-05	9.050E+04	996.00	5.514E-02
POW-ACT-5.0	5.01	5.719E-05	8.760E+04	959.00	5.485E-02
POW-ACT-5.0	5.01	1.020E-05	4.910E+05	772.00	7.877E-03
POW-ACT-5.0	5.01	6.807E-06	7.360E+05	1230.00	8.373E-03

<sup>a</sup> The concentrations listed are equilibrium values at the final state of the liquid solution.

Table F-4. Equilibrium data for cesium on CST engineered-form (IE-911 –38b) based on batch contact tests performed at 25 C in simulated and actual AW-101 solutions (Brown et al. (1996), 0.475 M potassium).<sup>a</sup>

Sample Description	Liquid Na <sup>+</sup> [M]	Liquid Cs <sup>+</sup> [M]	Liquid Na <sup>+</sup> /Cs <sup>+</sup> [ratio]	K <sub>d</sub> [ml/g]	Cs <sup>+</sup> loading [mmole/g <sub>CST</sub> ]
E38B-SIM-0.2	0.20	8.094E-04	2.471E+02	673.50	5.451E-01
E38B-SIM-0.2	0.20	7.460E-04	2.681E+02	743.80	5.549E-01
E38B-SIM-0.2	0.20	5.436E-06	3.679E+04	19190.00	1.043E-01
E38B-SIM-0.2	0.20	5.167E-06	3.871E+04	20760.00	1.073E-01
E38B-SIM-0.2	0.20	4.854E-07	4.120E+05	24620.00	1.195E-02

Sample Description	Liquid Na <sup>+</sup> [M]	Liquid Cs <sup>+</sup> [M]	Liquid Na <sup>+</sup> /Cs <sup>+</sup> [ratio]	K <sub>d</sub> [ml/g]	Cs <sup>+</sup> loading [mmole/g <sub>CST</sub> ]
E38B-SIM-0.2	0.20	6.129E-07	3.263E+05	16630.00	1.019E-02
E38B-SIM-0.2	0.20	4.250E-08	4.706E+06	28700.00	1.220E-03
E38B-SIM-0.2	0.20	4.277E-08	4.676E+06	28180.00	1.205E-03
E38B-SIM-0.2	0.20	3.490E-09	5.731E+07	43600.00	1.522E-04
E38B-SIM-0.2	0.20	4.314E-09	4.636E+07	28140.00	1.214E-04
E38B-SIM-1.0	1.00	1.660E-02	6.024E+01	34.51	5.729E-01
E38B-SIM-1.0	1.00	1.606E-02	6.225E+01	41.11	6.604E-01
E38B-SIM-1.0	1.00	1.549E-04	6.456E+03	2159.00	3.344E-01
E38B-SIM-1.0	1.00	1.473E-04	6.791E+03	2280.00	3.357E-01
E38B-SIM-1.0	1.00	8.953E-06	1.117E+05	4125.00	3.693E-02
E38B-SIM-1.0	1.00	8.340E-06	1.199E+05	4493.00	3.747E-02
E38B-SIM-1.0	1.00	6.305E-07	1.586E+06	6263.00	3.949E-03
E38B-SIM-1.0	1.00	6.116E-07	1.635E+06	6535.00	3.997E-03
E38B-SIM-1.0	1.00	7.369E-08	1.357E+07	5056.00	3.726E-04
E38B-SIM-1.0	1.00	7.210E-08	1.387E+07	5180.00	3.735E-04
E38B-SIM-3.0	3.00	5.663E-02	5.298E+01	10.06	5.696E-01
E38B-SIM-3.0	3.00	5.700E-02	5.263E+01	8.79	5.008E-01
E38B-SIM-3.0	3.00	3.422E-03	8.766E+02	126.60	4.333E-01
E38B-SIM-3.0	3.00	3.429E-03	8.748E+02	127.00	4.355E-01
E38B-SIM-3.0	3.00	6.241E-05	4.807E+04	1502.00	9.374E-02
E38B-SIM-3.0	3.00	6.180E-05	4.854E+04	1519.00	9.388E-02
E38B-SIM-3.0	3.00	6.537E-06	4.589E+05	1440.00	9.414E-03
E38B-SIM-3.0	3.00	5.299E-06	5.661E+05	1826.00	9.677E-03
E38B-SIM-3.0	3.00	5.308E-07	5.652E+06	1853.00	9.835E-04
E38B-SIM-3.0	3.00	3.779E-07	7.938E+06	2773.00	1.048E-03
E38B-SIM-5.0	5.00	9.619E-02	5.198E+01	6.74	6.481E-01
E38B-SIM-5.0	5.00	9.651E-02	5.181E+01	6.07	5.857E-01
E38B-SIM-5.0	5.00	7.423E-03	6.736E+02	58.81	4.365E-01
E38B-SIM-5.0	5.00	7.407E-03	6.750E+02	59.17	4.383E-01
E38B-SIM-5.0	5.00	1.987E-04	2.516E+04	700.30	1.392E-01
E38B-SIM-5.0	5.00	1.962E-04	2.549E+04	711.40	1.395E-01
E38B-SIM-5.0	5.00	1.486E-05	3.365E+05	998.40	1.484E-02
E38B-SIM-5.0	5.00	1.493E-05	3.350E+05	1001.00	1.494E-02
E38B-SIM-7.0	7.00	1.372E-01	5.101E+01	3.40	4.662E-01
E38B-SIM-7.0	7.00	1.373E-01	5.100E+01	3.39	4.650E-01
E38B-SIM-7.0	7.00	1.138E-02	6.149E+02	39.16	4.458E-01
E38B-SIM-7.0	7.00	1.137E-02	6.155E+02	39.11	4.448E-01
E38B-SIM-7.0	7.00	3.991E-04	1.754E+04	434.80	1.735E-01
E38B-SIM-7.0	7.00	3.919E-04	1.786E+04	442.20	1.733E-01
E38B-SIM-7.0	7.00	2.730E-05	2.564E+05	719.40	1.964E-02
E38B-SIM-7.0	7.00	2.696E-05	2.596E+05	724.20	1.953E-02
E38B-SIM-7.0	7.00	2.610E-06	2.682E+06	758.80	1.980E-03
E38B-SIM-7.0	7.00	2.613E-06	2.679E+06	764.60	1.998E-03
E38B-ACT-5.0	5.01	4.434E-02	1.130E+02	12.60	5.586E-01
E38B-ACT-5.0	5.01	4.514E-02	1.110E+02	9.82	4.432E-01
E38B-ACT-5.0	5.01	2.518E-03	1.990E+03	146.00	3.676E-01

Sample Description	Liquid Na <sup>+</sup> [M]	Liquid Cs <sup>+</sup> [M]	Liquid Na <sup>+</sup> /Cs <sup>+</sup> [ratio]	K <sub>d</sub> [ml/g]	Cs <sup>+</sup> loading [mmole/g <sub>CST</sub> ]
E38B-ACT-5.0	5.01	2.665E-03	1.880E+03	129.00	3.438E-01
E38B-ACT-5.0	5.01	9.210E-05	5.440E+04	646.00	5.949E-02
E38B-ACT-5.0	5.01	9.093E-05	5.510E+04	656.00	5.965E-02
E38B-ACT-5.0	5.01	1.136E-05	4.410E+05	782.00	8.884E-03
E38B-ACT-5.0	5.01	1.116E-05	4.490E+05	797.00	8.893E-03

<sup>a</sup> The concentrations listed are equilibrium values at the final state of the liquid solution.

Table F-5. Equilibrium data for cesium on CST engineered-form (IE-911 –08) based on batch contact tests performed at 25 C in simulated AW-101 solutions (Brown et al. (1996), 0.475 M potassium).<sup>a</sup>

Sample Description	Liquid Na <sup>+</sup> [M]	Liquid Cs <sup>+</sup> [M]	Liquid Na <sup>+</sup> /Cs <sup>+</sup> [ratio]	K <sub>d</sub> [ml/g]	Cs <sup>+</sup> loading [mmole/g <sub>CST</sub> ]
E08-SIM-0.2	0.20	3.982E-04	5.022E+02	1571.00	6.256E-01
E08-SIM-0.2	0.20	3.131E-04	6.387E+02	2081.00	6.516E-01
E08-SIM-0.2	0.20	4.240E-06	4.717E+04	29970.00	1.271E-01
E08-SIM-0.2	0.20	4.327E-06	4.622E+04	28710.00	1.242E-01
E08-SIM-0.2	0.20	4.442E-07	4.502E+05	31130.00	1.383E-02
E08-SIM-0.2	0.20	4.239E-07	4.718E+05	34430.00	1.460E-02
E08-SIM-0.2	0.20	3.706E-08	5.397E+06	39350.00	1.458E-03
E08-SIM-0.2	0.20	3.599E-08	5.557E+06	42060.00	1.514E-03
E08-SIM-0.2	0.20	4.337E-09	4.612E+07	23220.00	1.007E-04
E08-SIM-0.2	0.20	4.521E-09	4.424E+07	21810.00	9.860E-05
E08-SIM-1.0	1.00	1.597E-02	6.261E+01	41.91	6.694E-01
E08-SIM-1.0	1.00	1.595E-02	6.270E+01	42.14	6.721E-01
E08-SIM-1.0	1.00	9.881E-05	1.012E+04	3725.00	3.681E-01
E08-SIM-1.0	1.00	1.022E-04	9.781E+03	3580.00	3.660E-01
E08-SIM-1.0	1.00	6.460E-06	1.548E+05	6333.00	4.091E-02
E08-SIM-1.0	1.00	6.623E-06	1.510E+05	6149.00	4.072E-02
E08-SIM-1.0	1.00	6.301E-07	1.587E+06	6082.00	3.832E-03
E08-SIM-1.0	1.00	6.321E-07	1.582E+06	6048.00	3.823E-03
E08-SIM-1.0	1.00	6.192E-08	1.615E+07	6208.00	3.844E-04
E08-SIM-1.0	1.00	6.414E-08	1.559E+07	5921.00	3.798E-04
E08-SIM-3.0	3.00	5.640E-02	5.319E+01	10.66	6.012E-01
E08-SIM-3.0	3.00	5.659E-02	5.301E+01	10.08	5.705E-01
E08-SIM-3.0	3.00	2.910E-03	1.031E+03	177.90	5.177E-01
E08-SIM-3.0	3.00	2.918E-03	1.028E+03	178.50	5.209E-01
E08-SIM-3.0	3.00	5.393E-05	5.563E+04	1824.00	9.836E-02
E08-SIM-3.0	3.00	5.568E-05	5.388E+04	1740.00	9.688E-02
E08-SIM-3.0	3.00	5.054E-06	5.936E+05	1922.00	9.714E-03
E08-SIM-3.0	3.00	5.165E-06	5.808E+05	1909.00	9.861E-03
E08-SIM-3.0	3.00	5.512E-07	5.443E+06	1791.00	9.871E-04
E08-SIM-3.0	3.00	5.376E-07	5.580E+06	1791.00	9.629E-04
E08-SIM-5.0	5.00	9.625E-02	5.195E+01	6.67	6.422E-01
E08-SIM-5.0	5.00	9.575E-02	5.222E+01	7.42	7.102E-01
E08-SIM-5.0	5.00	6.780E-03	7.375E+02	77.63	5.263E-01
E08-SIM-5.0	5.00	6.806E-03	7.346E+02	75.98	5.172E-01

Sample Description	Liquid Na <sup>+</sup> [M]	Liquid Cs <sup>+</sup> [M]	Liquid Na <sup>+</sup> /Cs <sup>+</sup> [ratio]	K <sub>d</sub> [ml/g]	Cs <sup>+</sup> loading [mmole/g <sub>CST</sub> ]
E08-SIM-5.0	5.00	1.612E-04	3.102E+04	867.30	1.398E-01
E08-SIM-5.0	5.00	1.571E-04	3.183E+04	883.10	1.387E-01
E08-SIM-5.0	5.00	1.417E-05	3.528E+05	1041.00	1.475E-02
E08-SIM-5.0	5.00	1.454E-05	3.438E+05	1024.00	1.489E-02
E08-SIM-7.0	7.00	1.368E-01	5.118E+01	3.91	5.345E-01
E08-SIM-7.0	7.00	1.376E-01	5.089E+01	2.95	4.061E-01
E08-SIM-7.0	7.00	1.103E-02	6.347E+02	44.94	4.956E-01
E08-SIM-7.0	7.00	1.111E-02	6.299E+02	43.23	4.804E-01
E08-SIM-7.0	7.00	3.302E-04	2.120E+04	553.20	1.827E-01
E08-SIM-7.0	7.00	3.382E-04	2.070E+04	535.40	1.811E-01
E08-SIM-7.0	7.00	2.510E-05	2.789E+05	791.80	1.987E-02
E08-SIM-7.0	7.00	2.554E-05	2.741E+05	772.80	1.974E-02
E08-SIM-7.0	7.00	2.647E-06	2.645E+06	728.70	1.929E-03
E08-SIM-7.0	7.00	2.585E-06	2.708E+06	752.10	1.944E-03

<sup>a</sup> The concentrations listed are equilibrium values at the final state of the liquid solution.

Table F-6. ZAM predictions for cesium on CST powder (IE-910) based on simulated batch contact tests performed at 25 C in AW-101 solutions.<sup>a</sup>

Sample Description	Liquid Na <sup>+</sup> [M]	Liquid Cs <sup>+</sup> [M]	Liquid Na <sup>+</sup> /Cs <sup>+</sup> [ratio]	K <sub>d</sub> [ml/g]	Cs <sup>+</sup> loading [mmole/g <sub>CST</sub> ]
POW-ZAM-0.2	0.20	4.330E-09	4.619E+07	51400.00	2.226E-04
POW-ZAM-0.2	0.20	4.350E-08	4.598E+06	51300.00	2.232E-03
POW-ZAM-0.2	0.20	2.210E-07	9.050E+05	50500.00	1.116E-02
POW-ZAM-0.2	0.20	4.510E-07	4.435E+05	49500.00	2.232E-02
POW-ZAM-0.2	0.20	2.690E-06	7.435E+04	41500.00	1.116E-01
POW-ZAM-0.2	0.20	7.040E-06	2.841E+04	31600.00	2.225E-01
POW-ZAM-0.2	0.20	3.570E-05	5.602E+03	12300.00	4.391E-01
POW-ZAM-0.2	0.20	1.260E-04	1.587E+03	4240.00	5.342E-01
POW-ZAM-0.2	0.20	4.710E-04	4.246E+02	1200.00	5.652E-01
POW-ZAM-0.2	0.20	2.420E-03	8.264E+01	238.00	5.760E-01
POW-ZAM-1.0	1.00	2.280E-08	4.386E+07	9600.00	2.189E-04
POW-ZAM-1.0	1.00	2.290E-07	4.367E+06	9570.00	2.192E-03
POW-ZAM-1.0	1.00	1.160E-06	8.621E+05	9420.00	1.093E-02
POW-ZAM-1.0	1.00	2.360E-06	4.237E+05	9240.00	2.181E-02
POW-ZAM-1.0	1.00	1.400E-05	7.143E+04	7800.00	1.092E-01
POW-ZAM-1.0	1.00	3.580E-05	2.793E+04	6020.00	2.155E-01
POW-ZAM-1.0	1.00	1.510E-04	6.623E+03	2740.00	4.137E-01
POW-ZAM-1.0	1.00	6.350E-04	1.575E+03	834.00	5.296E-01
POW-ZAM-1.0	1.00	2.470E-03	4.049E+02	229.00	5.656E-01
POW-ZAM-1.0	1.00	7.430E-03	1.346E+02	77.40	5.751E-01
POW-ZAM-1.0	1.00	2.740E-02	3.650E+01	21.10	5.781E-01
POW-ZAM-1.0	1.00	4.740E-02	2.110E+01	12.20	5.783E-01
POW-ZAM-1.0	1.00	9.740E-02	1.027E+01	5.95	5.795E-01
POW-ZAM-3.0	3.00	7.440E-08	4.032E+07	2790.00	2.076E-04



Sample Description	Liquid Na <sup>+</sup> [M]	Liquid Cs <sup>+</sup> [M]	Liquid Na <sup>+</sup> /Cs <sup>+</sup> [ratio]	K <sub>d</sub> [ml/g]	Cs <sup>+</sup> loading [mmole/g <sub>CST</sub> ]
POW-ZAM-3.0	3.00	7.460E-07	4.021E+06	2780.00	2.074E-03
POW-ZAM-3.0	3.00	3.780E-06	7.937E+05	2740.00	1.036E-02
POW-ZAM-3.0	3.00	7.690E-06	3.901E+05	2690.00	2.069E-02
POW-ZAM-3.0	3.00	4.440E-05	6.757E+04	2300.00	1.021E-01
POW-ZAM-3.0	3.00	1.090E-04	2.752E+04	1830.00	1.995E-01
POW-ZAM-3.0	3.00	3.600E-04	8.333E+03	1020.00	3.672E-01
POW-ZAM-3.0	3.00	8.970E-04	3.344E+03	524.00	4.700E-01
POW-ZAM-3.0	3.00	2.600E-03	1.154E+03	206.00	5.356E-01
POW-ZAM-3.0	3.00	7.480E-03	4.011E+02	75.40	5.640E-01
POW-ZAM-3.0	3.00	2.740E-02	1.095E+02	21.00	5.754E-01
POW-ZAM-3.0	3.00	4.740E-02	6.329E+01	12.20	5.783E-01
POW-ZAM-3.0	3.00	9.740E-02	3.080E+01	5.94	5.786E-01
POW-ZAM-5.0	5.00	1.390E-07	3.597E+07	1390.00	1.932E-04
POW-ZAM-5.0	5.00	1.390E-06	3.597E+06	1390.00	1.932E-03
POW-ZAM-5.0	5.00	7.030E-06	7.112E+05	1370.00	9.631E-03
POW-ZAM-5.0	5.00	1.430E-05	3.497E+05	1350.00	1.931E-02
POW-ZAM-5.0	5.00	8.060E-05	6.203E+04	1170.00	9.430E-02
POW-ZAM-5.0	5.00	1.900E-04	2.632E+04	956.00	1.816E-01
POW-ZAM-5.0	5.00	5.390E-04	9.276E+03	606.00	3.266E-01
POW-ZAM-5.0	5.00	1.120E-03	4.464E+03	378.00	4.234E-01
POW-ZAM-5.0	5.00	2.750E-03	1.818E+03	183.00	5.033E-01
POW-ZAM-5.0	5.00	7.550E-03	6.623E+02	72.80	5.496E-01
POW-ZAM-5.0	5.00	2.740E-02	1.825E+02	20.80	5.699E-01
POW-ZAM-5.0	5.00	4.740E-02	1.055E+02	12.10	5.735E-01
POW-ZAM-5.0	5.00	9.740E-02	5.133E+01	5.93	5.776E-01
POW-ZAM-7.0	7.00	1.860E-07	3.763E+07	979.00	1.821E-04
POW-ZAM-7.0	7.00	1.870E-06	3.743E+06	976.00	1.825E-03
POW-ZAM-7.0	7.00	9.430E-06	7.423E+05	964.00	9.091E-03
POW-ZAM-7.0	7.00	1.910E-05	3.665E+05	948.00	1.811E-02
POW-ZAM-7.0	7.00	1.060E-04	6.604E+04	830.00	8.798E-02
POW-ZAM-7.0	7.00	2.440E-04	2.869E+04	693.00	1.691E-01
POW-ZAM-7.0	7.00	6.480E-04	1.080E+04	468.00	3.033E-01
POW-ZAM-7.0	7.00	1.250E-03	5.600E+03	315.00	3.938E-01
POW-ZAM-7.0	7.00	2.860E-03	2.448E+03	168.00	4.805E-01
POW-ZAM-7.0	7.00	7.600E-03	9.211E+02	70.80	5.381E-01
POW-ZAM-7.0	7.00	2.750E-02	2.545E+02	20.70	5.693E-01
POW-ZAM-7.0	7.00	4.740E-02	1.477E+02	12.10	5.735E-01
POW-ZAM-7.0	7.00	9.740E-02	7.187E+01	5.92	5.766E-01

<sup>a</sup> The concentrations listed are equilibrium values at the final state of the liquid solution.

Table F-7. AW-101 simulant and actual solution compositions used to perform ZAM predictions for cesium on CST powder (IE-910) at 25 C.<sup>a</sup>

Ion Category	Species	ZAM ID	0.2 M Na <sup>+</sup> Solution	1 M Na <sup>+</sup> Solution	3 M Na <sup>+</sup> Solution	5 M Na <sup>+</sup> Solution	7 M Na <sup>+</sup> Solution
<b>Cations</b>	Na <sup>+</sup>	3	2.000E-01	1.000E+00	3.000E+00	5.000E+00	7.000E+00
	K <sup>+</sup>	4	1.900E-02	9.500E-02	2.850E-01	4.750E-01	6.650E-01
	Cs <sup>+</sup> <sup>(b)</sup>	6	varies	varies	Varies	varies	varies
	H <sup>+</sup>	1	6.340E-17	3.170E-16	9.510E-16	1.585E-15	2.219E-15
	Ba <sup>2+</sup>	14	2.364E-08	1.182E-07	3.546E-07	5.910E-07	8.274E-07
	Ca <sup>2+</sup>	12	9.640E-06	4.820E-05	1.446E-04	2.410E-04	3.374E-04
	Sr <sup>2+</sup>	13	2.856E-09	1.428E-08	4.284E-08	7.140E-08	9.996E-08
<b>Anions</b>	OH <sup>-</sup> (free)	13	8.400E-02	4.200E-01	1.260E+00	2.100E+00	2.940E+00
	Cl <sup>-</sup> <sup>(b)</sup>	2	2.600E-03 + Cs conc	1.300E-02 + Cs conc	3.900E-02 + Cs conc	6.500E-02 + Cs conc	9.100E-02 + Cs conc
	F <sup>-</sup>	1	1.732E-03	8.660E-03	2.598E-02	4.330E-02	6.062E-02
	NO <sub>2</sub> <sup>-</sup>	27	3.760E-02	1.880E-01	5.640E-01	9.400E-01	1.316E+00
	NO <sub>3</sub> <sup>-</sup>	9	5.960E-02	2.980E-01	8.940E-01	1.490E+00	2.086E+00
	Al(OH) <sub>4</sub> <sup>-</sup>	28	1.988E-02	9.940E-02	2.982E-01	4.970E-01	6.958E-01
	SO <sub>4</sub> <sup>2-</sup>	15	5.040E-04	2.520E-03	7.560E-03	1.260E-02	1.764E-02
	CO <sub>3</sub> <sup>2-</sup>	19	5.600E-03	2.800E-02	8.400E-02	1.400E-01	1.960E-01
	HPO <sub>4</sub> <sup>2-</sup>	17	7.000E-04	3.500E-03	1.050E-02	1.750E-02	2.450E-02

<sup>a</sup> The species concentrations for simulants at sodium concentrations other than 5 M can be obtained by using a diluting factor (e.g., for a 2 M sodium case multiply the 5 M sodium simulant species concentrations by 2/5).

<sup>b</sup> Cesium and chlorine concentrations are varied in order to generate isotherm database over a wide cesium concentration range (i.e., 1x10<sup>-6</sup> M to 0.1 M) where CsCl is added to maintain an overall charge balance.

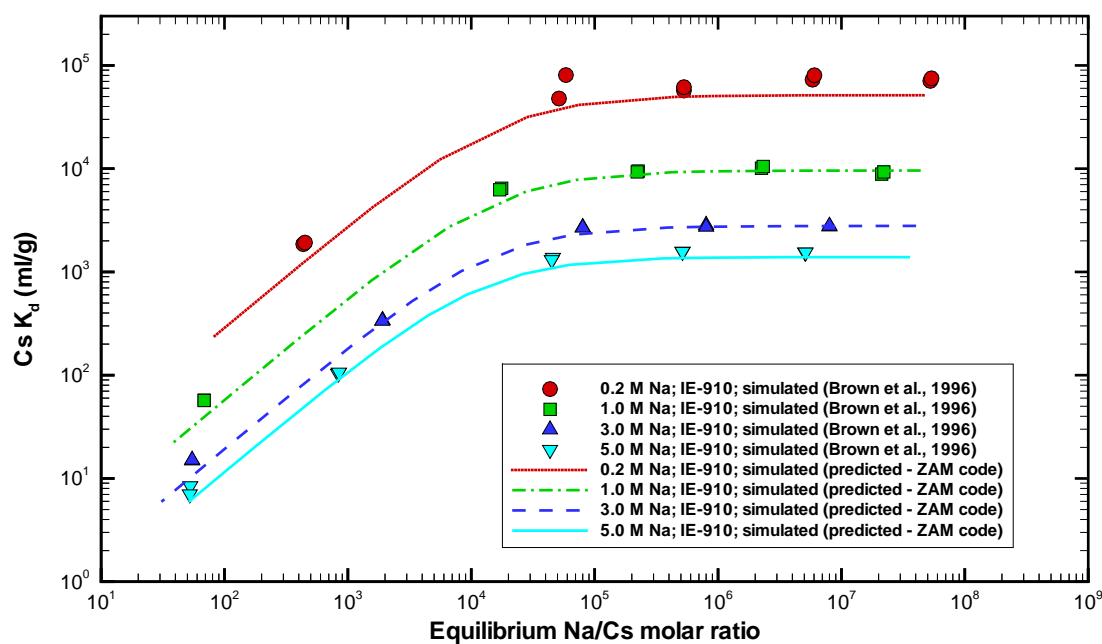


Figure F-1. A comparison of measured versus ZAM predicted cesium  $K_d$  values for simulated AW-101 feed in contact with CST in its power-form (IE-910) over a range of sodium concentration levels [data by Brown et al. (1996)].

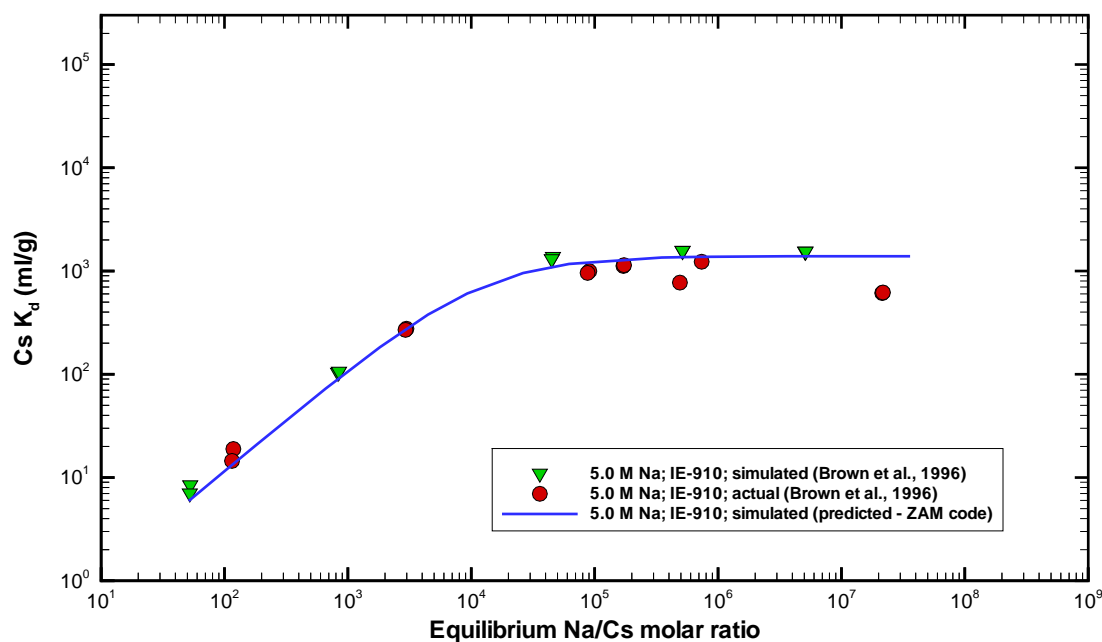


Figure F-2. A comparison of measured versus ZAM predicted cesium  $K_d$  values for 5 M sodium simulated and actual AW-101 feeds in contact with CST in its power-form (IE-910) [data by Brown et al. (1996)].

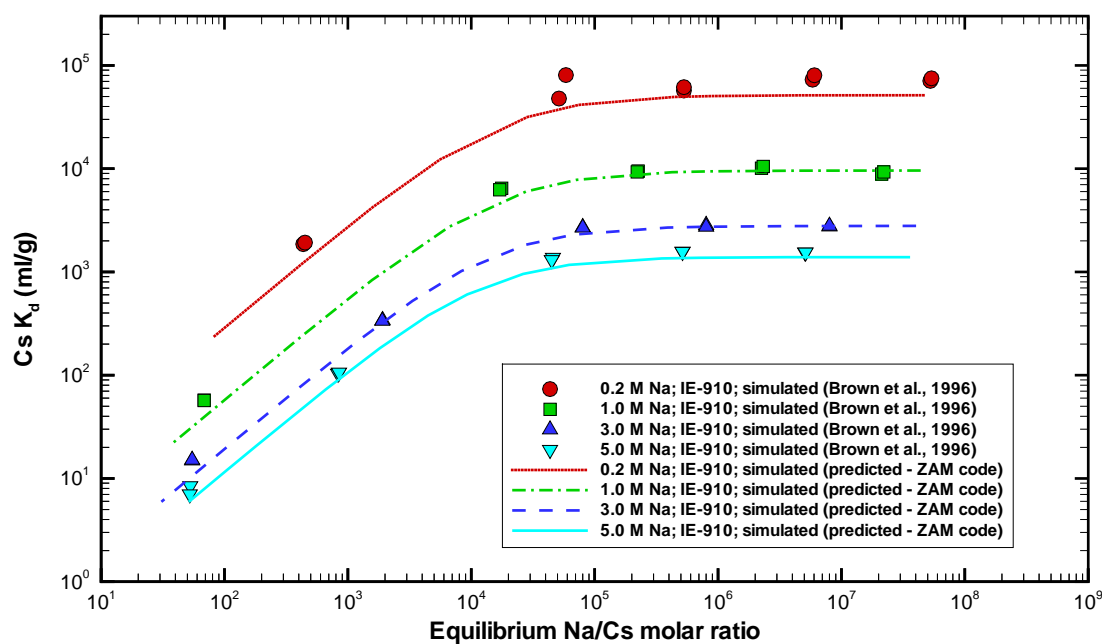


Figure F-3. A comparison of measured versus ZAM predicted cesium  $K_d$  values for simulated AW-101 feed in contact with CST in one of its engineered-forms referred to as “08” (IE-911) over a range of sodium concentration levels [data by Brown et al. (1996)].

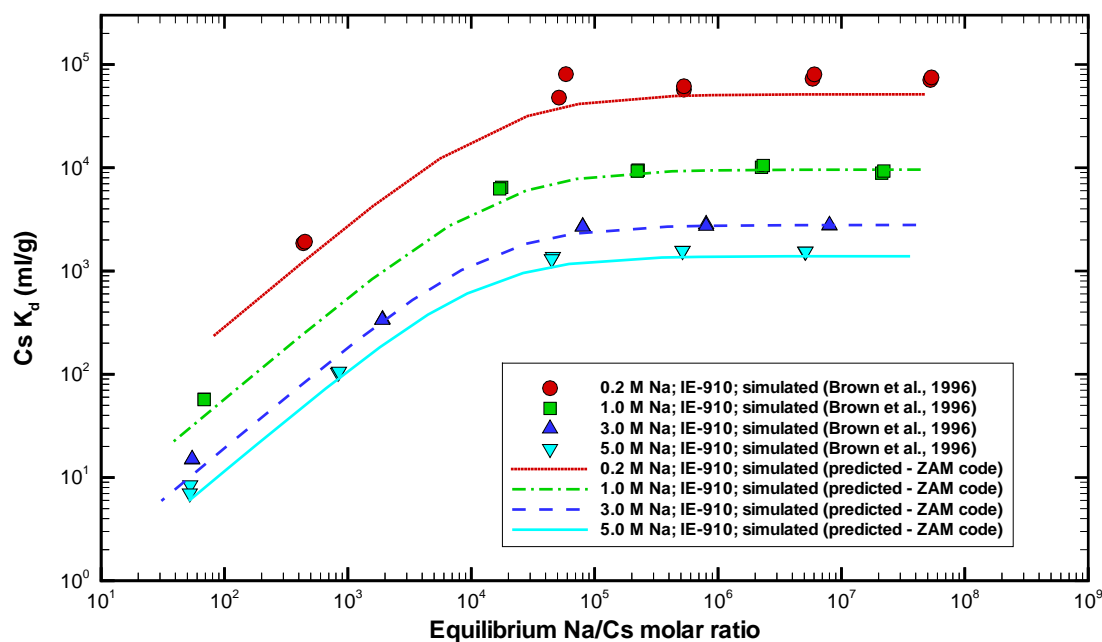


Figure F-4. A comparison of measured versus ZAM predicted cesium  $K_d$  values for simulated AW-101 feed in contact with CST in one of its engineered-forms referred to as “38b” (IE-911) over a range of sodium concentration levels [data by Brown et al. (1996)].

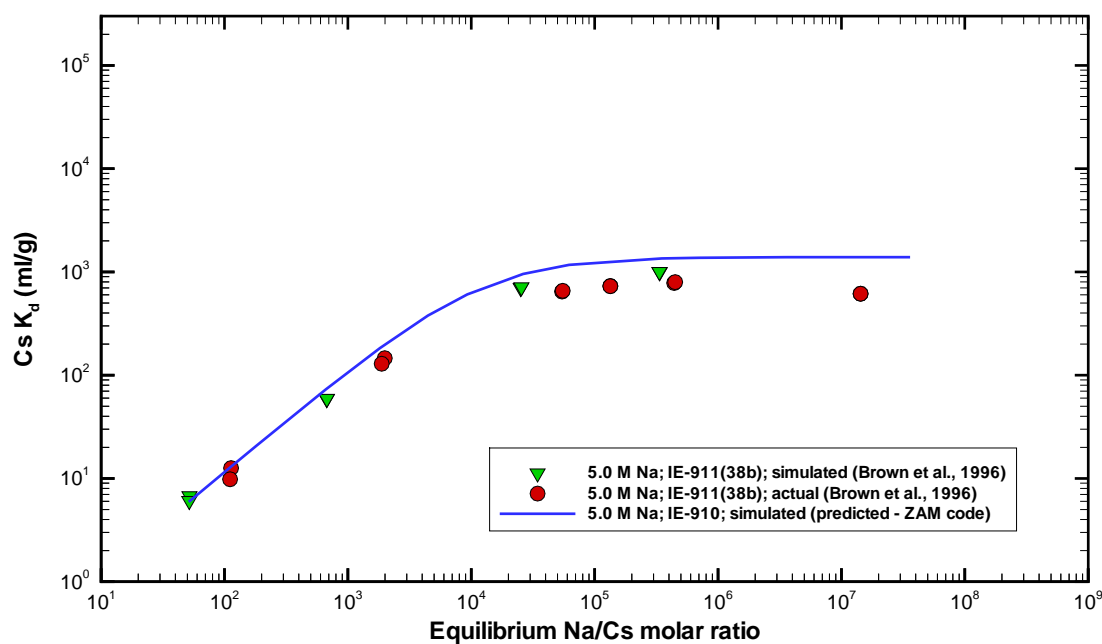


Figure F-5. A comparison of measured versus ZAM predicted cesium  $K_d$  values for 5 M sodium simulated and actual AW-101 feeds in contact with CST in one of its engineered-forms referred to as “038b” (IE-911) [data by Brown et al. (1996)].

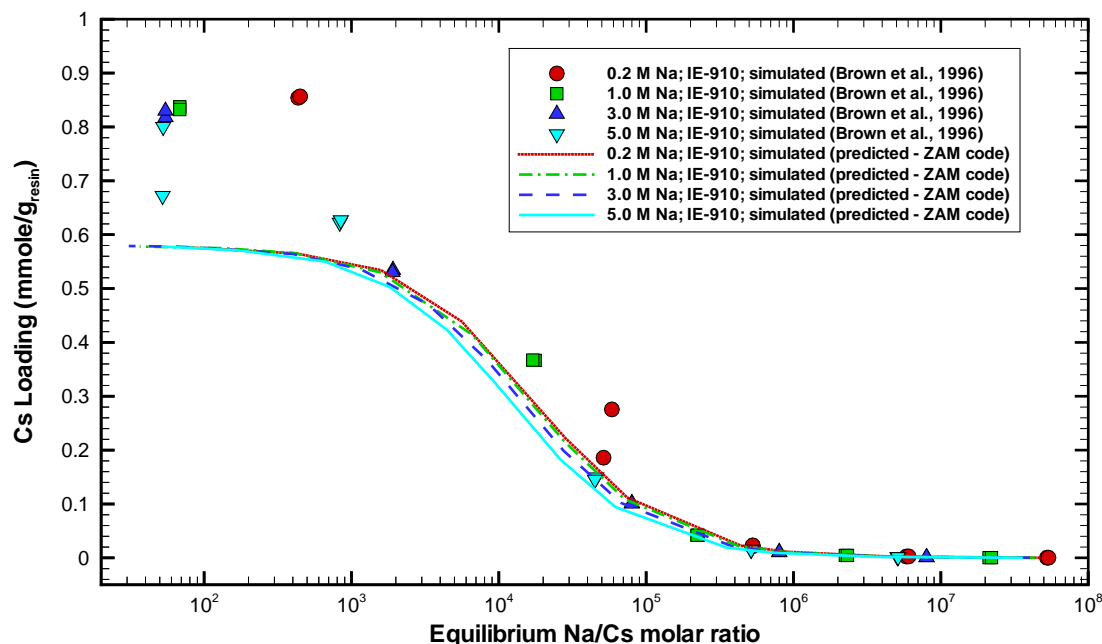


Figure F-6. A comparison of measured versus ZAM predicted cesium loadings for simulated AW-101 feed in contact with CST in its power-form (IE-910) over a range of sodium concentration levels [data by Brown et al. (1996)].

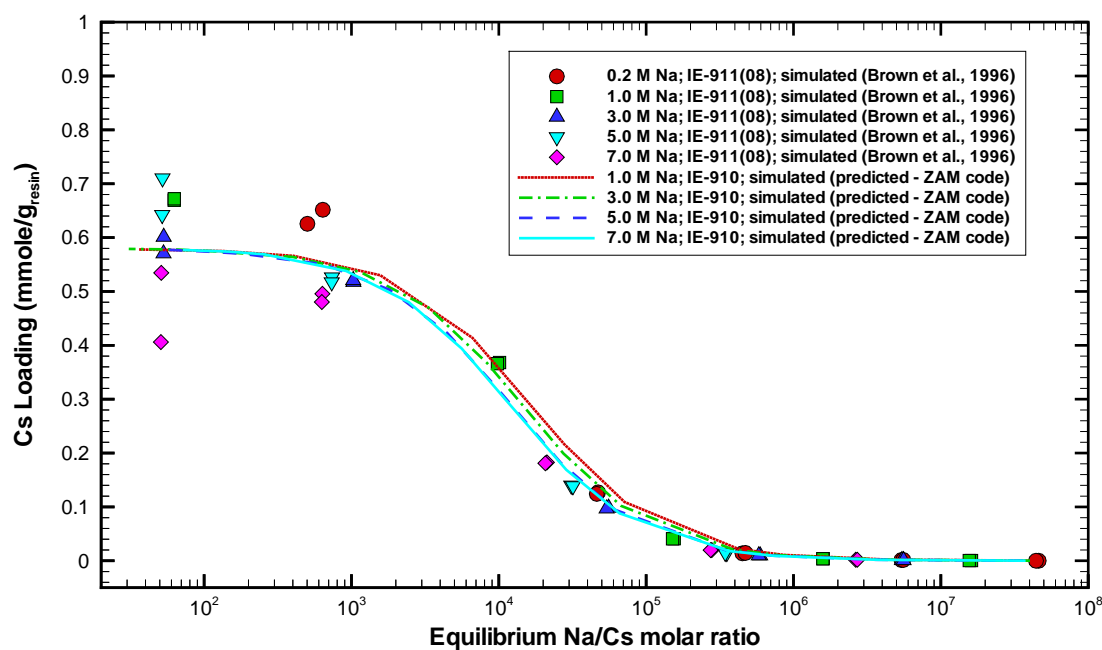


Figure F-7. A comparison of measured versus ZAM predicted cesium loadings for simulated AW-101 feed in contact with CST in one of its engineered-forms referred to as “08” (IE-911) over a range of sodium concentration levels [data by Brown et al. (1996)].

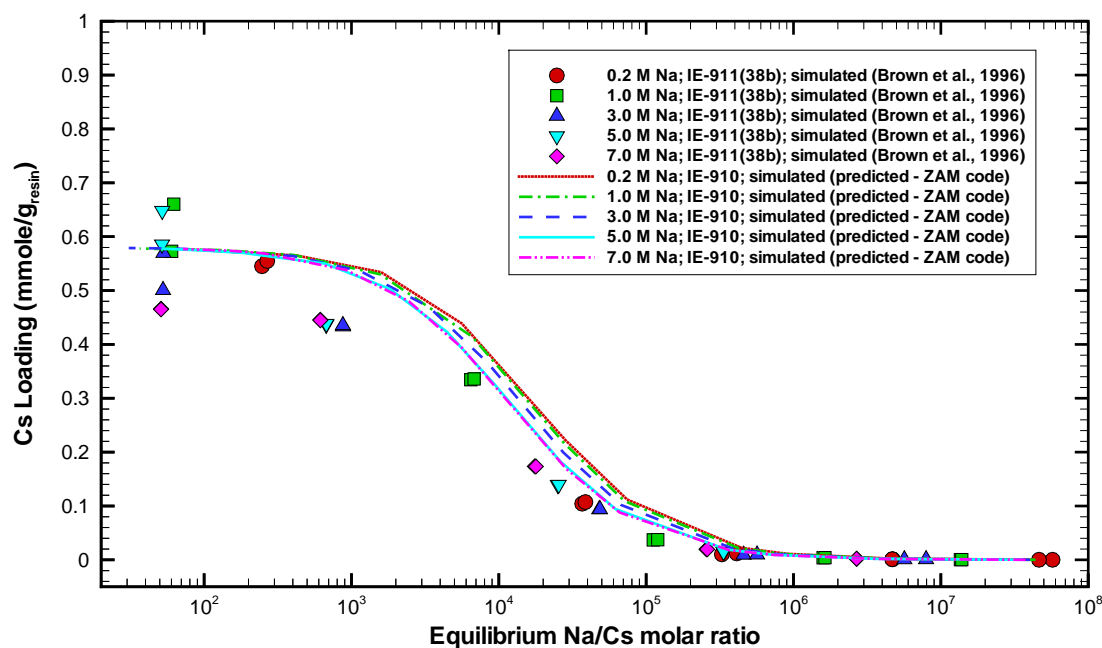


Figure F-8. A comparison of measured versus ZAM predicted cesium loadings for simulated AW-101 feed in contact with CST in one of its engineered-forms referred to as “38b” (IE-911) over a range of sodium concentration levels [data by Brown et al. (1996)].

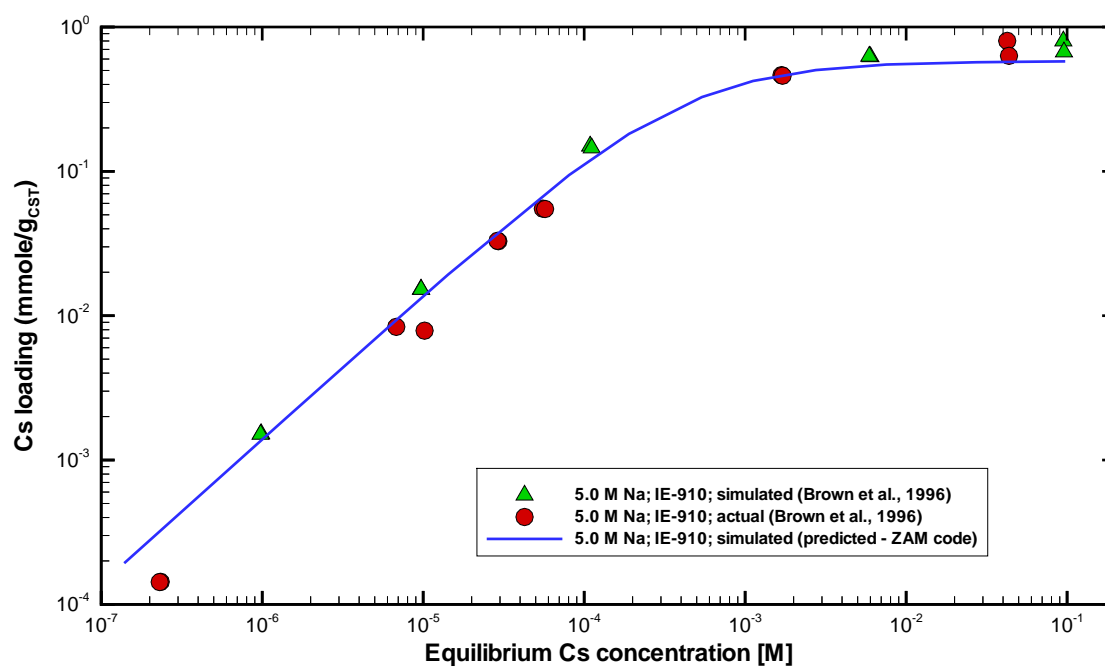


Figure F-9. A comparison of measured versus ZAM predicted cesium loading values for 5 M sodium simulated and actual AW-101 feeds in contact with CST in its power-form (IE-910) [data by Brown et al. (1996)].

## F.5 ZAM Version-4 or Version-5 Input for 5 M Na AW-101 Feed)

1, 298.15	Activity Coeff. Model, Temperature
CSTIX 101-AW (5.0 M Na;simulant)	Title
9,9	Number of Cations & Anions
1229	Density(kg/m3)
3, 6, 1, 5, 4, 40, 13, 14, 12	Names of Cations
13, 9, 2, 1, 27, 15, 19, 17, 28	Names of Anions
5.0, 1.0e-5, 1.585e-15, 0., 0.475, 0., 7.14e-8, 5.91e-7, 2.41e-4	Concentrations of Cations
2.1, 1.49, 0.06501, 0.0433, 0.94, 0.0126, 0.14, 0.0175, 0.497	Concentrations of Anions
0.015, 0.067	Liquid(L), Solid(g)
0	Initial solid Form
1.0	Calculation Adjustment

## F.6 ZAM Version-4 Output for 5 M Na AW-101 Feed)

Solution: CSTIX 101-AW (5.0 M Na;simulant)  
\*\*\*\*\*INPUT\*\*\*\*\*

Density= .1229E+04 kg/m3

	Molecular Wt.	Valance	Molarity(mol/L)
Na+....	22.9898	1.	.5000E+01
Cs+....	132.9054	1.	.1000E-04
H+....	1.0079	1.	.1585E-14
Rb+....	85.4678	1.	.0000E+00
K+....	39.0983	1.	.4750E+00
SrOH+...	105.0000	1.	.0000E+00
Sr++....	87.6200	2.	.7140E-07
Ba++....	137.3270	2.	.5910E-06
Ca++....	40.0780	2.	.2410E-03
OH-....	17.0073	-1.	.2100E+01
NO3-....	62.0049	-1.	.1490E+01
Cl-....	35.4527	-1.	.6501E-01
F-....	18.9984	-1.	.4330E-01
NO2-....	46.0000	-1.	.9400E+00
SO4--...	96.0636	-2.	.1260E-01
CO3--...	60.0092	-2.	.1400E+00
HPO4--..	95.9792	-2.	.1750E-01
Al(OH)4-	95.0000	-1.	.4970E+00

Liquid(L)= .1500E-01 Solid(g)= .6700E-01

Material: Na Form

\*\*\*\*\*OUTPUT\*\*\*\*\*

Ionic Strength= 6.665123171031650 mol/kg

	Q (mmol/gCST)	C (mmol/L)	Kd (ml/gCST)
Cs	.1928E-02	.1390E-02	.1386E+04
Rb	.0000E+00	.0000E+00	.0000E+00
Sr	.1593E-04	.2566E-06	.6208E+05
K	.8634E+00	.4711E+03	.1832E+01

## F.7 ZAM Version-4 or Version-5 Input for Phase 1 LAW-1 Batch Feed)

1, 298.15	Activity Coeff. Model, Temperature
CSTIX (5.0 M Na;LAW-1)	Title
20,10	Number of Cations & Anions
1255	Density(kg/m3)
3, 6, 1, 5, 4, 40, 13, 14, 12, 21, 15, 18, 23, 20, 16, 22, 25, 24, 28, 29	Names of Cations
13, 9, 27, 2, 1, 28, 4, 19, 15, 20	Names of Anions
5.000E+00, 3.433E-05, 1.150E-15, 0.000E+00, 3.601E-01, 0.000E+00, 0.000E+00, 2.052E-06, 7.575E-04,	Concentrations of Cations
7.276E-06, 0.000E+00, 8.433E-05, 8.377E-05, 4.086E-04, 5.448E-05, 1.194E-05, 0.000E+00, 0.000E+00,	
0.000E+00, 0.000E+00	



2.155E+00,1.666E+00,6.884E-01,2.910E-02,9.478E-02,2.834E-01,1.866E-06,1.828E-01,2.799E-02,  
8.209E-03  
1.0, 0.01  
0  
0.95

Concentrations of Anions  
Liquid(L), Solid(g)  
Initial solid Form  
Calculation Adjustment

## F.8 ZAM Version-4 Output for Phase 1 LAW-1 Batch Feed)

Solution: CSTIX (5.0 M Na;LAW-1)  
\*\*\*\*\*INPUT\*\*\*\*\*

Density= .1255E+04 kg/m3

	Molecular Wt.	Valance	Molarity(mol/L)
Na+.....	22.9898	1.	.5000E+01
Cs+.....	132.9054	1.	.3433E-04
H+.....	1.0079	1.	.1150E-14
Rb+.....	85.4678	1.	.0000E+00
K+.....	39.0983	1.	.3601E+00
SrOH+...	105.0000	1.	.0000E+00
Sr++.....	87.6200	2.	.0000E+00
Ba++.....	137.3270	2.	.2052E-05
Ca++.....	40.0780	2.	.7575E-03
Cd++.....	112.4110	2.	.7276E-05
Mn++.....	54.9309	2.	.0000E+00
Ni++.....	58.6934	2.	.8433E-04
UO2++...	270.0277	2.	.8377E-04
Zn++.....	65.3900	2.	.4086E-03
Fe++.....	55.8470	2.	.5448E-04
Pb++.....	207.2000	2.	.1194E-04
Al+++...	26.9815	3.	.0000E+00
Cr+++...	51.9961	3.	.0000E+00
La+++...	138.9055	3.	.0000E+00
Ce+++...	140.1150	3.	.0000E+00
OH-.....	17.0073	-1.	.2155E+01
NO3-.....	62.0049	-1.	.1666E+01
NO2-.....	46.0000	-1.	.6884E+00
Cl-.....	35.4527	-1.	.2910E-01
F-.....	18.9984	-1.	.9478E-01
Al (OH) 4-	95.0000	-1.	.2834E+00
I-.....	126.9045	-1.	.1866E-05
CO3--...	60.0092	-2.	.1828E+00
SO4--...	96.0636	-2.	.2799E-01
PO4---..	94.9712	-3.	.8209E-02

Liquid(L)= .1000E+01 Solid(g)= .1000E-01

Material: Na Form

\*\*\*\*\*OUTPUT\*\*\*\*\*

Ionic Strength= 6.303838137196418 mol/kg

	Q (mmol/gCST)	C (mmol/L)	Kd (ml/gCST)
Cs	.4694E-01	.3386E-01	.1386E+04
Rb	.0000E+00	.0000E+00	.0000E+00
Sr	.0000E+00	.0000E+00	.0000E+00
K	.8058E+00	.3601E+03	.2238E+01

## F.9 ZAM Version-5 Output for Phase 1 LAW-1 Batch Feed)

Solution: CSTIX (5.0 M Na;LAW-1)  
\*\*\*\*\*INPUT\*\*\*\*\*

Density= .1255E+04 kg/m3

	Molecular Wt.	Valance	Molarity(mol/L)
Na+.....	22.9898	1.	.5000E+01

Cs+....	132.9054	1.	.3433E-04
H+....	1.0079	1.	.1150E-14
Rb+....	85.4678	1.	.0000E+00
K+....	39.0983	1.	.3601E+00
SrOH+...	105.0000	1.	.0000E+00
Sr++....	87.6200	2.	.0000E+00
Ba++....	137.3270	2.	.2052E-05
Ca++....	40.0780	2.	.7575E-03
Cd++....	112.4110	2.	.7276E-05
Mn++....	54.9309	2.	.0000E+00
Ni++....	58.6934	2.	.8433E-04
UO2++...	270.0277	2.	.8377E-04
Zn++....	65.3900	2.	.4086E-03
Fe++....	55.8470	2.	.5448E-04
Pb++....	207.2000	2.	.1194E-04
Al+++...	26.9815	3.	.0000E+00
Cr+++...	51.9961	3.	.0000E+00
La+++...	138.9055	3.	.0000E+00
Ce+++...	140.1150	3.	.0000E+00
OH-....	17.0073	-1.	.2155E+01
NO3-....	62.0049	-1.	.1666E+01
NO2-....	46.0000	-1.	.6884E+00
Cl-....	35.4527	-1.	.2910E-01
F-....	18.9984	-1.	.9478E-01
Al (OH) 4-	95.0000	-1.	.2834E+00
I-....	126.9045	-1.	.1866E-05
CO3--...	60.0092	-2.	.1828E+00
SO4--...	96.0636	-2.	.2799E-01
PO4---..	94.9712	-3.	.8209E-02

Material: Na Form

\*\*\*\*\*OUTPUT\*\*\*\*\*

Ionic Strength= .630E+01 mol/kg  
Equilibrium pH= 14.6

	Q (mmol/gCST)	C (mmol/L)	Kd (ml/gCST)
Cs	.469E-01	.339E-01	.139E+04
Rb	.000E+00	.000E+00	.000E+00
SrOH	.000E+00	.000E+00	.000E+00
K	.806E+00	.360E+03	.224E+01

## Appendix G (ZAM Input Files for Phase 1 Batch Feeds)

For reference the ZAM input files for the 16 Phase 1 batch feeds are provided in this appendix. The input files for the nominal ZAM runs are provided. Other cesium concentration levels can be obtained by adding or reducing CsCl concentration within these input files. The ZAM results generated constitute our cesium isotherm database for the development of algebraic isotherm models for cesium loading that are used in VERSE-LC column transport simulation (i.e., full-scale column design studies). Also included are the ZAM input files for some of the sensitivity runs made. Note that nominal settings are 25 C, 5 M Na<sup>+</sup>, 0 M Rb<sup>+</sup>, and 0 M Sr<sup>+2</sup>.

Table E-1. Listing of ZAM input files provided in this appendix for reference.

Feed Category	Phase 1 LAW batch feeds considered
Nominal Envelope A	LAW-1 LAW-5 LAW-6 LAW-8 LAW-9 LAW-10 LAW-11 LAW-12 LAW-13 LAW-14 LAW-15
Nominal Envelope B	LAW-2a LAW-2b
Nominal Envelope C	LAW-3 LAW-4 LAW-7
Sensitivity Envelope A	LAW-1 (4 M Na <sup>+</sup> ) LAW-1 (6 M Na <sup>+</sup> )
Sensitivity Envelope C	LAW-3 (with Sr <sup>+2</sup> )

**ZAM Input for Phase 1 LAW-1 Batch Feed (Envelope A; nominal case)**

1, 298.15	Activity Coeff. Model, Temperature
CSTIX (5.0 M Na; LAW-1)	Title
20, 10	Number of Cations & Anions
1255	Density (kg/m3)
3, 6, 1, 5, 4, 40, 13, 14, 12, 21, 15, 18, 23, 20, 16, 22, 25, 24, 28, 29	Names of Cations
13, 9, 27, 2, 1, 28, 4, 19, 15, 20	Names of Anions
5.000E+00, 3.433E-05, 1.150E-15, 0.000E+00, 3.601E-01, 0.000E+00, 0.000E+00, 2.052E-06, 7.575E-04, 7.276E-06, 0.000E+00, 8.433E-05, 8.377E-05, 4.086E-04, 5.448E-05, 1.194E-05, 0.000E+00, 0.000E+00, 0.000E+00, 0.000E+00	Concentrations of Cations
2.155E+00, 1.666E+00, 6.884E-01, 2.910E-02, 9.478E-02, 2.834E-01, 1.866E-06, 1.828E-01, 2.799E-02, 8.209E-03	Concentrations of Anions
1.0, 0.01	Liquid(L), Solid(g)
0	Initial solid Form
1.0	Calculation Adjustment

**ZAM Input for Phase 1 LAW-5 Batch Feed (Envelope A; nominal case)**

1, 298.15	Activity Coeff. Model, Temperature
CSTIX (5.0 M Na; LAW-5)	Title
20, 10	Number of Cations & Anions
1232	Density (kg/m3)
3, 6, 1, 5, 4, 40, 13, 14, 12, 21, 15, 18, 23, 20, 16, 22, 25, 24, 28, 29	Names of Cations
13, 9, 27, 2, 1, 28, 4, 19, 15, 20	Names of Anions
5.0000E+00 6.2827E-05 1.0877E-15 0.0000E+00 6.0733E-02 0.0000E+00 0.0000E+00 5.9686E-05 4.7906E-04 7.3298E-06 3.4293E-05 6.1518E-05 3.0366E-05 0.0000E+00 1.6126E-04 9.3717E-05 0.0000E+00	Concentrations of Cations
0.0000E+00 6.0209E-06 1.5916E-19	Concentrations of Anions
8.6425E-01 1.3770E+00 1.1885E+00 1.0340E-01 1.4712E-02 5.7065E-01 8.1152E-06 3.9267E-01 4.8429E-02 2.0654E-02	Liquid(L), Solid(g)
1.0, 0.01	Initial solid Form
0	Calculation Adjustment
1.0	

**ZAM Input for Phase 1 LAW-6 Batch Feed (Envelope A; nominal case)**

1, 298.15	Activity Coeff. Model, Temperature
CSTIX (5.0 M Na; LAW-6 )	Title
20, 10	Number of Cations & Anions
1231	Density (kg/m3)
3, 6, 1, 5, 4, 40, 13, 14, 12, 21, 15, 18, 23, 20, 16, 22, 25, 24, 28, 29	Names of Cations
13, 9, 27, 2, 1, 28, 4, 19, 15, 20	Names of Anions
5.0000E+00, 6.3277E-05, 1.0890E-15, 0.0000E+00, 6.2429E-02, 0.0000E+00, 0.0000E+00, 6.3559E-05, 4.9718E-04, 7.6271E-06, 3.5876E-05, 6.4689E-05, 2.8192E-05, 0.0000E+00, 1.6949E-04, 9.7740E-05, 0.0000E+00, 0.0000E+00, 6.4972E-06, 1.7345E-19	Concentrations of Cations
9.5427E-01, 1.3588E+00, 1.1921E+00, 1.0311E-01, 1.3362E-02, 5.7606E-01, 8.4746E-06, 3.5876E-01, 4.4915E-02, 1.9802E-02	Concentrations of Anions
1.0, 0.01	Liquid(L), Solid(g)
0	Initial solid Form
1.0	Calculation Adjustment

**ZAM Input for Phase 1 LAW-8 Batch Feed (Envelope A; nominal case)**

1, 298.15	Activity Coeff. Model, Temperature
CSTIX (5.0 M Na; LAW-8)	Title
20, 10	Number of Cations & Anions
1225	Density (kg/m3)
3, 6, 1, 5, 4, 40, 13, 14, 12, 21, 15, 18, 23, 20, 16, 22, 25, 24, 28, 29	Names of Cations
13, 9, 27, 2, 1, 28, 4, 19, 15, 20	Names of Anions
5.0000E+00 4.3243E-05 1.0784E-15 0.0000E+00 7.2162E-02 0.0000E+00 0.0000E+00 9.0811E-05 1.0622E-03 2.4595E-05 7.9459E-05 2.6622E-04 2.7568E-05 0.0000E+00 2.8108E-04 1.3216E-04 0.0000E+00	Concentrations of Cations
0.0000E+00 3.1351E-13 0.0000E+00	Concentrations of Anions
1.3432E+00 1.2784E+00 1.1973E+00 1.2459E-01 1.6541E-02 6.3746E-01 2.1892E-05 2.0135E-01 2.1703E-02 1.0838E-02	Liquid(L), Solid(g)
1.0, 0.01	Initial solid Form
0	

1.0

Calculation Adjustment

**ZAM Input for Phase 1 LAW-9 Batch Feed (Envelope A; nominal case)**

1, 298.15	Activity Coeff. Model, Temperature
CSTIX (5.0 M Na; LAW-9)	Title
20, 10	Number of Cations & Anions
1238	Density (kg/m3)
3, 6, 1, 5, 4, 40, 13, 14, 12, 21, 15, 18, 23, 20, 16, 22, 25, 24, 28, 29	Names of Cations
13, 9, 27, 2, 1, 28, 4, 19, 15, 20	Names of Anions
5.0000E+00 4.4444E-05 1.0708E-15 0.0000E+00 6.0278E-02 0.0000E+00 0.0000E+00 4.1389E-05 1.0500E-03 4.1667E-06 2.1944E-05 7.7778E-05 4.4722E-06 0.0000E+00 9.2500E-05 7.2222E-05 0.0000E+00	Concentrations of Cations
0.0000E+00 1.7083E-12 0.0000E+00	Concentrations of Anions
5.7331E-01 1.4083E+00 1.2083E+00 1.2722E-01 4.4722E-02 4.5325E-01 1.0278E-05 5.4722E-01 3.6667E-02 2.6694E-02	Liquid(L), Solid(g)
1.0, 0.01	Initial solid Form
0	Calculation Adjustment
1.0	

**ZAM Input for Phase 1 LAW-10 Batch Feed (Envelope A; nominal case)**

1, 298.15	Activity Coeff. Model, Temperature
CSTIX (5.0 M Na; LAW-10)	Title
20, 10	Number of Cations & Anions
1237	Density (kg/m3)
3, 6, 1, 5, 4, 40, 13, 14, 12, 21, 15, 18, 23, 20, 16, 22, 25, 24, 28, 29	Names of Cations
13, 9, 27, 2, 1, 28, 4, 19, 15, 20	Names of Anions
5.0E+00, 3.6923E-05, 1.6327E-15, 0.0E+00, 4.1923E-02, 0.0E+00, 0.0E+00, 0.0E+00, 1.6308E-03, 0.0E+00, 6.6923E-05, 8.3462E-04, 7.4231E-05, 0.0E+00, 1.7385E-03, 1.5154E-03, 0.0E+00, 0.0E+00, 2.0385E-05, 2.5769E-05	Concentrations of Cations
8.6970E-01, 1.4308E+00, 1.3115E+00, 1.4000E-01, 2.4962E-02, 5.1500E-01, 1.3077E-05, 2.7846E-01, 3.7269E-02, 4.3462E-02	Concentrations of Anions
1.0, 0.01	Liquid(L), Solid(g)
0	Initial solid Form
1.0	Calculation Adjustment

**ZAM Input for Phase 1 LAW-11 Batch Feed (Envelope A; nominal case)**

1, 298.15	Activity Coeff. Model, Temperature
CSTIX (5.0 M Na; LAW-11)	Title
20, 10	Number of Cations & Anions
1232	Density (kg/m3)
3, 6, 1, 5, 4, 40, 13, 14, 12, 21, 15, 18, 23, 20, 16, 22, 25, 24, 28, 29	Names of Cations
13, 9, 27, 2, 1, 28, 4, 19, 15, 20	Names of Anions
5.0000E+00 3.7391E-05 1.0989E-15 0.0000E+00 4.1522E-02 0.0000E+00 0.0000E+00 1.9565E-06 2.2174E-03 2.1739E-07 8.4130E-05 1.4630E-03 4.2826E-05 0.0000E+00 3.0870E-03 1.7370E-04 0.0000E+00	Concentrations of Cations
0.0000E+00 2.1739E-07 4.3478E-07	Concentrations of Anions
9.3069E-01 1.2000E+00 1.3870E+00 1.3652E-01 3.1087E-02 4.9130E-01 7.3913E-06 3.6087E-01 2.3913E-02 3.6522E-02	Liquid(L), Solid(g)
1.0, 0.01	Initial solid Form
0	Calculation Adjustment
1.0	

**ZAM Input for Phase 1 LAW-12 Batch Feed (Envelope A; nominal case)**

1, 298.15	Activity Coeff. Model, Temperature
CSTIX (5.0 M Na; LAW-12)	Title
20, 10	Number of Cations & Anions
1221	Density (kg/m3)
3, 6, 1, 5, 4, 40, 13, 14, 12, 21, 15, 18, 23, 20, 16, 22, 25, 24, 28, 29	Names of Cations
13, 9, 27, 2, 1, 28, 4, 19, 15, 20	Names of Anions
5.0000E+00 4.8305E-05 1.1091E-15 0.0000E+00 1.2352E-01 0.0000E+00 0.0000E+00 5.5720E-05 3.3475E-04 9.5339E-06 2.0127E-05 4.1737E-05 5.9746E-06 0.0000E+00 9.5975E-05 1.1653E-04 0.0000E+00	Concentrations of Cations
0.0000E+00 1.6949E-06 0.0000E+00	Concentrations of Anions
1.5432E+00 1.2225E+00 1.1271E+00 8.6229E-02 1.8475E-02 7.5360E-01 7.4153E-06 1.6144E-01 1.1377E-02 9.3856E-03	Liquid(L), Solid(g)
1.0, 0.01	Initial solid Form
	Calculation Adjustment

0  
1.0Initial solid Form  
Calculation Adjustment**ZAM Input for Phase 1 LAW-13 Batch Feed (Envelope A; nominal case)**

1, 298.15	Activity Coeff. Model, Temperature
CSTIX (5.0 M Na; LAW-13)	Title
20, 10	Number of Cations & Anions
1221	Density(kg/m3)
3, 6, 1, 5, 4, 40, 13, 14, 12, 21, 15, 18, 23, 20, 16, 22, 25, 24, 28, 29	Names of Cations
13, 9, 27, 2, 1, 28, 4, 19, 15, 20	Names of Anions
5.0000E+00 4.8305E-05 1.1186E-15 0.0000E+00 1.2521E-01 0.0000E+00 0.0000E+00 5.4661E-05 3.1356E-04 9.1102E-06 1.8432E-05 3.4958E-05 5.3390E-06 0.0000E+00 9.0466E-05 1.1631E-04 0.0000E+00	Concentrations of Cations
0.0000E+00 1.9068E-06 0.0000E+00	Concentrations of Anions
1.5423E+00 1.2225E+00 1.1271E+00 8.5169E-02 1.8559E-02 7.6000E-01 6.9915E-06 1.6038E-01 1.1081E-02 9.3432E-03	Liquid(L), Solid(g)
1.0, 0.01	Initial solid Form
0	Calculation Adjustment
1.0	

**ZAM Input for Phase 1 LAW-14 Batch Feed (Envelope A; nominal case)**

1, 298.15	Activity Coeff. Model, Temperature
CSTIX (5.0 M Na; LAW-14)	Title
20, 10	Number of Cations & Anions
1234	Density(kg/m3)
3, 6, 1, 5, 4, 40, 13, 14, 12, 21, 15, 18, 23, 20, 16, 22, 25, 24, 28, 29	Names of Cations
13, 9, 27, 2, 1, 28, 4, 19, 15, 20	Names of Anions
5.0000E+00 4.5685E-05 1.0736E-15 0.0000E+00 3.1980E-01 0.0000E+00 0.0000E+00 1.0406E-05 9.0863E-04 1.0152E-06 5.0508E-05 1.0025E-04 2.9442E-04 0.0000E+00 2.3477E-04 1.3807E-04 0.0000E+00	Concentrations of Cations
0.0000E+00 4.7716E-12 0.0000E+00	Concentrations of Anions
1.7475E+00 1.3249E+00 1.0635E+00 8.4264E-02 4.0609E-02 4.8912E-01 9.3909E-06 2.5305E-01 1.7208E-02 1.0990E-02	Liquid(L), Solid(g)
1.0, 0.01	Initial solid Form
0	Calculation Adjustment
1.0	

**ZAM Input for Phase 1 LAW-15 Batch Feed (Envelope A; nominal case)**

1, 298.15	Activity Coeff. Model, Temperature
CSTIX (5.0 M Na; LAW-15)	Title
20, 10	Number of Cations & Anions
1235	Density(kg/m3)
3, 6, 1, 5, 4, 40, 13, 14, 12, 21, 15, 18, 23, 20, 16, 22, 25, 24, 28, 29	Names of Cations
13, 9, 27, 2, 1, 28, 4, 19, 15, 20	Names of Anions
5.0000E+00 4.5522E-05 1.0746E-15 0.0000E+00 4.0672E-01 0.0000E+00 0.0000E+00 8.6007E-04 0.0000E+00 6.0261E-05 1.0802E-04 3.9552E-04 0.0000E+00 2.8358E-04 1.6063E-04 0.0000E+00 5.8022E-12 0.0000E+00	Concentrations of Cations
2.1409E+00 1.2985E+00 1.0149E+00 6.9776E-02 3.9366E-02 5.0132E-01 9.1418E-06 1.5373E-01 1.0616E-02 5.6716E-03	Concentrations of Anions
1.0, 0.01	Liquid(L), Solid(g)
0	Initial solid Form
1.0	Calculation Adjustment

**ZAM Input for Phase 1 LAW-2a Batch Feed (Envelope B; nominal case)**

1, 298.15	Activity Coeff. Model, Temperature
CSTIX (5.0 M Na; LAW-2a)	Title
20, 10	Number of Cations & Anions
1254	Density(kg/m3)
3, 6, 1, 5, 4, 40, 13, 14, 12, 21, 15, 18, 23, 20, 16, 22, 25, 24, 28, 29	Names of Cations
13, 9, 27, 2, 1, 28, 4, 19, 15, 20	Names of Anions
5.0000E+00 4.6755E-04 6.2555E-14 0.0000E+00 1.2498E-01 0.0000E+00 0.0000E+00 2.0448E-05 1.2708E-05 4.3479E-05 2.5496E-07 9.2620E-07 2.2266E-05 0.0000E+00 2.0891E-04 0.0000E+00 0.0000E+00	Concentrations of Cations
0.0000E+00 2.3339E-10 0.0000E+00	Concentrations of Anions
1.5986E-01 1.2766E+00 1.4812E+00 5.8342E-03 1.0289E-01 4.3642E-01 3.9746E-02 5.9071E-01 1.9669E-01 1.6090E-02	Liquid(L), Solid(g)
	Initial solid Form
	Calculation Adjustment

1.0, 0.01  
0  
1.0Liquid(L), Solid(g)  
Initial solid Form  
Calculation Adjustment**ZAM Input for Phase 1 LAW-2b Batch Feed (Envelope B; nominal case)**

1, 298.15	Activity Coeff. Model, Temperature
CSTIX (5.0 M Na; LAW-2b)	Title
20,10	Number of Cations & Anions
1242	Density(kg/m3)
3, 6, 1, 5, 4, 40, 13, 14, 12, 21, 15, 18, 23, 20, 16, 22, 25, 24, 28, 29	Names of Cations
13, 9, 27, 2, 1, 28, 4, 19, 15, 20	Names of Anions
5.0000E+00 4.3110E-04 3.6771E-14 0.0000E+00 1.4295E-01 0.0000E+00 0.0000E+00 5.6007E-13 1.9760E-04 1.1913E-12 2.3439E-05 6.4344E-05 1.1586E-03 0.0000E+00 3.4076E-04 0.0000E+00 0.0000E+00	Concentrations of Cations
0.0000E+00 3.5152E-05 0.0000E+00	Concentrations of Anions
2.7195E-01 6.7357E-01 1.1815E+00 4.7250E-04 9.8670E-02 1.3419E-01 3.5026E-02 1.0349E+00 3.3690E-01 2.5378E-03	Concentrations of Anions
1.0, 0.01	Liquid(L), Solid(g)
0	Initial solid Form
1.0	Calculation Adjustment

**ZAM Input for Phase 1 LAW-3 Batch Feed (Envelope C; nominal case)**

1, 298.15	Activity Coeff. Model, Temperature
CSTIX (5.0 M Na; LAW-3)	Title
20,10	Number of Cations & Anions
1237	Density(kg/m3)
3, 6, 1, 5, 4, 40, 13, 14, 12, 21, 15, 18, 23, 20, 16, 22, 25, 24, 28, 29	Names of Cations
13, 9, 27, 2, 1, 28, 4, 19, 15, 20	Names of Anions
5.0000E+00 3.9675E-05 8.2892E-16 0.0000E+00 4.3926E-02 0.0000E+00 0.0000E+00 1.0013E-04 6.9195E-03 2.5978E-04 4.1328E-02 3.0701E-03 3.4007E-04 0.0000E+00 1.7429E-03 4.2981E-04 0.0000E+00	Concentrations of Cations
0.0000E+00 0.0000E+00 0.0000E+00	Concentrations of Anions
1.0328E+00 1.7370E+00 7.9586E-01 4.7941E-02 4.3454E-02 2.6103E-01 1.5823E-05 5.1011E-01 7.2737E-02 2.2860E-02	Concentrations of Anions
1.0, 0.01	Liquid(L), Solid(g)
0	Initial solid Form
1.0	Calculation Adjustment

**ZAM Input for Phase 1 LAW-4 Batch Feed (Envelope C; nominal case)**

1, 298.15	Activity Coeff. Model, Temperature
CSTIX (5.0 M Na; LAW-4)	Title
20,10	Number of Cations & Anions
1237	Density(kg/m3)
3, 6, 1, 5, 4, 40, 13, 14, 12, 21, 15, 18, 23, 20, 16, 22, 25, 24, 28, 29	Names of Cations
13, 9, 27, 2, 1, 28, 4, 19, 15, 20	Names of Anions
5.0000E+00 3.7786E-05 8.2892E-16 0.0000E+00 4.3926E-02 0.0000E+00 0.0000E+00 1.0013E-04 6.9195E-03 2.5741E-04 4.1328E-02 3.0701E-03 3.4007E-04 0.0000E+00 1.7429E-03 4.2981E-04 0.0000E+00	Concentrations of Cations
0.0000E+00 0.0000E+00 0.0000E+00	Concentrations of Anions
1.0328E+00 1.7370E+00 7.9586E-01 4.7941E-02 4.3454E-02 2.6103E-01 1.5823E-05 5.1011E-01 7.2737E-02 2.2860E-02	Concentrations of Anions
1.0, 0.01	Liquid(L), Solid(g)
0	Initial solid Form
1.0	Calculation Adjustment

**ZAM Input for Phase 1 LAW-7 Batch Feed (Envelope C; nominal case)**

1, 298.15	Activity Coeff. Model, Temperature
CSTIX (5.0 M Na; LAW-7)	Title
20,10	Number of Cations & Anions
1243	Density(kg/m3)
3, 6, 1, 5, 4, 40, 13, 14, 12, 21, 15, 18, 23, 20, 16, 22, 25, 24, 28, 29	Names of Cations
13, 9, 27, 2, 1, 28, 4, 19, 15, 20	Names of Anions
5.0000E+00 4.4548E-05 8.6392E-16 0.0000E+00 2.2274E-02 0.0000E+00 0.0000E+00 0.0000E+00 7.5573E-03 0.0000E+00 4.0571E-02 4.4389E-03 3.1025E-04 0.0000E+00 2.6570E-02 1.0151E-03 0.0000E+00	Concentrations of Cations
0.0000E+00 1.3174E-04 0.0000E+00	Concentrations of Anions

7.9429E-01 1.9673E+00 6.9527E-01 2.7843E-02 9.3869E-02 1.3912E-01 1.2728E-05 6.5549E-01 4.6935E-02 2.0365E-02	Concentrations of Anions
1.0, 0.01	Liquid(L), Solid(g)
0	Initial solid Form
1.0	Calculation Adjustment

**ZAM Input for Phase 1 LAW-1 Batch Feed (Envelope A; with 4 M Na<sup>+</sup>)**

1, 298.15	Activity Coeff. Model, Temperature
CSTIX (4.0 M Na; LAW-1)	Title
20, 10	Number of Cations & Anions
1224	Density(kg/m3)
3, 6, 1, 5, 4, 40, 13, 14, 12, 21, 15, 18, 23, 20, 16, 22, 25, 24, 28, 29	Names of Cations
13, 9, 27, 2, 1, 28, 4, 19, 15, 20	Names of Anions
4.0000E+00, 2.7463E-05, 9.2015E-16, 0.0000E+00, 2.8806E-01, 0.0000E+00, 0.0000E+00, 1.6418E-06, 6.0597E-04, 5.8209E-06, 0.0000E+00, 6.7463E-05, 6.7015E-05, 3.2687E-04, 4.3582E-05, 9.5522E-06, 0.0000E+00, 0.0000E+00, 0.0000E+00, 0.0000E+00	Concentrations of Cations
1.7240E+00, 1.3328E+00, 5.5075E-01, 2.3284E-02, 7.5821E-02, 2.2668E-01, 1.4925E-06, 1.4627E-01, 2.2388E-02, 6.5672E-03	Concentrations of Anions
1.0, 0.01	Liquid(L), Solid(g)
0	Initial solid Form
1.0	Calculation Adjustment

**ZAM Input for Phase 1 LAW-1 Batch Feed (Envelope A; with 6 M Na<sup>+</sup>)**

1, 298.15	Activity Coeff. Model, Temperature
CSTIX (6.0 M Na; LAW-1)	Title
20, 10	Number of Cations & Anions
1269	Density(kg/m3)
3, 6, 1, 5, 4, 40, 13, 14, 12, 21, 15, 18, 23, 20, 16, 22, 25, 24, 28, 29	Names of Cations
13, 9, 27, 2, 1, 28, 4, 19, 15, 20	Names of Anions
6.0000E+00, 4.1194E-05, 1.3802E-15, 0.0000E+00, 4.3209E-01, 0.0000E+00, 0.0000E+00, 2.4627E-06, 9.0896E-04, 8.7313E-06, 0.0000E+00, 1.0119E-04, 1.0052E-04, 4.9030E-04, 6.5373E-05, 1.4328E-05, 0.0000E+00, 0.0000E+00, 0.0000E+00, 0.0000E+00	Concentrations of Cations
2.5859E+00, 1.9993E+00, 8.2612E-01, 3.4925E-02, 1.1373E-01, 3.4002E-01, 2.2388E-06, 2.1940E-01, 3.3582E-02, 9.8507E-03	Concentrations of Anions
1.0, 0.01	Liquid(L), Solid(g)
0	Initial solid Form
1.0	Calculation Adjustment

**ZAM Input for Phase 1 LAW-3 Batch Feed (Envelope C; with Sr<sup>+2</sup>)**

1, 298.15	Activity Coeff. Model, Temperature
CSTIX (5.0 M Na; LAW-3)	Title
20, 10	Number of Cations & Anions
1237	Density(kg/m3)
3, 6, 1, 5, 4, 40, 13, 14, 12, 21, 15, 18, 23, 20, 16, 22, 25, 24, 28, 29	Names of Cations
13, 9, 27, 2, 1, 28, 4, 19, 15, 20	Names of Anions
5.0000E+00 3.9675E-05 8.2892E-16 0.0000E+00 4.3926E-02 0.0000E+00 1.633E-03 1.0013E-04 6.9195E-03 2.5978E-04 4.1328E-02 3.0701E-03 3.4007E-04 0.0000E+00 1.7429E-03 4.2981E-04 0.0000E+00 0.0000E+00 0.0000E+00 0.0000E+00	Concentrations of Cations
1.0328E+00 1.740266E+00 7.9586E-01 4.7941E-02 4.3454E-02 2.6103E-01 1.5823E-05 5.1011E-01 7.2737E-02 2.2860E-02	Concentrations of Anions
1.0, 0.01	Liquid(L), Solid(g)
0	Initial solid Form
1.0	Calculation Adjustment



## Appendix H (Column Test Input Files)

For reference the VERSE-LC input files for the laboratory-scale and pilot-scale test columns are provided in this appendix (output files are not shown but can be quickly generated based on the input files). The results of these VERSE-LC input files are discussed in Chapter 9. The column tests were performed using the single component modeling option (i.e., effective cesium isotherms and column transport simulations). Fifteen column simulation models were run. The input files for each case are listed below. Some of the key parameters and details of the experiments are listed in tables, along with the measured cesium breakthrough curves.

An “effective” single component transport analysis is used for all of the VERSE-LC column studies. When using this option a single component isotherm model for cesium loading is required. To estimate the cesium isotherms an algebraic model is fit to the ZAM generated database, where a beta factor for each column study is defined. The feed compositions for the column tests considered are listed in Table H-1.

In the majority of case runs a bed density of 1.0 g/ml and a cesium total ionic capacity of 0.58 mmole/g<sub>CST</sub> were assumed. For assessment and optimization purposes several VERSE-LC simulation runs were made for each column test while varying the dilution factor (i.e., typical values of either 68% or 100%) and the pore to free diffusion coefficient ratio (i.e., values of 10%, 20%, 26%, 30%, and 35%). The ratio value of 26% corresponds to pore diffusion coefficient values used in several earlier SRS analysis efforts.

### H.1 SRS Tank 44 Studies

Walker et al. (1999) performed batch contact and column tests using CST IE-911 (Lot number 98-05) with actual diluted Tank 44 supernate. Some of the key column parameters for these tests are given in Table H-2. The cesium breakthrough data at two axial locations (i.e., sampling points) are tabulated in Table H-3. Two different VERSE-LC models were used to simulate this data. The only difference between the two models being the column size considered. Example input files for each model is also provided in this appendix. The beta parameter used for the cesium isotherm is  $2.0486 \times 10^{-4}$  M based on a fit of data generated using the ZAM code at 31 C.

### H.2 SRS Average Simulant Studies

Several column tests using CST material were performed with SRS average simulant as the feed:

#### Wilmarth et al. (1999) Data Sets

Wilmarth et al. (1999) performed a series of column tests at ~25 C where the effects of CST pretreatment, superficial velocity, and the presence of organic constituents were considered. CST with Lot numbers 96-04 and 98-05 were tested. Some of the key column parameters for these tests are given in Table H-4. The cesium breakthrough data for these tests are tabulated in Tables H-5 and H-6. The beta parameter used for the cesium isotherm is  $2.4145 \times 10^{-4}$  M based on a fit of data generated using the ZAM code at 25 C.

For the SRS-Avg-Test2 test both single component and ternary column simulations were performed, as discussed in Chapter 3 for justifying the use of the single component modeling approach. The input file of both approaches is provided.

### **Walker et al. (1998) Data Sets**

Walker et al. (1998) performed several batch contact tests and three column tests using CST IE-911 (Lot numbers 96-02 and 96-04) with SRS-Avg simulant, as well. The column tests were performed at ~22 C. The beta parameter used for the cesium isotherm is  $2.4145 \times 10^{-4}$  M, the same value used for all of the seven SRS-Avg tests. The slight difference due to temperature was neglected. Some of the key column parameters for these tests are given in Table H-7. The cesium breakthrough data for the three column tests are tabulated in Table H-8. The VERSE-LC input file for each column test is also provided in this appendix.

## **H.3 SRS High OH Simulant Studies**

Walker et al. (1999) also performed batch contact and column tests using CST IE-911 (Lot number 98-05) with SRS high OH simulant. These tests are basically repeat tests where the feed was changed from SRS Tank44 supernate to SRS high OH simulant. Some of the key column parameters for these tests are also given in Table H-2. The cesium breakthrough data at the earlier two axial locations (i.e., sampling points) are tabulated in Table H-9. No breakthrough was observed at the 85 cm axial location over the time period of the testing. Two different VERSE-LC models were used to simulate this data. The only difference between the two models being the column length considered. Example input files for each model is also provided in this appendix. The beta parameter used for the cesium isotherm is  $2.0987 \times 10^{-4}$  M based on a fit of data generated using the ZAM code at 31 C.

## **H.4 PNNL AW-101 Sample Studies**

Hendrickson (1997) performed a column test using CST IE-911 (Lot number 96-01) with a diluted AW-101 sample. The column test was performed at ~25 C and the key features of these tests are listed in Table H-10. The cesium breakthrough data are tabulated in Table H-11. The beta parameter used for the cesium isotherm is  $4.7414 \times 10^{-4}$  M based on a fit of data generated using the ZAM code at 25 C.

## **H.5 ORNL MVST Sample Tests**

Several column tests using CST material were performed with MVST waste as the feed:

### **Lee et al. (1997) Data Sets**

Lee et al. (1997b) performed columns test using CST IE-911 (Lot number –38b) with a MVST W-27 sample. The column test was performed at ~25 C and the key features of these tests are listed in Table H-12. The cesium breakthrough data are tabulated in Table H-13. The beta parameter used for the cesium isotherm is  $9.3232 \times 10^{-4}$  M based on a fit of data generated using the ZAM code at 25 C.

### **Walker, Jr., et al. (1998) Data Sets**

Walker, Jr., et al. (1998) performed pilot-scale column testing using CST IE-911 (Lot number – 38b) with a MVST W-29 sample. The column tests were performed at ~25 C and the key features of these tests are listed in Table H-14. The cesium breakthrough data are tabulated in Tables H-15, H-16, H-17, and H-18. Since the composition of the feeds was not well defined within the Walker, Jr., et al. (1998) report, the limited  $K_d$  values reported were directly used to fit the isotherms where several beta values (feed dependent) were generated and used.

Table H-1. Ionic species molar concentrations for various simulated and actual waste solutions used in ZAM batch contact simulations to generate a cesium isotherm data used for estimating the beta factor.

Species ID	SRS Average simulant [M]	SRS High OH <sup>-</sup> simulant [M]	SRS Tank 44 sample [M]	PNNL AW-101 sample [M]	ORNL MVST W-27 sample [M]
<b>Cations</b>					
Na <sup>+</sup>	5.6	5.6	5.4	5.64	5.119
Cs <sup>+</sup>	$1.4 \times 10^{-4}$	$3.7 \times 10^{-4}$	$3.51 \times 10^{-4}$	$7.26 \times 10^{-5}$	$7.04 \times 10^{-6}$
K <sup>+</sup>	0.015	0.03	0.051	0.50	0.263
H <sup>+</sup>	$5.2 \times 10^{-15}$	$3.3 \times 10^{-15}$	$2.3 \times 10^{-15}$	$3.9 \times 10^{-15}$	$1.4 \times 10^{-13}$
Ca <sup>+2</sup>	-	-	-	-	$2.22 \times 10^{-3}$
<b>Anions</b>					
NO <sub>3</sub> <sup>-</sup>	2.14	1.1	0.37	1.53	5.194
NO <sub>2</sub> <sup>-</sup>	0.52	0.74	0.35	1.13	-
Cl <sup>-</sup>	0.025	$3.637 \times 10^{-2}$	0.009	0.0883	0.09
F <sup>-</sup>	0.032	0.01	-	0.0334	-
OH <sup>-</sup> (free)	1.938	3.05	4.3	2.541	0.0708
Al(OH) <sub>4</sub> <sup>-</sup>	0.31	0.27	0.126	0.574	$3.14 \times 10^{-5}$
CO <sub>3</sub> <sup>2-</sup>	0.16	0.17	0.1412	0.11	-
SO <sub>4</sub> <sup>2-</sup>	0.15	0.03	0.001	3.28	$1.60 \times 10^{-2}$
PO <sub>4</sub> <sup>3-</sup>	0.01	0.008	0.0001	$5.53 \times 10^{-3}$	-
Cations =	5.615	5.630	5.451	6.140	5.387
Anions =	-5.615	-5.630	-5.451	-6.140	-5.387
Sum =	0.000	0.000	0.000	0.000	0.000
Beta =	$2.4145 \times 10^{-4}$	$2.0987 \times 10^{-4}$	$2.0486 \times 10^{-4}$	$4.7414 \times 10^{-4}$	$9.3232 \times 10^{-4}$

Table H-2. Key column parameters for CST IE-911 packed columns using SRS high OH simulant and SRS Tank 44 supernate waste taken by Walker et al. (1999) at 31.<sup>a,b</sup>

Parameter	SRS-High-OH-Test1a	SRS-High-OH-Test1b	SRS-Tank44-Test1a	SRS-Tank44-Test1b
Column diameter (cm)	1.50	1.50	1.50	1.50
Axial sampling location (cm)	10.0	85.0	10.0	85.0
CST (Lot #)	98-05	98-05	98-05	98-05
Average superficial velocity (cm/min)	5.43	5.43	5.32	5.32
Average temperature (C)	31	31	31	31
Avg. Cs feed concentration (M)	3.70E-04	3.70E-04	3.51E-04	3.51E-04
Column volume (ml)	17.6714	150.2074	17.6714	150.2074
Flowrate Q (ml/min) [CV/hr]	9.60 [32.6]	9.60 [32.6]	9.40 [3.8]	9.40 [3.8]

<sup>a</sup> The SRS high OH simulant and SRS Tank 44 waste feed compositions are provided in Appendix C.

<sup>b</sup> Same basic columns and sampling locations used for both feed types.

Table H-3. Cesium breakthrough data for CST IE-911 (Lot 98-05) and actual SRS Tank 44 waste taken by Walker et al. (1999) at 31 C.

Effectively a Lead Column (10 cm down column length)		Effectively a Lag Column (85 cm down column length)	
Time (hrs)	Normalized cesium breakthrough (c/c <sub>0</sub> ) <sup>a</sup>	Time (hrs)	Normalized cesium breakthrough (c/c <sub>0</sub> ) <sup>a</sup>
0	0.000	0	0.000E+00
1.1	0.007	1.1	4.700E-07
3.9	0.067	7.9	1.200E-06
7.9	0.174	15.6	4.300E-07
11.7	0.279	23.5	1.100E-06
15.6	0.381	31.4	4.500E-07
19.4	0.487	39.2	1.500E-06
23.5	0.554	46.9	1.400E-06
27.4	0.631	54.7	4.900E-06
31.4	0.710	62.5	1.100E-07
35.3	0.732	70.3	2.900E-05
39.2	0.770	78.1	7.600E-05
43.1	0.770	86.0	1.700E-04
46.9	0.817	93.9	5.300E-04
50.8	0.880	101.9	7.300E-04
54.7	0.899	109.8	1.200E-03
58.7	0.897	113.8	1.600E-03

62.5	0.928	117.8	2.100E-03
66.4	0.918	125.7	3.400E-03
70.3	0.966		
74.2	0.961		
78.1	0.955		
82.0	0.955		
86.0	0.976		
90.0	0.946		
93.9	0.974		
97.9	0.997		
101.9	1.025		
105.9	0.992		
109.8	0.987		
113.8	0.982		
117.8	1.019		
121.7	1.221		
125.7	0.999		

<sup>a</sup> The inlet cesium feed concentration (i.e.,  $3.51 \times 10^{-4}$  M) was used to normalize the breakthrough data.

Table H-4. Key column parameters for CST IE-911 packed columns using SRS-Avg simulant taken by Wilmarth et al. (1999) at 25 C ( $\pm 5$  C).<sup>a</sup>

Parameter	SRS-Avg-Test 1	SRS-Avg-Test 2	SRS-Avg-Test 3 (a & b) <sup>b</sup>	SRS-Avg-Test 4
Column diameter (cm)	1.50	1.50	1.50	2.50
Column length (cm)	10.0	10.0	10.0	10.0
CST (Lot #)	98-05	98-05	98-05	98-05
Average superficial velocity (cm/min)	5.50	7.00	4.10	4.10
Average temperature (C)	25	25	25	25
Avg. Cs feed concentration (M)	1.30E-04	1.24E-04	1.43E-04	1.366E-04
Column volume (ml)	17.6714	17.6714	17.6714	49.0874
Flowrate Q (ml/min) [CV/hr]	9.7193 [33.0]	12.370 [42.0]	7.2453 [24.6]	20.1258 [24.6]

<sup>a</sup> The SRS-Avg simulant feed composition is provided in Appendix C.

<sup>b</sup> Same basic column test where for Test3a the CST had prior exposure to humid air, while Test3b did not.

Table H-5. Cesium breakthrough data for CST IE-911 and SRS-Avg waste simulant taken by Wilmarth et al. (1999) at ~25 C.

SRS-Avg-Test1 (CST lot 96-02)		SRS-Avg-Test2 (CST lot 96-02)		SRS-Avg-Test4 (CST lot 96-04)	
Time (hrs)	Normalized cesium breakthrough (c/c <sub>0</sub> ) <sup>a</sup>	Time (hrs)	Normalized cesium breakthrough (c/c <sub>0</sub> ) <sup>a</sup>	Time (hrs)	Normalized cesium breakthrough (c/c <sub>0</sub> ) <sup>a</sup>
0.0	0.000	0.0	0.000	0.0	0.000
4.0	0.184	8.0	0.390	0.0	0.033
16.0	0.488	16.0	0.553	8.0	0.184
28.0	0.574	20.0	0.615	20.0	0.307
36.0	0.661	28.0	0.720	32.0	0.438
44.0	0.701	36.0	0.756	44.0	0.534
52.0	0.801	40.0	0.793	56.0	0.691
60.0	0.857	48.0	0.824	68.0	0.736
72.0	0.895	56.0	0.864	80.0	0.873
84.0	1.039	60.0	0.867	92.0	0.694
96.0	0.974	64.0	0.869	104.0	0.718
108.0	1.031	68.0	0.875	116.0	0.742
120.0	1.004	76.0	0.916	128.0	0.802
132.0	1.004	80.0	0.886	140.0	0.754
140.0	1.018	88.0	0.882	152.0	0.823
		100.0	0.969	164.0	0.785
		104.0	0.936		
		112.0	0.957		
		120.0	0.950		
		124.0	0.957		
		132.0	0.900		

<sup>a</sup> The inlet cesium feed concentration (i.e.,  $1.30 \times 10^{-4}$  M for Test1,  $1.24 \times 10^{-4}$  M for Test2, and  $1.366 \times 10^{-4}$  M for Test4) was used to normalize the breakthrough data.

Table H-6. Cesium breakthrough data for CST IE-911 (with and without prior exposure to humid air) and SRS-Avg waste simulant taken by Wilmarth et al. (1999) at ~25 C.

SRS-Avg-Test3a (CST lot 98-05)		SRS-Avg-Test3b (CST lot 98-05)	
Time (hrs)	Normalized Cs breakthrough (c/c <sub>0</sub> ) <sup>a</sup>	Time (hrs)	Normalized Cs breakthrough (c/c <sub>0</sub> ) <sup>a</sup>
0.0	0.000	0.0	0.000
2.0	0.020	2.0	0.001
6.0	0.078	6.0	0.058
10.0	0.146	10.0	0.114
14.0	0.208	14.0	0.166
18.0	0.261	18.0	0.217
22.0	0.281	22.0	0.248
26.0	0.279	26.0	0.307
30.0	0.349	30.0	0.344
34.0	0.333	34.0	0.371
38.0	0.409	38.0	0.477
42.0	0.379	42.0	0.636
46.0	0.474	46.0	0.598
50.0	0.510	50.0	0.726
54.0	0.469	54.0	0.539
58.0	0.630	58.0	0.545
62.0	0.566	62.0	0.731
66.0	0.603	66.0	0.539
70.0	0.689	70.0	0.694
74.0	0.678	74.0	0.833
78.0	0.694	78.0	0.972
82.0	0.683	82.0	0.902
86.0	0.721	86.0	0.785
90.0	0.705	90.0	0.747
94.0	0.705	94.0	0.950
98.0	0.668	98.0	0.859
		102.0	0.783
		106.0	0.755
		110.0	0.745
		114.0	0.772
		118.0	0.761
		122.0	0.826
		126.0	0.848
		130.0	0.837
		134.0	0.886
		138.0	0.853
		142.0	0.821
		146.0	0.821
		150.0	0.832
		154.0	0.929
		158.0	0.946
		162.0	0.929
		166.0	0.891
		170.0	0.984
		174.0	0.880
		178.0	0.902
		182.0	0.880
		184.0	0.940
		188.0	0.935
		192.0	0.891
		196.0	0.902

<sup>a</sup> The inlet cesium feed concentration (i.e.,  $1.43 \times 10^{-4}$  M for both tests) was used to normalize the breakthrough data.

Table H-7. Key column parameters for CST IE-911 packed columns using SRS-Avg simulant taken by Walker et al. (1998) at 22 C.<sup>a,b</sup>

Parameter	SRS-Avg-Test 5	SRS-Avg-Test 6	SRS-Avg-Test 7
Column diameter (cm)	1.50	1.50	1.43
Column length (cm)	10.0	10.0	11.0
CST (Lot #)	96-02	96-02	96-04
Average superficial velocity (cm/min)	0.27	0.98	4.1
Average temperature (C)	22	22	22
Avg. Cs feed concentration (M)	1.40E-04	1.40E-04	1.40E-04
column volume (ml)	17.7	17.7	17.7
flowrate Q (ml/min) [CV/hr]	0.47 [1.59]	1.73 [5.88]	6.53 [22.1]

<sup>a</sup> These column tests were originally designed to only compare the effects of superficial velocity on CST column performance; however, due to availability limitations the third column had to be packed with a different CST material (i.e., a CST production-scale batch).

<sup>b</sup> The SRS-Avg simulant feed composition is provided in Appendix C.

Table H-8. Cesium breakthrough data for CST IE-911 and SRS-Avg waste simulant taken by Walker et al. (1998) at ~22 C.

SRS-Avg-Test5 (CST lot 96-02)		SRS-Avg-Test6 (CST lot 96-02)		SRS-Avg-Test7 (CST lot 96-04)	
Time (hrs)	Normalized cesium breakthrough (c/c <sub>0</sub> ) <sup>a</sup>	Time (hrs)	Normalized cesium breakthrough (c/c <sub>0</sub> ) <sup>a</sup>	Time (hrs)	Normalized cesium breakthrough (c/c <sub>0</sub> ) <sup>a</sup>
0.0	0.000E+00	0.0	1.571E-03	0.0	0.000E+00
1.6	1.500E-05	22.4	3.141E-03	1.0	1.890E-02
7.5	1.100E-05	57.3	1.518E-02	3.9	4.730E-02
21.5	2.000E-06	79.8	5.183E-02	6.9	1.094E-01
55.8	3.400E-05	103.2	1.005E-01	9.8	1.702E-01
143.2	4.000E-06	115.2	1.346E-01	12.8	2.374E-01
153.7	7.000E-06	138.9	1.671E-01	15.7	2.820E-01
198.0	1.600E-05	150.7	1.971E-01	18.7	3.427E-01
222.7	2.900E-05	162.6	2.551E-01	21.6	3.552E-01
249.7	1.100E-04	174.4	2.435E-01	24.7	4.777E-01
263.6	2.200E-04	198.1	4.821E-01	27.7	5.061E-01
304.4	4.600E-04	210.0	4.101E-01	30.7	5.128E-01
312.6	8.500E-04	221.9	5.809E-01	33.7	5.973E-01
337.5	1.630E-03	233.8	6.059E-01	36.7	6.716E-01
361.8	2.560E-03	245.6	6.558E-01	39.7	6.757E-01
391.8	4.161E-03	246.8	6.808E-01	42.7	7.027E-01
409.5	6.411E-03	259.9	6.246E-01	45.7	7.297E-01



433.9	8.747E-03	283.8	7.995E-01	48.5	6.533E-01
457.9	1.220E-02	295.8	8.182E-01	51.5	7.181E-01
481.1	1.722E-02	319.9	7.333E-01	54.5	7.049E-01
504.8	2.222E-02	344.0	7.641E-01	57.5	7.335E-01
530.0	2.957E-02	356.0	7.949E-01	60.5	7.221E-01
550.9	3.366E-02	367.9	6.513E-01	63.5	8.223E-01
575.2	4.455E-02	392.3	8.513E-01	66.5	7.450E-01
		416.6	8.615E-01	69.5	7.851E-01
		429.0	7.385E-01	72.7	7.332E-01
		441.4	7.692E-01	74.6	7.830E-01
		465.9	8.772E-01	77.6	7.880E-01
		490.8	9.006E-01	80.6	7.531E-01
		516.0	8.713E-01	83.5	7.930E-01
		540.2	8.655E-01	86.5	7.731E-01
		552.4	9.474E-01	89.5	8.080E-01
				92.4	7.930E-01
				94.4	8.922E-01
				97.4	8.824E-01
				100.4	8.971E-01
				103.4	9.020E-01
				106.4	9.265E-01
				109.4	8.971E-01
				112.3	8.725E-01
				115.3	8.971E-01
				117.3	9.375E-01
				120.4	9.615E-01
				123.4	1.024E+00
				126.4	9.327E-01
				129.5	9.038E-01
				132.5	1.000E+00
				135.5	9.135E-01
				138.6	9.327E-01
				140.6	9.417E-01
				143.6	9.806E-01
				146.6	1.015E+00
				149.7	9.709E-01
				152.7	1.000E+00
				155.7	9.563E-01
				158.8	1.005E+00

<sup>a</sup> The inlet cesium feed concentration (i.e.,  $1.40 \times 10^{-4}$  M) was used to normalize the breakthrough data.

Table H-9. Cesium breakthrough data for CST IE-911 (Lot 98-05) and SRS high OH simulant taken by Walker et al. (1999) at 31 C.

Effectively a Lead Column (10 cm down column length)		Effectively a Lag Column (85 cm down column length)	
Time (hrs)	Normalized cesium breakthrough (c/c <sub>0</sub> ) <sup>a</sup>	Time (hrs)	Normalized cesium breakthrough (c/c <sub>0</sub> ) <sup>a</sup>
0.0	0.000	0.0	0.000
2.9	0.042	2.9	0.000
6.4	0.126	6.4	0.000
10.1	0.262	10.1	0.000
14.0	0.364	14.0	0.000
17.8	0.424	17.8	0.000
21.6	0.470	21.6	0.000
25.3	0.550	25.3	0.000
29.1	0.623	29.1	0.000
32.8	0.622	32.8	0.000
36.6	0.678	36.6	0.000
40.5	0.748	40.5	0.000
44.3	0.704	44.3	0.000
48.1	0.741	48.1	0.000
52.0	0.790	52.0	0.000
55.7	0.827	55.7	0.000
59.6	0.820	59.6	0.000
63.4	0.850	63.4	0.000
67.3	0.840	67.3	0.000
72.6	0.852	72.6	0.000

<sup>a</sup> The inlet cesium feed concentration (i.e.,  $3.70 \times 10^{-4}$  M) was used to normalize the breakthrough data.

Table H-10. Key column parameters for CST IE-911 packed columns using PNNL diluted AW-101 sample taken by Hendrickson (1997) at 25 C.<sup>a</sup>

Parameter	PNNL-AW101-Test 1
Column diameter (cm)	1.0
Column length (cm)	10.0
CST (Lot #)	96-01
Average superficial velocity (cm/min)	1.06
Average temperature (C)	25
Avg. Cs feed concentration (M)	7.26E-05
Column volume (ml)	7.854
Flowrate Q (ml/min) [CV/hr]	0.83 [6.3]

<sup>a</sup> The PNNL AW-101 sample feed composition is provided in Appendix C.

Table H-11. Cesium breakthrough data for CST IE-911 and PNNL diluted AW-101 sample taken by Hendrickson (1997) at ~25 C.

PNNL-AW101-Test1 (CST lot 96-01)	
Time (hrs)	Normalized cesium breakthrough (c/c <sub>0</sub> ) <sup>a</sup>
0.4	0.000
5.8	0.000
15.1	0.000
19.6	0.000
24.3	0.000
28.7	0.001
32.3	0.002
36.0	0.005
39.6	0.008
43.6	0.013
44.9	0.019
51.4	0.027
55.3	0.038
59.6	0.056
63.5	0.071
67.5	0.102
71.6	0.136
75.6	0.163

80.0	0.182
83.4	0.231
87.8	0.263
91.8	0.309
95.7	0.347
99.4	0.399
103.7	0.430
108.0	0.460
111.8	0.470
115.7	0.571
119.6	0.682
124.2	0.656
128.3	0.674

<sup>a</sup> The inlet cesium feed concentration (i.e.,  $7.26 \times 10^{-5}$  M) was used to normalize the breakthrough data.

Table H-12. Key column parameters for CST IE-911 packed columns using MVST W-27 sample taken by Lee et al. (1997b) at 25 C. <sup>a,b</sup>

Parameter	ORNL-W27-Test 1	ORNL-W27-Test 2
Column diameter (cm)	1.50	1.50
Column length (cm)	5.659	5.659
CST (Lot #)	-38b	-38b
Average superficial velocity (cm/min)	0.283	0.566
Average temperature (C)	25	25
Avg. Cs feed concentration (M)	$7.04 \times 10^{-6}$	$7.04 \times 10^{-6}$
column volume (ml)	10.0	10.0
Bed density (g/ml)	1.15	1.15
Flowrate Q (ml/min) [CV/hr]	0.5 [3.0]	1.0 [6.0]

<sup>a</sup> The same column comparing the effect of superficial velocity on CST column performance.

<sup>b</sup> The MVST W-27 sample feed composition is provided in this appendix.

Table H-13. Cesium breakthrough data for CST IE-911 and MVST W-27 waste sample taken by Lee et al. (1997b) at ~25 C.

ORNL-W27-Test1 (CST lot -38b)		ORNL-W27-Test2 (CST lot -38b)	
Time (hrs)	Normalized cesium breakthrough (c/c <sub>0</sub> ) <sup>a</sup>	Time (hrs)	Normalized cesium breakthrough (c/c <sub>0</sub> ) <sup>a</sup>
0.0	0.000	0.0	0.000
16.7	0.002	8.3	0.003
33.3	0.005	10.0	0.004
50.0	0.039	13.3	0.009
66.7	0.121	16.7	0.019
83.3	0.245	25.0	0.070
100.0	0.389	33.3	0.160
116.7	0.523	41.7	0.300
133.3	0.631	50.0	0.400
146.0	0.694	58.3	0.510

<sup>a</sup> The inlet cesium feed concentration (i.e.,  $7.04 \times 10^{-6}$  M) was used to normalize the breakthrough data.

Table H-14. Key column parameters for CST IE-911 packed pilot-scale two-column carousel facility using MVST W-29 waste streams taken by Walker, Jr., et al. (1998) at 25 C.<sup>a</sup>

Parameter	ORNL-CsRD-Run2	ORNL-CsRD-Run3	ORNL-CsRD-Run4a	ORNL-CsRD-Run4b
Column diameter (cm)	30.6	1.50	1.50	1.50
Column length (cm)	51.672	5.659	5.659	5.659
CST (Lot #)	-38b (96-01)	-38b (96-01)	-38b (96-01)	-38b (96-01)
Average superficial velocity (cm/min)	2.584	5.167	5.167	5.167
Average temperature (C)	25	25	25	25
Avg. Cs feed concentration (M)	1.35E-05	1.35E-05	5.10E-06	5.10E-06
Column volume (L)	38.0	38.0	38.0	38.0
Bed density (g/ml)	1.0	1.0	1.0	1.0
Flowrate Q (ml/min) [CV/hr]	1900.0 [3.0]	3800.0 [6.0]	3800.0 [6.0]	3800.0 [6.0]

<sup>a</sup> The MVST W-29 sample feed compositions were not sufficiently defined.

Table H-15. Cycle 1 ORNL-CsRD-Run2 cesium breakthrough data for CST IE-911 and MVST W-29 waste streams taken by Walker, Jr., et al. (1998) at ~25 C.

<b>ORNL-CsRD-Run2 (fresh lead column) (CST lot –38b)</b>	
<b>Time (hrs)</b>	<b>Normalized cesium breakthrough (c/c<sub>o</sub>)<sup>a</sup></b>
8.3	0.014
16.7	0.007
25.0	0.014
33.3	0.024
41.7	0.043
50.0	0.085
58.3	0.113
66.7	0.151
75.0	0.193
83.3	0.231
91.7	0.113
100.0	0.302
108.3	0.293
116.7	0.354
125.0	0.425
133.3	0.425
141.7	0.472
150.0	0.467
158.3	0.509

<sup>a</sup> The inlet cesium feed concentration (i.e.,  $1.35 \times 10^{-5}$  M) was used to normalize the breakthrough data.

Table H-16. Cycle 1 ORNL-CsRD-Run3 cesium breakthrough data for CST IE-911 and MVST W-29 waste streams taken by Walker, Jr., et al. (1998) at ~25 C.

ORNL-CsRD-Run3 (fresh lead column) (CST lot –38b)		ORNL-CsRD-Run3 (fresh lag column) (CST lot –38b)	
Time (hrs)	Normalized cesium breakthrough (c/c <sub>0</sub> ) <sup>a</sup>	Time (hrs)	Normalized cesium breakthrough (c/c <sub>0</sub> ) <sup>a</sup>
8.3	0.038	8.3	0.003
16.7	0.114	16.7	0.006
25.0	0.162	25.0	0.011
33.3	0.210	33.3	0.020
41.7	0.286	41.7	0.034
50.0	0.371	50.0	0.057
58.3	0.333	58.3	0.109
66.7	0.324	66.7	0.097
75.0	0.429	75.0	0.111
83.3	0.424	83.3	0.143
91.7	0.562	91.7	0.177
100.0	0.543	100.0	0.211
108.3	0.591	108.3	0.229
116.7	0.657	116.7	0.269
125.0	0.705	125.0	0.383
133.3	0.700	133.3	0.360
141.7	0.752	141.7	0.371
150.0	0.743	150.0	0.394
158.3	0.781	158.3	0.469
166.7	0.733	166.7	0.451
172.0	0.791	172.0	0.486

<sup>a</sup> The inlet cesium feed concentration (i.e.,  $1.35 \times 10^{-5}$  M) was used to normalize the breakthrough data.

Table H-17. Cycle 1 ORNL-CsRD-Run4 cesium breakthrough data for CST IE-911 and MVST W-29 waste streams taken by Walker, Jr., et al. (1998) at ~25 C.

ORNL-CsRD-Run4a (fresh lead column) (CST lot –38b)		ORNL-CsRD-Run4a (fresh lag column) (CST lot –38b)	
Time (hrs)	Normalized cesium breakthrough (c/c <sub>0</sub> ) <sup>a</sup>	Time (hrs)	Normalized cesium breakthrough (c/c <sub>0</sub> ) <sup>a</sup>
8.3	0.014	8.3	0.002
16.7	0.031	16.7	0.002
25.0	0.071	25.0	0.004
33.3	0.120	33.3	0.004
41.7	0.186	41.7	0.011
50.0	0.249	50.0	0.017
58.3	0.291	58.3	0.031
66.7	0.331	66.7	0.045
75.0	0.411	75.0	0.069
83.3	0.434	83.3	0.086
91.7	0.474	91.7	0.116
100.0	0.514	100.0	0.142
108.3	0.534	108.3	0.174
116.7	0.554	116.7	0.193
124.3	0.555	124.3	0.205

<sup>a</sup> The inlet cesium feed concentration (i.e.,  $5.10 \times 10^{-6}$  M) was used to normalize the breakthrough data.

Table H-18. Cycle 2 ORNL-CsRD-Run4 cesium breakthrough data for CST IE-911 and MVST W-29 waste streams taken by Walker, Jr., et al. (1998) at ~25 C.

ORNL-CsRD-Run4b (lead column now cycle 1 lag column) (CST lot –38b)		ORNL-CsRD-Run4b (fresh lag column) (CST lot –38b)	
Time (hrs)	Normalized cesium breakthrough (c/c <sub>0</sub> ) <sup>a</sup>	Time (hrs)	Normalized cesium breakthrough (c/c <sub>0</sub> ) <sup>a</sup>
8.3	0.014	8.3	0.002
16.7	0.031	16.7	0.002
25.0	0.071	25.0	0.004
33.3	0.120	33.3	0.004
41.7	0.186	41.7	0.011
50.0	0.249	50.0	0.017
58.3	0.291	58.3	0.031
66.7	0.331	66.7	0.045
75.0	0.411	75.0	0.069
83.3	0.434	83.3	0.086
91.7	0.474	91.7	0.116
100.0	0.514	100.0	0.142
108.3	0.534	108.3	0.174
116.7	0.554	116.7	0.193
124.3	0.555	124.3	0.205

<sup>a</sup> The inlet cesium feed concentration (i.e.,  $5.10 \times 10^{-6}$  M) was used to normalize the breakthrough data.



**VERSE Input for SRS-Tank44-Test1a**


---

```

[Lab-Scale] Simulation of Cs removal on Baseline CST material singled column
1 component (Cs) isotherm (Na 5.4 M) (SRS Tank44 supernatant: Doug Walker Test1)
1, 50, 3, 6      ncomp, nelem, ncol-bed, ncol-part
FCWNA           isotherm,axial-disp,film-coef,surf-diff,BC-col  FCUNA
NNNNN          input-only,perfusable,feed-equil,datafile.yio
MM             comp-conc units
10.0, 1.50, 9.4, 3.534  Length(cm),Diam(cm),Q-flow(ml/min),CSTR-vol(ml)
172.0, 0.50, 0.240, 0.0  part-rad(um), bed-void, part-void, sorb-cap()
0.0            initial concentrations (M)
S             COMMAND - conc step change
1, 0.0, 3.51d-4, 1, 0.0  spec id, time(min), conc(M), freq, dt(min)
V             COMMAND - viscosity/density change
0.0260, 1.2015  fluid viscosity(posie), density(g/cm^3)
h            COMMAND - effluent history dump
1, 1.0, 1.0, 0.25, 0.1  unit op#, ptscale(1-4) filtering
h            COMMAND - effluent history dump
2, 1.0, 1.0, 0.25, 0.1  unit op#, ptscale(1-4) filtering
D
-1, 2000.0, 1, 0.0
D
-1, 4000.0, 1, 0.0
D
-1, 5600.0, 1, 0.0
-
8000.0, 1.0      end of commands
1.0d-7, 1.0d-4  end time(min), max dt in B.V.s
-              abs-tol, rel-tol
1.0d0          non-negative conc constraint
1.28d-4        size exclusion factor
5.963d-4       part-pore diffusivities(cm^2/min) 50% of free values 2.486d-5
0.58           Brownian diffusivities(cm^2/min)
1.0            Freundlich/Langmuir Hybrid a      (moles/L B.V.) rhob=1.0
1.0            Freundlich/Langmuir Hybrid b      (1/M)   Batch specific isotherm
1.0            Freundlich/Langmuir Hybrid Ma     (-)     ccap=0.580
1.0            Freundlich/Langmuir Hybrid Mb     (-)
2.0486d-4      Freundlich/Langmuir Hybrid beta   (-) "eff" isotherm Na = 5.6 M
-----

```

---

**VERSE Input for SRS-Tank44-Test1b**


---

```

[Lab-Scale] Simulation of Cs removal on Baseline CST material two columns (columns 1 +2)
1 component (Cs) isotherm (Na 5.4 M) (SRS Tank44 supernatant: Doug Walker Test1)
1, 50, 3, 6      ncomp, nelem, ncol-bed, ncol-part
FCWNA           isotherm,axial-disp,film-coef,surf-diff,BC-col  FCUNA
NNNNN          input-only,perfusable,feed-equil,datafile.yio
MM             comp-conc units
85.0, 1.50, 9.4, 3.534  Length(cm),Diam(cm),Q-flow(ml/min),CSTR-vol(ml)
172.0, 0.50, 0.240, 0.0  part-rad(um), bed-void, part-void, sorb-cap()
0.0            initial concentrations (M)
S             COMMAND - conc step change
1, 0.0, 3.51d-4, 1, 0.0  spec id, time(min), conc(M), freq, dt(min)
V             COMMAND - viscosity/density change
0.0260, 1.2015  fluid viscosity(posie), density(g/cm^3)
h            COMMAND - effluent history dump
1, 1.0, 1.0, 0.25, 0.1  unit op#, ptscale(1-4) filtering
h            COMMAND - effluent history dump
2, 1.0, 1.0, 0.25, 0.1  unit op#, ptscale(1-4) filtering
D
-1, 2000.0, 1, 0.0
D
-1, 4000.0, 1, 0.0
D
-1, 5600.0, 1, 0.0
-
8000.0, 1.0      end of commands
1.0d-7, 1.0d-4  end time(min), max dt in B.V.s
-              abs-tol, rel-tol
1.0d0          non-negative conc constraint
1.28d-4        size exclusion factor
part-pore diffusivities(cm^2/min) 50% of free values 2.486d-5

```

---

---

5.963d-4	Brownian diffusivities (cm <sup>2</sup> /min)
0.3944	Freundlich/Langmuir Hybrid a (moles/L B.V.) rhob=1.0
1.0	Freundlich/Langmuir Hybrid b (1/M) Batch specific isotherm
1.0	Freundlich/Langmuir Hybrid Ma (-) ccap=0.580
1.0	Freundlich/Langmuir Hybrid Mb (-)
2.0486d-4	Freundlich/Langmuir Hybrid beta (-) "eff" isotherm Na = 5.6 M

---

## VERSE Input for SRS-Avg-Test1

---

```
[Lab-Scale] Simulation of Cs removal on Baseline CST material lead column
1 component (Cs) isotherm (Na 5.6 M) (SRS Avg simulant: Bill Wilmart Test1)
1, 50, 3, 6      ncomp, nelelem, ncol-bed, ncol-part
FCWNA           isotherm, axial-disp, film-coef, surf-diff, BC-col  FCUNA
NNNNN          input-only, perfusable, feed-equil, datafile.yio
MM             comp-conc units
10.0, 1.50, 9.7193, 3.534  Length (cm), Diam (cm), Q-flow (ml/min), CSTR-vol (ml)
172.0, 0.50, 0.240, 0.0  part-rad (um), bed-void, part-void, sorb-cap ()
0.0            initial concentrations (M)
S             COMMAND - conc step change
1, 0.0, 1.30d-4, 1, 0.0  spec id, time (min), conc (M), freq, dt (min)
V             COMMAND - viscosity/density change
0.0278, 1.253  fluid viscosity (poise), density (g/cm^3)
h             COMMAND - effluent history dump
1, 1.0, 1.0, 0.25, 0.1  unit op#, ptscale (1-4) filtering
h             COMMAND - effluent history dump
2, 1.0, 1.0, 0.25, 0.1  unit op#, ptscale (1-4) filtering
D
-1, 2000.0, 1, 0.0
D
-1, 4000.0, 1, 0.0
D
-1, 5600.0, 1, 0.0
-
end of commands
8500.0, 1.0     end time (min), max dt in B.V.s
1.0d-7, 1.0d-4  abs-tol, rel-tol
-              non-negative conc constraint
1.0d0          size exclusion factor
4.972d-5       part-pore diffusivities (cm^2/min) 50% of free values 2.486d-5
4.972d-4       Brownian diffusivities (cm^2/min)
0.58           Freundlich/Langmuir Hybrid a (moles/L B.V.) rhob=1.0
1.0            Freundlich/Langmuir Hybrid b (1/M) Batch specific isotherm
1.0            Freundlich/Langmuir Hybrid Ma (-) ccap=0.580
1.0            Freundlich/Langmuir Hybrid Mb (-)
2.4145d-4      Freundlich/Langmuir Hybrid beta (-) "eff" isotherm Na = 5.6 M
-----
```

---

## VERSE Input for SRS-Avg-Test2 (single-component approach)

---

```
[Lab-Scale] Simulation of Cs removal on Baseline CST material lead column
1 component (Cs) isotherm (Na 5.6 M) (SRS Avg simulant: Bill Wilmart Test2)
1, 50, 3, 6      ncomp, nelelem, ncol-bed, ncol-part
FCWNA           isotherm, axial-disp, film-coef, surf-diff, BC-col  FCUNA
NNNNN          input-only, perfusable, feed-equil, datafile.yio
MM             comp-conc units
10.0, 1.50, 12.37, 3.534  Length (cm), Diam (cm), Q-flow (ml/min), CSTR-vol (ml)
172.0, 0.50, 0.240, 0.0  part-rad (um), bed-void, part-void, sorb-cap ()
0.0            initial concentrations (M)
S             COMMAND - conc step change
1, 0.0, 1.24d-4, 1, 0.0  spec id, time (min), conc (M), freq, dt (min)
V             COMMAND - viscosity/density change
0.0278, 1.253  fluid viscosity (poise), density (g/cm^3)
h             COMMAND - effluent history dump
1, 1.0, 1.0, 0.25, 0.1  unit op#, ptscale (1-4) filtering
h             COMMAND - effluent history dump
2, 1.0, 1.0, 0.25, 0.1  unit op#, ptscale (1-4) filtering
D
-1, 2000.0, 1, 0.0
D
-1, 4000.0, 1, 0.0
D
```

---

```

-1, 5600.0, 1, 0.0
-
8500.0, 1.0
1.0d-7, 1.0d-4
-
1.0d0
4.972d-5
4.972d-4
0.58
1.0
1.0
1.0
2.4145d-4
end of commands
end time(min), max dt in B.V.s
abs-tol, rel-tol
non-negative conc constraint
size exclusion factor
part-pore diffusivities(cm^2/min) 50% of free values 2.486d-5
Brownian diffusivities(cm^2/min)
Freundlich/Langmuir Hybrid a (moles/L B.V.) rhob=1.0
Freundlich/Langmuir Hybrid b (1/M) Batch specific isotherm
Freundlich/Langmuir Hybrid Ma (-) ccap=0.580
Freundlich/Langmuir Hybrid Mb (-)
Freundlich/Langmuir Hybrid beta (-) "eff" isotherm Na = 5.6 M
-----

```

## VERSE Input for SRS-Avg-Test2 (ternary-component approach)

```

[Lab-Scale] Simulation of Cs removal on Baseline CST material lead column
3 component (Cs,K,Na) isotherms (Na 5.6 M) (SRS Avg simulant: Bill Wilmart Test2)
3, 50, 3, 6
FCWNA
NNNNN
MM
10.0, 1.50, 12.37, 3.534
172.0, 0.50, 0.240, 0.0
0.0 0.0 0.25
S
1, 0.0, 1.24d-4, 1, 0.0
S
2, 0.0, 1.50d-2, 1, 0.0
S
3, 0.0, 5.60d-0, 1, 0.0
V
0.0278, 1.253
h
1, 1.0, 1.0, 0.25, 0.1
h
2, 1.0, 1.0, 0.25, 0.1
D
-1, 2000.0, 1, 0.0
D
-1, 4000.0, 1, 0.0
D
-1, 5600.0, 1, 0.0
-
8500.0, 1.0
1.0d-7, 1.0d-4
-
1.0d0 , 1.0d0 , 1.0d0
9.944d-5, 9.644d-5, 7.516d-5
4.972d-4, 4.822d-4, 3.758d-4
0.3944 , 2.8172d-4, 1.6250d-5
1.0 , 7.1429d-4, 4.1203d-5
1.0 , 1.0 , 1.0
1.0 , 1.0 , 1.0
0.0 , 0.0 , 0.0
ncomp, nelem, ncol-bed, ncol-part
isotherm,axial-disp,film-coef,surf-diff,BC-col FCUNA
input-only,perfusable,feed-equil,datafile.yio
comp-conc units
Length(cm),Diam(cm),Q-flow(ml/min),CSTR-vol(ml)
part-rad(um), bed-void, part-void, sorb-cap()
initial concentrations (M)
COMMAND - conc step change for Cs
spec id, time(min), conc(M), freq, dt(min)
COMMAND - conc step change for K
spec id, time(min), conc(M), freq, dt(min)
COMMAND - conc step change for Na
spec id, time(min), conc(M), freq, dt(min)
COMMAND - viscosity/density change
fluid viscosity(posie), density(g/cm^3)
COMMAND - effluent history dump
unit op#, ptscale(1-4) filtering
COMMAND - effluent history dump
unit op#, ptscale(1-4) filtering
end of commands
end time(min), max dt in B.V.s
abs-tol, rel-tol
non-negative conc constraint
size exclusion factor
part-pore diffusivities(cm^2/min) 20% of free values 2.486d-5
Brownian diffusivities(cm^2/min)
Freundlich/Langmuir Hybrid a (moles/L B.V.) rhob=1.0
Freundlich/Langmuir Hybrid b (1/M) Batch specific isotherm
Freundlich/Langmuir Hybrid Ma (-) ccap=0.580, df=0.68
Freundlich/Langmuir Hybrid Mb (-)
Freundlich/Langmuir Hybrid beta (-) "eff" isotherm Na = 5.6 M
-----

```

## VERSE Input for SRS-Avg-Test3

```

[Lab-Scale] Simulation of Cs removal on Baseline CST material lead column
1 component (Cs) isotherm (Na 5.6 M) (SRS Avg simulant: Bill Wilmart Test3)
1, 50, 3, 6
FCWNA
NNNNN
MM
10.0, 1.50, 7.2453, 3.534
172.0, 0.50, 0.240, 0.0
0.0
S
1, 0.0, 1.43d-4, 1, 0.0
ncomp, nelem, ncol-bed, ncol-part
isotherm,axial-disp,film-coef,surf-diff,BC-col FCUNA
input-only,perfusable,feed-equil,datafile.yio
comp-conc units
Length(cm),Diam(cm),Q-flow(ml/min),CSTR-vol(ml)
part-rad(um), bed-void, part-void, sorb-cap()
initial concentrations (M)
COMMAND - conc step change
spec id, time(min), conc(M), freq, dt(min)

```

---

```

V          COMMAND - viscosity/density change
0.0278, 1.253 fluid viscosity(posie), density(g/cm^3)
h          COMMAND - effluent history dump
1, 1.0, 1.0, 0.25, 0.1 unit op#, ptscale(1-4) filtering
h          COMMAND - effluent history dump
2, 1.0, 1.0, 0.25, 0.1 unit op#, ptscale(1-4) filtering
D
-1, 2000.0, 1, 0.0
D
-1, 4000.0, 1, 0.0
D
-1, 5600.0, 1, 0.0
-
end of commands
12000.0, 1.0 end time(min), max dt in B.V.s
1.0d-7, 1.0d-4 abs-tol, rel-tol
- non-negative conc constraint
1.0d0 size exclusion factor
1.28d-4 part-pore diffusivities(cm^2/min) 50% of free values 2.486d-5
4.972d-4 Brownian diffusivities(cm^2/min)
0.58 Freundlich/Langmuir Hybrid a (moles/L B.V.) rhob=1.0
1.0 Freundlich/Langmuir Hybrid b (1/M) Batch specific isotherm
1.0 Freundlich/Langmuir Hybrid Ma (-) ccap=0.580
1.0 Freundlich/Langmuir Hybrid Mb (-)
2.4145d-4 Freundlich/Langmuir Hybrid beta (-) "eff" isotherm Na = 5.6 M
-----

```

---

## VERSE Input for SRS-Avg-Test4

---

```

[Lab-Scale] Simulation of Cs removal on Baseline CST material lead column
1 component (Cs) isotherm (Na 5.6 M) (SRS Avg simulant: Bill Wilmart Test3)
1, 50, 3, 6 ncomp, nelem, ncol-bed, ncol-part
FCWNA isotherm,axial-disp,film-coef,surf-diff,BC-col FCUNA
NNNNN input-only,perfusable,feed-equil,datafile.yio
MM comp-conc units
10.0, 2.50, 20.12583, 3.534 Length(cm),Diam(cm),Q-flow(ml/min),CSTR-vol(ml)
172.0, 0.50, 0.240, 0.0 part-rad(um), bed-void, part-void, sorb-cap()
0.0 initial concentrations (M)
S COMMAND - conc step change
1, 0.0, 1.366d-4, 1, 0.0 spec id, time(min), conc(M), freq, dt(min)
V COMMAND - viscosity/density change
0.0278, 1.253 fluid viscosity(posie), density(g/cm^3)
h COMMAND - effluent history dump
1, 1.0, 1.0, 0.25, 0.1 unit op#, ptscale(1-4) filtering
h COMMAND - effluent history dump
2, 1.0, 1.0, 0.25, 0.1 unit op#, ptscale(1-4) filtering
D
-1, 2000.0, 1, 0.0
D
-1, 4000.0, 1, 0.0
D
-1, 5600.0, 1, 0.0
-
end of commands
11000.0, 1.0 end time(min), max dt in B.V.s
1.0d-7, 1.0d-4 abs-tol, rel-tol
- non-negative conc constraint
1.0d0 size exclusion factor
1.28d-4 part-pore diffusivities(cm^2/min) 50% of free values 2.486d-5
4.972d-4 Brownian diffusivities(cm^2/min)
0.58 Freundlich/Langmuir Hybrid a (moles/L B.V.) rhob=1.0
1.0 Freundlich/Langmuir Hybrid b (1/M) Batch specific isotherm
1.0 Freundlich/Langmuir Hybrid Ma (-) ccap=0.580
1.0 Freundlich/Langmuir Hybrid Mb (-)
2.4145d-4 Freundlich/Langmuir Hybrid beta (-) "eff" isotherm Na = 5.6 M
-----

```

---

## VERSE Input for SRS-Avg-Test5

---

```

[Lab-Scale] Simulation of Cs removal on Baseline CST material lead column
1 component (Cs) isotherm (Na 5.6 M) (SRS Avg simulant: Doug Walker Test5 WSRC-TR-98-00344-r1)
1, 50, 3, 6 ncomp, nelem, ncol-bed, ncol-part
FCWNA isotherm,axial-disp,film-coef,surf-diff,BC-col FCUNA

```

---

---

```

NNNNN      input-only,perfusable,feed-equil,datafile.yio
MM          comp-conc units
10.0, 1.50, 0.47, 3.534      Length(cm),Diam(cm),Q-flow(ml/min),CSTR-vol(ml)
172.0, 0.50, 0.240, 0.0     part-rad(um), bed-void, part-void, sorb-cap()
0.0          initial concentrations (M)
S           COMMAND - conc step change
1, 0.0, 1.40d-4, 1, 0.0     spec id, time(min), conc(M), freq, dt(min)
V           COMMAND - viscosity/density change
0.0278, 1.253              fluid viscosity(posie), density(g/cm^3)
h           COMMAND - effluent history dump
1, 1.0, 1.0, 0.25, 0.1     unit op#, ptscale(1-4) filtering
h           COMMAND - effluent history dump
2, 1.0, 1.0, 0.25, 0.1     unit op#, ptscale(1-4) filtering
D
-1, 2000.0, 1, 0.0
D
-1, 4000.0, 1, 0.0
D
-1, 5600.0, 1, 0.0
-
end of commands
35000.0, 1.0               end time(min), max dt in B.V.s
1.0d-7, 1.0d-4            abs-tol, rel-tol
-                           non-negative conc constraint
1.0d0                     size exclusion factor
4.972d-5                  part-pore diffusivities(cm^2/min) 50% of free values 2.486d-5
4.972d-4                  Brownian diffusivities(cm^2/min)
0.3944                   Freundlich/Langmuir Hybrid a      (moles/L B.V.) rhob=1.0
1.0                       Freundlich/Langmuir Hybrid b      (1/M)   Batch specific isotherm
1.0                       Freundlich/Langmuir Hybrid Ma      (-)     ccap=0.580
1.0                       Freundlich/Langmuir Hybrid Mb      (-)
2.4145d-4                 Freundlich/Langmuir Hybrid beta  (-) "eff" isotherm Na = 5.6 M
-----

```

---

## VERSE Input for SRS-Avg-Test6

---

```

[Lab-Scale] Simulation of Cs removal on Baseline CST material lead column
1 component (Cs) isotherm (Na 5.6 M) (SRS Avg simulant: Doug Walker Test6 WSRC-TR-98-00344-r1)
1, 50, 3, 6              ncomp, nelem, ncol-bed, ncol-part
FCWNA                    isotherm,axial-disp,film-coef,surf-diff,BC-col  FCUNA
NNNNN                    input-only,perfusable,feed-equil,datafile.yio
MM                        comp-conc units
10.0, 1.50, 1.73, 3.534   Length(cm),Diam(cm),Q-flow(ml/min),CSTR-vol(ml)
172.0, 0.50, 0.240, 0.0   part-rad(um), bed-void, part-void, sorb-cap()
0.0                       initial concentrations (M)
S                           COMMAND - conc step change
1, 0.0, 1.40d-4, 1, 0.0   spec id, time(min), conc(M), freq, dt(min)
V                           COMMAND - viscosity/density change
0.0278, 1.253             fluid viscosity(posie), density(g/cm^3)
h                           COMMAND - effluent history dump
1, 1.0, 1.0, 0.25, 0.1   unit op#, ptscale(1-4) filtering
h                           COMMAND - effluent history dump
2, 1.0, 1.0, 0.25, 0.1   unit op#, ptscale(1-4) filtering
D
-1, 2000.0, 1, 0.0
D
-1, 4000.0, 1, 0.0
D
-1, 5600.0, 1, 0.0
-
end of commands
35000.0, 1.0               end time(min), max dt in B.V.s
1.0d-7, 1.0d-4            abs-tol, rel-tol
-                           non-negative conc constraint
1.0d0                     size exclusion factor
1.28d-4                   part-pore diffusivities(cm^2/min) 50% of free values 2.486d-5
4.972d-4                  Brownian diffusivities(cm^2/min)
0.58                      Freundlich/Langmuir Hybrid a      (moles/L B.V.) rhob=1.0
1.0                       Freundlich/Langmuir Hybrid b      (1/M)   Batch specific isotherm
1.0                       Freundlich/Langmuir Hybrid Ma      (-)     ccap=0.580
1.0                       Freundlich/Langmuir Hybrid Mb      (-)
2.4145d-4                 Freundlich/Langmuir Hybrid beta  (-) "eff" isotherm Na = 5.6 M
-----

```

---

**VERSE Input for SRS-Avg-Test7**


---

```

[Lab-Scale] Simulation of Cs removal on Baseline CST material lead column
1 component (Cs) isotherm (Na 5.6 M) (SRS Avg simulant: Doug Walker Test7 WSRC-TR-98-00344-r1)
1, 50, 3, 6      ncomp, nelem, ncol-bed, ncol-part
FCWNA           isotherm,axial-disp,film-coef,surf-diff,BC-col  FCUNA
NNNNN          input-only,perfusable,feed-equil,datafile.yio
MM             comp-conc units
11.0, 1.43, 6.53, 3.534  Length(cm),Diam(cm),Q-flow(ml/min),CSTR-vol(ml)
172.0, 0.50, 0.240, 0.0  part-rad(um), bed-void, part-void, sorb-cap()
0.0            initial concentrations (M)
S             COMMAND - conc step change
1, 0.0, 1.40d-4, 1, 0.0  spec id, time(min), conc(M), freq, dt(min)
V             COMMAND - viscosity/density change
0.0278, 1.253      fluid viscosity(posie), density(g/cm^3)
h             COMMAND - effluent history dump
1, 1.0, 1.0, 0.25, 0.1  unit op#, ptscale(1-4) filtering
h             COMMAND - effluent history dump
2, 1.0, 1.0, 0.25, 0.1  unit op#, ptscale(1-4) filtering
D
-1, 2000.0, 1, 0.0
D
-1, 4000.0, 1, 0.0
D
-1, 5600.0, 1, 0.0
-
end of commands
10000.0, 1.0      end time(min), max dt in B.V.s
1.0d-7, 1.0d-4   abs-tol, rel-tol
-
non-negative conc constraint
1.0d0            size exclusion factor
4.972d-5         part-pore diffusivities(cm^2/min) 50% of free values 2.486d-5
4.972d-4         Brownian diffusivities(cm^2/min)
0.58            Freundlich/Langmuir Hybrid a      (moles/L B.V.) rhob=1.0
1.0             Freundlich/Langmuir Hybrid b      (1/M)   Batch specific isotherm
1.0             Freundlich/Langmuir Hybrid Ma     (-)     ccap=0.580
1.0             Freundlich/Langmuir Hybrid Mb     (-)
2.4145d-4       Freundlich/Langmuir Hybrid beta  (-) "eff" isotherm Na = 5.6 M
-----

```

---

**VERSE Input for SRS-High-OH-Test1a**


---

```

[Lab-Scale] Simulation of Cs removal on Baseline CST material lead column
1 component (Cs) isotherm (Na 5.6 M) (SRS High OH simulant: Doug Walker Test)
1, 50, 3, 6      ncomp, nelem, ncol-bed, ncol-part
FCWNA           isotherm,axial-disp,film-coef,surf-diff,BC-col  FCUNA
NNNNN          input-only,perfusable,feed-equil,datafile.yio
MM             comp-conc units
10.0, 1.50, 9.60, 3.534  Length(cm),Diam(cm),Q-flow(ml/min),CSTR-vol(ml)
172.0, 0.50, 0.240, 0.0  part-rad(um), bed-void, part-void, sorb-cap()
0.0            initial concentrations (M)
S             COMMAND - conc step change
1, 0.0, 3.70d-4, 1, 0.0  spec id, time(min), conc(M), freq, dt(min)
V             COMMAND - viscosity/density change
0.0310, 1.244      fluid viscosity(posie), density(g/cm^3)
h             COMMAND - effluent history dump
1, 1.0, 1.0, 0.25, 0.1  unit op#, ptscale(1-4) filtering
h             COMMAND - effluent history dump
2, 1.0, 1.0, 0.25, 0.1  unit op#, ptscale(1-4) filtering
D
-1, 2000.0, 1, 0.0
D
-1, 4500.0, 1, 0.0
-
end of commands
4500.0, 1.0      end time(min), max dt in B.V.s
1.0d-7, 1.0d-4   abs-tol, rel-tol
-
non-negative conc constraint
1.0d0            size exclusion factor
5.425d-5         part-pore diffusivities(cm^2/min) 50% of free values 2.486d-5
5.425d-4         Brownian diffusivities(cm^2/min)
0.58            Freundlich/Langmuir Hybrid a      (moles/L B.V.) rhob=1.0
1.0             Freundlich/Langmuir Hybrid b      (1/M)   Batch specific isotherm

```

---

---

```

1.0      Freundlich/Langmuir Hybrid Ma      (-)      ccap=0.580
1.0      Freundlich/Langmuir Hybrid Mb      (-)
2.0987E-04 Freundlich/Langmuir Hybrid beta (-) "eff" isotherm Na = 5.6 M
-----

```

---

## VERSE Input for SRS-High-OH-Test1b

---

```

[Lab-Scale] Simulation of Cs removal on Baseline CST material two columns (1+2)
1 component (Cs) isotherm (Na 5.6 M) (SRS High OH simulant: Doug Walker Test)
1, 50, 3, 6      ncomp, nelem, ncol-bed, ncol-part
FCWNA            isotherm,axial-disp,film-coef,surf-diff,BC-col FCUNA
NNNNN           input-only,perfusable,feed-equil,datafile.yio
MM              comp-conc units
85.0, 1.50, 9.60, 3.534 Length(cm),Diam(cm),Q-flow(ml/min),CSTR-vol(ml)
172.0, 0.50, 0.240, 0.0 part-rad(um), bed-void, part-void, sorb-cap()
0.0              initial concentrations (M)
S               COMMAND - conc step change
1, 0.0, 3.70d-4, 1, 0.0 spec id, time(min), conc(M), freq, dt(min)
V               COMMAND - viscosity/density change
0.0310, 1.244    fluid viscosity(posie), density(g/cm^3)
h               COMMAND - effluent history dump
1, 1.0, 1.0, 0.25, 0.1 unit op#, ptscale(1-4) filtering
h               COMMAND - effluent history dump
2, 1.0, 1.0, 0.25, 0.1 unit op#, ptscale(1-4) filtering
D
-1, 2000.0, 1, 0.0
D
-1, 4500.0, 1, 0.0
-               end of commands
4500.0, 1.0      end time(min), max dt in B.V.s
1.0d-7, 1.0d-4  abs-tol, rel-tol
-               non-negative conc constraint
1.0d0           size exclusion factor
1.28d-4         part-pore diffusivities(cm^2/min) 50% of free values 2.486d-5
5.425d-4        Brownian diffusivities(cm^2/min)
0.58            Freundlich/Langmuir Hybrid a      (moles/L B.V.) rhob=1.0
1.0             Freundlich/Langmuir Hybrid b      (1/M) Batch specific isotherm
1.0             Freundlich/Langmuir Hybrid Ma      (-)      ccap=0.580
1.0             Freundlich/Langmuir Hybrid Mb      (-)
2.0987E-04      Freundlich/Langmuir Hybrid beta (-) "eff" isotherm Na = 5.6 M
-----

```

---

## VERSE Input for PNNL-AW101-Test1

---

```

[Lab-Scale] Simulation of Cs removal on CST (96-01 engr) material lead column
1 component (Cs) isotherm (Na 5.64 M) (Hendrickson AW-101 sample: Hendrickson reports)
1, 50, 3, 6      ncomp, nelem, ncol-bed, ncol-part
FCWNA            isotherm,axial-disp,film-coef,surf-diff,BC-col FCUNA
NNNNN           input-only,perfusable,feed-equil,datafile.yio
MM              comp-conc units
10.0, 1.0, 0.83, 1.6 Length(cm),Diam(cm),Q-flow(ml/min),CSTR-vol(ml)
172.0, 0.50, 0.24, 0.0 part-rad(um), bed-void, part-void, sorb-cap()
0.0              initial concentrations (M)
S               COMMAND - conc step change
1, 0.0, 7.26d-5, 1, 0.0 spec id, time(min), conc(M), freq, dt(min)
V               COMMAND - viscosity/density change
0.0294, 1.287    fluid viscosity(posie), density(g/cm^3)
h               COMMAND - effluent history dump
1, 1.0, 1.0, 0.25, 0.1 unit op#, ptscale(1-4) filtering
h               COMMAND - effluent history dump
2, 1.0, 1.0, 0.25, 0.1 unit op#, ptscale(1-4) filtering
D
-1, 2000.0, 1, 0.0
D
-1, 4000.0, 1, 0.0
D
-1, 5600.0, 1, 0.0
-               end of commands
7700.0, 1.0      end time(min), max dt in B.V.s
1.0d-7, 1.0d-4  abs-tol, rel-tol
-               non-negative conc constraint

```

---

---

```

1.0d0                size exclusion factor
1.264d-4            part-pore diffusivities(cm^2/min) 50% of free values 1.264d-4
4.863d-4            Brownian diffusivities(cm^2/min)
0.58                Freundlich/Langmuir Hybrid a      (moles/L B.V.) rhob=1.0
1.0                Freundlich/Langmuir Hybrid b      (1/M)   Batch specific isotherm
1.0                Freundlich/Langmuir Hybrid Ma     (-)     ccap=0.580
1.0                Freundlich/Langmuir Hybrid Mb     (-)     rhob=1.15; df=0.68
4.7414d-4          Freundlich/Langmuir Hybrid beta  (-) "eff" isotherm Na = 4.935 M
-----

```

---

## VERSE Input for ORNL-W27-Test1

---

```

[Lab-Scale] Simulation of Cs removal on CST (-38b) material lead column
1 component (Cs) isotherm (Na 4.935 M) (ORNL W27 simulant: Lee et al., 1997)
1, 50, 3, 6                ncomp, nelem, ncol-bed, ncol-part
FCWNA                      isotherm,axial-disp,film-coef,surf-diff,BC-col  FCUNA
NNNNN                     input-only,perfusable,feed-equil,datafile.yio
MM                          comp-conc units
5.6588, 1.50, 0.5, 2.0    Length(cm),Diam(cm),Q-flow(ml/min),CSTR-vol(ml)
172.0, 0.50, 0.240, 0.0  part-rad(um), bed-void, part-void, sorb-cap()
0.0                        initial concentrations (M)
S                          COMMAND - conc step change
1, 0.0, 7.04d-6, 1, 0.0  spec id, time(min), conc(M), freq, dt(min)
V                          COMMAND - viscosity/density change
0.0278, 1.253            fluid viscosity(posie), density(g/cm^3)
h                          COMMAND - effluent history dump
1, 1.0, 1.0, 0.25, 0.1  unit op#, ptscale(1-4) filtering
h                          COMMAND - effluent history dump
2, 1.0, 1.0, 0.25, 0.1  unit op#, ptscale(1-4) filtering
D
-1, 2000.0, 1, 0.0
D
-1, 4000.0, 1, 0.0
D
-1, 5600.0, 1, 0.0
-
end of commands
9000.0, 1.0              end time(min), max dt in B.V.s
1.0d-7, 1.0d-4          abs-tol, rel-tol
-
non-negative conc constraint
1.0d0                    size exclusion factor
2.48d-4                  part-pore diffusivities(cm^2/min) 50% of free values 2.486d-5
4.062d-4                  Brownian diffusivities(cm^2/min)
0.45356                  Freundlich/Langmuir Hybrid a      (moles/L B.V.) rhob=1.0
1.0                      Freundlich/Langmuir Hybrid b      (1/M)   Batch specific isotherm
1.0                      Freundlich/Langmuir Hybrid Ma     (-)     ccap=0.580
1.0                      Freundlich/Langmuir Hybrid Mb     (-)     rhob=1.15; df=0.68
9.3232d-4                Freundlich/Langmuir Hybrid beta  (-) "eff" isotherm Na = 4.935 M
-----

```

---

## VERSE Input for ORNL-W27-Test2

---

```

[Lab-Scale] Simulation of Cs removal on CST (-38b) material lead column
1 component (Cs) isotherm (Na 4.935 M) (ORNL W27 simulant: Lee et al., 1997)
1, 50, 3, 6                ncomp, nelem, ncol-bed, ncol-part
FCWNA                      isotherm,axial-disp,film-coef,surf-diff,BC-col  FCUNA
NNNNN                     input-only,perfusable,feed-equil,datafile.yio
MM                          comp-conc units
5.6588, 1.50, 1.0, 2.0    Length(cm),Diam(cm),Q-flow(ml/min),CSTR-vol(ml)
172.0, 0.50, 0.240, 0.0  part-rad(um), bed-void, part-void, sorb-cap()
0.0                        initial concentrations (M)
S                          COMMAND - conc step change
1, 0.0, 7.04d-6, 1, 0.0  spec id, time(min), conc(M), freq, dt(min)
V                          COMMAND - viscosity/density change
0.0278, 1.253            fluid viscosity(posie), density(g/cm^3)
h                          COMMAND - effluent history dump
1, 1.0, 1.0, 0.25, 0.1  unit op#, ptscale(1-4) filtering
h                          COMMAND - effluent history dump
2, 1.0, 1.0, 0.25, 0.1  unit op#, ptscale(1-4) filtering
D
-1, 2000.0, 1, 0.0
D

```

---



```

-1, 4000.0, 1, 0.0
D
-1, 5600.0, 1, 0.0
-
end of commands
9000.0, 1.0
end time(min), max dt in B.V.s
1.0d-7, 1.0d-4
abs-tol, rel-tol
-
non-negative conc constraint
1.0d0
size exclusion factor
2.48d-4
part-pore diffusivities(cm^2/min) 50% of free values 2.486d-5
4.062d-4
Brownian diffusivities(cm^2/min)
0.45356
Freundlich/Langmuir Hybrid a (moles/L B.V.) rhob=1.0
1.0
Freundlich/Langmuir Hybrid b (1/M) Batch specific isotherm
1.0
Freundlich/Langmuir Hybrid Ma (-) ccap=0.580
1.0
Freundlich/Langmuir Hybrid Mb (-) rhob=1.15; df=0.68
9.3232d-4
Freundlich/Langmuir Hybrid beta (-) "eff" isotherm Na = 4.935 M
-----

```

## VERSE Input for ORNL-CsRD-Run2

```

[CsRD-Scale] Simulation of Cs removal on CST material (96-01) single column
1 component (Cs) isotherm (feed point fit) (CsRD Run 2 avgerage waste supernatant: Walker Run 2)
1, 50, 3, 6
ncomp, nelem, ncol-bed, ncol-part
FCWNA
isotherm,axial-disp,film-coef,surf-diff,BC-col FCUNA
NNNNN
input-only,perfusable,feed-equil,datafile.yio
MM
comp-conc units
51.672, 30.6, 1900.0, 7600.0
Length(cm),Diam(cm),Q-flow(ml/min),CSTR-vol(ml)
172.0, 0.50, 0.240, 0.0
part-rad(um), bed-void, part-void, sorb-cap()
0.0
initial concentrations (M)
S
COMMAND - conc step change
1, 0.0, 1.35d-5, 1, 0.0
spec id, time(min), conc(M), freq, dt(min)
V
COMMAND - viscosity/density change
0.0278, 1.253
fluid viscosity(posie), density(g/cm^3)
h
COMMAND - effluent history dump
1, 1.0, 1.0, 0.25, 0.1
unit op#, ptscale(1-4) filtering
h
COMMAND - effluent history dump
2, 1.0, 1.0, 0.25, 0.1
unit op#, ptscale(1-4) filtering
D
-1, 2000.0, 1, 0.0
D
-1, 4000.0, 1, 0.0
D
-1, 5600.0, 1, 0.0
-
end of commands
10000.0, 1.0
end time(min), max dt in B.V.s
1.0d-7, 1.0d-4
abs-tol, rel-tol
-
non-negative conc constraint
1.0d0
size exclusion factor
4.062d-5
part-pore diffusivities(cm^2/min)
4.062d-4
Brownian diffusivities(cm^2/min)
0.3944
Freundlich/Langmuir Hybrid a (moles/L B.V.) rhob=1.0
1.0
Freundlich/Langmuir Hybrid b (1/M) Batch specific isotherm
1.0
Freundlich/Langmuir Hybrid Ma (-) ccap=0.580
1.0
Freundlich/Langmuir Hybrid Mb (-)
6.50473d-4
Freundlich/Langmuir Hybrid beta (-) "eff" isotherm Na = unknown
-----

```

## VERSE Input for ORNL-CsRD-Run3

```

[CsRD-Scale] Simulation of Cs removal on CST material (96-01) two columns single cycle
1 component (Cs) isotherm (feed point fit) (CsRD Run 3 avgerage waste supernatant: Walker Run 3)
1, 100, 3, 6
ncomp, nelem, ncol-bed, ncol-part
FCWNA
isotherm,axial-disp,film-coef,surf-diff,BC-col FCUNA
NNNNN
input-only,perfusable,feed-equil,datafile.yio
MM
comp-conc units
103.344, 30.6, 3800.0, 7600.0
Length(cm),Diam(cm),Q-flow(ml/min),CSTR-vol(ml)
172.0, 0.50, 0.240, 0.0
part-rad(um), bed-void, part-void, sorb-cap()
0.0
initial concentrations (M)
S
COMMAND - conc step change
1, 0.0, 1.35d-5, 1, 0.0
spec id, time(min), conc(M), freq, dt(min)
V
COMMAND - viscosity/density change
0.0278, 1.253
fluid viscosity(posie), density(g/cm^3)

```

---

```

m          COMMAND - subcolumns
50, 100, 0, 1, 1.0d+8, 0.0, 50000.0 elem-shift,elem-watch,pp-watch,c-watch,c-thresh,t-e,t-ee
h          COMMAND - effluent history dump
0, 1.0, 1.0, 0.25, 0.1 unit op#, ptscale(1-4) filtering
h          COMMAND - effluent history dump
1, 1.0, 1.0, 0.25, 0.1 unit op#, ptscale(1-4) filtering
h          COMMAND - effluent history dump
2, 1.0, 1.0, 0.25, 0.1 unit op#, ptscale(1-4) filtering
h          COMMAND - effluent history dump
3, 1.0, 1.0, 0.25, 0.1 unit op#, ptscale(1-4) filtering
h          COMMAND - effluent history dump
4, 1.0, 1.0, 0.25, 0.1 unit op#, ptscale(1-4) filtering
D
-1, 2000.0, 1, 0.0
D
-1, 4000.0, 1, 0.0
D
-1, 5600.0, 1, 0.0
-
end of commands
12000.0, 1.0 end time(min), max dt in B.V.s
1.0d-7, 1.0d-4 abs-tol, rel-tol
- non-negative conc constraint
1.0d0 size exclusion factor
6.093d-5 part-pore diffusivities(cm^2/min)
4.062d-4 Brownian diffusivities(cm^2/min)
0.3944 Freundlich/Langmuir Hybrid a (moles/L B.V.) rhob=1.0
1.0 Freundlich/Langmuir Hybrid b (1/M) Batch specific isotherm
1.0 Freundlich/Langmuir Hybrid Ma (-) ccap=0.580
1.0 Freundlich/Langmuir Hybrid Mb (-)
6.50473d-4 Freundlich/Langmuir Hybrid beta (-) "eff" isotherm Na = unknown
-----

```

---

## VERSE Input for ORNL-CsRD-Run4a

---

```

[CsRD-Scale] Simulation of Cs removal on CST material (96-01) two columns first cycle
1 component (Cs) isotherm (feed point fit) (CsRD Run 4 average waste supernatant: Walker Run 4)
1, 100, 3, 6 ncomp, nelelem, ncol-bed, ncol-part
FCWNA isotherm,axial-disp,film-coef,surf-diff,BC-col FCUNA
NNNNY input-only,perfusable,feed-equil,datafile.yio
MM comp-conc units
103.344, 30.6, 3800.0, 7600.0 Length(cm),Diam(cm),Q-flow(ml/min),CSTR-vol(ml)
172.0, 0.50, 0.240, 0.0 part-rad(um), bed-void, part-void, sorb-cap()
0.0 initial concentrations (M)
S COMMAND - conc step change
1, 0.0, 5.10d-6, 1, 0.0 spec id, time(min), conc(M), freq, dt(min)
V COMMAND - viscosity/density change
0.0278, 1.253 fluid viscosity(posie), density(g/cm^3)
m COMMAND - subcolumns
50, 100, 0, 1, 1.0d+8, 0.0, 50000.0 elem-shift,elem-watch,pp-watch,c-watch,c-thresh,t-e,t-ee
h COMMAND - effluent history dump
0, 1.0, 1.0, 0.25, 0.1 unit op#, ptscale(1-4) filtering
h COMMAND - effluent history dump
1, 1.0, 1.0, 0.25, 0.1 unit op#, ptscale(1-4) filtering
h COMMAND - effluent history dump
2, 1.0, 1.0, 0.25, 0.1 unit op#, ptscale(1-4) filtering
h COMMAND - effluent history dump
3, 1.0, 1.0, 0.25, 0.1 unit op#, ptscale(1-4) filtering
h COMMAND - effluent history dump
4, 1.0, 1.0, 0.25, 0.1 unit op#, ptscale(1-4) filtering
D
-1, 2000.0, 1, 0.0
D
-1, 4000.0, 1, 0.0
D
-1, 5600.0, 1, 0.0
-
end of commands
7460.0, 1.0 end time(min), max dt in B.V.s
1.0d-7, 1.0d-4 abs-tol, rel-tol
- non-negative conc constraint
1.0d0 size exclusion factor
6.093d-5 part-pore diffusivities(cm^2/min)
4.062d-4 Brownian diffusivities(cm^2/min)

```

---

---

0.3944	Freundlich/Langmuir Hybrid a	(moles/L B.V.) rhob=1.0
1.0	Freundlich/Langmuir Hybrid b	(1/M) Batch specific isotherm
1.0	Freundlich/Langmuir Hybrid Ma	(-) ccap=0.580
1.0	Freundlich/Langmuir Hybrid Mb	(-)
5.37403d-4	Freundlich/Langmuir Hybrid beta	(-) "eff" isotherm Na = unknown

---

## VERSE Input for ORNL-CsRD-Run4b

---

```
[CsRD-Scale] Simulation of Cs removal on CST material (96-01) two columns second cycle
1 component (Cs) isotherm (feed point fit) (CsRD Run 4 average waste supernatant: Walker Run 4)
1, 100, 3, 6          ncomp, nele, ncol-bed, ncol-part
FCWNA                isotherm, axial-disp, film-coef, surf-diff, BC-col  FCUNA
NNNYN                input-only, perfusable, feed-equil, datafile.yio
MM                   comp-conc units
103.344, 30.6, 3800.0, 7600.0  Length(cm), Diam(cm), Q-flow(ml/min), CSTR-vol(ml)
172.0, 0.50, 0.240, 0.0      part-rad(um), bed-void, part-void, sorb-cap()
0.0                     initial concentrations (M)
S                        COMMAND - conc step change
1, 0.0, 5.10d-6, 1, 0.0      spec id, time(min), conc(M), freq, dt(min)
V                        COMMAND - viscosity/density change
0.0278, 1.253           fluid viscosity(posie), density(g/cm^3)
m                        COMMAND - subcolumns
50, 100, 0, 1, 1.0d+8, 0.0, 50000.0  elem-shift, elem-watch, pp-watch, c-watch, c-thresh, t-e, t-ee
h                        COMMAND - effluent history dump
0, 1.0, 1.0, 0.25, 0.1      unit op#, ptscale(1-4) filtering
h                        COMMAND - effluent history dump
1, 1.0, 1.0, 0.25, 0.1      unit op#, ptscale(1-4) filtering
h                        COMMAND - effluent history dump
2, 1.0, 1.0, 0.25, 0.1      unit op#, ptscale(1-4) filtering
h                        COMMAND - effluent history dump
3, 1.0, 1.0, 0.25, 0.1      unit op#, ptscale(1-4) filtering
h                        COMMAND - effluent history dump
4, 1.0, 1.0, 0.25, 0.1      unit op#, ptscale(1-4) filtering
D
-1, 2000.0, 1, 0.0
D
-1, 4000.0, 1, 0.0
D
-1, 5600.0, 1, 0.0
-
end of commands
8000.0, 1.0              end time(min), max dt in B.V.s
1.0d-7, 1.0d-4          abs-tol, rel-tol
-                          non-negative conc constraint
1.0d0                    size exclusion factor
4.062d-5                 part-pore diffusivities(cm^2/min)
4.062d-4                 Brownian diffusivities(cm^2/min)
0.3944                   Freundlich/Langmuir Hybrid a      (moles/L B.V.) rhob=1.0
1.0                      Freundlich/Langmuir Hybrid b      (1/M) Batch specific isotherm
1.0                      Freundlich/Langmuir Hybrid Ma      (-) ccap=0.580
1.0                      Freundlich/Langmuir Hybrid Mb      (-)
4.71229d-4              Freundlich/Langmuir Hybrid beta    (-) "eff" isotherm Na = unknown
-----
```

---

(This Page Intentionally Left Blank)